

Endurance

Lunar South Pole-Aitken Basin Traverse and Sample Return Rover

Mission Concept Study Report for the 2023–2032 Planetary Science
and Astrobiology Decadal Survey

James Tuttle Keane (JPL)

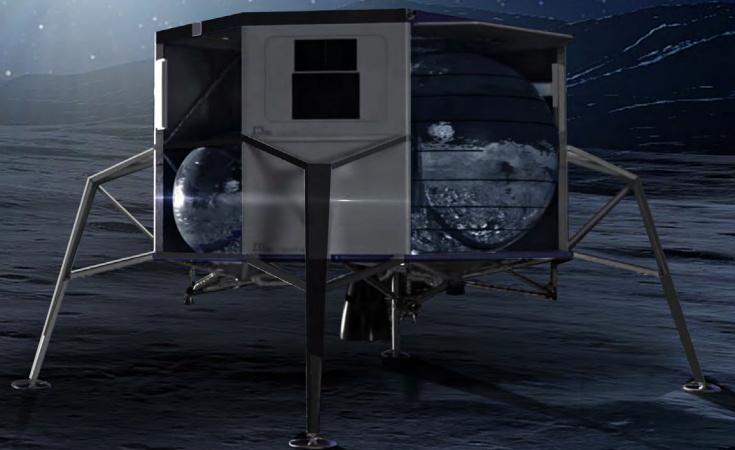
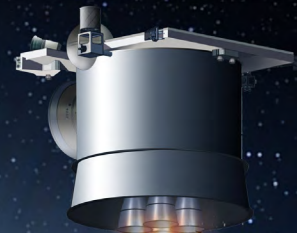
Science Champion, james.t.keane@jpl.nasa.gov

Sonia M. Tikoo (Stanford)

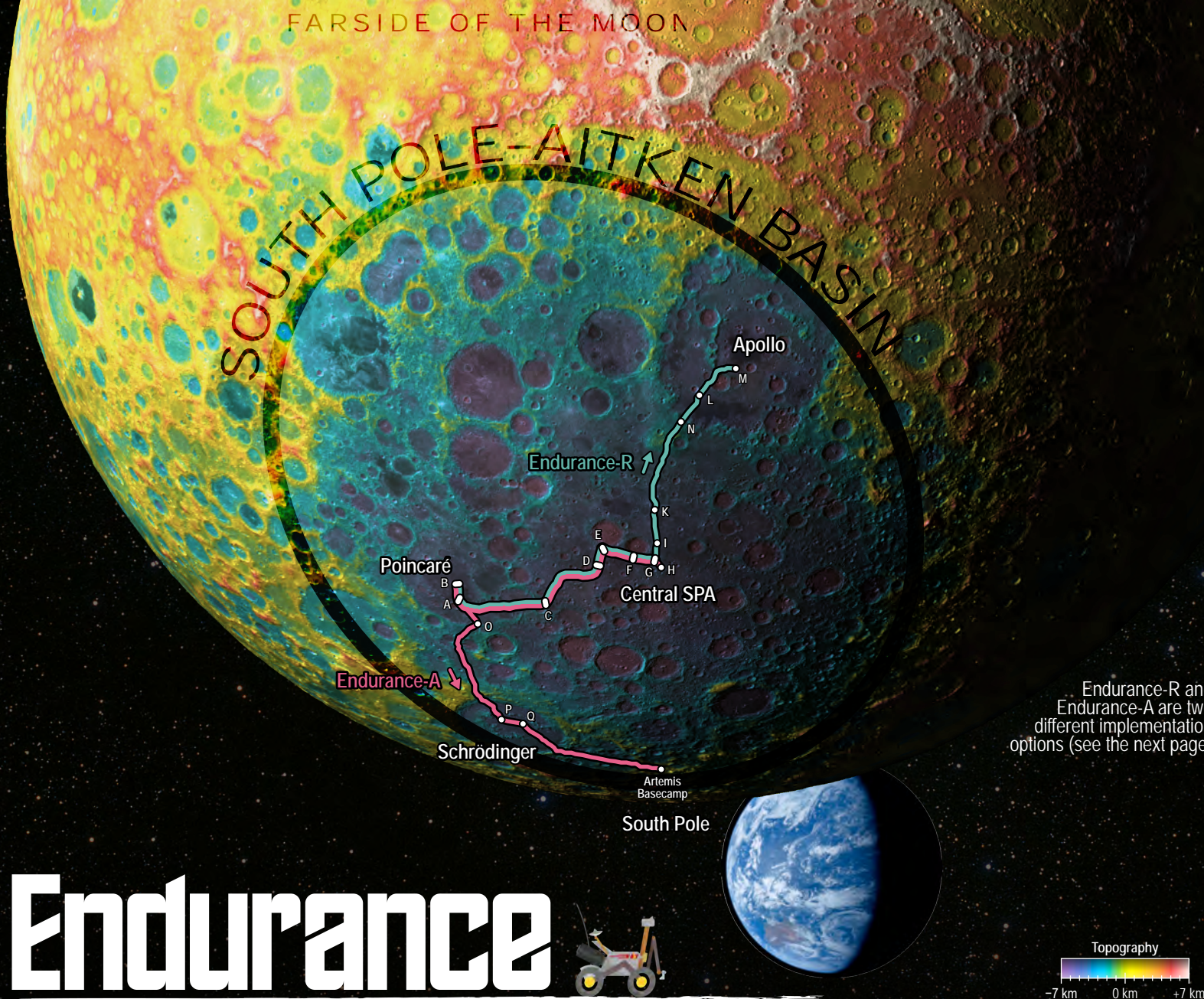
Deputy Science Champion, smtikoo@stanford.edu

John Elliott (JPL)

Study Lead, john.o.elliott@jpl.nasa.gov



SOUTH POLE-AITKEN BASIN



Endurance-R and Endurance-A are two different implementation options (see the next page)

Endurance



Lunar South Pole-Aitken Basin Traverse and Sample Return Rover

2023–2032 Planetary Science and Astrobiology Decadal Survey Mission Concept Study

Earth image: Apollo 11 / NASA / JSC;
Moon topography: LRO LOLA;
Moon image mosaic: LRO WAC / LRO LOLA /
NASA's Scientific Visualization Studio;
Sky: Taurus / NSF NOIRLab / Akira Fujii.
Composited by James Tuttle Keane.

Science Objectives:

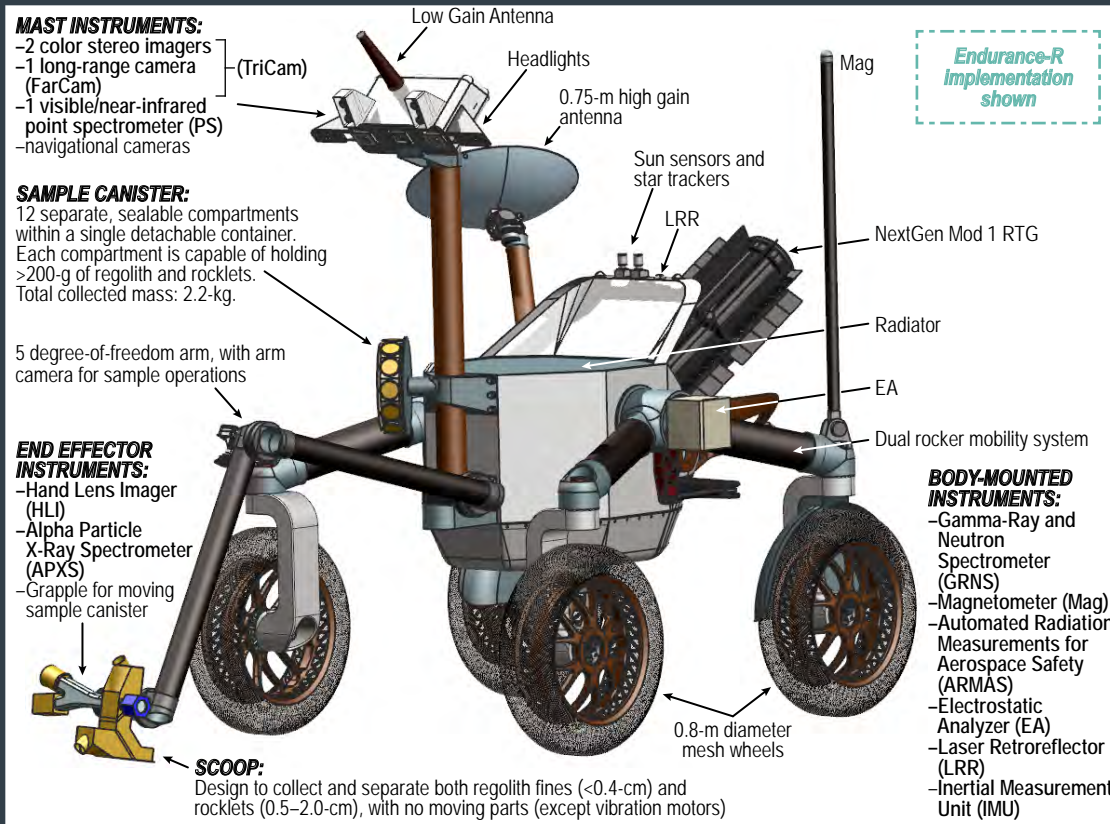
Endurance is a mission concept for a long-range rover (capable of traversing nearly 2,000 km) designed to explore and ultimately collect, cache, and return 12 samples from the South Pole-Aitken (SPA) basin on the farside of the Moon.

SPA is the largest and oldest (undisputed) impact basin on the Moon, and holds critical answers to Solar System chronology and planetary evolution.

SCIENCE THEME 1
SOLAR SYSTEM CHRONOLOGY

SCIENCE THEME 2
PLANETARY EVOLUTION

- 1.1 **Anchor the earliest impact history of the Solar System** by determining the age of the largest and oldest impact basin on the Moon: South Pole-Aitken basin.
Key Sample Sites: Central SPA (C, D, E, F, G, H, I, K), Poincaré and Apollo peak ring material (A, M), Lyman ejecta (O)
- 1.2 **Test the giant planet instability, impact cataclysm, and late heavy bombardment hypotheses** by determining when large farside lunar impact basins formed.
Key Sample Site: Poincaré basin (A, B), Apollo basin (M, N), Lyman basin (O), Schrödinger basin (P, Q)
- 1.3 **Anchor the "middle ages" of Solar System chronology (between 1 and 4 billion years ago)** by determining the absolute age of a cratered, farside lunar mare basalt.
Key Sample Sites: mare basalts (A, B, D, L, M), SPA resurfacing material (K)
- 2.1 **Test the magma ocean paradigm and characterize the thermochemical evolution of terrestrial planets** by determining the age and nature of volcanic features and compositional anomalies on the farside of the Moon.
Key Sample Sites: mare basalts (A, B, D, L, M), SPA ejecta (C), SPA resurfacing material (E, F, G, H, I, K), pyroclastics (Q)
- 2.2 **Explore a giant impact basin from floor to rim** by characterizing the geologic diversity across the gigantic South Pole-Aitken basin.
Key Sample Sites: all



Endurance-R Implementation shown

IMPLEMENTATION HIGHLIGHTS:

The Endurance mission concept relies on high-TRL hardware, advanced autonomy, detailed traverse pre-planning, and night-operations that enable traversing ~2,000-km across the lunar farside within four years.

- Rover Mass:** 487-kg (fully margined).
- Rover Size:** 2.7-m (length) x 1.8-m (width) x 2.5-m (height).
- Mobility:**
 - 4-wheeled driving and steering.
 - Large (80-cm diameter) mesh compliant wheels for mobility and longevity.
 - Maximum Traverse Speed: 1 kilometer per hour.
 - Average Traverse Speed: 0.5 kilometers per hour.
 - Capable of traversing slopes up to 20°.
 - Ground clearance: 0.6-meters.
- Power:** NextGen Mod 1 RTG (245 W at beginning of life), with secondary battery.
- Communications:**
 - 2-axis gimbaled 0.75-m S-band high gain antenna.
 - S-band omni directional low-gain antenna.
 - Farside communications enabled by an orbital relay (not costed or designed in this study). At least three relays are anticipated to be available in this timeframe (including Gateway).
- Launch date:** 2030 (based on the earliest availability of the RTG).
- Lunar Landing:** Delivered by a NASA Commercial Lunar Payload Service (CLPS) lander. Commercial landers with this capability are expected to be in regular operation in this timeframe (e.g., VIPER, a 500-kg rover, will be delivered to the lunar south pole by a CLPS lander in 2023).

SAMPLE CANISTER:
12 separate, sealable compartments within a single detachable container. Each compartment is capable of holding >200-g of regolith and rocklets. Total collected mass: 2.2-kg.

5 degree-of-freedom arm, with arm camera for sample operations

END EFFECTOR INSTRUMENTS:
-Hand Lens Imager (HLI)
-Alpha Particle X-Ray Spectrometer (APXS)
-Grapple for moving sample canister

SCOOP:
Design to collect and separate both regolith fines (<0.4-cm) and rocklets (0.5-2.0-cm), with no moving parts (except vibration motors)

BODY-MOUNTED INSTRUMENTS:
-Gamma-Ray and Neutron Spectrometer (GRNS)
-Magnetometer (Mag)
-Automated Radiation Measurements for Aerospace Safety (ARMAS)
-Electrostatic Analyzer (EA)
-Laser Retroreflector (LRR)
-Inertial Measurement Unit (IMU)

Endurance — One Concept with Two Implementation Options:



Endurance-R
R is for "Robotic"

Endurance-R would land on a CLPS lander in Poincaré basin, traverse through central SPA, collect a total of 2.2-kg of samples from 12 sites, and rendezvous with a second CLPS lander in Apollo basin carrying a robotic Earth Return Vehicle, which receives the samples and brings them to Earth.



Endurance-A
A is for "Astronaut"

Endurance-A would land on a CLPS lander in central SPA, traverse out of SPA through the Poincaré and Schrödinger basins, collect a total of 100-kg of samples from 12 sites, and deliver those samples to Artemis astronauts at the south pole, who retrieve the samples and bring them to Earth.

COST

Development Cost (A-D):	Phase E:	Launch Vehicles and CLPS Landers (x2):	Total Project Cost:
\$1,778 M	\$252 M	\$400 M	\$2,430 M

Flagship Class

Development Cost (A-D):	Phase E:	Launch Vehicles and CLPS Landers (x1):	Total Project Cost:
\$1,105 M	\$233 M	\$200 M	\$1,538 M

New Frontiers Class

Endurance is effectively a sample collection campaign in one mission, and it would address the highest priority questions in lunar science, with enormous implications for Solar System science. Endurance would capitalize on partnerships with commercial partners through the NASA CLPS program. The Endurance-A option would create a new paradigm for collaboration between NASA's Science Mission Directorate (SMD), and Human Exploration and Operations Mission Directorate (HEOMD)—achieving more science for less cost.

Science Champion: James Tuttle Keane (JPL, james.t.keane@jpl.nasa.gov). Deputy Science Champion: Sonia M. Tikoo (Stanford, smtikoo@stanford.edu). JPL Study Lead: John Elliott (JPL, john.o.elliott@jpl.nasa.gov). Science Team: Pamela Clark (JPL), Brett Denevi (JHUAPL), Alex Evans (Brown), Caleb Fassett (NASA Marshall), Jennifer Heldmann (NASA Ames), Francis McCubbin (NASA Johnson), Dan Moriarty (NASA Goddard), Mark Robinson (ASU). JPL Study Team: Mineh Badalian, John Baker, Paul Briggs, Mark Chodas, Faramaz Davarian, Martin Feather, Michael Fong, Natalie Gallegos, Ron Hall, David Hinkle, Jim Jackson, Richard Kim, Emily Law, Heather Leihco, Shan Malhotra, Larry Matthies, Kristine McGowan, Joe Melko, Rudranarayan Mukherjee, Charles Nainan, Hari Nayyar, Issa Nesnas, Hiro Ono, Raul Polit-Casillas, Miles Smith, Catherine Suh, Eric Sunada, Thaddeus Voss, and JPL's A-Team and Team-X. Pre-Decisional Information — For Planning and Discussion Purposes Only



Disclaimers/Acknowledgements

Pre-Decisional Information – For Planning and Discussion Purposes Only

The research was carried out at the Jet Propulsion Laboratory, California Institute of Technology, under a contract with the National Aeronautics and Space Administration (80NM0018D0004).

The cost information contained in this document is of a budgetary and planning nature and is intended for informational purposes only. It does not constitute a commitment on the part of JPL and/or Caltech.

© 2021. All rights reserved.



Study Participants

Endurance Science Team

Pamela Clark	Jet Propulsion Laboratory
Brett Denevi	Johns Hopkins University Applied Physics Laboratory
Alex Evans	Brown University
Caleb Fassett	NASA Marshall Space Flight Center
Jennifer Heldman	NASA Ames Research Center
James Tuttle Keane	Jet Propulsion Laboratory
Francis McCubbin	NASA Johnson Space Center
Dan Moriarty	NASA Goddard Space Flight Center
Mark Robinson	Arizona State University
Sonia M. Tikoo	Stanford University

JPL Study Team

Mineh Badalian	Shan Malhotra
John Baker	Larry Matthies
Paul Briggs	Joe Melko
Mark Chodas	Rudra Mukherjee
Faramaz Davirian	Kristine McGowan
John Elliott	Charles Nainan
Martin Feather	Hari Nayar
Michael Fong	Issa Nesnas
Natalie Gallegos	Hiro Ono
Ron Hall	Raul Polit-Casillas
David Hinkle	Miles Smith
Jim Jackson	Catherine Suh
Richard Kim	Eric Sunada
Emily Law	Thaddaeus Voss
Heather Lethcoe	

With significant additional participation from the members of JPL's A-Team and Team X.



PLANETARY SCIENCE DECADAL SURVEY

Mission Concept Study Final Report

Table of Contents

EXECUTIVE SUMMARY.....	vii
1 SCIENTIFIC OBJECTIVES	1
1.1 Science Background.....	1
1.2 What is South Pole–Aitken (SPA), and Why Go There?.....	2
1.3 Overview and Ground Rules of the Endurance Concept Study.....	3
1.4 Endurance Science Themes and Objectives	4
1.4.1 Science Theme #1: Solar System Chronology.....	4
1.4.2 Science Theme #2: Planetary Evolution	5
1.5 Endurance and the Long-Range Traverse of South Pole–Aitken Basin.....	5
1.6 Endurance Sample Science	7
1.7 Endurance Instrument Suite.....	8
1.8 Expected Significance.....	8
2 HIGH-LEVEL MISSION CONCEPT.....	9
2.1 Concept Maturity Level (CML).....	9
2.2 Technology Maturity.....	10
2.3 Key Trades	11
2.3.1 Mobility.....	11
2.3.2 Sampling	12
2.3.3 Sample Return.....	12
2.3.4 Autonomy/Localization.....	13
2.3.5 Power	14
3 TECHNICAL OVERVIEW	14
3.1 Instrument Payload Description.....	14
3.2 Flight System.....	14
3.2.1 Overview	14
3.2.2 Rover Subsystems	15
3.2.3 Earth Return Vehicle (ERV)	19
3.3 Concept of Operations and Mission Design.....	21
3.3.1 Launch, Cruise, and Landing Phase.....	21
3.3.2 Checkout.....	21
3.3.3 Traverse	21
3.3.4 Traverse Plan	22
3.3.5 Sample Acquisition.....	22
3.3.6 Sample Transfer.....	23
3.3.7 Sample Return.....	23
3.3.8 Telecom Strategy	23
3.3.9 Operations Strategy.....	24
3.4 Risk List.....	25
4 DEVELOPMENT SCHEDULE AND SCHEDULE CONSTRAINTS.....	25
4.1 High-Level Mission Schedule.....	25
4.2 Technology Development Plan.....	26
4.3 Development Schedule and Constraints.....	28



5 MISSION LIFE-CYCLE COST.....28

5.1 Costing Methodology and Basis of Estimate28

5.2 Cost Estimate(s)29

5.3 Potential Cost Savings30



Appendices

A	ACRONYMS	A-1
B	SCIENCE	B-1
B.1	Developing Endurance’s Long-Range Traverse.....	B-1
B.2	Geology of Endurance’s Long-Range Traverse	B-16
B.2.1	Central South Pole–Aitken	B-35
B.2.2	Poincaré Basin	B-35
B.2.3	Apollo Basin.....	B-36
B.2.4	Schrödinger Basin.....	B-36
B.2.5	High-Thorium Anomalies.....	B-37
B.2.6	Other Destinations on the South Pole–Aitken Basin Traverse	B-37
B.3	Science Operations	B-38
B.3.1	Endurance’s science instruments	B-38
B.3.2	Science Operations at Sample Sites	B-40
B.3.3	Target Lithologies	B-42
B.3.4	Identifying Target Lithologies with Spectroscopy.....	B-43
B.4	Sample Science	B-45
B.5	Science Frequently Asked Questions (FAQs):.....	B-50
B.5.1	How does Endurance address the priority science questions of the Decadal Survey?	B-50
B.5.2	What Decadal Survey white papers informed the Endurance concept?	B-51
B.5.3	How does Endurance compare to the other sample return (and in situ analysis) mission concepts, like the South Pole–Aitken Basin Sample Return concept in Vision and Voyages, In Situ Geochronology, and Artemis?	B-51
B.5.4	How does Endurance compare with Intrepid?.....	B-54
B.5.5	What is the nature of lunar regolith, and what are the challenges with sampling it?.....	B-54
B.5.6	What is the lunar mantle made of?	B-55
B.5.7	What instruments could Endurance descope?	B-55
B.5.8	What could Endurance do with an extended mission?	B-56
C	JPL TEAM X REPORTS.....	C-1
C.1	Rover Report	C-2
C.2	ERV Report	C-17
C.3	Combined Mission Report.....	C-41
D	MOBILITY.....	D-1
E	AUTONOMY.....	E-1
F	AUTONOMY RELIABILITY	F-1
G	ESTIMATING MISSION DURATION.....	G-1
G.1	Communication Constraints.....	G-1
G.2	Sloped-Terrain Mobility	G-1
G.3	Driven Path Inefficiency (Path tortuosity)	G-2
G.4	Autonomy Reliability (fault rates)	G-4
G.5	ConOps	G-5
G.6	Effective Traverse Rate	G-5
H	SAMPLING	H-1
H.1	Sample Chain Trades.....	H-1

- I TELECOMMUNICATIONS..... I-1
 - I.1 Lunar Relay Services for the 2030s..... I-1
 - I.1.1 Coverage I-3
 - I.1.2 Emergencies I-6
 - I.2 Communications Link I-6
 - I.2.1 The Radio I-7
 - I.2.2 The Antenna I-8
 - I.2.3 Functional Block Diagram of the Communications System I-8
- J THERMAL DESIGN J-1
- K PATH PLANNING K-1
 - K.1 Northern Traverse K-2
 - K.2 Southern Traverse K-4
 - K.3 Tools K-6
 - K.3.1 Lunar Reconnaissance Orbiter (LRO) NAC Search..... K-6
 - K.3.2 DEM / Mosaic Pipeline K-7
 - K.3.3 Lighting..... K-8
 - K.3.4 Communications K-10
 - K.4 Craters and Rocks K-12
 - K.5 Visualization K-15
- L ROVER ARCHITECTURE L-1
 - L.1 Block Diagram..... L-1
 - L.2 Configuration L-3
 - L.2.1 Endurance-A: Astronaut Version L-3
 - L.2.2 Endurance-R: Robotic Sample Return..... L-13
 - L.2.3 Endurance Rover (A and R Versions) Thermal System..... L-28
 - L.2.4 Endurance Rover (A and R Versions) Masthead L-30
- M ADDITIONAL COST MODELING INFORMATION M-1
 - M.1 Wrap factors..... M-3
 - M.2 SEER..... M-3
 - M.3 TruePlanning..... M-8
 - M.4 SOCM M-16
- N REFERENCES..... N-1
 - N.1 Sections 1 – 5..... N-1
 - N.2 Appendices N-5



EXECUTIVE SUMMARY

Since the last Decadal Survey, new ideas have emerged about the timing and nature of planet migration and impact bombardment, suggesting that the redistribution of primordial comets, asteroids, and other planetesimals may have happened earlier in Solar System history than previously expected. At the same time, new geologic evidence suggests that radiometric ages obtained from Apollo samples may be biased by a single impact basin (Imbrium), providing an incomplete and incorrect view of Solar System chronology. Finally, exploration of worlds across the Solar System—from Mercury to Pluto—have revealed the prevalence of giant, planetary-scale impacts, but only hint at the possible effects such impacts have on their target bodies.

The lunar farside and, in particular, the gigantic (~2,500-km diameter) South Pole–Aitken (SPA) basin provide a unique opportunity to address this confluence of problems. SPA is the largest and most ancient (undisputed) impact basin on the Moon—if not the entire Solar System. As the oldest basin on the Moon, SPA is a critical datum constraining the impact history of the Solar System and the formation of the Earth–Moon system. Determining the age of SPA, and the other large basins superposing it, would provide critical new constraints on the Earth and Moon’s bombardment history during the time when life first emerged on Earth, providing unparalleled insights into the formation and evolution of a habitable worlds that would serve as our touchstone to the emergence of life elsewhere in the Solar System. Moreover, determining the age of SPA would singularly revolutionize our ability to calibrate with exceptional certainty the timing of events across the Solar System. Additionally, SPA almost certainly excavated the lunar mantle, providing a window into the early thermochemical evolution of a rocky world.

Endurance is a mission concept for a long-range rover designed to address high priority planetary science questions by exploring and ultimately collecting, caching, and returning samples from SPA. The rover is an evolution of the Intrepid planetary mission concept study [1], and is capable of traversing nearly 2,000-km of lunar terrain in under four years, owing to a high degree of pre-planning and automation. As Endurance traverses this terrain, it will collect scientific measurements along the entire traverse using a suite of remote sensing instruments, with hundreds of stops for investigating the local geology, geochemistry, and geophysics. Along its journey, Endurance would collect samples from 12 key, pre-identified locations across SPA which would then be returned to Earth for analyses in terrestrial laboratories, enabling transformative advances in the understanding of solar system chronology and planetary evolution.

We formulated two variants of Endurance: Endurance-R and Endurance-A. These two variants both address the same motivating science questions, although they have different traverses, sample collection systems, and costs.

- **Endurance-R** (R is for “Robotic”) would deliver the sample cache to a separately landed robotic Earth Return Vehicle (ERV), which would deliver the sample back to Earth in a Stardust/Genesis/OSIRIS-REx-like sample return capsule. Endurance-R would return 2.2-kg of material from 12 sites spanning 1,750-km of SPA, with a development cost (A–D) of \$1.8B (FY25)—placing it firmly in the Flagship mission class.
- **Endurance-A** (A is for “Astronaut”) would deliver the sample cache to Artemis astronauts near the lunar south pole. Endurance-A would deliver 100-kg of material from 12 sites spanning 2,000-km of SPA to astronauts, with a development cost (A–D) of \$1.1B (FY25)—commensurate with a New Frontiers-class mission. The mass of samples collected by Endurance-A is comparable to the return from a single J-Class Apollo mission (Apollo 17 returned 110-kg of material).

Both variants of Endurance would yield transformative, flagship-caliber planetary science, far exceeding the science requirements for the highly recommended SPA sample return concept in previous Decadal Surveys [2, 3]. Both variants would return samples from priority sites spanning ~2,000-km, comparable to the distances between multiple Apollo landing sites (the greatest distance between two Apollo sites is 1,750-km). Endurance is effectively a sample return campaign in one mission. The Endurance-A concept demonstrates that if planetary science can partner with human exploration, we can achieve transformative planetary science at greatly reduced cost.



1 SCIENTIFIC OBJECTIVES

1.1 SCIENCE BACKGROUND

Over the past two decades, new ideas have emerged about the timing and nature of planetary bombardment and the early restructuring of the Solar System. It is now generally agreed that the giant planets (Jupiter, Saturn, Uranus, Neptune) formed in a more compact configuration—with quasi-circular, coplanar orbits between 5–20 Astronomical Units (AU) (Neptune is currently at 30 AU). Dynamical interactions between these planets and the remnant disk of planetesimals (comets, asteroids, etc.) led to the outward migration of the giant planets, eventually triggering a dynamical **giant planet instability** where the giant planets rapidly reorganized (in tens to hundreds of millions of years), leaving them closer to their present-day orbital configuration [4, 5]. During this evolution, once stable reservoirs of planetesimals were swiftly destabilized—sending them careening throughout the Solar System, increasing the impact bombardment rate across the Solar System. While the giant planet instability hypothesis has been used to explain many aspects of the Solar System—from the orbital architecture of the giant planets, and the properties of small body populations (see reviews in [4], [6])—the original primary piece of evidence for this hypothesis lies in the lunar impact record [7].

The lunar impact record is constrained by laboratory analyses of samples returned from the Apollo and Luna missions, and lunar meteorites. These analyses reveal a pronounced spike in large impact events near 3.9 billion years ago, called the **late heavy bombardment (LHB)** or **lunar cataclysm** [8–11]. The lunar cataclysm hypothesis posits that most large lunar impact basins (impact craters with diameters >300 kilometers) formed in a single spike around 3.9 billion years ago, lasting roughly a hundred million years, amidst what is otherwise a smooth decay of impacts following the formation of the Solar System (Figure 1-1). This spike is naturally explained by the giant planet instability hypothesis, which predicts similar spike of high impact rates when the orbits of the giant planets destabilize. However, the late heavy bombardment hypothesis has been contentious since its inception during the Apollo era. In the past decades, there has been growing concern that the perceived spike in impact flux may represent repeated dating of a single large impact basin, Imbrium [8, 12–15]. Imbrium dominates the lunar nearside, and its ejecta may similarly dominate the lunar sample collection. While additional constraints can be gleaned from geochronology analyses of other planetary materials (e.g., meteorites, returned samples and/or in situ geochronology analyses across the Solar System), the Moon—with its ancient surface and intimate ties to the Earth—will forever remain a critical cornerstone of Solar System chronology. As these hypotheses evolve and shift, it is clear that without new constraints on the ages of lunar impact basins, we will be unable to determine the true nature of the earliest history of the Solar System.

As our understanding of Solar System chronology has evolved, so too has our understanding of planetary evolution. Laboratory analyses during the Apollo era led to the development of the **magma ocean** hypothesis, where the Moon formed with an initially thick layer of melt (>100s of kilometers thick), which crystallized in sequences building the layered structure we observe on the Moon today (e.g., [16, 17]). Most terrestrial planets in the Solar System are thought to have gone through a magma ocean phase like the early Moon—including Mercury, Venus, Earth, and Mars [18]. Jupiter's moon Io may support a present-day subsurface magma ocean from tidal heating (e.g., [19, 20]). Many rocky exoplanets also likely went through a magma ocean phase, and some present-day magma ocean exoplanets are known (e.g., 55 Cancri e; [21]). Despite the ubiquity of magma oceans, the Moon is the best-preserved primordial magma ocean world, as most other rocky planets have been substantially reworked since these early epochs (e.g., Earth's plate tectonics has erased most of this time period, and Io's prolonged activity has evolved it far beyond a primordial rocky world). While the basic hypothesis has remained, the details have become complicated. Classic magma ocean crystallization models predict a very particular initial compositional stratigraphy within the Moon (Appendix B). While this is consistent with the composition of the Moon's uppermost layers (i.e., crust), it is unclear if these models accurately predict layering at depth. The largest basins, like the South Pole–Aitken basin, almost certainly excavated large volumes of lunar mantle—yet the lunar mantle predicted by magma ocean crystallization models has not been unambiguously observed in remote sensing datasets or returned samples [22–24]. There are major questions about whether the layering predicted by

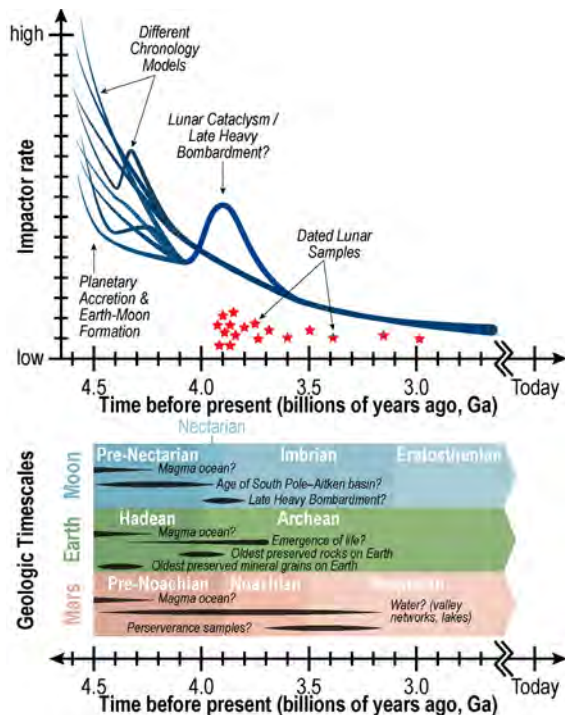


Figure 1-1. Qualitative illustration of the early impact record of the Moon. As you go further back in time (to the left), possible chronologies (blue lines) diverge, revealing our lack of knowledge of the earliest epochs of Solar System formation and evolution—when life was emerging on the Earth (and possibly elsewhere in the Solar System). Endurance would provide critical data points in these earliest epochs (before 3.9 Ga), testing competing hypotheses. Figure by J.T. Keane.

[36]; Caloris, Mercury [37]; Sputnik, Pluto [38]), causing global reorientation (e.g., Sputnik, Pluto [39, 40]), and more. Impacts of this scale are challenging to simulate numerically (e.g., [23, 41], and interpretation of remote sensing datasets are limited by the lack of samples to provide ground truth.

1.2 WHAT IS SOUTH POLE-AITKEN (SPA), AND WHY GO THERE?

Despite the breadth of the aforementioned, outstanding science questions—from Solar System chronology, to magma oceans, and giant impacts—there is one location in the Solar System that holds the answers all of these questions: the SPA basin on the farside of the Moon. SPA is the largest, deepest, and most ancient (undisputed) impact basin on the Moon—and possibly the entire Solar System (Figure 1-2A). SPA spans >2,000 kilometers on the lunar farside, from nearly the south pole to low latitudes, and has a depth of ~8 kilometers [42].

Exploration of SPA presents a unique opportunity to address a broad swath of priority themes in Planetary Science (e.g., [43]). As the oldest preserved lunar impact basin, SPA is a critical datum for constraining Solar System chronology. SPA effectively sets the “ $t = 0$ ” of the lunar and Solar System impact record—both because it is the oldest recognized stratigraphic unit, and because the impact itself may have resurfaced a large portion of the Moon, providing a “clean slate” for later impacts. Subsequent large impact basins superposed on SPA—like Poincaré, Apollo, and Ingenii—provide critical tests of the Late Heavy Bombardment, far from the possible contamination of nearside impact basins (i.e., Imbrium). Additionally, due to its large size, SPA almost certainly excavated the lunar mantle, which when coupled with analyses of the volcanic material in the basin, would provide an

magma ocean crystallization models was gravitationally stable or overturned (e.g., [23]). Moreover, classic magma ocean crystallization is generally assumed to be a globally uniform process, yet the Moon has an ancient, pronounced nearside-farside asymmetry—where the lunar nearside has a thinner crust and more extrusive volcanism than the farside—which has remained unexplained since its discovery. Hypotheses range from asymmetric thermal evolution due to Earth-shine [25], to asymmetric convection of the mantle [26–28], asymmetric crystallization of the magma ocean [29], tidal processes (e.g., [30, 31], giant impacts like South Pole–Aitken (e.g., [23, 32]), and even larger impacts (e.g., [33, 34]). None of these processes can be separated from questions about Solar System chronology, as some of these events (e.g., magma ocean crystallization, mantle overturn, lunar volcanism, late heavy bombardment, giant planet instability) may have occurred around the same time. For example, as the lunar magma ocean crystallized, it is unclear if the Moon would preserve the evidence of impacts into a magma ocean or slushy crust and mantle.

Finally, continued exploration of the Solar System over the last decade has revealed the ubiquity of **giant impacts**—where the resulting crater is comparable to the target body’s radius—from Mercury to Pluto (Figure 1-2). Despite their prevalence, giant impacts produce wildly varying outcomes on different bodies, and even different outcomes for different giant impacts on the same body, ranging from reshaping global crustal structure (e.g., Borealis, Mars [35]), triggering volcanism and tectonism (e.g., South Pole–Aitken, Moon

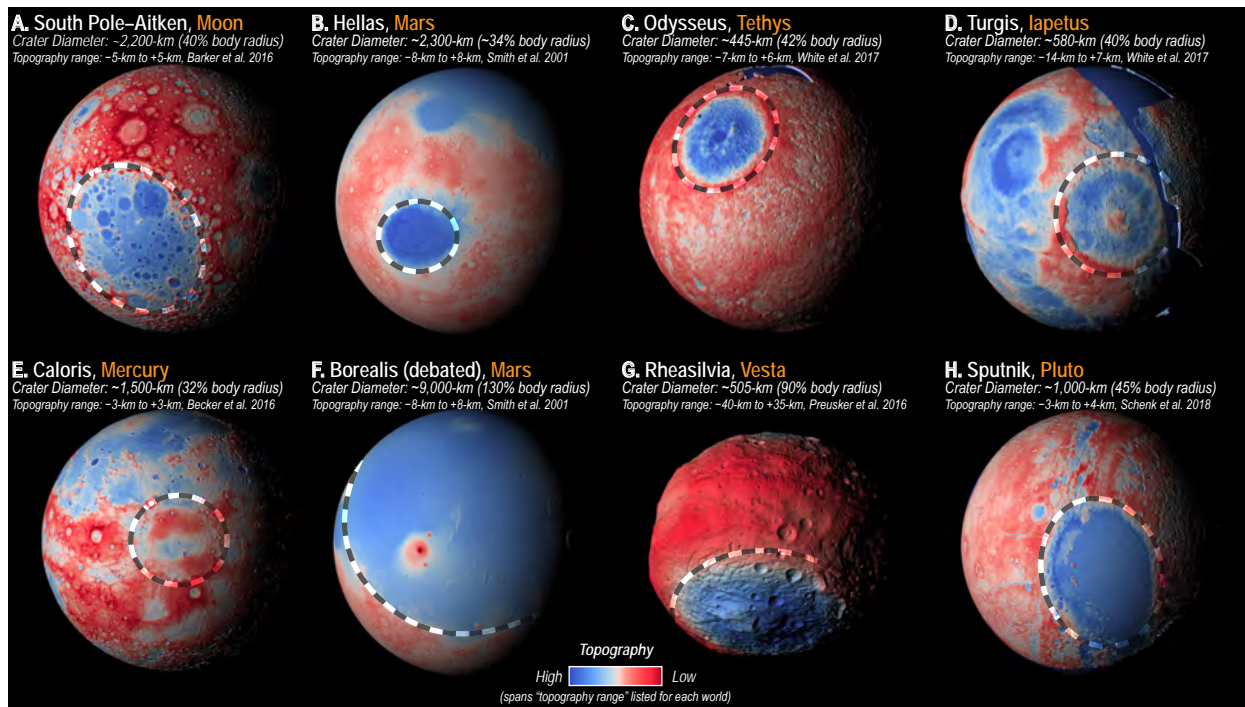


Figure 1-2. Giant impacts dominate bodies across the Solar System. Endurance would provide the first in situ exploration, from floor to rim, of a giant impact basin. Figure by J.T. Keane.

unprecedented view into the interior structure and thermochemical evolution of a terrestrial world. Nowhere else in the Solar System is this record so well preserved and readily accessible.

The importance of SPA has been long recognized, and SPA Sample Return (SPA-SR) has consistently ranked as one of the top priorities for planetary exploration in the two previous Decadal Surveys [2, 3], and the top priority for lunar exploration [44, 45]. While motivated by many of the same science questions, Endurance is very different, and more comprehensive than previous SPA-SR concepts.

1.3 OVERVIEW AND GROUND RULES OF THE ENDURANCE CONCEPT STUDY

Endurance is a mission concept for a long-range rover designed to address high priority planetary science questions by exploring and ultimately collecting, caching, and returning samples from the SPA basin on the farside of the Moon.

The Endurance concept was requested by the panel on Mercury and the Moon of 2023–2032 Planetary Science and Astrobiology Decadal Survey. Endurance is an evolution of the Intrepid planetary mission concept study [1], which was designed to traverse >1,800 kilometers on the lunar nearside in order to address priority science questions focused on lunar magmatism. Intrepid utilized solely remote sensing instruments, and did not collect, cache, or return samples. The Mercury and the Moon panel was impressed by the Intrepid concept and sought to understand if an Intrepid-like architecture could be applied to addressing the longstanding goal of SPA sample return.

Key *a priori* assumptions and guidelines for the Endurance mission concept study were:

- The study shall consider at least two architectures for returning samples: (1) Deliver samples to Artemis astronauts near the lunar south pole who would return the samples to Earth (Endurance-A), (2) Deliver the samples to a robotic Earth return vehicle (Endurance-R).
- The study shall assume that Endurance’s instrument suite is identical to the suite of scientific instruments on Intrepid, with the addition of sample collection and caching system. The concept study shall not consider adding or removing instruments.
- The study shall assume that a communications relay is in place and capable of supporting Endurance’s operations on the lunar farside (consistent with the plans of NASA and commercial providers in this timeframe), and shall not design or cost the development of a communications relay.



- The study shall assume that Endurance is delivered to the lunar surface by NASA Commercial Lunar Payload Service (CLPS) provider, and shall not design or cost the development of this lander. The CLPS program is anticipated to have appropriate payload capabilities in the near future. For example, NASA’s ~500-kg Volatiles Investigating Polar Exploration Rover (VIPER) will be delivered by a CLPS lander to the lunar south pole in 2023. Intrepid also used this assumption.
- For the option where Endurance returns samples via a robotic Earth return vehicle (Endurance-R), the study shall assume that the Earth return vehicle is delivered to the lunar surface by a second CLPS lander, and shall not design or cost the development of this lander.

Key goals and anticipated outcomes from the Endurance mission concept study were:

- The concept study shall evaluate the methodology for collecting, caching, and returning samples with a modified version of the Intrepid rover.
- The concept study shall evaluate the sample mass and characteristics that would be required to address priority science questions.
- The concept study shall evaluate the scientific and cost trades between the two sample return architectures: delivering samples to astronauts (Endurance-A), or delivering samples to a robotic Earth return vehicle (Endurance-R).
- The concept study shall evaluate the feasibility and scientific merit of a long-range rover traverse of the South Pole–Aitken basin.

Endurance vs. Endurance-R vs. Endurance-A

As described above, the Endurance concept includes two rover concepts: **Endurance-R** (R is for “Robotic”) refers to the rover that delivers its sample cache to a robotic Earth return vehicle. **Endurance-A** (A is for “Astronaut”) is the rover that delivers its sample cache to Artemis astronauts. Endurance-R and Endurance-A are largely identical from an engineering perspective, although they have different traverses, slightly different sample collection and caching systems, and ultimately different costs. Throughout this report, when referring to a specific concept, we will use “Endurance-R” or “Endurance-A”; when referring to the overall project, or an aspect that is identical between the two concepts, we will use “Endurance.”

1.4 ENDURANCE SCIENCE THEMES AND OBJECTIVES

Endurance’s science objectives are designed around two science themes: Solar System Chronology and Planetary Evolution. Themes and objectives are listed in priority order, and are enumerated in the **Science and Traverse Traceability Matrix** (Foldout, Table 1-1).

1.4.1 SCIENCE THEME #1: SOLAR SYSTEM CHRONOLOGY

Objective 1.1: Anchor the earliest impact history of the Solar System by determining the age of the largest and oldest impact basin on the Moon: South Pole–Aitken (SPA).

As the oldest undisputed impact basin in the Solar System, SPA provides a critical datum to understanding Solar System bombardment. SPA constrains how far back the lunar impact chronology—and by extension, the Solar System chronology—goes (Figure 1-1). This is reflected in three competing hypotheses that could be tested with returned samples from the basin: (1) If SPA formed ~4.5 billion years ago, shortly after the Moon’s formation, it implies that the Moon retains a nearly complete record of Solar System bombardment. Additionally, an age for SPA of ~4.5 billion years would provide new strict bounds on the age of the Moon and the Moon-forming impact. (2) If SPA formed ~4.3 billion years ago, then this implies that many (if not most) of the early impact basins on the Moon were erased by some process(es), ranging from basin erasure due to a hot and weak crust/mantle, to erasure by the SPA impact itself. (3) If SPA formed ~4.0 billion years ago, this would make SPA part of the lunar cataclysm, implying that the cataclysm was even more pronounced than previously hypothesized. Validation of any one of these hypotheses would have a ripple effect throughout all of planetary science, establishing a reliable paradigm for our understanding of Solar System chronology.

Objective 1.2: Test the giant planet instability and impact cataclysm hypotheses by determining when farside lunar basins formed.

Since the last Decadal Survey, new ideas have emerged about the timing and nature of planetary



migration and giant planet instability, suggesting that the redistribution of comets, asteroids, and other planetesimals may have occurred earlier in Solar System history. At the same time, new geologic evidence suggests that Apollo samples may date only a single basin—Imbrium—thus adding further uncertainty about the existence of the Lunar Cataclysm hypothesis or Late Heavy Bombardment (LHB). As these theories evolve and shift, it is clear that without new constraints on the ages of lunar basins, we will be unable to determine the true nature of the early history of Solar System bombardment. This bombardment record is best preserved and most accessible on the Moon, and acquiring the age of a single farside impact basin would readily test these hypotheses.

Objective 1.3: Anchor the "middle ages" of Solar System chronology (between 1 and 4 billion years ago) by determining the absolute age of a cratered, farside lunar mare basalt.

Returning samples from a young, but cratered surface on the lunar farside, like a volcanic deposit (i.e., a mare basalt), would provide a critical new datum for calibrating our capability of relating impact crater statistics (e.g., size-frequency distributions), and absolute ages. Improved understanding of these “middle ages” of lunar history would propagate throughout Solar System chronologies.

1.4.2 SCIENCE THEME #2: PLANETARY EVOLUTION

Objective 2.1: Test the magma ocean paradigm and characterize the thermochemical evolution of terrestrial worlds by determining the age and nature of volcanic features and compositional anomalies on the farside of the Moon.

As the largest and oldest (undisputed) impact basin in the Solar System, SPA provides a unique view into the lunar interior and the overall thermochemical evolution of rocky worlds. SPA almost certainly excavated large volumes of lunar mantle [23], however there is debate about what and where that material is, revealing a fundamental uncertainty about the composition and state of the lunar mantle. Samples returned from targeted regions within SPA would provide the first direct samples of a rocky planetary mantle. Furthermore, samples from SPA would be the first returned samples from the farside of the Moon (with a known provenance), and would shed light on the nature of global asymmetries in heat-producing elements, volcanism, and crustal structure—providing new constraints on the bulk composition, origin, and evolution of the Moon—and by extension, many rocky worlds.

Objective 2.2: Explore a giant impact basin from floor to rim by characterizing the geologic diversity across the South Pole–Aitken Basin.

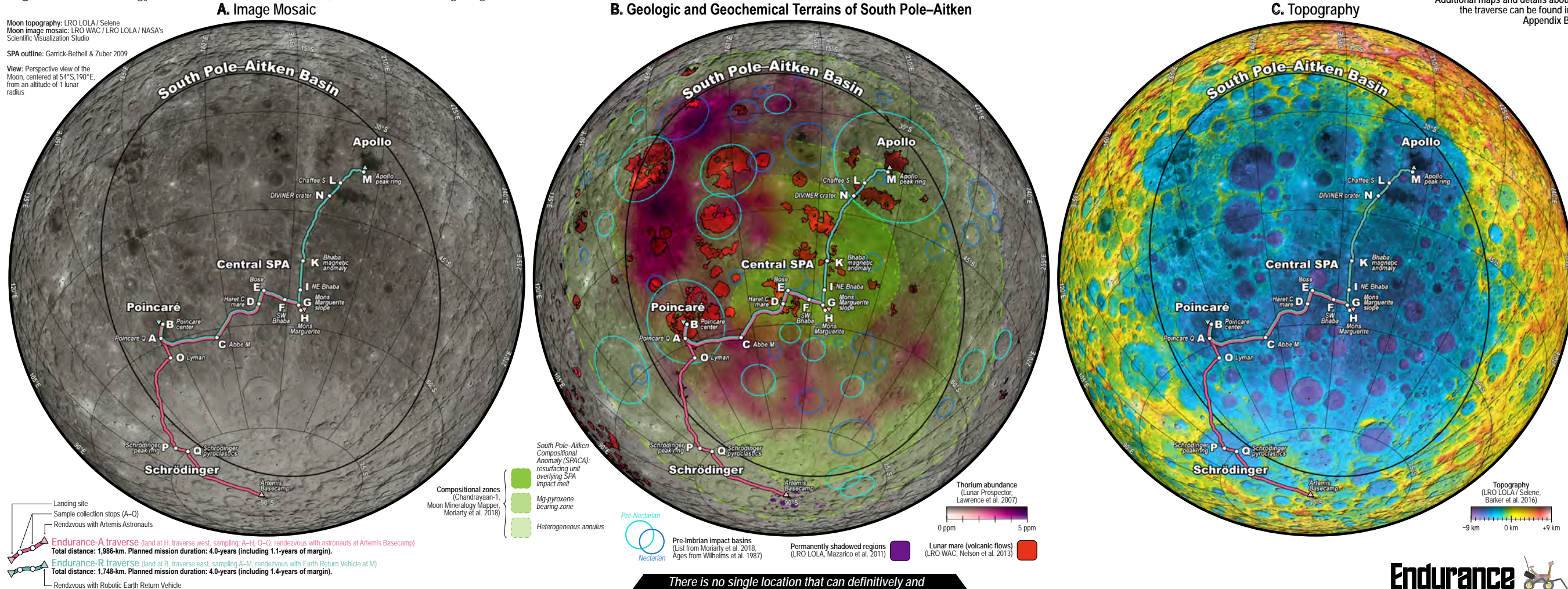
Planetary scale impacts like SPA are found throughout the Solar System (Figure 1-2). In many cases, these impacts are hypothesized to have substantial (if not catastrophic) effects on their host planets—from the hypothesized Borealis creating Mars’s global asymmetry, to the Sputnik impact reorienting Pluto and triggering cryovolcanism. Despite their ubiquity, planetary scale impacts are poorly understood, and they are harder to probe with computer simulations. A traverse across SPA would provide transformative ground-truth to both orbital remote sensing data and theoretical simulations, while also providing new data to constrain hypotheses about impact processes at a fundamental level.

1.5 ENDURANCE AND THE LONG-RANGE TRAVERSE OF SOUTH POLE–AITKEN BASIN

While the lunar farside and SPA hold the answers to many priority planetary science questions, the challenge is that no single site that can definitively and conclusively address all of the Science Objectives outlined here. Figure 1-3 shows maps of SPA and its different geologic and geochemical terrains, and Endurance’s Science and Traverse Traceability Matrix. Each of Endurance’s Science Objectives flows to different sample location requirements. For example, to date SPA (Objective 1.1) it necessary to go to central SPA (bright green in Figure 1-3B), where SPA impact melt is excavated by smaller craters, whereas to test for the Late Heavy Bombardment (Objective 1.2), it is necessary to go to a large impact basin like Poincaré or Apollo (blue circles in Figure 1-3B). Previous SPA sample return concepts (e.g., [3]) assumed a single lander, which would only capable of addressing a fraction of Endurance’s Science Objectives. To do all of these Science Objectives requires long-range mobility—over 1,000-km. This motivates the Endurance mission concept.

Endurance is a long-range rover concept that would address all of the aforementioned Science Objectives by traversing >1,700-km of lunar terrain in under four years. We planned two

Figure 1-3. The Geology of the South Pole–Aitken Basin, and Endurance's long range traverse.



View: Perspective view of the Moon, centered at 54°S, 190°E, from an altitude of 1 lunar radius

SPA outline: Garrick-Bethell & Zuber 2009

Endurance-A traverse (land at H, traverse west, sampling A–H, O–Q, rendezvous with astronauts at Artemis Basecamp)
Total distance: 1,986-km. Planned mission duration: 4.0-years (including 1.1-years of margin).

Endurance-R traverse (land at B, traverse east, sampling A–M, rendezvous with Earth Return Vehicle at M)
Total distance: 1,748-km. Planned mission duration: 4.0-years (including 1.4-years of margin).

There is no single location that can definitively and conclusively answer all of the science questions outlined here—motivating Endurance's long-range traverse.

Table 1-1. Endurance science and traverse traceability matrix.

SCIENCE OBJECTIVES:	MEASUREMENT REQUIREMENTS:	SAMPLE SITE REQUIREMENTS:	Core Traverse (both Endurance-A and Endurance-R)							North Traverse (Endurance-R only):				South Traverse (Endurance-A only):				
			A	B	C	D	E	F	G	I	K	N	L	M	H	O	P	Q
SCIENCE THEME 1: SOLAR SYSTEM CHRONOLOGY	1.1. Anchor the earliest impact history of the Solar System by determining the age of (perhaps) the largest and oldest impact basin on the Moon: South Pole–Aitken (SPA).	Determine the age of SPA to within ±0.05 Ga.	≥1 sample from the SPA melt sheet, as exposed by craters excavating through the SPA compositional anomaly (SPACA).	Contributing		X		X	X	Contributing	Contributing			Contributing	Contributing	X	Contributing	
	1.2. Test the giant planet instability and impact cataclysm hypotheses by determining when farside lunar basins formed.	Determine the age of ≥1 farside, pre-Imbrian impact basin to within ±0.05 Ga.	≥1 sample from the impact melt sheet and/or peak ring of a farside, pre-Imbrian impact basin.	X	X								X	X		Contributing	Contributing	Contributing
	1.3. Anchor the "middle ages" of Solar System chronology (between 1 and 4 billion years ago) by determining the absolute age of a cratered, farside lunar mare basalt.	Determine the age of ≥1 cratered, farside mare basalt flow to within ±0.05 Ga.	≥1 sample from a cratered farside mare basalt.	X	X		X				Contributing	Contributing	X	X				
SCIENCE THEME 2: PLANETARY EVOLUTION	2.1. Test the magma ocean paradigm and characterize the thermochemical evolution of terrestrial worlds by determining the age and nature of volcanic features and compositional anomalies on the farside of the Moon.	Determine the age of ≥2 distinct volcanic samples from the lunar farside to within ±0.05 Ga. Determine the composition of ≥2 volcanic samples from the lunar farside.	≥2 samples from a farside volcanic deposit, including mare basalts, pyroclastics, or other volcanic units.	X	X	Contributing	X	X	X	X	X		X	X	X		Contributing	X
	2.2. Explore a giant impact basin from floor to rim by characterizing the geologic diversity across the South Pole–Aitken Basin.	Determine the composition and characteristics of the major geochemical terrains across SPA, including SPA impact melt, SPA ejecta, and post-SPA volcanic products.	≥1 sample from a Thorium hot-spot (>3 ppm) materials on the lunar farside. ≥1 sample from each of the three geochemical major terrains within SPA: (1) SPACA, (2) Pyroxene Bearing Zone, and (3) Heterogenous Annulus.			X												
				X	X	X	X	X	X	X	X	X	X	X	X	X	X	X

1 sample is defined as 200-grams of regolith, including ≥20 rocklets between 0.5–2.0 cm. Sample science traceability is defined in Table 1-2. Samples also require both local-scale and regional scale geologic context measurements utilizing Endurance's remote sensing suite listed as described in Table 1-3. More details are in Appendix B.

Threshold Requirement: 6 samples
Baseline Requirement: 12 samples

X Samples from this location can meet the Sample Requirements, and would substantially address the motivating Science Objectives.

Contributing Samples from this location would contribute to addressing the motivating Science Objectives, but may not completely address them.

Additional information about each Sample Site can be found in Appendix B.



traverses—one for each of the Endurance implementation options—as shown in Figure 1-3. Endurance-R would be delivered by a CLPS lander in central Poincaré basin, traverse east into central SPA passing “Mons Marguerite” (informally named volcanic dome near the center of SPA), before traversing north to the Apollo. Endurance-A would land on a CLPS lander in central SPA, near Mons Marguerite, traversing west to Poincaré, and then south via Schrödinger basin, before arriving at the Artemis basecamp near the south pole. Along each traverse, Endurance would collect samples from 12 key, pre-selected sites that would uniquely and completely address all of the Science Questions and Objectives outlined here. Details of this traverse are provided in Appendix B.

While Endurance’s samples motivate the long-range traverse, Endurance would collect important data over the entire traverse using its instrument suite (Section 1.7). Many instruments would remain on continuously, including radiation monitors, magnetometer, and gamma-ray and neutron spectrometer. Endurance would have frequent pre-planned stops to collect data with its other instruments, including stops every 2-km for acquiring panoramas, microscopic images, and long-integrations with alpha particle x-ray, gamma-ray, and neutron spectrometers. In effect, Endurance would collect a high-resolution swath of in situ data across SPA that provides geologic context for the samples, addresses new science questions, and ground-truths orbital datasets. Details of the Endurance concept of operations are in Section 3.2, and Appendix B.

1.6 ENDURANCE SAMPLE SCIENCE

The majority of Endurance’s science objectives are addressed through detailed analyses of returned samples in laboratories here on Earth. While in situ radiometric dating, mineralogy, and geochemistry of planetary materials is possible (see the In Situ Geochronology PMCS report [46, 47]), analyses in Earth-based laboratories can achieve much higher precision than in situ measurements. Detailed characterization of returned samples, including determining lithologies, mineral compositions, and abundances, can ensure the best possible specimens are selected for radiometric dating. Earth-based studies also enable reproducibility by use of various geochronometers (e.g., U-Pb, Pb-Pb, ⁴⁰Ar/³⁹Ar, Rb-Sr, Sm-Nd, and Lu-Hf) to obtain multiple ages for an individual sample. Furthermore, recently developed methods such as laser probe analysis may be used to study heterogeneities in ages recorded within a single rock sample that may result from exposure to multiple impact events over lunar history [48].

Table 1-2 summarizes a range of laboratory analyses that could be performed to address the motivating science objectives (see Appendix B for a more detailed description). We provide this overview as a framework for any future mission proposals, which would select a refined suite of sample investigations. Each of these different analyses have different requirements for samples; for example, U-Pb and Pb-Pb dating require sifting through ~40-g of regolith to obtain the necessary number of zircons for statistically significant results [49], while the remaining geochronology methods require

Table 1-2. Samples returned by Endurance would be analyzed in state-of-the-art laboratories on Earth, capable of addressing the mission’s highest priority planetary science questions. More details about sample science can be found in Appendix B.

Analysis	Science Motivation	Analytical Approach	Sampling Requirements, Per Sample Site	
GEOCHRONOLOGY	Determine the age of SPA, other basins, and igneous rocks (basalts, crustal, pyroclastic) to ±0.05 Ga.	U-Pb, Pb-Pb	Collection of zircons from 40-g of regolith fines for either method	From each sample site, Endurance shall collect ≥200-grams of sample, including: ≥20 rocklets (0.5-cm to 2.0-cm diameter) and un-sieved regolith fines
		Ar-Ar, Rb-Sr, Sm-Nd, Lu-Hf	10-g of regolith rocklets (>4-mm diameter) for all methods combined	
PETROGRAPHY AND MINERAL COMPOSITION	Determine mineral occurrences and abundances, petrographic textures, elemental and oxide abundances Study trace elements to understand igneous rock petrogenesis, bulk composition, and mantle geochemistry	Optical microscopy, electron microprobe (EDS/WDS), SEM, FIB/TEM, SIMS, XANES	20-g of regolith rocklets (>4-mm diameter) for all methods combined	
		Inductively coupled plasma mass spectrometry (ICP-MS)	6-g of regolith fines or rocklets (>4-mm diameter)	
STABLE ISOTOPE GEOCHEMISTRY AND VOLATILES	Determine the global abundance and distribution of volatile elements, which ultimately provide key insights into the origin of the Moon and mantle geochemistry and degree of heterogeneity	Volatile abundances (C, F, Cl, S, OH in mineral phases and glasses) by SIMS	0.3-g of regolith rocklets (>4-mm diameter) for all methods combined	
		OH, H, Cl, S, Zn, K, N, and other stable isotope systems	15-g of regolith rocklets (>4 mm diameter rocklets) for all methods combined	
			13-g of regolith fines for all methods combined	



preparation of subsamples from initially intact rocklets. Some materials may be re-used for multiple investigations using different approaches.

1.7 ENDURANCE INSTRUMENT SUITE

In addition to its sampling system, the Endurance rover incorporates the complete suite of nine instruments used in the earlier Intrepid mission concept. **As stated in the study guidelines (Section 1.3), Endurance did not consider an instrument trade.** This decision, mandated by the Mercury and the Moon panel of the Decadal Survey, was based on the assumption that Intrepid’s instrument suite was more than capable of supporting Endurance’s science investigations—even though Intrepid’s payload was optimized for different science investigations (e.g., magmatism, swirls). In short, the panel felt that the Intrepid was a robust and adaptable rover suitable for investigating a range of science questions (analogous to how the Mars Exploration Rovers, Spirit and Opportunity, utilized identical payloads to explore different terrains on Mars). The Endurance payload suite would acquire the geochemistry, mineralogy, geology, magnetic, radiation, and solar wind observations required to meet the science objectives while maintaining high-Technology Readiness Level (TRL) and a simple ConOps. The instruments are summarized in Table 1-3 and Figure 1-4, and additional details can be found in Appendix B and the Intrepid report [1].

1.8 EXPECTED SIGNIFICANCE

Endurance was conceived and designed to address some of the highest priority questions in planetary science, and the highest priority questions in lunar science—which have been called out repeatedly in numerous community documents over at least three decades, and yet never addressed head on. The most comprehensive prioritization of lunar science goals was completed in 2007 [45], and included in the top five (of 35 total) were: (1) Test the cataclysm hypothesis by determining the spacing in time of the lunar basins; (2) Anchor the early Earth-Moon impact flux curve by determining the age of the oldest lunar basin (South Pole–Aitken Basin); (3) Establish a precise absolute chronology; (4) Determine the composition of the primary feldspathic crust, KREEP layer, and other products of planetary differentiation. Endurance would directly address these goals.

By embarking on a comprehensive tour of the only remaining unsampled lunar terrain type [50], and collecting samples from locations that can now be carefully selected based on the revolutionary remote sensing data collected by multiple nations over the last 15 years, Endurance would provide the means to directly address these questions. At the same time, Endurance would also provide new value to all past remote sensing datasets of the lunar farside.

While Endurance is framed around a small number of specific Science Objectives and testable hypotheses (consistent with the scope of New Frontiers-class mission), it is important to note the transformative amount of “spin-off” science that would be enabled by a ~2,000-km traverse through South Pole–Aitken. Additionally, Endurance-A’s large mass of returned samples (100 kg) would provide even more science and opportunities for unanticipated discoveries for laboratories across the globe.

Endurance also capitalizes on NASA’s investments in and partnerships with commercial providers through utilization of CLPS lander(s). Endurance-A would additionally provide a new paradigm for collaboration between NASA’s Science Mission Directorate (SMD) and Human Exploration and Operations Mission Directorate (HEOMD).

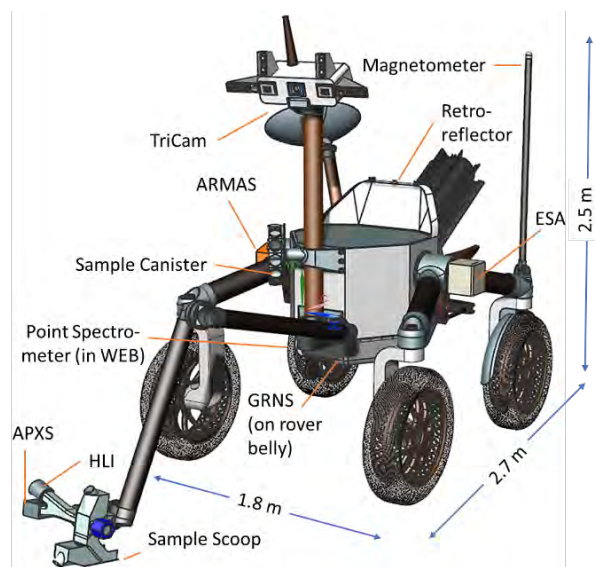


Figure 1-4. Rover configuration showing instrument accommodation. Endurance-R implementation shown.



Table 1-3. Endurance Instrument Suite. Power and mass estimates are from high TRL instruments. Total standby power: 30-W. Total instrument mass: 19.8-kg. Note: these are instrument capabilities, not requirements. Additional details about this instrument suite can be found in the Intrepid PMCS report [1].

Instrument		Key Parameters and Capabilities	Heritage	Data	Peak (Standby) Power	Mass	Rover Accommodation
TriCam	Stereo Imagers	<p>Pair of color stereo imaging cameras to characterize local geology</p> <ul style="list-style-type: none"> • 3 color bands (RGB) • FOV: 50° × 37.5° (>180° with mosaicking) • IFOV: 220-μradians (1-mm pixel scale at 4-m range, 1-cm pixel scale at 45-m range) 	MSL, LRO LROC, MSSS, ECAM, others	up to 8.5-MBytes per obs.	12-W (9-W)	5.9-kg (3.5-kg on mast)	<p>Mast viewing requirements:</p> <ul style="list-style-type: none"> • Yaw: $\pm 90^\circ$ • Pitch: -60° to $+15^\circ$ • Pointing accuracy: $\pm 2^\circ$ • Height: >1.4-m
	FarCam	<p>Monochromatic narrow angle camera for long-range reconnaissance</p> <ul style="list-style-type: none"> • FOV: 6.7° × 5° (>180° with mosaicking) • IFOV: 50-μradians (5-cm pixel scale at 1-km range) 					
PS: Point Spectrometer		<p>Near-infrared spectra for determining mineralogy</p> <ul style="list-style-type: none"> • 16 color bands (300-nm to 1,400-nm) • FOV: <0.3° (3-m spot size at 100-m range) 	MSL, SELENE	~35-Bytes per obs.	4-W (4-W)	2-kg (1-kg on mast)	
HLI: Hand Lens Imager		<p>Hand lens imager for imaging lunar regolith and rocks at the microscopic scale</p> <ul style="list-style-type: none"> • 3 color bands (red, green, blue [RGB]) • 2-cm to infinite focal range (15-μm pixel scale at 23-mm range) • Active focus and illumination (for day & AE33:AE34night operations) 	MSL MAHLI	5.4-Mbytes per obs.	12-W (1-W)	0.6-kg	Position accuracy: 2-cm off surface or rock
APXS: Alpha Particle X-Ray Spectrometer		<p>X-ray spectra for determining elemental abundances</p> <ul style="list-style-type: none"> • Energy range: 0.4-MeV to 10-MeV • Sensing depth: 2-cm (below space weathering rind) 	MSL APXS	~30-kBytes per obs.	8-W (8-W)	2.3-kg (0.9-kg on arm)	Position accuracy: 5-cm on surface or rock
Mag: Magnetometer		<p>Magnetometer</p> <ul style="list-style-type: none"> • Magnetic field intensity: $\pm 100,000$-nT • Precision: 0.2-nT • Sampling rate: 1-Hz 	MESSENGER, others	60-kBytes per hour	1.7-W (1.7-W)	0.5-kg	Mounted >1-m away from magnetic sources on the rover
GRNS: Gamma Ray and Neutron Spectrometer		<p>Gamma-ray and neutron spectra for determining elemental abundances</p> <ul style="list-style-type: none"> • Energy range: 0.4-MeV to 10-MeV • Sensing depth: 30-cm 	MESSENGER, Lunar Prospector, others	4-kBytes per obs.	4-W (4-W)	3-kg	Mounted on the bottom of the rover, <70-cm from the surface with clear view to the surface
ARMAS: Automated Radiation Measurements for Aerospace Safety		<p>Radiation monitor for measuring heavy ions, alphas, protons, neutrons, electrons, and gamma-rays</p> <ul style="list-style-type: none"> • Absorbed energy: 60-keV to >15-MeV 	LRO CRaTER	~300-kBytes per hour	0.3-W (0.3-W)	1-kg	Requires mostly unobstructed, omni-directional zenith viewing
ESA: Electrostatic Analyzer		<p>Radiation monitor to characterize solar wind ions and other ionizing radiation</p> <ul style="list-style-type: none"> • Energy range: 200-eV to 20-keV • Energy resolution: 8% 	THEMIS	500-kBytes per hour	2-W (2-W)	4.2-kg	Mounted with upward facing view
LRR: Laser Retro-Reflector		<p>Passive laser retroreflector for geodetic measurements from other spacecraft</p>	SpacEL Beresheet	N/A	N/A	0.5-kg	On top of rover, visible from an orbiting, nadir-pointed laser
IMU: Inertial Measurement Unit		<p>LN-200S accelerometer, for measuring gravitational accelerations</p> <ul style="list-style-type: none"> • Sensitivity: 10 mGal • Sampling rate: <400 Hz 	Curiosity	N/A	N/A	N/A	N/A

2 HIGH-LEVEL MISSION CONCEPT

2.1 CONCEPT MATURITY LEVEL (CML)

The Endurance concept as presented in this study is at CML 4, per the definitions presented in the Decadal Survey mission concept study ground rules. The initial rover concept began with the CML 4 Intrepid design and was modified to meet the particular requirements of the Endurance mission given the difference in location on the lunar farside and the components needed to accomplish the sample collection objectives. In addition, an ERV system point design and operations concept was developed



and costed to support the full autonomous sample return mission option. Each mission element was defined at the assembly level and was estimated for mass, power, data volume, link rate, and cost by Team X using JPL's institutionally endorsed design and cost tools. Following this an in-depth configuration, design and operations refinement effort was conducted by the study team.

2.2 TECHNOLOGY MATURITY

The Endurance rover design leverages the Intrepid PMCS design trades adapting to a new mission to explore the South Pole–Aitken basin. It also benefits from significant prior art, robust engineering processes and design practices, and a large body of knowledge generated in developing and successfully operating Mars rovers over the last two decades. It leverages experience from past and current lunar rovers (Apollo Lunar Roving Vehicle [LRV], Lunokhod, Yutu) and builds on current lunar development activities including the VIPER lunar rover, as well as significant advances in capabilities from other space and terrestrial applications. As is the case with any new mission concept, the Endurance rover will need specific engineering developments and the application of key technologies.

Lunar Dust Environment: Lunar dust is a potential hazard with unique challenges posed by abrasive particles, electrostatic charging of surfaces, and differential charging effects over the day/night cycle. Our current understanding of lunar dust challenges for rovers is built on experience gained from past lunar surface missions and is informed by continuing technology efforts [51] as well as current plans for the upcoming commercial (CLPS) landers and VIPER rover missions. Given that dust deposition in the lunar environment primarily results from the interactions of the wheels with terrain the system is designed to keep all dust-sensitive surfaces well above the height of the wheels to minimize dust accumulation at Endurance's low mobility speed (<1 km/hr). The slow mobility together with frequent hourly stops minimize wheel triboelectric charging and enhances charge dissipation. Arm-mounted instruments are equipped with dust covers and are kept as far off the regolith as possible during sampling operations. Further, sampling operations will be conducted with slow sampling arm motions to minimize lofting of dust. Sample transfer operations are designed to take place away from sensitive surfaces. While engineering development activities and validation to mitigate dust remain and are planned for, especially for the long-distance traverse, there are no new technologies that are anticipated beyond what has been employed by prior missions (including Mars) and those being addressed by the upcoming VIPER rover.

Science Instruments: The Endurance rover mission objectives are met using the same high-heritage instrument suite that has been identified for the Intrepid mission (Table 1-3). The HLI and APXS are based on those currently in use on MSL. ARMAS has flown on high-altitude balloons, sounding rockets, Unity Space Ship Two, New Shepard, and CubeSats. All components of TriCam have heritage with MSSS ECAM, MSL and LRO imaging systems. While standard engineering will be needed to adapt these instruments to the Endurance mission, none of them require new technologies. Only the point spectrometer and its integration with the FarCam will require flight qualification since it is based on a new combination of existing product-line elements.

Mobility and Manipulation System: Endurance's mobility system has a four-wheel-drive, all-wheel-steered vehicle with compliant wheels, which is similar to Intrepid. However, unlike Intrepid, which had a single passive front rocker suspension for the lowest mass, Endurance uses a dual-side rocker suspension which better accommodates the sampling system in front of the rover. The dual-rocker design has been part of the suspension that has proven effective for all of NASA's Mars rovers. Endurance's 0.8 m compliant wheels are similar in both size and design to the LRV mesh wheels. NASA Glenn Research Center has conducted a detailed design, development, and testing campaign (currently at TRL 6 for Mars environment) that improved this design to extend durability and traversability (rocks and craters). Further maturation of the wheel design and materials for the lunar environment for this mission will be needed (See Appendix D).

The manipulation system on Endurance serves two primary functions: (1) sample collection, caching, and cache transfer¹ and (2) instrument placement. It comprises a 5 degree-of-freedom robotic

¹ The cache transfer is only relevant to the Robotic Return option. The rover-mounted sample caching system is different between the Robotic and Astronaut Return options, with the latter accommodating a larger mass without a robotic cache transfer option.



arm with a turret end effector that hosts the sampling scoop and two instruments: the HLI and APXS. The sampling system design, informed by prior MoonRise studies for sampling and sample return from the South Pole–Aitken basin, consists of a scoop for sampling, sieving, and regolith/rocklet transfer, a sample cache, and mechanisms to transfer the cache to the lander. The sampling scoop and scooping operation for collecting regolith and small rocks is a new design that will need to be further developed and tested. The sample cache will also be transferred to the ERV in a coordinated process between the vehicle, arm and ERV. The technologies associated with these operations will need to be matured in preparation for the Endurance mission (See Appendix H). Actuator technology is adequately mature from prior martian and lunar missions and motor controllers are based on the maturation of the distributed Europa motor controllers, whose specifications would encompass the needs of this mission.

2.3 KEY TRADES

2.3.1 MOBILITY

Table 2-1 captures Endurance’s key mobility requirements and expected terrain characteristics. They are similar to the traverse requirements for Intrepid except that Endurance requires significantly longer distance and faster night driving to free the daytime for sampling operations. Night driving is slower than day driving because the visible horizon is limited by onboard lighting requiring additional stops with long camera exposures.

For the mobility trade, key drivers are robustness and durability, long-traverse distance, energy efficiency, low power, and the ability to traverse expected terrain. The Northern Route (Endurance-R) is relatively flat with 88% of the route at less than 5° in slope and 98% at less than 10°. The Southern Route (Endurance-A) has 84% of its route at less than 5° and 98% at less than 10° (see Appendix D, Table D-2).

Mobility designs with different wheel/steering configurations, suspension (passively compliant or actuated) [52], and wheel types and sizes, leveraging Apollo wheel-design data (see Appendix D) were examined based on these requirements. Table 2-2 summarizes the selection for the mobility system and corresponding rationale. The selected architecture is four-wheel drive, all-wheel steering with a passive, dual-rocker suspension that balances the weight of the vehicle among its four wheels. The wheels are large for better traction and narrow to reduce mass. Compliant wheel rims improve traction and reduce wear [53].

The choice of the dual-rocker suspension was primarily driven by the need to accommodate the

Table 2-1. Key Mobility Requirements and Constraints.

		Requirements	Comments
Rover	Endurance-R: Northern Route		
	Nominal Distance	1,750 km	Based 59 m/pixel DEM
	Actual Distance	2,050 km	Accounting for terrain tortuosity
	Endurance-A: Southern Route		
	Nominal Distance	2,000 km	Based 59 m/pixel orbital map
	Actual Distance	2,350 km	Accounting for terrain tortuosity
	Both		
	Max wheel speed	1 km/hr	Mechanical speed (or 28 cm/s)
Ave traverse rate (day)	0.65 km/hr	Incl. eng. stops for localization	
Ave traverse rate (night)	0.35 km/hr	Also incl. long-exposure imaging	
Max slope	15°	Actual route at rover scale	
Environment	Characteristics		Comments
	Surface properties	Regolith	Largely ubiquitous
	Max slope	15°	From 3×3 grid (20 m/px) DEM
	Rock distribution (area coverage)	1%	Most of the traverse route
	Crater distribution (areal coverage)	~10%	Around crater rims

Table 2-2. Mobility Trades, Selection, and Rationale.

		Key Trades	Selection	Rationale
Configuration	Type	Wheeled vs. tracked	Wheeled	Lower mass, larger ground clearance and lower risk of rocks entrapment
	Configuration	Drive + steering wheels: 3-wheel (1 steering) 4- and 6-wheel config (see Figure 2-1)	4-wheel (4-steering)	Adequate stability (low tip-over risk) and best maneuverability at lower mass and power; resilient to single-steering failure.
		Suspension: Active vs. passive vs. spring-loaded	Passive	Balanced weight on wheels,
Wheels	Wheels	Dual-sided rocker vs. single-sided rocker	Dual-sided rocker	Keeps front available for sampling system. Reduces chassis tilt over rockier/undulating terrain relative to single rocker.
		Diameter: Large vs. small Narrow vs. wide (large: ~1½ x MSL) (narrow: ½ x MSL)	Large Narrow	Superior traction, energy efficient, enhanced obstacle traversal; fewer rotations and terrain contacts for longer life.
	G	Rigid vs. compliant	Compliant	Improved mobility in soft regolith and over rocks, improved wear resistance
G	G	Lunar rover to operate under Earth gravity vs. only lunar gravity	Earth-gravity Rover	Enables end-to-end testing of rover in different terrains without complex gravity offloading aids



sampling system at the front of the vehicle². For Endurance, the sampling system had to be mounted at the front of the vehicle for visibility with the front-facing perception system, and maneuverability for positioning with respect to sampling locations. This requirement drove the Endurance vehicle suspension design to adopt a side-mounted dual-rocker mechanism design that wraps around the vehicle chassis. The dual-rocker design has heritage from the successful Mars rovers, as it was part of their rocker-bogie suspension. For Endurance, the rocker differential that connects the left and right sides of the mechanism uses the same design as the Curiosity and Perseverance rovers, but this differential link is mounted below the vehicle chassis to accommodate the lunar rover radiator to accommodate the top-mounted radiator. The differential was incorporated toward the back of the chassis to minimize impact on ground clearance. This change did not add significantly to the mass or volume of the vehicle. A dual rocker suspension halves the tilt that the vehicle chassis experiences when traversing wheel-surmountable terrain features.

2.3.2 SAMPLING

Trades supported two separate sample chain options of robotic and astronaut-based sample return. For Endurance-R, the sampling system must (i) collect 12 separate 200 g surface samples of rocklets and loose regolith totaling 2.4 kg mass, (ii) transfer samples to a cache for separately storing the 12 samples, and (iii) transfer the cache for sample return. For Endurance-A, the sampling system collects and stores 100 kg of samples, but eliminates the requirement for robotic sample cache transfer. Trades were also carried out on accommodating the APXS and HLI instruments within the sample chain or using a separate manipulation system.

The key trades included (i) the manipulation system configuration, (ii) the design of the end effector to collect the samples using a scoop, accommodate the APXS and HLI instruments, and host a gripper to transfer the cache, (iii) the design of the sample cache on the rover, and (iv) the associated concept of operations for the different options. For the manipulation system, we considered trades for one or two arms and investigated different arm topologies, kinematic configurations, and degrees of freedom. These were subject to constraints of manipulability and reachability for operations, stowage, and observability from rover cameras. Similar trades were considered for the manipulation requirement to transfer the cache from the rover to the sample return capsule (SRC) on the ERV.

The end effector design was five major considerations (i) scoop design for lunar-surface sample collection, (ii) retention of samples of science relevant sizes (5–20 mm) and rejecting others, (iii) sample flow within and out of the scoop into the cache, (iv) protection of the science instruments from lunar dust, and (v) gripper for transferring the cache from the rover to the SRC. Risks of clogging or blockage of sample flow and uncertainty in regolith properties were significant considerations in these trades leading to designs that simplified sample flow, maximized flow areas, avoided sharp features, and minimized contact surfaces.

The trades for the sample cache design for Endurance-R were informed by considerations, among others, of (i) accommodation on the SRC, (ii) ease of sample transfer from scoop to cache, (iii) means for securely storing 12 different samples, (iv) accommodation on the rover with sufficient workspace for sample transfer from the arm. For Endurance-A, the primary considerations were the accommodation of the total 100 kg samples, the reachability of the arm, and the observability of the arm operations from the rover cameras. Appendix H discusses the trades in more detail.

2.3.3 SAMPLE RETURN

For the Endurance-R mission variant sample return trades centered around 1) destination of sample, and 2) where and when the ERV would be deployed to meet the rover.

For the first trade, possible sample return scenarios were considered involving (i) placing the sample in lunar orbit for later pickup, either by astronauts or robotic vehicle; (ii) delivering the sample to Gateway for retrieval by astronauts; and (iii) direct return to Earth. The team determined that the

² The Intrepid design chose a single-rocker to minimize mass and reduce the energy required for the long traverse. The rocker was located on the front of the rover to accommodate the RTG on the backside.



lowest risk and most straightforward option for the study to consider was direct Earth return using an OSIRIS-REx type SRC carried by an ERV.

The main architectural trade for Endurance-R was whether to bring the ERV with the rover on the same lander or deliver it on a separate lander at the end of mission. Bringing the ERV as part of a single landed mission has the advantage of requiring only one CLPS delivery mission, however numerous disadvantages were identified as well. Having the ERV at the rover landing site would require a traverse to return to the lander, limiting the area open for exploration. It would also require the ERV to be designed to survive four years in the harsh lunar environment before initiating its return mission. By sending the ERV on a separate lander the science traverse can be relatively unconstrained, with the ERV able to meet the lander at the end of mission for sample transfer. This also allows the ERV to be designed to operate for a single day on the lunar surface, eliminating requirements for overnight survival, thus simplifying the design. An additional degree of robustness is also added by building the ERV at the same time as the rover. Having the ERV available early opens the possibility of meeting the rover at any point in the traverse should problems arise that might prevent the rover from completing the full mission.

2.3.4 AUTONOMY/LOCALIZATION

For the autonomy trade, key constraints that drive the viability of the operation modes listed in Table 2-3 include: (1) the visibility and availability of the orbiting communication relay satellite, (2) bandwidth and latency of the end-to-end communication link between the rover and the ground, (3) the cadence of required rover motions (day/night traverse and instrument placement), and (4) the nominal workday ground operations schedule following the initial phase of surface operations. Unlike Intrepid, Endurance will conduct a significant portion of its traverse operations during the night. To identify the required level of autonomy, we examined trades ranging from ground-based human control, similar to the joystick operations of the Lunokhod rover, to onboard autonomous control for mobility, instrument placement and system management. Table 2-3 summarizes the autonomy-related trades. Throughput analyses based on sensors dataflow, onboard computation performance, and communication bandwidths showed that this mission has to rely on the *onboard decide* mode for a significant portion of its nominal operations and on the *human-decide* mode for handling contingencies. Furthermore, after the first four weeks of 24/7 mission operations, the project transitions to a normal workday schedule, where mobility, traverse, arm, and science operations would inevitably fall outside the workday schedule, requiring autonomy for a significant portion.

Key capabilities needed for autonomous surface operations include: navigation (hazards assessment, motion planning, and hazard avoidance), pose estimation (dead-reckoning), global localization (determining the vehicle’s location relative to orbital maps), and instrument deployment and placement on targets. Heritage navigation, pose estimation, and manipulation algorithms would be

Table 2-3. Autonomy-related Trades, Selection, and Rationale.

	Key Trades	Selection	Rationale
Operation Modes	<ul style="list-style-type: none"> • Human control: operators joystick every action • Human decide: ground computers assess w/ humans deciding on actions • Ground compute: computers assess and decide w/ limited async human oversight • Onboard decide: onboard computer controls w/ limited async human oversight 	Main: Onboard decide Backup: Human decide	Visibility and availability of the relay orbiter (nominal 4 hours every 12 hours) and the need to drive for hundreds of hours during lunar day and night (Earth day/night) using daytime operations left the <i>onboard-decide</i> mode as the only viable option for nominal operations to meet traverse rate. Slower operations can use <i>human-decide</i> mode.
Sensors	<u>Exteroceptive</u> <ul style="list-style-type: none"> • Cameras (stereo) • LIDARs (flash, spinning) • Star tracker • Sun sensor 	Stereo cameras w/ Lighting + Sun sensor + Star tracker	Lower power and mass; mature capability; wide field-of-view.
	<u>Perception Sensor Mounting</u> <ul style="list-style-type: none"> • Front only vs. front/rear perception • Body mounted vs. articulated mast mounted 	Front/rear perception Articulated front + body-mounted back	Bi-directional driving allows retracting the rover from entrapments Primary forward driving direction requires situational-awareness of a wide area for path planning
	<u>Proprioceptive</u> <ul style="list-style-type: none"> • Inertial • Resolvers, encoders, hall effect • Motor currents 	IMU + hall-effect (all) + resolvers (arm/steer only) + current	IMU complement visual odometry for low textured terrains, provides vehicle tilt; hall-effect sensors and resolvers are more reliable than encoders at high temperatures.
Compute	<u>Main Processor:</u> <ul style="list-style-type: none"> • LEON3 (dual-core) / Sphinx • LEON4 (quad-core) / Sabertooth <u>Aux Processor:</u> <ul style="list-style-type: none"> • Virtex 5 	LEON 4 Sabertooth Virtex 5	Quadruple compute and more Input/Output (I/O) Mars 2020 heritage



leveraged from the Mars rovers, but these rovers use ground-based global localization. Similar to the Mars rovers, Endurance would have to update its global localization every ~300 m. Given the ground-operations schedule and communication constraints, onboard global localization becomes necessary to meet the traverse rate and distances. Optical, radiometric, or hybrid techniques can be used for onboard global localization but require further investigation to assess accuracy based on the number of available relay orbiters and the quality of the orbital map data and rover-lit surface images at night. Optical techniques would image unique surface features, such as craters or boulders and map them to lower-resolution orbital images to correct the drift in the rover's pose estimate (dead reckoning). Periodic stops every 300 m for global localization would be necessary to maintain an error of < 10 m relative to the orbital maps. Since Endurance will be covering greater distance at night than Intrepid, global localization at night would have to rely on longer exposures of illuminated images to increase the perception horizon. Alternatively, radiometric techniques would use the known ephemerides of the orbiting satellite(s) for Doppler ranging and time-of-flight measurements to localize the rover. Depending on the precision of the inputs, the estimated localization accuracy may range between 5–15 meters. But because of the uncertainty associated with the number and availability of orbital assets at the time of the mission, an optical-based approach was baselined for this mission.

2.3.5 POWER

The Endurance mission concept was based closely on the design developed earlier in the Intrepid PMCS concept. In that earlier study two rover options were developed; one using a radioisotope power system (RPS) and one using solar power combined with batteries for overnight survival. To accommodate daytime sampling, Endurance's long-distance night driving favored an RPS option to maintain a shorter mission duration, although the solar powered option remains a viable backup at the expense of additional mission duration—at least for Endurance-R. For Endurance-A, which traverses to the south pole, RPS is strongly favored owing to the low solar elevation and prevalence of long shadows (even though Endurance-A does not drive through permanently shadowed regions.)

Changes in the Next Gen RTG program have resulted in a slightly different menu of RTGs available for the Endurance design, as detailed in the study ground rules. The choices now include Mod-0, Mod-1 and Mod-2 Next Gen RTGs, as well as the Dynamic Radioisotope Power System (DRPS).

To match the beginning of life (BOL) output power of the Intrepid 12-General Purpose Heat Source (GPHS) modular unit (300 W BOL), the Mod-0 Next Gen RTG would be a natural choice, however the limited availability of this model (only one will be produced) led the team to evaluate other options to ensure a viable design. The Mod 2 Next Gen RTG promises significant performance improvement, but its later predicted availability date (2034) might unnecessarily delay the implementation of this mission. While the DRPS falls into the right range of power as well and would apparently be a relatively straightforward implementation, concerns regarding the significantly increased mass of this option led the team to baseline the Mod-1 Next Gen RTG as the optimal choice. The Mod-1 has a BOL power output of 245 W, a power level that readily meets the mission needs as shown in Table 3-3.

It should be noted that the type of RPS is somewhat flexible for the Endurance design. While the Mod-1 RTG has been baselined, the Mod-0 or Mod-2 RTGs would be a drop-in replacement with no impact on system mass or design and would provide increased power for the mission. The DRPS could also be readily accommodated with a mass increase, but also a resultant benefit in power.

3 TECHNICAL OVERVIEW

3.1 INSTRUMENT PAYLOAD DESCRIPTION

In addition to its sampling system, the Endurance rover incorporates the complete suite of 8 instruments (plus the passive lunar retroreflector) used in the earlier Intrepid mission concept. These instruments are described in Section 1.7, Table 1-3, Appendix B, and the Intrepid report.

3.2 FLIGHT SYSTEM

3.2.1 OVERVIEW

The Endurance rover design began with the long-range rover concept developed for the earlier Intrepid PMCS. Changes were made to those subsystems where the unique requirements of the

Endurance mission warranted them, as listed in Table 3-1. Most of these changes stemmed from the addition of sample collection and transfer capability, a change in performance of available RTGs, and the communications implications of operating on the lunar far side.

As discussed in Section 2, the Endurance rover chose to look only at an RTG-powered option to enable the mission, but two slight variants of the configuration resulted from the two concepts for sample return; astronaut and robotic. In terms of rover design, these options differ only in the details of their sample acquisition and handling subsystems as illustrated in Figure 3-1. System mass and power modes are shown in Tables 3-2 and 3-3 and are the same for both variants. The rover launch mass maximum expected value (MEV) is 488 kg. Carrying the suggested 30% margin on this rover mass results in a requirement that the CLPS lander capability be at least 570 kg, which should be well within the range of medium- or large-class cargo landers expected to be available in this timeframe. Power output of the Mod-1 RTG provides robust margins in all power modes through end of mission. Rover characteristics are summarized in Table 3-4.

3.2.2 ROVER SUBSYSTEMS

Subsystem elements for Endurance were derived from the design of the original Intrepid rover concept using proven, heritage designs as well as product lines currently in late stages of development.

3.2.2.1 Mobility

The mobility system is designed for the expected terrain along two possible routes (see Appendix D, Table D-2). Both routes are designed to maintain slope angles that do not exceed 15°,

Table 3-1. Endurance Rover Design Changes from Intrepid.

Subsystem	Intrepid	Endurance
ACS	Cameras, IMUs, SS	Add headlights and ST for night driving
Telecom	CXS-610 radio, LGAs, Omnis	UST-Lite radio, 0.75 m steerable HGA, LGAs to accommodate relay
C&DH	Dual string Sabertooth	Same
Power	12-GPHS Next Gen RTG with 300 W BOL	Mod 1 Next Gen RTG with 245 W BOL
Thermal	Radiator, thermal switch, etc.	Same
Structures/Mechanisms	Aluminum/composite, one 5-DOF arm	Similar structure. Arm is longer and includes sampling system on end effector + sample canister
Mobility	4 80-cm mesh wheels, all driven and steered, single front rocker	Same but with two-side rockers and differential to accommodate the sampling and storage system
Ground System	DTE using DSN (near-side)	Relay using orbital relay asset based on commercial "lunar pathfinder" system (far-side)

For definitions of acronyms used in tables, see Appendix A.

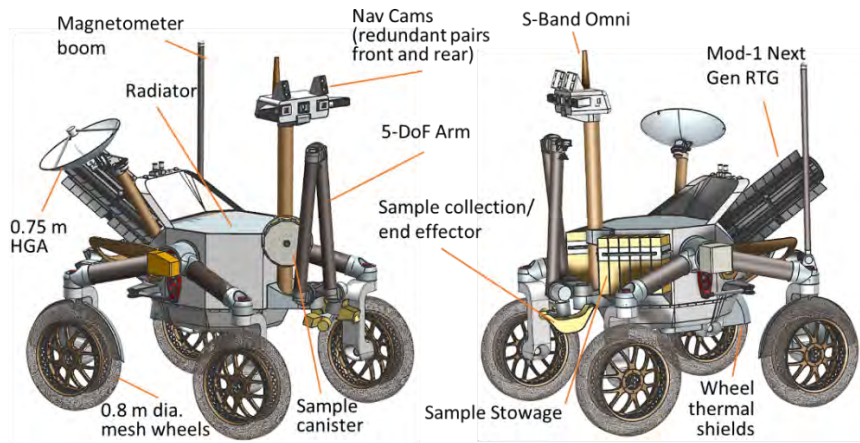


Figure 3-1. Rover overview (Endurance-R on left, Endurance-A on right). The rover designs are identical other than sample collection and caching systems.

Table 3-2. Summary MEL.

Subsystem	Mass (kg)		
	CBE	Cont.	MEV
Instruments	20.0	12%	22.4
C&DH	13.7	13%	15.5
Telecom	20.7	20%	24.8
GNC	8.4	11%	9.3
Power	65.9	29%	85.3
Thermal	12.8	30%	16.6
Structures	124.4	22%	151.9
Mobility	111.9	21%	135.3
Harness	20.4	30%	26.5
Rover Total	398.2	22%	487.6
Lander Allocation (MPV) ¹			570
Margin (MPV-CBE)/MPV			30%

¹ Allocation represents minimum capability of lander to meet 30% mass margin

Table 3-3. Endurance Power Modes.

Subsystem	Power Modes				
	Traverse Day (W)	Traverse Night (W)	Mobility Warmup (W)	Stop w/Telcom (W)	Charge (Safe) (W)
Instruments	10	8	0	30	0
GNC	20	22	12	15	12
C&DH	29	29	15	23	1
Power	11	11	10	10	10
Mobility/Mech	94	94	0	8	0
Telecom	10	10	10	31	10
Thermal	0	3	20	0	0
Rover total	174	177	67	118	33
Contingency	43%	43%	43%	43%	43%
MEV Power	249	252	96	168	47
Avail. Power ¹	213	213	213	213	213
Margin²	18%	17%	69%	45%	85%

¹ Represents end-of-mission (EOM) power from RTG

² Traverse modes are augmented with battery to ensure MEV power

which are expected to be traversed at rates shown in Appendix G, Tables G-8 and G-9. The mobility system uses a four-wheel drive, all-wheel steering configuration with a passive dual-sided rocker suspension. Two rocker mechanisms pivot on the left and right sides of the vehicle. The two sides are connected to each other by a differential mechanism that kinematically couples them under the vehicle chassis so the motion on one side causes the opposite motion on the other side. The rover is designed to drive in either direction supported by front and back stereo cameras. With all wheel steering, the rover can also drive sideways at different angles. The rover has >0.6 m ground clearance and large-diameter compliant wheels to improve rock traversal, traction on regolith, and energy efficiency [53-55]. The 0.8 m-diameter wheels use a mesh structure, similar to the Apollo LRV, to traverse rocks that are less than 30 cm in height and drive through smaller craters not apparent in orbital data (<5 m in diameter).

3.2.2.2 Manipulation and Sampling

Endurance has a 5 degree-of-freedom arm (shoulder: yaw-pitch, elbow: pitch, wrist: pitch-yaw) with two, 1-m size links. The actuators are based on NASA Space Technology Mission Directorate (STMD) developed ColdArm technology that uses bulk metallic gears (BMG) for cold temperature operations. The Endurance-R end effector, shown in Figure 3-2, houses a scoop with built-in sample-separation features, APXS and HLI instruments, and a gripper for sample cache transfer. The arm also has a camera at the elbow and a force-torque sensor at the wrist. Each joint has encoders, brakes, and resolvers.

As seen in Figure 3-2, the scoop for surface sampling (not digging) is a structure with metal tines for scraping the lunar surface to collect samples, a sieve for separating rocks from regolith, and a plate with an array of 20 mm holes for rejecting larger rocks from being cached. It has simple structural pathways for sample flow, which maximize flow areas, avoid sharp features, and minimize contact surfaces. It also has a vibration mechanism (eccentric mass on an actuator) to easily separate regolith from rocks and mitigate any sample flow issues with 10 g vibrations. There is also a mechanical feature that the arm can use to remove any clogs or jams in the sample flow. The sample transfer pathway is storyboarded in Appendix H.

The HLI and APXS have dust covers, are placed in structural enclosures, and are oriented such that they are shielded from any ballistic particles ejected during sampling. The scoop and the instruments are mounted on the yaw joint of the wrist to alternate their pointing at the ground. The end effector also has a gripper for grabbing the sample canister to transfer to the SRC. The design of the gripper and its mating part are based on those used on International Space Station payloads.

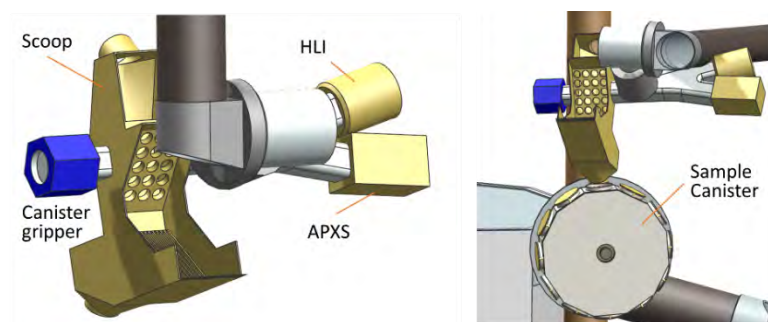


Figure 3-2. Endurance-R End Effector (left) and Sample Canister (right).

Table 3-4. Endurance Rover Characteristics.

Flight System Element Parameters	Value/Summary, Units
General	
Design Life	48 months
Structure	
Structure material	Aluminum and composite
Number of deployed structures	2 (magnetometer boom, arm)
Mobility/Articulation	
Control method	4-wheeled rover, 4-wheel steering
Control reference	Solar, stellar, terrain recognition
Slope capability	20 degrees
Max rover speed on flat terrain	1.0 km/hr
Number of degrees of freedom	24 (mobility, arm, pointing, sampling)
Thermal Control	
Type of thermal control used	Passive/heat pipes/radiators/electric heaters/thermal switches
Command & Data Handling	
Rover housekeeping data rate	2 kbps
Data storage capacity	128,000 Mbits
Max. storage record/playback rate	700 kbps
Power	
Expected generation at BOL and EOM	RTG: 245 W BOL, 213 W EOM
Average power consumption	249 W (day driving mode)
Battery type	Li-ion
Battery storage capacity	20 amp-hr

The instruments are mounted on the yaw joint of the wrist to alternate their pointing at the ground. The end effector also has a gripper for grabbing the sample canister to transfer to the SRC. The design of the gripper and its mating part are based on those used on International Space Station payloads.

The sample canister, shown in Figure 3-2, is a hollow circular disk



consisting of 12 separate radial chambers with built-in lids. The canister is mounted vertically to the side of the rover and can be rotated about a horizontal axis using a single actuator. The canister rotation incrementally indexes its empty chambers to point vertically up to receive the samples. The rotation also opens the lid of the chamber being indexed into the vertical position. Once the sample is transferred from the arm, subsequent rotation of the canister closes the lid and secures the sample. The rotation of the canister also allows dumping a sample and retrying in the event the lid cannot be closed, which ensures the canister with all-closed-lids can fit in the sample return module. The canister has a vibration mechanism for ease of sample flow to avoid clogs and jams. It also has a mating feature for the arm’s gripper to grasp it for transfer to the SRC. The canister is separated from the rover using a wire-cutter when it is grasped by the arm.

Sampling operations can be observed by both the mast cameras and the arm-mounted camera for redundancy. Along with guides and structural alignment features, there are also fiducials for vision-based alignment of the arm during the sample transfer and sample cache transfer maneuvers. All moving joints have dust seals. The arm camera also has a dust cover.

The Endurance-A variant has the same robotic arm. The end effector has a simple scoop, shown on the right side of Figure 3-1, and also accommodates the HLI and APXS. The scoop is similar to the one flown on the Mars Phoenix mission and has a built-in vibration mechanism. The 100 kg samples are stored in 12 astronaut-removable containers mounted on the sides of the rover. Details of design and operation of the sampling systems are provided in Appendix H.

3.2.2.3 Autonomous Surface Operations

The overall science objective of the mission is to visit specified target sites along a pre-planned path. Due to limited communication windows, an Earth-based operations schedule, and the required traverse distances and science observations, these activities must be executed autonomously and reliably with only infrequent ground oversight to track progress, re-adjust the plan, and support fault handling (for more details, see Table 3-5 and Table E-2 in Appendix E).

The rover’s sensors, avionics, and software are designed to support onboard autonomous operations with ground oversight. The rover has two redundant stereo camera pairs (Mars 2020 EECAM) mounted on a pan-tilt mast and a second redundant pair mounted on the rear of the rover, making bidirectional driving fully redundant. With a height over 2 m above the ground, dust covers for the cameras were deemed unnecessary. All navigation cameras have 90° field-of-view lenses and a ~25-cm

baseline to enable bi-directional surface navigation without mast articulation. Short exposures (~10–20 ms) allow imaging while driving during the lunar daytime (similar to the Perseverance rover). At night, Endurance will use high-intensity LED lights to image the terrain frequently while driving. It will stop for longer exposures and some panoramic images every 10–15 m in order to reconstruct a 3D model of its environment and plan its next steps. The mast-mounted cameras also support autonomous manipulation operations. The rover uses an Adcole pyramid-type coarse sun sensor and redundant heritage LN200 IMUs for navigation purposes.

In nominal situations, autonomous operations use vision-based waypoint navigation that respects keep-in and keep-out zones to reach targets of interest. Resources and activities are managed onboard and monitored by the system-health manager (fault protection), which has to detect and identify all faults/failures but only respond to a subset. For off-nominal situations that cannot be handled onboard, operations fall back

Table 3-5. Onboard and ground activities.

Onboard and Ground Functions	
Onboard Rover	<p><u>While driving</u></p> <ul style="list-style-type: none"> • Surface navigation (stereo imaging, 3D mapping, hazard assessment (rocks, craters), path planning, path following) • Dead reckoning pose estimation (visual/inertial/wheel odometry ego-motion estimation)
	<p><u>While stopped</u></p> <ul style="list-style-type: none"> • Global localization (Sun sensing (daytime), star tracking (night), crater detection from rover and registration with orbital imagery) • Safe target selection for instrument placement (thermal hazard assessment, arm (self) and environment collisions) • Arm instrument placement on selected targets (collision-free motion planning)
	<p><u>Both</u></p> <ul style="list-style-type: none"> • Reliable operations (mean-distance between faults > 6 km; mean-time for recovery < 3 hours) • System health management (monitoring devices and activities, assessing health, limited diagnosing and response) • Activity and resource planning, scheduling and execution
Ground	<p><u>24/7 Operations (first 4 weeks)</u></p> <ul style="list-style-type: none"> • 75% coverage and continuous oversight • Checkouts and shakedown of remaining bugs • Rapid fault response (min 1-hour turn around)
	<p><u>Workday schedule (remaining 4 years)</u></p> <ul style="list-style-type: none"> • Ground-based monitoring and health assessment • On-call fault diagnosis and response



on ground-in-the-loop control. Table 3-5 summarizes the functions for autonomous operations.

3.2.2.4 C&DH

The Endurance rover's C&DH subsystem consists of three assemblies: a compute element, an instrument interface and motor controllers. All are JPL-designed and have heritage traceable to flight units. A block diagram of the C&DH system is shown in Appendix L.

The compute element is built around redundant GR740, Quad-core LEON4 processor boards, redundant power supplies and a fault management unit that facilitates timer, sleep functions, and swap-over between the processor boards. Redundant Virtex 5 navigation boards are connected to the processors to implement specific autonomous functions. The redundant instrument interface units are built around the GR712 Dual-core LEON 3 processor and control and collect data from the science instruments. The motor drivers were developed for the Europa Lander and built using the same processing board as the instrument interface. These control the mobility, arm, and mast, and HGA. Each motor control board can control three motors, but only one motor at a time; the current configuration supports sixteen simultaneous motor operations.

The Flight Software (FSW) for the compute element is direct heritage from JPL's Psyche FSW product with modifications from the Mars 2020 rover software. The FSW heritage includes not only the flight code, but also the software development and management processes required for a class B flight software deliverable. Over 99% of the inherited flight software is written in the C programming language. The remainder is written in assembly to cover niche areas in SUROM and operating system routines. The basic FSW architectural principles have remained the same for years with successful architectural reuse across MSL, M2020 and Psyche missions. The FSW for the motor controller and instrument interface units uses the C++ F⁷ (F Prime) framework developed at JPL to facilitate embedded software development. It provides features such as message queues, threading, OS abstraction and generic components for commands, memory management and event logging. F⁷ has flown on the Mars Helicopter and the ASTERIA CubeSat.

3.2.2.5 Telecom

Because the Endurance rover mission will take place on the far side of the Moon, no direct-to-Earth communications will be possible, necessitating use of a relay satellite. The Lunar Communications Pathfinder relay network by Surrey Satellite Technology Limited (SSTL), a UK commercial company with ties to the European Space Agency (ESA), has been baselined as the relay service for Endurance. The trade that resulted in this choice is detailed in Appendix I. Analyses of relay visibility, coverage statistics, and link throughput indicate that Pathfinder can support the requirements of the mission, as detailed in Appendix I. The rover telecommunications subsystem supports all mission uplink and downlink requirements using S-band frequencies and components. A 75-cm directional antenna with 22.5 dBi gain combined with a 5 W power amplifier supports the 2 Mbps data rate of Pathfinder with 3 dB margin; it also supports a commanding (receive) rate of 128 kbps with 3-dB margin. The antenna tracks the relay satellite while uplinking data for return to Earth as well as receiving commands from Earth. A capable radio, UST-Lite, is chosen to support the required data rates. This radio, currently under development at JPL, is a lighter variant of the JPL-built Universal Space Transponder (UST). For emergencies and safe mode, a low-gain 3-dBi antenna supports a transmit data rate of 128 bps and a commanding rate of 22 kbps. The radio uses Proximity-1 protocol for communicating with the relay. This standard will allow the radio to communicate with other relay systems as they become available. The telecom subsystem is redundant, carrying two USTs and two 5 W SSPAs.

3.2.2.6 Power

The Mod-1 Next Generation RTG provides sufficient power for all operating modes at end of mission per Table 3-3. The battery is sized to absorb power transients and provide margin during driving modes. The design includes three power control modules to support the ~245 W capability at BOL as well as providing the battery charge/discharge control interface.

Power electronics are based on a SmallSat avionics architecture currently in development at JPL. This includes RTG power control functionality as well as power distribution for loads and pyro events. This distribution functionality has a fault tolerant control interface to C&DH. Further, switches can be placed in parallel to mitigate stuck-open faults or in series to mitigate stuck-on faults.

3.2.2.7 Thermal

The thermal control subsystem is required to maintain hardware within allowable flight temperatures (shown in Table J-1 in Appendix J). The system is challenged by not only the need to survive the lunar night, but also the lunar day where regolith temperatures and high relative solar angles combine into extreme hot scenarios at mission latitudes as low as 35°. Building on past rover experience, Endurance employs a Warm Electronics Box (WEB) design, as illustrated in Appendix J, Figure J-2.

During the lunar day, a zenith-facing radiator is employed to reject heat from rover internals. Barring articulation or complex orientation restrictions for the rover, this implementation provides the best performance throughout the lunar day with the design allowing some degradation depending on rover tilt angles and terrain features. To conserve heater power during the lunar night, WEB internals are thermally co-located and insulated with MLI. The thermal path to the radiator via a set of constant conductance heat pipes embedded in the WEB structure is essentially removed if hardware temperatures drop below $-10\text{ }^{\circ}\text{C}$ through the action of a set of passive thermal switches. Each switch is capable of turning down its thermal conductance from 5 to 0.002 W/K. Each switch is associated with a flexible thermal strap that accommodates its linear actuation of 0.13 mm.

Mobility and arm actuators are allowed to freeze during the night and are warmed prior to use to their minimum operating allowable flight temperatures (AFTs). Those elements external to the WEB, such as instruments, have local thermal control consisting of heaters to maintain nighttime temperatures and a local zenith-facing radiator to maintain temperatures during the day. Note that some operational scenarios may dictate that instruments are powered down to prevent overheating.

3.2.2.8 Structures

The structure configuration employs a lightweight approach using a combination of carbon fiber composite struts, aluminum brackets, and aluminum honeycomb panels. These materials are compatible with all radiation and thermal conditions during the traverse (details are presented in Appendix L).

The rover incorporates a honeycomb chassis, as well as metal fixtures using aluminum metal sheet bending techniques for instruments and cameras. The chassis provides mechanical attachments as well as space for the thermal system and attachment points for interface with the lander. The rocker system is made of large-diameter hollowed composite rods and metal fittings. The rest of the rocker mechanisms, as well as the attachment to the chassis are made of machined aluminum parts. The radiator is mounted on top of the chassis and all electronics are placed on a horizontal plate accessible from the bottom to facilitate integration and thermal performance.

3.2.3 EARTH RETURN VEHICLE (ERV)

The ERV for the Endurance-R variant was designed by JPL's Team X to meet the requirements of the mission. A summary of the design study may be found in Appendix C.

The ERV would be delivered by a CLPS lander, landing in the lunar morning at a site near the rover. The rover would then drive to the ERV and use its arm to grapple the filled sample canister. The canister would be separated from the rover by a pyro device and the arm would then transfer the canister to a single degree-of-freedom transfer link integral with the ERV interface on the lander. The transfer link would swing up and place the sample canister in the SRC attached to the side of the ERV. The SRC would be closed and the ERV would launch and execute a return trajectory for the Earth. All activities related to sample transfer and launch take place during the course of a single lunar day, hence no overnight survival capability is required. An overview of the ERV is shown in Figure 3-4 and characteristics are summarized in Table 3-6. Subsystems are described below:

Payload: Primary payload on the ERV is the SRC. The SRC is based on the design used for OSIRIS-REx. Additional payload includes two cameras; one on the transfer link to ensure proper placement of the sample canister in the SRC and a second on the ERV to view separation of the SRC.

C&DH: The basic functions of the ERV necessary for executing the sample transfer and Earth-return mission are handled by a dual-string system consisting of two JPL-developed Sphinx computers and a pair of interface cards for communication with GNC components. Motor controllers are also included for the sample transfer link, the SRC lid, and the spin-up device for SRC release.

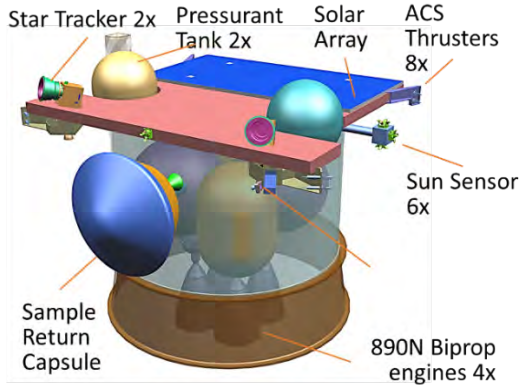


Figure 3-4. ERV Overview.

Telecom: Telecommunications are required for the SRC during two phases of flight. First, from launch through ERV ascent, a telecom link through the orbiting relay asset will be required. Post-ascent and during the cruise to Earth, telecom will be DTE using the DSN. To meet these requirements the ERV incorporates a dual string S-band radio similar to that used on the rover comprising two UST-Lite transponders operating in the S-band and two 5 W SSPAs. An S-band omnidirectional antenna is provided for both relay and DTE communications.

Power: Power is available from the delivery lander for pre-ascent activities, with an assumed capability of up to 150 W. From ascent through Earth-return, the ERV is provided with a fixed solar array with 1.55 m² total area producing 424 W at EOM. This array is augmented with a 16 A-hr Li-ion battery to handle peak loads and eclipse periods.

GNC: The GNC subsystem provides the basic functions necessary to ensure the ERV can execute its ascent and transfer trajectory with required accuracy to deliver the SRC to Earth. The ERV is three-axis stabilized during launch and SRC-release and spin stabilized during cruise. Components making up the GNC subsystem include dual redundant stellar reference units, IMUs and sun sensors.

Thermal: The thermal control subsystem (TCS) for the ERV is designed to maintain all components and propellant at allowable flight temperatures during all mission phases. The TCS is a passive design using thermostatically-controlled heaters, radiators MLI to meet design requirements.

Propulsion: The ERV makes use of a dual-mode bipropellant propulsion system to provide the large amount of Delta-V needed for ascent and Earth-injection burns (biprop) as well as the RCS for attitude control during large burns and cruise. The system uses four 890 N main biprop engines for high thrust maneuvers (sized to provide >2:1 thrust to weight ratio at launch) and four 90 N and eight 1 N monoprop thrusters for attitude control. Two fuel and two oxidizer tanks provide sufficient capacity to support a total Delta-V capability of >2,500 m/s.

Structures/Mechanisms: The ERV was designed with a conventional aluminum structure to support loads through all mission phases. Mechanisms on the ERV are minimal, limited to the spin-up and release device for the SRC, and ERV launch locks. Additionally, the SRC will have its own set of mechanisms (as assumed in the OSIRIS-REx design, which formed the basis for the Endurance SRC concept) associated with sample-canister retention and the SRC door.

Because the configuration of the CLPS lander that will be used for delivery of the ERV is not known, the deck height may preclude direct transfer of the sample canister to the SRC. As such, the ERV support includes a 1-DOF transfer link, which remains on the lander post launch, to receive the

Table 3-6. ERV Flight System Characteristics.

Flight System Element Parameters	Value/Summary, units
General	
Design Life	7 months
Structure	
Structure material	Aluminum/composite
Number of articulated structures	2 (transfer link, SRC door)
Number of deployed structures	2 (canister transfer link, SRC)
Aeroshell diameter	0.81 m (SRC)
Thermal Control	
Type of thermal control used	Passive (radiator, heaters)
Propulsion	
Estimated delta-V budget	2536 m/s
Propulsion type(s) and associated propellant(s)/oxidizer(s)	Dual mode biprop (hydrazine/NTO)
Number of thrusters and tanks	4 bi, 4 90N, 8 1N monoprop
Specific impulse of each mode	320 s biprop, 230 s monoprop
Attitude Control	
Control method	3-axis with spin during cruise
Control reference	inertial
Articulation/#-axes	none
Command & Data Handling	
Housekeeping data rate	2 kbps
Data storage capacity	4 Gb
Power	
Type of array structure	Rigid, body mounted
Array size	1.55 m ²
Solar cell type	Triple junction GaAs
Expected generation at BOL and EOL	474 (BOL), 424 (EOL)
On-orbit ave power consumption	352 W
Battery type	Li-ion
Battery storage capacity	16 A-hr

canister from the rover’s arm at a reasonable height (Figure 3-5). The transfer link swings the canister directly up to mate with the SRC, then folds back out of the way prior to SRC closure and ascent burn.

3.3 CONCEPT OF OPERATIONS AND MISSION DESIGN

The Endurance mission combines advanced autonomy with targeted ground-in-the-loop operations to traverse over 1,750 km across the South Pole–Aitken Basin, collect samples from 12 separate sites, and return them to Earth. As in the Intrepid mission, the incorporation of advanced autonomy vastly increases the distance that can be covered over the course of the mission and arm-based measurements along the way. Real-time operations, facilitated by a relay satellite orbiting the Moon, enable efficient ground-in-the-loop sample acquisition and transfer. In addition to collecting samples, Endurance conducts continuous science observations along its path to provide context and to explore the Moon’s history. The mission takes place over the course of four years, including over one year of margin. The ERV used to return samples to Earth in the Endurance-R option has a total mission duration of seven months and all ERV lunar surface operations are performed during a single daylight period.

The Endurance concept of operations can be divided into six phases: Launch, Cruise, and Landing; Checkout; Traverse; Sample Acquisition; Sample Transfer; and Sample Return as shown in Figure 3-6.

3.3.1 LAUNCH, CRUISE, AND LANDING PHASE

In the Launch, Cruise, and Landing Phase, the rover or ERV launches from Earth, cruises to Moon, and lands on the Moon’s surface while attached to the CLPS lander. The rover or ERV are in an idle state during this phase while all critical functions are performed by the CLPS lander.

3.3.2 CHECKOUT

The Checkout phase describes initial operations of the rover or ERV once landed on the Moon’s surface. For the rover, instruments are checked out, launch locks are released, and the rover disembarks from the CLPS lander onto the lunar surface. For the ERV, Checkout proceeds similarly except that once Checkout has been completed, the ERV sits idle.

3.3.3 TRAVERSE

In the Traverse phase, the rover drives across the SPA between sampling regions. The rover takes measurements with ARMAS, the Magnetometer, GRNS, and ESA continuously throughout this phase. TriCam stereo and FarCam images are collected every ten minutes while driving.

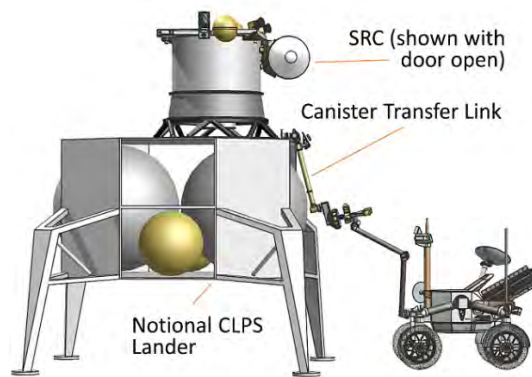


Figure 3-5. View showing canister transfer configuration.

The rover makes repeated stops in order to perform more detailed investigations, recharge its batteries if required, and communicate through the relay satellite. Every 2 km, the rover performs a 1-hr Interval Stop to quickly characterize its surroundings at times deploying its robotic arm for APXS and HLI measurements on regolith and rock samples. Every 20 km, the rover performs a longer, 48-hr Deep Interval Stop to acquire more detailed measurements. The science measurements made during Interval Stops and Deep Interval stops are shown in Table 3-7.

The rover covers ground at an average rate of 220 m/hr during the daytime accounting for engineering and

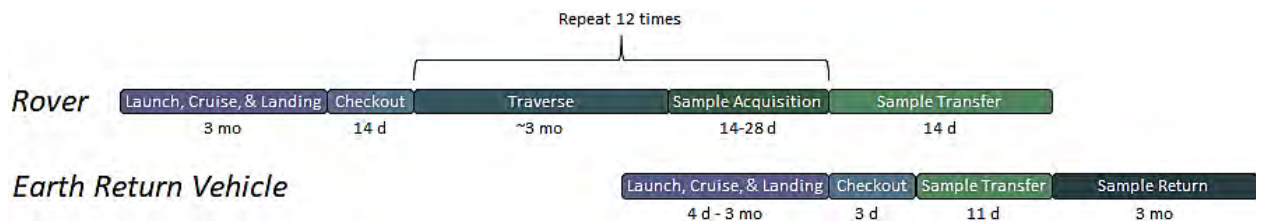


Figure 3-6. Endurance mission phases and durations. ERV phases apply only to the Endurance-R option.



Table 3-7. Traverse phase observations

Instrument	Interval Stop	Deep Interval Stop
TriCam	1 Stereo 360° panorama	3 Stereo 360° panoramas
Point Spectrometer	50 spectra	150 spectra
FarCam	18 images	54 images
GRNS	1 hr integration	48 hr integration
APXS	1 hr integration	48 hr integration
HLI	1 image of APXS measurement area	1 image of APXS measurement area

science Interval and Deep Interval Stops. Night time driving is slower, at 160 m/hr, due to the need to stop every 10-m to take a set of navigation images under long-exposure illumination of with rover’s headlights. A typical lunar day during the Traverse phase is shown in Figure 3-7.

Traverse length and predicted mission duration differ between the Endurance-R and Endurance-A options. For Endurance-R, the rover is delivered to Poincaré crater and journeys north across the SPA, ending in Apollo crater where the rover meets the ERV (see Figure 1-3). The total

traverse length is 1,750 km and the planned mission duration is four years (2.7 years to execute the baseline traverse plus 1.3 years margin). For Endurance-A, the lander is delivered to the central SPA, traverses east to Poincaré, and then heads south towards the expected Artemis base located near the South Pole. The total traverse length for this option is 2,000 km and the expected mission duration is 2.9 years (also baselined as four years with margin).

3.3.4 TRAVERSE PLAN

The Endurance traverses are designed to visit scientifically compelling sampling sites across the SPA. Both traverses were planned using digital-elevation maps (DEMs) generated from LOLA data, Kaguya, and Chang’e. A merge of Kaguya and LOLA data was used to generate a 59-m resolution DEM covering areas north of 60°S latitude. For more southerly portions of the Endurance-A traverse, a 20-m resolution DEM using Chang’e data was used. Traverse paths were found through these DEMs that limited slopes to less than 15°. Details on traverse planning can be found in Appendix K.

The only location constraints for the traverses are the pre-identified sampling regions. The path between those regions is flexible. The rover’s onboard autonomy and the operations team will work together to identify the most expeditious path between sampling regions. In addition to contingencies based on an expected fault rate and ground-in-the-loop driving for portions of the steepest slopes, Endurance carries >25% margin on its mission duration in order to account for unforeseen situations that may cause replanning of the traverse.

3.3.5 SAMPLE ACQUISITION

The Sample Acquisition Phase begins when the rover arrives at a pre-identified 100-m x 100-m sampling site. Upon arriving at each region, the rover drives to the first of five candidate sampling areas within the region and performs a Candidate Sampling Area Reconnaissance observation. Upon down-link of this initial dataset to Earth, the science team can command the rover to conduct up to three Candidate Sampling Area Survey observations for each candidate area. These are more detailed observations intended to characterize possible sampling locations at the candidate site. While driving between candidate sampling areas, the rover stops every 10 m to conduct a Between-Area Survey observation in order to image its surroundings. This 10-min observation may help the science team identify additional candidate sampling areas that could not be identified from orbit. Measurements gathered during these observations are described in Table 3-8. The Magnetometer, ARMAS, and ESA remain on and collecting data during all observations.

Once the science team identifies the desired sampling area, the rover drives to that location and begins real-time sample acquisition operations. In the case of Endurance-R, the rover is commanded to acquire a sample with its scoop, present the acquired sample to its cameras for evaluation, separate the sample into regolith and rocklets using its sieve, and present the sieved sample for another inspection by its cameras. If the remaining sample is of high value, then the rover is commanded to deposit

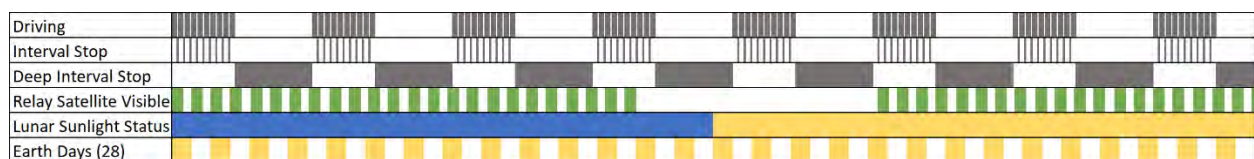


Figure 3-7. A typical lunar day during the Traverse phase. Note the 6-day relay satellite gap that occurs monthly.



the sample into the canister. If multiple scoops are required to fill the chamber, then the scooping activity is repeated until the required volume has been collected. Sampling for Endurance-A eliminates sieving and simply fills each sample chamber with mixed material (Section 3.2.2.2 and Appendix H).

3.3.6 SAMPLE TRANSFER

In the Sample Transfer Phase, the collected samples are transferred to the system that will return them to Earth. In the case of Endurance-R, the rover must rendezvous with the ERV. The ERV lands at a safe distance from the rover to avoid damage by high velocity dust from the landing event. Once the ERV has landed, the rover traverses to the ERV’s location. Rover and ERV operations are performed by two separate teams working in close coordination. The relay satellite can only communicate with one vehicle at a time and so communication passes are tightly coordinated between the two vehicles.

Transfer and storage of the Endurance-R sample canister is performed in two sub-phases, each performed in real-time. In the first sub-phase, the rover grapples the sample canister with its arm, activates a separation mechanism to separate the sample canister from its body, moves the sample canister into the grasp of the ERV transfer link, confirms that the ERV has grappled the sample canister, then releases its grip and stows its arm. Each action is initiated upon command from the ground but is performed autonomously with monitoring from images and real-time telemetry. In the second sub-phase, the ERV actuates its canister transfer link to swing the sample canister up into the SRC and seal the capsule. Again, each action is initiated by command but is performed autonomously. Monitoring is provided by cameras onboard the ERV and the rover. Throughout, operators have the ability to halt operations at any point in order to investigate and resolve anomalies. Once the sample canister is sealed in the SRC, the rover drives away from the ERV to protect itself from debris generated by the launch of the ERV.

Sample transfer and storage in the case of Endurance-A is a matter of the rover driving to a location that is accessible by astronauts. The astronauts are responsible for removing the samples from the rover and storing them for transfer to Earth.

3.3.7 SAMPLE RETURN

In the Sample Return Phase, the samples collected by the rover are returned to Earth via either a robotic sample return vehicle or a crewed vehicle. For Endurance-R, after transfer of the sample canister to the ERV, the ERV launches from its CLPS lander onto a return trajectory to Earth. Mission design for the ERV decreases the delta V requirements through a low-energy trajectory that takes 137 days to Earth. This trajectory requires about 2536 m/s of delta V. The ERV is sunlit throughout the entire trajectory. The SRC is spun up and separated from the ERV shortly before entry. The SRC lands in the Utah Test and Training Range and is immediately transported to a curation facility after landing. Sample return trajectory characteristics are summarized in Table 3-9.

For Endurance-A, once the sample containers are in the possession of astronauts, they are carried with the astronauts on a return trip from the Moon’s surface to Earth.

3.3.8 TELECOM STRATEGY

Communications with the rover and ERV occurs only through a relay satellite orbiting the Moon. Uplink and downlink strategies differ from phase to phase, depending on the goals of each phase. The telecom strategy assumes an average duration of contact between the rover and the relay satellite at the worst-case, most northerly latitude of 7 hours and an average of 1.6 contacts per Earth day (See Appendix I for more information).

Table 3-8. Sample Acquisition phase observations.

Instrument	Candidate Sampling Site Reconnaissance	Candidate Sampling Site Survey	Between-Site Survey
TriCam	One stereo 360° panorama		
Point Spectrometer	50 spectra	45 spectra	50 spectra
FarCam	18 images	18 images	18 images
GRNS	1 hr integration	12 hr integration	-
APXS	1 hr integration	12 hr integration	-
HLI	1 image of APXS measurement area		-

Table 3-9. Earth Return Vehicle sample return trajectory mission design table.

Parameter	Value	Units
Sample Return Trajectory Duration	3	mos
Maximum Eclipse Period	0	min
Launch Site (from moon)	-35 S	Deg Latitude
Total ERV Mass with contingency	526	kg
Propellant Mass with contingency	711	kg
Total Launch Mass with contingency	1,237	kg



During the Launch, Cruise, and Landing phase, communications occur through the CLPS lander. During the Checkout phase, communications initially occur through the CLPS lander until reliable communication between the rover or ERV and the relay satellite can be established. Communication windows while attached to the CLPS lander are set by the CLPS provider. Once the rover separates from the lander, it will communicate with Earth whenever the relay satellite is visible for the remainder of the Checkout Phase. The CLPS lander is assumed to not need significant communication time after the rover has been successfully delivered to the Moon’s surface.

After beginning its Traverse, the rover communicates with Earth for 8-hrs each day for the first year of the mission in order to provide frequent opportunities to identify and mitigate faults. For the remainder of the mission, the rover communicates through the relay satellite for 3-hrs each day, which provides ~60% margin over worst-case daily science data volume. For the first year of the mission, communications may occur both while stopped, and at a reduced data rate while driving. After the first year, communications occur only when the rover is stopped.

At high latitudes near the end of the Endurance-R traverse, the relay satellite may be out of view for up to six days at a time every month (see Appendix I). During this period, the rover will continue to operate normally, storing data in the rover’s memory until a fault occurs that requires ground engagement. Depending on the fault, the rover may halt its traverse but has to manage its health until the remainder of that blackout period or until the fault has been resolved by backup communication (e.g. Gateway). Endurance has 128 Gbit of memory while only ~55 Gbit of data will accumulate over this six-day period, providing over 120% margin.

Real-time communication is necessary during parts of the Sample Acquisition and Sample Transfer phases. All real-time operations are designed to be completed within the duration of an average contact (7 hours). Uplink and downlink telecom characteristics are summarized in Table 3-10.

3.3.9 OPERATIONS STRATEGY

Rover and ERV operations are commanded from JPL with co-located science and engineering teams. A nominal plan is uplinked to the rover that contains the science goals and engineering constraints. The rover can autonomously alter its path and its operations to avoid obstacles, take advantage of benign terrain, and determine the best arm placement to investigate an interesting science target. Telemetry is continuously recorded and stored onboard the rover until the next downlink opportunity. Anomalies are handled hierarchically: onboard the rover if possible and only through ground intervention when necessary. Rapid response to faults is enabled by on-call personnel on the ground who can rapidly evaluate the rover’s state and restore nominal operations quickly using real-time interactions. Some challenging terrains may require the operations team to take over control of the rover. Because the rover can be controlled in near real-time as long as the relay link is available, the Endurance rover is able to traverse relatively quickly over challenging terrain as compared to Mars rovers.

The science and engineering teams operate largely in parallel with the science team establishing long-term goals and traverse paths while the engineering team focuses on monitoring rover health and resource status. The two teams work together during real-time operations to make timely decisions about whether to proceed with critical activities like sample stowage. The ~12-hr orbital

Table 3-10. Endurance communication between the rover and relay satellite at different phases including ERV during Sample Return. Communication periods during Launch, Cruise, and Landing are scheduled by the CLPS provider.

Downlink Information	Units	Checkout	Traverse (1st Year)	Traverse (2 nd –4 th year)	Sample Acquisition	Sample Transfer	Sample Return
Number of Contacts	#/ week	~11	~11	21	~11		7-21
Downlink Contact Duration	hours	~7	~5	1	~7		8
Mission Phase Duration	weeks	4	~29	~84	24	2	12
Downlink Frequency Band		S					S
Telemetry Data Rate(s)	kps	HGA: 2000, LGA: 22					LGA: 8
Total Daily Data Volume	MB/day	183	1145		780	515	11
Uplink Information		Checkout	Traverse (1st Year)	Traverse (2 nd –4 th year)	Sample Acquisition	Sample Transfer	Sample Return
Number of Uplinks	#/day			~2			1-3
Uplink Contact Duration	hours	~7	~5	1	~7		8
Uplink Frequency Band		S					S
Telecommand Data Rate	kbps	HGA: 128, LGA: 1.2					LGA: 2



period of the relay satellite enables communications passes to be scheduled on a daily basis at times that are convenient to the operations teams. Operations in the vicinity of the CLPS lander or astronauts are closely coordinated with those teams to ensure the safety of the vehicles and crew.

3.4 RISK LIST

The Endurance concept takes a conservative approach to engineering, mission planning and operations, informed by experience from past lunar and Mars missions. New technology is limited and the operating environment and traverse is reasonably understood. Significant risks identified by the team are shown in Table 3-11.

Table 3-11. Endurance's adoption of existing technologies and proven instrument designs facilitates a high-performance mission with manageable risks.

Risk	C*	L*	Mitigation
Mod-1 Next Gen RTG not available in time for launch	3	2	<ul style="list-style-type: none"> Design could use Mod-0 Next Gen RTG or DRPS, if available, with minimal impact to mission Design could be adapted to MMRTG with significant impact to mission duration to meet baseline science objectives Solar-powered option (see Intrepid PMCS report) could be adopted with commensurate increase in mission duration Mission opportunity is not time-critical and could accommodate some slip in Next Gen schedule
Accommodation of lunar dust environment requires additional qualification and design changes to ensure reliable operation	3	2	<ul style="list-style-type: none"> Seal all exposed joints: use three-stage seal derived from Mars rovers. Raise height of sensitive surfaces (optical/thermal) and instruments (currently higher than the wheels to mitigate the effect of dust and debris). Place body-mounted instruments at least 60 cm above regolith. Perform testing of sampling system with variety of regolith simulants to characterize dust migration Account for dust in performance analysis and design: all thermal analyses assume a mono-layer of dust at all times
Reliability of autonomous operations cannot be made sufficiently high during lunar day and night to ensure execution of mission within allotted time	2	2	<ul style="list-style-type: none"> Mature integrated autonomous capabilities on relevant prototype rovers with flight-relevant components (h/w and s/w) Test day/night driving and arm operations in high-fidelity simulations informed by data from VIPER's PSR operations Conduct extensive field-testing complemented with a validated simulation to collect adequate statistics Increase ground engagement in autonomous operations that have the least reliable performance. Include significant margin and flexibility in mission plan to allow for anomaly resolution in operations ERV rendezvous with rover can be adjusted for timing and landing site to provide mission flexibility
Rover encounters lunar terrain with unexpected trafficability features	2	2	<ul style="list-style-type: none"> Include worst-case terrain types in rover mobility test plans Design mobility system with multiple ways to detect mobility problems and back out of hazardous areas Include timeline margin for alternate route planning, should hazardous terrains be encountered on planned path
Thermal design does not perform as expected	2	2	<ul style="list-style-type: none"> Begin thermal design and testing early in Phase A. Increase battery capacity or radiator area (currently includes margin above design principles)

* C=Consequences; L=Likelihood, in accordance with the NASA 5x5 Table. Consequence and Likelihood criteria defined per SOMA Cost Threat Matrix (ref. Discovery 2014 Transition Briefing, 3/3/2017). Consequence criteria (C): cost impact to complete Phases A-D: 1=Very Minimal (<\$10M). 2=Minimal (\$10-20M). 3=Limited (\$20-40M). 4=Moderate (\$40-80M). 5=Significant (\$80-\$120M). 6=Very Significant (>\$120M). Likelihood criteria (L): % probability of occurrence: 1=Unlikely (<10%). 2=Possible (10-30%). 3=Likely (30-60%). 4=Very Likely (60-75%). 5=Almost Certain (>75%).

4 DEVELOPMENT SCHEDULE AND SCHEDULE CONSTRAINTS

4.1 HIGH-LEVEL MISSION SCHEDULE

Figure 4-1 presents a feasible high-level schedule for the Endurance mission. It shows the full mission Endurance-R variant, including development and launch of the ERV. Schedule for the Endurance-A variant would be the same, with the exclusion of the activities involving the ERV.

While the development for the ERV could potentially be carried out in series with the rover as a subsequent project (as was the assumption used in the ERV Team X study), given the four-year separation of launch dates, it was found that concurrent development under a single project structure provides cost benefits resulting from efficiencies in management. An additional benefit is that the ERV will be fully built and tested at the beginning of the rover's mission, enabling the option of an early launch and sample retrieval should the rover mission require it.

The mission complexity falls in the range of a New Frontiers-class development. The reference schedules used for this study were derived from the JPL mission schedule database, informed by recent rover developments, past sample return mission concepts, and the unique schedule features associated with the use of radioisotope power systems.

The Endurance mission has a direct analog to rover-specific aspects of MER/MSL/2020 and ERV aspects of OSIRIS-REx. Overall mission architecture is significantly simplified for both the -A and -R variants through use of the CLPS provider for cruise and landing. The mobility range for Endurance

Endurance Plan (B/C/D 61 mo)

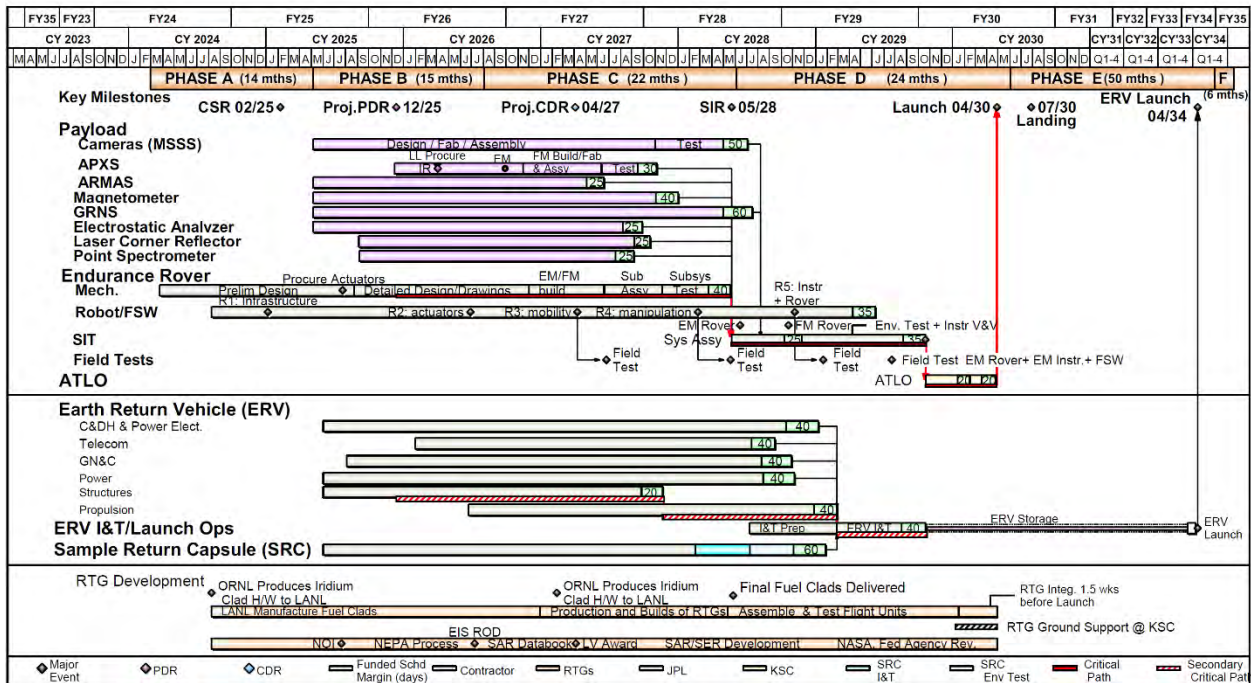


Figure 4-1. Notional High-Level Schedule Assuming a 2030 Launch (Endurance-R shown; Endurance-A would eliminate the lines associated with the ERV and SRC).

is significantly beyond that of previous rover missions, and that is reflected in the number of field tests and component life tests planned to begin early in the development cycle (see Table 4-2).

No major schedule drivers or long-lead items need to be addressed beyond the proposed schedule. Table 4-1 provides key phase durations for the project. Since the mission is targeted as a New Frontiers competed mission, all instruments and instrument providers are selected during proposal preparation and the schedule need not accommodate a competitive Instrument Announcement of Opportunity (AO).

4.2 TECHNOLOGY DEVELOPMENT PLAN

As identified in Section 2, two technologies need to be matured to higher technology readiness levels: (i) reliable and extended autonomous surface operations and (ii) the point spectrometer instrument.

Autonomous surface operations leverage several Mars-heritage autonomous functions but need to provide integrated mobility, target selection, instrument placement, perception, and localization for extended durations and when there is little or no natural illumination. The 12 sampling operations are planned to frequently engage ground operators at every step from sample selection through caching. However, primitive robotic arm motions such as sampling, sieving, or transferring the sample would be executed onboard by the rover as some involve force control such as digging. Sampling aside, the placements of the arm-mounted instruments on rocks and regolith targets every two kilometers have to execute autonomously, as such operations occurs during both the lunar day and night and may not coincide with ground-operations. In addition to their robotic motions, autonomous surface operations require onboard activity planning and resource/health management, relying only on

Table 4-1. Key Phase Duration Table.

Project Phase	Duration (Months)
Phase A – Conceptual Design	14
Phase B – Preliminary Design	15
Phase C – Detailed Design	22
Phase D – Integration & Test	23
Phase E – Primary Mission Operations	50
Phase F – Extended Mission Operations	6
Start of Phase B to Preliminary Design Review (PDR)	8
Start of Phase B to Critical Design Review (CDR)	23
Start of Phase B to Delivery of Instrument #1-8	37
Start of Phase B to Delivery of Flight Element #1	54
System Level Integration & Test	17
Project Total Funded Schedule Reserve	6 (120 days)
Total Development Time Phase B - D	61



Table 4-2. Technology Development Plan.

Justification (completed activities)	Maturation Plan (work to go)	Duration	ROM Cost	
Reliable Integrated Autonomous Operations				
Endurance needs integrated and reliable autonomous operations for traverse, target selection, instrument placement, and system management. Preliminary models long-traverse indicate that Intrepid requires the following mean-distance-between-faults (MDBF) with fault-recovery response time (RT): MDBF > 6 km w/ ave. RT < 3 hours MDBF > 16 km w/ ave. RT < 7 hours (see Appendix F)	Phase I: Pre-Phase A (FY21–24) (feasibility assessment) Integrated autonomy framework: set up framework for integration of all functions Function adaptation: adapt/update Perseverance rover autonomy functions (surface navigation (perception, hazard assessment, pose estimation, path planning, mobility), instrument placement (target selection, self- and terrain-collision, arm motion planning), activity planning, and system health into framework to execute without ground ops the full cycle of repeated driving and arm placement science Night navigation: develop from TRL 3 to 6 Investigate trades for night perception (LIDAR vs. stereo), assess quality of night stereo (near-range and mid-range) for short and long exposures; for stationary and for imaging while driving; assess hazards based on night perception. Develop capability, mature, and test <i>Fallback:</i> reduce percent of night driving to available ground-in-the-loop rates and extend mission duration (50% night driving requires 3 more months; no night driving requires 2 more years). Day global localization: develop from TRL 3 to 6; funded by NASA STMD GCD ('21–24); <i>Fallback:</i> use ground-based localization techniques used in current Mars missions every 10 km. Night global localization: investigate trades for optical, radiometric, and hybrid techniques for global localization. Develop capability (possibly hybrid), mature, simulate, and test <i>Fallback:</i> use ground-based localization techniques used in current Mars missions every 10 km. Demonstration: demonstrate integrated functions in existing simulation or on existing rover prototypes	4 years 2 years 3 years 3 years 3 years 3 years 1 year	\$8.0 M \$2.0 M \$2.5 M \$1.5M Funded \$1.5M \$0.5 M	
	Phase II: Pre-Phase A (FY23–FY26) (reliability assessment) Rover prototype: develop prototype with similar mechanical configuration, sensing, and avionics SW Bench top: set up equivalent bench top system for software/autonomy development Simulation: increase fidelity of simulation and validate against field campaigns MOS/GDS: mature MOS/GDS tools to support rapid anomaly identification and resolution Validation campaigns: conduct 10s of km of autonomous full-cycle driving and science ops to collect statistics to mature and validate integrated capabilities; fully characterize reliability; inform hw changes <i>Fallback:</i> extend mission duration to accommodate the achievable reliability performance metrics	4 years 3 years 1 year 3 years 2 years 2 years	\$8.6 M \$3.5 M \$0.8 M \$2.3 M \$1.0 M \$1.0 M	
	Instrument Development			
	Point Spectrometer	Before PDR – 3 years MSSS led activity integrated with cameras, likely a DALI/ MatISSE		

the strategic science plan but without daily tactical planning as neither nor ground operations schedule nor mission timeline allow for a daily ground-based tactical planning. Furthermore, this mission requires extended autonomous operations, whose activities, unlike its martian counterparts, will not be planned daily. The performance metric needed for Endurance to complete its mission is a combination of mean-distance-between-faults and fault-recovery response time. A preliminary model based on Intrepid’s fault frequency and recovery times provided insight into the reliability performance metrics needed for this mission. Parametric data for this model was based on fault rates and response times of prior Mars missions adjusted for the cadence of lunar communication. A Monte-Carlo statistical analysis indicated that for minor faults, the rover needs a mean distance-between-faults of > 6 km with an average response time of 3 hours and for major faults a mean distance-between-faults of 16 km with an average response time of 7 hours (see more details in Appendix E – Autonomy Reliability). This level of reliability for autonomous operations would allow Endurance to complete its baseline science in a manner consistent with the current concept of operations and within the planned 2.7-year period, leaving the remaining 1.3 years as unallocated margin.

Ground-operation tools, matured for Mars rovers, are expected to have the needed functionality to support the rapid response. The plan is to adapt and integrate flight-matured autonomous functions that include surface navigation (Mars 2020: 3D perception, hazard assessment, motion planning, visual/wheel/inertial odometry), instrument placement (MER/research development: target tracking, approach, rover positioning, hazard assessment (self- and surface collision), arm deployment), and activity/resource planning (Mars 2020), with system health management and global localization into an autonomous system and deploy it in simulation and on a prototype rover with relevant sensing, mobility, controls, and compute avionics. Night driving would be critical for the Endurance mission as more than 60% of the total distance would be driven at night since 12 lunar days are set aside for sampling. Unlike Intrepid’s limited night driving (1–2 km per lunar night), Endurance is covering a total of 1,200 km at night, thus requiring frequent imaging and global localization stops to keep the



rover on the planned route. Initial maturation of the integrated autonomy capabilities for long-duration, long-distance, day/night driving, day/night instrument operations, and fault recovery can be demonstrated in simulation (*e.g.*, the Mars 2020 rover simulation used for autonomous navigation) as well as on existing rover prototypes. To validate the required Endurance performance, a combination of flight-relevant rover prototype and validated high-fidelity Endurance simulation would be necessary. The use of the relevant prototype in relevant environments to validate the simulation is similar to the approach adopted by the Mars 2020 mission for entry, descent and landing and for autonomous rover traverse. Table 4-2 provides a development plan for a focused technology program, which is similar to the multi-year programs that preceded MER, MSL and Mars 2020. Trends to reduce mean-distance-between-interruptions have been well-documented for the autonomous vehicle industry [56], which similarly, complemented road testing on relevant hardware with high-fidelity simulations.

The point-spectrometer design is well understood and uses components from an existing product line. As the current TRL is at 4, the instrument would have to be fabricated and flight qualified for operations on the Moon. NASA has instrument development programs (*e.g.* PICASSO and MatISSE) that can be exercised for the flight qualification for TRL 6. We also propose a phase A activity for any residual activities to get to TRL 6 prior to PDR.

4.3 DEVELOPMENT SCHEDULE AND CONSTRAINTS

The development schedule including Phases C and D is shown in Figure 4-1. The schedule represents a relatively straightforward completion of design and transition to integration and test (I&T) through launch operations for a rover of this type. Instrument development is complete for all instruments prior to start of Phase D. The critical path runs through the rover mechanical system which is necessary to begin I&T. Rover field tests to validate mobility and autonomy continue throughout these phases and feed into FSW builds. The RTG development line is representative of the typical activities associated with an MMRTG mission and may need to be revisited should there be any changes associated with use of the NextGen RTG.

The schedule is tied to a launch date in April of 2030, representing an early opportunity for execution given the timing of advanced RPS development. It should be noted that the Endurance mission schedule is flexible and can be adapted to any CLPS payload opportunity in this timeframe.

5 MISSION LIFE-CYCLE COST

5.1 COSTING METHODOLOGY AND BASIS OF ESTIMATE

Endurance developed its cost estimate using JPL's cost estimation process for early formulation. The Endurance team initiates this process by describing the project in a technical data package (TDP) containing the science requirements, technical design, instrument design, and project schedule. An initial estimate is generated using JPL Institutional Cost Models (ICM) in a focused Team X session that allows the Endurance team to perform subsequent design-to-cost trades.

This study generated cost estimates for the two lunar sample return options: Endurance-R and Endurance-A. The JPL Team X has estimated the lifecycle cost for these Endurance concepts to be \$2,430M and \$1,538M FY25 respectively, as detailed in Table 5-1. The estimate is organized by NASA's standard Work Breakdown Structure (WBS).

Team X estimates are generally model-based, and generated from a series of instrument and mission-level studies. The costs herein are ROM estimates and do not constitute an implementation or cost commitment. It is possible that each estimate could range from as much as 20% higher to 10% lower. The costs presented are based on Pre-Phase A design information, which is subject to change.

The instruments were estimated using the NICM System Tool which primarily relies on mass and power. Lifetime also impacts cost for ARMAS, GRNS and Electrostatic Analyzer. The rover was estimated assuming an in-house build and the ERV and SRC are assumed to be contractor developed.

Flight software was assessed based on analogy to the MSL and Mars2020 rover missions. One key difference and a significant cost driver is Endurance's required degree of autonomy.



Table 5-1. JPL Team X and cost model estimates for Endurance (FY25\$M).

WBS Element	Endurance-R Option		Endurance-A Option	
	Team X	Cost Models	Team X	Cost Models
Phase A Concept Study	Incl. below	5.0	Incl. below	5.0
01/02/03 PM/PSE/SMA	148.8	142.4	84.9	86.1
04 Science	35.0	28.6	32.2	18.9
05 Payload	77.1	97.6	73.5	93.2
06 Flight System	795.3	729.6	471.6	410.9
07 Mission Ops System	43.7	41.1	32.8	24.8
09 Ground Data System	47.4	42.2	32.3	25.8
10 Project System I&T	61.5	98.0	32.8	56.3
Total Dev. w/o Reserves	1,208.8	1,184.6	760.0	720.9
Development Reserves (50%)	569.4	557.3	345.0	325.5
Total A-D Development Cost	1,778.2	1,741.9	1,105.0	1,046.4
01/02 PM/PSE	11.0	2.2	6.7	2.0
04 Science	81.6	105.2	78.2	97.6
07 Mission Ops System	79.5	77.2	70.8	61.6
09 Ground Data System	33.1	27.8	32.5	24.5
Total Ops w/o Reserves	205.2	212.4	188.2	185.7
Operations Reserves (25%)	47.0	48.8	44.9	44.3
Total E-F Operations Cost	252.1	261.2	233.1	230.0
08 Launch System	400.0	400.0	200.0	200.0
Total Cost	2,430.3	2,403.2	1,538.1	1,476.4

The RTG is based on the NextGen RTG with 12 general purpose heat source modules. The \$70M cost is derived from the “Groundrules For Mission Concept Studies in Support of Planetary Decadal Survey”, Appendix A, Nov. 2019.

Planetary Protection is accounted for under WBS 02.

As required for this study, reserves were applied at 50% for Phase A-D development (excluding launch vehicle [LV] and the RTG) and 25% for Phase E operations (excluding tracking costs).

The LV value of \$200M is based on the expected delivery cost for a medium class CLPS lander as estimated by the NASA CLPS Program Office. For the robotic option, two LVs

are required for the mission.

As another step to validate these costs, JPL’s business organization evaluated the Endurance options using parametric models supplemented with analogies and wrap factors based on historical data. The cost model used include SEER and TruePlanning for Phase B-D, and SOCM for Phase E. Launch system, Phase E tracking costs, and sample curation costs were a passthrough from Team X. Phase A costs were assumed to be \$5M based on the value of the Phase A cost from a pre-release draft of the NF 5 AO. The details for each of the cost model estimates is provided in Appendix K.

Table 5-1 shows the mission cost breakdown for the JPL Team X cost estimate, as well as the average from the cost model estimates. The bottom line total costs for Team X and the cost models differ by 1-4% (see Appendix K). The flight system cost (WBS 06) shows the greatest numeric difference between the two estimates (\$66M and \$61M) with the cost model being lower. One factor that contributes to this difference is the flight software. SEER and TruePlanning can model software based on lines of code. Since this information was not available in Pre-Phase A, a factor was applied to the hardware costs based on a historical average. Because of Endurance’s requirement for autonomous surface operations, this is not well represented by historical data and is possibly underestimated in the cost model.

WBS 10 has the largest percentage difference (59% and 72%) with the cost model estimate higher than Team X. This is especially observable with the TruePlanning estimate. A possible explanation is that Team X carries the cost for a mechanical integration testbed and the robotics tests as part of WBS 06 whereas TruePlanning captures this under WBS 10. Because of this mapping difference, it is better to compare WBS 06 and 10 together, which makes the percentage delta 3% and 7%.

5.2 COST ESTIMATE(S)

The Endurance team has adopted the Team X cost as the more conservative estimate. To create a mission cost funding profile, historical missions were analyzed to define representative profiles by phase. The analogous mission set includes the MER and MSL rovers, and a selection of competed Discover and New Frontiers missions. The normalized percentage spreads were then used to phase the Team X estimate over the duration of 61 months for Phase B-D development and similarly for the 4-year duration for Phase E. The base year profile was then escalated to real year dollars using the



JPL Composite Inflation Index. Table 5-2 and Table 5-3 shows the total mission cost funding profile for both options, assuming a Phase A start date of March 2024 and a launch date of April 2030.

5.3 POTENTIAL COST SAVINGS

In addition to developing a cost estimate for the Endurance concept, Team X also provided feedback on potential ways to lower costs. These include:

- A simpler mobility system, especially if the loads are low and the touchdown is soft.
- The use COTS or existing cameras to observe placement and stowage of sample canister (<\$1M).
- Reduction in contamination-control cost if requirements are confirmed to be low for the cameras and sample-adjacent hardware.
- Optimization of SRC location and possible elimination of canister transfer arm.
- Smaller rover battery based on more detailed analysis of specific battery characteristics

Table 5-2. Endurance-R: Mission Cost Funding Profile (FY costs¹ in Real Year \$, Totals in Real Year and FY25 \$).

Item	FY24	FY25	FY26	FY27	FY28	FY29	FY30	FY31	FY32	FY33	FY34	Total (RY\$M)	Total (FY25\$M)	
Cost														
Phase A Concept Study	2.1	2.9	-	-	-	-	-	-	-	-	-	4.9	5.0	
Technology Development	-	-	-	-	-	-	-	-	-	-	-	-	-	
Phase B-D Development ²	-	95.0	324.2	410.4	251.4	139.2	56.9	-	-	-	-	1,277.1	1,203.8	
Phase B-D Reserves	-	44.9	153.4	194.1	118.9	65.8	26.9	-	-	-	-	604.1	569.4	
Total A-D Development Cost	2.1	142.7	477.6	604.5	370.3	205.0	83.9	-	-	-	-	1,886.1	1,778.2	
Launch services	-	-	68.5	70.5	72.5	74.5	76.6	78.8	-	-	-	441.5	400.0	
Phase E Science	-	-	-	-	-	-	15.6	20.1	20.7	21.3	21.9	99.5	81.6	
Other Phase E Cost	-	-	-	-	-	-	23.6	30.5	31.3	32.2	33.1	150.8	123.6	
Phase E Reserves	-	-	-	-	-	-	9.0	11.6	11.9	12.2	12.6	57.3	47.0	
Total Phase E Cost	-	-	-	-	-	-	48.2	62.1	63.9	65.7	67.6	307.6	252.1	
Education/Outreach	-	-	-	-	-	-	-	-	-	-	-	-	-	
Other (specify)	-	-	-	-	-	-	-	-	-	-	-	-	-	
Total Cost	2.1	142.7	546.1	675.0	442.8	279.6	208.8	141.0	63.9	65.7	67.6	2,635.2	2,430.3	
¹ Costs should include all costs including any fee												Total Mission Cost	2,635.2	2,430.3
² MSI&T - Mission System Integration and Test and preparation for operations included														

Table 5-3. Endurance A Mission Cost Funding Profile (FY costs¹ in Real Year \$, Totals in Real Year and FY25 \$).

Item	FY24	FY25	FY26	FY27	FY28	FY29	FY30	FY31	FY32	FY33	FY34	Total (RY\$M)	Total (FY25\$M)	
Cost														
Phase A Concept Study	2.1	2.9	-	-	-	-	-	-	-	-	-	4.9	5.0	
Technology Development	-	-	-	-	-	-	-	-	-	-	-	-	-	
Phase B-D Development ²	-	59.6	203.4	257.4	157.7	87.3	35.7	-	-	-	-	801.0	755.0	
Phase B-D Reserves	-	27.2	92.9	117.6	72.0	39.9	16.3	-	-	-	-	366.0	345.0	
Total A-D Development Cost	2.1	89.6	296.3	375.0	229.7	127.2	52.0	-	-	-	-	1,171.9	1,105.0	
Launch services	-	-	34.3	35.2	36.2	37.3	38.3	39.4	-	-	-	220.8	200.0	
Phase E Science	-	-	-	-	-	-	16.3	18.9	19.5	20.0	20.6	95.3	78.2	
Other Phase E Cost	-	-	-	-	-	-	23.0	26.6	27.4	28.2	29.0	134.1	110.0	
Phase E Reserves	-	-	-	-	-	-	9.4	10.9	11.2	11.5	11.8	54.7	44.9	
Total Phase E Cost	-	-	-	-	-	-	48.7	56.4	58.0	59.7	61.4	284.1	233.1	
Education/Outreach	-	-	-	-	-	-	-	-	-	-	-	-	-	
Other (specify)	-	-	-	-	-	-	-	-	-	-	-	-	-	
Total Cost	2.1	89.6	330.6	410.2	266.0	164.5	139.0	95.8	58.0	59.7	61.4	1,676.8	1,538.1	
¹ Costs should include all costs including any fee												Total Mission Cost	1,676.8	1,538.1
² MSI&T - Mission System Integration and Test and preparation for operations included														



A ACRONYMS

ACS	Attitude Control Subsystem
AFT	Allowable Flight Temperature
AO	Announcement of Opportunity
APL	Applied Physics Laboratory
APXS	Alpha Particle X Ray Spectrometer
ARMAS	Automated Radiation Measurements for Aerospace Safety
ASCE	American Society of Civil Engineers
ASTERIA	Arcsecond Space Telescope Enabling Research in Astrophysics
AU	Astronomical Unit
B-CPX	Basaltic Clinopyroxene
BMG	Bulk Metallic Gears
BOL	Beginning of Life
BW	Black and White
C&DH	Command & Data Handling
CA	California
CBE	Current Best Estimate
CCD	Charge-coupled Device
CCHP	Constant Conductance Heat Pipe
CCSDS	Consultative Committee for Space Data Systems
CDH	Command and Data Handling
CDR	Critical Design Review
CDS	Command and Data Subsystem
CEPCU	Compute Element Power Control Unit
CFA	Cumulative Fractional Area
CLPS	Commercial Lunar Payload Service
CML	Concept Maturity Level
CMOS	Complementary Metal Oxide Semiconductor
COTS	Commercial Off the Shelf
CPX	Clinopyroxene
CRaTER	Cosmic Ray Telescope for the Effects of Radiation
CT	Computed Tomography
CXS	Coax Transfer Switch
DALI	Development and Advancement of Lunar Instrumentation
DC	District of Columbia
DEM	digital elevation map
DM	Dual Mode
DOF	Degrees of Freedom
DRPS	Dynamic Radioisotope Power System
DSN	Deep Space Network
DTE	Direct to Earth
DTM	Digital Terrain Model
EBC	Estimated Band Center
EBD	Estimated Band Depth



ECAM	Electronic Camera
EDL	Entry, Descent, and Landing
EDS	Energy Dispersive X-ray Spectroscopy
EECAM	Enhanced Engineering Camera
EIRP	Effective Isotropic Radiated Power
EM	Engineering Model
Endurance-A	Variant of the Endurance rover that delivers samples to Artemis astronauts (“A” is for “Astronaut”)
Endurance-R	Variant of the Endurance rover that delivers samples to a robotic Earth return vehicle (“R” is for “Robotic”)
EOL	End of Life
EOM	End of Mission
EOS	Earth Observing System
ERV	Earth Return Vehicle
ESA	Electrostatic Analyzer
ESA	European Space Agency
EVA	Extravehicular Activity
FAQ	Frequently Asked Question
FIB/TEM	Focused Ion Beam/Transmission Electron Microscope
FoV	Field of View
FSW	Flight Software
FY	Fiscal Year
G/T	Gain-to-noise Temperature
GaAs	Gallium Arsenide
GDS	Ground Data System
GNC	Guidance Navigation and Control
GPHS	General Purpose Heat Source
GRAIL	Gravity Recovery and Interior Laboratory
GRNS	Gamma Ray and Neutron Spectrometer
HCP	high Ca Fe pyroxene NM
HEO	Human Exploration and Operations
HEOMD	Human Exploration and Operations Mission Directorate
HGA	High Gain Antenna
HLI	Hand Lens Imager
HP	High Pressure
HSE	Highly Siderophile Elements
HST	Hubble Space Telescope
I/F	interface
I/O	Input/Output
I&T	Integration and Test
ICM	Institutional Cost Model
ICP-MS	Inductively Coupled Plasma-Mass Spectrometry
IEEE	Institute of Electrical and Electronics Engineer
IFOV	Instantaneous Field of View
IMU	Inertial Measurement Unit



INSPIRE	In Situ Solar system Polar Ice Roving Explorer
IOAG/LCAWG	Interagency Operations Advisory Group Lunar Communications Architecture Working Group
IPN	Interplanetary Network
IR	infrared
JPL	Jet Propulsion Laboratory
JSC	Johnson Space Center
KaM	Ka-band Modulator
KOZ/KIZ	Keep Out/In Zone
KREEP	K-potassium, REE-rare earth elements, and P-phosphorus
LEAG	Lunar Exploration Analysis Group
LED	Light Emitting Diode
LGA	Low Gain Antenna
LHB	Late Heavy Bombardment
Li-Ion	Lithium-Ion
LIDAR	Light Detection and Ranging
LM	Lunar Module
LOLA	Lunar Orbiter Laser Altimeter
LP	Low Pressure
LRO	Lunar Reconnaissance Orbiter
LROC	Lunar Reconnaissance Orbiter Camera
LRR	Laser Retro Reflector
LRV	Lunar Roving Vehicle
LSSM	Local Scientific Survey Module
LV	Launch Vehicle
M2020	Mars 2020
M3	Moon Mineralogy Mapper
MAHLI	Mars Hand Lens Imager
MatISSE	Maturation of Instruments for Solar System Exploration
MDBF	Mean Distance Between Faults
MEL	Master Equipment List
MER	Mars Exploration Rover
MEV	maximum expected value
MeV	Megaelectron Volt
Mg-Px	Mg-rich proxene
MIMU	Miniature Inertial Measurement Units
MLI	Multi-Layer Insulation
MMRTG	Multi Mission Radioisotope Thermoelectric Generator
MOS	Mission Operations System
MOU	Memorandum of Understanding
MPF	Mars Pathfinder
MPV	Maximum Possible Value
MPV-CBE	Maximum Possible Value-Current Best Estimate
MS ³	Meter per Second Squared



MSI&T	Mission System Integration and Test
MSL	Mars Science Laboratory
MSSS	Malin Space Science Systems
MTBF	Mean Time Between Faults
MUX	Multiplexer
N/A	Not Applicable
NAC	Narrow Angle Camera
NAIF	Navigation and Ancillary Information Facility
NASA	National Aeronautics and Space Administration
NC	Normally Closed
NE	Northeast
NICM	NASA Instrument Cost Model
NIR	Near-Infrared
NISAR	NASA ISRO Synthetic Aperture Radar
NLSI	NASA Lunar Science Institute
NM	Nonmare high-Ca/Fe pyroxene
NM-CPX	non-mare clinopyroxene
NRC	National Research Council
NTO	Nitrogen Tetroxide
OH	Hydroxide
OS	Operating System
OSIRIS	Origins Spectral Interpretation Resource Identification Security
OSIRIS-REx	Origins, Spectral Interpretation, Resource Identification, Security, Regolith Explorer
PBC	Power Bus Control
PDR	Preliminary Design Review
PICASSO	Planetary Instrument Concepts for the Advancement of Solar System Observations
PKT	Procellarum KREEP Terrane
PM	Project Manager
PM/PSE	Project/Program Manager Project System Engineer(ing)
PMCS	Planetary Mission Concept Study
POV	Persistence of Vision Ray Tracer
Prox-1	Proximity-1
PRT	Platinum Resistance Thermometer
PS	Point Spectrometer
PSE	Project Systems Engineering
PSR	Pre-ship Review
RCS	Reaction Control Subsystem
REE	Rare Earth Elements
RF	Radio Frequency
RGB	Red, Green, Blue
RHU	Radioisotope Heater Unit
ROM	Rough Order of Magnitude
RPS	Radioisotope Power System



RT	Response Time
RTG	Radioisotope Thermoelectric Generator
RX	Receive
RY	Real Year
S/C	Spacecraft
SAIRAS	International Symposium on Artificial Intelligence, Robotics and Automation in Space
SDT	Science Definition Team
SEER	System Evaluation and Estimate of Resources
SELENE	Selenological and Engineering Explorer
SEM	Scanning Electron Microscope
SfM	Structure from Motion
SHRIMP	Sensitive High-Resolution Ion Microprobe (Mass Spectrometer)
SIMS	Secondary Ion Mass Spectrometry
SMA	Safety & Mission Assurance
SMAP	Soil Moisture Active Passive
SMD	Science Mission Directorate
SOCM	Space Operations Cost Model
SOMA	Science Office for Mission Assessments
SPA	South Pole–Aitken
SPA-SR	South Pole–Aiken Sample Return
SPACA	South Pole–Aiken Compositional Anomaly
SpaceIL	Space Israel
SPICE	Spacecraft ephemeris, Planetary/satellite ephemeris and constants, Instruments, C Pointing Matrix, Event Info. (Kernels)
SRC	Sample Return Capsule
SRU	Stellar Reference Units
SS	Sun Sensor
SSPA	Solid State Power Amplifier
SSTL	Surrey Satellite Technology Limited
SSTMP	Solar System Treks Mosaic Pipeline
ST	Star Tracker
STMD	Space Technology Mission Directorate
SUROM	Start Up Read Only Memory
SW	Software
TBD	To Be Determined
TCS	Thermal Control Subsystem
TDP	Technical Data Package
THEMIS	Time History of Events and Macroscale Interactions during Substorms mission
TID	Total Ionizing Dose
TJ	Triple Junction
TRCTL	Terrain Adaptive Wheel Speed Control
TRL	Test Readiness Level
TX	Texas
UK	United Kingdom



UST	Universal Space Transponder
UV	Ultraviolet
UV/IR	Ultraviolet/Infrared
VIPER	Volatiles Investigating Polar Exploration Rover
VO	Visual Odometry
W/K	Watts per Meter per Degree Kelvin
WAC	Wide Angle Camera
WBS	Work Breakdown Structure
WDS	Wavelength Dispersive X-ray Spectroscopy
WEB	Warm Electronics Box
WES	Waterways Experiment Station
WFOV	Wide Field of View
XANES	X-ray Absorption Near Edge Structure
YPPPY	Yaw-Pitch-Pitch-Pitch-Yaw



B SCIENCE

B.1 DEVELOPING ENDURANCE'S LONG-RANGE TRAVERSE

From its inception, a key component of the Endurance mission concept study was the development of its long-range traverse across South Pole–Aitken (SPA) and the lunar farside. The Intrepid planetary mission concept study [1], demonstrated the credibility of a long-range (>1,800-km) lunar rover—albeit on different terrain on the lunar nearside. One of the central challenges of the Endurance concept study was to identify potential waypoints where returned samples could address the motivating science goals, and to identify a feasible traverse connecting those waypoints.

In this section, we describe the process by which the science team identified the waypoints (Section B.1). In the subsequent section, we detail the geology of the different regions along Endurance's traverses (Section B.2). Section K describes the process by which the traverse route between sample site waypoints was planned utilizing available lunar datasets.

Figure 1-3, Table 1-1, and Table B-1 detail Endurance's science objectives, and how they trace to sample site requirements. In short, to accomplish Endurance's science objectives, Endurance must acquire at least one sample capable of dating SPA (Objective 1.1), at least one sample capable of dating a farside, pre-Imbrian impact basin (Objective 1.2), at least two samples from a farside volcanic deposit, one of which must be a cratered mare basalt (Objectives 1.3, 2.1), at least one sample from a farside thorium hot-spot (Objective 2.1), and at least one sample from each of SPA's distinct geochemical terrains. In many cases, a single sample from one site can address more than one objective. In total, Endurance's threshold requirement is to acquire samples from 6 distinct sites, and the baseline threshold is to acquire samples from 12 distinct sites. 12 distinct sites ensure ample science margin; for example, Endurance collects samples from at least two different sites within each large basin it visits, samples far more than two volcanic deposits, and samples multiple terrains within SPA. Moreover, Endurance-R samples *two* pre-Imbrian basins (Poincaré and Apollo).

With these science requirements, there are no lack of candidate sample sites and notional traverses that could address Endurance's science objectives. The science team developed a variety of candidate traverses during the study, utilizing a combination of different orbital datasets and past research (Figure B-1). Despite the various candidate traverses, there were substantial similarities between all candidate traverses. All candidate traverses explored central SPA—including the SPA compositional anomaly (SPACA), the volcanic feature informally named Mons Marguerite (also known as Mafic Mound), and the surrounding regions. These regions were considered the highest priority for acquiring samples of SPA impact melt exposed by smaller impact craters (e.g., Bose, Bhaba), and subsequent volcanic products that trace the thermochemical evolution of SPA and the Moon as a whole. Beyond central SPA, candidate traverses were pinned by one of four large impact basins in the region: Ingenii, Apollo, Poincaré, and Schrödinger. Of these four, Ingenii, Apollo, and Poincaré are all large pre-Imbrian basins satisfying Objective 1.2. Schrödinger represents a target of opportunity, on the route towards the south pole, with its own scientific merit relevant for Objective 2.1, but not 1.2. There are smaller pre-Imbrian impact basins in SPA, like Leibnitz, Von Kármán, and Minnaert, although these were not favored due to their smaller size (which likely reflects shallower excavation depths) and comparatively rougher terrain (in Ingenii, Apollo, and Poincaré, it is relatively easy to traverse in and out of the basin and access peak rings and other important destinations). Additionally, many of the smaller pre-Imbrian basins are extensively superposed by extensive ejecta blankets from nearby younger craters (e.g., Minnaert is superposed by Antoniadi ejecta). Of the remaining three large basins, Ingenii represented a tempting target due to the presence of swirls and magnetic anomalies. Swirls featured prominently in the Intrepid mission concept [1], and one could imagine addressing some of Intrepid's science objectives with a traverse into Ingenii. However, Ingenii was ultimately not favored because it is nearly antipodal to Imbrium (meaning that Imbrium ejecta may focus in this region), and so there is a chance that Ingenii samples could still suffer the Imbrium bias that is feared to exist in Apollo samples. This ultimately resulted in favoring Poincaré and Apollo basins. While the final traverses for Endurance-R



(Robotic) and Endurance-A (Astronaut) are capable of addressing all of the motivating science objectives, they should not be considered the only possible traverse. A future proposal may find alternative traverses and destinations that satisfy the science objectives.

Once these broad regions were determined, the science team set about identifying specific candidate sample sites. These sites ranged from generalized regions (e.g., Site O: sample the ejecta of Lyman), to sites defined by single pixels of remote sensing data (e.g., Site C: sample the highest thorium anomaly outside of Abbe M crater; Site F: sample noritic material identified by M³). Details about these sites are displayed in Table B-1. Our final list consists of 17 sample sites (1 of which was descoped), labeled A-Q. Sites A-G are common to both the traverses of Endurance-A and Endurance-R (referred to as the “core traverse”). Sites I-N are unique to Endurance-R, and sites H and O-Q are unique to Endurance-A. The sites are not visited in alphabetical order with either variant of Endurance: Endurance-A traverses, in order: B, A, C, D, E, F, G, I, K, L, M; Endurance-R traverses, in order: H, G, F, E, D, C, A, B, A, O, P, Q. Sites J and N were considered, but ultimately descoped to meet the 12-sample limit of the Endurance-R sample canister.

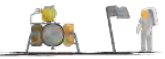


Table B-1. Expanded Endurance Science and Traverse Traceability Matrix (see Table 1-1 for a trimmed down version).

					Core Traverse (both Endurance-A and Endurance-R)																																										
					A	B	C	D	E	F	G																																				
					Poincaré Q	Poincaré center	Abbe M	Haret C mare	SW Bose	SW Bhaba	Mons Marguerite slope																																				
					LATITUDE, LONGITUDE:	-59.12448°N, 161.05104°E	-57.2223°N, 162.6293°E	-61.2595°N, 176.5608°E	-57.2341°N, -171.9308°E	-55.4248°N, -170.8276°E	-56.6008°N, -166.6533°E	-57.3560°N, 197.2267°E																																			
					NOTES:	Ideal location at the contact between Poincaré mare basalts, Poincaré peak ring material, and material excavated from depth by the Poincaré Q crater. A date from this region may be able to date Poincaré Q, Poincaré, the mare basalts, and SPA (as Poincaré likely excavated SPA impact melt).						This small unnamed crater likely excavated through the mare in the center of Poincaré, and samples from this region would likely date the unnamed crater, the mare basalts, and Poincaré itself.						The ejecta around Abbe M is associated with the highest thorium abundances (>3-ppm) on either traverse of Endurance. This may be the best location for acquiring exposed mantle and SPA ejecta.						This site is associated with a large mare basalt flow, with superposed craters, that would be ideal for establishing an absolute crater chronology.						Based on M3 data, this location is the best plausible location for sampling noritic impact melt excavated by the Bose crater.						Based on M3 data, this location is the best plausible location for sampling noritic impact melt excavated by the Bhaba crater.						This small unnamed crater on the slopes of Mons Marguerite (informal name) likely excavated pristine material from within Mons Marguerite, and may also excavate SPA impact melt from depth.					
SCIENCE OBJECTIVES:	SCIENCE QUESTIONS:	MEASUREMENT REQUIREMENTS:	SAMPLE SITE REQUIREMENTS:																																												
SCIENCE THEME 1: SOLAR SYSTEM CHRONOLOGY	1.1. Anchor the earliest impact history of the Solar System by determining the age of (perhaps) the largest and oldest impact basin on the Moon: South Pole–Aitken (SPA).	<ul style="list-style-type: none"> Hold old is SPA? Does the Moon retain a complete record of all impact basins, or were most early impact basins erased—either due to SPA itself, the magma ocean, or some other process(es)? To what degree did SPA formation obscure the earlier bombardment history? 	Determine the age of SPA to within ±0.05 Ga.	≥1 sample from the SPA melt sheet, as exposed by craters excavating through the SPA compositional anomaly (SPACA).	Contributing		X		X	X	Contributing																																				
	1.2. Test the giant planet instability and impact cataclysm hypotheses by determining when farside lunar basins formed.	<ul style="list-style-type: none"> Was there a lunar cataclysm (i.e., late heavy bombardment) caused by the reorganization of the Solar System? If there was a lunar cataclysm, when did occur, and for how long? Are all of our samples from the nearside really just dating the same thing: the Imbrium impact? 	Determine the age of ≥1 farside, pre-Imbrian impact basin to within ±0.05 Ga.	≥1 sample from the impact melt sheet and/or peak ring of a farside, pre-Imbrian impact basin.	X	X																																									
	1.3. Anchor the "middle ages" of Solar System chronology (between 1 and 4 billion years ago) by determining the absolute age of a cratered, farside lunar mare basalt.	<ul style="list-style-type: none"> What is the relationship between crater size-frequency distributions and absolute ages on the Moon and across the Solar System? 	Determine the age of ≥1 cratered, farside mare basalt flow to within ±0.05 Ga.	≥1 sample from a cratered farside mare basalt.	X	X		X																																							
SCIENCE THEME 2: PLANETARY EVOLUTION	2.1. Test the magma ocean paradigm and characterize the thermochemical evolution of terrestrial worlds by determining the age and nature of volcanic features and compositional anomalies on the farside of the Moon.	Why are the nearside and farside different? <ul style="list-style-type: none"> What is the age, composition, and source of diverse manifestations of lunar farside volcanism—and is it different than nearside volcanism? Is there a causal relationship between SPA and the nearside Procellarum KREEP Terrane (PKT)? Was the lunar magma ocean a global event? Was urKREEP (the last dregs of magma ocean crystallization) globally distributed? What is the composition and structure of the Moon's lower crust and mantle? Did the lunar mantle overturn? 	Determine the age of ≥2 distinct volcanic samples from the lunar farside to within ±0.02 Ga.	≥2 samples from a farside volcanic deposit, including mare basalts, pyroclastics, or other volcanic units.	X	X	Contributing	X	X	X	X																																				
			Determine the composition of ≥2 volcanic samples from the lunar farside.				X																																								
	Determine the composition of ≥1 Thorium hot-spot (>3 ppm) materials on the lunar farside.	≥1 sample from a Thorium hot-spot (>3ppm) from the lunar farside.																																													
2.2. Explore a giant impact basin from floor to rim by characterizing the geologic diversity across the South Pole–Aitken Basin.	<ul style="list-style-type: none"> How do planetary-scale impacts reshape planets and moons? 	Determine the composition and characteristics of the major geochemical terrains across SPA, including SPA impact melt, SPA ejecta, and post-SPA volcanic products.	≥1 sample from each of the three geochemical major terrains within SPA: (1) SPACA, (2) Pyroxene Bearing Zone, and (3) Heterogenous Annulus.	X	X	X	X	X	X	X																																					



Table B-1. Expanded Endurance Science and Traverse Traceability Matrix (see Table 1-1 for a trimmed down version).

					North Traverse (Endurance-R only):						
					I NE Bhaba	J Smooth SPACA plains	K Bhaba magnetic anomaly	L Chaffee S	M Apollo peak ring	N DIVINER-identified crater	
					LATITUDE, LONGITUDE:	-54.6008°N, -162.5337°E	-53.2858°N, -160.2125°E	-51.1017°N, -162.3162°E	-40.3708°N, -157.2198°E	-37.7115°N, -153.0430°E	-42.5305°N, -158.8416°E
					NOTES:	Bhaba exhibits a substantial east-west compositional variation, perhaps reflecting variations in excavation depth or subsurface heterogeneity. Based on M3, this region is more gabbroic than the western rim sampled at Site F	This region is associated with the smooth, young plains of SPACA. A sample from this region may date the youngest resurfaced areas of SPA. Ultimately this site was descoped, in part because it may be redundant to samples from elsewhere in central SPA.	This is the strongest magnetic anomaly along the Endurance-R traverse.	Chaffee S almost certainly excavated Apollo impact melt. A sample from its ejecta blanket may date Chaffee S, Apollo, and the nearby mare basalts.	Ideal location at the contact between Apollo mare basalts and Apollo peak-ring material, presenting the opportunity to potentially date Apollo, the mare basalts, and SPA melt excavated by Apollo's peak ring.	This is the lone DIVINER-identified young crater (<1 Myr old) on the Endurance-R traverse, and an excellent opportunistic target.
SCIENCE OBJECTIVES:		SCIENCE QUESTIONS:	MEASUREMENT REQUIREMENTS:	SAMPLE SITE REQUIREMENTS:							
SCIENCE THEME 1: SOLAR SYSTEM CHRONOLOGY	1.1. Anchor the earliest impact history of the Solar System by determining the age of (perhaps) the largest and oldest impact basin on the Moon: South Pole–Aitken (SPA).	<ul style="list-style-type: none"> • How old is SPA? • Does the Moon retain a complete record of all impact basins, or were most early impact basins erased—either due to SPA itself, the magma ocean, or some other process(es)? • To what degree did SPA formation obscure the earlier bombardment history? 	Determine the age of SPA to within ±0.05 Ga.	≥1 sample from the SPA melt sheet, as exposed by craters excavating through the SPA compositional anomaly (SPACA).	Contributing				Contributing		
	1.2. Test the giant planet instability and impact cataclysm hypotheses by determining when farside lunar basins formed.	<ul style="list-style-type: none"> • Was there a lunar cataclysm (i.e., late heavy bombardment) caused by the reorganization of the Solar System? • If there was a lunar cataclysm, when did occur, and for how long? • Are all of our samples from the nearside really just dating the same thing: the Imbrium impact? 	Determine the age of ≥1 farside, pre-Imbrian impact basin to within ±0.05 Ga.	≥1 sample from the impact melt sheet and/or peak ring of a farside, pre-Imbrian impact basin.				X	X		
	1.3. Anchor the "middle ages" of Solar System chronology (between 1 and 4 billion years ago) by determining the absolute age of a cratered, farside lunar mare basalt.	<ul style="list-style-type: none"> • What is the relationship between crater size-frequency distributions and absolute ages on the Moon and across the Solar System? 	Determine the age of ≥1 cratered, farside mare basalt flow to within ±0.05 Ga.	≥1 sample from a cratered farside mare basalt.	Descoped	Contributing	X	X	X	Contributing	
SCIENCE THEME 2: PLANETARY EVOLUTION	2.1. Test the magma ocean paradigm and characterize the thermochemical evolution of terrestrial worlds by determining the age and nature of volcanic features and compositional anomalies on the farside of the Moon.	Why are the nearside and farside different? • What is the age, composition, and source of diverse manifestations of lunar farside volcanism—and is it different than nearside volcanism? • Is there a causal relationship between SPA and the nearside Procellarum KREEP Terrane (PKT)? • Was the lunar magma ocean a global event? • Was urKREEP (the last dregs of magma ocean crystallization) globally distributed? • What is the composition and structure of the Moon's lower crust and mantle? • Did the lunar mantle overturn?	Determine the age of ≥2 distinct volcanic samples from the lunar farside to within ±0.02 Ga.	≥2 samples from a farside volcanic deposit, including mare basalts, pyroclastics, or other volcanic units.	X		X	X	X		
			Determine the composition of ≥2 volcanic samples from the lunar farside.								
	Determine the composition of ≥1 Thorium hot-spot (>3 ppm) materials on the lunar farside.	≥1 sample from a Thorium hot-spot (>3ppm) from the lunar farside.									
2.2. Explore a giant impact basin from floor to rim by characterizing the geologic diversity across the South Pole–Aitken Basin.	<ul style="list-style-type: none"> • How do planetary-scale impacts reshape planets and moons? 	Determine the composition and characteristics of the major geochemical terrains across SPA, including SPA impact melt, SPA ejecta, and post-SPA volcanic products.	≥1 sample from each of the three geochemical major terrains within SPA: (1) SPACA, (2) Pyroxene Bearing Zone, and (3) Heterogenous Annulus.	X	X	X	X	X			



Table B-1. Expanded Endurance Science and Traverse Traceability Matrix (see Table 1-1 for a trimmed down version).

					South Traverse (Endurance-A only):							
					H Mons Marguerite	O Lyman	P Schrodinger north	Q Schrodinger pyroclastic				
					LATITUDE: -57.8621°N, -161.8022°E	-64.9294°N, 162.4302°E	73.4034°N, 135.3675°E	-75.2993°N, 139.3307°E				
					NOTES:	Mons Marguerite (informal name) is a unique volcanic feature in SPA that may trace the later evolution of SPA.	Lyman may be the youngest complex crater in the SPA region, and an excellent opportunistic target. Endurance shall not drive into Lyman.	Ideal location to both sample Schrodinger peak-ring material and impact melt in central Schrodinger.	The best exposure of pyroclastic deposits (a unique type of volcanism) on the entire Endurance-A traverse.			
					SCIENCE OBJECTIVES:	SCIENCE QUESTIONS:	MEASUREMENT REQUIREMENTS:	SAMPLE SITE REQUIREMENTS:				
SCIENCE THEME 1: SOLAR SYSTEM CHRONOLOGY	1.1. Anchor the earliest impact history of the Solar System by determining the age of (perhaps) the largest and oldest impact basin on the Moon: South Pole–Aitken (SPA).	<ul style="list-style-type: none"> Hold old is SPA? Does the Moon retain a complete record of all impact basins, or were most early impact basins erased—either due to SPA itself, the magma ocean, or some other process(es)? To what degree did SPA formation obscure the earlier bombardment history? 	Determine the age of SPA to within ±0.05 Ga.	≥1 sample from the SPA melt sheet, as exposed by craters excavating through the SPA compositional anomaly (SPACA).	Contributing	X	Contributing					
	1.2. Test the giant planet instability and impact cataclysm hypotheses by determining when farside lunar basins formed.	<ul style="list-style-type: none"> Was there a lunar cataclysm (i.e., late heavy bombardment) caused by the reorganization of the Solar System? If there was a lunar cataclysm, when did occur, and for how long? Are all of our samples from the nearside really just dating the same thing: the Imbrium impact? 	Determine the age of ≥1 farside, pre-Imbrian impact basin to within ±0.05 Ga.	≥1 sample from the impact melt sheet and/or peak ring of a farside, pre-Imbrian impact basin.		Contributing	Contributing	Contributing				
	1.3. Anchor the "middle ages" of Solar System chronology (between 1 and 4 billion years ago) by determining the absolute age of a cratered, farside lunar mare basalt.	<ul style="list-style-type: none"> What is the relationship between crater size-frequency distributions and absolute ages on the Moon and across the Solar System? 	Determine the age of ≥1 cratered, farside mare basalt flow to within ±0.05 Ga.	≥1 sample from a cratered farside mare basalt.								
SCIENCE THEME 2: PLANETARY EVOLUTION	2.1. Test the magma ocean paradigm and characterize the thermochemical evolution of terrestrial worlds by determining the age and nature of volcanic features and compositional anomalies on the farside of the Moon.	Why are the nearside and farside different? <ul style="list-style-type: none"> What is the age, composition, and source of diverse manifestations of lunar farside volcanism—and is it different than nearside volcanism? Is there a causal relationship between SPA and the nearside Procellarum KREEP Terrane (PKT)? Was the lunar magma ocean a global event? Was urKREEP (the last dregs of magma ocean crystallization) globally distributed? What is the composition and structure of the Moon's lower crust and mantle? Did the lunar mantle overturn? 	Determine the age of ≥2 distinct volcanic samples from the lunar farside to within ±0.02 Ga.	≥2 samples from a farside volcanic deposit, including mare basalts, pyroclastics, or other volcanic units.	X		Contributing	X				
			Determine the composition of ≥2 volcanic samples from the lunar farside.									
			Determine the composition of ≥1 Thorium hot-spot (>3 ppm) materials on the lunar farside.	≥1 sample from a Thorium hot-spot (>3ppm) from the lunar farside.								
	2.2. Explore a giant impact basin from floor to rim by characterizing the geologic diversity across the South Pole–Aitken Basin.	<ul style="list-style-type: none"> How do planetary-scale impacts reshape planets and moons? 	Determine the composition and characteristics of the major geochemical terrains across SPA, including SPA impact melt, SPA ejecta, and post-SPA volcanic products.	≥1 sample from each of the three geochemical major terrains within SPA: (1) SPACA, (2) Pyroxene Bearing Zone, and (3) Heterogenous Annulus.	X	X	X	X				



GLOBAL MAP SET 1: Color and albedo

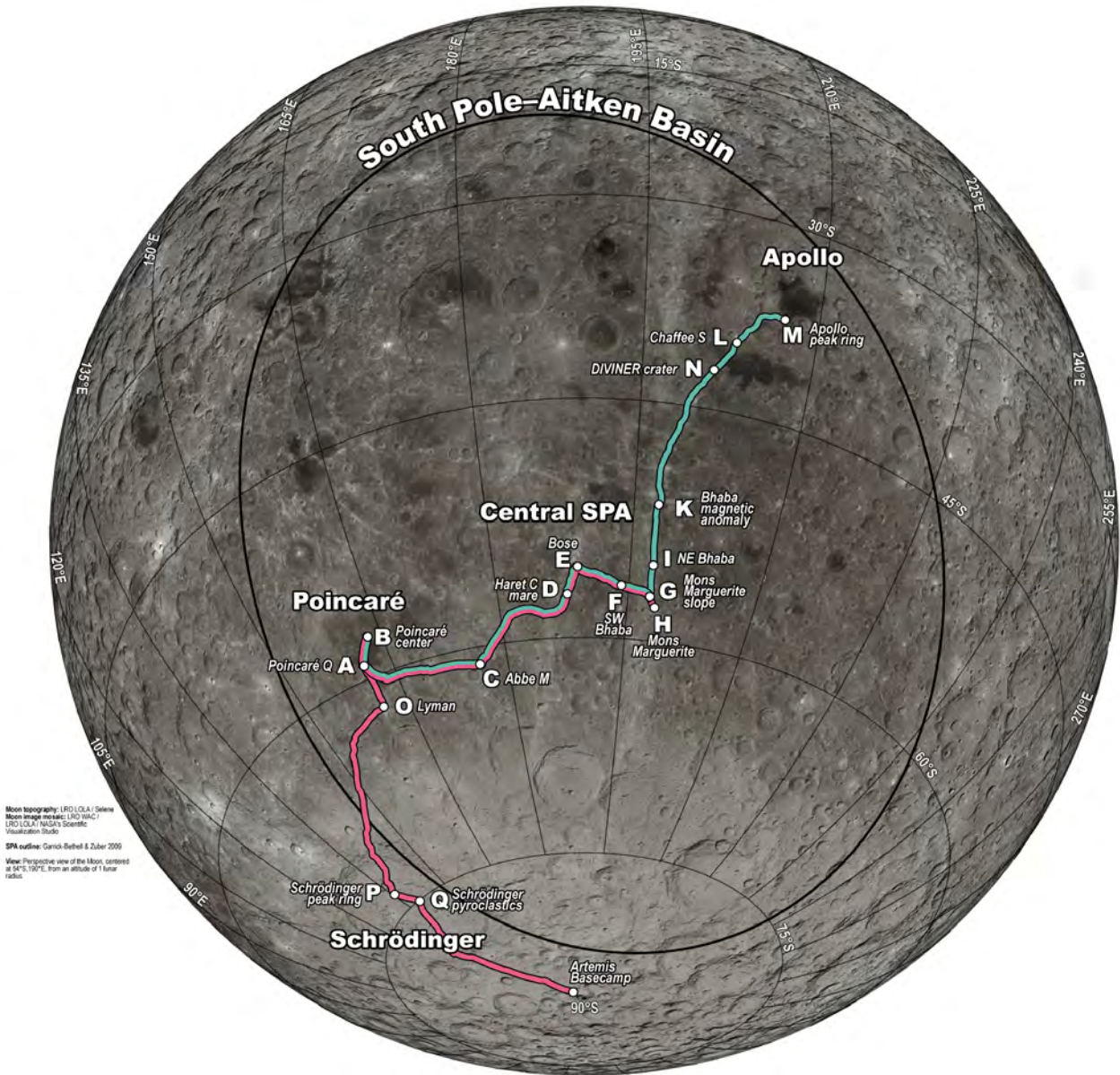
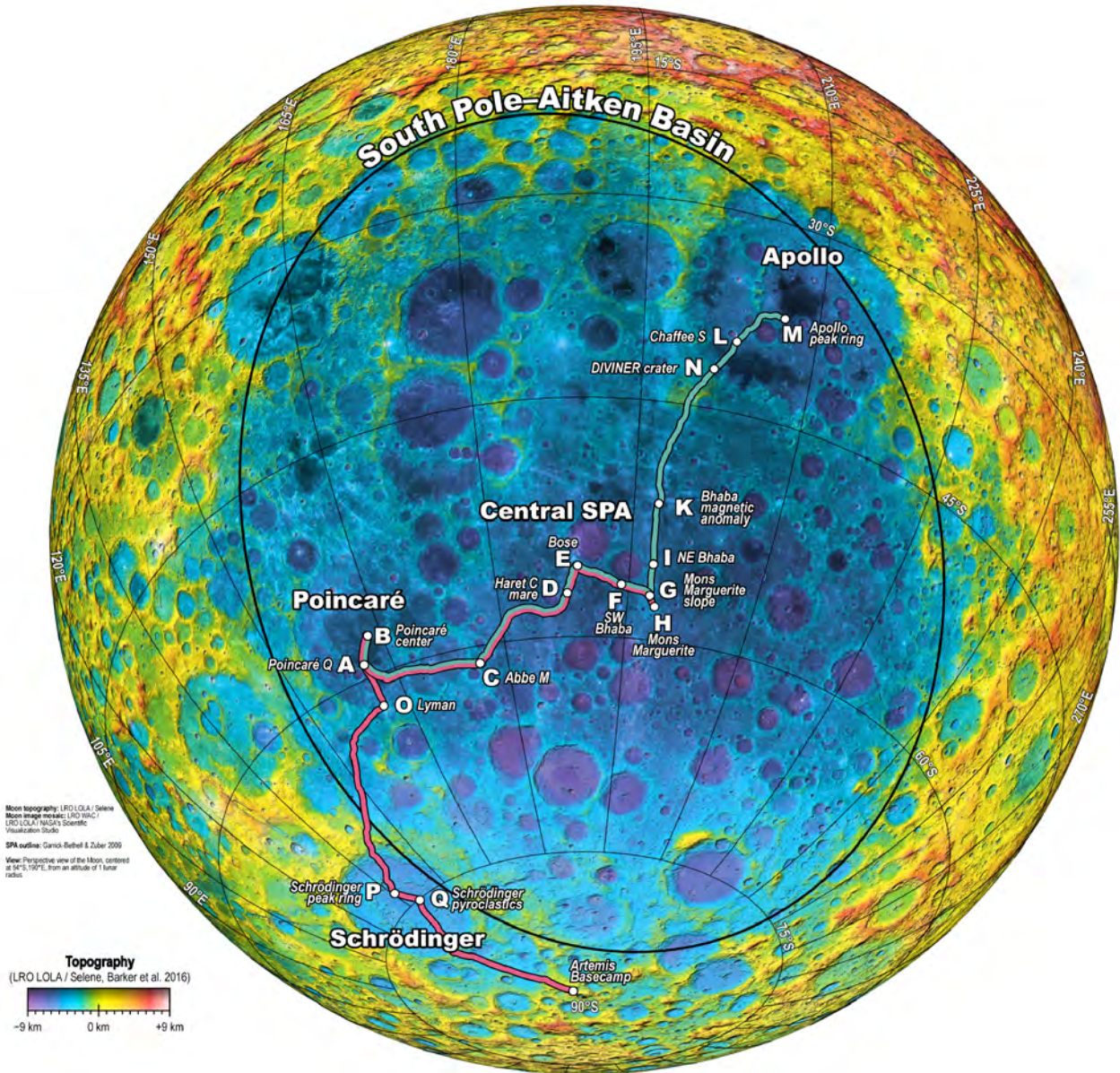


Figure B-1. Datasets used in early traverse planning by the science team (continued on following pages).

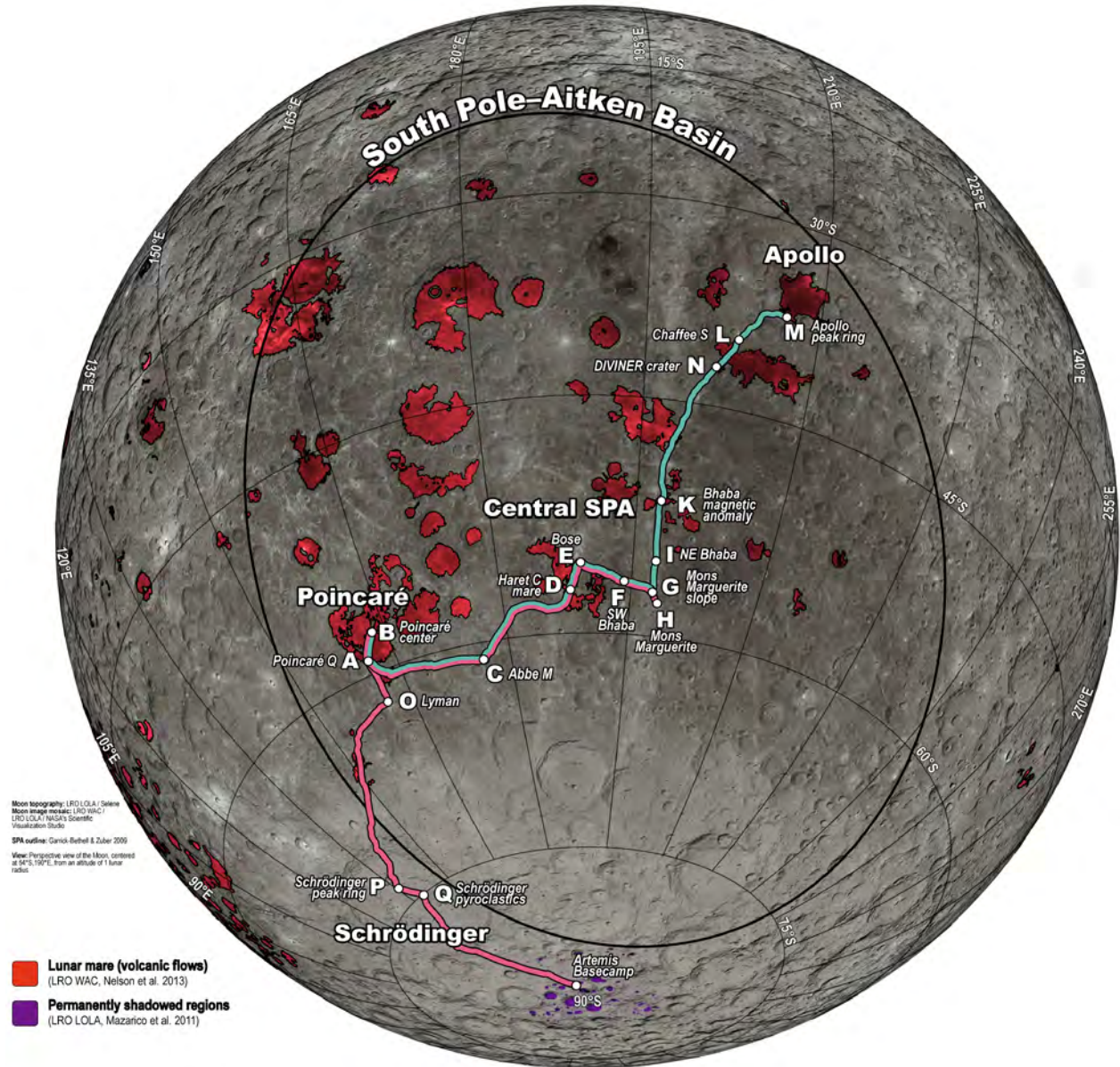


GLOBAL MAP SET 2: Topography



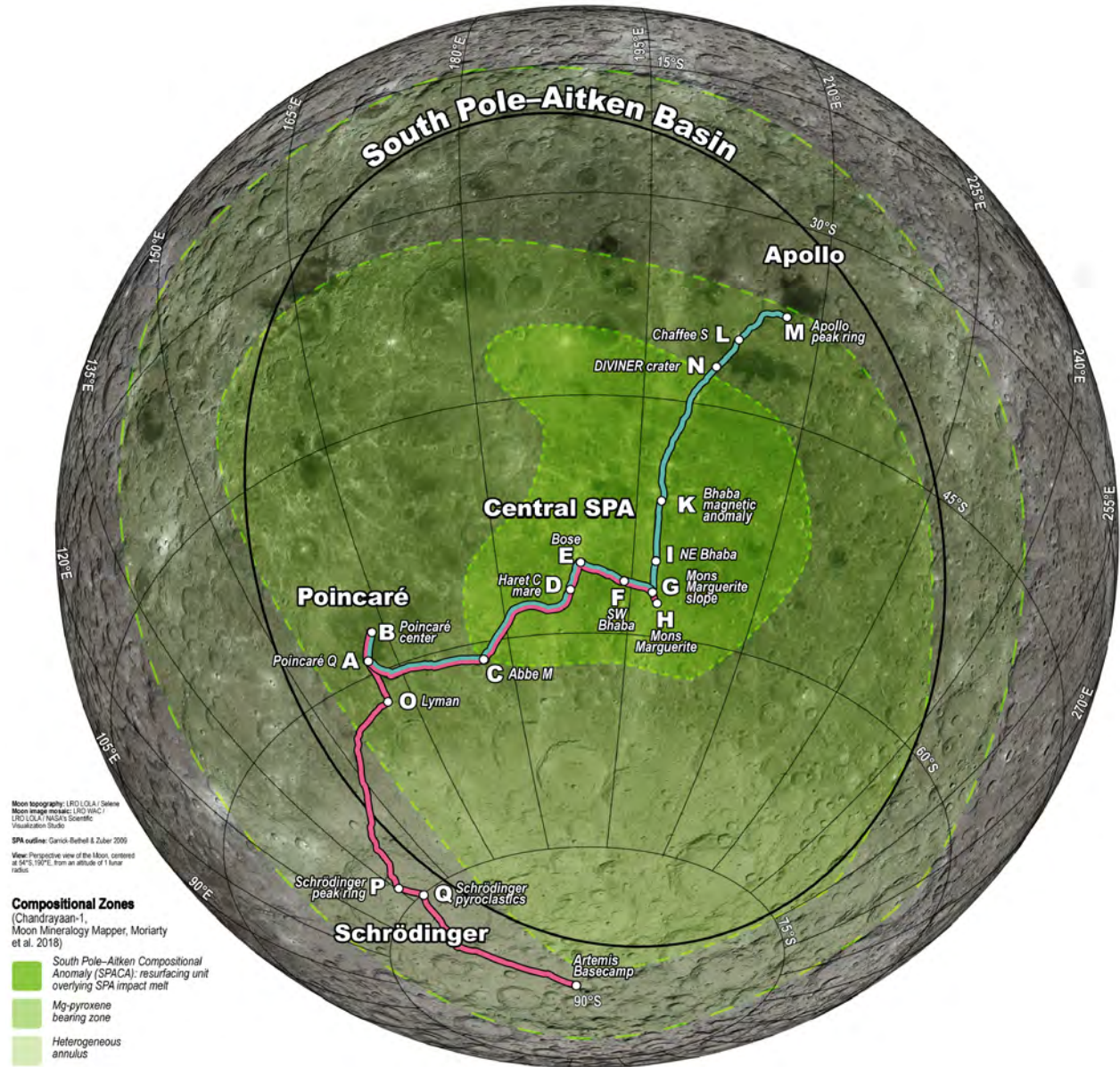


GLOBAL MAP SET 3: Mare and permanently shadowed regions (PSRs)



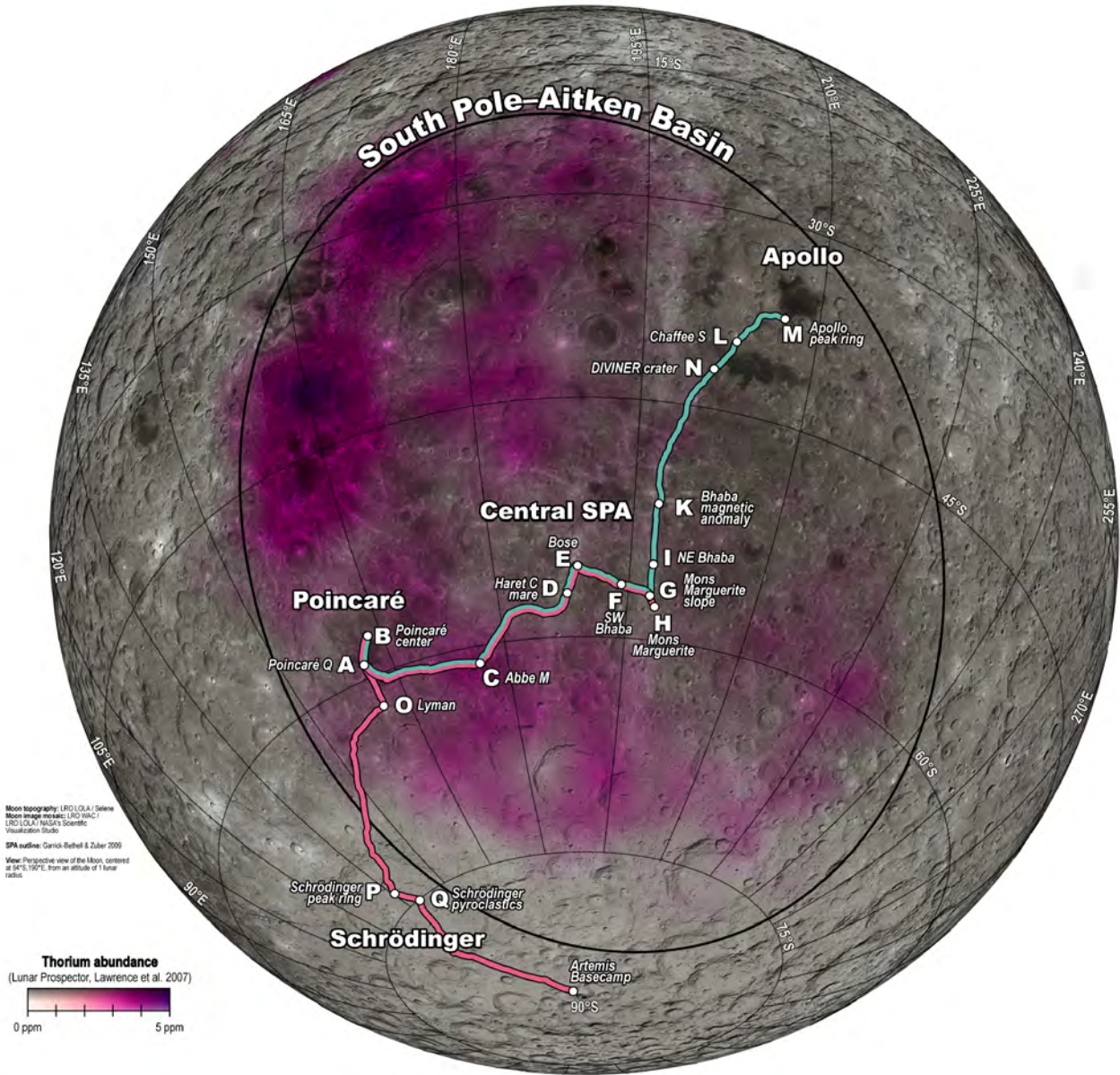


GLOBAL MAP SET 4: Compositional zones



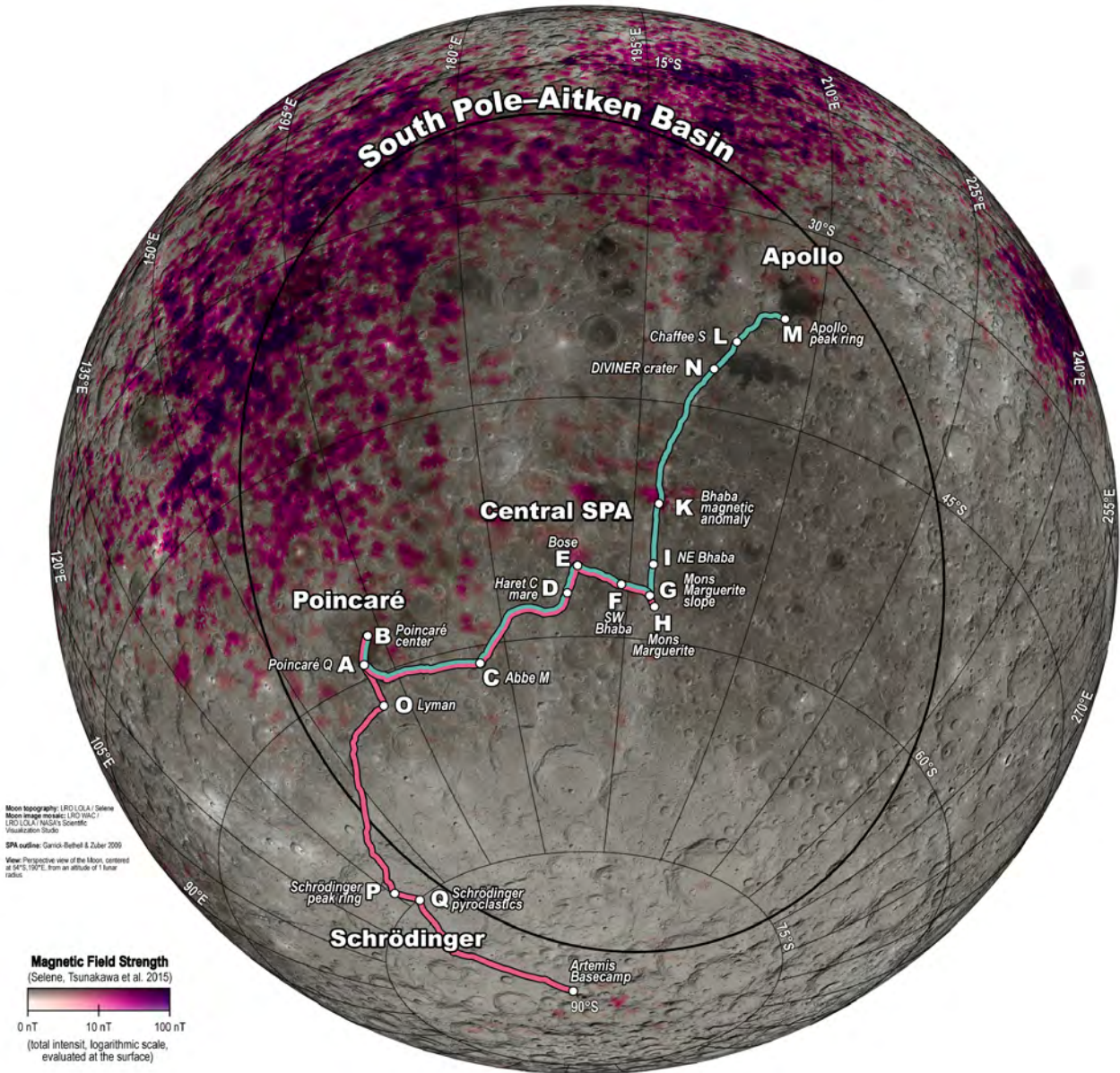


GLOBAL MAP SET 5: Thorium abundance



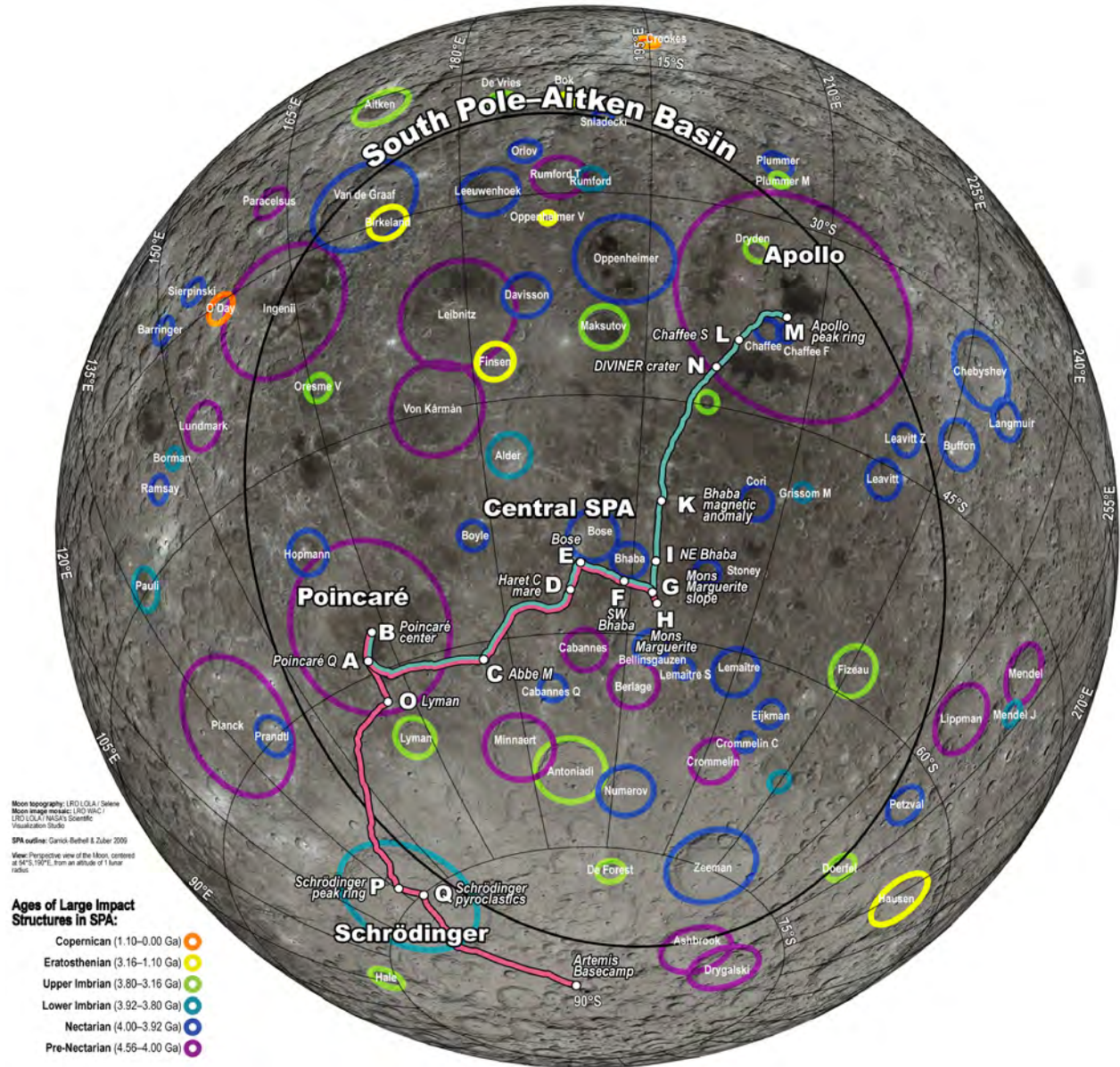


GLOBAL MAP SET 6: Magnetic field strength



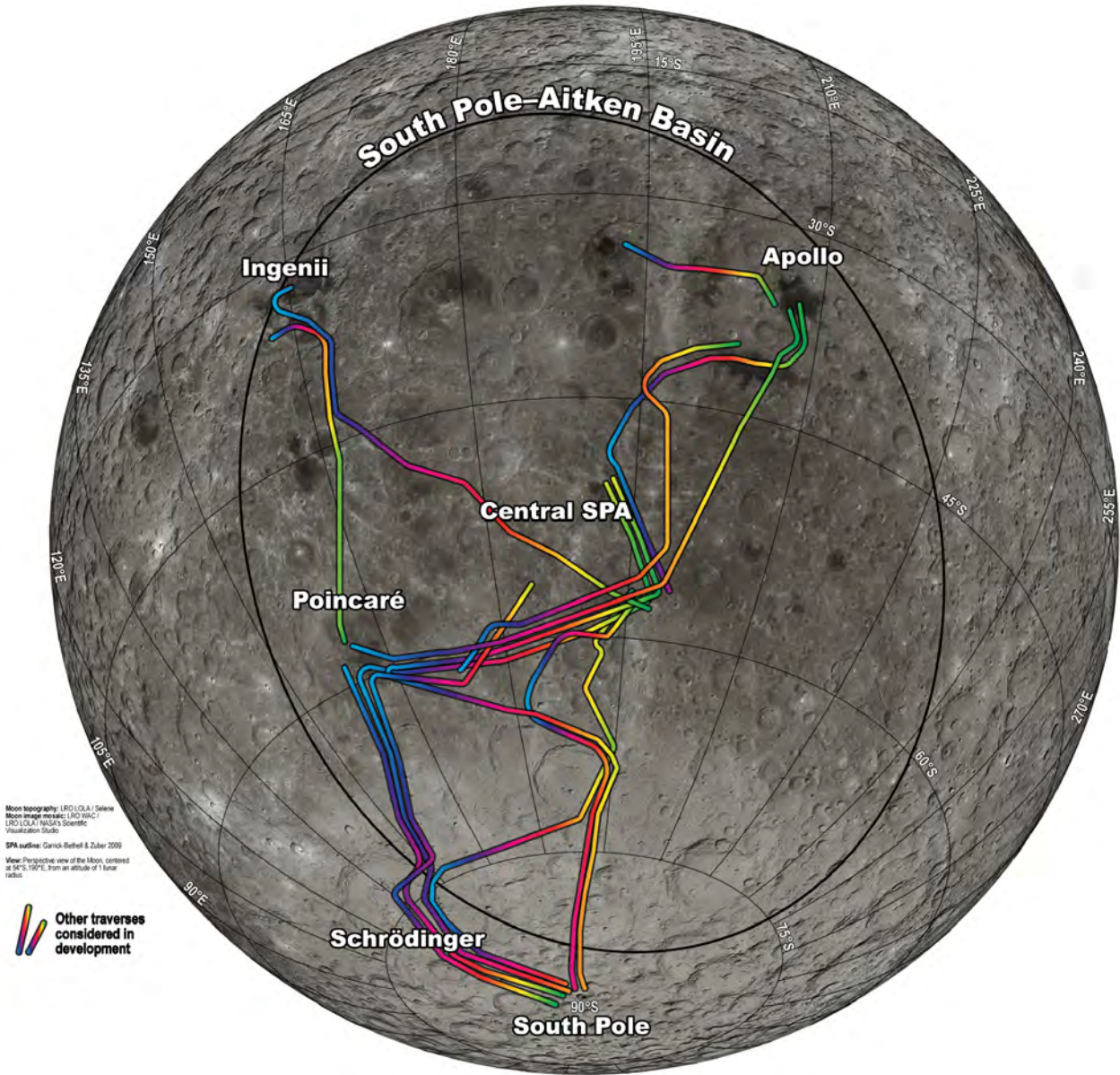


GLOBAL MAP SET 7: Impact basins



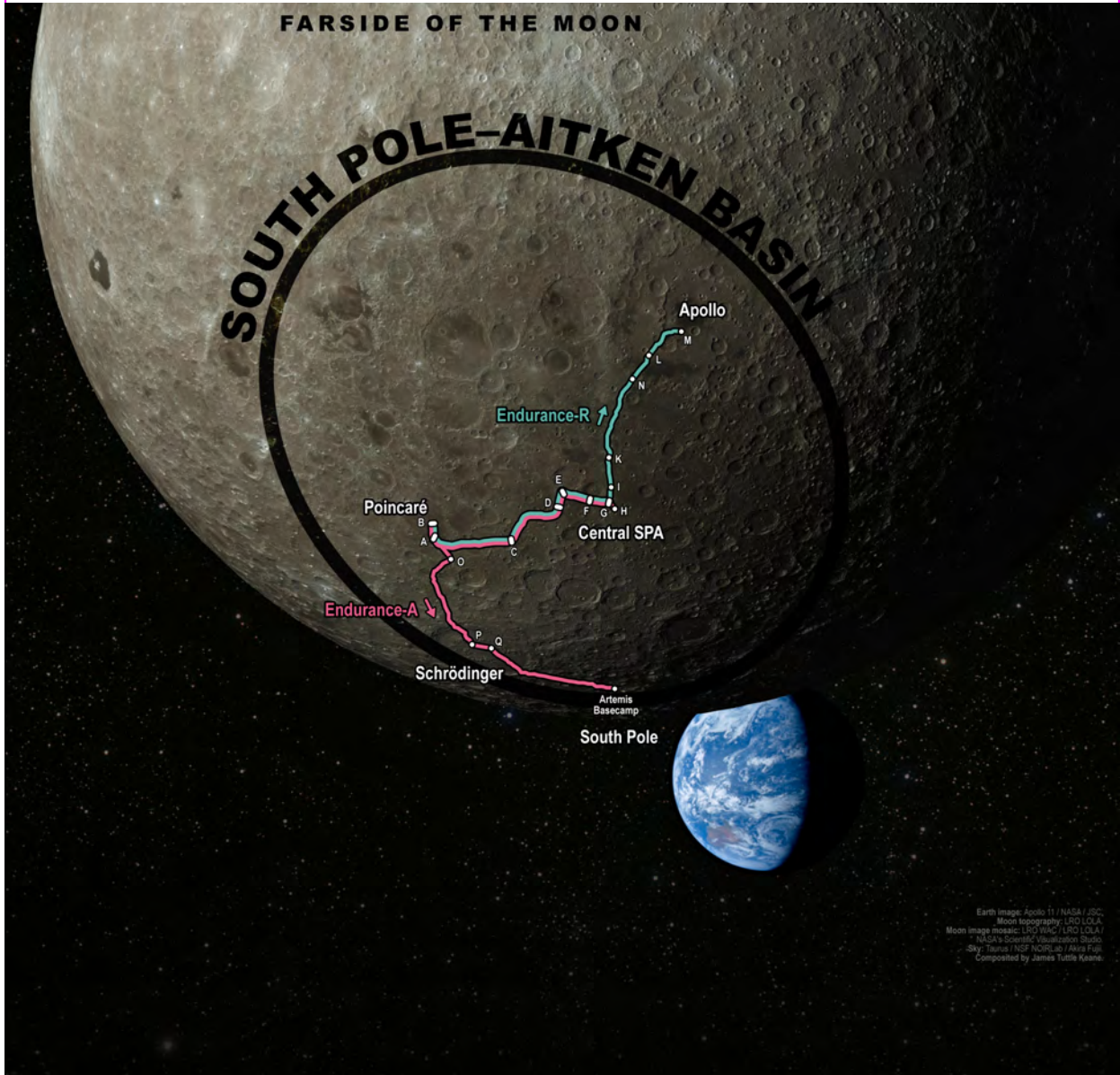


GLOBAL MAP SET 8: Candidate traverses



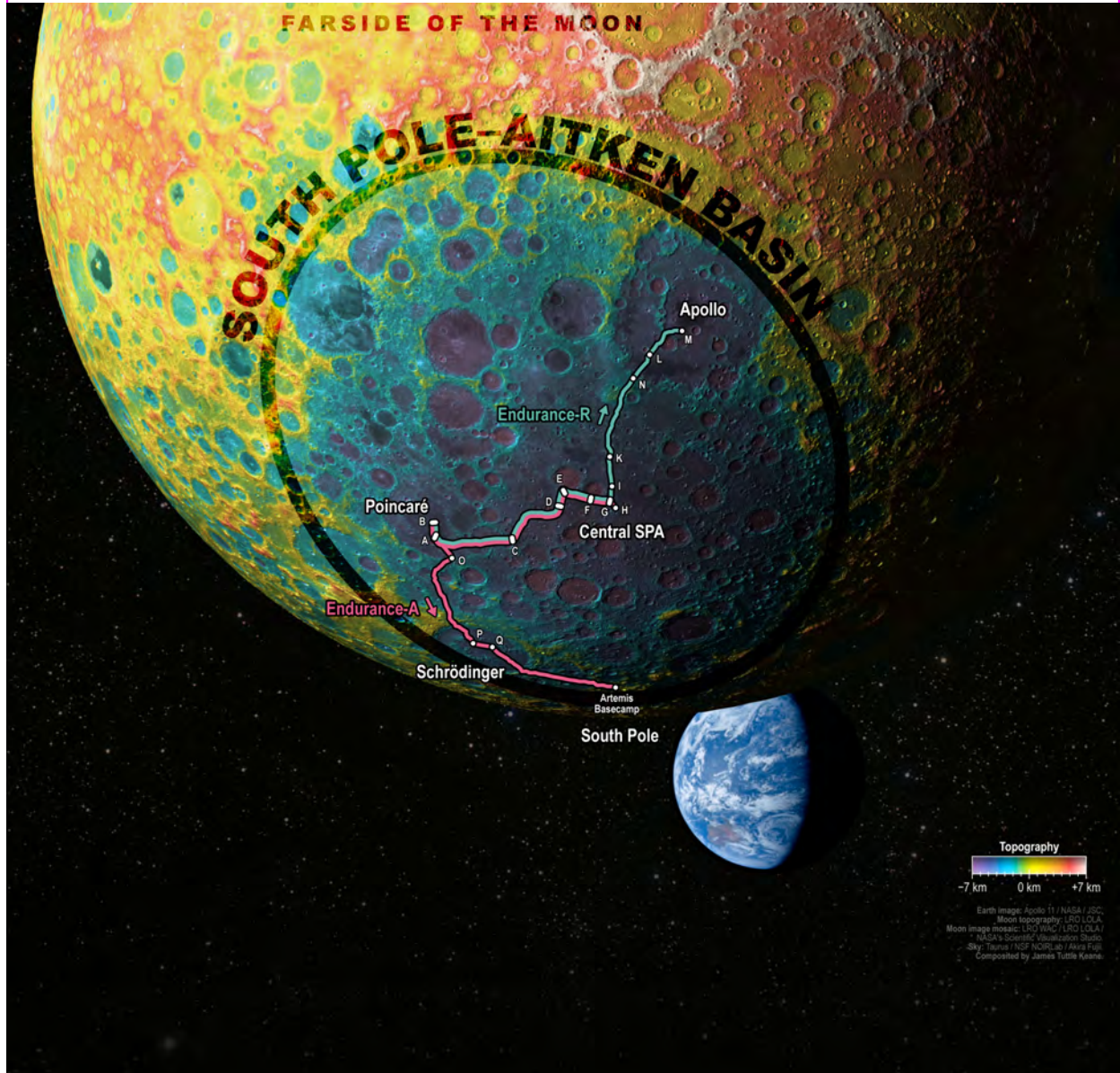


GLOBAL MAP SET 9: Simulated view of the farside of the Moon, Endurance's traverse, and the Earth





GLOBAL MAP SET 10: Simulated view of the farside of the Moon, Endurance's traverse, and the Earth





B.2 GEOLOGY OF ENDURANCE'S LONG-RANGE TRAVERSE

In this section, we detail the geology of the different regions along Endurance's traverses, including Central South Pole–Aitken (Section B.2.1), Poincaré basin (Section B.2.2), Apollo basin (Section B.2.3), and Schrödinger basin (Section B.2.4). Global maps of this traverse are shown in Figure 1-3 and Figure B-1. Local-scale maps covering the traverse can be found in Figure B-2.

TRAVERSE MAP SET TABLE OF CONTENTS

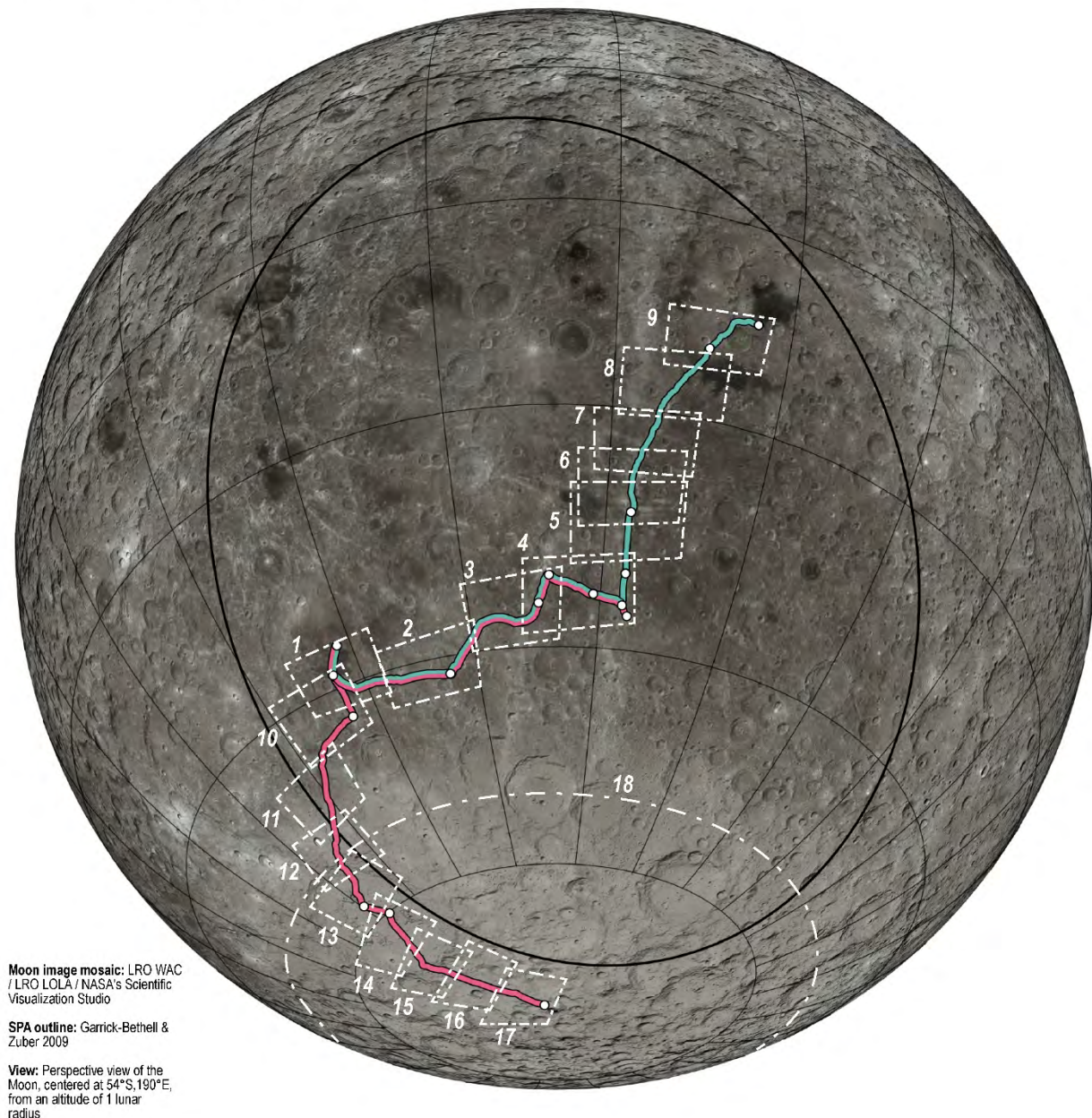
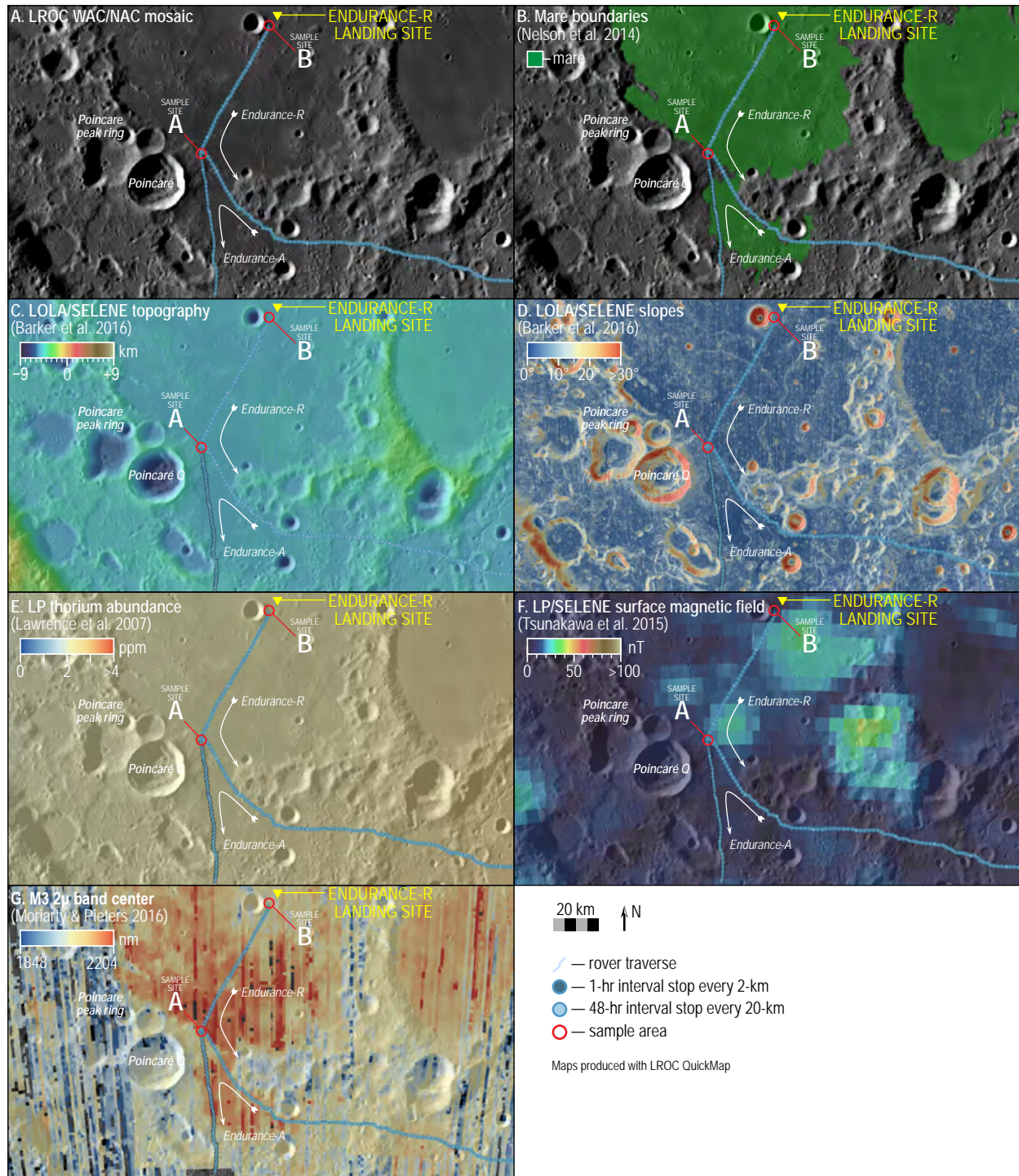


Figure B-2. Maps of Endurance's traverse (continued on subsequent pages).

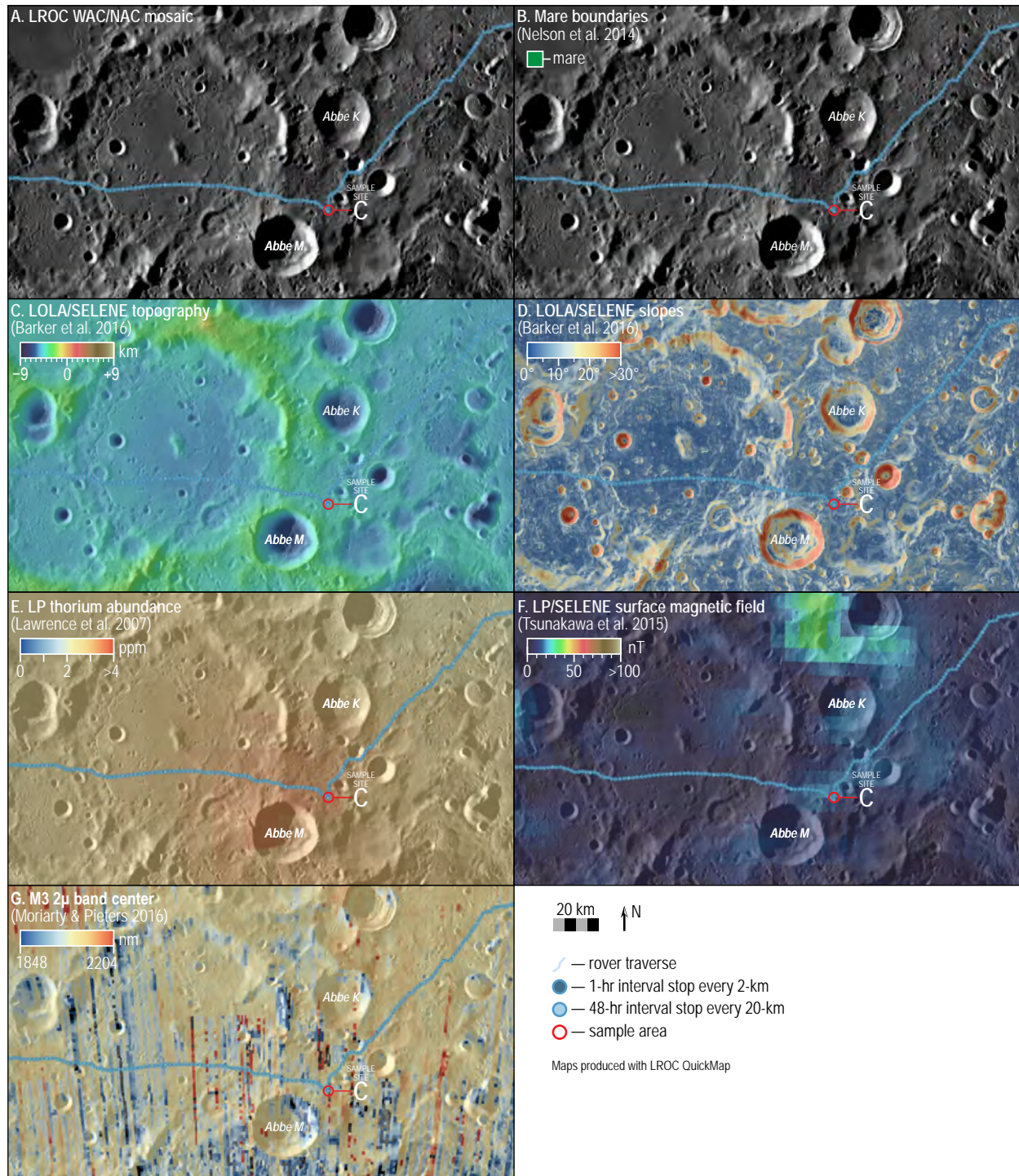


TRAVERSE MAP SET 1: Poincaré basin



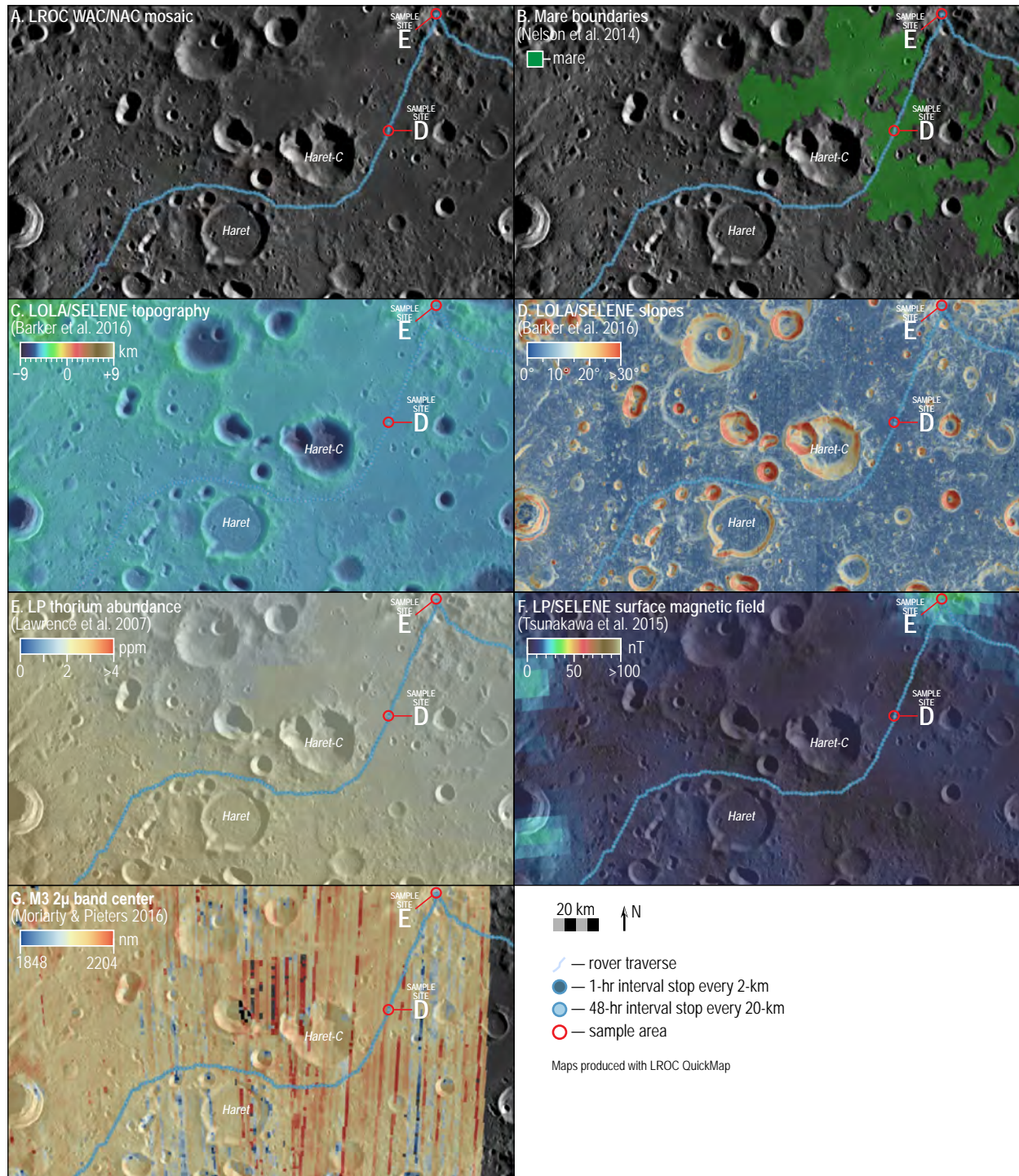


TRAVERSE MAP SET 2: East of Pointcaré, near Abbe M crater



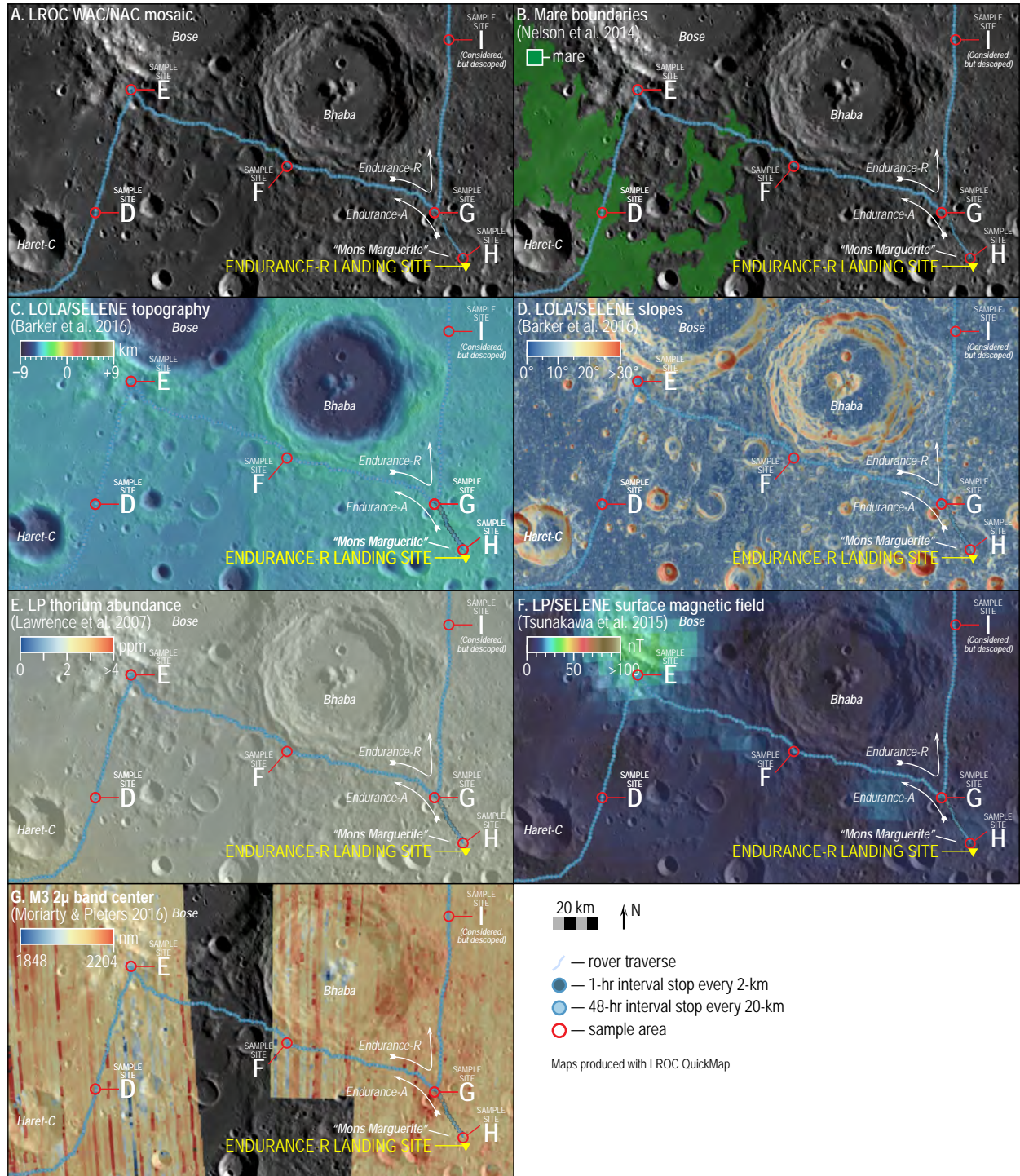


TRAVERSE MAP SET 3: Central SPA, near Haret crater



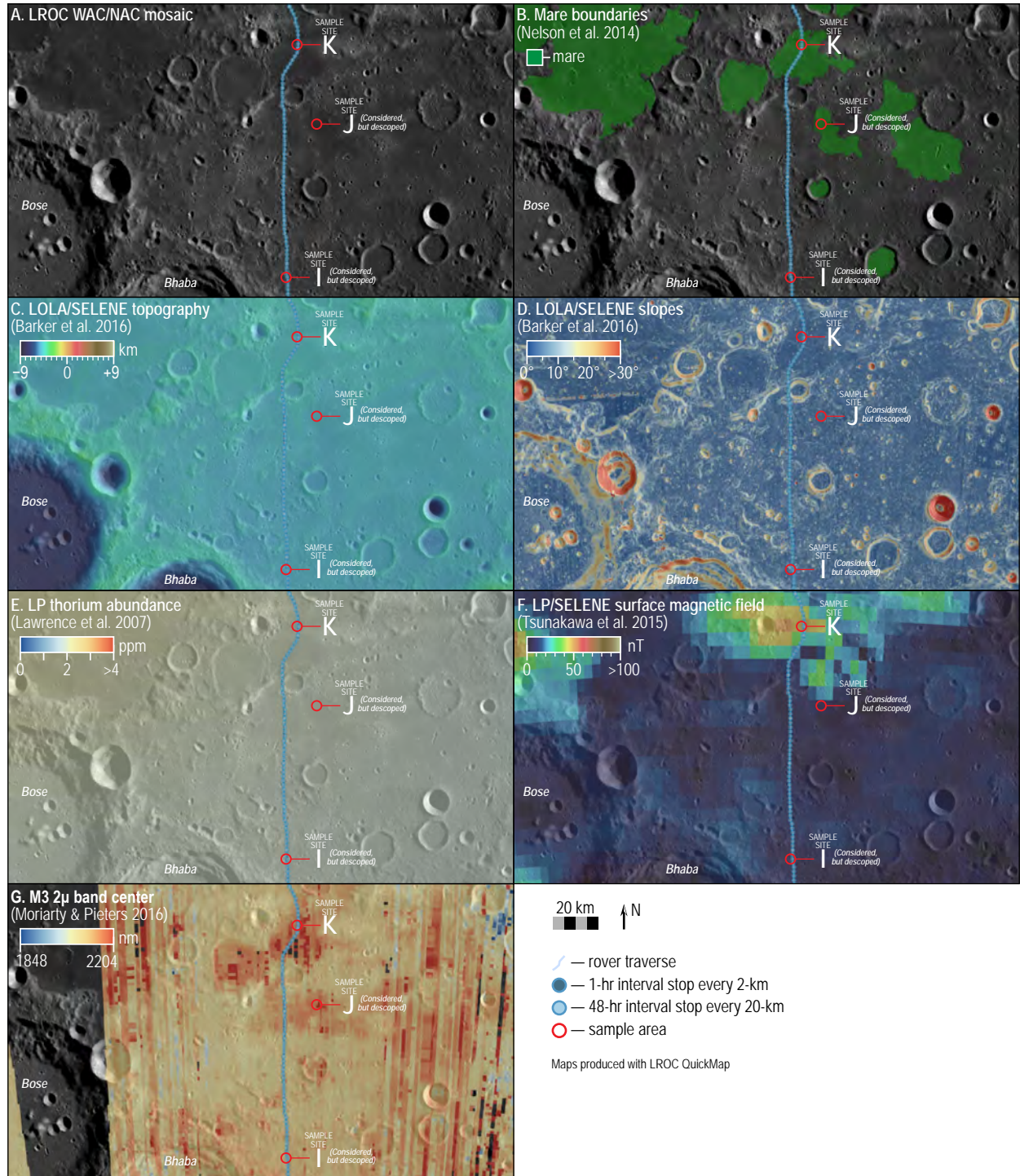


TRAVERSE MAP SET 4: Central SPA, south of Bose crater & Bhaba crater



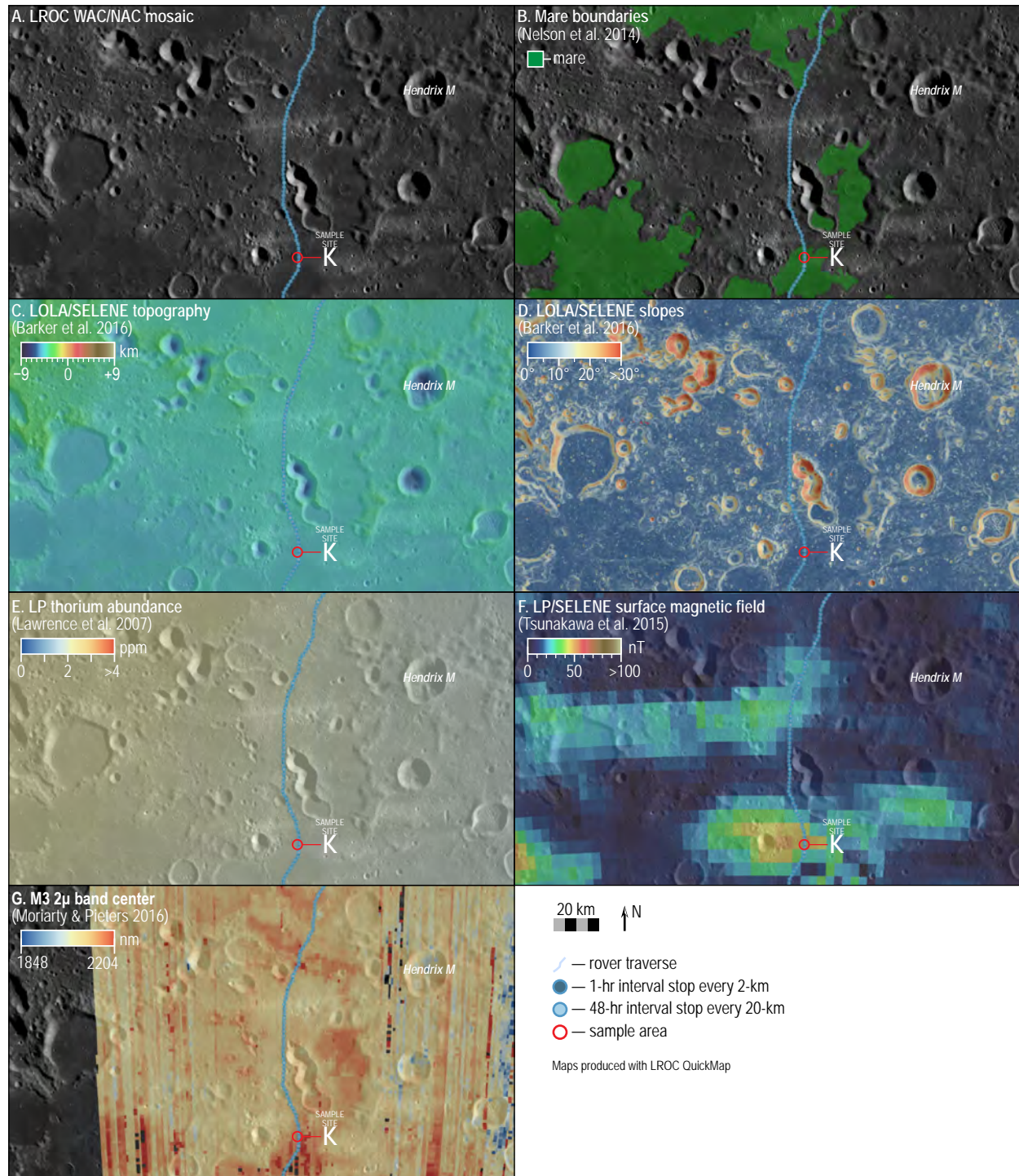


TRAVERSE MAP SET 5: Central SPA, northeast of Bose crater & Bhaba crater



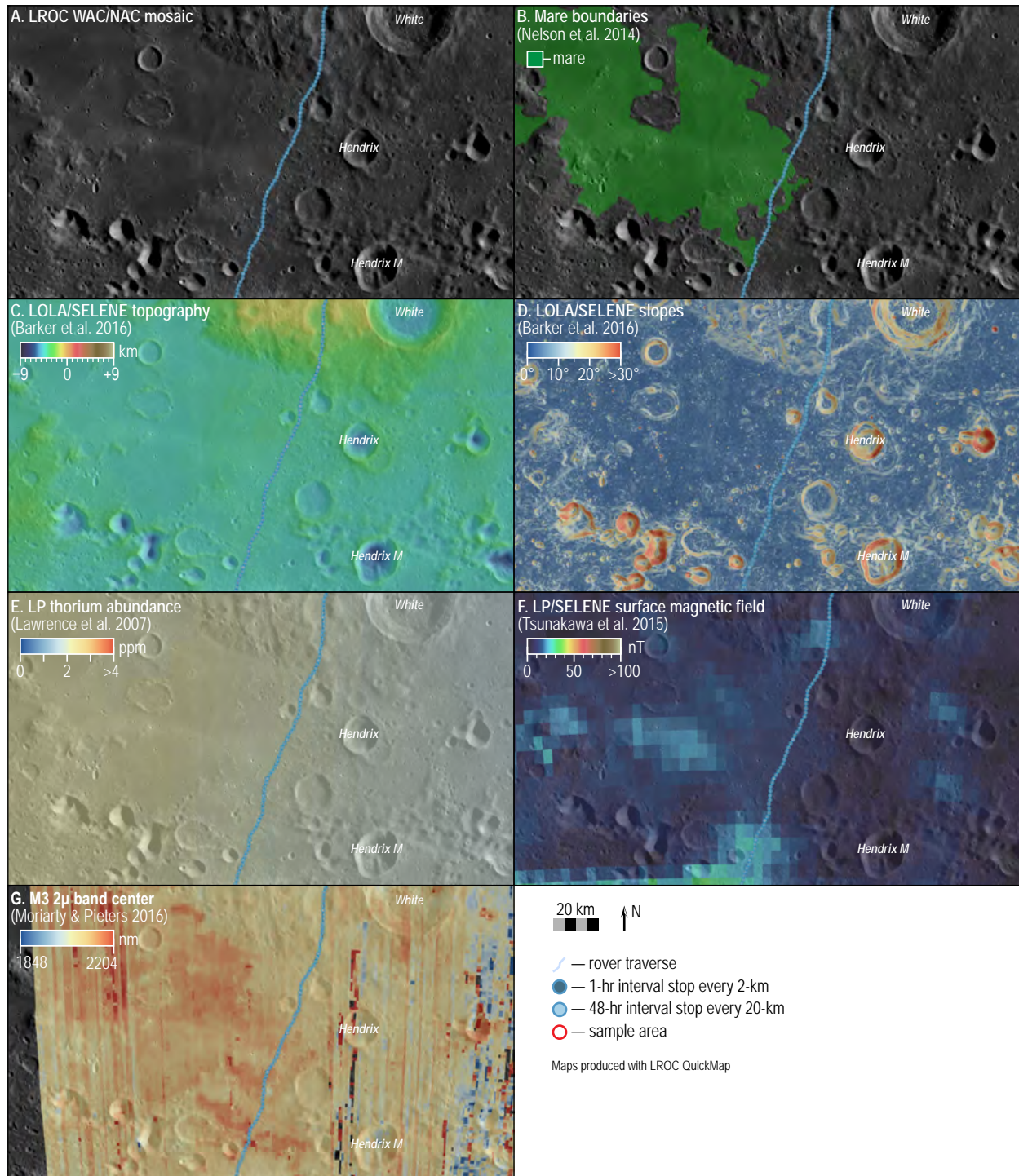


TRAVERSE MAP SET 6: Central SPA, north of Bose crater and Bhaba crater



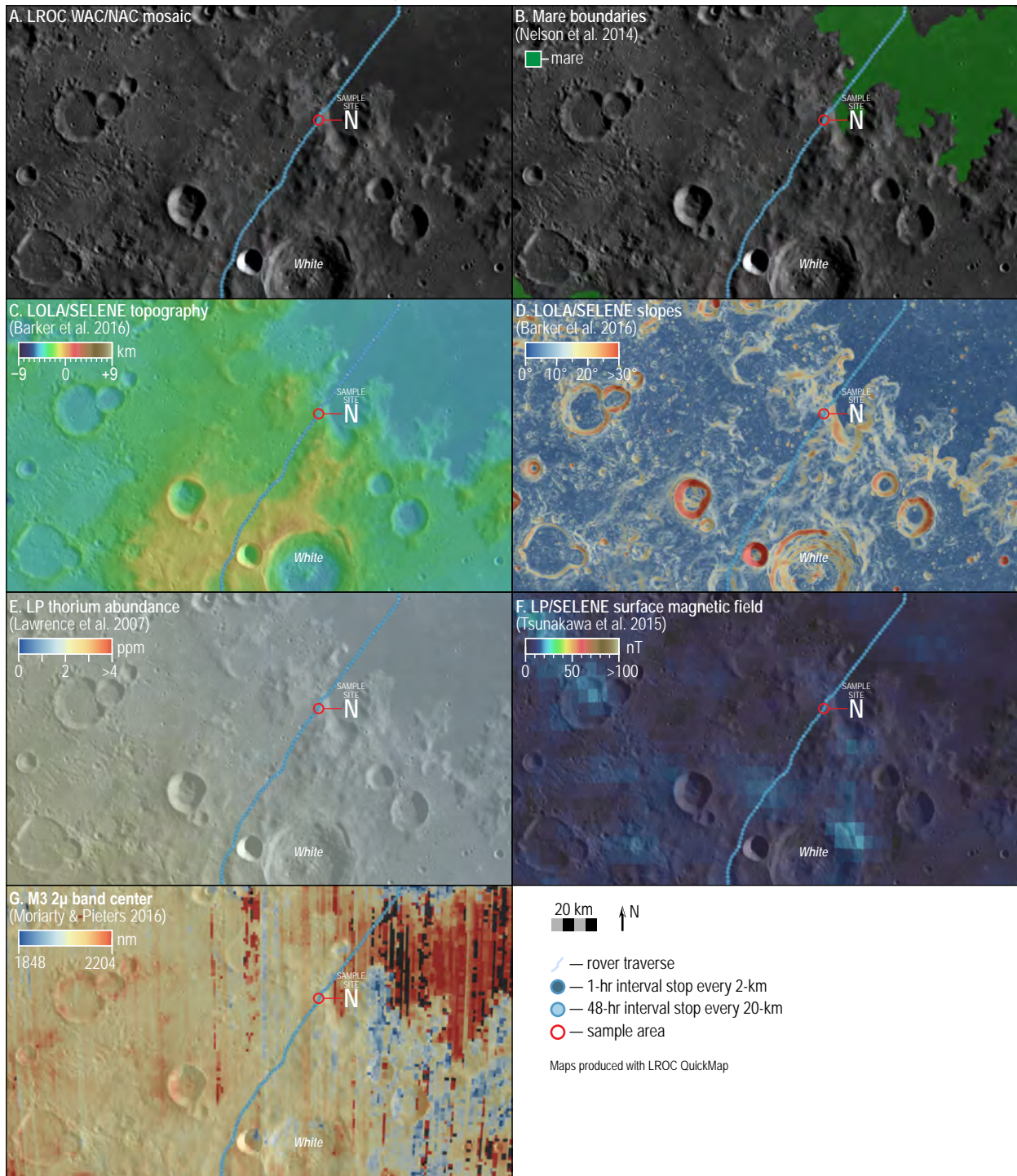


TRAVERSE MAP SET 7: Central SPA, near White crater



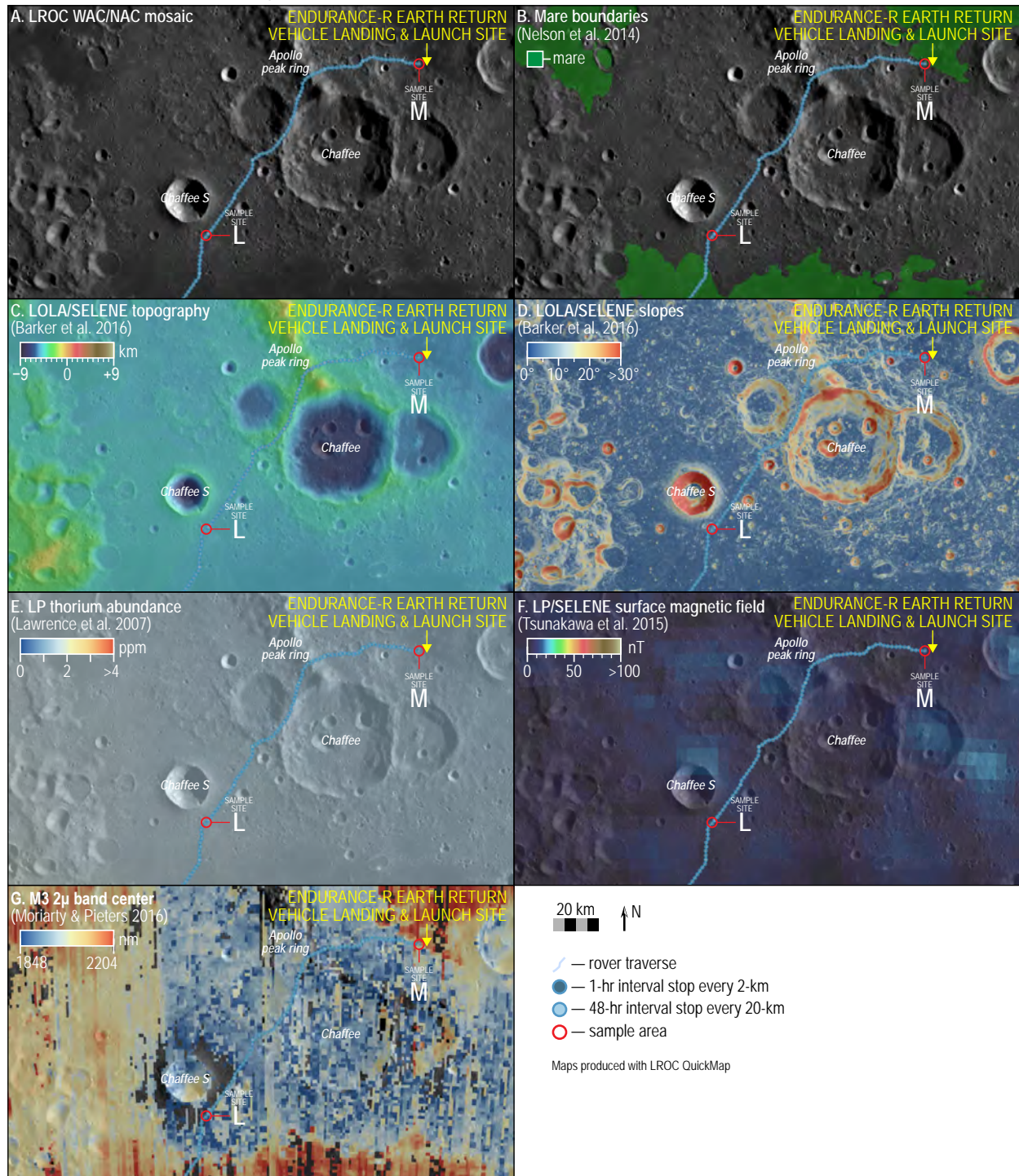


TRAVERSE MAP SET 8: Southwest of Apollo basin



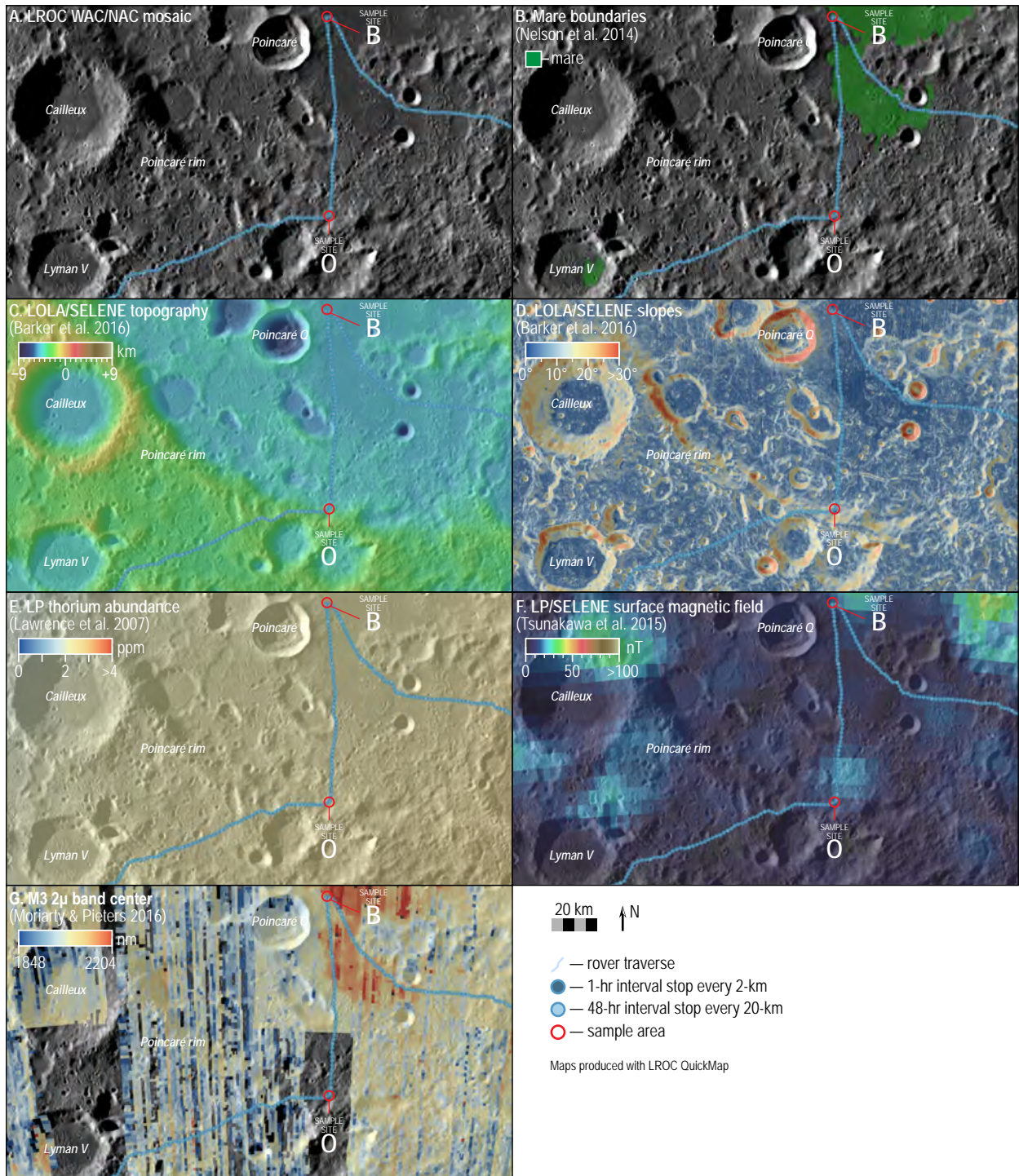


TRAVERSE MAP SET 9: Apollo basin



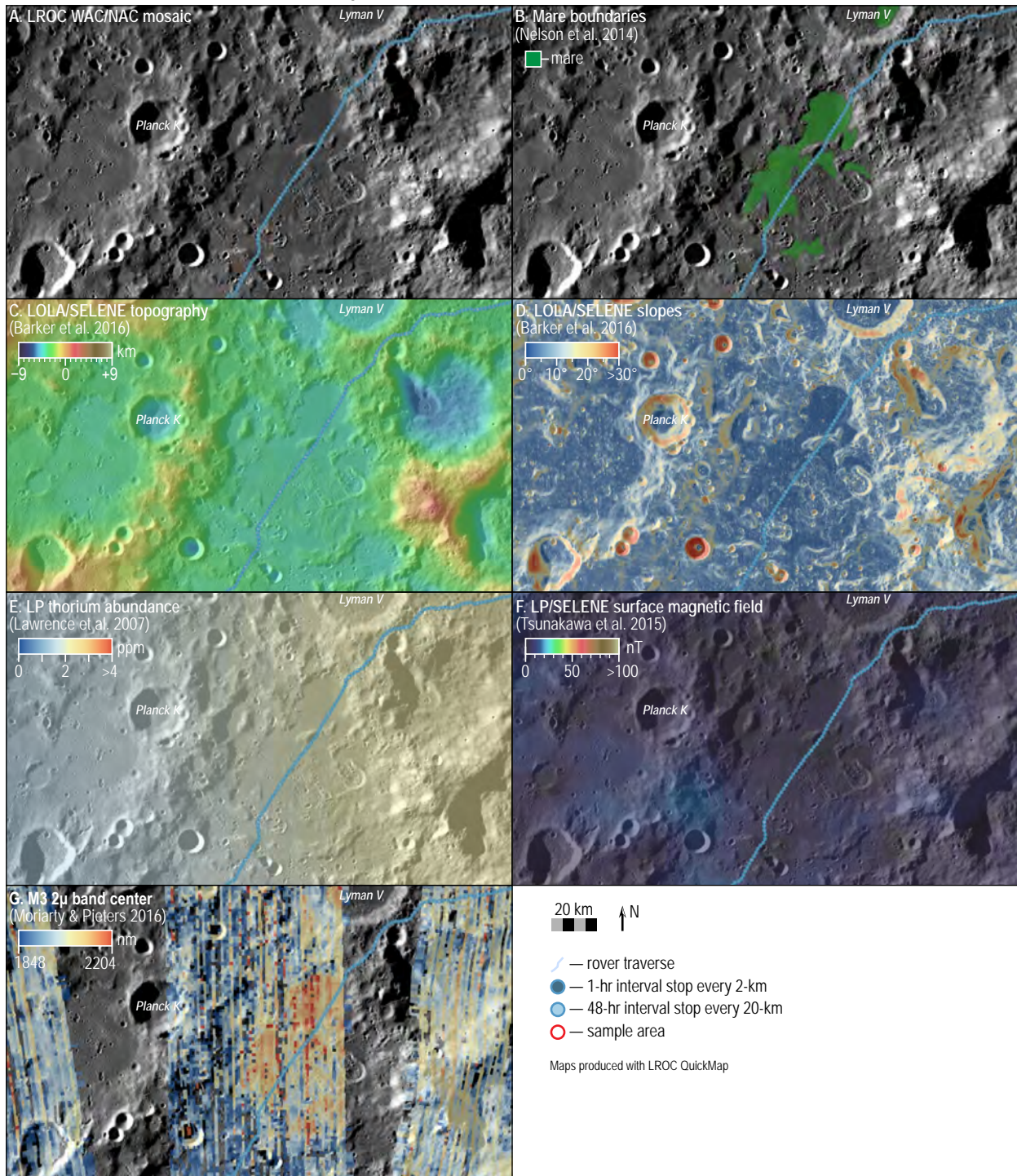


TRAVERSE MAP SET 10: Southern Poincaré basin



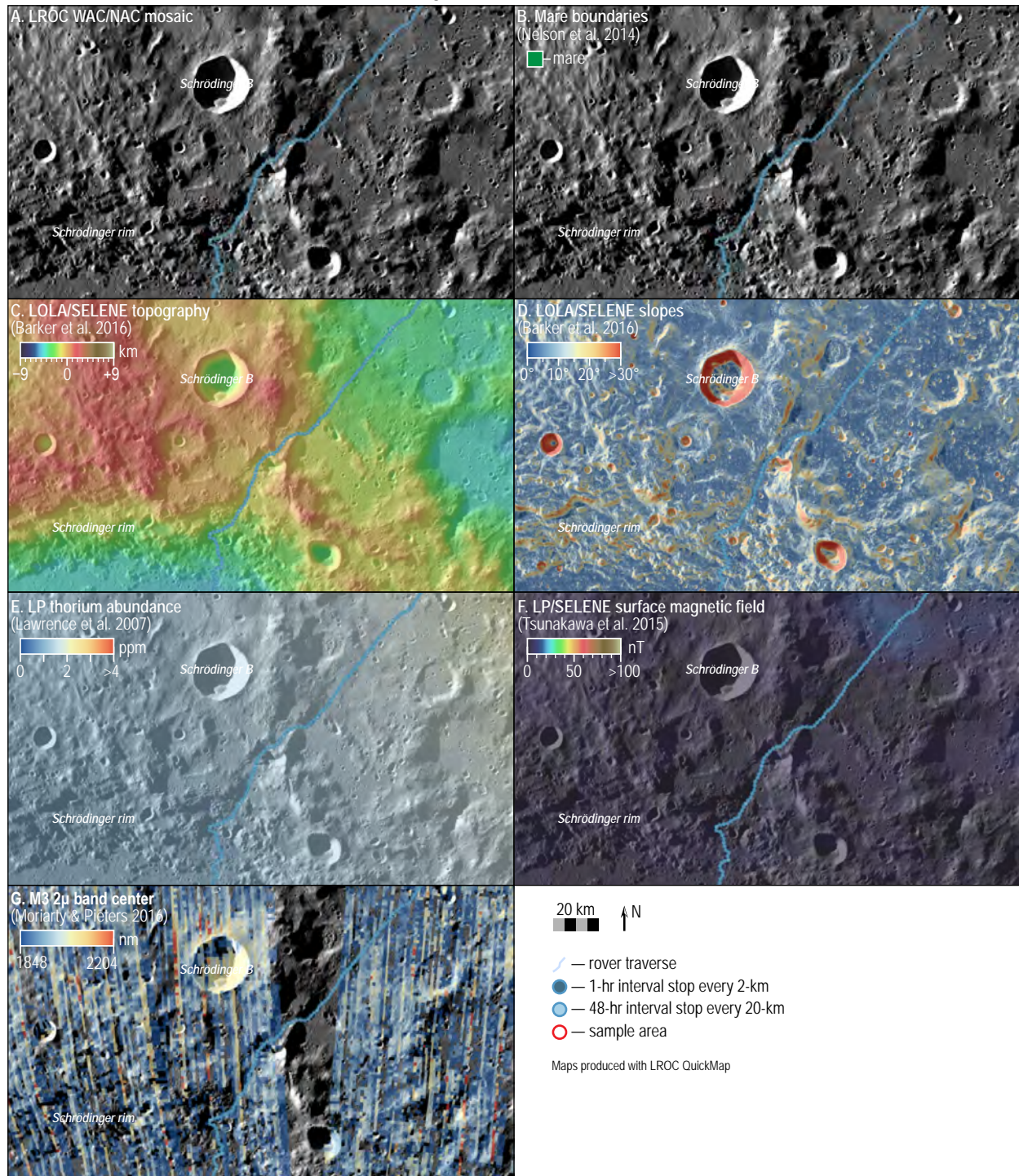


TRAVERSE MAP SET 11: West of Lyman crater



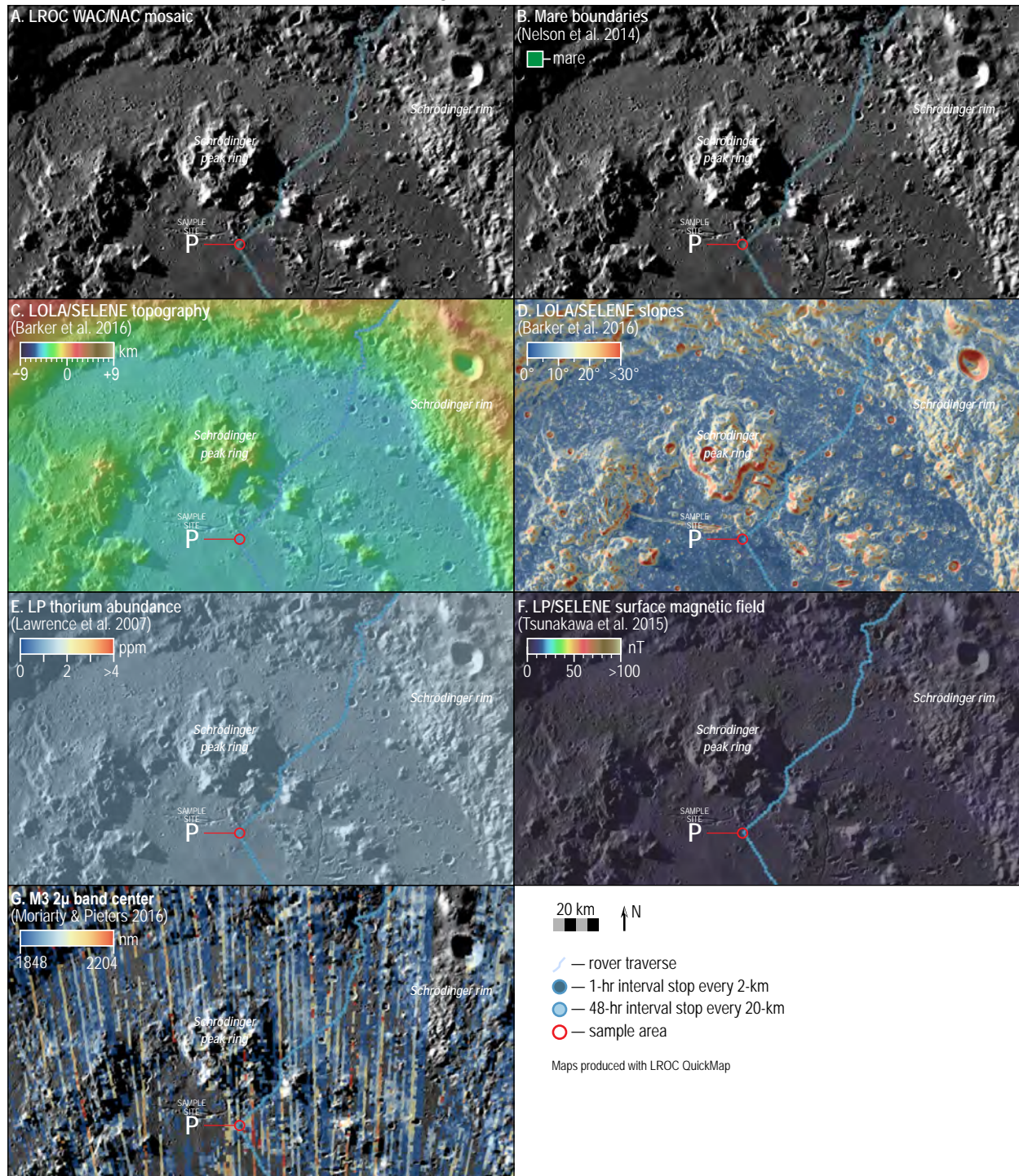


TRAVERSE MAP SET 12: North of Schrödinger basin



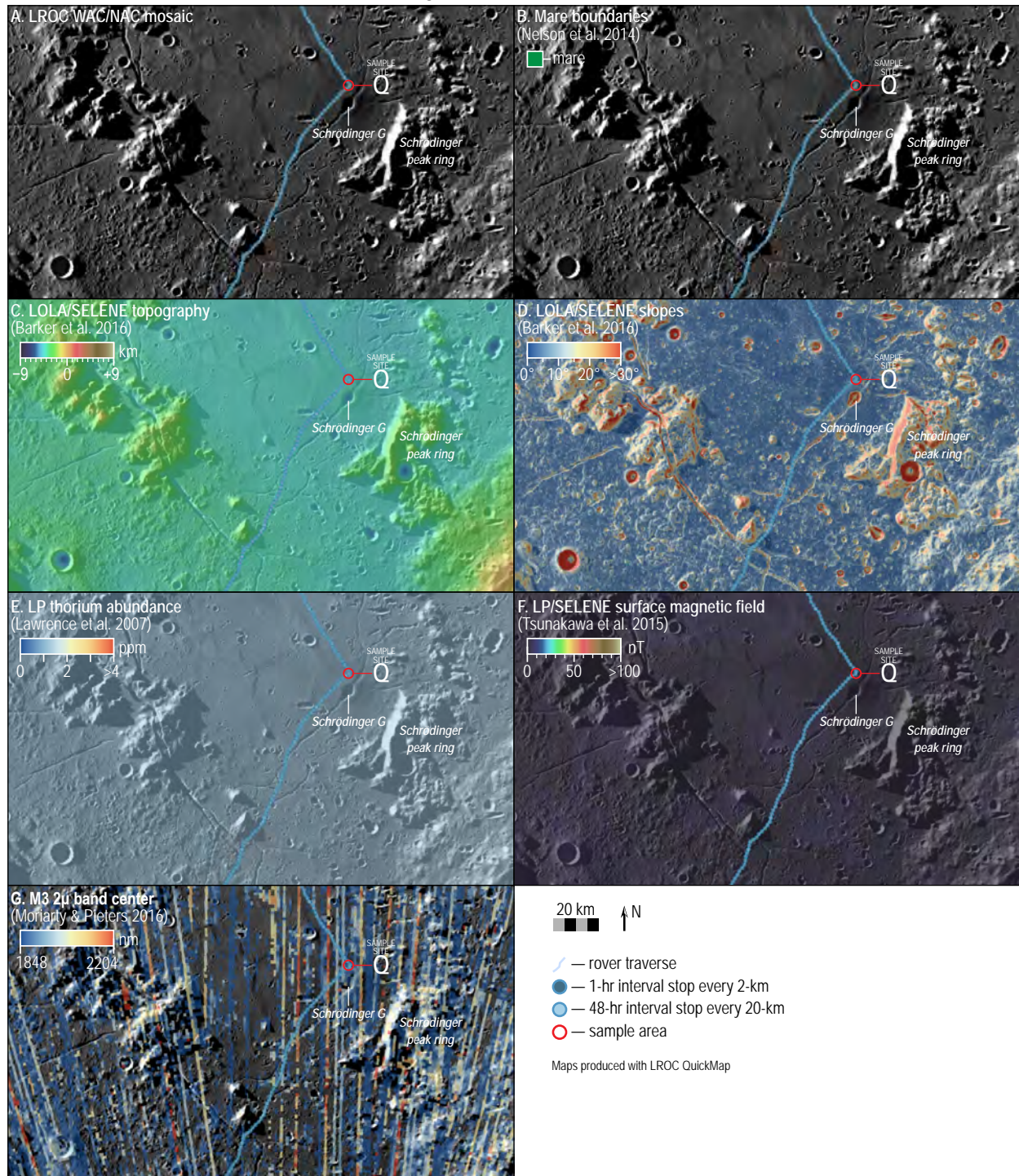


TRAVERSE MAP SET 13: Northern Schrödinger basin



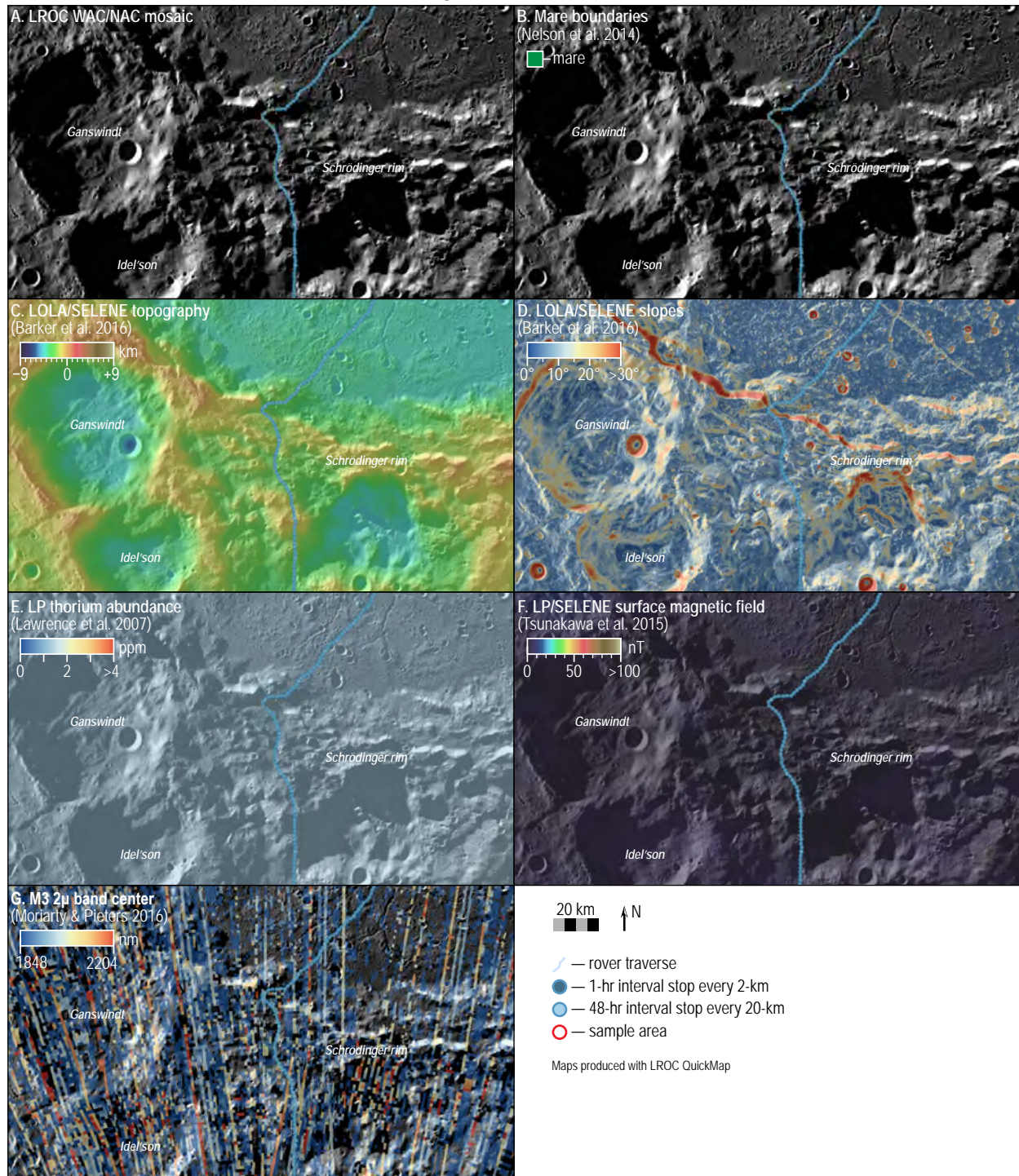


TRAVERSE MAP SET 14: Central Schrödinger basin



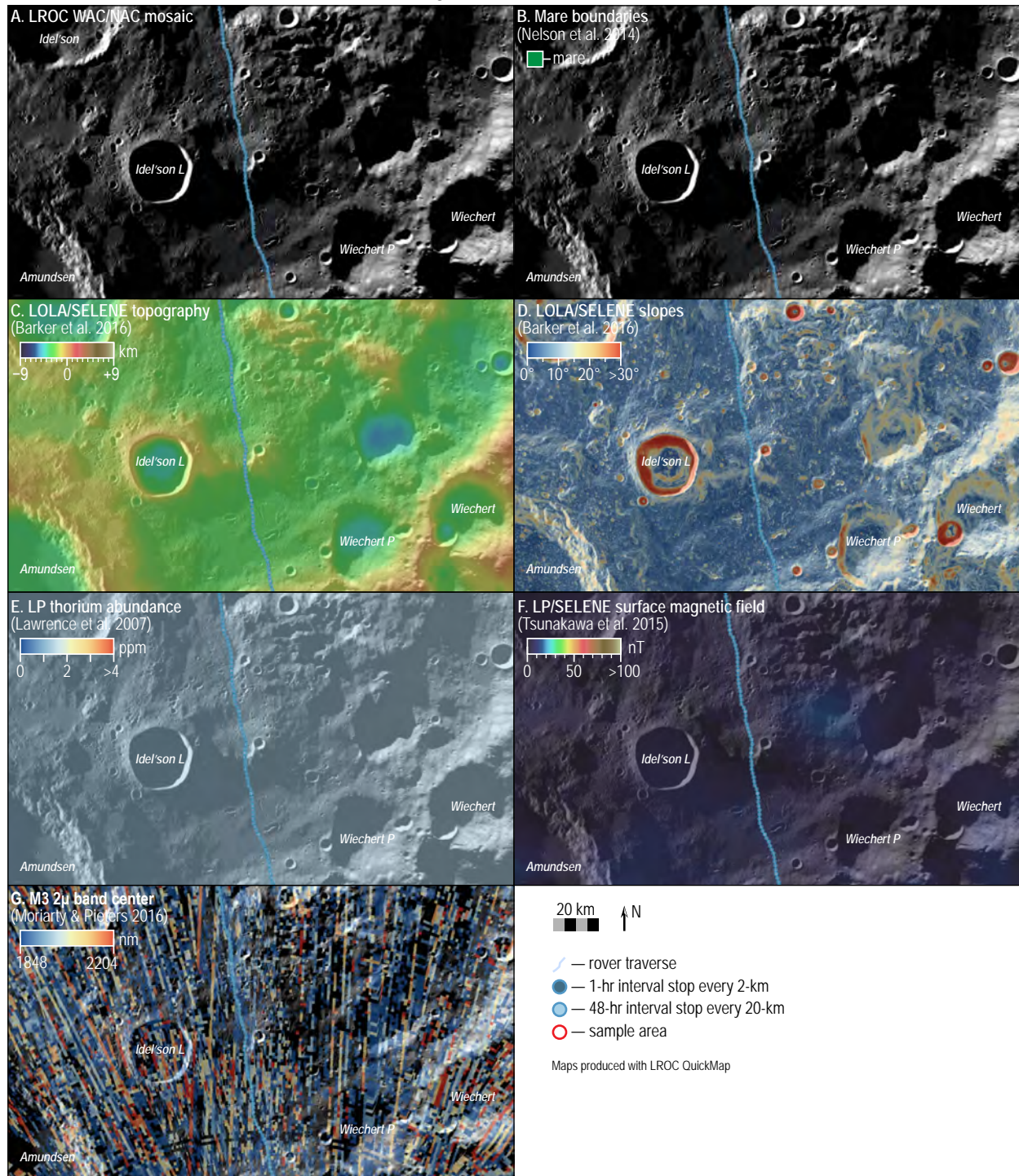


TRAVERSE MAP SET 15: Southern Schrödinger basin



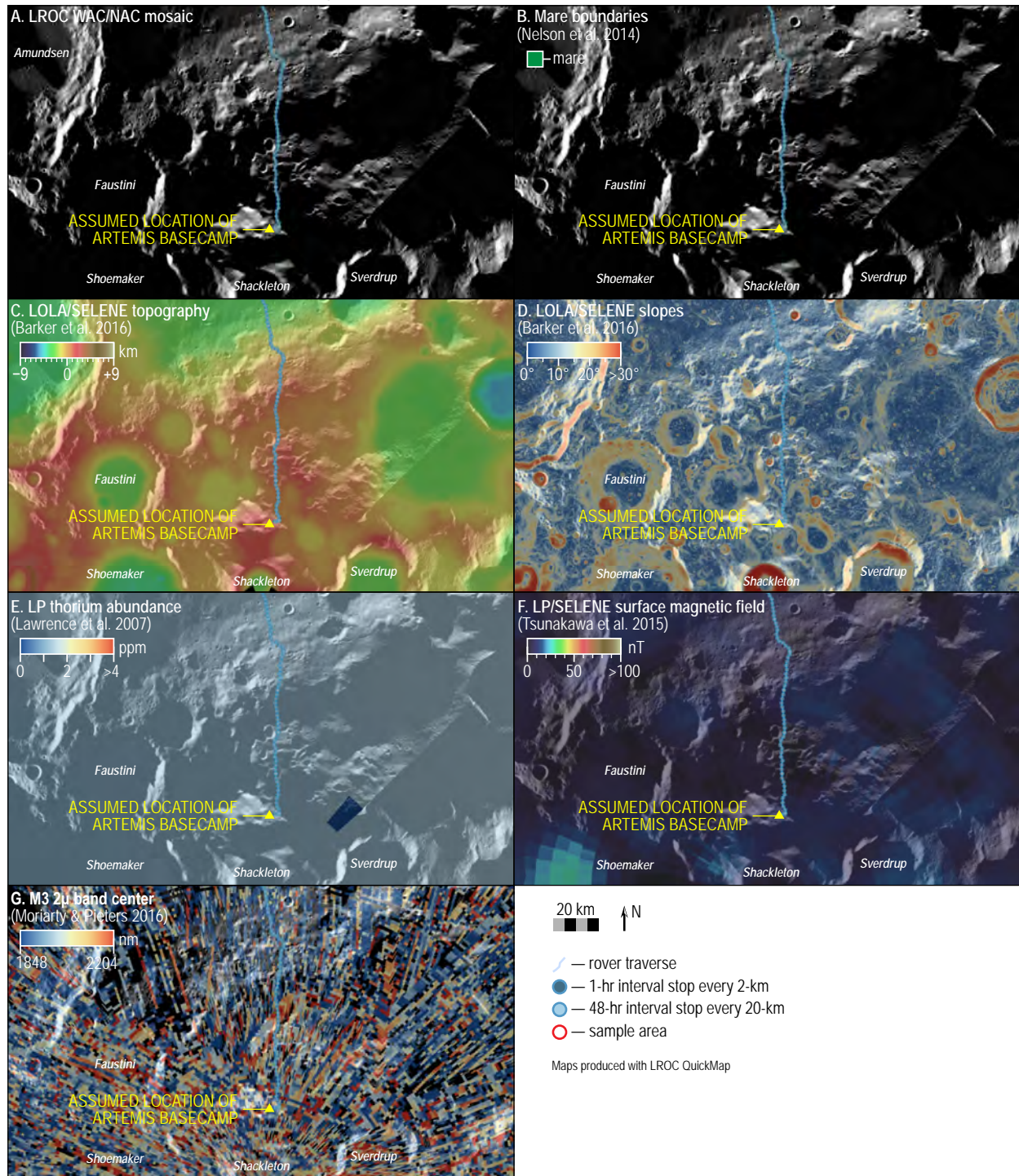


TRAVERSE MAP SET 16: South of Schrödinger basin



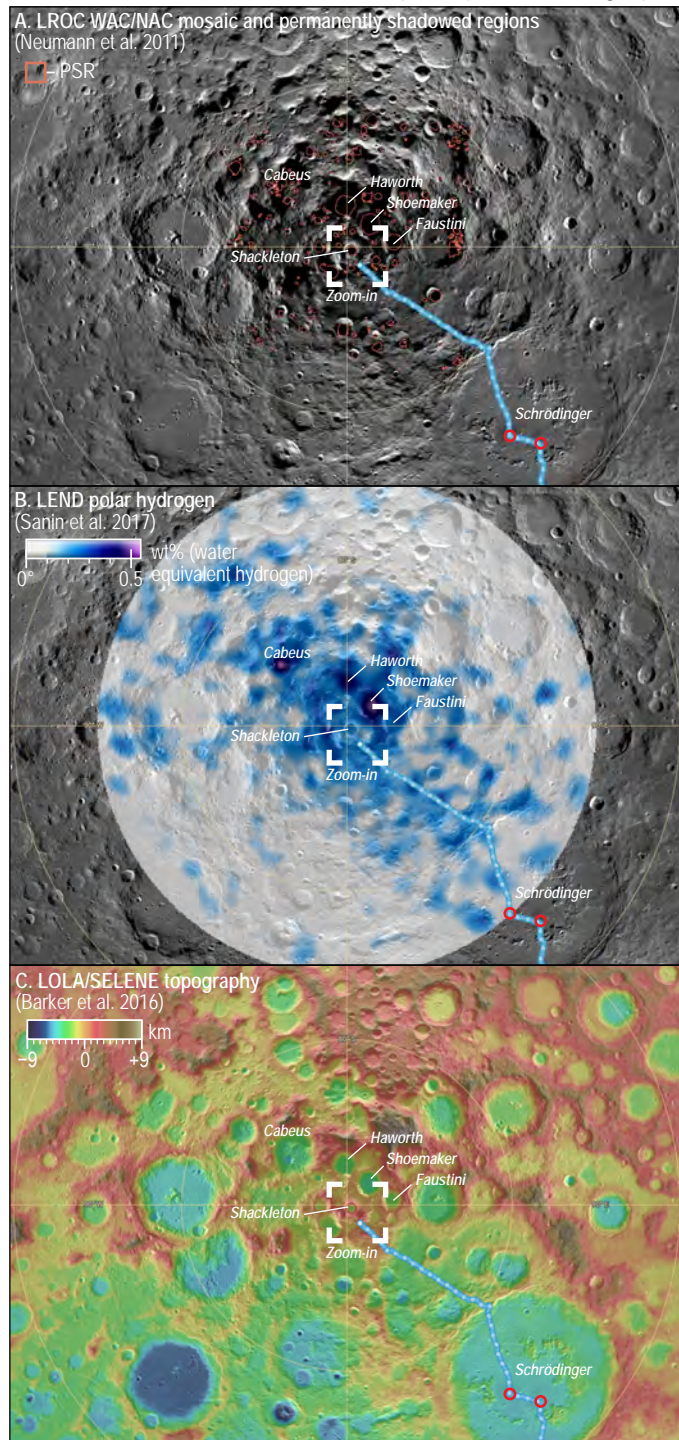


TRAVERSE MAP SET 17: South pole

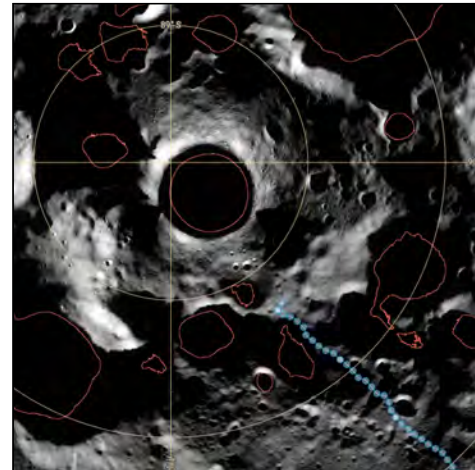




TRAVERSE MAP SET 18: South pole (polar stereographic projection)



D. Zoom-in on the final leg of Endurance-A's traverse



Endurance never drives through a permanently shadowed region.

E. Candidate Artemis south pole landing sites
(NASA's Plan for Sustained Lunar Exploration and Development, 2020)



Figure 5: A South Pole landing site has not been determined, but this image shows sites of interest near permanently shadowed regions, which may contain mission-enhancing volatiles. These sites may also offer long-duration access to sunlight, direct-to-Earth communication, surface slope and roughness that will be less challenging for landers and astronauts.

- rover traverse
- 1-hr interval stop every 2-km
- 48-hr interval stop every 20-km
- sample area

Maps produced with LROC QuickMap



B.2.1 CENTRAL SOUTH POLE–AITKEN

At the heart of the Endurance traverse is the central region of SPA, an area exhibiting a complex geologic history and numerous sites of high scientific interest. Central SPA is a compositionally and geologically diverse region, enabling this segment of the Endurance traverse to address six of eight science goals, including sampling SPA impact melt, low-Th material, young impact crater ejecta, material associated with a magnetic anomaly, and both mare and nonmare volcanic emplacements.

The SPA-basin-forming impact melted staggering volumes of target rock, forming an extensive, thick melt sheet spanning the basin center (e.g., [2]). This material is of high scientific interest, as it records the age of SPA formation in its isotopic systems. However, much of central SPA also exhibits evidence of extensive resurfacing, burying SPA melt rock under volcanic materials up to several km thick [3]. The resurfaced zone in central SPA exhibits various volcanic flows and constructs, numerous buried, flooded, and/or embayed impact structures, and a distinct compositional signature, and has been referred to as the SPA Compositional Anomaly (SPACA) [3, 4]. Fortunately, several large impacts (including Bose and Bhabha) expose SPA impact melt from beneath SPACA resurfacing materials [3, 5, 6]. Sampling site selection for Endurance leverages this geologic and compositional diversity to address multiple science priorities within this region.

Bose and Bhabha craters: Bose (91-km diameter, Site E) and Bhabha (64-km diameter, Sites F+I) are centrally located within SPA. Both craters exhibit compositional distinctions between their walls/rims and central peaks. For both craters, noritic central peak materials are uplifted from depths >5-km, in the heart of the SPA impact melt sheet. Wall/rim materials are excavated from shallow (<~5-km) depths and exhibit mostly gabbroic mineralogies similar to SPACA resurfacing materials. However, certain sections of the walls/rims (Sites E+F) exhibit noritic mineralogies, suggesting excavation from similar strata as their central peaks. These sites are the most accessible confidently identifiable exposures of SPA impact melt sheet material in central SPA. Site I targets more typical gabbroic Bhabha ejecta, which may represent SPACA resurfacing material [3] or upper strata of a differentiated impact melt sheet [7].

Mons Marguerite: Spanning ~70-km and standing ~1-km above the local terrain, the informally named Mons Marguerite (and formerly informally named “mafic mound”; Sites G+H) features a central circular depression with several asymmetric emanating lobes. The structure exhibits a gabbroic mineralogy spectrally distinct from typical mare basalts, exhibiting a higher albedo and Mg content characteristic of SPACA resurfacing materials. Recent analyses of the topography, morphology, mineralogy, and gravity signature of Mons Marguerite indicate that it is a volcanic construct, and is perhaps the single best piece of evidence indicating that SPACA resurfacing materials are a distinct igneous product distinct from typical mare basalts. Mons Marguerite is therefore an important target for understanding the thermal history of the lunar farside as well as the volcanological and geophysical consequences of large basins. Site G targets a small crater on the northeastern slope of Mons Marguerite, which may expose pristine material from within the mound and possibly SPA impact melt from depth. Site H would sample the top of Mons Marguerite.

Other sites: Central SPA hosts several additional sampling opportunities addressing Endurance science priorities. Sites D+J target mare basalt emplacements, while Site K targets a local magnetic anomaly. Samples throughout central SPA exhibit low Th abundances (<3 ppm), and young impact craters are distributed across the region.

B.2.2 POINCARÉ BASIN

Poincaré is a ~340-km diameter, Pre-Nectarian peak-ring basin (e.g., [8]) and one of the oldest large basins within SPA. The basin’s western rim and peak ring are preserved, and sampling these materials would provide access to ancient highlands crust with clear provenance. Its eastern half is superposed by multiple younger craters of 70–100-km diameter that have substantially reworked the material in that part of the basin. Both the central floor of Poincaré and the floors of some of the larger craters on its eastern rim (Poincaré E, Poincaré F) are buried by younger mare basalt (Imbrian; model age ~3.4–3.6 Ga; [9]). Sampling this mare (Sites A+B) would address questions related to the generation



and eruption of basalts, and how volcanism on the farside differed from on the lunar nearside. Site B targets a small crater in the central mare basalts, and samples from this region would likely trace both the mare basalts and the Poincaré impact melt excavated from depth.

Poincaré peak ring material (Site A) is a particularly important target because it has the potential to provide two key geochronology results: an age for Poincaré itself and an age for SPA. This would have widespread implications for lunar science, as well as the impact history of the Solar System, because Poincaré basin's crater density suggests that it is older than any landform on the Moon with a well-established age. Dating its formation would provide a critical test for models of the Late Heavy Bombardment that is hypothesized to have affected not just the Moon, but also the Earth and other bodies in the inner Solar System. Poincaré's peak-ring is expected to contain abundant SPA basin ejecta uplifted during the formation of the peak-ring. Comparing the geochemistry and mineralogy of this peak-ring material with SPA impact melt that Endurance obtained elsewhere would provide additional confidence of obtaining a SPA sample, as well as provide a sample of SPA basin material with different provenance (from the deep crust; 20–30-km depth; e.g. [10]).

B.2.3 APOLLO BASIN

Apollo basin is a ~500-km diameter basin superposed on the northeastern margin of SPA and is the largest post-SPA impact basin (e.g., [2]). Like Poincaré, Apollo is mapped as Pre-Nectarian, although its superposed crater frequency is only slightly higher than the near-side Nectaris basin [8]. The Apollo basin interior has extensive areas of rugged highlands plains exposed in the areas surrounding its peak ring. The crater size-frequency distribution superposed on these rugged plains is consistent with the Apollo basin as a whole [11], supporting the idea that these interior plains are a direct result of Apollo's formation (perhaps the gardened remnant of the basin's impact melt sheet). This provides confidence that samples of the Apollo-forming event should be accessible, enabling determination of an age of Apollo on the basis of the returned samples. A determination of Apollo basin's age would be valuable for similar reasons as an age for Poincaré: it would be a pre-Imbrian data point directly constraining the magnitude of the basin formation rate and impactor flux during the hypothesized Late Heavy Bombardment. Moreover, Apollo's large size makes its superposed crater population statistically robust, helping to calibrate the formation rate for smaller craters ($D \sim 20\text{--}100$ km) as well. Such a determination may also be possible for Poincaré but with lower confidence. Site L would sample material in the outer regions of Poincaré, excavated by the Chaffee S crater—which would likely exhume Poincaré impact melt from depth, while also containing mare basalts. Site M would sample material at the base of Poincaré's peak ring, and from the central mare basalts.

Mare basalt with low titanium abundances and model ages of ~2.3–3.5 Ga [9] are also easily accessible in Apollo, particularly in its central interior (Site M) and southwestern quadrant (Site L). The fraction of the basin surface covered by maria is somewhat less than in Poincaré, but the total volume erupted may have been comparable [12]. Both were likely erupted through very thin crust (<5 km; [13]). Looking at Apollo's mare deposits (Sites L+M) would again enable sample interrogation of important questions related to magmatogenesis, migration, and eruption on the lunar farside.

B.2.4 SCHRÖDINGER BASIN

Schrödinger basin is a ~320-km diameter peak-ring basin near the southwest rim of SPA that has been extensively studied as an exploration site (e.g., [14, 15]). Schrödinger is Imbrian in age and the second-youngest large impact basin on the Moon (pre-dating only Orientale). Basin facies and ejecta are both well-preserved. Key targets for sampling include Schrödinger's impact melt, as well as possible SPA-derived material (ejecta and/or impact melt) in Schrödinger's peak ring (Site P) or southern rim [7, 16]. For geochronology purposes, the precise age for Schrödinger is scientifically interesting, but of less significance than an age for Apollo or Poincaré, as morphology and superposed crater-size frequency distributions indicate that Schrödinger is younger than Imbrium (<3.9-Ga), so it post-dates the unconstrained part of lunar cratering chronology. However, an advantage of any impact materials



returned from Schrödinger is that there will not be ambiguity distinguishing Schrödinger basin materials from those reset by SPA, because the basins bracket the preserved basin-forming era on the Moon, and should be significantly separated in time.

Both mare-style volcanism and pyroclastic vents are found in Schrödinger as well (Site Q). Samples of these eruptive products would provide insight into the source depth of magma, eruption mechanisms, and lunar thermal evolution, as well as how these differ between the nearside and farside regions. The volatile enrichment of the Schrödinger pyroclastic materials is of particular interest for understanding the lunar interior. Additionally, these pyroclastic eruptions may have been a volumetrically significant source of indigenous volatiles to the South Pole (e.g., [17]), so understanding their composition and abundance may have broader implications for understanding the history of volatiles on the Moon.

B.2.5 HIGH-THORIUM ANOMALIES

Across the lunar nearside hemisphere, thorium abundance serves as the chief proxy for a geochemical component in select lunar rocks and breccias known as KREEP—material enriched in potassium (K), rare earth elements (REE), and Phosphorus (P). KREEP material is a secondary melt product derived from the dregs of the primordial global lunar magma ocean that formed ~4.5 Ga. Although KREEP-rich samples have yet to be returned from the lunar farside hemisphere, a broad, crescent-shaped Th-rich region within SPA is hypothesized to be a surface exposure of KREEP excavated during the SPA impact event (e.g., [18]). The identification of samples from the farside Th-rich region within SPA would conclusively determine the degree to which KREEP was excavated by impacts on the lunar farside, in comparison to that of the lunar nearside hemisphere. Additionally, the classification of the Th-rich signature within SPA as KREEP or non-KREEP would provide vital information to constrain the nature, asymmetry, and evolution of the lunar magma ocean and the post-magma-ocean evolution of the Moon. Ultimately, identifying the origin and nature of the thorium-rich signature on the farside hemisphere of the Moon is critical to understanding the earliest stages of planetary evolution and differentiation, and would advance our understanding on the thermal and compositional evolution of planetary interiors. Endurance would sample high-Th material at Abbe M (Site C), which has the highest thorium abundance of any location along Endurance's two traverses.

B.2.6 OTHER DESTINATIONS ON THE SOUTH POLE–AITKEN BASIN TRAVERSE

The Endurance traverse presents the opportunity to conduct a variety of additional science investigations. These other destinations were considered opportunistic targets, did not guide the overall traverse plan.

Magnetic anomalies: The Endurance traverse presents the opportunity to conduct continuous series of surface magnetic field measurements crossing magnetic anomalies in the vicinity of Bhabha and Bose craters. Such measurements, in combination with regolith sample collection from within the anomaly would elucidate the intensity and spatial heterogeneity of lunar crustal fields. This information would help distinguish whether magnetic source bodies are magmatic or impact-related in origin. Magnetometer data, coupled with particle and radiation data from the electrostatic analyzer and ARMAS and spectroscopy data, may also reveal to what extent crustal fields (that are not lunar swirls) can mitigate space weathering of the regolith. Site K would sample material with the highest expected crustal magnetic field along the entire traverse, based on orbital magnetic field data.

Young craters: Over its long traverse, Endurance would pass by countless smaller, younger craters. These smaller craters present an opportunity to both understand impact processes, and to probe material excavated from depth. As a general rule of thumb, the deepest material is excavated from about one-tenth of the diameter of the crater, and is deposited closest to the rim of the resulting crater. By traversing the ejecta blankets of various craters with diameters ranging from meters to kilometers, Endurance would sample underlying stratigraphy, from different times. Samples returned from smaller, younger craters also have the potential to address priority planetary science goals (e.g., [19]). There are multiple lines of evidence suggesting that the impact rate on the Moon has changed over the past 1 billion years, and sample return from younger craters could pin the recent impact flux.



Sample return from a younger crater could pin the recent impact flux. Site N represents on such potential target: a DIVINER-identified fresh crater on the rim of Apollo that is likely less than 1 million years old [20].

B.3 SCIENCE OPERATIONS

B.3.1 ENDURANCE'S SCIENCE INSTRUMENTS

Endurance's instrument suite is summarized in Section 1.7 and Table 1-2. **As stated in the study guidelines (Section 1.3), the Endurance rover incorporates the same suite of nine instruments used in the earlier Intrepid mission concept, and Endurance did not consider an instrument trade.**

Endurance's instruments would provide essential geological context for samples, particularly in the SPA region, of great interest and distinctively different from other regions but previously unvisited. This is true not only on a local scale, in the immediate vicinity of the sampling sites themselves, but on a regional scale along traverses between sampling sites. Endurance's instruments fall into two categories: imaging and spectrometer instruments, and fields and particle instruments. In this section, we provide more details about the science instruments—first starting with the two categories of instruments, and then more detailed information about each instrument. Even more information about these instruments and their capabilities are detailed in the Intrepid mission concept [1].

Summary of Endurance's imaging and spectrometer instruments: The mast-mounted camera system (**TriCam**), which includes a color stereo imager (**stereo cameras**), a monochrome imager (**FarCam**), and a visible/near-infrared point spectrometer (**PS**), would allow photogeological characterization of the surrounding terrain, including its topography and morphology (e.g., the character and distribution of slopes, distinctive impact or volcanic features, and exposed stratigraphy) on scales ranging from kilometers to meters). These data would be collected at Interval Stops every 2-km (within distance to horizon) along the traverse routes. In the immediate vicinity of the rover, when stopped, the camera system would allow determination of the textural character of the surface (variations in color, albedo, and rock distribution) as well as in variations in the compositional character, size, and density of surface rocks, on scales ranging from meters to millimeters. The arm-mounted hand lens imager (**HLLI**), would provide essential context for understanding the nature of the regolith, on the scale of microns to tens of microns, including its size-particle distribution, shapes diagnostic of impact or volcanic events, agglutinate content and age/maturity, mineralogy (from color and cleavage of crystalline rock fragments). Such imaging would also provide essential mineralogical context for understanding the elemental abundance measurements provided by the alpha-particle x-ray spectrometer (**APXS**) and the gamma-ray and neutron spectrometer (**GRNS**), and vice versa. X-ray and gamma-ray derived elemental abundance measurements, from which cation ratios could be derived, would enhance understanding of potential samples origin and history. Neutron derived subsurface proton (volatile) measurements would also provide information on the nature of the subsurface in terms of volatile content. As a whole, these spectrometer and camera measurements would provide a basis for understanding anomalous or systematic variations along a traverse, between or within sampling sites, and their relationship to underlying stratigraphy and their origin, and characterization with the combined spectrometer suite would be crucial for the optimal down selection process.

Summary of Endurance's fields and particle instruments: Endurance's magnetometer (**Mag**) and accelerometer (**Inertial Measurement Unit [IMU]**) provide information on the variations in the underlying regolith and bedrock on a scale of meters to hundreds of kilometers, including its density, structure, depth (when combined with stratigraphy), and origin (via amplitude and direction of associated magnetic fields). The two particle analyzers (**Electrostatic Analyzer [ESA]** and **Automated Radiation Measurements for Aerospace Safety [ARMAS]**), will characterize the flux, energy and angular distribution of the energetic ion flux in two energy regions, representing the lower energy range solar wind and higher energy range galactic cosmic rays. Such measurements will provide an important context for understanding observed variations in space weathering of regolith grains and



rocks resulting from differential exposure to surrounding charged particle environment induced impact feature induced shadowing or by magnetic anomalies.

In the following sections, we describe the individual instruments in more detail.

TriCam: TriCam consists of three cameras mounted side-by-side on the mast, and is capable in pointing in almost any direction. Two Bayer pattern 3-color **stereo cameras** each have a field-of-view (FoV) of 50° horizontal by 37.5° vertical, providing 3D context around the rover while also supporting arm and sample collection, caching, and transfer operations. The stereo cameras have sufficient resolution (instantaneous field-of-view [iFoV]: 2.2×10^{-4} radians) to image sampleable material within the entire arm workspace: down to 0.2-cm rocklets at a range of 2-m (the arm reach), assuming 3-pixels are required to identify a rocklet. **FarCam** [21] is mounted between the two stereo cameras and is an adaptation of the 100-mm focal length Mars Science Laboratory (MSL) MastCam instrument. It is a monochrome imaging system (FoV: $6.7^\circ \times 5.0^\circ$) providing high resolution (5-cm at 1-km) images for geologic context and close-up inspection of landforms the rover cannot access. FarCam also serves as the telescope of the Point Spectrometer; there is a fiber optic pickup on the FarCam focal plane. TriCam shares a common electronics box (commanding, compression, and buffering) with the Hand Lens Imager and Point Spectrometer. All components of TriCam have heritage with various Malin Space Science Systems imaging systems.

PS: The Point Spectrometer provides spectral reflectance in 16 bands across the wavelength range 300–1,400-nm enabling mineralogic abundance estimates (clinopyroxene vs orthopyroxene, spinel, glasses, olivine, shocked plagioclase, and maturity). Spectra would have a spot size of 3-m at 100-m, or 30-cm at 10-m. The fiber optic pickup on the focal plane of FarCam is routed to the detectors in the warm electronics box in the body of the rover. The PS requires the most development of all the instruments, however it is entirely built of high Technology Readiness Level (TRL) components, including the detectors.

GRNS: The Gamma Ray Neutron Spectrometer provides the primary geochemical measurements with integration collected while in motion and when stopped. It returns Si, O, Fe, Mg, K, Al, Ca, Ti, Th abundances to better than 3% (in 6 to 48-hour integrations), and it enables estimates of H abundance to 50-ppm (from neutron absorption). The instrument senses elements throughout the top 30-cm of regolith. The ARMAS provides simultaneous measurements of the Galactic Cosmic Ray environment which improves the GRNS calibration ensuring the 3% absolute accuracy is met.

APXS: The arm mounted Alpha Particle X-ray Spectrometer provides close-up elemental abundances (Si, O, Fe, Mg, K, Al, Ca) to $\leq 3\%$ accuracy in 1-hour integrations, and all elements with atomic numbers between 11 and 40 (Na through Zr) in 4-hours. The APXS requires temperatures $< 0^\circ\text{C}$; a cryocooler would maintain the detector at its operating temperature during most of the day (with some exceptions due to rover position, local topography and time of day). The instrument senses elements in the top 2-cm of the target (regolith or rock) which complements the GRNS measurements which sense the top 30-cm of the target.

HLI: The Hand Lens Imager is mounted on the arm and has active focus and active illumination (for close up targets), providing flexibility to image the surface at 15-micron pixel scale night and day. The pixel scale was selected due to the average grain size of most lunar soils between 45–100 microns [22]. Its Bayer pattern 3-color capability is a powerful tool for investigating color differences known to exist within lunar materials (e.g., [22]).

Mag: The Magnetometer is a dual ring-core triaxial fluxgate instrument that would determine the strength, orientation, polarity and depth of the magnetic field. Mag would measure the intensities and directions of remnant crustal fields over the traverse, and explore questions such as the evolution of the core dynamo (in terms of both intensity and field geometry) and test whether crustal magnetic anomalies are endogenic or exogenic in origin ([23], and references therein).

ESA: The ElectroStatic Analyzer measures ions (200 eV to 20 keV; 9% accuracy) impinging on the surface. Its key role is providing the means to determine the relative importance of solar wind in space weathering processes across the traverse.



ARMAS: The Automated Radiation Measurements for Aerospace Safety records the Total Ionizing Dose (TID) from all sources including heavy ions, alphas, protons, neutrons, electrons, and gamma rays, provided they be energetic enough to deposit at least 60 keV in the sensor and up to 15 MeV. ARMAS would provide critical information regarding the primary and secondary radiation environment, and key information for planning future human exploration of the Moon as well as extending our characterization of the space weathering environment and its effect on surface materials. Additionally, ARMAS would play a significant role in calibrating the GRNS observations.

LRR: The Laser Retro-Reflector is passive, using no power and producing no onboard data. It simply reflects laser shots back to an orbiting spacecraft as part of ranging geophysics experiments, which can also supply precise geographic coordinates of the rover.

IMU: The LN-200S Inertial Measurement Unit is not strictly a science instrument but it allows estimates of the local gravity field, which in turn are used to estimate density contrasts in the subsurface [24]. This capability provides the ability to detect dikes and subsurface voids. For example, a dike that begins at the base of the crust (~30 km depth) and extends to within 0.5 km of the surface, width of 250 m, and a density contrast of 500 kg/m³ (density difference between the upper crust (2550 kg/m³, [13]) and the bulk densities of Apollo lunar basalts (~3010–3247 kg/m³) would produce a gravity anomaly of ~600 mGal. This signal is detectable with margin (IMU/accelerometer performance ~10 mGal).

B.3.2 SCIENCE OPERATIONS AT SAMPLE SITES

The centerpieces of Endurance’s long traverse are the sample sites. Endurance would collect samples containing both regolith and rocklets would be collected from each of 12 sites over the course of its long traverse, aimed at sampling specific geological features, as detailed in Section B.1 and B.2. In this section, we describe the science operations that would occur when Endurance arrives at one of those sampling sites.

At an individual sample site, Endurance would perform a localized survey to identify sampleable material, and if possible, material with appropriate lithologies to address the motivating science. The overall sample site survey strategy is shown in Figure B-3. Sampling sites were selected based on orbital datasets, and are only precisely defined to within ~100-meters at best (comparable to the resolution of M3 compositional data). To further refine our knowledge of the site, Endurance would perform a ~100-m traverse to ~5 pre-selected, candidate sample areas. These areas would be chosen prior to arrival based on orbital datasets, extrapolated to the highest resolution possible (at best: LRO NAC, ~0.5-m/pixel). At each candidate sample area, Endurance would perform two sets of operations in sequence. First, Endurance a 1-hour “Candidate Sample Area Reconnaissance” investigation, which is analogous to an Endurance Interval Stop. This would include ~50-point spectrometer measurements to determine mineralogy, and full-color stereo imaging campaigns to identify material that is sampleable with Endurance’s sample scoop (i.e., appropriate rocklet sizes, abundance of regolith fines, etc.), and 1-hour integrations with APXS and GRNS measurements to determine elemental composition. This data would then be transmitted to Earth, where the ground team would decide which regions in the sample area immediately surrounding the rover merited deeper investigations. Then, Endurance would perform up to three more focused “Candidate Sample Area Survey” investigation, which is analogous to an Endurance Deep Interval Stop. This would more than double the amount of imaging and spectra in that area, and provide 48-hour long integrations with the APXS and GRNS—yielding the elemental composition to much higher precision. The data would be transmitted to Earth and analyzed over the subsequent days to determine the detailed characteristics and sampleability of that area—including analyses to determine if the lithologies and composition are appropriate to address the science motivating samples at that location (Section B.3.3 and B.3.4).

Regolith processing by hypervelocity impacts of varying scales reduces exposed surface rocks to scales that are readily analyzed by rover instrumentation, enabling quick characterization and precluding the need for digging, drilling, or grinding boulders or outcrops and the associated instrumentation required to complete those tasks. Weathering rinds are typically confined to the exterior <100-microns

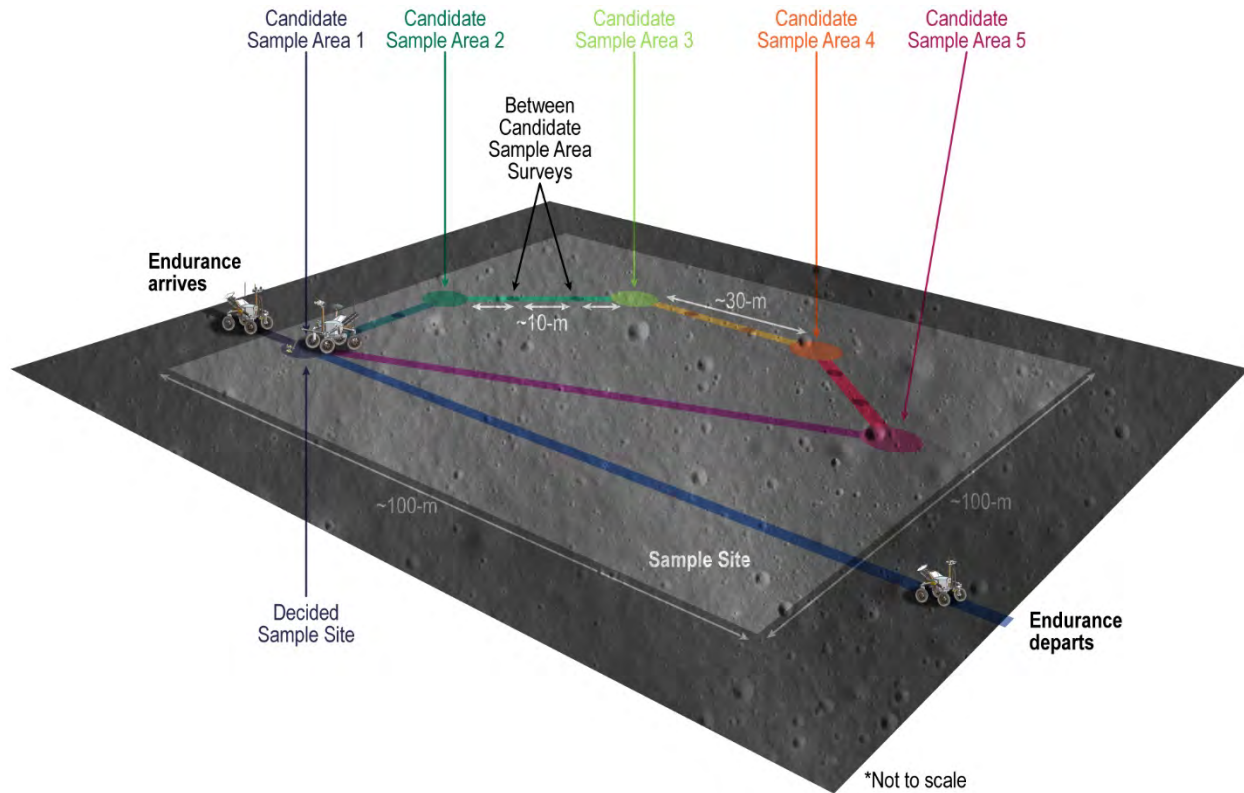


Figure B-3. Endurance concept of operations at a sample site.

of rocks and hence does not alter the bulk chemistry of lunar materials, and thus would not compromise APXS or GRNS measurements would not be compromised [25]. Processing by repeated impacts also facilitates lateral mixing of regolith materials. For example, ~30% of regolith material at a particular spot will be sourced from greater than >10-m of its final location, and >1% will be sourced from distances >10 km [26]. Therefore, an individual scooped sample of regolith and rocklets from each location should in principle capture the targeted rock types in addition to permitting sampling of small amounts of material sourced from farther away.

Upon completing Candidate Sample Area Reconnaissance and Survey, Endurance would move to the next candidate sample area. Between each candidate sampling area, Endurance would perform between-area surveys—stopping every ~10-meters to acquire more images and spectra—both to provide added geologic context and to determine if the optimal sample area is really between pre-defined candidate sample areas.

After surveying all ~5 pre-selected candidate sample areas, the ground team will decide which candidate area will be sampled, and command the rover to head to that location and collect samples. In the schematic illustration in Figure B-3, the rover returns to Candidate Sample Area 1 (now the Decided Sample Area), and collects samples. Sample collection is described in more detail in Section 2.3.2 and Section H.

Based on the operations described here and in Section 2.3.2 and Section H, we estimate that sample site survey would take approximately 170-hours (~7 earth days), and the sample collection activities would take approximately 24-hours. To ensure ample margin, we allocated one full lunar daylight period (14 earth days) to do sampling operations at each sample site. Sample site survey and collection are the only part of the mission where ground is substantially “in the loop,” frequently making decisions about rover operations—although even then, Endurance drives autonomously between areas. (Endurance-R would have ground “in the loop” during sample hand-off to the Earth Return Vehicle.)



B.3.3 TARGET LITHOLOGIES

As detailed in Tables 1-1 and B-1, Endurance is required to collect samples capable of addressing very specific science objectives, including dating SPA and other impact basins, and investigating the thermochemical evolution of the Moon. Not all samples are equally capable of addressing these objectives. For example, a sample of young mare basalt collected in a region where we are trying to date an old impact basin, may not be desired. Thus, Endurance's sample objectives flow down to desired lithologies. In this section, we describe the general lithologies desired for addressing these objectives. In Section B.3.3, we summarize how Endurance's instrument package could be used to identify these lithologies.

Sample the SPA melt sheet (Objective 1.1): This might be the most complicated to evaluate, as there is a great diversity of materials that were melted by the SPA-forming impact and could be good candidates to obtain a radiogenic age for the basin. The impact excavated and melted material over a huge depth range, from the pre-impact target feldspathic crust, the entire crustal column, and a stratified upper mantle (e.g., [2, 3, 18, 27]).

Accessing SPA melt sheet materials offers the highest degree of confidence for measuring the age of SPA, but there are a few complicating factors. SPA likely formed a broad, thick impact melt sheet in the central region of the basin, which may be roughly bound by transient cavity diameter, somewhere between ~800-km and 1,500-km [27]. The impact melt sheet should be thickest and most coherent towards the basin center, and become thinner and more diluted towards the edges [4, 28]. The impact melt sheet may have differentiated due to its enormous thickness [7, 29], or it may have become homogenized through convection [30]. The resulting lithologies in the top few kilometers could vary based on a number of factors, including the bulk composition and degree of differentiation. However, the most likely components are norite, gabbro, and/or pyroxenite [3, 7].

An additional complicating factor is that the central region of SPA (roughly corresponding to the extent of the impact melt sheet) is extensively resurfaced. This region exhibits a distinct gabbroic signature and is known as the South Pole Aitken Compositional Anomaly (SPACA) (Figure 1-3, Figure B-1; [3]). Evidence for resurfacing comes from the widespread nature of filled, embayed, modified, and buried impact craters in this region, and its overall paucity of impact craters [3, 31]. Additionally, a ~70-km feature informally known as Mons Marguerite (also known as Mafic Mound) near the basin center is consistent with a volcanic construction formed from this gabbroic magma [31]. Constraints on the thickness of the SPACA resurfacing deposit as well as the composition of the underlying SPA melt sheet are imposed by the 64-km Bhabha Crater near the basin center. The walls, rim, and proximal ejecta of Bhabha exhibit a gabbroic composition, while the central peak is noritic [3]. Based on crater scaling laws [32, 33], this indicates the gabbroic material is up to ~5-km thick and is underlain by a noritic layer. Five kilometers seems unusually thick for a lunar resurfacing deposit, so perhaps there is a differentiated melt sheet with gabbroic upper strata spectrally similar to the resurfacing material. This is an area of active research. There may be a few ways to tell these units apart: differentiated melt sheet cumulates should exhibit larger grain sizes than extrusive volcanic materials, and melt sheet materials may be enriched in siderophile elements compared to mantle-derived melts, although the magnitude and distribution of this enrichment is unclear.

The most confident sample of SPA impact melt would come from the central peak of a crater such as Bhabha, which almost assuredly uplifted material from the interior of the impact melt sheet. Since central peaks are challenging to access due to the steep slopes on the peak, Endurance focused on sampling noritic material ejected from Bhabha or similar large craters, similar in mineralogy to the noritic central peaks [3, 5, 6]. Bhabha and its neighboring crater, Bose, have noritic exposures around their rims and in their proximal ejecta blankets—making them good candidate for sampling SPA impact melt. The gabbroic material that dominates the wall, rim, and ejecta of Bhabha may also be SPA impact melt, if the melt sheet differentiated to form a gabbroic unit at the top of the cumulate pile. If this is the case, sampling gabbroic ejecta from such craters would also contain SPA impact melt. However, this is not as confident as the norites.



In short, different lithologies across SPACA may correspond to impact melt:

- Norite is most traditionally assumed to be SPA impact melt. Noritic signatures are observed in the central peaks and ejecta blankets of several craters in central SPA (Bose, Bhaba) that are expected to tap into the SPA impact melt sheet.
- Clinopyroxenite or Pyroxenite may represent impact melt if the SPA impact melt sheet differentiated. These materials are unlikely to be found in SPACA resurfacing material.
- Orthopyroxenite may represent impact melt if the impact melt sheet differentiated, but could also be unmelted mantle ejecta.
- Gabbro could represent impact melt if the melt sheet differentiated, although it is difficult to differentiate from SPACA resurfacing material in remote sensing data.

A potentially concerning issue is considering how radiogenic ages may have been reset in these materials by the post-SPA cratering. In terrestrial studies, there is evidence both for and against resetting of radiogenic ages in central peak materials [34, 35]. For Endurance, this will need to be considered further, specifically considering crater and basin ejecta. Both terrestrial analogs and impact models will be helpful.

Sample SPA Ejecta (Objectives 2.1 and 2.2): SPA ejecta and/or ejected melt may also record the age of SPA. This material is present in an annulus surrounding central SPA (Figure 1-3 and Figure B-1; [3, 18]). Immediately outside of SPACA lies the Mg-Pyroxene Annulus, which is dominated by noritic and/or orthopyroxenitic impact melt and/or ejecta [3]. Just outside of this is the Heterogeneous Annulus, which corresponds to a thick blanket of mixed SPA ejecta [18]. Based on its high Th, Fe, Ti, and K content and its gabbro-noritic signature, this material seems to have been excavated from the uppermost mantle near the end of lunar magma ocean crystallization, from a dregs layer sometimes referred to as urKREEP [18].

Radiogenic ages were likely reset in much of this ejected material, although the extent to which this happened is unclear. However, these areas do offer a potential advantage, in that they underwent a significantly lower degree of volcanic resurfacing than the central SPA melt sheet. It is therefore less confident that any individual sample was reset by SPA formation, but somewhat more confident that it might not have been reset by a later impact, depending on the geologic setting.

Sample a large, pre-Imbrian impact basin (Objective 1.2): Relevant Poincaré material (Sites A+B) exhibits a noritic composition, although it is reasonable that impact melts could also include low-Ca pyroxenite and/or anorthositic norite. Relevant Apollo materials should exhibit similar compositional properties, with perhaps lower mafic content.

Sample a volcanic feature (Objectives 1.3, 2.1, and 2.2): This is a fairly broad category that could be satisfied by a number of different materials. (1) Mare basalts are characterized by basaltic mineralogy, low albedo, grain sizes and crystallization textures consistent with extrusive magmatism, and elevated iron and sometimes titanium abundances. (2) Pyroclastic volcanic deposits are characterized by broad, long-wavelength 1-micron band, and bead-like texture. (3) Non-Mare volcanic deposits are characterized by gabbroic mineralogy, intermediate albedo, grain sizes and crystallization textures consistent with extrusive magmatism, and elevated iron and low titanium abundances.

Sample a high-Thorium region (Objective 2.1 and 2.2): High-Th materials across SPA seem to be associated with a specific mineralogy, specifically anorthositic gabbro-norite. These materials are also associated with elevated Ti, K, and Fe. It is possible that the anorthite content is due to mixing between anorthosite and gabbro-norite below the scale of remote sensing data. But the defining characteristic will be Th content, which might be higher in individual samples than the regional character measured in remote sensing data.

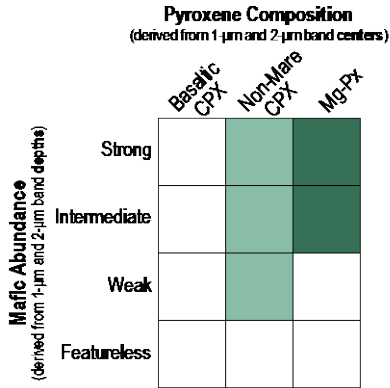
B.3.4 IDENTIFYING TARGET LITHOLOGIES WITH SPECTROSCOPY

Endurance's instrument suite (Section 1.7) is well-suited for identifying lithologies of lunar materials. In particular, Endurance's point spectrometer (PS) is ideally suited for determining target composition, following the generalized SPA material classification scheme by [3]. This scheme separates materials

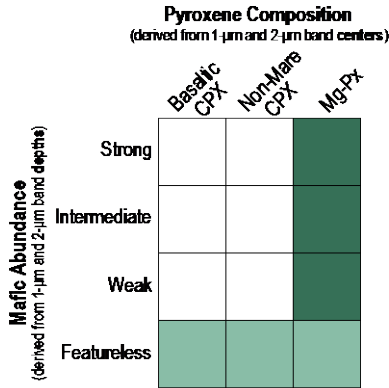


based on spectral characteristics in continuum-removed spectra, including estimated band depths (EBD, tracing mafic abundance) and estimated band centers (EBC, tracing pyroxene composition). Figure B-4 shows how these classification schemes map to target lithologies described in Section B.3.2.

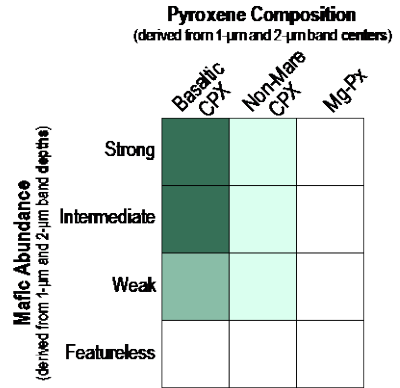
A. Spectral assessment for samples of SPA impact melt
(Objective 1.1)



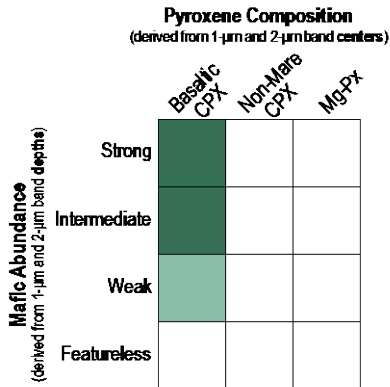
B. Spectral assessment for samples from a large, pre-Imbrian impact basin
(Objective 1.2)



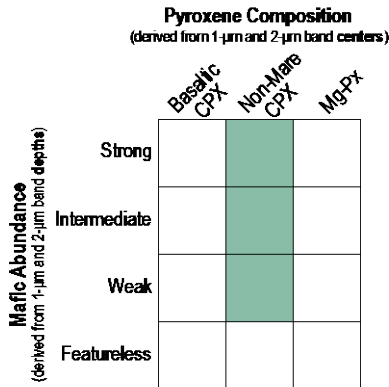
C. Spectral assessment for samples from a volcanic feature
(Objectives 1.3, 2.1, 2.2)



D. Spectral assessment for samples from a mare basalt
(Objective 1.3, 2.1, 2.2)



E. Spectral assessment for samples from a high-Th region
(Objective 2.1)



F. Spectral assessment for samples from a low-Th region
(Objective 2.2)

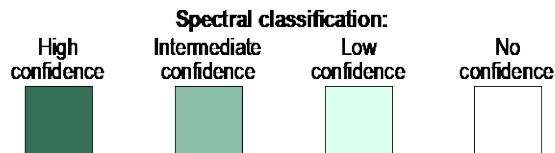
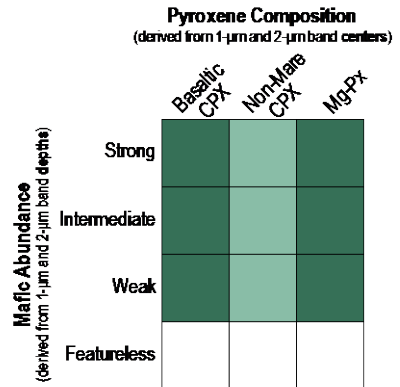


Figure B-4. Spectral assessment of target lithologies in SPA, based on the [3].

Band depth classes (mafic abundance):

- **Strong:** (EBD2 > ~0.1) Optically immature pyroxene-dominated materials. These exposures are mostly confined to central SPA and are associated with fresh craters and highly sloped surfaces such as crater walls and central peaks. These materials represent the freshest exposures of pyroxene-dominated materials in SPA.
- **Intermediate:** (EBD2 > ~0.05) Relatively optically mature pyroxene-dominated materials. These materials are pervasive throughout the SPA interior and appear to represent pyroxene-rich soils and older, degraded crater structures.



- **Weak:** ($EBD2 < \sim 0.05$): Mixed mafic/feldspathic materials. These materials are prevalent in the outer reaches of the SPA interior and probably represent feldspathic materials with a small but nonzero mafic component, likely the result of mixing between mafic and feldspathic materials.
- **Featureless:** ($EBD2 \sim 0$) Highly feldspathic materials. These materials exhibit no detectible mafic minerals and appear highly feldspathic in nature. They are common throughout the rim and exterior of SPA.

Band Center Classes (pyroxene composition):

- **Basaltic clinopyroxene (B-CPx):** Materials with 1- μm band centers $>980\text{-nm}$ and 2- μm band centers $>2,100\text{-nm}$. Most exposures of these materials also exhibit relatively low reflectance in M^3 data. Mare basalts in SPA exhibit similar band centers to nearside mare and basaltic samples, indicating similar average pyroxene compositions. Through laboratory analysis of returned samples, the average pyroxene compositions of mare materials are fairly well defined, although individual pyroxene components span a wide range of compositions [36]. SPA mare exhibit a very similar range in band centers as the nearside mare and basaltic samples, and therefore have a very similar range of average pyroxene compositions. Therefore, we interpret the dominant mafic mineral in SPA mare to be clinopyroxene, similar to the basaltic lunar samples.
- **Nonmare high-Ca/Fe pyroxene (NM-HCP):** Materials with 1 μm band centers $>960\text{-nm}$ and 2- μm band centers $>2,050\text{-nm}$. NM-HCP pyroxenes are the dominant mafic component of SPACA surface materials. SPACA materials exhibit somewhat shorter-wavelength band centers than mare basalts, but with some overlap in the distributions. Performing Welch's unequal variance t-test on the 1- μm band centers for SPACA materials and SPA mare basalts results in a P value of less than 0.0001, indicating that the difference in band centers for these materials is highly statistically significant. The somewhat shorter-wavelength band centers imply that the range of NM-HCP pyroxene compositions is somewhat lower in average Ca (or Fe) content than B-CPx. In the pyroxene composition quadrilateral of Figure 8c, the range in average pyroxene compositions for SPACA NM-HCP materials is therefore inferred to be slightly below and/or to the left of the B-CPx range (representing slightly lower Ca/Fe content). Furthermore, the NM-HCP materials are significantly brighter than B-CPx materials (Figure 6), indicating an overall different mineralogy. The petrological character and origin of these unusual NM-HCP materials are uncertain, and they likely represent either (1) a mixture of B-CPx compositions, Mg-pyroxenes, and other crustal materials or (2) a distinct igneous rock type [31, 37].
- **Mg-rich pyroxene (Mg-Px):** These nonmare materials appear blue/purple in Figure 5, indicating 1 μm band centers $<960\text{ nm}$ and 2 μm band centers $<2,050\text{ nm}$. Mg-Px materials are pervasive throughout the Mg-pyroxene annulus and appear locally within the heterogeneous annulus and within several central peaks across SPACA. Due to their average short-wavelength band centers, Mg-Px materials are inferred to be dominated by Mg-rich pigeonites and orthopyroxenes. The most likely range of average pyroxene compositions is significantly below and to the left of the mare basalt range in Figure 8c, shifted toward the Mg end-member.

Mg-Px includes a range of mineralogies and can probably be further broken down into two classes, based on Mg# (See the distinction between the central peaks of Finsen, Bhabha, and Lyman in [5] and some of the crater analyses from [3]). Some further work needs to be done to better understand these differences, but in general it seems like Mg-Px materials exhibit lower Mg# with increasing distance from the basin center, perhaps reflecting a transition between impact melt sheet materials and upper mantle/lower crust ejecta and/or quenched melt. But this probably won't be a relevant distinction for any of our sample requirements.

B-CPX and NM-CPX overlap a bit, but can be differentiated by albedo. B-CPX typically exhibits lower albedo than NM-CPX.

B.4 SAMPLE SCIENCE

The overarching goals of the Endurance mission are to: (1) establish a more accurate solar system chronology and (2) to elucidate long-term planetary evolution. In this section, we describe sample



collection requirements and the nature of associated sample investigations that would be conducted in Earth-based labs in pursuit of those goals.

The first objective requires radiometric dating of impact melt-containing rocks and ejecta from SPA, younger basins and smaller craters, and rocks of magmatic origin (i.e., lunar crustal rocks, basalts, and pyroclastic deposits). While in situ radiometric dating, mineralogy, and geochemistry analyses of planetary crustal rocks are possible [38, 39], analyses in Earth-based laboratories can achieve much higher precision than currently yielded by in-situ instruments. Detailed sample characterization to assign accurate lithologies to samples and determine mineral compositions and abundances prior to dating samples can ensure that the best possible specimens are selected for radiometric dating. Earth-based studies also enable reproducibility by use of various geochronometers (e.g., U-Pb, Pb-Pb, $^{40}\text{Ar}/^{39}\text{Ar}$, Rb-Sr, Sm-Nd, and Lu-Hf) to obtain multiple ages for an individual sample. Furthermore, recently developed methods such as laser probe analysis may be used to study heterogeneities in ages recorded within a single rock sample that may result from exposure to multiple impact events over lunar history [40]. As summarized in Table B-2, multiple rock types are needed for different geochronology studies. For example, U-Pb and Pb-Pb dating require sifting through $\sim 40\text{-g}$ of regolith to obtain the necessary number of zircons for statistically significant results [41], while the remaining methods require preparation of subsamples from initially intact rocklets.

Endurance would also facilitate understanding of long-term planetary evolution by collecting components of primary crust (e.g., magma ocean crystallization products) and secondary crust (mantle-derived materials and volcanic rocks such as basalts and pyroclastic deposits). Sampling these sites will answer questions such as to what degree igneous materials on the lunar farside differ from those collected by Apollo on the nearside, and may also reveal how the compositions and petrogenesis of magmatic products have evolved over geologic time. Most detailed petrographic characterization studies (e.g., optical microscopy, SEM, electron microprobe) require study of $>4\text{-mm}$ rocklets to ensure intra-sample heterogeneity is appropriately characterized [42]. Trace element and isotopic (i.e., mass spectrometer) measurements required for studying the geochemical evolution of the lunar crust and interior may require specimen preparation from either rocklets or regolith fragments, depending on the specific methods used.

Measurement of physical properties such as density, porosity, rock magnetism, and paleomagnetism typically require larger ($>1\text{-cm}$ diameter) samples. However, collection of such samples by Endurance would permit research into several secondary objectives tied to lunar geophysics. Density and porosity measurements of lunar materials are needed for correct application of gravity data to understand the nature of the lunar lithosphere [43]. Magnetic measurements may be used to understand the paleointensity history of the lunar dynamo, which reflects the thermal evolution of the Moon [23]. Rock magnetic properties characterization can also be used to study space weathering products (i.e., nanophase iron formation) and identify lithologies that may be responsible for producing strong crustal magnetic anomalies like those observed near Bhabha crater (e.g., Sample Site K).

Based on our science objectives and current laboratory capabilities (Table B-2) we developed the sample requirements for Endurance. Our primary science investigations focus on exploring solar system chronology and planetary evolution via laboratory analyses of returned lunar samples. The required analyses would involve petrographic observations, mineral identification, isotope geochemistry, and age determinations using a variety of geochronometers. Many of these analyses (petrographic studies in particular) require intact $>4\text{-mm}$ diameter rocklets to account for intra-sample heterogeneity, while other analyses may be conducted on unsieved regolith or from rocklet mineral separates. Noting that multiple nondestructive analyses can often be conducted on an individual rocklet sample, we estimated that our range of proposed analyses would require ~ 20 rocklets of $0.5\text{--}2.0\text{-cm}$ in diameter. Assuming a rocklet diameter of 0.5-cm and a bulk density of $3\text{-g}/\text{cm}^3$ translates to a rocklet mass requirement of 31.4-g per sample site. Allocating an additional 18.6-g of mass for unsieved regolith for other analyses and placing a requirement that 75% of the total mass would be preserved for future analyses results in a threshold requirement of 200-g of material per sample site. For the baseline requirement of 12 sample sites, this results in a total returned mass of 2.4-kg (1.2-kg for the threshold

requirement of 6 sample sites). This returned mass is consistent with past lunar sample return goals (e.g., the Moonrise concept aimed to return ~1-kg; [42]) and current asteroid sample return efforts (e.g., the threshold requirement of 60-g from (101955) Bennu from OSIRIS-REx; [44]).

The Endurance-A option would return ~100 kg of lunar samples from SPA, permitting scientific investigations of a scale comparable to that of a single large Apollo mission (e.g., Apollo 17 returned 110 kg of lunar materials). This would permit analyses of more material to address the core Endurance mission science goals, increasing the statistical robustness of obtained results. The additional mass facilitated by Artemis sample return would also allow material to be studied to address science questions that transcend the stated mission goals. Because $\geq 75\%$ by mass of returned materials would be preserved in a pristine state after the initial mission-oriented studies, a ~100 kg sample return would ensure that enough material will remain for future investigators, some of whom have not yet been born, and who could pursue novel science questions or employ analytical techniques yet to be developed.



Table B-2. Summary of potential sample-based investigations to be conducted in Earth-based laboratories to address the primary (Table A) and secondary (Table B) science goals for the Endurance mission concept. Columns 1-3 describe broader science themes, analytical categories, and the scientific motivation for each approach. Columns 4-5 detail specific proposed laboratory measurements and their associated sampling requirements. Columns 6-8 further specify the targeted sample types (regolith vs. rocklets), required masses, and a recommended number of discrete analyses to be conducted for an individual sampling site. Columns 9-11 designate whether a given analysis is nondestructive (materials may be reused) or destructive (materials cannot be reused by subsequent investigators for other analyses) and provide constraints on the amount of mass that could be either reused or destroyed. Column 12 details the desired outcomes and, if applicable, the precision level for each measurement. References providing an example of each type of lunar sample science study are provided in column 13.

TABLE A. PRIMARY SAMPLE SCIENCE INVESTIGATIONS

SCIENCE THEME:	ANALYTICAL CATEGORY:	SCIENTIFIC MOTIVATION	ANALYTICAL APPROACH:	SAMPLE REQUIREMENTS:	Does the analysis require regolith rocklets (diameter > 4-mm), regolith fines, or either?	Mass required per analysis (g):	Number of discrete analyses required per sampling site:	Is the analysis destructive (i.e., does this analysis prevent other analyses)?	SAMPLE MASS REQUIRED PER SITE FOR NON-DESTRUCTIVE ANALYSES:	SAMPLE MASS REQUIRED PER SITE FOR DESTRUCTIVE ANALYSES:	ANTICIPATED MEASUREMENT & PRECISION:	REFERENCES:	
1: SOLAR SYSTEM CHRONOLOGY	Geochronology	Determine the age of SPA and other younger impacts; determine ages for igneous rocks (basalts, crustal, pyroclastic) to constrain surface ages and magmatic evolution of the Moon.	40Ar/39Ar geochronology	10-30 mg for whole rock analyses, depending on lithology (mafic rocks require less mass than more felsic ones). Laser probe dating also possible on thick sections for impactite rocks.	rocks	0.03	3	destructive	0.00	0.09	Age ± 50 Myr	[40, 45]	
			U-Pb or Pb-Pb geochronology	collect zircons from approx. 40 g of regolith "per study" (most of this regolith could remain w/curation). Spot measurements via SHRIMP may be possible on zircons in thick section.	regolith	40.00	1	not destructive (once zircons are selected (<0.5 g, the 39.5 g of remaining materials may remain in curation for other studies)	0.00	0.50	Age ± 20 Myr	[46] (refs therein)	
			Rb-Sr geochronology	200-300 mg for a typical basalt, and more for cumulates	rocks	0.30	3	destructive	0.00	0.90	Age ± 10s to 200 Myr	[46, 47]	
			Sm-Nd geochronology	0.5-1 g (less if there is a KREEP component)	rocks	1.00	3	destructive	0.00	3.00	Age ± 20-50 Myr	[46-48]	
			Lu-Hf geochronology	1-2 g (much less if there is a KREEP component i.e., ~200 mg if KREEPy)	rocks	2.00	3	destructive	0.00	6.00	Age ± 20-60 Myr	[47, 49]	
2: PLANETARY EVOLUTION	Petrography and mineral composition	Understand the compositions and petrologic history and diversity of lunar materials. These analyses are also usually done on splits from samples allocated for isotopic work to place them in petrologic context.	Optical microscopy	>4 mm diameter, requires preparation of polished thin section	rocks	0.10	2	not destructive	0.20	0.00	mineral occurrences and abundances ± 5% estimation	many studies	
			Electron Microprobe (EDS, WDS)	>4 mm diameter, requires preparation of polished thin or thick section	rocks	0.10	2	not destructive	0.20	0.00	elemental and oxide wt. % abundances w/<10 micron resolution	many studies	
			SEM	>4 mm diameter, requires preparation of polished thin or thick section	rocks	0.10	2	not destructive	0.20	0.00	images of minerals and textures w/ 1 micron resolution	many studies	
			FIB/TEM	>4 mm diameter, requires extensive surface polishing	rocks	0.10	3	not destructive	0.30	0.00	images of minerals and textures + composition with 10 nm to 1 micron resolution	[50]	
			SIMS	>4 mm diameter, requires preparation of polished thin or thick section	rocks	0.10	3	not destructive	0.30	0.00	isotopic ratios and chemical abundances, precision varies by system	[51, 52]	
			XANES	>4 mm diameter, requires preparation of polished thin or thick section	rocks	0.10	3	not destructive	0.30	0.00	determination of oxidation states, which are useful for mineral identification and oxygen fugacities	[53]	
	Stable Isotope Geochemistry & Volatiles	Understand the diverse petrology and geochemistry of regolith, crustal, and mantle materials.	ICP-MS (composition)	1-2 g for HSE and bulk composition	either	2.00	3	destructive	0.00	6.00	measurements of trace elements	[54]	
			Understand mantle geochemistry and the overall degree of volatile depletion in the bulk Moon.	Volatile abundances by SIMS	>4 mm diameter, requires preparation of polished thin section	rocks	0.00	3	not destructive	0.00	0.00	C, F, Cl, S, OH abundances in mineral phases and glasses	[55, 56]
		Understand the origin of the Moon and mantle geochemistry.		O isotopes	1-10 mg for laser fluorination	either	0.01	3	not destructive	0.03	0.00	δ18O, δ17O, Δ17O	[57]
				H isotopes	100-200 mg for bulk and >4 mm diameter, requires preparation of polished thin section for in situ	rocks	0.2	3	not destructive	0.60	0.00	δD	[58, 59]
				Cl isotopes	1-3 grams for bulk measurements of KREEP-poor samples, 0.5 g for KREEP-rich; >4 mm diameter, requires preparation of polished thin section for in situ	rocks	3	3	not destructive	9.00	0.00	δ37Cl	[60]
				S isotopes	1g for bulk analysis and 1.5mg for sulfide mineral separates	either	1	3	not destructive	3.00	0.00	δ34S, Δ33S, Δ36S	[61]
		Determine the global abundance and distribution of volatile elements, which ultimately provide key insights into the origin of the Moon and mantle geochemistry and degree of heterogeneity.	Zn isotopes	0.5-1g for bulk measurements	rocks	1	3	destructive	0.00	3.00	δ66Zn	[62, 63]	
K isotopes	100 mg for bulk measurements		either	0.1	3	destructive	0.00	0.30	δ41K	[64]			
N isotopes	5-50 mg for bulk measurements		either	0.05	3	destructive	0.00	0.15	δ15N	[65]			
Other stable isotope systems	0.2-3.0 g for each bulk measurement	either	3	3	destructive	0.00	9.00	e.g., δ65Cu, δ71Ga, δ87Rb, δ124Sn, δ82/78Se	(Se) [66]; (Sn) [67]; (Rb) [68]; [69]; (Ga) [70]; (Cu) [71]				

TOTAL MASS REQUIRED PER SITE FOR PRIMARY SAMPLE SCIENCE INVESTIGATIONS: 14.1 g (nondestructive), 28.9 g (destructive)



TABLE B. SECONDARY SAMPLE SCIENCE INVESTIGATIONS

SCIENCE THEME:	ANALYTICAL CATEGORY:	SCIENTIFIC MOTIVATION	ANALYTICAL APPROACH:	SAMPLE REQUIREMENTS:	Does the analysis require regolith rocklets (diameter > 4-mm), regolith fines, or either?	Mass required per analysis (g):	Number of discrete analyses required per sampling site:	Is the analysis destructive (i.e., does this analysis prevent other analyses)?	SAMPLE MASS REQUIRED PER SITE FOR NON-DESTRUCTIVE ANALYSES:	SAMPLE MASS REQUIRED PER SITE FOR DESTRUCTIVE ANALYSES:	ANTICIPATED MEASUREMENT & PRECISION:	REFERENCES:
LUNAR GEOPHYSICS	Physical Properties	Understand the paleointensity evolution of the ancient lunar dynamo; understand the origins of strong lunar crustal magnetic anomalies, which in turn have applications for solar wind standoff	Paleomagnetism + rock magnetism	bulk samples >1 cm diameter (ideally 2 cm) stored in non-magnetic container, further sample preparation on Earth needed to obtain non-space-weathered interior of rocks. Final paleomagnetic subsamples should be >100 mg each, with associated geochronology study to establish age.	rocks	3.00	2	not destructive	5.40	0.60	dynamo field paleointensity (within factor 2 uncertainty); magnetic mineral composition and grain sizes	[23, 72]
		Density and porosity measurements are important for constructing gravity models of the Moon's crust and lithosphere.	Density, Porosity	1 g whole rock samples via classical bead method and He pycnometry, or smaller for estimates from micro-CT analyses.	rocks	1.00	2	not destructive	2.00	0.00	density ± 50 kg/m ³ ; porosity ± 2% via Bead method or He pycnometry	[43]
LUNAR PETROLOGY & GEOCHEMISTRY	Isotope Geochemistry	Determine abundance of impactor components in samples	Various metal isotope systems	5-10 g (less for metal-rich samples)	either	10.00	2	destructive	0.00	20.00	isotopic abundances and ratios (precision depends on specific systems)	[73, 74]

TOTAL MASS REQUIRED PER SITE FOR SECONDARY SAMPLE SCIENCE INVESTIGATIONS: 7.4 g (nondestructive), 20.6 g (destructive)



B.5 SCIENCE FREQUENTLY ASKED QUESTIONS (FAQS):

B.5.1 HOW DOES ENDURANCE ADDRESS THE PRIORITY SCIENCE QUESTIONS OF THE DECADAL SURVEY?

Endurance’s science objectives (Section 1) were formulated from the outset to explicitly address a preponderance of the priority planetary science questions identified by the Planetary Science and Astrobiology Decadal Survey 2023–2032. Table B-3 details Endurance’s relevance to the priority science question (i.e., chapters) of the decadal survey. Endurance’s goals are also responsive to the highest

Table B-3. Relevance between Endurance and the priority planetary science questions identified by the Planetary Science and Astrobiology Decadal Survey 2023–2032. “Critical” indicates that Endurance would provide potentially paradigm-changing insight relevant to addressing that priority science question. “Contributing” indicates that Endurance would support addressing that priority science question.

Decadal Survey Priority Science Questions:		Relevance:	
1	Evolution of the Protoplanetary Disk	Contributing	<ul style="list-style-type: none"> Endurance would return samples of the lunar mantle exposed in SPA, which would constrain the bulk composition of the Moon, the early Earth, and their building blocks. Endurance would likely serendipitously return meteoritic material in impact breccias, which would improve our understanding of planetesimal compositions.
2	Accretion in the Outer Solar System	Critical	<ul style="list-style-type: none"> Endurance would return samples from large pre-Imbrian (>3.9 Gyr age) impact basins (Poincaré, Apollo), which would provide critical tests of the “late heavy bombardment” and giant planet migration and instability hypotheses. Endurance would return samples of SPA material that could provide an age for the largest and oldest impact basin on the Moon, providing a critical constraint on the earliest bombardment and organization of the Solar System.
3	Origin of the Earth and Inner Solar System Bodies	Critical	<ul style="list-style-type: none"> Endurance would return samples, and provide in situ geochemical and geophysical measurements, that would provide constraints on the chemical, thermal, and physical evolution of the Earth and Moon, with broad implications for the formation and evolution of other rocky worlds. Endurance would return samples of the lunar mantle exposed in SPA, which would constrain the bulk composition of the Moon, the early Earth, and their building blocks.
4	Impacts and Dynamics	Critical	<ul style="list-style-type: none"> Endurance’s returned samples would provide critical new constraints on the impact bombardment history of the Moon, including dating the largest basin (SPA), other large basins (Poincaré, Apollo, Schrödinger), and younger surfaces (mare basalts, young craters). Endurance’s long traverse and in situ geochemical, geological, and geophysical measurements would provide fundamental insight to impact cratering processes at all scales—from simple craters, to complex craters, and planetary-scale basins.
5	Solid Body Interiors and Surfaces	Critical	<ul style="list-style-type: none"> Endurance would characterize the geologic processes across a large, poorly understood lunar terrain (SPA and the lunar farside), elucidating the geologic processes that shaped the formation and evolution of rocky bodies—including magma oceans, impacts, magmatism and volcanism, and more. Endurance’s long traverse and in situ geochemical, geological, and geophysical measurements would provide fundamental insight to impact cratering processes at all scales—from simple craters, to complex craters, and planetary-scale basins. Endurance would return samples of the lunar mantle exposed in SPA, which would constrain the overall thermochemical evolution of the Moon and other rocky worlds.
6	Atmosphere and Climate Evolution on Solid Bodies	Contributing	<ul style="list-style-type: none"> Endurance’s particles and fields measurements would characterize the incident solar flux across both magnetized and unmagnetized regions of SPA—a needed input for understanding exosphere formation and loss across different airless bodies. Endurance would characterize magmatic deposits across the lunar farside, providing key insight into how volcanic outgassing may contribute to planetary atmospheres.
7	Giant Planet Structure and Evolution		
8	Circumplanetary Systems	Contributing	<ul style="list-style-type: none"> Endurance would characterize the lunar farside and a giant impact basin in great detail, and test hypotheses for forming planetary scale asymmetries—a common phenomenon in circumplanetary systems. Endurance would characterize volcanic and magmatic processes in an unexplored terrain on the Moon, which is important for understanding if circumplanetary processes (e.g., tides) shaped the crustal structure of the Moon and other worlds.
9	Insights from Terrestrial Life	Contributing	<ul style="list-style-type: none"> Endurance’s returned samples would determine the timing and magnitude of impact bombardment of the Earth–Moon system, which is critical to understanding the early conditions and processes conducive to the emergence and evolution of terrestrial life.
10	Dynamic Habitability	Contributing	<ul style="list-style-type: none"> Endurance’s returned samples would constrain the earliest impact history of the Earth–Moon system, and shed light on the evolution of habitable conditions on the early Earth. Endurance’s returned samples and in situ measurements would characterize the fundamental process of flood volcanism—which can both create and destroy habitable environments on rocky worlds.
11	Search for Life Elsewhere		
12	Exoplanets	Contributing	<ul style="list-style-type: none"> Endurance’s returned samples and in situ measurements would yield substantial advancements across many fields in planetary science, which would have implications to a variety of exoplanet studies—from improving our understanding the thermochemical evolution of rocky exoplanets (and potential magma ocean exoplanets), to testing our ideas for the dynamical evolution of solar systems, and more.



priority questions in lunar science—which have been called out repeatedly in numerous community documents over at least three decades, and yet never addressed head on [75].

B.5.2 WHAT DECADAL SURVEY WHITE PAPERS INFORMED THE ENDURANCE CONCEPT?

The Endurance concept was informed by a number of white papers submitted to the Planetary Science and Astrobiology Decadal Survey 2023–2032, including:

- Bailey (#414), Will Key Lunar Decadal Objectives be Missed in the Lunar Land Rush?
- Bottke (#249), Exploring the Bombardment History of the Moon.
- Cohen (#28), Geochronology as a Framework for Inner Solar System History and Evolution.
- Cohen (#356), Lunar Missions for the Decade 2023–2033.
- Costello (#146), Investigating Impact Processes at all Scales: The Moon as a Laboratory.
- Ghentz & Zellner (#212), Assessing the Recent Impact Flux in the Inner Solar System: 1 Ga to Present.
- Jolliff (#332), Sample Return from the Moon’s South Pole-Aitken Basin.
- Moriarty (#244), The Moon is a Special Place.
- Moriarty (#400), Lunar Sample Return from Multiple Locations is a Critical Capability for Addressing High-Priority Planetary Science Goals.
- Rufu (#270), The Origin of the Earth-Moon System as Revealed by the Moon.
- Valencia (#111), High Priority Returned Lunar Samples.

B.5.3 HOW DOES ENDURANCE COMPARE TO THE OTHER SAMPLE RETURN (AND IN SITU ANALYSIS) MISSION CONCEPTS, LIKE THE SOUTH POLE-AITKEN BASIN SAMPLE RETURN CONCEPT IN VISION AND VOYAGES, IN SITU GEOCHRONOLOGY, AND ARTEMIS?

Endurance is one of many concepts that have been proposed to address outstanding questions related to solar system chronology, and the thermochemical evolution of the Moon and rocky worlds. Table B-4 outlines how Endurance-R and Endurance-A compare with related New Frontiers class missions, including the *Vision and Voyages* Lunar South Pole–Aitken Basin Sample Return concept (henceforth, SPA-SR; [76]), the lunar concept in the In Situ Geochronology planetary mission concept study [38, 39], and sample return with Artemis astronauts from either the Artemis III mission or a future Artemis south pole basecamp.

The central difference between Endurance and previously considered planetary missions (e.g., SPA-SR, In Situ Geochronology) is Endurance’s mobility—which enables addressing broader science questions. Both SPA-SR and In Situ Geochronology traditionally assume a single static lander. Previously proposed SPA-SR concepts (e.g., MoonRise, [42]) considered landing sites in central SPA, near Bose and Bhaba craters, and near Endurance sample sites E, F, G, H, and I [77]; The In Situ Geochronology mission concept study considered landing sites on the nearside of the Moon, including the Crisium or Nectaris basins (to address an analog of Endurance Science Objective 1.2) or volcanic features in central Procellarum or Serenitatis (to address an analog Endurance Science Objective 1.3). The In Situ Geochronology concept study considered a hopper mobility systems to visit multiple sites separated by several hundreds of kilometers, but ultimately found that concept infeasible due to the large propellant mass. It is important to note that the In Situ Geochronology mission concept study did not consider farside landing sites (to avoid requiring a communications relay) which makes it incapable of addressing Endurance Science Objective 1.1. However, if a communications relay exists in this timeframe (as we assume in the Endurance concept study), then it is conceivable that a mission like In Situ Geochronology could land in SPA and address some of Endurance’s SPA-centric Science Objectives. In any event, a single lander would likely only be able to address a subset of Endurance’s Science Objectives.



The lack of mobility makes it challenging for a single lander (e.g., SPA-SR or In Situ Geochronology) to *completely and confidently* address the full breadth of Endurance’s science objectives. Impact gardening does act to mix lunar material over long-distances (even hundreds of kilometers), so it is not impossible for a mission to a single location to address multiple objectives if it collects and returns/analyzes sufficient volume of regolith (hence why SPA-SR can “contribute” to addressing other Endurance Objectives in Table B-4, even if it cannot completely address them). However, the lack of clear provenance and geological context for samples collected as fragments

Table B-4. Comparison of the science return and cost between different lunar mission concepts, including the Vision and Voyages South Pole–Aitken Basin Sample Return (SPA-SR) concept [76], the Planetary Mission Concept Study (PMCS) for In Situ Geochronology [38], the two variants of Endurance, and sample return with Artemis astronauts making trips to a future south pole basecamp. “X”s indicate that the concept would substantially address the motivating Endurance Science Objective, and “contributing” indicate that the concept may partially address the motivating Endurance Science Objective. Single landers like SPA-SR and In Situ Geochronology can only address a subset of Endurance’s Science Objectives. The planned location for the Artemis basecamp precludes it from confidently addressing any of Endurance’s Science Objectives.

			Vision and Voyages SPA Sample Return (SPA-SR)	PMCS In Situ Geochronology	Endurance-R (Robotic Sample Return Option)	Endurance-A (Astronaut Sample Return Option)	Artemis South Pole Basecamp
Endurance Science Objectives:	Science Theme 1: Solar System Chronology	1.1. Anchor the earliest impact history of the Solar System by determining the age of (perhaps) the largest and oldest impact basin on the Moon: South Pole–Aitken (SPA).	X		X	X	Contributing
		1.2. Test the giant planet instability and impact cataclysm hypotheses by determining when farside lunar basins formed.	Contributing	X	X	X	Contributing
		1.3. Anchor the “middle ages” of Solar System chronology (between 1 and 4 billion years ago) by determining the absolute age of a cratered, farside lunar mare basalt.	Contributing	X	X	X	
	Science Theme 2: Planetary Evolution	2.1. Test the magma ocean paradigm and characterize the thermochemical evolution of terrestrial worlds by determining the age and nature of volcanic features and compositional anomalies on the farside of the Moon.	X	Contributing	X	X	
		2.2. Explore a giant impact basin from floor to rim by characterizing the geologic diversity across the South Pole–Aitken Basin.			X	X	
	Development (A-D) Cost (FY25):		\$1.1B (this concept has not been fully costed by a decadal survey)	\$1.1B	\$1.8B	\$1.1B	Unknown
Total Project Cost (FY25):		Unknown (this concept has not been fully costed by a decadal survey)	\$1.2B	\$2.4B	\$1.5B (if HEO costs are not included)	Unknown	
Mission Class:		New Frontiers	New Frontiers	Flagship	New Frontiers (if HEO costs are not included)	N/A	
Sample Area:		1 site (~2 × 2 meters)	1 site (~2 × 2 meters)	12 sites along ~1,800 km traverse	12 sites along ~2,000 km traverse	Unknown	
Returned Mass:		~1 kg	~0 kg	~2 kg	~100 kg (contingent on Artemis return capability)	Unknown (Artemis III SDT: minimum mass: 25 kg, nominal mass: 83 kg)	



within the regolith will add uncertainty to the interpretation of their origin and significance. Endurance’s long-range mobility, capability of collecting multiple samples, and acquiring geological, geochemical, and geophysical measurements at (and between) sampling sites mitigates these issues.

Endurance’s long-range traverse also enables new and valuable science beyond just collecting more varied samples. Endurance’s remote sensing instruments (Section 1.7, Table 1-3, Section B.5.5) would acquire a variety of geological, geochemical, and geophysical measurements across an enormous (>1,700-km) swath of South Pole–Aitken basin. Endurance would have 1-hour “Interval Stops” every 2 kilometers, and 48-hour “Deep Interval Stops” every 20 kilometers, where the rover would acquire panoramas, hand-lens images, spectra, and long-integrations with the gamma-ray and neutron spectrometer (GRNS) and alpha-particle x-ray spectrometer (APXS). Each of the 12 sample sites would also be characterized in even greater detail. In total, Endurance would have nearly 800 Interval Stops, and nearly 100 Deep Interval Stops, as shown in Figure B-2. These measurements would provide ultra-high-quality stripes of data across SPA, which would be capable of addressing a variety of broad science questions (e.g., Endurance Objective 2.2) that are simply out of reach of single landers. Moreover, these datasets would provide ground-truth to countless orbital datasets, thereby extending and strengthening their novelty. We believe that this combination of sample science and traverse science elevates Endurance’s potential science impact to the level of a Flagship class mission.

In the forthcoming decade, it is anticipated that humans will return to the surface of the Moon with the NASA Artemis program. The details of this program are still in flux, but at present it is expected that the first human mission, Artemis III, will land at the lunar south pole (see [78]). Subsequent missions may land in the same region, building a south pole basecamp. The exact location for these landings and planned basecamp has not yet been defined, but is currently anticipated to be within 6° of the south pole. Candidate sites are shown in Figure B-2. Artemis astronauts will return substantial amounts of sample to the Earth; the Artemis SDT report estimates a minimum mass of 25-kg, and a nominal mass of 83-kg. While samples returned from the lunar south pole have potential to address some important planetary science questions (particularly related to volatiles in the Moon’s permanently shadowed craters), the south pole is *not* the ideal location to acquire samples to address Endurance’s Science Objectives. The south pole is beyond (or on) the rim of SPA, far from any large, pre-Imbrian basins, and far from the most important geological and geochemical terrains that hold the answers to the thermochemical evolution of rocky worlds. Thus, it is unlikely that samples returned from the south pole will substantially address any of Endurance’s Science Objectives. The one exception could be if astronauts process or return an exceptionally large volume of regolith—in which case it may be possible to identify fragments in the regolith that have been transported large distances by impact events from within SPA to the south polar region. However, these samples will again lack geologic context, making it challenging to confidently interpret their significance. The Endurance-A concept presented in this report, which would collect samples from across SPA and deliver them to astronauts at the south pole, would more completely and confidently address the motivating Science Objectives, with a budget that is still commensurate with a New Frontiers mission.

If Artemis astronauts land at other locations in SPA (e.g., Central SPA, Poincaré, Apollo, Schrödinger), they may be able to address more of Endurance’s Science Objectives. However, such missions are not currently planned. Additionally, like any single lander mission, a single Artemis mission to a region within SPA would likely only be capable of addressing a subset of Endurance’s Science Objectives, again motivating consideration of Endurance-like mission concepts. If the Artemis program performs an exploration campaign that includes more broadly distributed landing sites (akin to the Apollo missions), Endurance-like rovers landed at key sites ahead of time could effectively increase the reach of the Artemis astronauts who could retrieve the samples later. Such partnership would provide a new paradigm for collaboration NASA’s Science Mission Directorate (SMD), and Human Exploration and Operations Mission Directorate (HEOMD), and substantially enhance science outcomes.



B.5.4 HOW DOES ENDURANCE COMPARE WITH INTREPID?

The Endurance mission concept is derived from the Intrepid mission concept study implementation [1]. Endurance thus has incorporated many of the engineering solutions developed for Intrepid, including the overall configuration, traverse length, and instrument suite (as mandated by the guidelines from the Decadal Survey: Section 1.3). In addition to hardware, Endurance also follows Intrepid's strategy for rover operations along an extended traverse, including developing an extensively detailed pre-planned route, relying on autonomy, and using streamlined, focused operations.

While Endurance derives its engineering lineage and operations philosophy from the Intrepid rover concept, it addresses fundamentally different science objectives. Intrepid investigates planetary **magmatism** by exploring diverse geologic regions in the Procellarum region of the lunar nearside. Endurance investigates Solar System **chronology** and the **thermochemical evolution** of rocky worlds by exploring diverse regions within South Pole–Aitken basin on the lunar farside. Intrepid would not address a preponderance of Endurance's Science Objectives (in particular, Intrepid would not address Solar System chronology), and Endurance would not address a preponderance of Intrepid's Science Objectives (in particular, Endurance would not address the same diversity of magmatic processes, and Endurance would not investigate lunar swirls).

One interesting result from the Endurance concept study was that it was possible to add a sample collection and caching system to an Intrepid-like rover while still remaining within the New Frontiers cost cap (\$1.1B). Samples collected by an Intrepid-like concept traversing Procellarum—delivered either to a robotic Earth Return Vehicle (an “Intrepid-R” analogous to Endurance-R) or a future Artemis mission (an “Intrepid-A” analogous to Endurance-A)—would both enhance the science outcomes of the Intrepid concept, and potentially address some (but not all) of the Solar System chronology objectives of either Endurance or In Situ Geochronology.

B.5.5 WHAT IS THE NATURE OF LUNAR REGOLITH, AND WHAT ARE THE CHALLENGES WITH SAMPLING IT?

The tools and procedures for their use developed for the Apollo program provide important lessons for future lunar sampling tools. The successful ones (scoops, rakes, core tubes, sample bags) were simple, robust, and designed to be used in a heavily constrained fashion due to limited mobility of astronaut hands and arms within a space suit. These lessons factored heavily into the development of Endurance's sample collection and caching system—where we favored simplified scoops and rakes with no moving parts (other than vibration motors to facilitate clearing clogs). Endurance's sampling system also benefited from years of experience with sampling martian material with Curiosity and Perseverance, although we note that martian material is systematically different than lunar material. The sampling system is detailed in Section K.

Even with the Apollo “baseline” there will be additional challenges of remote operation and fewer degrees of freedom. Thus, it is important that the sampling system be tested with simulants that closely resemble real lunar soil, and in particular, its physical characteristics. Here is a summary of characteristics:

- **Sizes:** The lunar regolith is an impact-generated soil-like layer above the bedrock, and it is dominated by particles ranging in size from centimeter to submicron scales. 10-20% of the regolith consists of fine particles or dust, below 10 microns in size. Fines are systematically less mafic, higher in silicic and felsic components [79-81].
- **Morphology:** Extensive re-melting generates abrasive, shard-like particles, which are highly irregular, angular, elongated (1:3 aspect ratio), with high specific surface area (eight times the surface area as spheres with equivalent particle size distribution). Many fragments are entirely melted or containing amorphous glass (agglutinate). Reentrant hook-like projections, anisotropic, porous, compressible, aligning along long axes. In short, lunar regolith behaves like abrasive Velcro.
- **Composition:** There are three major rock “suites” and variations that, including classic mare volcanism (basalts), gabbros/anorthosites, and Mg-suite/Fra Mauro basalts which include early volcanic produces including KREEP materials. Volatiles can be bound in and/or adsorbed on mineral



grains. Most lunar regolith is substantially space weathered due to the combined effects of solar wind and micrometeorite bombardment, which produce rings of nanophase iron on grains.

The Endurance sampling system should be tested with materials that simulate the lunar regolith. In particular, the aspects of a lunar regolith that control geotechnical properties should be closely simulated: the particle size–frequency distribution, grain morphology, and compaction. Current work is evaluating the efficacy of available simulants for a range of uses, including geotechnical properties (e.g., [82]).

B.5.6 WHAT IS THE LUNAR MANTLE MADE OF?

The moon crystallized a lunar magma ocean early in its history (4.38 to 4.45 billion years ago). The depth of the magma ocean is not agreed upon but estimates range from 300 to 600 km (some suggest that it was 1000 km and some suggest that the entire moon was melted). Within the magma ocean cumulates, the last liquids to crystallize formed dense, ilmenite-rich cumulates that contain high concentrations of incompatible radioactive elements (KREEP). The underlying olivine-orthopyroxene cumulates were also stratified with later crystallized, denser, more Fe-rich compositions at the top. As one went deeper into the magma ocean cumulate pile the density decreased further and the lower 50% of the pile is thought to be all olivine (dunite).

At the end of magma ocean solidification Rayleigh-Taylor instability likely caused the dense ilmenite-rich cumulate layer and underlying Fe-rich cumulates to sink downward, leading to a late-stage lunar magma ocean cumulate overturn event. This overturn was proposed by [83] and much has been written about the efficiency of the process and the depth to which the dense cumulates sunk into the deep mantle. If an overturn event occurred the rocks (“mantle”) under the lunar anorthosite crust could be: (a) Late-stage iron-rich cumulates that “stuck” to the underlying crust and are still in their original stratigraphic position. (b) Deeper Mg-rich cumulates (dunites) that were advected upwards to replace the shallower ones that sank. (c) Deep, primitive, un-melted lunar mantle that ascended to replace the shallower denser cumulates that had sunk to a depth below the bottom of the original magma ocean.

There is evidence to suggest that some of the ilmenite-rich cumulates did sink to great depth. The depth to the source region of lunar high-Ti ultramafic glasses has been determined in laboratory high-pressure, high-temperature melting experiments to be 300 to 400 km [84]. There is also evidence that some of the ilmenite-rich cumulates did not sink much, if at all. The same high-pressure, high-temperature melting experiments performed on Apollo 11 and Apollo 17 high-Ti basalts give much shallower source region depths of ~100 km. On the near-side of the moon are mare basalts enriched in high concentrations of incompatible elements (KREEP) and these basalts also have a shallow mantle source.

At South Pole–Aitken, the material that is thought to have been excavated from the “mantle” shows only a small enrichment in KREEP, so it might be that the mantle sampled by the impact might be of type (b) or even (c). We won’t know until we go there!

B.5.7 WHAT INSTRUMENTS COULD ENDURANCE DESCOPE?

Per the ground rules of the Endurance concept study (Section 1.3), we did not consider an instrument trade when developing Endurance. This decision flowed from an assumption by the Mercury and the Moon panel of the decadal survey that Intrepid’s instrument suite was more than capable of supporting Endurance’s science investigations. Nonetheless, Intrepid’s instrument suite was selected to address different science investigations (e.g., magmatism and swirls on the lunar nearside), and therefore not all of Intrepid’s instruments may be required to successfully complete the Endurance mission concept. In particular, since there are no swirls in the region of SPA explored by Endurance, it may be reasonable to descope the radiation instruments (electrostatic analyzer and ARMAS). Additionally, since Endurance would return substantial samples (either 2.2-kg for Endurance-R or ~100-kg for Endurance-A), some in situ analyses may be superseded by laboratory analyses. The highest priority instruments for Endurance are the stereo cameras and visible/near-infrared spectrometer (which are



important for identifying sampleable material and geologic context), and the APXS and GRNS which provide geochemical data along the traverse. A future study or proposal would need to investigate descopes in more detail.

B.5.8 WHAT COULD ENDURANCE DO WITH AN EXTENDED MISSION?

NASA planetary rovers have historically exceeded their planned lifespans and drive distances—sometimes by orders of magnitude (e.g., Opportunity). If Endurance completed its prime mission and remained in good health, there may be potential for an extended mission. A detailed investigation of possible extended missions was beyond the scope of this study. Nonetheless, interesting opportunities exist for additional high-science return extended missions.

Endurance-R would end its prime mission in the Apollo basin, after transferring its samples to the Earth Return Vehicle. Without a sample canister, Endurance-R would no longer be capable of collecting and caching samples. Nonetheless, Endurance-R's suite of remote sensing instruments have potential to do transformative science, and many extended mission traverses could be considered, including: (1) An in-depth survey of the Apollo basin. (2) A traverse to Oppenheimer basin. (3) A traverse out of Apollo into the lunar farside highlands.

Endurance-A would end its prime mission near the Artemis basecamp at the lunar south pole, after Artemis astronauts retrieve its samples. Unlike Endurance-R, Endurance-A's sample canisters could be emptied and re-attached to the rover by the astronauts—potentially readying it for additional sample collection and caching expeditions. One could imagine Endurance-A repeatedly departing the Artemis basecamp on sample collection sorties, visiting regional sites of interest, collecting samples, and returning them to the basecamp for collection and return to Earth by different Artemis astronaut crews. This would effectively increase the reach of the Artemis astronauts. Potential sites of interest could span the south pole, ranging from visiting unexplored terrains to returning to the Schrödinger basin for a more detailed survey. Alternatively, Endurance-A could become part of the Artemis infrastructure, directly supporting human operations by scouting locations for future Artemis astronaut extravehicular activities (EVAs). Endurance's gamma-ray and neutron spectrometer would be capable of identifying subsurface water ice, although Endurance was not designed for sustained operations in permanently shadowed regions—so additional study is required before considering using Endurance as an “ice prospecting” rover. (See the In Situ Solar system Polar Ice Roving Explorer, INSPIRE, decadal survey mission concept study report for a more focused investigation of a lunar polar volatiles rover.) Finally, with the recent selection of the SpaceX Starship human landing system, even more imaginative extended missions could be possible. For example, Starship could return Endurance to Earth, where the rover could either be refueled and refit for another voyage to the Moon, or it could retire comfortably in the Smithsonian National Air and Space Museum and inspire future generations of planetary explorers.

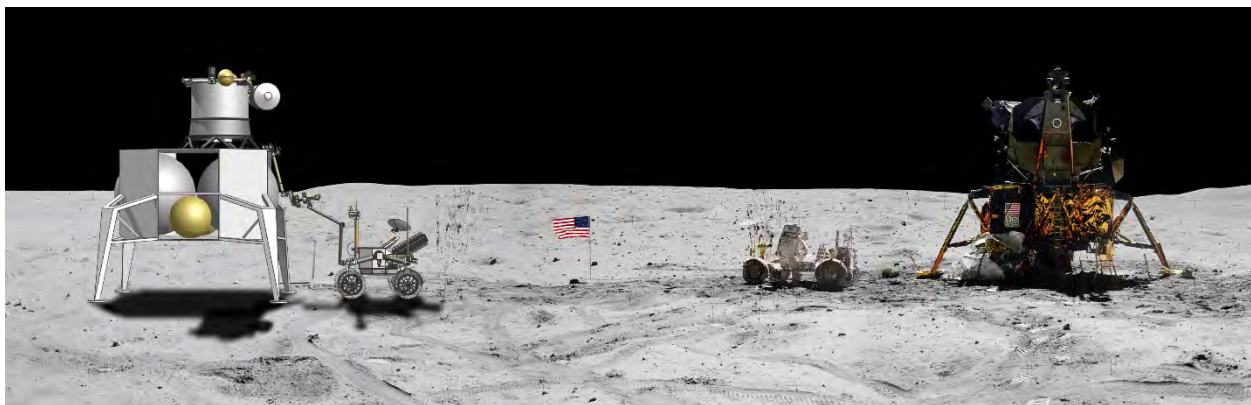


Figure B-5. Endurance-R, roughly to scale with the Apollo 16 lunar rover vehicle (LRV), lunar module (LM), and astronaut John Young. Adapted from Apollo images AS16-116-18573 to AS16-116-18582 (file number JSC2011e118363), available: <https://www.lpi.usra.edu/resources/apollopanoramas/pans/?pan=JSC2011e118363>.

C JPL TEAM X REPORTS

Three Team X studies were held in support of the Endurance mission concept development. One Team X study was held for the rover, primarily for costing purposes, based on the Endurance team design and using prior work from the Intrepid study to inform the process. The second study involved a complete design of the Earth Return Vehicle for the Endurance-R variant. This element of the mission was not separately developed by the Endurance team, thus this was a more involved Team X design involving both design and costing. Finally, a brief Team X study was held to assemble the results of the first two studies into an overall mission cost for the Endurance-R variant including all mission elements and science operations through sample curation.

This appendix provides the Executive Summary and Systems Engineering sections from the Endurance (formerly called Intrepid +) rover and ERV Team X Study Reports, and the full report from the Endurance-R full mission cost exercise.

Note that rover detailed design activities by the Endurance team continued following this study, resulting in values for some parameters (e.g., total mass, power modes, etc.) being slightly different from those in the body of the report.

C.1 ROVER REPORTC-2

C.2 ERV REPORT..... C-17

C.3 COMBINED MISSION REPORT C-41



C.1 ROVER REPORT



Lunar Intrepid+ Rover

Customers: James Keane, John Elliott

Facilitator: Al Nash

Session Dates: March 16 – March 17, 2021

Study ID: 370





Data Use Policy



- The information and data contained in this document may include restricted information considered JPL/Caltech Proprietary, Proposal Sensitive, Third-party Proprietary, and/or Export Controlled. This document has not been reviewed for export control. It may not be distributed to, or accessed by, foreign persons.
- The data contained in this document may not be modified in any way.
- Distribution of this document is constrained by the terms specified in the footer on each page of the report.



Team X Participants



- **Al Nash**(Facilitator)
- **Mason Takidin** (Cost)
- **Serena Ferraro** (Deputy Systems)
- **Greg Welz** (Ground Systems)
- **Chris Landry** (Mechanical)
- **Ronald Hall** (Power)
- **William Smythe** (Science)
- **Eddie Benowitz** (Software)
- **Jonathan Murphey** (Systems)
- **Thaddaeus Voss** (Telecommunications)



Table of Contents



- 1. Systems
- 2. Cost
- 3. Science
- 4. Mechanical
- 5. Power
- 6. Telecom
- 7. Ground Systems
- 8. Software



Systems Report

Author: Jonathan Murphy

Email: Jonathan.Murphy@jpl.nasa.gov

Phone: (818) 354 - 0360





Systems

Study Overview



- The goal of this study was to estimate the *cost* of the Lunar Intrepid+ Rover concept, for a NASA mid-decadal study. Intrepid+ would be a long-duration RTG-powered rover to explore the lunar South Pole Aiken basin (SPA). It would do in-situ science as well as collecting samples from diverse SPA locations for return to Earth. This study was *not* primarily a design exercise; the customer provided a MEL and design, and Team X used it to estimate a project cost, for the rover portion of the mission (though there were some minor design changes made in Team X). The larger Intrepid+ mission also involves either a) a return of samples to Earth by Artemis astronauts or b) a separate robotic sample return element. The robotic sample return component was studied in a previous Team X study, #369. The full project cost rollups, including both rover and sample return components, are outside the scope of this study, but are to be part of a small addendum study.
- Customer Inputs
 - Rover design description, including MEL
- Team X Outputs
 - Project-level cost (and WBS) for Rover portion only
 - Team X design (primarily customer-supplied design, with minor modifications, entered into Team X's format)

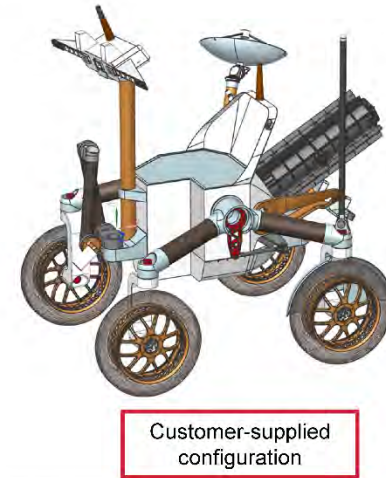
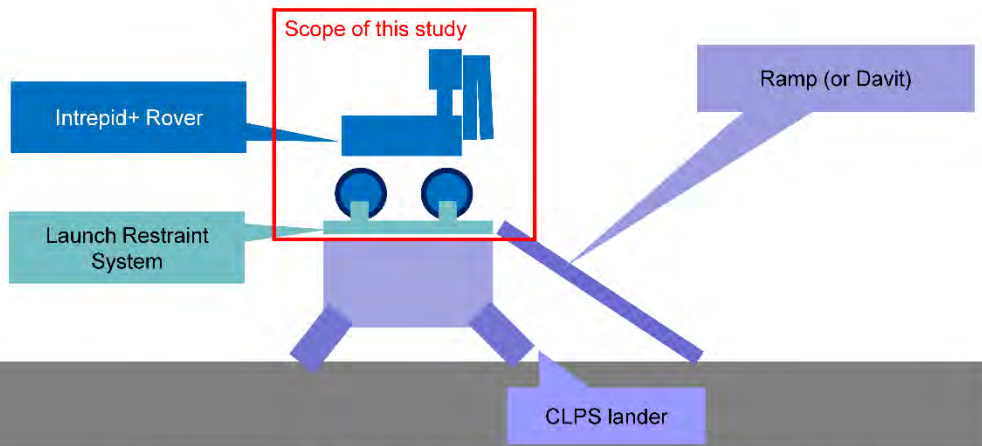


Systems

Architecture



- Team X costed the **Intrepid+ Rover**
 - The design (MEL and configuration) was supplied by the customer; image at lower right
- The cost and mass also includes a **Launch Restraint System** (to hold the rover during flight, and to release it)
- The rover will be delivered by a **Commercial Lunar Payload Service (CLPS) lander**
 - CLPS delivery was treated only as a pass-through launch cost in our WBS
 - The target mass allocation was 500kg, though if this were broken, we were simply to report the final required mass allocation
 - The lander was assumed to provide a **Ramp (or possibly a davit)** (to get to the surface)





Systems

Concept of Operations



- As a cost-only exercise, this study did not examine the concept of operations, nor did it attempt to model the ConOps for the purposes of data or power sizing.



Systems

Design Assumptions



- Most of the design was taken directly from the customer-supplied MEL
- There were several changes that were made during the study
 - The Telecom design was revised; some changes were requested by the customer (removal of an antenna); other changes were made on the recommendation of the Telecom chair
 - A hazard camera was added for the robotic arm
 - A pyro device was added for detaching the sample canister
 - The number of motor driver cards was increased (from 10 to 14, with 3 channels per card), to account for the large number of actuators required. However, the number of cards is still not enough for a 100% redundant system. Customer will continue to work motor card design and redundancy story. See “Notes about CDS Design” slide for more details.



Systems

System Guidelines

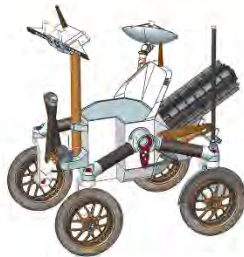


Team X Study Guidelines		Spacecraft	
<p>370 4X Planetary Decadal - Lunar Intrepid+ Rover 2021-03 Rover</p>		<p>Spacecraft Instruments</p>	<p>Rover ARMAS, Magnetometer, Gamma Ray Neutron Spectrometer (GRNS), TriCam, Point Spectrometer, Hand Lens Imager (HLI), APXS-cryocooler, Elect Analyzer, Laser Corner Reflector, ..., etc</p>
<p><i>Project - Study</i></p>		<p>Redundancy</p>	<p>Dual (Cold)</p>
<p>Customer</p>	<p>John Elliott</p>	<p>Heritage</p>	<p>Minimal</p>
<p>Study Lead</p>	<p>Alfred Nash</p>	<p>P/L Mass CBE, kg</p>	<p>19.6 kg Payload CBE</p>
<p>Study Type</p>	<p>Lunar Study</p>	<p><i>Project - Cost and Schedule</i></p>	
<p>Report Type</p>	<p>Standard Report</p>	<p>Cost Target</p>	<p>\$900M</p>
<p><i>Project - Mission</i></p>		<p>Mission Cost Category</p>	<p>Large - e.g. New Frontiers</p>
<p>Mission</p>	<p>370 4X Planetary Decadal - Lunar Intrepid+ Rover 2021-03</p>	<p>FY\$ (year)</p>	<p>2025</p>
<p>Target Body</p>	<p>Moon</p>	<p>Include Phase A cost estimate?</p>	<p>Yes</p>
<p>Science</p>	<p>South Pole Aiken Basin (SPA) sample return</p>	<p>Phase A Start</p>	<p>March 2024</p>
<p>Launch Date</p>	<p>30-Apr-30</p>	<p>Phase A Duration (months)</p>	<p>14</p>
<p>Mission Duration</p>	<p>4.25 years</p>	<p>Phase B Duration (months)</p>	<p>15</p>
<p>Mission Risk Class</p>	<p>B</p>	<p>Phase C/D Duration (months)</p>	<p>45</p>
<p>Planetary Protection</p>	<p>Outbound: II, Inbound: N/A</p>	<p>Review Dates</p>	<p>PDR - August 2026, CDR - July 2027, ARR - June 2028</p>
<p>Flight System Development Mode</p>	<p>In-House</p>	<p>Phase E Duration (months)</p>	<p>50</p>
<p><i>Project - Architecture</i></p>		<p>Phase F Duration (months)</p>	<p>6</p>
<p>Rover</p>	<p>on CLPS Lander</p>		
<p>CLPS Lander</p>	<p>on Launch Vehicle</p>		
<p>Launch Vehicle</p>	<p>Delivered by CLPS Lander</p>		
<p>Tracking Network</p>	<p>NEN/SN</p>		
<p>Contingency Method</p>	<p>Apply Total System-Level</p>		



Systems

Design Summary



Customer-supplied configuration

- Instruments
 - ARMAS
 - Magnetometer
 - Gamma Ray Neutron Spectrometer (GRNS)
 - TriCam
 - Point Spectrometer
 - Hand Lens Imager (HLI)
 - APXS-cryocooler
 - Elect Analyzer
 - Laser Corner Reflector
- CDS
 - Sabertooth (Sphinx successor) avionics
 - Motor Control box (Sphinx-based)
 - Instrument interface box (Sphinx-based)
- Ground Systems
 - Ground Network = Lunar relay satellite
 - Daily 4hr passes (DSN analog used for costing)
- Telecom
 - S-band HGA (0.75m)
 - S-band omni LGA
 - 2x UST-Lite transponders
 - 2x 5W SSPAs
- ACS
 - 2x IMUs
 - 2x Sun Sensors
 - 9x total Nav Cameras
 - 5x Illuminators
- Structures
 - Primary Structure Mass MEV= 70.3 kg
 - Secondary Structure Mass MEV = 6.7 kg
 - Mobility System total MEV = 145.4kg
 - Telecom articulation (2-axis)
 - Mast (2-axis)
 - Arm with end effector
 - Sample handling and "pizza" sample container
 - Harness/Cabling MEV = 26.5kg
 - Launch restraint
- Thermal
 - MLI, heaters, radiator
 - Thermal switch, heat pipes, and flexible strap
- Power
 - NextGen Mod 1 RTG (245W BOM)
 - Secondary battery



Systems

Note About CDS Design



- The CDS design was primarily left as-is from the customer inputs and previous design exercises
 - The CDS chair was minimally involved in the study, and there is no CDS subsystem report
- The number of motor control cards was changed from 10 to 14 to account for the large number of actuators required
 - There are two motor control boxes; each box has a Sphinx card controlling it
 - Each card can control up to 3 motors, though only 1 at a time
 - Each box has 7 cards
- However, the number of cards is still not enough for a 100% redundant system. The customer will continue to work motor card design and the redundancy story.
 - Note that simply operating the mobility system requires 8 simultaneous motors (4 for drive motors, 4 for steering), so if one of the two Sphinx controller cards fails, there is no redundancy approach that allows all 8 motors to run
 - Note also that it may be required for the 2-axis HGA articulation to run simultaneously with driving, which increases the total required simultaneous channels to 10
 - A fully redundant design would require $25 / 3 \approx 9$ cards in each box (a standard A/B redundancy approach)
- Actuations required include:
 - 8 = (1 wheel motor and 1 steering motor per wheel) * (4 wheels)
 - 5 = number of DOF on Arm
 - 2 = Mast (pan/tilt)
 - 2 = HGA (pan/tilt)
 - 3 = sample canister (pizza): rotation, opening/closing door, vibrating
 - Note that there is also a release mechanism, but that is a pyro, not a motor
 - 5 = end effector: gripper, vibration, "thwacker", motorized covers for 2 instruments
 - ... for a total of 25 actuations



Systems Summary Sheet



	Mass Fraction	Mass (kg)	Subsys Cont. %	CBE+ Cont. (kg)
<i>Power Mode Duration (hours)</i>				
Payload on this Element				
Instruments	5%	19.6	24%	24.4
Payload Total	5%	19.6	24%	24.4
Spacecraft Bus				
Attitude Control	2%	7.7	10%	8.4
Command & Data	3%	13.6	13%	15.3
Power	16%	65.9	29%	85.3
Structures & Mechanisms	62%	251.6	30%	327.1
S/C-Side Adapter	0%	0.0	0%	0.0
Cabling	5%	20.4	30%	26.5
Telecom	3%	14.1	15%	16.2
Thermal	4%	14.4	30%	18.7
Bus Total		387.7	28%	497.6
<i>Thermally Controlled Mass</i>				
Spacecraft Total (Dry): CBE & MEV		407.3	28%	521.9
Subsystem Heritage Contingency	28%	114.7	SEP Cont	10%
System Contingency	15%	60.4		
Total Contingency <input type="checkbox"/> Include Carried?	43%	175.1		
Spacecraft with Contingency:		582	of total	w/o addl pid
Spacecraft Total with Contingency (Wet)		582		
LV-Side Adapter		0.0		Wet Mass for Prop Sizing
Launch Mass		582		Dry Mass for Prop Sizing
CLPS Capability Required		582		
Launch Vehicle Margin		0.0		Mission Unique LV F
Dry Mass Allocation: MPV		582.4		
JPL Design Principles Margin		175.1	30% (MPV - CBE)/MPV	
NASA Margin		60.4	12% (MPV - MEV)/MEV	

- Note that this study was primarily concerned with costing, so Power Modes were not used
- With this design, a total CLPS payload mass allocation of 582kg would be required to provide for 30% JPL Design Principles Margin (which is equivalent to the 30% Margin required in the study ground rules)



Systems

Margin and Contingency Guidelines



- To ensure compliance with JPL's Design Principles (v8), we asserted a 30% JPL Dry Mass Margin on launch mass
 - $\text{JPL Dry Mass Margin} = (\text{Dry Capability} - \text{CBE Dry Mass}) / (\text{Dry Capability})$
 - Dry Capability = Launch Allocation – Propellant Mass (in this case propellant mass was zero)
 - In the case of this study, the Launch Allocation was allowed to “float” such that the design converged with 30% JPL Dry Mass Margin
 - 30% JPL Dry Mass Margin corresponds to a 43% increase over the CBE dry mass
 - Margined Dry Mass = 1.43 * CBE Dry Mass
 - The final Margined Wet Mass of 582kg is what would be required as a CLPS payload allocation, to allow for 30% JPL Dry Mass Margin
- NASA Margin was also calculated and is shown in mass tables; however, it did not drive the design
 - $\text{NASA Dry Mass Margin} = (\text{Dry Capability} - \text{MEV Dry Mass}) / (\text{MEV Dry Mass})$
- Payload power values were also assigned 30% JPL Margin (43% over CBE) for the purposes of sizing
- For the purposes of the Decadal Study, the 30% JPL Margin appears to be equivalent to the required 30% Margin listed in the Ground Rules, page 3:
 - $\text{Margin} = \text{Max Possible Resource Value} - \text{Proposed Resource Value}$
 - $\text{Margin (\%)} = (\text{Margin} / \text{Max Possible Resource Value}) \times 100$



Systems

Conclusions, Risks, and Recommendations



- The design came in at 582kg margined launch mass, which is over the 500kg target allocation
 - There may however be other CLPS landers which are capable of higher payload masses
 - The CBE mass is 407kg; there may be paths to pulling the design under a 500kg launch mass, though there is no obvious approach besides reducing the payload mass
- The mobility system mass was taken from the customer inputs; depending on whether it comes from a structural analysis based on the current total rover mass or not, there may be a mass upper risk (or an opportunity)
- The development cost (A-D), without Launch (CLPS), and with 50% reserves, comes to \$1.1B (FY25), which is compatible with a NF-class mission



Lunar Intrepid + Sample Return

Customers: John Elliott, John Baker

Facilitator: Alfred Nash

Session Dates: 23-Feb-2021 – 25-Feb-2021 Afternoons

Study ID: 369





Data Use Policy



- The information and data contained in this document may include restricted information considered JPL/Caltech Proprietary, Proposal Sensitive, Third-party Proprietary, and/or Export Controlled. This document has not been reviewed for export control. It may not be distributed to, or accessed by, foreign persons.
- The data contained in this document may not be modified in any way.
- Distribution of this document is constrained by the terms specified in the footer on each page of the report.



Team X Participants



- Alfred Nash (Facilitator)
- David Sternberg (ACS)
- William Jones-Wilson (ACS)
- Roger Klemm (CDS)
- Sun Matsumoto (CDS)
- Sherry Stukes (Cost)
- Steve Zusack (Deputy Systems)
- Greg Welz (Ground Systems)
- Melora Larson (Instruments)
- Steve Coffed (Mechanical)
- Reza Karimi (Mission Design)
- Laura Newlin (Planetary Protection)
- Ronald Hall (Power)
- Shelly Sposato (Power)
- Frank Picha (Propulsion)
- William Smythe (Science)
- Eddie Benowitz (Software)
- Ban Tieu (SVIT)
- Jonathan Murphy (Systems)
- Thaddaeus Voss (Telecom)
- Eric Sunada (Thermal)
- Mary Magiligan (Configuration)



Table of Contents



- 1. Executive Summary
- 2. Systems
- 3. Science
- 4. Instruments
- 5. Mission Design
- 6. Configuration
- 7. Mechanical
- 8. ACS
- 9. Power
- 10. Propulsion
- 11. Thermal
- 12. CDS
- 13. Telecom
- 14. Ground Systems
- 15. Software
- 16. SVIT
- 17. Planetary Protection
- 18. Cost



Executive Summary

Author: Alfred Nash
Email: Alfred.E.Nash@JPL.NASA.Gov
Phone: (818) 458-0501





Executive Summary

Study Overview



- Goals
 - The goal of this study is to generate a subsystem level point design and cost estimate for the Sample Return Element of the Lunar Intrepid Plus Sample Return Planetary Decadal Concept
- Objectives
 - From customer supplied requirements and references (which may include the MoonRise designs), Team-X shall design at a subsystem level, and estimate the costs of:
 - a) a Earth Return Vehicle (ERV), and
 - b) an Sample Return Capsule (SRC)



Executive Summary

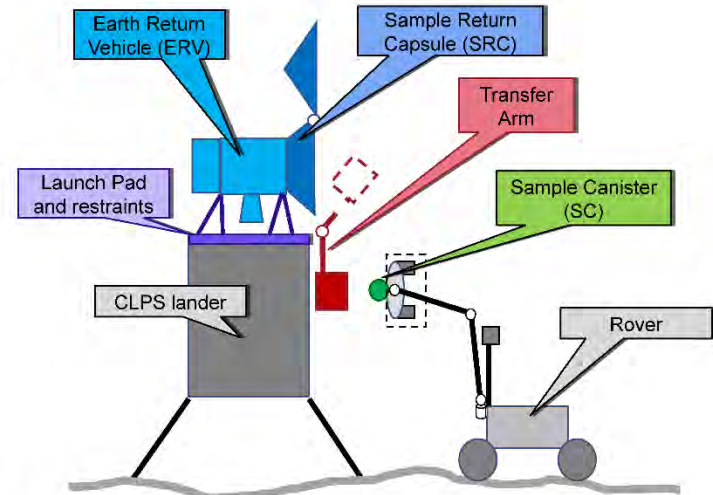
Mission Architecture and Assumptions



- The goal of this study was to design and cost a *robotic Earth-return* component for the **Lunar Intrepid+ Rover** concept, as a mid-decadal study for the Planetary Science decadal survey process. Lunar Intrepid+ would be a multi-lunar-day rover mission to the lunar far side south polar region, to collect regolith and rock samples over a large region, for return to Earth. Two approaches are being considered for Earth return: either return by astronauts, or a robotic return. This study is *just* for the robotic return component, including:
 - An atmospheric entry system (the “**Sample Return Capsule**” or **SRC**), launched from the lunar surface by...
 - An **Earth Return Vehicle (ERV)** which would launch from...
 - A **Launch Pad** with launch restraints, to hold and release the ERV
 - A **Transfer Arm** would transfer the **Sample Canister (SC)** (customer pass-through mass) from the Rover to the ERV
- ... with all of this (except the Sample Canister) to be delivered to the Lunar surface by a **Commercial Lunar Payload Service (CLPS)** lander
- **Customer Inputs**
 - Architecture description
 - Assumptions about the samples and their container
 - Concept of operations
- **Team X Outputs**
 - Cost for the robotic Earth return component (SRC, ERV, Launch Pad, Arm, Delivery by CLPS)
 - Estimate for Science cost of the Earth-based sample analysis
 - Design for the ERV, Launch Pad, and Arm; with assumptions for the SRC (based on OSIRIS-ReX Sample Return Capsule)

Architecture

(Cartoon adapted from customer inputs)



Colored elements are within the scope of this study; items in gray are not

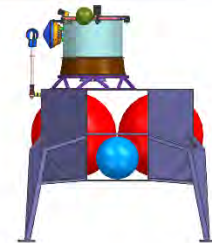


Executive Summary

Technical Findings



- The table below summarizes the architectural components of the spacecraft
- The rows in blue are what launch as a CLPS payload, and drive the required CLPS mass allocation
- The rows in red are what launch from the surface of the Moon, and drive the ERV's propulsion design
- Rows in purple are common to both the CLPS payload and the lunar launch



	Name	Dry Mass					Propellant Mass	Wet Mass Allocation	
		CBE	Contingency	MEV	Allocation	JPL Margin			NASA Margin
		kg	%	kg	kg	%			%
>	Total CLPS Payload	434.4	23%	534.7	619.6	30%	16%	710.9	1320.0
>	Launchpad and Arm	65.5	30%	85.2	93.7	30%	10%	0.0	93.7
>	ERV + SRC (no SC, no samples)	360.9	22%	439.9	515.5	30%	17%	710.9	1226.4
	ERV + SRC + SC + Samples	368.9	22%	449.6	525.9	30%	17%	710.9	1236.8
Launches on CLPS	ERV (Earth Return Vehicle)	314.3	21%	379.5	449.1	30%	18%	710.9	1159.9
	ERV Instruments	0.8	15%	0.9	1.1	30%	24%	0.0	1.1
	Carried SRC spin-up device - bus side	2.1	30%	2.8	3.0	30%	10%	0.0	3.0
	Carried SRC release device - bus side	4.1	30%	5.3	5.8	30%	10%	0.0	5.8
	Carried SRC mounting	2.3	30%	3.0	3.3	30%	10%	0.0	3.3
	ERV Bus	305.1	20%	367.5	435.8	30%	19%	710.9	1146.7
	SRC (Sample Return Capsule)	46.5	30%	60.5	66.4	30%	10%	0.0	66.4
	SC + Samples	8.0	21%	9.7	10.4			0.0	10.4
	SC (Sample Canister)	5.6	30%	7.3	8.0	30%	10%	0.0	8.0
	Lunar Sample	2.4	0%	2.4	2.4	0%	0%	0.0	2.4

Launches from Moon



Executive Summary

Programmatic Findings



COST SUMMARY (FY2025 \$M)	Team X Estimate	
	CBE	PBE
Project Cost	\$711.2 M	\$957.9 M
Launch Vehicle	\$200.0 M	\$200.0 M
Project Cost (w/o LV)	\$511.2 M	\$757.9 M
Development Cost	\$477.1 M	\$715.6 M
Phase A	\$4.8 M	\$7.2 M
Phase B	\$42.9 M	\$64.4 M
Phase C/D	\$429.4 M	\$644.0 M
Operations Cost	\$34.2 M	\$42.3 M



Executive Summary

Risks



- At \$716M (FY25) for A-D, not including launch costs, including 50% reserves, the cost of this mission fits comfortably in a New Frontiers allocation. See Cost report for full bookkeeping.
- This concept closed at 1321kg wet (including 30% JPL Margin), considerably over the 500kg target mass
 - 500kg was considered “safe” as a minimum CLPS capability; however, there may at some point be CLPS landers that can deliver more mass, and 1321kg may well be eventually feasible
 - The result is not surprising, as this design is similar in both mass and function to the ascent vehicle for the MoonRise concept
- Except for the higher-than-desired launch mass, there do not appear to be any major technical risks for this sample return portion of the mission
- As a high ΔV mission (essentially a launch vehicle), the design was driven primarily by propulsion and structures
 - It is very sensitive to changes in propulsion design
 - It is very sensitive to changes in structural mass fraction, which ripple through the Propulsion design with a feedback loop. Since the Team X design is based on historical structural mass fractions rather than on a specific structural design, there may be opportunities to reduce the overall mass through a careful structural design (possibly including a coupled propulsion/structural optimization approach)



Systems Report

Author: Jonathan Murphy
Email: Jonathan.Murphy@jpl.nasa.gov
Phone: (818) 354-0360





Systems

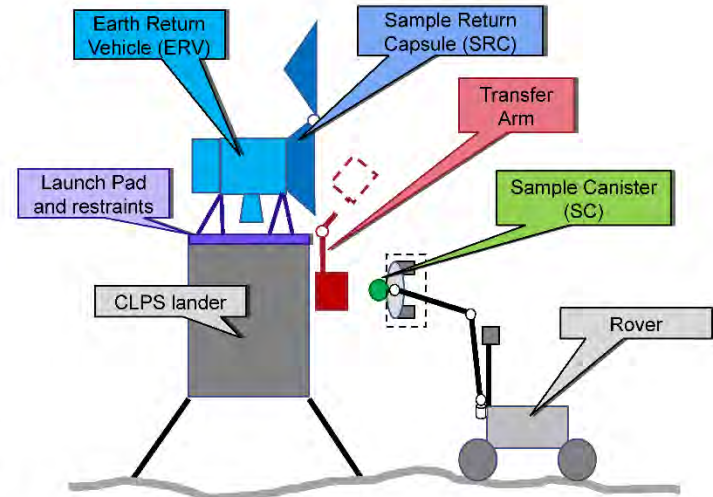
Study Overview



- The goal of this study was to design a *robotic Earth-return* component for the **Lunar Intrepid+ Rover** concept, as a mid-decadal study for the Planetary Science decadal survey process. Lunar Intrepid+ would be a multi-lunar-day rover mission to the lunar far side south polar region, to collect regolith and rock samples over a large region, for return to Earth. Two approaches are being considered for Earth return: either return by astronauts, or a robotic return. This study is *just* for the robotic return component, including:
 - An atmospheric entry system (the “**Sample Return Capsule**” or **SRC**), launched from the lunar surface by...
 - An **Earth Return Vehicle (ERV)** which would launch from...
 - A **Launch Pad** with launch restraints, to hold and release the ERV
 - A **Transfer Arm** would transfer the **Sample Canister (SC)** (customer pass-through mass) from the Rover to the ERV
- ... with all of this (except the Sample Canister) to be delivered to the Lunar surface by a **Commercial Lunar Payload Service (CLPS)** lander
- **Customer Inputs**
 - Architecture description
 - Assumptions about the samples and their container
 - Concept of operations
- **Team X Outputs**
 - Cost for the robotic Earth return component (SRC, ERV, Launch Pad, Arm, Delivery by CLPS)
 - Estimate for Science cost of the Earth-based sample analysis
 - Design for the ERV, Launch Pad, and Arm; with assumptions for the SRC (based on OSIRIS-ReX Sample Return Capsule)

Architecture

(Cartoon adapted from customer inputs)



Colored elements are within the scope of this study; items in gray are not

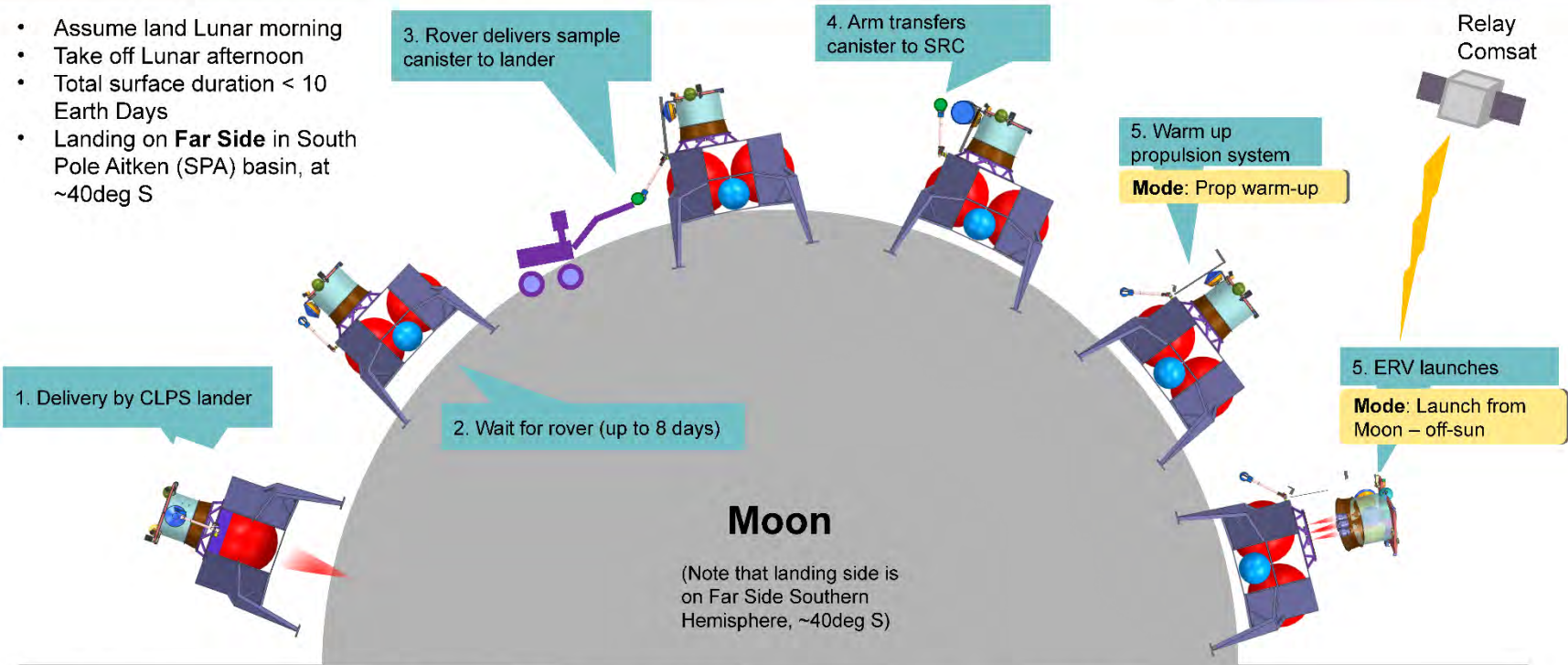


Systems

Concept of Operations (1/2)



- Assume land Lunar morning
- Take off Lunar afternoon
- Total surface duration < 10 Earth Days
- Landing on **Far Side** in South Pole Aitken (SPA) basin, at ~40deg S



Study ID: 369

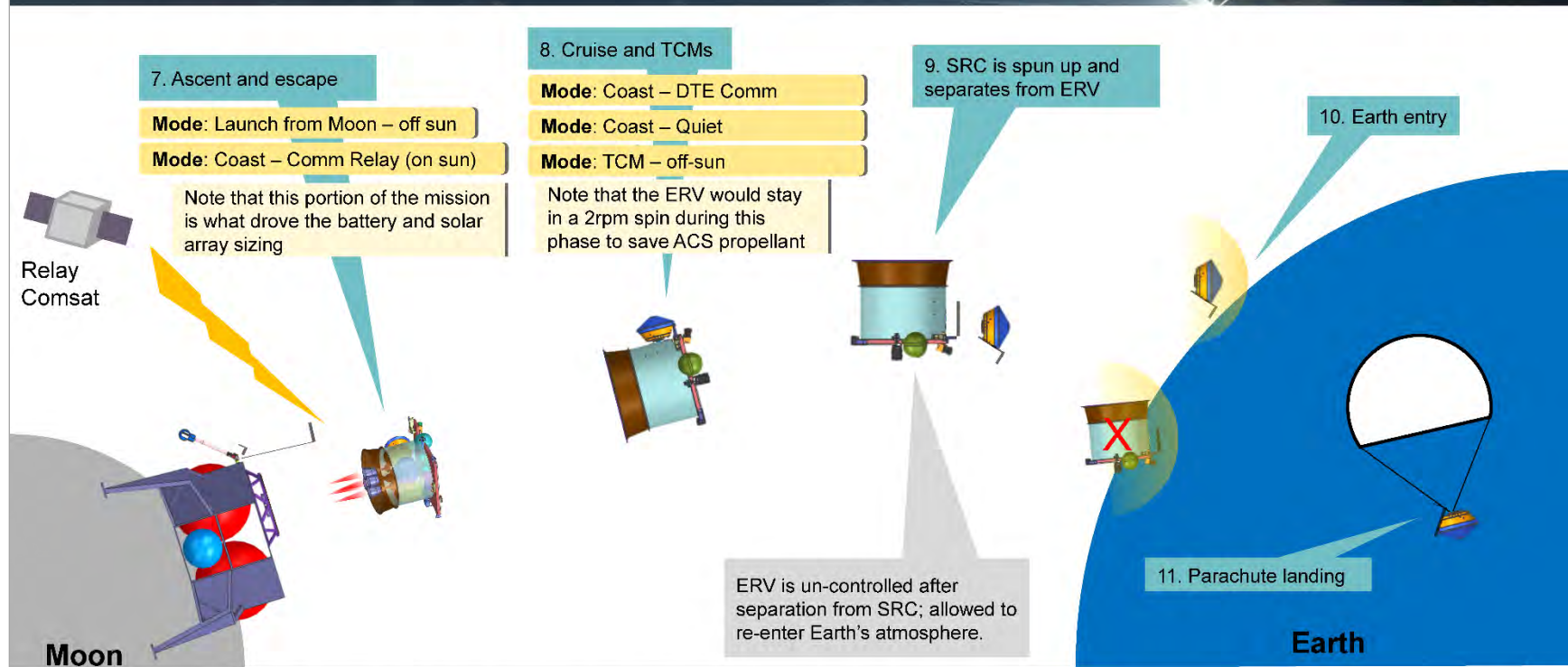
JPL/Caltech Proprietary, for JPL internal release only by 4X Planetary Decadal – Concept 4 Team, JPL customer team lead: John Elliott

13



Systems

Concept of Operations (2/2)



Study ID: 369

JPL/Caltech Proprietary, for JPL internal release only by 4X Planetary Decadal – Concept 4 Team, JPL customer team lead: John Elliott

14



Systems

Design Assumptions



- The Sample Return Capsule (SRC) was based on the OSIRIS-ReX Sample Return Capsule
 - The OSIRIS-ReX SRC is itself based on the Stardust SRC
 - The OSIRIS-ReX as-launched CBE mass was used as the CBE mass for this SRC (46.5kg)
 - Given the uncertainty in the Sample Canister (SC), and given that the actual mass of samples (2.4kg) is slightly higher than the OSIRIS-ReX sample size (2kg), standard JPL Margin policies were applied (30% JPL Margin, equivalent to 43% of CBE mass, see Margin Policy slide)
 - At first glance, it seems quite likely that the OSIRIS-ReX SRC could be used with minimal modification. See Configuration report for CAD sketches.
- 500kg used as an initial mass allocation for launching as a CLPS payload. However, the design did not close under that mass, and the mass was allowed to grow until we had a self-consistent “converged” design.



Systems

System Guidelines



Team X Study Guidelines		Spacecraft												
<p>4X Planetary Decadal - Lunar Intrepid + Sample Return Earth Return Vehicle</p> <p><i>Project - Study</i></p> <p>Customer: John Elliott Study Lead: Alfred Nash Study Type: Lunar Study Report Type: Standard Report</p> <p><i>Project - Mission</i></p> <p>Mission: 4X Planetary Decadal - Lunar Intrepid + Sample Return Target Body: Moon Launch Date: 1-Apr-34 Mission Duration: 7 months Mission Risk Class: B Technology Cutoff: 2031 Planetary Protection: Outbound: II, Inbound: V Unrestricted Flight System Development Mode: In-House</p> <p><i>Project - Architecture</i></p> <table border="1"> <tr> <td>Sample Return Capsule (SRC)</td> <td>on</td> <td>Earth Return Vehicle (ERV)</td> </tr> <tr> <td>Earth Return Vehicle (ERV)</td> <td>on</td> <td>Launchpad (with Arm)</td> </tr> <tr> <td>Launchpad (with Arm)</td> <td>on</td> <td>CLPS lander</td> </tr> <tr> <td>CLPS lander</td> <td>on</td> <td>Launch Vehicle</td> </tr> </table> <p>Launch Vehicle: (Unknown; contracted to CLPS lander) Contingency Method: Apply Total System-Level</p>		Sample Return Capsule (SRC)	on	Earth Return Vehicle (ERV)	Earth Return Vehicle (ERV)	on	Launchpad (with Arm)	Launchpad (with Arm)	on	CLPS lander	CLPS lander	on	Launch Vehicle	<p>Spacecraft Instruments</p> <p>Redundancy</p> <p>Stabilization</p> <p>Radiation Total Dose</p> <p>Type of Propulsion Systems</p> <p>Post-Launch Delta-V, m/s</p> <p>P/L Mass CBE, kg</p> <p>Cost Target</p> <p>Mission Cost Category</p> <p>FY\$ (year)</p> <p>Include Phase A cost estimate?</p> <p>Phase A Start</p> <p>Phase A Duration (months)</p> <p>Phase B Duration (months)</p> <p>Phase C/D Duration (months)</p> <p>Review Dates</p> <p>Phase E Duration (months)</p> <p>Phase F Duration (months)</p>
Sample Return Capsule (SRC)	on	Earth Return Vehicle (ERV)												
Earth Return Vehicle (ERV)	on	Launchpad (with Arm)												
Launchpad (with Arm)	on	CLPS lander												
CLPS lander	on	Launch Vehicle												
		<p>Earth Return Vehicle</p> <p>Camera</p> <p>Dual (Hot)</p> <p>3-Axis</p> <p>3.6 krad behind 100 mil. of Aluminum, with an RDM of 2 added.</p> <p>System 1 - Biprop</p> <p>2523.84</p> <p>0.8 kg Payload CBE + 60 kg Sample Return Capsule (SRC) without samples (alloc) + 2 kg SRC Spin-up device - Bus side (alloc) + 5 kg SRC Release Device - Bus Side (alloc) + 2 kg SRC Mounting (alloc) + 7 kg Sample Canister without Samples (alloc) + 2 kg Lunar Samples (alloc)</p> <p><i>Project - Cost and Schedule</i></p> <p>\$500 M</p> <p>Medium - e.g. Discovery, Scout, ESSP</p> <p>2025</p> <p>Yes</p> <p>November 2029</p> <p>9</p> <p>9</p> <p>36</p> <p>PDR - May 2031, CDR - March 2032, ARR - January 2033</p> <p>7</p> <p>4</p>												

Note: the Earth Return Vehicle (ERV) would be 3-axis stabilized during Launch and for SRC release. It would be a slow spinner (rotational axis through the solar array on the “top” of the ERV) during the cruise phase.



Systems

Power Modes



- The table below lists the “Power Modes” that were used for sizing the spacecraft’s power system
- Note that the two modes highlighted blue constituted the driving power sizing scenario; the two in sequence sized the solar array, and the “Launch from Moon – off sun” mode sized the battery
- The “Coast – Eclipse” mode (in gray) ended up not being used, because a mission design was chosen that did not go into eclipse

Mode Name	Prop Warm-up	Launch from Moon - off sun	Coast - Comm Relay	Coast - DTE comm	Coast - Quiet	Coast - Eclipse	TCM - off sun
Duration (hrs)	1.5	0.13*	0.23	8	24	0	0.029
Assumptions	Still on CLPS power	Sun not on arrays Mode applies only for duration of burn Battery sizing mode	Return cruise, after shutting off engines, but before DSN is in view S/C is communicating via comm relay	Return cruise, and DSN is in view S/C is communicating via DSN	Return cruise, and S/C is not communicating	This mode was unused, as mission design was selected to avoid eclipses	S/C is firing engines for Trajectory Correction Maneuver during return cruise (106 seconds)

* Note that due to a late design change, the duration of the Launch from Moon mode should be 10 rather than 8 minutes. This would have a non-zero but small ripple effect through battery size (currently 4.8kg) and the rest of the system.



Systems

Summary MEL - Stack



- The table below summarizes the architectural components of the spacecraft
- The rows in blue are what launch as a CLPS payload, and drive the required CLPS mass allocation
- The rows in red are what launch from the surface of the Moon, and drive the ERV's propulsion design
- Rows in purple are common to both the CLPS payload and the lunar launch

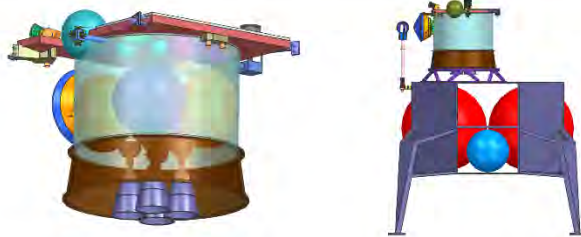
	Name	Dry Mass						Propellant	Wet Mass
		CBE	Contingency	MEV	Allocation	JPL Margin	NASA Margin	Mass	Allocation
		kg	%	kg	kg	%	%	kg	kg
>	Total CLPS Payload	434.4	23%	534.7	619.6	30%	16%	710.9	1320.0
>	Launchpad and Arm	65.5	30%	85.2	93.7	30%	10%	0.0	93.7
>	ERV + SRC (no SC, no samples)	360.9	22%	439.9	515.5	30%	17%	710.9	1226.4
	ERV + SRC + SC + Samples	368.9	22%	449.6	525.9	30%	17%	710.9	1236.8
Launches on CLPS	ERV (Earth Return Vehicle)	314.3	21%	379.5	449.1	30%	18%	710.9	1159.9
>	ERV Instruments	0.8	15%	0.9	1.1	30%	24%	0.0	1.1
>	Carried SRC spin-up device - bus side	2.1	30%	2.8	3.0	30%	10%	0.0	3.0
>	Carried SRC release device - bus side	4.1	30%	5.3	5.8	30%	10%	0.0	5.8
>	Carried SRC mounting	2.3	30%	3.0	3.3	30%	10%	0.0	3.3
>	ERV Bus	305.1	20%	367.5	435.8	30%	19%	710.9	1146.7
>	SRC (Sample Return Capsule)	46.5	30%	60.5	66.4	30%	10%	0.0	66.4
	SC + Samples	8.0	21%	9.7	10.4			0.0	10.4
	SC (Sample Canister)	5.6	30%	7.3	8.0	30%	10%	0.0	8.0
	Lunar Sample	2.4	0%	2.4	2.4	0%	0%	0.0	2.4

Launches from Moon



Systems

Design Summary – Earth Return Vehicle (ERV)



- **Carried Payload**
 - Sample Return Capsule (SRC) with Sample Canister (SC) and Lunar Samples
 - SRC spin-up, release, and mounting hardware
- **Instruments**
 - Engineering camera
- **CDS**
 - Sphinx-based avionics
 - Motor control boards
- **Ground Systems**
 - Relay Satellite during launch from moon
 - DSN during remainder of return trip
 - 2x 8hr passes per day around launch
 - 1x 8hr passes per day during cruise
 - Continuous coverage for 4 weeks leading to EDL
- **Telecom**
 - S-band LGA
 - UST-Lite
- **ACS**
 - Sun sensors, star trackers, IMUs
- **Structures**
 - Primary Structure Mass MEV= 122 kg
 - Secondary Structure Mass MEV = 6.3 kg
 - Harness MEV = 20kg
- **Thermal**
 - MLI, heaters
- **Power**
 - Fixed array, facing up: 1.55m²
 - Battery sized for launch
 - High-efficiency electronics
- **Propulsion**
 - Biprop dual-mode system
 - 4x main engines (for launch)
 - 4x RCS engines (for launch and TCMs)
 - 8x small RCS engines (for ACS)



Systems

Summary Sheet – ERV (and carried elements)



	Mass Fraction	Mass (kg)	Subsys Cont. %	CBE+ Cont. (kg)	Mode 1 Power (W) Prop Warm-up	Mode 2 Power (W) Launch from Moon	Mode 3 Power (W) Coast - Comm Relay	Mode 4 Power (W) Coast - DTE comm	Mode 5 Power (W) Coast - Quiet	Mode 6 Power (W) Coast - Eclipse	Mode 7 Power (W) TCM - off sun
Power Mode Duration (hours)					1.5	0.13333	0.23333	8	24	0	0.02944
Payload on this Element											
Instruments	0%	0.8	15%	0.9	0	0	0	0	0	0	0
Payload Total	0%	0.8	15%	0.9	0	0	0	0	0	0	0
Additional Elements Carried by this Element											
Sample Return Capsule (SRC) without samples	13%	46.5	30%	60.5							
SRC Spin-up device - Bus side	1%	2.1	30%	2.8							
SRC Release Device - Bus Side	1%	4.1	30%	5.3							
SRC Mounting	1%	2.3	30%	3.0							
Sample Canister without Samples	2%	5.6	30%	7.3							
Lunar Samples	1%	2.4	0%	2.4							
Carried Elements Total	17%	63.0	29%	81.2	0	0	0	0	0	0	0
Spacecraft Bus											
Altitude Control	4%	15.4	10%	16.9	0	43	43	43	43	43	43
Command & Data	2%	8.3	17%	9.7	10	21	10	10	10	10	10
Power	6%	20.9	39%	29.1	15	22	20	20	20	20	23
Propulsion <input type="checkbox"/> SEP1	29%	105.4	6%	111.5	47	184	3	3	3	3	138
Structures & Mechanisms	30%	110.0	30%	143.0	0	0	0	0	0	0	0
S/C-Side Adaptor	0%	0.0	0%	0.0							
Cabling	4%	15.5	30%	20.1							
Telecom	2%	8.3	16%	9.7	30	30	30	30	10	10	30
Thermal	6%	21.2	30%	27.5	8	8	140	140	140	140	108
Bus Total		305.1	20%	367.5	111	307	246	246	226	226	351
Thermal Subsystem Mass											
Spacecraft Total (Dry): CBE & MEV		368.9	22%	449.6	111	307	246	246	226	226	351
Subsystem Heritage Contingency	22%	80.7			0	0	0	0	0	0	0
System Contingency	21%	76.3			48	132	106	106	97	97	151
Total Contingency <input type="checkbox"/> Include Carried?	43%	157.1									
Spacecraft with Contingency:		526	of total	w/o ardl pkl	159	439	352	352	323	323	502
Propellant & Pressurant with residuals:1	57%	710.9									
Spacecraft Total with Contingency (Wet)		1237			1240.0						10.5
LV-Side Adaptor		0.0			1237		BOL Power: 474.3	W			
S/C Launches from Earth without Samples		-10.4									
Launchpad and Arm (Margined)		93.7									
Launch Mass (on CLPS)		1320			526		EOL Power: 424.0	W			
CLPS Capability Required		1320									
Dry Mass Allocation: MPV		609.2									
JPL Design Principles Margin		182.8	30%	(6%)							
NASA Margin		84.1	16%	(6%)							

The table at left shows a high-level mass and power summary of the ERV component of the mission, along with the components that the ERV must be sized to carry from the Lunar surface.

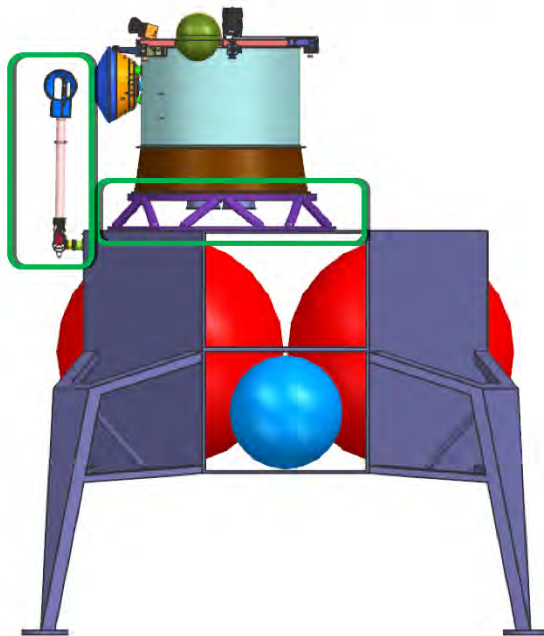
At the bottom, the launch mass has been adjusted to reflect the mass that the CLPS lander will need to launch with.

Systems Note: The Thermal subsystem mass and power on this table is slightly higher than the final values due to a technical error with the workbooks during the study. The correct values are lower and should have an overall positive effect on the converged design. The correct values are reported in the Thermal Section and are 20.8kg / 27.0kg CBE/MEV mass and a max of 129.5W Power.



Systems

Design Summary – Launch Pad and Arm



The Launch Pad and Arm consisted only of structural and mechanical elements.

- Structures and Mechanisms
 - Transfer arm MEV = 13 kg
 - Launch platform, support, & locks MEV = 59.2 kg
 - Harness MEV = 13 kg



Systems

Summary Sheet – Launch pad and Arm



	Mass Fraction	Mass (kg)	Subsys Cont. %	CBE+ Cont. (kg)
Spacecraft Bus				
Structures & Mechanisms	85%	55.5	30%	72.2
Cabling	15%	10.0	30%	13.0
Bus Total		65.5	30%	85.2
Thermally Controlled Mass				85.2
Spacecraft Total (Dry): CBE & MEV		65.5	30%	85.2
Subsystem Heritage Contingency	30%	19.7		
System Contingency	13%	8.5		
Total Contingency <input type="checkbox"/> Include Carried?	43%	28.2		
Spacecraft with Contingency:		94	of total	w/o addl pld
Spacecraft Total with Contingency (Wet)		94		

The Launch pad and robotic transfer arm were modeled as a separate element. The table at left shows a high-level summary of the mass of that element. See Mechanical report for a detailed breakdown.



Systems

Margin and Contingency Guidelines



- To ensure compliance with JPL's Design Principles (v8), we asserted a 30% JPL Dry Mass Margin on launch mass
 - JPL Dry Mass Margin = $(\text{Dry Capability} - \text{CBE Dry Mass}) / (\text{Dry Capability})$
 - Dry Capability = Launch Allocation – Propellant Mass
 - In the case of this study, the Launch Allocation was allowed to “float” such that the design converged with 30% JPL Dry Mass Margin
 - 30% JPL Dry Mass Margin corresponds to a 43% increase over the CBE dry mass
 - Margined Dry Mass = $1.43 * \text{CBE Dry Mass}$
 - Margined wet mass (margined dry mass (payload+bus) plus propellant) was used to size the propulsion system
 - No margin was added on the 2.4kg of rock samples; all other dry masses were margined
- NASA Margin was also calculated and is shown in mass tables; however, it did not drive the design
 - NASA Dry Mass Margin = $(\text{Dry Capability} - \text{MEV Dry Mass}) / (\text{MEV Dry Mass})$
- Payload power values were also assigned 30% JPL Margin (43% over CBE) for the purposes of sizing



Systems

Conclusions, Risks, and Recommendations



- At \$716M (FY25) for A-D, not including launch costs, including 50% reserves, the cost of this mission fits comfortably in a New Frontiers allocation. See Cost report for full bookkeeping.
- This concept closed at 1321kg wet (including 30% JPL Margin), considerably over the 500kg target mass
 - 500kg was considered “safe” as a minimum CLPS capability; however, there may at some point be CLPS landers that can deliver more mass, and 1321kg may well be eventually feasible
 - The result is not surprising, as this design is similar in both mass and function to the ascent vehicle for the MoonRise concept
- Except for the higher-than-desired launch mass, there do not appear to be any major technical risks for this sample return portion of the mission
- As a high ΔV mission (essentially a launch vehicle), the design was driven primarily by propulsion and structures
 - It is very sensitive to changes in propulsion design
 - It is very sensitive to changes in structural mass fraction, which ripple through the Propulsion design with a feedback loop. Since the Team X design is based on historical structural mass fractions rather than on a specific structural design, there may be opportunities to reduce the overall mass through a careful structural design (possibly including a coupled propulsion/structural optimization approach)



C.3 COMBINED MISSION REPORT



Lunar Intrepid+ Follow-On

Customers: James Keane, John Elliott

Facilitator: Al Nash

Session Dates: April 7, 2021





Data Use Policy



- The information and data contained in this document may include restricted information considered JPL/Caltech Proprietary, Proposal Sensitive, Third-party Proprietary, and/or Export Controlled. This document has not been reviewed for export control. It may not be distributed to, or accessed by, foreign persons.
- The data contained in this document may not be modified in any way.
- Distribution of this document is constrained by the terms specified in the footer on each page of the report.



Team X Participants



- **Al Nash**(Facilitator)
- **Mason Takidin** (Cost)
- **Greg Welz** (Ground Systems)
- **Alex Austin** (Systems)



Table of Contents



- 1. Systems
- 2. Ground Systems
- 3. Cost



Systems Report

Author: Alex Austin

Email: Alexander.Austin@jpl.nasa.gov

Phone: (818) 393-7521





Systems

Study Overview



- The goal of this study was to estimate the total cost of a mission which includes both the Intrepid+ Rover and a Sample Return Vehicle.
- The rover comes from the Team X Lunar Intrepid+ Rover Study (Team X ID: 370)
- The Sample Return Vehicle comes from the Team X Lunar Intrepid+ Sample Return Study (Team X ID: 369)

- This was a **cost only** study. No technical design work was done beyond what was previously finalized in the earlier Team X studies.

- Team X costed 4 options:
 1. Customer specified project schedule (approximately New Frontiers class) with 50% Phase A-D Reserves and 25% Phase E-F Reserves
 2. Customer specified project schedule (approximately New Frontiers class) with 30% Phase A-D Reserves and 15% Phase E-F Reserves
 3. Team X recommended project schedule (approximately Flagship class) with 50% Phase A-D Reserves and 25% Phase E-F Reserves
 - The schedules for the individual elements (rover and sample return vehicle) were unchanged, with the assumption that they would be phased within the total project schedule.
 4. Team X recommended project schedule (approximately Flagship class) with 30% Phase A-D Reserves and 15% Phase E-F Reserves
 - The schedules for the individual elements (rover and sample return vehicle) were unchanged, with the assumption that they would be phased within the total project schedule.



Cost Report

Author: Mason Takidin
Email: mason.r.takidin@jpl.nasa.gov
Phone: (626) 567 - 6123





Cost

Disclaimer



The costs presented in this report are ROM estimates, not point estimates or cost commitments. It is likely that each estimate could range from as much as 20% percent higher to 10% lower. The costs presented are based on Pre-Phase A design information, which is subject to change.



Cost

Cost Requirements



- Constant/Real Year Dollars: FY25
- Estimates are generated using the TeamX ICMs
- Cost estimates are lifecycle costs provided at WBS level 2 and WBS level 3 for the Flight System
- Launch date is 4/30/2030

- Total Mission cost for a Rover and a Earth Return Vehicle.



Cost

Cost Assumptions



- Fiscal Year: FY25
- Mission Class: A
- Cost Category: New Frontiers

- Wrap Factors
 - Mission Assurance 4%
 - Phases A-D Reserves 50% and 30% - Not calculated on LV and Tracking costs
 - Phases E-F Reserves 25% and 15% - Not calculated on LV and Tracking costs

- \$70M included for RTG and Launch Vehicle Nuclear Payload Support



Cost

Cost Assumptions – Schedule



- Based on **New Frontiers class** mission schedule
 - Development schedule duration - **75 months**
 - Mission Operations duration - **50 months**, plus **6 months** for Phase F

Phase	Duration (Mo.)
A-D	75
E	50
F	6

Phase	Duration
Phase A	14 mo.
Phase B	15 mo.
Phase C	22 mo.
Design	11 mo.
Fabrication	6 mo.
Subsystem I&T	5 mo.
Phase D	24 mo.
System I&T	18 mo.
Launch Operations	6 mo.
Phase E	50 mo.
Phase F	6 mo.



Cost

Cost Assumptions



- Costing Methods:
 - Project (WBS 01) – Calculated using Team X Institutional Cost Model.
 - PSE (WBS 02) – Calculated using Team X Institutional Cost Model.
 - Science (WBS 04) - Estimate provided by Team X Science Chair
 - Payload (WBS 05) – Estimate provided by Team X Instrument Chair.
 - Flight System (WBS 06) – Estimate provided by Team X Chairs.
 - RPS Cost for rover included (\$70M). Reserve not calculated for this element.
 - MOS (WBS 07) - Estimate provided by Team X MOS Chair.
 - GDS (WBS 09) - Estimate provided by Team X GDS Chair.
 - ATLO (WBS 10) - Estimate provided by Team X Chair
 - Mission Design (WBS 12) not included in study.



Cost

Total Cost



- Assuming 50% Development and 25% Operations Reserves

COST SUMMARY (FY2025 \$M)	Team X Estimate		
	CBE	Res.	PBE
Project Cost	\$1814.0 M	34%	\$2430.3 M
Launch Vehicle	\$400.0 M	0%	\$400.0 M
Project Cost (w/o LV)	\$1414.0 M	44%	\$2030.3 M
Development Cost	\$1208.8 M	47%	\$1778.2 M
Phase A	\$12.1 M	47%	\$17.8 M
Phase B	\$108.8 M	47%	\$160.0 M
Phase C/D	\$1087.9 M	47%	\$1600.4 M
Operations Cost	\$205.2 M	23%	\$252.1 M

- Includes \$400M LV for 2 CLPS Landers



Cost

Cost A-D with 50% reserves



WBS Elements	ProPricer Input	NRE	RE	1st Unit
Project Cost (including Launch Vehicle)		\$2011.3 M	\$419.0 M	\$2430.3 M
Development Cost (Phases A - D)		\$1359.2 M	\$419.0 M	\$1778.2 M
01.0 Project Management		\$44.8 M		\$44.8 M
02.0 Project Systems Engineering		\$41.7 M	\$1.2 M	\$42.9 M
03.0 Mission Assurance		\$39.7 M	\$11.9 M	\$51.7 M
04.0 Science		\$35.0 M		\$35.0 M
05.0 Payload System		\$51.7 M	\$25.3 M	\$77.0 M
5.01 Payload Management		\$9.9 M		\$9.9 M
5.02 Payload Engineering		\$8.3 M		\$8.3 M
Instruments		\$33.5 M	\$25.3 M	\$58.8 M
ARMAS		\$1.2 M	\$0.9 M	\$2.1 M
Magnetometer		\$1.8 M	\$1.3 M	\$3.1 M
Gamma Ray Neutron Spectrometer (GRNS)		\$5.2 M	\$3.7 M	\$8.9 M
TriCam		\$8.2 M	\$6.0 M	\$14.2 M
Point Spectrometer		\$3.7 M	\$2.6 M	\$6.3 M
Hand Lens Imager (HLI)		\$3.0 M	\$2.2 M	\$5.2 M
APXS cryocooler		\$4.7 M	\$3.4 M	\$8.1 M
Elect Analyzer		\$4.1 M	\$3.0 M	\$7.1 M
Laser Corner Reflector		\$0.1 M	\$0.1 M	\$0.3 M
Cameras (ERV)		\$1.5 M	\$2.1 M	\$3.6 M

WBS Elements	ProPricer Input	NRE	RE	1st Unit
06.0 Flight System		\$575.1 M	\$220.2 M	\$795.3 M
6.01 Flight System Management		\$6.1 M		\$6.1 M
6.02 Flight System Systems Engineering		\$61.6 M		\$61.6 M
6.03 Flight System Reserves (includes In-CAL)				
Rover		\$301.0 M	\$120.0 M	\$421.0 M
6.04 Power		\$15.2 M	\$10.4 M	\$25.6 M
6.04B RPS		\$70.0 M	\$0.0 M	\$70.0 M
6.05 C&DH		\$24.7 M	\$44.2 M	\$68.9 M
6.06 Telecom		\$17.7 M	\$10.1 M	\$27.8 M
6.07 Structures (includes Mech. I&T)		\$88.6 M	\$28.0 M	\$116.6 M
6.08 Thermal		\$2.6 M	\$4.4 M	\$7.0 M
6.09 Propulsion		\$0.0 M	\$0.0 M	\$0.0 M
6.10 ACS		\$16.3 M	\$14.0 M	\$30.3 M
6.11 Harness		\$5.7 M	\$5.3 M	\$11.0 M
6.12 S/C Software		\$53.8 M	\$2.8 M	\$56.6 M
6.13 Materials and Processes		\$6.4 M	\$0.7 M	\$7.2 M
Earth Return Vehicle		\$140.0 M	\$87.4 M	\$227.4 M
Launch Pad and Arm		\$20.5 M	\$8.5 M	\$28.9 M
Sample Return Capsule		\$32.7 M	\$0.0 M	\$32.7 M
6.14 Spacecraft Testbeds		\$13.2 M	\$4.4 M	\$17.7 M
07.0 Mission Operations Preparation		\$43.7 M		\$43.7 M
7.0 MOS Teams		\$42.8 M		\$42.8 M
7.03 Tracking (Launch Ops.)		\$0.0 M		\$0.0 M
7.06 Navigation Operations Team		\$1.0 M		\$1.0 M
7.08 Mission Planning Team		\$0.0 M		\$0.0 M
09.0 Ground Data Systems		\$47.4 M		\$47.4 M
10.0 ATLO		\$40.9 M	\$20.6 M	\$61.5 M
11.0 Education and Public Outreach		\$0.0 M	\$0.0 M	\$0.0 M
12.0 Mission and Navigation Design		\$9.4 M		\$9.4 M
Development Reserves		\$429.7 M	\$139.7 M	\$569.4 M

370 Lunar Intrepid+ Follow-On

JPL/Caltech Proprietary, for JPL internal release only by Lunar Intrepid+ Follow-On, JPL customer team lead: James Keane



Cost

Cost E-F with 25% Reserves



WBS Elements	ProPricer Input	NRE	RE	1st Unit
Operations Cost (Phases E - F)		\$252.1 M	\$0.0 M	\$252.1 M
01.0 Project Management		\$11.0 M		\$11.0 M
02.0 Project Systems Engineering		\$0.0 M	\$0.0 M	\$0.0 M
03.0 Mission Assurance		\$0.0 M	\$0.0 M	\$0.0 M
04.0 Science		\$81.6 M		\$81.6 M
06.0 Flight System		\$0.0 M		\$0.0 M
07.0 Mission Operations		\$79.5 M		\$79.5 M
09.0 Ground Data Systems		\$33.1 M		\$33.1 M
11.0 Education and Public Outreach		\$0.0 M	\$0.0 M	\$0.0 M
12.0 Mission and Navigation Design		\$0.0 M		\$0.0 M
Operations Reserves		\$47.0 M	\$0.0 M	\$47.0 M
8.0 Launch Vehicle		\$400.0 M		\$400.0 M
Launch Vehicle and Processing		\$0.0 M		\$0.0 M
CLPS Lander		\$400.0 M		\$400.0 M



Cost

Total Cost



- **Assuming 30% Development and 15% Operations Reserves**

COST SUMMARY (FY2025 \$M)	Team X Estimate		
	CBE	Res.	PBE
Project Cost	\$1814.0 M	20%	\$2183.8 M
Launch Vehicle	\$400.0 M	0%	\$400.0 M
Project Cost (w/o LV)	\$1414.0 M	26%	\$1783.8 M
Development Cost	\$1208.8 M	28%	\$1550.4 M
Phase A	\$12.1 M	28%	\$15.5 M
Phase B	\$108.8 M	28%	\$139.5 M
Phase C/D	\$1087.9 M	28%	\$1395.4 M
Operations Cost	\$205.2 M	14%	\$233.4 M

- **Includes \$400M LV for 2 CLPS Landers**



Cost

Cost A-D with 30% reserves



WBS Elements	ProPricer Input	NRE	RE	1st Unit
Project Cost (including Launch Vehicle)		\$1820.6 M	\$363.1 M	\$2183.8 M
Development Cost (Phases A - D)		\$1187.3 M	\$363.1 M	\$1550.4 M
01.0 Project Management		\$44.8 M		\$44.8 M
02.0 Project Systems Engineering		\$41.7 M	\$1.2 M	\$42.9 M
03.0 Mission Assurance		\$39.7 M	\$11.9 M	\$51.7 M
04.0 Science		\$35.0 M		\$35.0 M
05.0 Payload System		\$51.7 M	\$25.3 M	\$77.0 M
5.01 Payload Management		\$9.9 M		\$9.9 M
5.02 Payload Engineering		\$8.3 M		\$8.3 M
Instruments		\$33.5 M	\$25.3 M	\$58.8 M
ARMAS		\$1.2 M	\$0.9 M	\$2.1 M
Magnetometer		\$1.8 M	\$1.3 M	\$3.1 M
Gamma Ray Neutron Spectrometer (GRNS)		\$5.2 M	\$3.7 M	\$8.9 M
TriCam		\$8.2 M	\$6.0 M	\$14.2 M
Point Spectrometer		\$3.7 M	\$2.6 M	\$6.3 M
Hand Lens Imager (HLI)		\$3.0 M	\$2.2 M	\$5.2 M
APXS-cryocooler		\$4.7 M	\$3.4 M	\$8.1 M
Elect Analyzer		\$4.1 M	\$3.0 M	\$7.1 M
Laser Corner Reflector		\$0.1 M	\$0.1 M	\$0.3 M
Cameras (ERV)		\$1.5 M	\$2.1 M	\$3.6 M

WBS Elements	ProPricer Input	NRE	RE	1st Unit
06.0 Flight System		\$575.1 M	\$220.2 M	\$795.3 M
6.01 Flight System Management		\$6.1 M		\$6.1 M
6.02 Flight System Systems Engineering		\$61.6 M		\$61.6 M
6.03 Power, Robotics, Instrumentation, etc.				
Rover		\$301.0 M	\$120.0 M	\$421.0 M
6.04 Power		\$15.2 M	\$10.4 M	\$25.6 M
6.04B RPS		\$70.0 M	\$0.0 M	\$70.0 M
6.05 C&DH		\$24.7 M	\$44.2 M	\$68.9 M
6.06 Telecom		\$17.7 M	\$10.1 M	\$27.8 M
6.07 Structures (includes Mech. I&T)		\$88.6 M	\$28.0 M	\$116.6 M
6.08 Thermal		\$2.6 M	\$4.4 M	\$7.0 M
6.09 Propulsion		\$0.0 M	\$0.0 M	\$0.0 M
6.10 ACS		\$16.3 M	\$14.0 M	\$30.3 M
6.11 Harness		\$5.7 M	\$5.3 M	\$11.0 M
6.12 S/C Software		\$53.8 M	\$2.8 M	\$56.6 M
6.13 Materials and Processes		\$6.4 M	\$0.7 M	\$7.2 M
Earth Return Vehicle		\$140.0 M	\$87.4 M	\$227.4 M
Launch Pad and Arm		\$20.5 M	\$8.5 M	\$28.9 M
Sample Return Capsule		\$32.7 M	\$0.0 M	\$32.7 M
6.14 Spacecraft Testbeds		\$13.2 M	\$4.4 M	\$17.7 M
07.0 Mission Operations Preparation		\$43.7 M		\$43.7 M
7.0 MOS Teams		\$42.8 M		\$42.8 M
7.03 Tracking (Launch Ops.)		\$0.0 M		\$0.0 M
7.06 Navigation Operations Team		\$1.0 M		\$1.0 M
7.08 Mission Planning Team		\$0.0 M		\$0.0 M
09.0 Ground Data Systems		\$47.4 M		\$47.4 M
10.0 ATLO		\$40.9 M	\$20.6 M	\$61.5 M
11.0 Education and Public Outreach		\$0.0 M	\$0.0 M	\$0.0 M
12.0 Mission and Navigation Design		\$9.4 M		\$9.4 M
Development Reserves		\$257.8 M	\$83.8 M	\$341.6 M

370 Lunar Intrepid+ Follow-On

JPL/Caltech Proprietary, for JPL internal release only by Lunar Intrepid+ Follow-On, JPL customer team lead: James Keane



Cost

Cost E-F with 15% Reserves



WBS Elements	ProPricer Input	NRE	RE	1st Unit
Operations Cost (Phases E - F)		\$233.3 M	\$0.0 M	\$233.4 M
01.0 Project Management		\$11.0 M		\$11.0 M
02.0 Project Systems Engineering		\$0.0 M	\$0.0 M	\$0.0 M
03.0 Mission Assurance		\$0.0 M	\$0.0 M	\$0.0 M
04.0 Science		\$81.6 M		\$81.6 M
06.0 Flight System		\$0.0 M		\$0.0 M
07.0 Mission Operations		\$79.5 M		\$79.5 M
09.0 Ground Data Systems		\$33.1 M		\$33.1 M
11.0 Education and Public Outreach		\$0.0 M	\$0.0 M	\$0.0 M
12.0 Mission and Navigation Design		\$0.0 M		\$0.0 M
Operations Reserves		\$28.2 M	\$0.0 M	\$28.2 M
8.0 Launch Vehicle		\$400.0 M		\$400.0 M
Launch Vehicle and Processing		\$0.0 M		\$0.0 M
CLPS Lander		\$400.0 M		\$400.0 M



Cost

Cost Rationale



- Cost Drivers
 - \$70M included in 06 FS under 06.04B for RPS. (Reserve not included in this amount)
 - 50 Months costed for Operations (Phase E)
 - Assumed 2 CLPS Landers for transportation to landing site (\$400M under LV)



Cost

Cost Assumptions – Schedule



It was noted that the New Frontiers project schedule may be short for this mission, so a cost was generated with a Flagship project schedule as well. The schedules for the individual elements (rover and sample return vehicle) were unchanged, with the assumption that they would be phased within the total project schedule.

- Based on **Flagship class** mission schedule
 - Development schedule duration - **96 months**
 - Mission Operations duration - **50 months**, plus **6 months** for Phase F

Phase	Duration (Mo.)
A-D	96
E	50
F	6

Phase	Duration
Phase A	14 mo.
Phase B	18 mo.
Phase C	41 mo.
Design	20 mo.
Fabrication	12 mo.
Subsystem I&T	9 mo.
Phase D	23 mo.
System I&T	17 mo.
Launch Operations	6 mo.
Phase E	50 mo.
Phase F	6 mo.



Cost

Total Cost – Assuming a Flagship Class Schedule



- **Assuming 50% Development and 25% Operations Reserves**

COST SUMMARY (FY2025 \$M)	Team X Estimate		
	CBE	Res.	PBE
Project Cost	\$1873.3 M	34%	\$2519.3 M
Launch Vehicle	\$400.0 M	0%	\$400.0 M
Project Cost (w/o LV)	\$1473.3 M	44%	\$2119.3 M
Development Cost	\$1268.1 M	47%	\$1867.1 M
Phase A	\$12.7 M	47%	\$18.7 M
Phase B	\$114.1 M	47%	\$168.0 M
Phase C/D	\$1141.3 M	47%	\$1680.4 M
Operations Cost	\$205.2 M	23%	\$252.1 M

- **Includes \$400M LV for 2 CLPS Landers**



Cost

Cost A-D with 50% reserves



WBS Elements	ProPricer Input	NRE	RE	1st Unit
Project Cost (including Launch Vehicle)		\$2097.1 M	\$422.1 M	\$2519.3 M
Development Cost (Phases A - D)		\$1445.0 M	\$422.1 M	\$1867.1 M
01.0 Project Management		\$54.3 M		\$54.3 M
02.0 Project Systems Engineering		\$53.5 M	\$1.2 M	\$54.7 M
03.0 Mission Assurance		\$44.8 M	\$12.8 M	\$57.6 M
04.0 Science		\$35.0 M		\$35.0 M
05.0 Payload System		\$51.7 M	\$25.3 M	\$77.0 M
5.01 Payload Management		\$9.9 M		\$9.9 M
5.02 Payload Engineering		\$8.3 M		\$8.3 M
Instruments		\$33.5 M	\$25.3 M	\$58.8 M
ARMAS		\$1.2 M	\$0.9 M	\$2.1 M
Magnetometer		\$1.8 M	\$1.3 M	\$3.1 M
Gamma Ray Neutron Spectrometer (GRNS)		\$5.2 M	\$3.7 M	\$8.9 M
TriCam		\$8.2 M	\$6.0 M	\$14.2 M
Point Spectrometer		\$3.7 M	\$2.6 M	\$6.3 M
Hand Lens Imager (HLI)		\$3.0 M	\$2.2 M	\$5.2 M
APXS-cryocooler		\$4.7 M	\$3.4 M	\$8.1 M
Elect Analyzer		\$4.1 M	\$3.0 M	\$7.1 M
Laser Corner Reflector		\$0.1 M	\$0.1 M	\$0.3 M
Cameras (ERV)		\$1.5 M	\$2.1 M	\$3.6 M

WBS Elements	ProPricer Input	NRE	RE	1st Unit
06.0 Flight System		\$602.8 M	\$220.6 M	\$823.4 M
6.01 Flight System Management		\$8.0 M		\$8.0 M
6.02 Flight System Systems Engineering		\$86.3 M		\$86.3 M
6.03 Payload Engineering (includes Mech. I&T)				
Rover		\$301.0 M	\$120.0 M	\$421.0 M
6.04 Power		\$15.2 M	\$10.4 M	\$25.6 M
6.04B RPS		\$70.0 M	\$0.0 M	\$70.0 M
6.05 C&DH		\$24.7 M	\$44.2 M	\$68.9 M
6.06 Telecom		\$17.7 M	\$10.1 M	\$27.8 M
6.07 Structures (includes Mech. I&T)		\$88.6 M	\$28.0 M	\$116.6 M
6.08 Thermal		\$2.6 M	\$4.4 M	\$7.0 M
6.09 Propulsion		\$0.0 M	\$0.0 M	\$0.0 M
6.10 ACS		\$16.3 M	\$14.0 M	\$30.3 M
6.11 Harness		\$5.7 M	\$5.3 M	\$11.0 M
6.12 S/C Software		\$53.8 M	\$2.8 M	\$56.6 M
6.13 Materials and Processes		\$6.4 M	\$0.7 M	\$7.2 M
Earth Return Vehicle		\$140.0 M	\$87.4 M	\$227.4 M
Launch Pad and Arm		\$20.5 M	\$8.5 M	\$28.9 M
Sample Return Capsule		\$32.7 M	\$0.0 M	\$32.7 M
6.14 Spacecraft Testbeds		\$14.3 M	\$4.8 M	\$19.1 M
07.0 Mission Operations Preparation		\$43.7 M		\$43.7 M
7.0 MOS Teams		\$42.8 M		\$42.8 M
7.03 Tracking (Launch Ops.)		\$0.0 M		\$0.0 M
7.06 Navigation Operations Team		\$1.0 M		\$1.0 M
7.08 Mission Planning Team		\$0.0 M		\$0.0 M
09.0 Ground Data Systems		\$47.4 M		\$47.4 M
10.0 ATLO		\$44.1 M	\$21.5 M	\$65.6 M
11.0 Education and Public Outreach		\$0.0 M	\$0.0 M	\$0.0 M
12.0 Mission and Navigation Design		\$9.4 M		\$9.4 M
Development Reserves		\$458.3 M	\$140.7 M	\$599.0 M

370 Lunar Intrepid+ Follow-On

JPL/Caltech Proprietary, for JPL internal release only by Lunar Intrepid+ Follow-On, JPL customer team lead: James Keane



Cost

Cost E-F with 25% Reserves



WBS Elements	ProPricer Input	NRE	RE	1st Unit
Operations Cost (Phases E - F)		\$252.1 M	\$0.0 M	\$252.1 M
01.0 Project Management		\$11.0 M		\$11.0 M
02.0 Project Systems Engineering		\$0.0 M	\$0.0 M	\$0.0 M
03.0 Mission Assurance		\$0.0 M	\$0.0 M	\$0.0 M
04.0 Science		\$81.6 M		\$81.6 M
06.0 Flight System		\$0.0 M		\$0.0 M
07.0 Mission Operations		\$79.5 M		\$79.5 M
09.0 Ground Data Systems		\$33.1 M		\$33.1 M
11.0 Education and Public Outreach		\$0.0 M	\$0.0 M	\$0.0 M
12.0 Mission and Navigation Design		\$0.0 M		\$0.0 M
Operations Reserves		\$47.0 M	\$0.0 M	\$47.0 M
8.0 Launch Vehicle		\$400.0 M		\$400.0 M
Launch Vehicle and Processing		\$0.0 M		\$0.0 M
CLPS Lander		\$400.0 M		\$400.0 M



Cost

Total Cost – Assuming a Flagship Class Schedule



- **Assuming 30% Development and 15% Operations Reserves**

COST SUMMARY (FY2025 \$M)	Team X Estimate		
	CBE	Res.	PBE
Project Cost	\$1873.3 M	21%	\$2260.9 M
Launch Vehicle	\$400.0 M	0%	\$400.0 M
Project Cost (w/o LV)	\$1473.3 M	26%	\$1860.9 M
Development Cost	\$1268.1 M	28%	\$1627.5 M
Phase A	\$12.7 M	28%	\$16.3 M
Phase B	\$114.1 M	28%	\$146.5 M
Phase C/D	\$1141.3 M	28%	\$1464.8 M
Operations Cost	\$205.2 M	14%	\$233.4 M

- **Includes \$400M LV for 2 CLPS Landers**



Cost

Cost A-D with 30% reserves



WBS Elements	ProPricer Input	NRE	RE	1st Unit
Project Cost (including Launch Vehicle)		\$1895.0 M	\$365.9 M	\$2260.9 M
Development Cost (Phases A - D)		\$1261.7 M	\$365.8 M	\$1627.5 M
01.0 Project Management		\$54.3 M		\$54.3 M
02.0 Project Systems Engineering		\$53.5 M	\$1.2 M	\$54.7 M
03.0 Mission Assurance		\$44.8 M	\$12.8 M	\$57.6 M
04.0 Science		\$35.0 M		\$35.0 M
05.0 Payload System		\$51.7 M	\$25.3 M	\$77.0 M
5.01 Payload Management		\$9.9 M		\$9.9 M
5.02 Payload Engineering		\$8.3 M		\$8.3 M
Instruments		\$33.5 M	\$25.3 M	\$58.8 M
ARMAS		\$1.2 M	\$0.9 M	\$2.1 M
Magnetometer		\$1.8 M	\$1.3 M	\$3.1 M
Gamma Ray Neutron Spectrometer (GRNS)		\$5.2 M	\$3.7 M	\$8.9 M
TriCam		\$8.2 M	\$6.0 M	\$14.2 M
Point Spectrometer		\$3.7 M	\$2.6 M	\$6.3 M
Hand Lens Imager (HLI)		\$3.0 M	\$2.2 M	\$5.2 M
APXS-cryocooler		\$4.7 M	\$3.4 M	\$8.1 M
Elect Analyzer		\$4.1 M	\$3.0 M	\$7.1 M
Laser Corner Reflector		\$0.1 M	\$0.1 M	\$0.3 M
Cameras (ERV)		\$1.5 M	\$2.1 M	\$3.6 M

WBS Elements	ProPricer Input	NRE	RE	1st Unit
06.0 Flight System		\$602.8 M	\$220.6 M	\$823.4 M
6.01 Flight System Management		\$8.0 M		\$8.0 M
6.02 Flight System Systems Engineering		\$86.3 M		\$86.3 M
6.03 Flight System Assembly (includes Mech. I&T)				
Rover		\$301.0 M	\$120.0 M	\$421.0 M
6.04 Power		\$15.2 M	\$10.4 M	\$25.6 M
6.04B RPS		\$70.0 M	\$0.0 M	\$70.0 M
6.05 C&DH		\$24.7 M	\$44.2 M	\$68.9 M
6.06 Telecom		\$17.7 M	\$10.1 M	\$27.8 M
6.07 Structures (includes Mech. I&T)		\$88.6 M	\$28.0 M	\$116.6 M
6.08 Thermal		\$2.6 M	\$4.4 M	\$7.0 M
6.09 Propulsion		\$0.0 M	\$0.0 M	\$0.0 M
6.10 ACS		\$16.3 M	\$14.0 M	\$30.3 M
6.11 Harness		\$5.7 M	\$5.3 M	\$11.0 M
6.12 S/C Software		\$53.8 M	\$2.8 M	\$56.6 M
6.13 Materials and Processes		\$6.4 M	\$0.7 M	\$7.2 M
Earth Return Vehicle		\$140.0 M	\$87.4 M	\$227.4 M
Launch Pad and Arm		\$20.5 M	\$8.5 M	\$28.9 M
Sample Return Capsule		\$32.7 M	\$0.0 M	\$32.7 M
6.14 Spacecraft Testbeds		\$14.3 M	\$4.8 M	\$19.1 M
07.0 Mission Operations Preparation		\$43.7 M		\$43.7 M
7.0 MOS Teams		\$42.8 M		\$42.8 M
7.03 Tracking (Launch Ops.)		\$0.0 M		\$0.0 M
7.06 Navigation Operations Team		\$1.0 M		\$1.0 M
7.08 Mission Planning Team		\$0.0 M		\$0.0 M
09.0 Ground Data Systems		\$47.4 M		\$47.4 M
10.0 ATLO		\$44.1 M	\$21.5 M	\$65.6 M
11.0 Education and Public Outreach		\$0.0 M	\$0.0 M	\$0.0 M
12.0 Mission and Navigation Design		\$9.4 M		\$9.4 M
Development Reserves		\$275.0 M	\$84.4 M	\$359.4 M

370 Lunar Intrepid+ Follow-On

JPL/Caltech Proprietary, for JPL internal release only by Lunar Intrepid+ Follow-On, JPL customer team lead: James Keane



Cost

Cost E-F with 15% Reserves



WBS Elements	ProPricer Input	NRE	RE	1st Unit
Operations Cost (Phases E - F)		\$233.3 M	\$0.0 M	\$233.4 M
01.0 Project Management		\$11.0 M		\$11.0 M
02.0 Project Systems Engineering		\$0.0 M	\$0.0 M	\$0.0 M
03.0 Mission Assurance		\$0.0 M	\$0.0 M	\$0.0 M
04.0 Science		\$81.6 M		\$81.6 M
06.0 Flight System		\$0.0 M		\$0.0 M
07.0 Mission Operations		\$79.5 M		\$79.5 M
09.0 Ground Data Systems		\$33.1 M		\$33.1 M
11.0 Education and Public Outreach		\$0.0 M	\$0.0 M	\$0.0 M
12.0 Mission and Navigation Design		\$0.0 M		\$0.0 M
Operations Reserves		\$28.2 M	\$0.0 M	\$28.2 M
8.0 Launch Vehicle		\$400.0 M		\$400.0 M
Launch Vehicle and Processing		\$0.0 M		\$0.0 M
CLPS Lander		\$400.0 M		\$400.0 M



Ground Systems Report

Author: Greg Welz
Email: gwelz@jpl.nasa.gov
Phone: 818 393-4978





Ground Systems

Design Requirements



- Lunar Rover + Earth Return Element
- Assume there can be some sharing of development between Rover and Earth Return Vehicle mission system
 - Sort of reverse Mars Rover mission
 - Will require separate MSA facility and Test/ATLO equipment from Rover
 - Shared leadership
 - Key to maintain Operations knowledge for the ERV while it is in storage



Ground Systems

Cost Assumptions



- Full MOS/GDS cost for Rover Mission
- 80% of ERV Dev + 100% of ERV ops + \$4M for ops retention
 - Assumes sharing of leadership and taking advantage of commonality with rover during development, some reduction in ATLO activity since this is deferred
 - Ops retention assume 3 FTE of effort for 4 years. FTE would be split across several people to maintain all of the ops support knowledge learned during ATLO.
 - May need to add a little more for doing additional ORTs prior to ERV mission operations, not sure where this was book kept in ERV study. Could shift them from late Dev phase in to Phase E.

D MOBILITY

Requirements: We examined mobility trades for the requirements described in Table D-1. While terrain information at the scale of the mobility system is not available for the planned route, it can be inferred from available data and current knowledge of lunar surface formation process. This information includes data from the Apollo missions, full coverage of orbital imagery at 0.5–2 m resolution at different incidence angles from the Lunar Reconnaissance Orbiter Narrow Angle Camera (LRO NAC), derived high-resolution digital-elevation map (DEM) at 2–5 m scale for ~10–25% of the path, 7 m/pixel DEM from Chang-E, lower-resolution DEM from Kaguya Terrain Camera at 60 m scale for the entire path, thermal imaging from Diviner on LRO, and HST (Hubble-Space Telescope) Ultraviolet (UV) and Red, Blue, Green (RBG) imagery of the lunar surface. For the mobility trades, we drew on mobility and navigation expertise from the lunar (Apollo) and martian surface missions. Table D-2 shows the terrain types along the rover’s route.

Based on test data from the Apollo program, mobility on 15°–20° is possible in lunar simulant [85], which exceeds the maximum slope requirement for Endurance. However, for angles exceeding 15°, slip would likely exceed 30% (see Figure G-1).

Mobility configuration: Based on the key requirements of distance, speed, and anticipated terrain properties (topography, regolith properties) (Table D-2), we examined vehicle designs with different wheel/steering configurations (skid-steered, Ackermann-steered, and omni-directional) and with different suspension types (passively and actively articulated). Figure D-1 shows examples of different mobility wheel configurations and suspensions with examples from both flight and research rovers [86].

Table D-1. Mobility Requirements.

Requirement		Comments
Endurance-R: Northern Route		
Nominal Distance	1,750 km	Based 59 m/pixel DEM
Actual Distance	2,050 km	Accounting for terrain tortuosity
Endurance-A: Southern Route		
Nominal Distance	2,000 km	Based 59 and 20 m/pixel DEMs
Actual Distance	2,350 km	Accounting for terrain tortuosity
Rover		
Max wheel speed	1 km/hr	Mechanical speed (or 28 cm/s)
Ave traverse rate (day)	0.65 km/hr	Incl. eng. stops for localization
Ave traverse rate (night)	0.35 km/hr	Also incl. long-exposure imaging
Max slope	20°	Unobservable at rover scale
Environment for both		
Nominal regolith (largely ubiquitous)	Fine Coarse	30%: 40–100 μm angular fines 70%: mm – cm regolith
Worst terrain	Interior crater walls	
Nominal sinkage	2 – 5 cm	In regolith
Crater distribution	10% 20%	Diameter: 5 m < φ < 35 m Diameter: φ < 5 m
Small crater slopes	7° – 8°	Depth = 0.17 φ (diameter) at formation w/ rapid degradation
Rock distribution (area coverage)	1% 10%	Most of the traverse route Around crater rims
Obstacle height	±0.25 m	Max traversable ± obstacle

Table D-2. Terrain types for mobility and navigation.

Direction	Slope Range	Northern Route (Endurance-R)	Southern Route (Endurance-A)	% Skid or Slip (estimate)	Likely Rock Abundance		Source
		% of Path	% of Path		< 1 m	> 1 m	
Downslope	-15° ≤ α < -13°	0.4%	0%	-15%	Medium	2–15%	DEM 59 m/pixel
	-13° ≤ α < -10°	0.4%	1.0%	-12%	Medium-low	2–15%	
	-10° ≤ α < -5°	4.6%	6.1%	-9%	Low	< 2%	
	-5° ≤ α < 0°	47.3%	39.0%	-4%	Low	< 2%	
Upslope	0° ≤ α < 5°	40.9%	44.8%	8%	Low	< 2%	DEM 20 m/pixel at < -60° lat. 59 m/pixel elsewhere
	5° ≤ α < 10°	5.5%	7.6%	17%	Low	< 2%	
	10° ≤ α < 13°	1.2%	1.5%	25%	Medium-low	2–15%	
	13° ≤ α < 15°	0.3%	0%	30%	Medium	2–15%	

Table D-3 captures the pros and cons of skid-steered vehicles that have four or more wheels, where none of the wheels can steer. Figure D-2 shows an example of how a skid-steered vehicle is amenable

to walking out of entrapments. With an articulated suspension, the vehicle can lean forward and then use its link suspension to flip one wheel a time clockwise to overcome a difficult terrain. Wheels with walking abilities can be made smaller and lighter since the rover can walk out of areas of higher sinkage.

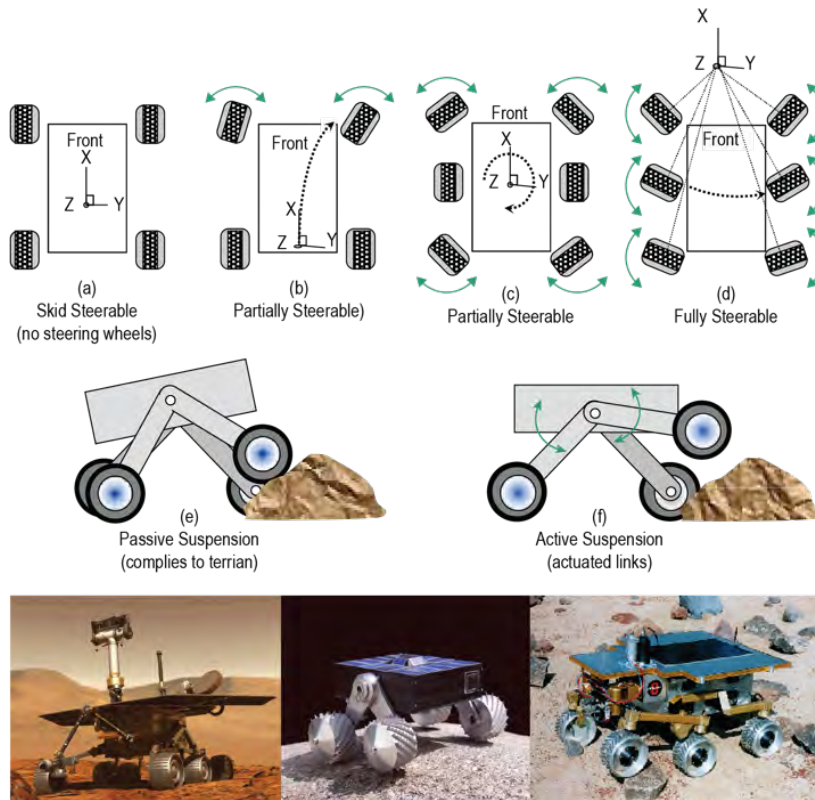


Figure D-1. Examples of different mobility configurations (drive wheels and steering) (top), active vs. passive suspension (middle), and examples from flight and research rovers (bottom). MER is a six-wheel-drive, four-wheel steering with passive suspension (bottom left), Nanorover is a four-wheel drive skid-steered vehicle with active suspension (bottom middle), and Rocky 8 is a six-wheel drive, six-wheel steering with passive suspension (bottom right).

Table D-3. Skid (no steering) pros and cons.

Pros	Cons
<ul style="list-style-type: none"> • Has fewer actuators (no steering actuators) • Is amenable to larger wheels (no sweeping volume needed for steering) • Is no susceptible to steering failure • Is amenable to walking • Can steer and drive simultaneously (by differentially driving each side) 	<ul style="list-style-type: none"> • Cannot position vehicle predictably (but may be able to use control to compensate) • Experiences high sinkage during turn-in-place • Slides downslope when turning • Turning is friction dependent • Uses more power (may be negligible) • Turning is sensitive to small terrain variation. Cannot turn with rocks adjacent to wheels (<i>i.e.</i>, cannot steer wheels to roll over adjacent rocks) • Experiences higher wheel wear from turning • <i>Has stability concerns if front/back wheels are closely placed*</i> • <i>Experiences high loads on frame (not quantified yet)*</i>

* There is disagreement among subject-matter experts about these cons.

A variant of skid-steered and partially-steered vehicles is one with toe-in steering. In this configuration, the steerable wheels can toe in to allow the vehicle to rotate around a point at the center of the non-steerable wheels (Figure D-3). The advantage of toe-in steering is that it does not require a clear sweep volume for the motion of the steerable wheels, yet it allows turns-in-place without the slip experienced by skid-steered vehicles. Table D-4 captures the pros and cons of this configuration.

Table D-5 looks at the trades of partially-steered vehicles. One of the key benefits of this configuration is that it can drive along arcs. Partially steered vehicles allow the use of large wheels for the non-steered wheels, which have the advantage of improved trafficability over rocky and loose terrains and without loss of maneuverability (Figure D-4). Table D-6 captures the trades associated with the configuration of large non-steerable wheels and smaller steerable wheels. Figure D-5 shows a prototype that preceded the LRV with larger non-steerable front wheels.

Vehicles with all-wheel drive, whether four-wheeled, or six-wheeled and so on, are capable of omni-directional driving, also known as crabbing. This additional maneuverability that comes at a



Figure D-2. Four-wheeled skid vehicle with active suspension (amenable to walking)

cost of additional actuation offers functional redundancy and can handle a loss of a single steering wheel. The Spirit rover’s maneuverability was impacted when the steering wheel froze at a fixed angle.

In all-wheel-steering vehicles, one can overcome such constraint by orienting the vehicle along the direction of the failed steering angle and then drive. Figure D-6 shows two examples of all-wheel steered vehicles with different suspensions. Table D-7 outlines the trade related to all-wheel (omni-directional) vehicles. Figure D-7 depicts a six-wheel drive vehicle with all-wheel steering, which is capable of arc-crabbing by rotating the vehicle around any single point in the plane it drives on. Table D-8 examines the trades associated with six-wheel omni-directional vehicles, such as the Rock 8 rover shown in Figure D-1.

Wheel design: We also examined wheel types and sizes (stiff vs. compliant, small vs. large), leveraging Apollo wheel-design data (Table D-10) [87-89]. Tracked vehicles were excluded from the trade due to their low-ground clearance, large mass, and high risks associated with rock entrapment in the tracks of lighter versions.

Larger wheel diameters with narrower widths were favored over smaller wider wheels because of their superior traverse performance (traction, energy efficiency, and obstacle traversal) [90]. Larger wheels have lower coefficient of rolling resistance and a larger contact area for the same wheel width, offering improved traction. When compared to a rigid wheel, compliant wheels have better performance in wear resistance and soft-regolith mobility and slightly better performance in rock traverses.

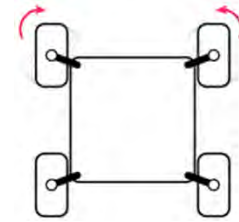


Figure D-3. Four-wheeled skid steered vehicle with toe-in steering.

Table D-4. Skid with toe-in steering pros and cons.

Pros	Cons
<ul style="list-style-type: none"> Is amenable to using large wheels for better traversal Enables turn-in-place for predictable pointing Eliminates many cons of skid-steered vehicles 	<ul style="list-style-type: none"> Does not offer more benefit over same design with full front-wheel steering Increased number of actuators compared to skid while remaining a skid vehicle Risks steering failure Slides downslope when turning (unless you turn in place)



Figure D-5. An example of a lunar rover prototype with different sized front and rear wheels: the Local Scientific Survey Module (LSSM) developed in 1965 by Brown Engineering (NASA).

Table D-5. Partial steering pros and cons.

Pros	Cons
<ul style="list-style-type: none"> Improves maneuverability (allows arc drives) – all wheels moving in the rolling direction Improves directionality for driving on slopes Requires only partial steering Steering fails gracefully to skid steer 	<ul style="list-style-type: none"> Requires more actuation than and complexity than skid-steered vehicles to support steering Needs large sweep volume for steering Is less amenable to large wheels (requires a large sweep volume that moves with the suspension)

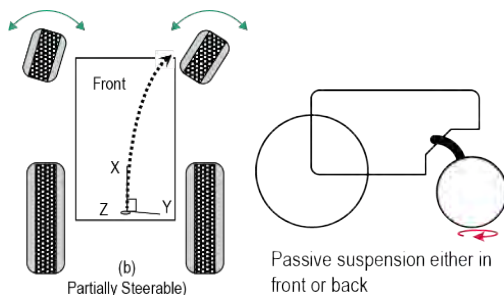


Figure D-4. Partially steerable vehicles with different sized wheels.

Table D-6. Partially steered: race car/tractor pros and cons.

Pros	Cons
<ul style="list-style-type: none"> Improves back-wheel rock traversal (rough terrain) Can house rear actuators inside thermally controlled electronics box Is volumetrically compact Improves maneuverability over skid; provides directionality for driving on slopes Has fewer actuators than fully-steerable Fails gracefully to skid steer Could be more energy efficient with larger wheels (requires further analysis) 	<ul style="list-style-type: none"> Has higher cost due to different front/rear actuator gear-train types Has more actuation and complexity than skid Needs large sweep volume for front steering Has some drawbacks to being asymmetric: <ul style="list-style-type: none"> Uneven performance for bidirectional mobility Could lead to higher structural mass May be more susceptible to tip over when compared to using equal-size wheels

Larger wheels, however, require large sweep volumes to support vehicle suspension and steering motions, which impact vehicle design. However, for long traverses, large wheels undergo fewer actuator rotations, which extends their lifetime and reduces wheel wear.

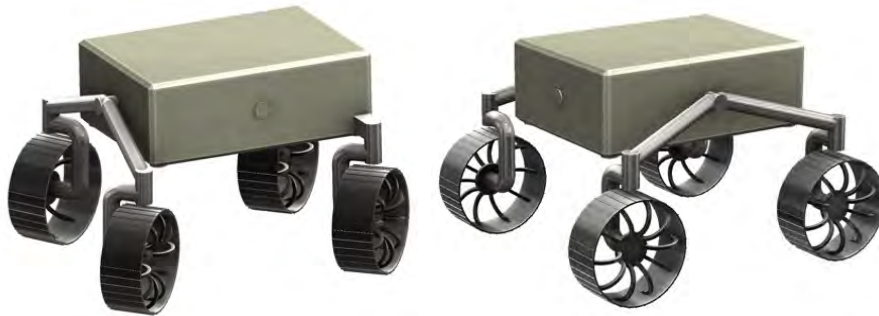
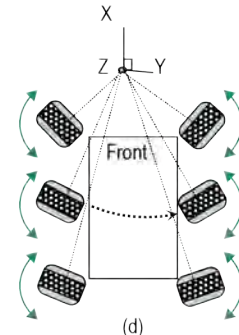


Figure D-6. Examples of a four-wheel drive, all-wheel steering vehicle with front rocker (top) and a side rocker (bottom).



(d) Fully Steerable

Figure D-7. Figure caption.





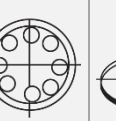

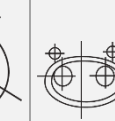
Table D-7. Crabbing (full steering, omni-directional, four-wheels) pros and cons.

Pros	Cons
<ul style="list-style-type: none"> • Allows fine positioning • Can tolerate a single steering failure with minimal impact on mobility • Allows changing drive direction on steep slopes • Has improved maneuverability for getting out of trouble (out of a rut if rover slides into it) 	<ul style="list-style-type: none"> • Is not amenable to very large wheels • Steering sweeps large volumes • Has more actuation than partially steerable • Forces either a higher center of gravity to accommodate the large wheels or forces the wheels out to accommodate the sweep volume for steering.

Table D-8. Crabbing (full steering, six wheels) pros and cons.

Pros	Cons
<ul style="list-style-type: none"> • Additional drive wheels allow improved traction on steep, rocky, and fine regolith terrains • Allows fine positioning for arm placement • Can tolerate a single steering failure with minimal impact on mobility • Allows changing drive direction on steep slopes • Has improved maneuverability for getting out of trouble (out of a rut if rover slides into it) 	<ul style="list-style-type: none"> • Is not amenable to large wheels • Requires more complex suspension design (larger mass) • Steering sweeps large volumes • Has more actuation than partially steerable • Forces either a higher center of gravity for large wheels or forces the wheels out to accommodate sweep volume for steering.

Table D-10. The Development of a Moon Rover [88].

Criteria	Relative Value Factors								
		Rigid Wheel	Pneumatic Tire	Wire Mesh Tire	Metal-elastic Tires		Elliptical Wheel	Hemispherical Tire	Hubless Wheel
Mechanical Reliability	15	90.0	67.5	75.0	70.5	70.5	25.5	60.0	28.5
Weight	14	92.0	46.2	121.8	35.0	63.0	14.0	81.2	7.0
Soft Ground Performance*	14	53.0	101.5	101.5	121.1	121.1	114.8	116.4	121.1
Obstacle Performance**	10	68.0	74.0	74.0	64.0	64.0	68.0	74.0	64.0
Steerability	6	43.8	34.8	34.8	12.0	12.0	24.6	39.6	12.0
Ride Comfort	13	ZERO	104.0	117.0	39.0	65.0	78.0	26.0	39.0
Stability	8	64.0	56.0	56.0	22.4	45.6	34.4	56.0	22.4
Wear Resistance	8	24.0	12.0	42.0	48.0	48.0	48.0	42.0	48.0
Environment Compatibility	6	48.0	ZERO	36.0	42.0	42.0	36.0	36.0	18.0
Development Risk & Cost	6	64.0	8.0	48.0	48.0	48.0	24.0	32.0	16.0
Total	100	Eliminated	Eliminated	706.0	502.0	579.0	467.0	553.0	376.0

*Includes Slopes and Slip; **Includes vertical obstacles and crevasses.

Rover selection: Considering the traverse requirements (distance/speed) and the expected terrain properties (slopes, crater abundance, regolith, and other hazards) (Table D-2), designs with fewer wheels offers several advantages. They have: (1) enhanced maneuverability with fewer steering actuators, (2) lower mass with less complex mechanisms, and (3) lower power and higher energy efficiency compared to rovers with more wheels.

As such, a four-wheeled design with all-wheel steering was favored over six-wheel designs. Among the four-wheeled vehicles with large narrow wheels, three designs emerged as contenders for the baseline: (1) a four-wheeled vehicle with one-sided toe-in steering, (2) a four-wheeled vehicle with one-sided full-range steering, and (3) a four-wheeled vehicle with two-sided full-range steering. Each of these configurations offer non-skid steering for improved heading control and non-skid driving, which is necessary for maneuvering on rocky crater rim slopes and for pointing and placing instrument on targets. The first two options allow for even larger wheel diameters and fewer actuators since the wheels on one side do not steer. However, option (3) with its all-wheel drive, all-wheel steering is selected for the baseline because it affords some steering redundancy and has improved maneuverability for negotiating terrains around crater rim. The vehicle is designed to drive and steering in either directions. With all wheel steering, the rover can also drive sideways at different angles. Descopes reduce the design to option (2).

A four-wheeled vehicles requires only a single passive degree-of-freedom to ensure that all wheels remain in contact with the terrain and support equal weight on each wheel. While a three-wheeled vehicle conforms to the terrain without any suspension, it is less stable, risking tip over. Endurance's suspension uses a dual-sided rocker with a single passive degree of freedom. The two rocker mechanisms that pivot on the left and right sides of the vehicle are connected to each other by a differential mechanism that kinematically couples them under the vehicle chassis, resulting in a single passive degree-of-freedom suspension. With this mechanism, a motion on one rocker (one side of the vehicle) causes the opposite motion on the other side. The dual rockers were selected over a single front rocker, like the one chosen for the Intrepid rover, primarily to accommodate Endurance's sampling system, which is mounted on the front side of the rover. The dual-sided rocker has the benefit of minimizing the side-to-side rolling when traversing rocky or undulated terrain, compared to a single rocker design. However, that benefit comes at a cost of a slight increase (~10%) in the mass of the mobility subsystem.

The baseline uses large-diameter compliant wheels to improve rock traversal, traction on regolith, and energy efficiency [87, 89, 90]. The 0.8 m-diameter wheels use a mesh structure, similar to the LRV, to traverse rocks that are less than 0.3 m in height and drive through smaller craters not apparent in orbital data (<5 m in diameter with slopes below 10°). The vehicle is designed with a ground clearance of > 0.6 m.

The drive wheels use magnetic detent in lieu of brakes to reduce power draw and increase robustness to failures. Steering wheels do use brakes nor detent to minimize power draw and maintain smooth steering motions. The rover is designed to drive in either direction supported by front and back stereo cameras.

Figure D-8 summarizes the aforementioned mobility configuration trades that were considered for this type of terrain and Table D-9b summarizes the selections and offers rationale for that selection. The elaboration of the trade space, the selection, the rationale were informed by subject matter experts that drew from prior analyses, designs, implementations, and lessons learned.

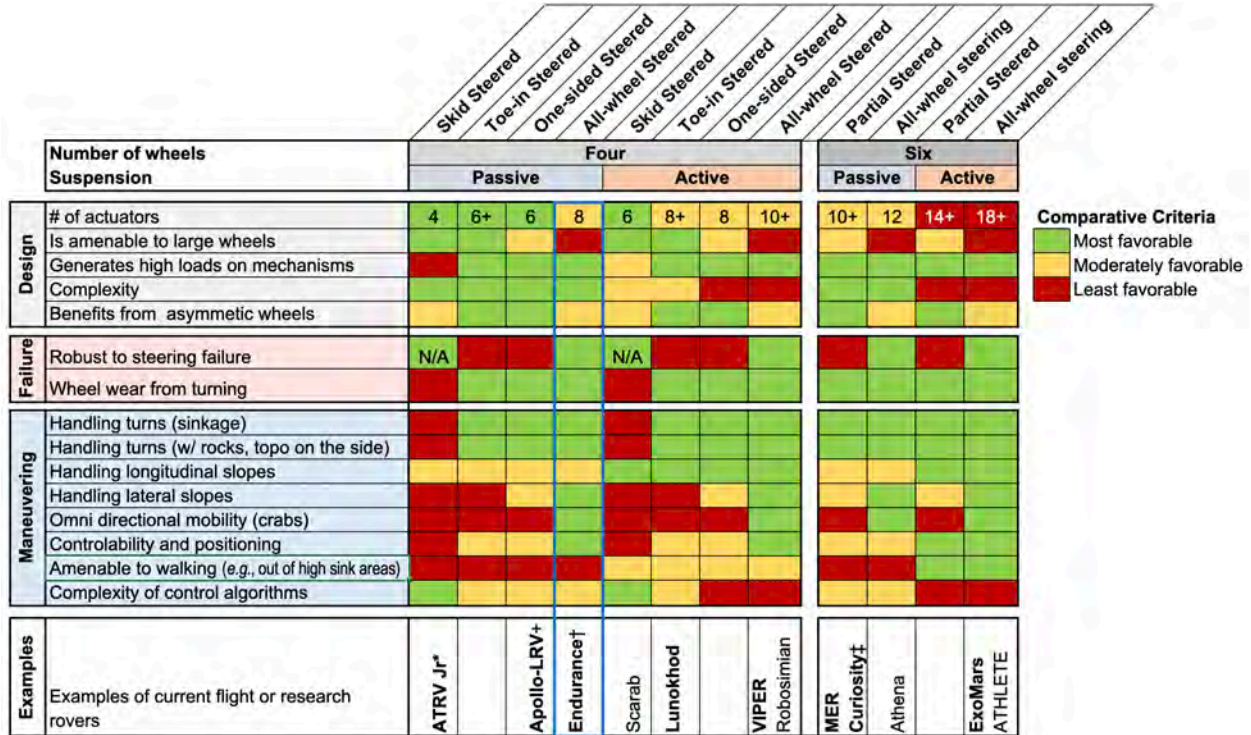


Figure D-8. Summary of the mobility trades for Endurance, which would traverse thousands of kilometers across largely benign lunar terrain. Bold in the examples are flight rovers while non-bold are research rovers; +LRV uses spring in lieu of passive suspension; † includes Intrepid and INSPIRE; ‡ includes Perseverance, Yutu, Yutu-2.

Table D-9. Wheel design.

Pros	Cons
Wheel diameter (large vs. small)	
<ul style="list-style-type: none"> • Larger contact length and area for same width (key) • Lower coefficient of rolling resistance • Lower wheel contact angle 	<ul style="list-style-type: none"> • Large steerable wheels sweep large volumes (larger accommodations) • Large wheels are harder to turn
Wheel width (narrow vs. wide)	
<ul style="list-style-type: none"> • Lower mass with lower impact on mobility performance 	<ul style="list-style-type: none"> • Lower ground pressure, but that is no longer a good metric to use
Grouser (stiff vs. compliant)	
Third order effect	
Further requires analyses	
Quantifying impact of wheel diameter/width on power, energy, thermal, wear, and mass for long lunar traverses	

Table D-9b. Summary of mobility trades, selection, and rationale.

	Key Trades	Selection	Rationale
Type	Wheeled vs. tracked	Wheeled	Lower mass, larger ground clearance and lower risk of rocks entrapment
Configuration	Drive + steering wheels: 3-wheel (1 steering) 4-wheel (0 steering) 4-wheel (2 steering) 4-wheel (4 steering) 6-wheel (4 steering) 6-wheel (6 steering)	4-wheel (4-steering)	Adequate stability (low tip-over risk) and best maneuverability at lower mass and power; resilient to single-steering failure.
	Suspension: Active vs. passive vs. spring-loaded Dual-sided rocker vs. single-sided rocker	Passive Dual-sided rocker	Balanced weight on wheels, lower mass and volume in rover body, fewer failure modes, adequate for expected terrain difficulty and rock traversal. Dual-sided rocker to accommodate sampling.
Wheels	Diameter: Large vs. small Narrow vs. wide (large: ~1½ x MSL) (narrow: ½ x MSL) Rigid vs. compliant	Large Narrow Compliant	Superior traction, energy efficient, enhanced obstacle traversal; fewer rotations and terrain contacts for longer life. Improved mobility in soft regolith and over rocks, improved wear resistance
Gravity	Lunar rover to operate under Earth gravity vs. only lunar gravity	Earth-gravity Rover	Enables end-to-end testing of rover in different terrains without complex gravity offloading aids

E AUTONOMY

To identify the required level of autonomy, we examined trades from ground-based human control, similar to the joystick operations of the Lunokhod rover back in the 1970s, to onboard autonomous control for mobility, instrument placement and system management. The trades are summarized in Table E-1.

Key constraints that determine the viability of the operations modes include: (1) the visibility and availability of lunar relay orbiter and associated ground stations, (2) the uplink and downlink bandwidth and latency of the communication infrastructure from the lunar rover to the ground operations center, (3) the cadence of rover motions (traverse and instrument placement) throughout the lunar day and night, and (4) the nominal operations schedule. Figure E-1 summarizes the required operations and operational constraints in a lunar day and night for two representative examples.

Sustained *ground control* was deemed too cognitively taxing and not viable for the four-year operations period. *Ground decide* and *ground compute* modes were also not viable because they are unable to meet even the average traverse. Table E-2 estimates the throughput based on sensors' dataflow, onboard computation performance, and communication bandwidths. As a result, this mission has to rely on *onboard decide* for a significant portion of its nominal operations and on the *ground decide* for the remaining portions. Leveraging ground-based computing infrastructure (*ground compute*) to supplement the onboard computing does not offer an advantage due to the communication availability and bandwidth.

As shown in Figure E-1, after mission operations transition to an Earth-based schedule, both traverse and instrument-placement arm operations

Table E-1. Operations modes and trades.

Mode	Downlink	Ground	Uplink
Human control	Stereo imagery and rover telemetry	Human assesses and controls rover, arm, and instruments	Actions for every step
<i>Sustained human control was deemed too cognitively taxing and not viable to sustain for the four-year operations (24/7).</i>			
Human decide	Stereo imagery and rover telemetry	Ground computer assesses and generates actions. Extensive synchronous human selection/oversight.	Actions for every step
Ground compute	Stereo imagery and rover telemetry	Ground computer assesses and generates actions autonomously. Limited asynchronous human oversight.	Actions for every step
<i>Human decide and ground compute modes were also not viable because they are unable to meet even the average traverse. Leveraging ground-based computing infrastructure (ground compute) to supplement the onboard computing does not offer an advantage due to the communication availability and bandwidth.</i>			
Onboard decide	Thumbnail imagery and rover telemetry	Onboard computer assesses and generates actions autonomously. Limited asynchronous human oversight.	Route plan and goals
<i>Onboard decide was the only viable option for nominal operations. Contingencies and off-nominal operations can leverage ground-based human decide option.</i>			

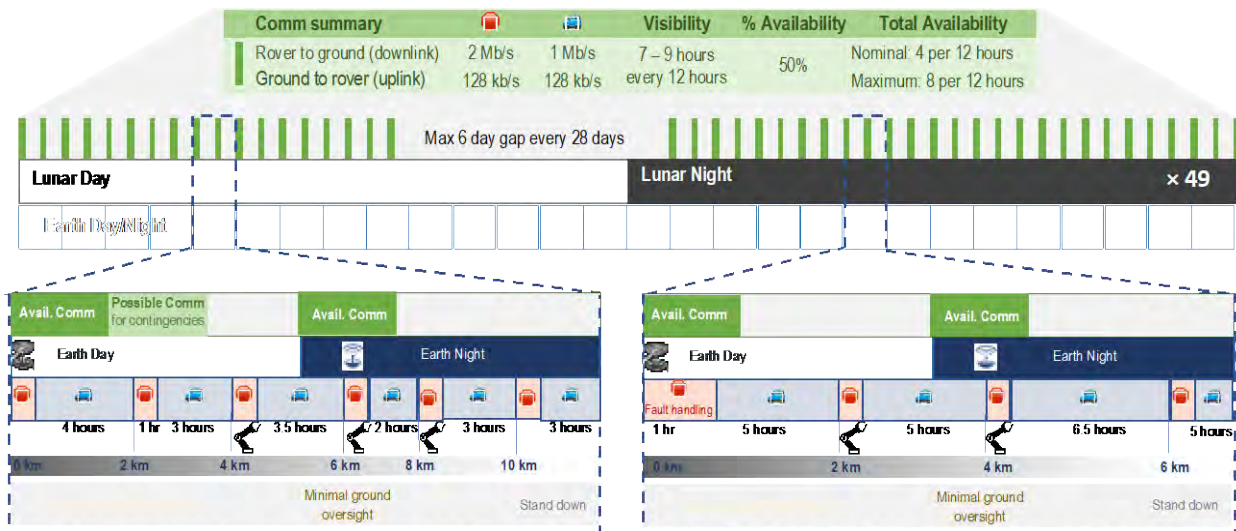


Figure E-1. Examples of operations from a lunar day and night across an Earth day that shows drive/arm operations with communication constraints and operation shifts.

Table E-2. Assessing viability of ground-based compute mode.

Mode	Time for human confirmation (s)	Distance between onboard images (m)	Distance between images sent to ground (m)	Image Resolution (pixels)	Traverse Rate (m/hour)		Required Traverse Rate (m/hour)		
					Possible (comm visible)	Possible (comm not visible)	Daytime	Nighttime	
Nominal Comm Window: 4 hours per 12 hour period with up to 6-day gap every 28 days					Downlink Rate: 2 Mb/s 1 Mb/s				
Ground Compute	60	1.7-2.3	10-m drive steps	1280×960	208	0	Effective 600	Effective 300	
				640×480	219	0			
Onboard decide	N/A	1.7-2.3	continuous drive	128×96 thumbnails	1,018	1,018	Max 900		
Backup Comm Window: when nominal comm not visible					Downlink rate: 200 kb/s 100 kb/s				
Ground Compute	60	1.7-2.3	10-m drive steps	1280×960	119	0	Effective 600	Effective 300	
				640×480	183	0			
Onboard decide	N/A	1.7-2.3	continuous drive	128×96 thumbnails	1,018	1,018	Max 900		

would inevitably fall outside the nominal operations schedule. Therefore, a significant portion mobility and instrument placements has to be conducted through autonomous operations.

Special accommodations would be necessary for the twelve sampling operations. Ground operations would switch to a 24/7 for the duration of each sampling site, which is allocated a full lunar day for selecting and caching the sample. The sampling operations have significant ground engagement³ when compared to mobility and instrument placement between sampling sites.

The long-traverse path necessitates a level of reliability in autonomous surface navigation and instrument placement to complete the mission within the planned four years. The mean-distance-between-faults maintains the required traverse rate for the different terrains (Table E-2). Table E-3 captures the required capabilities for autonomous operations that encompasses surface navigation, localization, identifying safe regolith and rock targets for placing instruments and acquiring measurements. Throughout, the rover has to plan and manage its shared resources and monitor its health to achieve the rate of faults for such operations shown in Table E-2.

Sensor selection and placement. Sensors are selected and mounted on the rover to support both autonomous and ground-assisted operations, simplify operations, provide adequate sensing coverage with minimal articulation of the mast and arm, and offer robustness through functional of physical redundancy (see Redundancy Section).

Tables E-4 and E-5 examine the trades of passive (cameras) and active imaging (LIDAR).

Stereo cameras in the visible range are selected over LIDAR options (both spinning and flash) and Near-Infrared cameras for traverse and arm operations. Despite their superior 3D range and being agnostic to sun angle and shadows, LIDARs require higher power, have limited resolution in, at least, one dimension (vertical for spinning), and are currently at a lower TRL for lunar surface applications than cameras. Lunar regolith tend to be more reflective in the near infrared but Near Infrared (NIR) cameras are usually less optimal overall. The plan is to select a visible-range camera that has the best NIR response among that class of cameras.

³ During sampling operations that only occur during the lunar day, the science team would be engaged in all key sampling-related decisions: sample selection, sample confirmation, sieving, caching or discarding the sample, repeating to increase cached sample volume, confirming the cached sample prior to sealing it.

Table E-3. Autonomy Requirements

	Requirement	Description
Surface navigation	Effective Rate	1 km/hour max during daytime; 0.4 km/hour max during nighttime
	Hazard assessment	Detection and avoidance for all hazards that include: <ol style="list-style-type: none"> 1. terrain topography (positive: untraversable rocks, negative: deep depressions or craters), 2. lateral slip toward a terrain hazard, 3. sink hazards in soft terrain, and 4. power/thermal hazards that occlude solar panels or block radiator
	Path planning	Route path around hazards
Instr. Placement (excludes sampling)	Target identification	Autonomous regolith patch or rock selection based on intent
	Approach target	Tracking and approach of selected target while avoiding navigation hazards along the way
	Hazard assessment	Hazard assessment at the target's vicinity prior to final positioning and placement <ul style="list-style-type: none"> • Assess lighting/thermal hazards from environment • Estimate surface normal of target patch • Maneuver rover to approach target to match surface normal and optimal sun angle • Assess clearance around target surface area for collision-free placement
	Arm deployment and instrument placement	<ul style="list-style-type: none"> • Deploy arm and align other surface normal angle to turret's pitch angle • Place on regolith or small/large rock targets • Acquire measurements from multiple instruments • Retract and stow the arm
System	Health management	Continuously monitor the health of the hardware and software components
	Resource management	Plan and schedule activities based on intent and available resources

arm operations. The wide field of view allows rover navigation without the need to articulate and point the mast during nominal traverses. At the maximum traverse rate, short exposures (~10–20 ms) allow imaging-while-driving during the lunar daytime. At night, the rover flashes its LED lights for short-exposure imaging while driving (1.7–2.3 m/image) and stops its drive every 10 m for long and multiple-exposure imaging with enough time to allow mast slew for mini-panoramas (imaging the sides of the rover in addition to the front). Approaching and placing instruments on regolith and rocks at night would use the same capabilities as those during the daytime, supported by rover-based lights.

With the cameras mounted at ~1.5 m off the ground, articulated covers for the camera lenses are not necessary. Arm-based instrument placements are slow and do not require contact with the surface. All sampling operations will occur with ground in the loop. Because of the sampling operations and the proximity of the arm-mounted during to the surface, the instrument heads would be covered. Further assessment of the impact dust on lenses after prolonged exposure and the effects of sun glints on the camera images is warranted. In addition to these perception sensors, the arm can be stowed such that the Hand Lens Imager (HLI) can image the wheels on the arm-mounted side with only a rotation of the wrist pitch.

Table E-6 captures the trade for inertial sensors which are using for pose (position and attitude) estimation of the rover. Selection favored low mass and power options.

In addition to the perception and inertial sensors, all actuators use hall-effect sensors in lieu of encoders to estimate and control wheel/joint motions. Hall-effect sensors are more tolerant to higher temperatures experienced by components outside the thermally managed electronics box. In addition

Table E-4. Active imaging pros and cons.

Pros	Cons
LIDARs	
<ul style="list-style-type: none"> • High range • High accuracy at range • Works at night • Data can be used for science • Agnostic to shadow • Agnostic to sun angle • Could filter out dust (like snow from blizzard in terrestrial apps) 	<ul style="list-style-type: none"> • High power • Low TRL for lunar environment • Higher cost • Laser life • Localization accuracy • Dust accumulation on optics • Motion distortion
Spinning LIDAR	
<ul style="list-style-type: none"> • 360° coverage (no mast articulation) 	<ul style="list-style-type: none"> • Low vertical resolution • Moving parts
Flash LIDAR	
	<ul style="list-style-type: none"> • Small FOV (50° –60°)

Table E-5. Passive imaging pros and cons.

Pros	Cons
Stereo vision	
<ul style="list-style-type: none"> • Low power • No moving parts • High heritage (TRL9 hw/sw) • High-density point cloud • Intensity + 3D data • Data can be used for science • Dust tolerant (quantified by MS³) • Functional redundancy (SfM) 	<ul style="list-style-type: none"> • Texture dependent • Limited range (especially with night imaging) • Dependent on incident/phase angles • Lens distortion for WFOV lenses • Requires calibration • Requires large computation and memory for stereo • Motion smear/blur at higher speeds

Redundant high-resolution stereo-camera pairs with 90° field-of-view lenses and a ~25 cm baseline are mounted on either end of the rover to accommodate driving in either direction as well as

Table E-6. Internal sensing. Limited options for low-mass, low-power, reliable long-duration Class B IMUs.

	Power	Mass	Rationale
Miniature Inertial Measurement Units (MIMU)	22 W ave 32 W max	4.5 kg*	High mass and power compared to other options. Used on M2020 entry, descent and landing (EDL); baselined for Mars Sample Return Ascent Vehicle
LN200**	15 W	0.6 kg	Has reliability problems; will be discontinued
ASTERIX 120	6 W × 3	6.5 kg	Large mass
Siru	43 W max	5.5 kg	High cost; used for classified work
SmallSat IMUs	1.5 W ave 2 W max	0.06 kg	Not available in Class B (e.g. STIM300)
Accels only			Allows recovery of rover tilt, but without gyros, rover loses ability to accurately control its heading.

to these relative-position sensors, the steering and arm joints use resolvers on the joint outputs for absolute positioning. Torques on the wheels and arm are inferred from the motor winding currents and is sufficient since the arm does not require contact for instrument placement.

Arm operations and instrument placement. The arm, which carries the sampling/sieving scoop and two turret-mounted instruments, the APXS and the HLI. It has four primary functions: (1) collecting, sieving, and depositing rocklets and regolith samples into caches, (2) transferring the filled cache canister to an Earth return vehicle (Endurance-R only), (3) placing these instruments at centimeters distance above their surface targets, and (4) inspecting the sample canister, the rover, its wheels, and underbelly using the HLI. The details of the sampling is described in Appendix H. Both the rover and the arm position and orient the instruments on either regolith or rock targets. The APXS places its head 2 cm above the surface. For rocks greater than 60 cm in diameter, the required lateral placement accuracy from rover-based images is ± 15 cm from the middle of the rock. Orientations errors of up to 30° can be tolerated by both instruments [91]. Targets are selected either by ground operators based on high-resolution orbital data with positional accuracy of > 1 m relative to the rover or by an onboard algorithm based on intent from ground operator. The science measurements do not necessitate surface preparation nor do they constrain a specific location or face on the rock for instrument placement. Therefore, onboard autonomy algorithms are driven only by engineering considerations such as lighting, thermal, and geometric consideration for safe placement and arm retraction in the event of a failure. Targets identified by ground operators or onboard algorithms from 10 m away will have a placement accuracy of < 5 cm [92], well-within the science requirement. To minimize orientation errors in placement, the rover/arm has to match the two angles of the target surface normal, which it can achieve with its five-degree-of-freedom arm.

System-level autonomy: The long traverse requires a level of reliability that exceeds that of prior Mars missions. System health, shared resource and activities are managed using an onboard autonomous system that can plan activities based on intent from the ground, available onboard resources, and the health of the components of the systems. Fault protection is integrated with the system manager to handle both nominal and off-nominal conditions through the same control-flow. Robustness of performance both at the function and system levels for a range of uncertainties is critical to successfully meet the objectives of the mission.

Redundancy

The Endurance rover features numerous physical and functional redundancy ensuring a robust system. For example, in addition to the physical redundancy of two front and two rear stereo cameras, 3D information can also be generated using functional redundancy such as generating 3D information from a single camera using structure-from-motion. The stereo cameras on both side of the rover have redundant pairs. The compute elements, motor controllers, and IMU are all redundant. For localization, the rover relies on both visual odometry as well as wheel and inertial dead reckoning.

Localization

Localization requires knowledge of rover position, which is coupled with knowledge of heading. Heading knowledge also serves antenna pointing, but this is not a driver with the relatively wide antenna beams; therefore, heading knowledge requirements and trades were assessed as part of meeting position knowledge requirements.

Position knowledge error will likely be similar to that of the Intrepid rover, which is on the order of a few meters 1,000 m of traverse in order to see science targets identified from orbital maps in the rover imagery. However, tighter requirements derive from rover hazard avoidance processes. Rover navigation follows routes designated with orbital imagery and must respect human-specified keep-in and keep-out zones, which keep the rover safely away from navigation hazards that are visible from orbit. The most frequent hazards on the Moon are craters; absolute position knowledge on the order of the smallest crater reliably detectable from orbit (5 m diameter) is required at all times to respect these zones.

Potential sources of absolute position knowledge include radiometric sensing from lunar relay orbiter if they are equipped with such capability, co-registration of DEMs created onboard the rover to DEMs created from orbit, recognizing and co-registering skyline landmarks, and recognizing crater landmarks near the rover. In between absolute position corrections, relative position updates are possible from wheel odometry, visual odometry, and an inertial measurement unit (IMU). Potential sources of absolute heading knowledge include sensing directions to the sun, the Earth, and stars; relative heading updates are possible from an IMU and from wheel and visual odometry.

Since Endurance will be traversing long distances during both the lunar day and night, both sun sensors (e.g., Adcole pyramid-type coarse sun sensor) and star trackers are used for correcting absolute heading during the day and night respectively. It is possible to only rely on star tracker for both day and night. A typical star tracker would operate with the sun within 26° of boresight and 18° of Earth. It is possible to operate a star tracker with decreased accuracy with the Earth in the FOV. The Sun exclusion angle can also be made smaller with bigger baffles. By pointing the redundant star trackers in different directions (or changing the rover's heading), it is possible to avoid the Sun in at least one of the sensors at all times. Since the rover's absolute heading would not be adequately known, it is not possible to always avoid the sun in the star tracker's FOV. However, having the sun in a star tracker's FOV would not damage the sensor.

To correct for absolute position, in addition to the necessary aforementioned absolute heading correction, surface landmarks detected from the rover stereo cameras are be matched with orbital maps to correct dead reckoning errors from relative updates of wheel odometry, visual odometry, and the IMU. Example of landmark detection is detecting ~ 10 m diameter craters, which appear every ~ 100 m along the route. When the sun is near zenith, absolute heading updates are still available from crater landmarks and can be obtained by observing direction to the Earth with the mast cameras.

F AUTONOMY RELIABILITY

To assess the required autonomous traverse performance for long-distance lunar roving for Endurance, Inspire, and Intrepid, we studied data from past Mars rovers (the MER rovers and Curiosity) and created a simulation to investigate the effect of drive interruptions on planned the planned traverse.

Past Mars rovers: We analyzed faults that resulted in an incomplete traverse of the Curiosity rover, which has been operating on Mars since August 2012. This reports Curiosity drove a total of 21,318.5 meters during its first seven years, in 738 drives ranging in length from 2.6 centimeters to 142.5 meters. Of those, 622 completed successfully, 26 were halted by time (the end of the driving day occurred before it could cover the over-ambitiously set planned distance), 25 were not allowed to start due to rover conditions (e.g., the robotic arm had not been stowed at the end of the preceding science), and the remaining 65 were interrupted during driving for the reasons shown in Figure F-1. Each such interruption terminated the rover’s drive, requiring operators on Earth to diagnose the situation and develop a plan to resume driving on the next sol (Mars day) that a drive was requested.

We are interested in similar interruptions to Endurance’s autonomous driving, those requiring operator intervention. However, the majority of the time Curiosity was not being driven completely autonomously. Instead, operators planned the route the rover would drive over the next Sol (or sometimes several Sols), and estimated the terrain conditions (e.g., slope) it would experience. When Curiosity then followed this route, any conditions causing exceedances of the rover’s self-monitoring (e.g., tilt) would interrupt the drive, after which Curiosity made no attempt to autonomously recover. Since operators were predicting terrain conditions from already returned camera images, accurate estimation at longer distances was challenging, and the primary cause of drive interruptions.

We also looked history of the two MER rovers to see the trend in software anomalies due to all causes (not just those triggered by driving). The data shows that *within a few months of operation, the frequency of anomalies drops by an order of magnitude.*

Simulating drive interruptions

Endurance’s science plan calls for approximately 33 lunar days and nights of activities. A typical day involves a series of autonomous drives alternating with stops for science measurements. The rover drives significant distances during both the lunar day and night. As shown in Figure E-1, the rover would stop every 2 km for one hour to acquire science measurements using the arm-mounted instruments (APXS and HLI). The duration between stops varies since the effective traverse rate varies based on the time of the day (day/night), the terrain slope and direction (upslope vs. downslope), the hazard density, and the engineering stops for localization and for long-exposure imaging to the visible horizon at night.

The Endurance rover is designed to autonomously drive between locations, i.e., without guidance from operators back on Earth. As it does so, Endurance’s driving software continually checks for anomalous conditions, its response to which is to: cease movement; transmit data on its condition and surroundings to Earth; and rely on the operators to analyze the situation and direct Endurance’s actions necessary to recover and resume driving. Such interruptions consume time, and depending on how frequent they are and how long it takes the operators to direct recovery, the lunar day’s schedule may not be attainable. We simulated

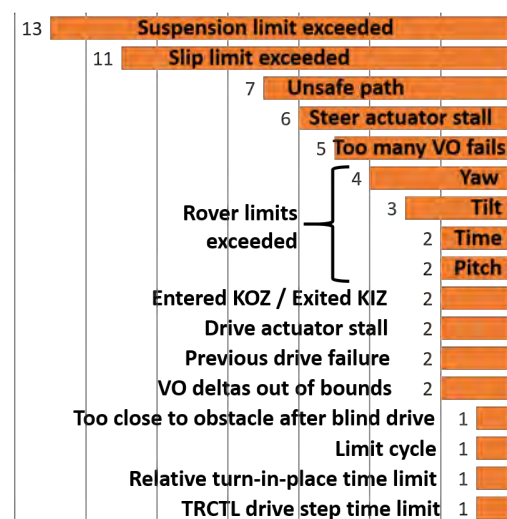


Figure F-1. Causes of interruptions to Curiosity’s drives
 KOZ/KIZ = Keep Out/In Zone; TRCTL = Terrain-adaptive wheel speed control; VO = Visual Odometry.

interruptions and their effects on this schedule based on two key parameters, as follows:

Interruption rate: we used a distance-dependent rate of interruptions, characterized by the mean distance between interruptions. Figure F-2 plots the distribution of interruption distances (in km) from a sample of 10,000, based on a mean of 10 km.

Recovery time: we used an exponential distribution of recovery times, with a minimum of one hour, characterized by the mean recovery time. Figure F-3 plots the distribution of recovery times (in hours) for a sample of 10,000 based on a mean of 5 hours.

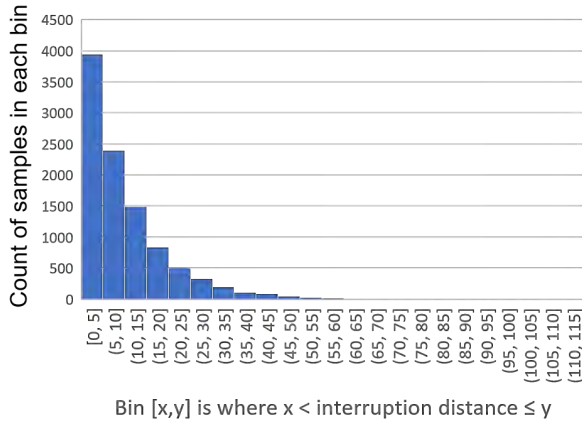


Figure F-2. The distribution of interruption distances.

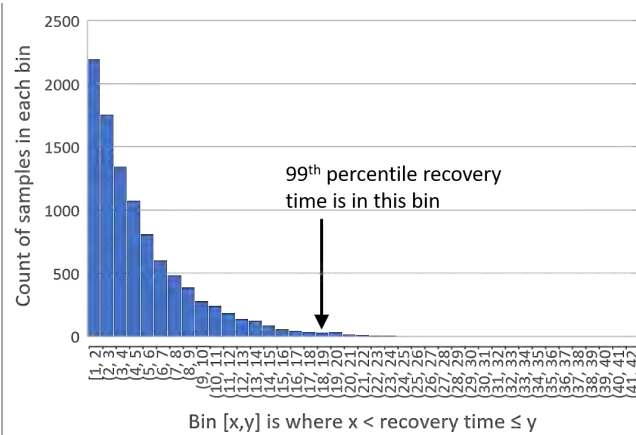


Figure F-3. The distribution of recovery times.

The simulation mimics an entire mission based on the detailed science plan’s daytime drives (distances and speeds) and science stops (minimum stop times). In each Monte Carlo run of the simulation, drive interruptions occur as drawn from the interruption distribution, incurring a delay whose length is the time drawn from the recovery distribution. Inability to get to a daytime stop for sampling with night driving hours counts as a “failed” lunar day, requiring an extra lunar day to be spent getting there in the worst case, after which the mission continues. The outcome of a Monte Carlo simulation run is the count of such “failed” lunar days. Once a more detailed science route plan is in place, one can use such simulations to inform science planners where their lunar activities may have ambitious schedules. If a sampling site is not reached during the lunar night traverse, some science stops could be skipped to catch up. The current alternating two-kilometer traverse followed by a one-hour science top provides flexibility in the plan. The simulation takes these into account.

Figure F-4 shows results of simulation runs for combinations of mean recovery time and mean distance between interruptions. Each small dot and number to its right reports the result of 10,000 Monte Carlo simulation runs. The number indicates that over the Monte Carlo runs, 90% of them had no more than this many “failed” lunar days. Blue lines connect points of zero “failed” lunar days, red lines connect points of three, and green lines connect points of six. These results show, for example, that to have zero “failed” lunar days 90% of the time could be achieved with a mean interruption distance of 4 km and mean recovery time of 2 hours, or 8 km and 4 hours, etc.

Conclusions

It is challenging to extrapolate the experience of Curiosity’s driving on Mars to lunar driving needs. Curiosity has been predominantly directed by ground controllers identifying a path forward between waypoints 10s of meters apart for the rover to then follow. Interruptions to Curiosity’s drives have occurred due to mismatches between the controllers’ predictions of ground characteristics, based on camera images taken from only where the drive starts, and the actual terrain conditions experienced. This is obviously limited by the view ahead, the fidelity of which diminishes over distance. In contrast, Endurance’s long drives will be done by having the rover itself direct its path forward based on repeatedly taking images of the upcoming terrain, enabling it to accurately assess those terrain conditions

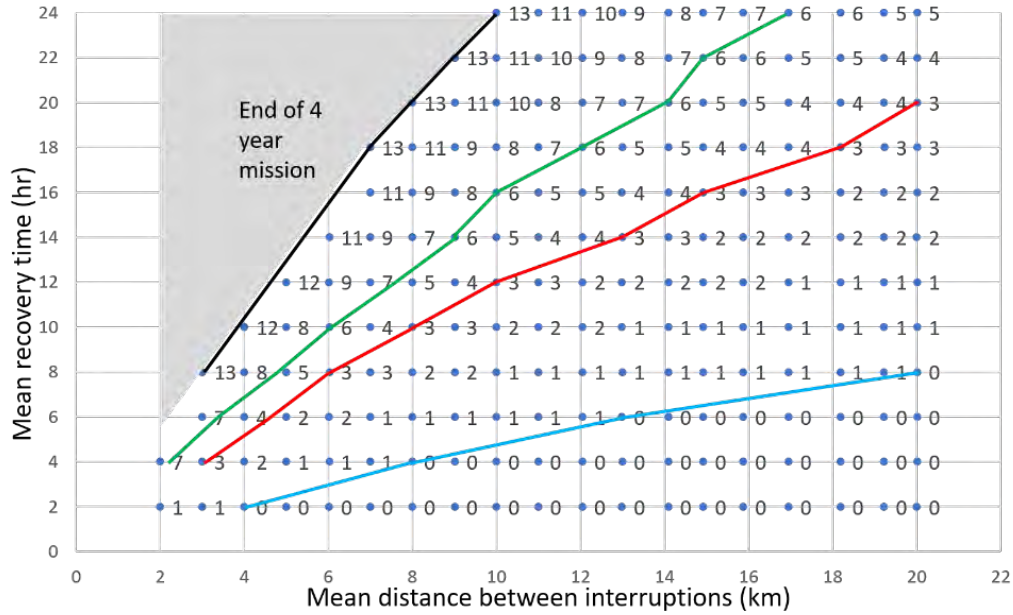


Figure F-4. “Failed” lunar days for recover x interruption combinations.

and directing itself accordingly. As long as safety limits are adhered to, such as avoiding overly steep slopes and large boulders, Endurance should not be subject to Curiosity’s kinds of drive interruptions.

Nevertheless, mid-drive interruptions to Endurance’s progress may occur from time to time (e.g., from sensory glitches, hardware transients, or software bugs). When Endurance itself is not able to resolve the problem and resume progress, it will need to call home for ground operators’ help. We developed a simulation to explore the consequences of such interruptions on fulfilling the mission science plan’s driving needs. Its results suggest the following (Table F-1):

Table F-1. Effect of recovery time on mission duration.

Mission duration beyond 3 years	Allowable mean recovery time between faults (MTBF) for a given mean distance between faults (MDBF) (points from Figure F-4)					
	MDBF km	MTBF hours	MDBF km	MTBF hours	MDBF km	MTBF hours
0 months	4	2	6	3	16	7
3 months	4	5	6	8	16	16.8
6 months	4	7	6	10	16	23
13 months	4	10.5	6	15.5	16	36

For example, a middle-of-the-road goal could be to allow the mission to continue six months beyond its initial three years. To achieve this, Figure F-4 shows if drive interruptions can be expected to occur on average no more than every 6 km, then the mean recovery time must be held to no more than 10 hours or if it occurs on average no more than every 16 km, then mean recovery time must be held to no more than 23 hours.

A final note: these results may be slightly pessimistic. The simulation has incorporated only an initial attempt at identifying flexibility in the science schedule. It also does not consider the phenomenon seen on Mars rovers of “teething” troubles being found and eliminated early in the mission.

G ESTIMATING MISSION DURATION

Below, we summarize the key drivers that impact mission durations: (1) communication constraints, (2) mobility on sloped terrain and associated skid/slip, (3) estimated path tortuosity (or path inefficiency), and the (4) reliability of autonomous surface operations.

G.1 COMMUNICATION CONSTRAINTS





Based on the analysis in Appendix I, below is summary of the key relevant information relevant to estimating mission duration.

Assumptions:

- The lunar relay orbiter can talk to rover and ground simultaneously
- The initial ground antenna will have visibility of the orbiter 8 hours every 24 hours
- With increase in distributed antennae, visibility of orbiter will increase to full coverage
- Communication gaps for the Northern Route would range from 0.4 days to nearly 6 days every 28 days for latitudes between -52° and -37° .

Table G-1 summarizes the communication constraints:

Table G-1. Summary of communication constraints.

	Communication	Mode	Latency (minutes)	LGA Rate		HGA Rate		Visibility (geometry)				Availability (other users)		Comments
								%	Min (hours)	Max (hours)	Period (hours)	%	Ave Duration per period	
Endurance	Rover to Ground (downlink)	Normal	1	22 kb/s	22 kb/s	2 Mb/s	1 Mb/s	76%	7	9	12	50%	4.0	6 day gap every 28 days
		Max	1440									100%	8.0	
	Ground to rover (uplink)	Normal	1	128 kb/s	128 kb/s	50%	4.0							
		Max	1440					100%	8.0					

G.2 SLOPED-TERRAIN MOBILITY

The traverse rate is impacted by the terra-mechanical properties, the terrain slope angle, and the distribution of hazards. While we attempt to estimate traverse rate for the purpose of estimating total mission duration, there are a few caveats to keep in mind.

Caveats

- The terra-mechanical properties are *unknown in PSRs*. The agglutinates in the polar regions would vary depending on impact history.
- The interaction of the warm wheel on ice-cold regolith with a composition of 1–10% wt. water abundance has not yet been characterized.
- Lunar regolith has angular particles when compared to sand used for martian/terrestrial testing; slip estimates are adjusted from analyses done for Mars rovers to account for that [93]. When testing with lunar simulant, it is critical to keep in mind that the knee in the slip/slope curve is dependent on the simulant type [94].

Based on the *Lunar Sourcebook* [22], the wheel-slip on the lunar surface was measured to be between only 2–3%, which allowed for reasonably accurate navigation by dead-reckoning. However, slip is very *non-linear*. We estimated the skid (downward slip) and slip (upwards) of a four-wheel vehicle in lunar regolith based on experimental results provided by [93–96], tests conducted in support of the Mars Sample Return fetch rover studies, and inputs from subject matter experts.

Table G-2. Estimates of skid/slip vs. slope for lunar regolith.

Slope Direction	Angle	% Slip		Comments
Downslope	-25° – -20°	-40%	-26%	Skid (based on Ding's paper below)
Downslope	-20° – -18°	-26%	-20%	Skid
Downslope	-18° – -15°	-20%	-15%	Skid
Downslope	-15° – -13°	-15%	-12%	Skid
Downslope	-13° – -10°	-12%	-9%	Skid
Downslope	-10° – -5°	-9%	-4%	Skid
Flat	-5° – 0°	-4%	-3%	
Flat	0° – 5°	3%	8%	2–3% on lunar surface (Lunar sourcebook p 524)
Upslope	5° – 10°	8%	17%	Slip
Upslope	10° – 13°	17%	25%	Slip
Upslope	13° – 15°	25%	30%	Slip
Upslope	15° – 18°	30%	60%	Slip
Upslope	18° – 20°	60%	80%	Untraversable
Upslope	20° – 25°	80%	100%	Untraversable

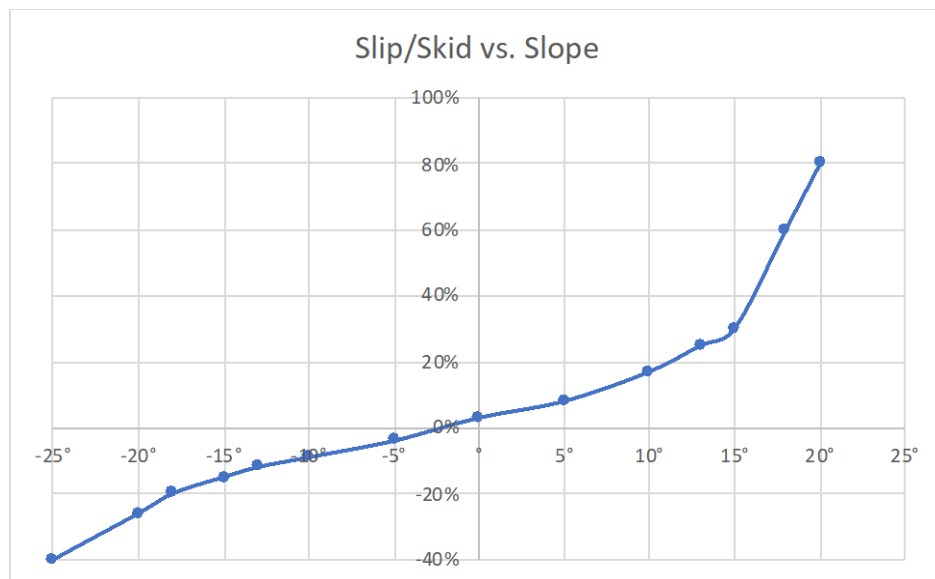


Figure G-1. Estimates of skid/slip vs. slope for lunar regolith.

G.3 DRIVEN PATH INEFFICIENCY (PATH TORTUOSITY)

The nominal path defined for Endurance-R (Northern Route) and Endurance-A (Southern Route) were based on an iterative A* path planning algorithm that connected waypoints identified by the science team using mobility constraints of maintaining finding short routes on slopes below 15° in angle. The algorithm operated on a map of 59 m/pixel resolution for the Northern Route and 20 m/pixel resolution for the Southern Route below -60° and 59 m/pixel elsewhere for the Southern Route. Path inefficiency captures the increase in the traverse path based on the actual route the rover is likely to take to account for terrain topography at the scale of the rover to avoid hazards. As such the driven path inefficiency, which accounts for actual rover driven path, is given by the following equation:

$$\eta_{driven} = \frac{L_{driven} - L_{straight}}{L_{straight}} \times 100$$

The commanded path inefficiency is the difference between the commanded path based on rover images and the straight line path to a given waypoint.

$$\eta_{\text{commanded}} = \frac{L_{\text{commanded}} - L_{\text{straight}}}{L_{\text{straight}}} \times 100$$

There are several factors that impact path inefficiencies (tortuosity). These include:

- **Orbital map resolution.** Paths planned at lower pixel resolution DEMs would increase in length when planned at higher resolution or when driven, as the actual path would need to avoid craters and rocks not resolved in the path when planned at lower resolution.
- **Wheel diameter/ground clearance.** Rovers with larger wheels and larger ground clearance can drive over smaller rocks and through small craters that have to be avoided by rovers with small wheels. E.g., tortuosity for VIPER rover would be higher than that of the Endurance rover.
- **Perception horizon.** Rovers with a limited visible horizon (e.g., rovers that use lights when driving at night) would be more myopic than ones that drive in daylight. Limited horizons results in planning shorter paths, which would increase path inefficiency. E.g., rovers with limited perception horizon may end up driving up to craters and then circumnavigating them to avoid driving through them rather than being able to see these craters and avoid them from a farther distance. Other factors such as navigation camera height and terrain topography impact this as well.
- **Slip.** Slip impacts “commanded path inefficiency.” This is a concern in high-slip areas where the progress the rover makes is not always in the direction it was commanded. As a result, the rover ends up meandering more to traverse a path. This is the case of a rover climbing a slope at a lateral angle and keeps slipping a downhill. The rover then has to correct for that slip. If the rover is doing all this onboard, then the tortuosity due to side slip will be less than if ground is in the loop because of the minimum step size for every ground-in-the-loop command.

We leveraged information from subject matter experts, data from simulation of the VIPER rover mission, and that from the Mars rover missions to estimate path tortuosity for Endurance.

Perseverance Simulation Data

Benign Terrains: (CFA: 7%, slope < 15 deg)

Driven path tortuosity: **3%** (requirement < 15%)
 % paths driven with < 15% tortuosity: **98%**

Complex Terrains (sim results): (CFA: 15%, slope < 20 deg)

Driven path tortuosity: **16%** (requirement < 35%)
 % paths driven with < 15% tortuosity: **90%**

CFA: Cumulative Fractional Area, a metric for rock distribution

Caveats:

- The above are simulation results
- Simulates Mars terrain with mainly rock hazards and not small crater hazards; the latter occupy a larger area

VIPER Simulation Data

- The tortuosity factor for the VIPER rover have large variability
- Path tortuosity for VIPER was estimated to range from 1–3x (or 50% to 200% path inefficiency). The analysis was based on a 1 m DEM upscaled to 4 cm using crater and rock abundance profiles.

Actual traverses driven on that simulated terrain ranged from 1.3 - 1.5x longer, which is typical of highland terrains.

Caveats:

- The above are simulation results
- The tortuosity is impacted by the diameter of the wheels and the suspension mechanism

Table G-3. Estimated tortuosity for different slope ranges.

Slope Range	Comments	% Nominal Inefficiency	Nominal Tortuosity Factor
0°–5°	Double MoonTrek estimate	15%	1.15
5°–10°		25%	1.25
10°–13°		50%	1.50
13°–15°		75%	1.75
15°–18°	More hazards	150%	2.50
18°–20°	Incl. zig-zag motion	200%	3.00

G.4 AUTONOMY RELIABILITY (FAULT RATES)

Based on the autonomy reliability analysis presented in Appendix E, below we summarize the average fault rates and average recovery times for minor and major faults. This is based on a preliminary analysis of faults from the Mars rovers adjusted for shorter and more frequent ground-in-the-loop lunar cycles.

Definitions

- **MDBF:** mean distance between faults
- **MTBF:** mean time between faults
- **Minor fault:** a fault that can be rapidly fixed without requiring convening a larger multi-discipline team of domain experts. Examples include faults that can be adjusted by changing a parameter by the operations team.
- **Major fault:** a fault that would require assembling a team of experts, conducting some analysis, and generating a plan to resolve the fault

For Endurance, faults would occur on the rover or on the relay orbiter. The tables below summarize the average fault rates and average and maximum recovery times that the system would have to meet in order to complete the mission within the planned four-year duration.

Table G-4. Rover-based fault rate and recovery times requirement based on distance traversed.

	Fault type	MDBF		Ave Recovery Duration		Max Recovery Duration		Recovery Strategy
		Value	Unit	Value	Unit	Value	Unit	
Rover	Minor fault	6	km	3	hours	24	hours	Ground operators diagnose fault in near real-time
	Major fault	16	km	7	hours	72	hours	

Table G-5. Lunar Relay Orbiter estimated fault frequency.

	Fault type	MTBF		Ave Recovery Time		Max Recovery Time		Recovery Strategy
		Value	Unit	Value	Unit	Value	Unit	
Orbiter	Relay fault	3	Months	1	day	2	day	Multiple relays would ensure continuity

G.5 CONOPS

During the concept of operations, the rover alternates between fast traverses (max 1 km/hr) and stops. Stops are required for science and engineering purposes. During the lunar day and night, the rover stops every 300 m for up to 10 minutes to image its surroundings and correct its global position and heading. At night the rover would have to make additional stops every 10 m for one minute to acquire long exposure images in front and to the side of the rover to plan its path. Night traverses include imaging while driving (short exposure and hence short horizon imaging) as well as long-exposure imaging while the rover has come to a halt. In addition to these engineering stops, the rover stops every 2 km for one hour to deploy its arm on the regolith or auto-selected rocks to acquire measurements by the APXS and HLI. A 48-hour stop occurs every 20 km for longer integration of the APXS measurement. Sampling occurs at twelve distinct sites throughout the entire mission but all occur during the lunar day and with ground in the loop. Table G-6 summarizes the rover stops.

Table G-5. Endurance’s science and engineering stops.

Rover stops	Lunar Time	Stop Every	Stop Duration	Reason	Comments
For mobility	Both	300 m	10.0 mins	Localization (account for day and night localization where visibility is more limited)	Dead reckoning error 2% of distance travelled. Error tolerance 6 m
	Night	10 m	1.0 mins	Imaging for navigation (long exposure ~1 sec)	Assumes two extra wedges (-90° – 90° @12 s for slew 90° slew per. Curiosity for a total of 36 s of slew and 4 seconds for stabilization).
For comm	Both	2 km	1 hrs	2 Mb/s of rover-to-Earth may not be enough to download 35 Gb/day+ pictures	Maybe (if 1 Mb/s if not enough) (35 Gb/day (does not incl pictures). Doing comm while at the science and engineering stop. (2 hours every 8 hours) Data volume 2 G/day
For science	Both	2 km	1 hrs	APXS, HLI, and panorama	Makes more sense to be distance based
	Both	20 km	48 hrs	APXS (long integration) and HLI	New type of stop - (could be changed to 24 hours)
	Day	12 samples	336 hrs	Sampling (rocklets and regolith)	

Table G-6. Endurance’s science stops for the Northern Route (Endurance-R).

Science Stop Duration	Every	Each Duration	#	Total Hours
Short science stops	2 km	1 hrs	923.38	923
Long science stops	20 km	48 hrs	102.60	4,925
Sampling		336 hrs	12	4,032
Total Science				9,880

Table G-7. Endurance’s science stops for the Southern Route (Endurance-A).

Science Stop Duration	Every	Each Duration	#	Total Hours
Short science stops	2 km	1 hrs	1,048	1,048
Long science stops	20 km	48 hrs	116	5,589
Sampling		336 hrs	12	4,032
Total Science				10,669

G.6 EFFECTIVE TRAVERSE RATE

The effective traverse rate (a.k.a. speed-made-good) accounts for terrain topography and associated skid/slip, rover science and engineering stops, path tortuosity, and ground-take-over during the terrain is too difficult for the onboard autonomous system. Below is a summary of the day/night traverse rates for different portions of the path. Note in Tables G-8 and G-9, the majority of the path is on flat terrain with ±5° slope.

Table G-8. Endurance’s traverse rates for the Northern Route (Endurance-R) of 1,748 km.

T Type	Slope Information			Traverse Rates (m/hr)					
	Slope Angle*	% of Path	Skid/Slip	w/ Slip/Skid		+ w/localz		+ science stops/no sampling	
				Day Rate	Night Rate**	Day Rate	Night Rate**	Day Rate	Night Rate**
Down-slope	-15°	0.4%	-15%	529	281	409	243	187	143
	-13°	0.4%	-12%	511	276	398	239	185	141
	-10°	4.6%	-9%	495	271	388	236	183	140
	-5°	47.3%	-4%	938	366	616	304	221	162
Upslope	5°	40.9%	8%	833	349	570	292	215	158
	10°	5.5%	17%	769	337	539	284	210	156
	13°	1.2%	25%	720	327	514	277	206	154
	15°	0.3%	30%	692	321	500	273	204	152
Total		100%		863	353	582	295	217	159
* negative slope is downs			9			439			
** night rate includes imaging stops									

Table G-9. Endurance’s traverse rates for the Southern Route (Endurance-A) of 1,986 km.

T Type	Slope Information			Traverse Rates (m/hr)					
	Slope Angle*	% of Path	Skid/Slip	w/ Slip/Skid		+ w/localz		+ science stops/no sampling	
				Day Rate	Night Rate**	Day Rate	Night Rate**	Day Rate	Night Rate**
Down-slope	-15°	0.0%	-15%	529	281	409	243	187	143
	-13°	1.0%	-12%	511	276	398	239	185	141
	-10°	6.1%	-9%	495	271	388	236	183	140
	-5°	39.0%	-4%	938	366	616	304	221	162
Upslope	5°	44.8%	8%	833	349	570	292	215	158
	10°	7.6%	17%	769	337	539	284	210	156
	13°	1.5%	25%	720	327	514	277	206	154
	15°	0.0%	30%	692	321	500	273	204	152
Total		100%		844	349	572	292	215	158
* negative slope is downslope						432			
** night rate includes imaging stops									

Because the rover stops more frequently at night, the effective traverse rate at night is lower than during the day, the sampling occurs during the lunar day, a higher percentage of the distance is in fact traversed at night. The derivation below shows how the percentages of the distance traversed during the day and at night are calculated.

d_d : day drive distance

d_n : night drive distance

d : total drive distance

t_d : day drive time

t_n : night drive time

t : total drive time

$$t = t_d + t_n$$

$$f_n = \frac{t_n}{t}$$

$$d_n = v_n t_n = v_n f_n t$$

$$d = d_a + d_n = v_a(1 - f_n)t + v_n f_n t$$

$$\frac{d_a}{d} = \frac{v_a(1 - f_n)}{v_n f_n + v_a(1 - f_n)}$$

$$\frac{d_n}{d} = \frac{v_n f_n}{v_n f_n + v_a(1 - f_n)}$$

Table G-10. Endurance's distance percentages and ground-in-the-loop engagement for the Northern Route (Endurance-R) of 1,748 km.

Type	Slope Information			Path Information				Ground in the loop Driving	
	Slope Angle*	% of Path	Skid/Slip	Inefficiency (tortuosity)	Path Length (km)	Day& % Distance	Night % Distance	Likely to Engage (L, M, H)	% Path with Ground Drive
Down-slope	-15°	0.4%	-15%	75%	12	36.6%	63.4%	M	20%
	-13°	0.4%	-12%	50%	10	36.5%	63.5%	ML	15%
	-10°	4.6%	-9%	25%	100	36.4%	63.6%	L	10%
	-5°	47.3%	-4%	15%	950	37.5%	62.5%	LL	0%
Upslope	5°	40.9%	8%	15%	822	37.4%	62.6%	LL	0%
	10°	5.5%	17%	25%	119	37.2%	62.8%	L	10%
	13°	1.2%	25%	50%	31	37.1%	62.9%	ML	15%
	15°	0.3%	30%	75%	8	37.1%	62.9%	M	20%
Total		100%		17%	2,052	37.0%	63.0%		
* negative slope is downs			9			& Reduced by allocation for day-only sampling			
** night rate includes imaging stops									

Table G-11. Endurance's distance percentages and ground-in-the-loop engagement for the Southern Route (Endurance-A) of 1,986 km.

Type	Slope Information			Path Information				Ground in the loop Driving	
	Slope Angle*	% of Path	Skid/Slip	Inefficiency (tortuosity)	Path Length (km)	Day& % Distance	Night % Distance	Likely to Engage (L, M, H)	% Path with Ground Drive
Down-slope	-15°	0.0%	-15%	75%	0	39.6%	60.4%	M	20%
	-13°	1.0%	-12%	50%	30	39.5%	60.5%	ML	15%
	-10°	6.1%	-9%	25%	151	39.5%	60.5%	L	10%
	-5°	39.0%	-4%	15%	890	40.6%	59.4%	LL	0%
Upslope	5°	44.8%	8%	15%	1023	40.4%	59.6%	LL	0%
	10°	7.6%	17%	25%	189	40.3%	59.7%	L	10%
	13°	1.5%	25%	50%	45	40.2%	59.8%	ML	15%
	15°	0.0%	30%	75%	0	40.1%	59.9%	M	20%
Total		100%		17%	2,329	40.4%	59.6%		
* negative slope is downslope						& Reduced by allocation for day-only sampling			
** night rate includes imaging stops									

Table G-12. Endurance's drive durations for the Northern Route (Endurance-R) of 1,748 km.

Type	Slope Information			Durations (hours)					
	Slope Angle*	% of Path	Skid/Slip	Nominal Drive		Drive w/ ground in the loop		Drive w/ gil+science stops	
				Day Duration	Duration	Day Duration	Night Duration	Day Duration	Duration
Down-slope	-15°	0.4%	-15%	11	31	33	67	43	85
	-13°	0.4%	-12%	9	27	24	50	33	66
	-10°	4.6%	-9%	93	269	185	418	280	583
	-5°	47.3%	-4%	579	1952	579	1952	1613	3673
Upslope	5°	40.9%	8%	539	1762	539	1762	1430	3255
	10°	5.5%	17%	83	264	198	446	314	642
	13°	1.2%	25%	22	70	66	140	94	187
	15°	0.3%	30%	6	18	21	43	28	54
Total				1,342	4,393	1,644	4,877	3,835	8,545
* negative slope is downs			9	5,735		6,521		12,379	

Table G-13. Endurance's drive durations for the Southern Route (Endurance-A) of 1,986 km.

Type	Slope Information			Durations (hours)					
	Slope Angle*	% of Path	Skid/Slip	Nominal Drive		Drive w/ ground in the loop		Drive w/ gil+science stops	
				Day Duration	Duration	Day Duration	Night Duration	Day Duration	Duration
Down-slope	-15°	0.0%	-15%	0	0	0	0	0	0
	-13°	1.0%	-12%	30	76	75	141	105	186
	-10°	6.1%	-9%	153	388	304	602	459	841
	-5°	39.0%	-4%	587	1739	587	1739	1636	3272
Upslope	5°	44.8%	8%	727	2086	727	2086	1927	3854
	10°	7.6%	17%	141	396	338	669	536	963
	13°	1.5%	25%	35	98	106	196	151	263
	15°	0.0%	30%	0	0	0	0	0	0
Total				1,673	4,783	2,136	5,433	4,813	9,378
* negative slope is downslope				6,456		7,569		14,191	
** night rate includes imaging stops									

Table G-14. Endurance's communication gaps for the Northern Route (Endurance-R).

	Comm Gaps	Value
Average across entire path	Average day/night drive speed	188 m/hr
	Average gap duration	1.98 days
	Average distance before minor faults	N/A
	Average distance before major fault	8 km
	Average time before major fault (MTBMF)	1.77 days
	# of gap occurrences across entire path	17.49
	Total days lost in gaps due to major faults	34.62 days
	Total hours lost in gaps due to major faults	831 hrs
Average across path with gaps > MTBMF	% of path with gap > MTBMF	38%
	Total distance in gaps > MTBMF	774 km
	Average gap duration for gaps > MTBMF	4.60 days
	Lost days per gap for gaps > MTBMF	2.83 days
	# of gap occurrences > MTBMF	7.33
	Total hours lost in gaps due to major faults	497 hrs

Table G-15. Endurance's average speed for the Northern Route (Endurance-R).

Summary	Value	Comments
Average speed	0.17 km/hr	Includes fault recover

Table G-16. Endurance's average speed for the Southern Route (Endurance-A).

Summary	Value	Comments
Average speed	0.17 km/hr	Includes fault recovery

Table G-17. Endurance's fault recovery durations for the Northern Route (Endurance-R).

Fault Statistics	Every	Ave. Recovery Duration	#	w/ comm constants	Total Hours
Minor faults	6 km	3 hrs	342	11 hrs	3,762
Major faults	16 km	7 hrs	128	15 hrs	1,924
Total fault recovery					5,686

Table G-18. Endurance's fault recovery durations for the Southern Route (Endurance-A).

Fault Statistics	Every	Ave. Recovery Duration	#	w/ comm constants	Total Hours
Minor faults	6 km	3 hrs	388	11 hrs	4,269
Major faults	16 km	7 hrs	146	15 hrs	2,183
Total fault recovery					6,452

Table G-19. Endurance's total durations for the Northern Route (Endurance-R).

Description	Duration (hours)	Comments
Drive: total day hours	1,644	Incl. localization, imaging, GIL
Drive: total night hours	4,877	
Science: total day hours	2,162	
Science: total night hours	3,686	Excluding sampling
Sampling: total hours	4,032	
Recovery: total day hours	2,102	
Recovery: total night hours	3,583	
Communication (gaps)	831 hrs	Lost time in comm gaps
Commissioning	336	
Rendezvous and handoff	336	
Subtotal	23,590	Day+Night hours
	10,613	Day hours operations
	12,146	Night hours operations
Margin	33%	One year for 3 years
Total lunar day/night cycle	33.32	Max of 1/2 total hours or lunar day
	2.69	Years (w/o margin)
	3.579	Years (w margin)

Table G-20. Endurance's total durations for the Southern Route (Endurance-A).

Description	Duration (hours)	Comments
Drive: total day hours	2,136	Incl. localization, imaging, GIL
Drive: total night hours	5,433	
Science: total day hours	2,683	
Science: total night hours	3,953	Excluding sampling
Sampling: total hours	4,032	
Recovery: total day hours	2,609	
Recovery: total night hours	3,844	
Communication		Incl.
Commissioning	336	
Rendezvous and handoff	336	
Subtotal	25,362	Day+Night hours
	12,132	Day hours operations
	13,230	Night hours operations
Margin	33%	One year for 3 years
Total lunar day/night cycle	35.82	Max of 1/2 total hours or lunar day
	2.89	Years (w/o margin)
	3.848	Years (w margin)

Endurance-R's four-year mission will provide an unallocated margin of ~50% for its 2.7 year-mission. For Endurance-A, its four-year mission would provide a 38% equivalent margin.

Table G-21. Comparison of Endurance-R and Intrepid mission durations.

Description	Units	Endurance	Intrepid	Comments
Total drive distance	km	2,052	1,768	
Total drive time	hours	6,521	5,234	
Ave lunar day drive time	%	28%	60%	Includes only short (eng.) stop and excludes everything else
Ave lunar night drive time	%	46%	11%	Includes only short (eng.) stop and excludes everything else
Average speed	km/hr	0.315	0.338	Excludes science stops and faults
Average speed w/ faults	km/hr	0.168	0.257	Excludes science stops and faults
between eng. stops	km	2	1.35	
Total eng. stops	#	1,026	1,173	
Mission duration	years	2.7	3.0	
Mission duration w Margi	years	3.6	4.0	

Table G-22. Comparison of Endurance-A and Intrepid mission durations.

Description	Units	Endurance	Intrepid	Comments
Total drive distance	km	2,329	1,768	
Total drive time	hours	7,569	5,234	
Ave lunar day drive time	%	32%	60%	Includes only short (eng.) stop and excludes everything else
Ave lunar night drive time	%	48%	11%	Includes only short (eng.) stop and excludes everything else
Average speed	km/hr	0.308	0.338	Excludes science stops and faults
Average speed w/ faults	km/hr	0.166	0.257	Excludes science stops and faults
between eng. stops	km	2	1.35	
Total eng. stops	#	1,164	1,173	
Mission duration	years	2.9	3.0	
Mission duration w Margi	years	3.8	4.0	

H SAMPLING

H.1 SAMPLE CHAIN TRADES

Two separate sample handling approaches were studied for the Endurance viz., (a) a robotic sample return approach and (b) an astronaut-based sample return. In both cases, the goal is to collect lunar rocklets and regolith.

Sampling Approach: In both cases, sample acquisition method was the first trade, i.e., whether to dig deep into the surface or collect samples that are exposed on the surface. Digging in a specific region was an architectural choice for past lander-based sampling studies. This typically required sieving a large volume of regolith to find rocklets. It also resulted in higher loads on the robotic arm from digging deeper into the terrain. To mitigate both these issues, we decided to use the mobility system of Endurance to go to specific locations where rocklets are exposed on the surface and can be identified using Endurance's mast cameras. The robotic manipulator on Endurance would then scrape the surface to collect samples rather than digging and sieving a large volume. This would result in lower interaction loads and be a more efficient way of sampling.

Manipulator: The nature of the manipulation system had a number of options. These included:

- Number of arms: we discussed prospect of putting the APXS and the HLI on a separate robotic arm than the one used for sampling.
- Topology of the arm: We discussed a tree topology of the robotic arm as opposed to a traditional serial link topology. We explored whether an additional link and joint could be added in a Y configuration to the sampling arm to accommodate the instruments.
- Joint configurations: We discussed the different combinations of Yaw, Pitch, and Roll degrees of freedom for the manipulator configuration in tandem with different link lengths to achieve the different behaviors in the sample chain.
- Joint actuators: We discussed different types of joint actuators ranging from those used on the Mars Curiosity and Perseverance arms as well as new technologies from the ColdArm being developed by NASA STMD specifically for surviving lunar nights.
- Accommodation: We discussed various options for accommodating the robotic arm on the rover and configurations in which it can be launch locked and stowed.

We evaluated the different options using criteria such as objectives and constraints of manipulability and reachability for operations, stowage, observability from rover cameras, engineering experience on ease of implementation and design of mechanisms, and cost ranges. We chose to use a 5 degree of freedom robotic arm with two 1m long links in a Yaw-Pitch-Pitch-Pitch-Yaw (YPPPY) configuration with joints based on the ColdArm actuators using bulk metallic material technology. The ColdArm technology does not require additional heaters to operate in the lunar temperature ranges. The 5-dof YPPPY resulted in sufficient manipulability for sample acquisition, storage, transfer behaviors as well as instrument placement. The final Yaw degree of freedom rotates the end effector to alternately use the sampling tool and the instruments. This provides the ability to accommodate the instruments on the same arm while also keeping them shielded from the sampling.

End Effector: For the end effector, we considered different options including:

- Sampling tools used by the Apollo program,
- The simple structural scoop with tines used for Mars Phoenix
- A more capable scoop used by 2010/2018 Moonrise Lunar Sample Return New Frontiers Step 2 proposal that had built in sample flow pathways for scooping and sieving
- The Mars rover end effector design principles (not the specific designs)

The functional goals of collecting the right amounts and types of samples, and accommodating the instruments were fundamental to this trade. The end effector for the robotic sample return option needs to sieve and separate rocklets from the regolith to collect the 60g samples while the astronaut option does not have to do this due to the large volume of samples being collected (~8kg) at each

sampling region. Risks of clogging or blockage of sample flow and uncertainty in regolith properties were significant considerations in these trades leading to designs that simplified sample flow, provided large areas for sample flow to avoid jams/clogs, avoided sharp features, and minimized number of contact surfaces. The end effector also had to fit within the architecture of the entire sample chain and be consistent with the robotic arm, sample cache, and sample transfer.

We chose two different designs for the two approaches. For the astronaut approach, we used a simple scoop similar to the one used in Mars Phoenix. This is a hollow structure with tines at the end to scrape the surface. We made this scoop double ended to ensure the samples could be transferred to the caches located on either side of the rover (reachability consideration). The dimensions of the scoop were sized to collect a large volume of sample while still being small enough to fit in the openings of the sample cache. There are no internal obstructing walls or pathways. We added a mechanism (eccentric mass on actuator) that induces up to 10-g vibrations for ease of sample acquisition and sample transfer.

For the robotic sample return approach, we adopted a sampling approach of first collecting the rocklets and caching them to ensure requisite amount of rocklets were collected. The cache chamber would then be filled with regolith. Our scoop, shown in Figure H-2, has the following features:

- Tines at the sampling end which would scrape the surface for exposed rocklets and regolith.
- A slanted plate with wire mesh to allow any collected regolith or rocklets smaller than 4mm to be separated from the rocklets under the effect of gravity and vibrations. An actuated mechanism is mounted on the scoop which winds up a sprung mass and releases it to apply a large impulse load (thwack) to the scoop and intermittently clean the wire mesh.
- A plate with 20mm circular holes in an array. When the scoop is rotated, the smaller rocklets would pass through these holes (under effect of gravity and vibrations) and be separated from any larger rocklets.
- An open, wide temporary sample collecting area with a wide circular opening for transferring the samples to the cache. The collecting area is open at the top to avoid clogs and for cleaning in case of one. The rocklets can also be imaged when in this area from the open end. The circular opening is short and is 50mm in diameter (>2x the largest rocklet). The circular opening as well as the collecting area can be mechanically unclogged. A slender rod is mounted on the rover body onto which the arm can place either the open collecting area or the circular opening to mechanically remove any clogs with arm motions and vibrations.
- A separate pathway for transferring the regolith. After the required amount of rocklets have been collected, the scoop is used to collect loose regolith from the surface. This regolith passes through the wire mesh and accommodates on another, separate collecting area which also has a 50mm diameter opening. The regolith is transferred to the cache through the 50mm short circular opening. Both the circular opening and the collecting area can also be robotically unclogged using the slender rod mounted on the rover body.

The HLI and the APXS instruments are mounted on the end effector using vibration isolators as used on the Mars rovers to isolate the vibrations used during sampling. They are housed in closed structures with the open end pointing away from the sampling end at approximately 90 degrees. This keeps the open end away from the ballistic pathways of any regolith or dust ejected during sampling. The instruments also have actuated dust covers. Further, for measurements, the instruments are not required to be placed in contact with the surface. These steps ensure the instruments are not adversely impacted by the lunar dust.

The end effector for the robotic sample return option also has an actuated gripper for sample cache transfer to the sample return lander. Its design is based on the grippers used by robots on the International Space Station with mechanical guiding features for alignment with the gripping feature on the cache. The arm can align the gripper on the cache initial with vision guided alignment followed by compliance-controlled alignment arising from mating loads on the mechanical guides.

Sample Cache: Endurance has two separate options for sample cache. For the astronaut-based approach, the cache accommodates 12 different samples amounting to a net 100kg of samples. The robotic sample return option accommodates 12 different samples amounting to 2.4kg net samples.

The astronaut-based sample cache trade was mostly dominated by the goal to accommodate 100kg of sample and the uncertainty on how the astronauts may want to manipulate the cache. Our concept design is made of two separate boxes mounted on either side of the rover. Each box has six separate sample chambers which are open at the top for sample ingress. The scoop of the robotic arm is placed on the opening of each of the chambers and samples transferred under the effect of gravity and vibrations. Cross contamination is not a critical concern, but is addressed using a predefined sample transfer sequence, deep chamber openings, and keeping the scoop size smaller than the opening of the chambers. The deep chambers also ensures that samples do not bounce out during driving. While an actuated lid for each of the boxes can be accommodated, we kept that option open given the uncertainty on how astronauts may want to bring back the samples. There can also be bags mounted in each of the chambers if that is preferred by the astronauts. The boxes have handles for astronauts to grab and remove them.

The robotic sample return option sample cache trades were much richer with various considerations for sample transfer, storage, portioning, cache transfer to return lander, mitigating clogging and jams, dexterity of robotic behaviors needed, ease of implementation of electromechanical design among others. The size of the cache was constrained by what may fit in a sample return capsule and we used the OSIRIS-REx sample canister as a guide for notional bounding volume. We used a disk of 32cm diameter and 10cm height. Given this size and the approximate estimated density of lunar samples, accommodation of 12 sample chambers was volumetrically fairly tight. We also wanted the openings to these individual sample chambers to be as large as possible to ease sample transfer. Moreover, we wanted the sample transfer to be visible to the mast cameras. Further, the desire to take advantage of gravity to transfer samples meant the chamber openings had to be pointed upwards during the transfer. The portioning of the samples was another concern as overfills could cause jams in closing the sample cache lid and prevent correct insertion into the sample return module, thereby ending the mission. Following were some of the different options discussed:

- Horizontally mounted disk with the 12 chambers on the flat face of the disk with their open ends pointing up. We considered different options for lids for the cache as well as various options for passive and actuated lids for the individual chambers. We considered different arrangements of the 12 chambers and their shapes to fit in the allocated volume.
- Vertically mounted disk with 12 radial chambers with openings along the circular periphery. Here also we considered different approaches for lids for the chambers.
- Use of external funnels or guides to ease the sample transfer and portioning.
- We considered various options of moving the arm, moving the cache, moving the funnels, and other options for transferring, storing, portioning, and securing 12 distinct samples.

While the horizontally mounted disk design initially looked like an attractive option, several key challenges arose on closer inspection. Compared to the vertical disk, this option had less volume and smaller openings for the sample transfer for the 12 chambers. Accommodation of individual lids for the chambers was also challenging. Overfilled chambers posed challenges of jams and obstacles for cache lid closure. The arm would have to reach to a different location on the cache for every sample transfer and there would be alignment challenges given the small openings of individual chambers. Further, accommodating a horizontal footprint on the rover within reach of the arm was challenging.

The use of funnels and guides was also found to be challenging as they posed additional areas for sample clog and jams while also needing additional actuators and moving parts, accommodation on the rover, additional mass, and other challenges. This was particularly acute for the horizontally mounted disk option as there would have to either be 12 different funnels for the 12 different chambers or the funnel would have to be itself moved and aligned with the chambers.

We chose the vertically mounted disk with radial chambers open at the circular edge (circumference) as it provided larger sample volume, larger openings for sample transfer, easier accommodation on the rover, and relatively easier accommodation of lid mechanisms. As the openings are along the circumference, they are large enough to not need guides or funnels and also provides margin for arm alignment. The disk is mounted on a single actuator that rotates it about a horizontal axis. This indexes each radial chamber to point its lid vertical upwards to receive the samples. This also ensures the arm can deposit the samples from the same pose for the 12 different chambers. Each chamber has its own lid and the lids are all mounted via a cam driven mechanism to the actuator that rotates the cache. Thus, as the cache is rotated to align a chamber with the vertical, the lid of that specific chamber also opens due to the mechanically coupled cam drive. Similarly, the chamber that is rotating off the vertical alignment also has its lid closed due to the cam drive and rotation of the cache. This makes the sample cache a mechanically coupled and synchronized mechanism that can function deterministically without needing different actuators, sensors, and controls. The design also enables any overflow to fall off as the cache rotates off the vertical before the lid closes. This mitigates any portioning concerns. Further, the mechanisms can be reversible to undo any jams or sample transfer anomalies. A vibration mechanism is also mounted on the cache to assist with sample transfer in the chamber.

The cache also has grasping and guiding features for the robot arm end effector gripper to align and grasp the cache. When the arm has grasped the cache and secured it, the cache can be detached from its rover mount using a pyro device that is not in the load path.

Sample Cache Transfer: The return lander has a single degree of freedom link with an end effector for receiving the cache from the rover arm. Before launch from Earth, the link is aligned with the sample return module's sample retention volume and launch locked to prevent any misalignment. The end effector has a gripper to secure the cache on the link, and guides and visual fiducials to aid in the alignment during sample cache transfer. When the sample cache is securely grasped in its end effector, the launch locks are released. The link is then rotated which causes the link to insert the cache into the sample return module. When cameras on the lander confirm the cache is secured in place, the link end effector releases the sample cache and the link rotates out of the way for the sample return capsule's door to close.

Endurance drives up to the sample return lander and uses its mast cameras and fiducials on the lander to align itself for sample cache transfer. The robotic arm on the rover reaches to the cache, grasps it, and confirms the cache is secure through a deliberate behavior observed by the mast cameras and recorded by the arm force-torque sensor. The pyro device is fired to release the cache and the arm slowly removes the cache from the rover mount. The arm then changes pose to a predefined sample cache transfer configuration. Following this, the arm slowly approaches the end effector on the lander link using a series of small moves that are guided by vision-based estimation of relative pose and distance between the arm and the lander. Operators on the ground monitor the progress with the ability to abort the move and retry if any anomalies are encountered. This arm behavior is somewhat similar to APXS placement on a rock on the surface as the lander link remains passive through the entire sequence.

The trades in this phase included weighing various aspects of the concept of operations, the size and configuration of the link, and the design of the various interfaces for transferring the samples among other considerations.

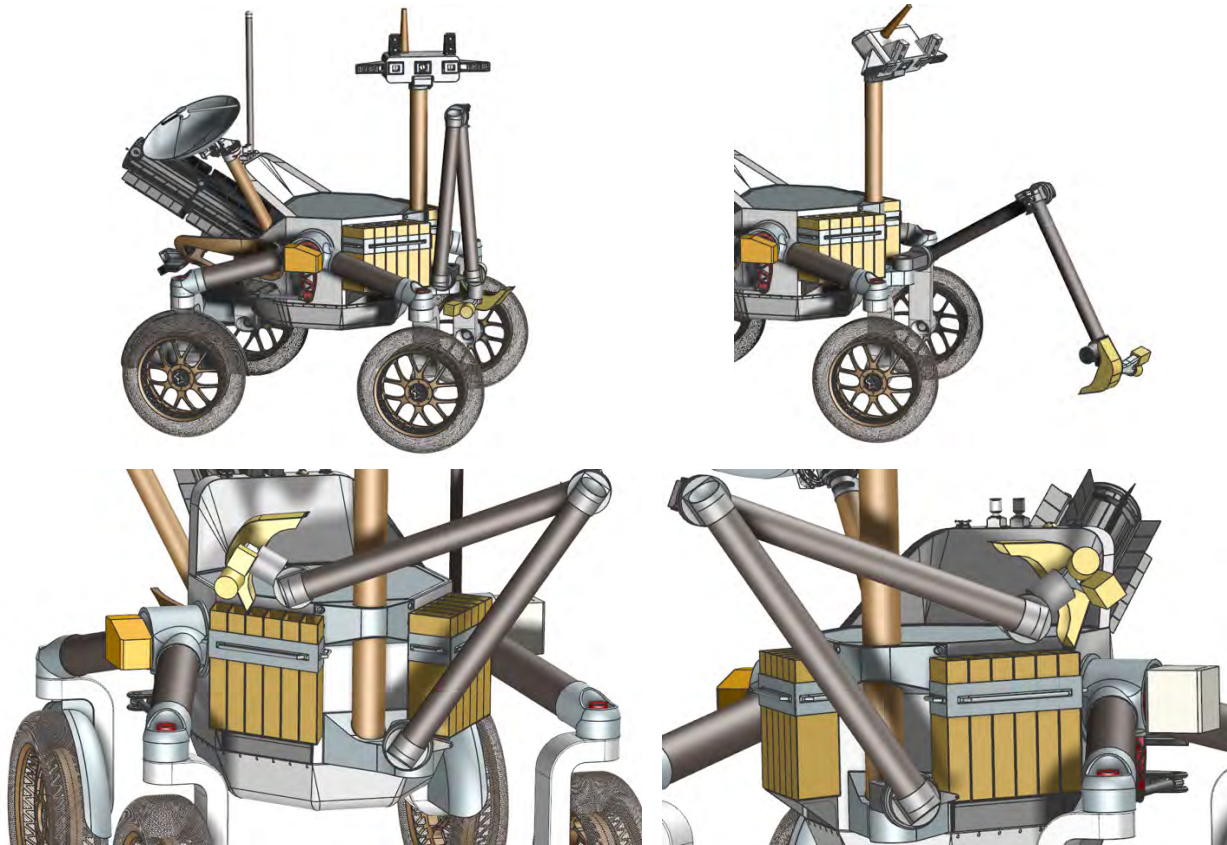


Figure H-1. The sequence of images shows the manipulation and sample cache for the astronaut-based sample return option. The robotic arm with the dual ended scoop is shown in the top row in stowed and sampling configuration. The sample transfer to caches located on either side of the rover is shown in the bottom row. These operations are observable by the mast cameras.

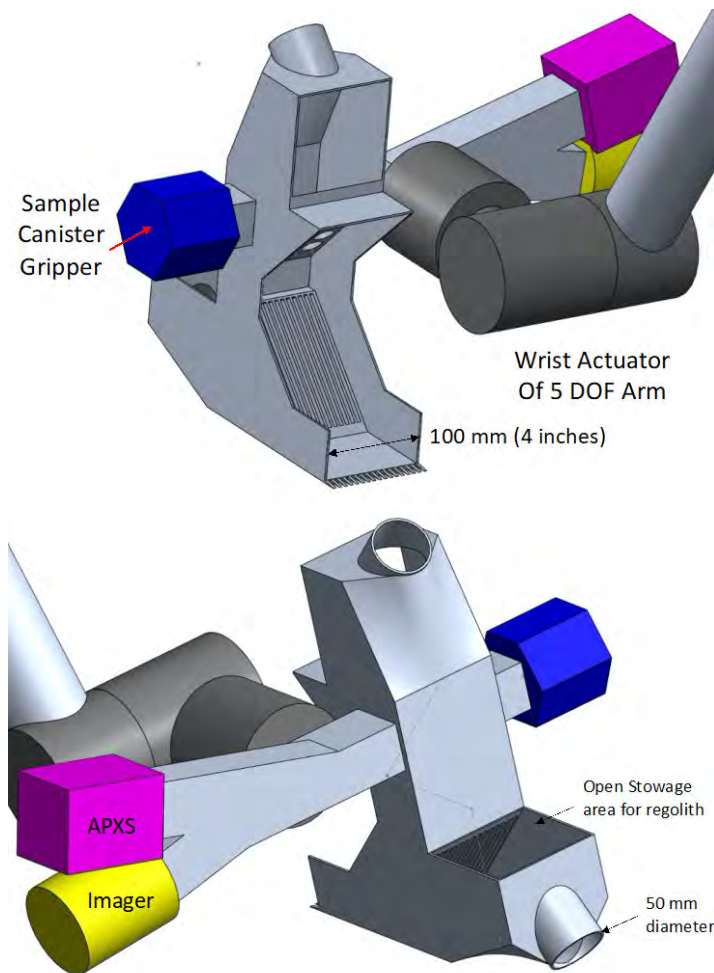


Figure H-2. Two views of the end effector for the robotic sample return option. Top figure shows the various features for rocklet and regolith collection including the open-faced temporary stowage area of the rocklets. Bottom figure shows the instruments and the regolith stowage and transfer features.

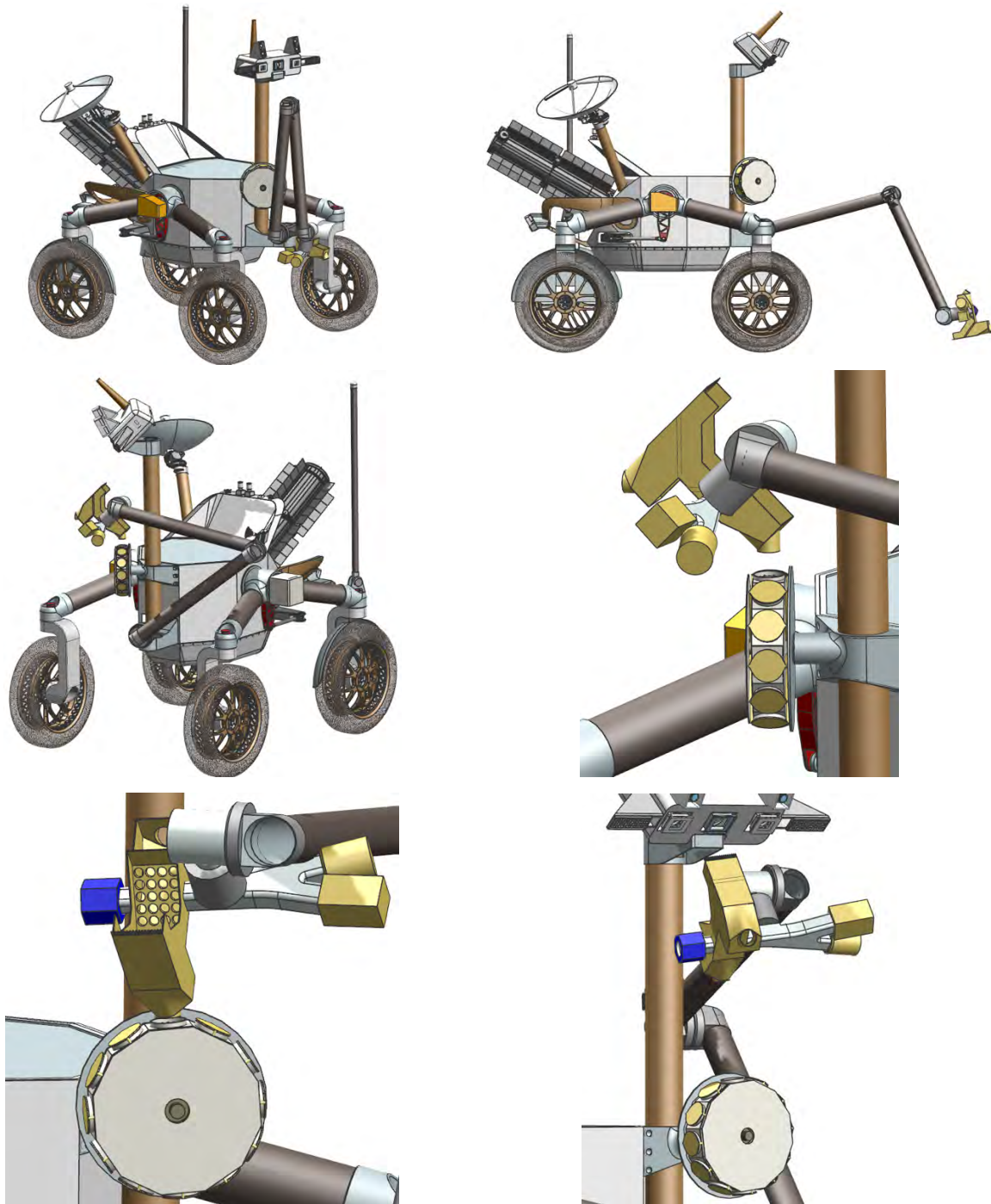


Figure H-3. Top row shows the robotic sample return rover configurations with the sample cache and manipulation system stowed and deployed for sampling. Three different views of the configuration for sample transfer from the arm into the sample cache are shown. The bottom right figure shows the configuration in which the arm retracts and the mast cameras are used to inspect samples in the cache to validate sample caching.

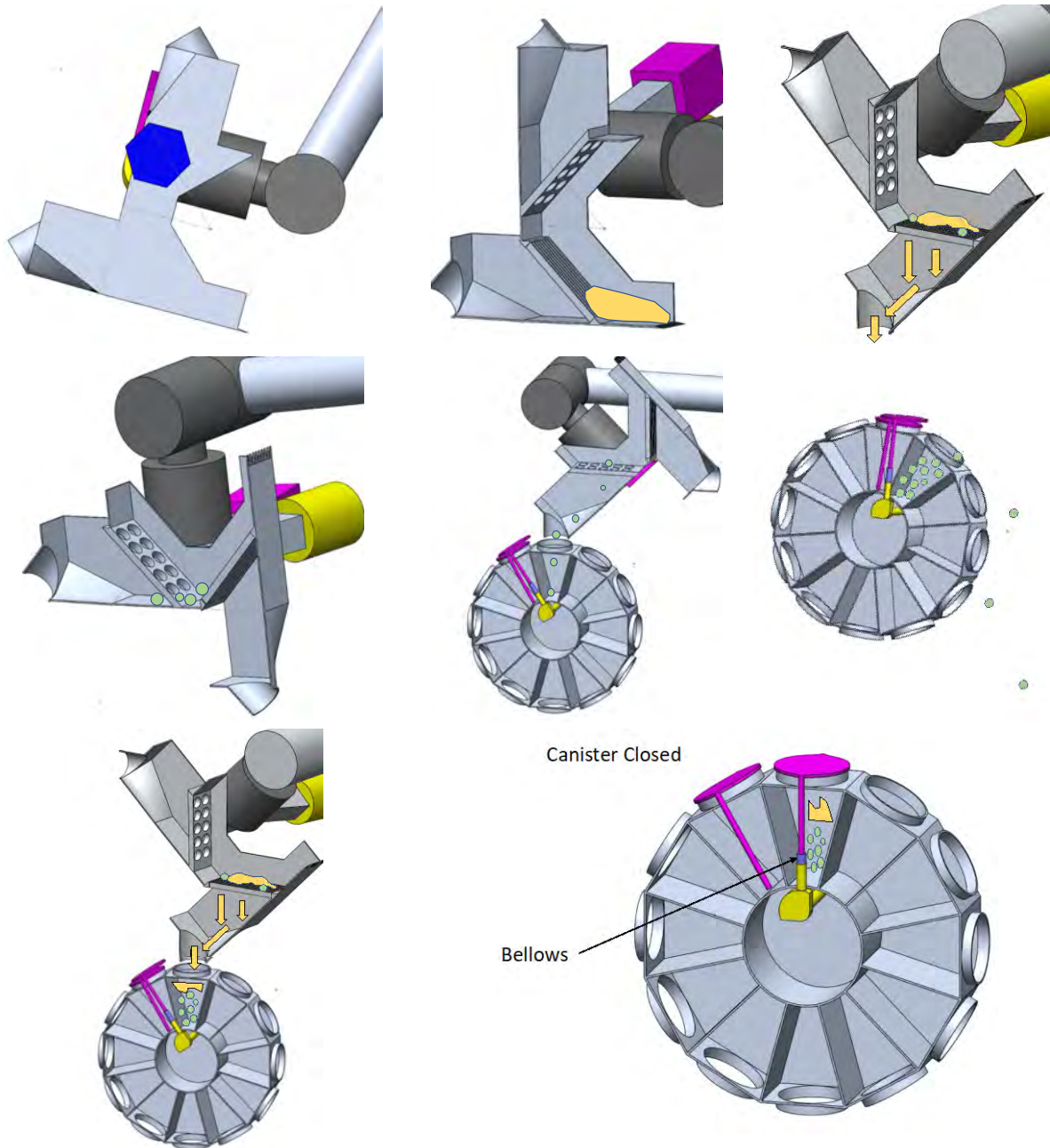


Figure H-4. Figure shows the storyboard of scoop operations and sample pathways for caching. The scoop is shown in sampling configuration followed by cut cross-sections that show how the regolith is discarded through the wire mesh and larger rocklets are stopped by the plate with array of holes. The next image shows the rocklet transfer to the cache chamber where the lid has been pushed open by the cam drive mechanism. It also shows the case of discarding overfilled rocklets by rotating the cache. Finally, the last two pictures show the regolith transfer and closing of the lid for securing the samples in the chamber.

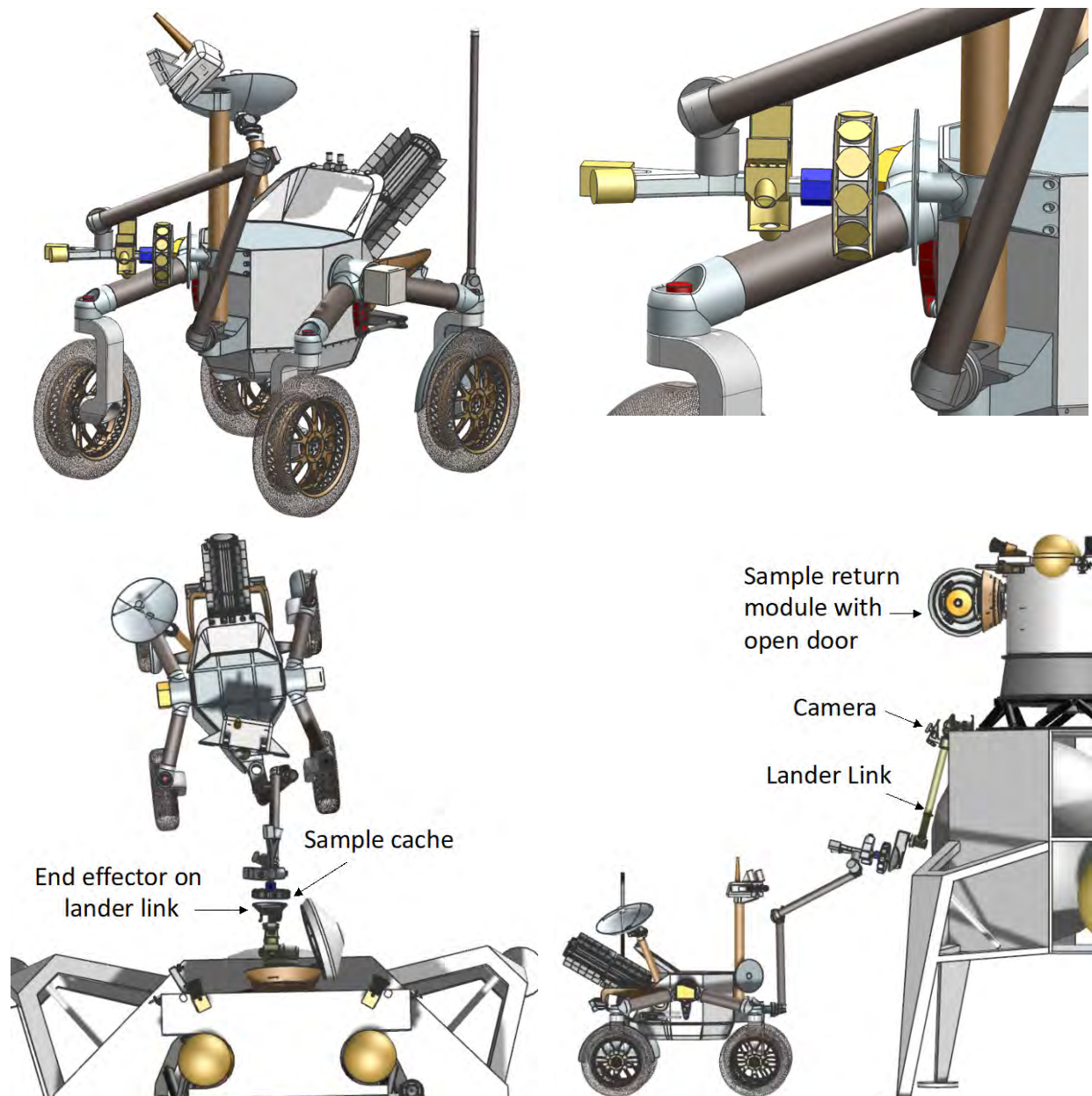


Figure H-5. Figure shows two views of sample cache transfer from Endurance to sample return module. The left is the view from the lander camera. Note, with a 5dof arm, Endurance has a large allocation in its alignment budget on rover pose relative to the lander. The right shows the lander link onto which the cache is transferred and the sample return module with its door open ready to receive the cache. The link rotates through 1 dof after receiving the cache from Endurance and inserts the cache in the return module.

I TELECOMMUNICATIONS

This appendix addresses the communication needs of the Endurance rover. The objective is to design a communications system that meets the science requirements of the mission. The rover will operate on the far side of the Moon, traversing the SPA impact basin on one of two possible routes. The southern route will bring the rover close to the South Pole, and the northern route will traverse up to -35° latitude—it will not go further north than -35° latitude. The region that the rover will operate, the far side, does not have a view of the Earth and therefore no direct line of site to earth is possible. Hence, the rover has to communicate through a relay satellite. The notional launch date of the Endurance mission is 2030 with approximately four years of mission duration.

In this appendix, we establish a baseline end-to-end communications system for Endurance with the understanding that, by the time of the launch of the mission, a more capable communications system is likely to be available. This understanding is critical because the baseline relay, as will be discussed later, is a single satellite network, and, thus, does not offer redundancy. However, there are strong indications that by 2030 there will be multiple relay networks in the cislunar region providing more than one relay satellite option to connect with Endurance [97]. The landscape around 2030 seems promising for easily meeting mission data communication requirements in a reliable and robust fashion.

I.1 LUNAR RELAY SERVICES FOR THE 2030S

The next decade is expected to see a major increase in lunar exploration [97]. These ventures will include both robotic and human activities with science and commercial flavors. NASA and other space agencies have plans to explore the Moon with emphasis given to the poles and the far side. It is safe to assume that the majority of lunar hot spots will be located in areas where direct communications with earth will be difficult or will not be possible. NASA has proposed a communication and navigation infrastructure to lower the barriers to entry for new missions and capabilities to support expanding robotic and human activities at the Moon with emphasis on commercialization [98]. Therefore, it is likely that several relay providers will offer service in the lunar theater for the time frame of interest to us. Currently, there are several lunar relay systems that are being planned or discussed. Among the potential future relay systems, only one has reached the implementation phase: a relay system, called Lunar Communications Pathfinder, is being developed by SSTL, a UK commercial company, to be launched in late 2023 (see Table I-1). This table illustrates the capabilities of three lunar relay systems planned to be launched in the next decade.

No relay system will provide 100% coverage of all the lunar surface. Because of the Moon's size, a relay network with 100% coverage may be cost prohibitive. However, it is possible to provide great coverage to certain parts of the Moon, such as the South Pole region, with reasonable cost. While the first two relays in the above table are single satellite systems, the third one, Andromeda, will have multiple satellites, hence providing better coverage than the other two. The first two relay systems provide good coverage near the Lunar South Pole. Andromeda, on the other hand, will provide 100% coverage of the areas near the South Pole and good coverage for the rest of the Moon. As mentioned above, Pathfinder is currently under development, whereas Andromeda is in the study phase. Pathfinder is scheduled to be launched in late 2023 or early 2024 with a lifetime of 8 years. The service provider, SSTL, is also planning to expand its service in the future by launching additional satellites, assuming their lunar commercial investment will prove profitable. Therefore, we have selected the Pathfinder as the baseline relay service for Endurance because this relay system is highly likely to be available for the time frame of interest to us.

The majority of the relays being planned assume a risk posture of Class D. Therefore, although we are baselining the Pathfinder, we realize that a Class B mission, such as Endurance, will need to have access to two relay satellites in order to meet its risk requirements. It is our belief that more relay satellites are very likely to be available during Endurance's operational life time to fulfil redundancy requirements of Endurance.

Table I-1. Examples of lunar relay orbiters to be launched during 2021–2030 period.

Relay Orbiter	Lunar Gateway (single satellite)	Lunar Communications Pathfinder (single satellite)	Andromeda (Multiple satellites)
Launch Year	After 2024	Late 2023	After 2024
Agency	NASA	Goonhilly/SSTL/ESA	Argotec
Earth Station	DSN, NEN, ESTRACK	Goonhilly, ESTRACK	DSN, Commercial
Orbit type	Near-Rectilinear Halo Orbit (NRHO)	12-hour Frozen Orbit	12-hour Frozen Orbit
Orbital parameters	Max range from S. Pole: 71,000 km	Max range from S. Pole: ~8,400 km	Max range from S. Pole: ~8,400 km
Coverage performance	Orbital period ~6.56 days. Continuous coverage of S.Pole for 144.6 hours with a gap of 5.4 hours	Orbital period 12 hours. Single satellite with continuous coverage of S. Pole for 9.13 hours with a gap of 2.87 hours.	Orbital period 12 hours. Multiple satellite with zero coverage gap at S. Pole
Frequencies and Max Data Rates	Earth to Relay	X-band: 10 Msps; K-band: at least 10 Mbps (may be 30 Mbps);	X-band: 30 Kbps K-band: 16 Mbps
	Relay to Earth	X-band: 4 Msps; K-Band: at least 100 Mbps (may be 300 Mbps)	X-band: 5 Mbps K-band: 100Mbps
	Relay to Lunar surface or orbital user	S-band: 10 Msps; K-band: 10 Mbps; Optical: TBD	S-band and UHF: 128 Kbps S-band and K-band Max:16Mbps
	Lunar surface or orbital user to Relay	S-band: 4 Msps; K-band: 100 Mbps; Optical: rate TBD	S-band and UHF: 2 Mbps S-band and K-band Max:100Mbps
Relay Services	Store-&-forward and bent pipe, In-situ tracking service, In-situ navigation service (TBC).	Store-&-forward communications (Phase I); bent pipe and navigation services will be added in Phase II	Store-&-forward and bent pipe services, navigation services

The European Space Agency (ESA) has invested in the Pathfinder lunar relay and has a close relationship with SSTL. The plan is for NASA to launch the spacecraft. Moreover, NASA intends to use the relay for CLPS landers, and is about to sign a MOU with ESA to have access to the Pathfinder network [99]. The MOU will address the near-term needs of NASA beginning in 2024 and will not explicitly address Endurance.

SSTL has secured a suitable ground station (Goonhilly, UK) for its relay operation. At the start of operations in 2024, the ground antenna will be available 8-hours a day, hence, not able to provide near-real-time communications for most of a 24-hour period. SSTL claims an average data delivery latency of 24 hours [100] during the first phase of its service. However, during the 8-hours-per-day that the ground antenna is available, near-real-time communication may be possible. Moreover, SSTL intends to expand its network and improve network functionality over time (Phase 2 of the relay service), examples of which are launching additional orbiters, acquiring additional ground antennas, and improving the overall performance of the network. For initial Pathfinder operations, the service will be limited to communications only; the expanded capability will also offer navigation services [101]. Improvements planned for Phase 2 provide multiple advantages that include relay redundancy, shortened data delivery period for better near-real-time service, and increased relay coverage and availability. Moreover, additional ground stations will be added to increase relay-Earth contact time. Another possibility regarding ground stations is NASA's Deep Space Network (DSN). Fortunately Pathfinder has been designed to be compatible with the DSN, thus it will be possible to use the DSN when Pathfinder is serving Endurance. Although not a requirement, the use of the DSN can shorten data delivery latency, hence improving on near-real-time operations. In this report, we are assuming that,

by the time of the launch of Endurance, near-real-time operation will be possible for close to 24 hours a day whenever the rover-to-relay link is available.

The Pathfinder relay operates in a 12-hour frozen orbit² that favors the lunar southern hemisphere [101]. It covers the far side of the Moon and benefits from long access times to Earth for relaying back customer data. Since the orbit is frozen, the Moon turns slowly under the orbit making one complete cycle in about 28 days. Therefore, the coverage scenario repeats itself every 28 days. Figure I-1 shows Pathfinder's orbit.

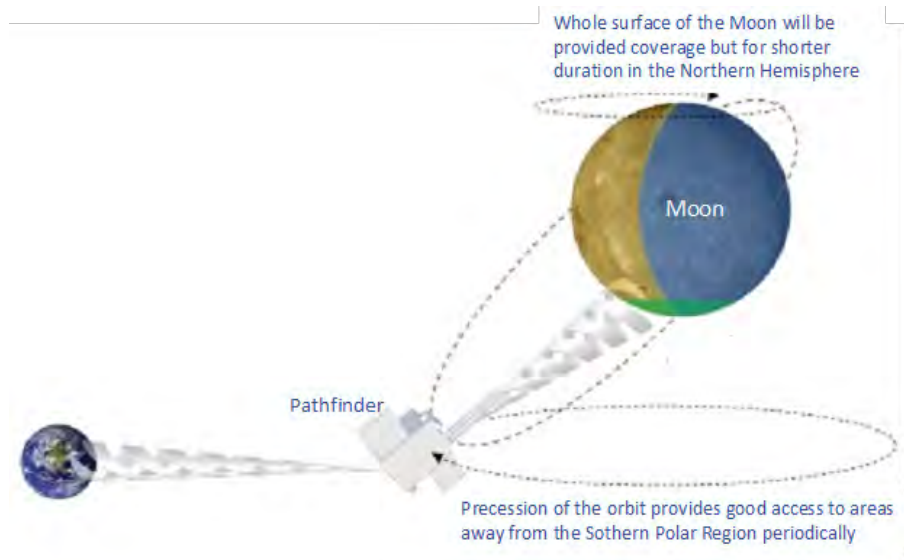


Figure I-1. Pathfinder's 12-hour frozen orbit provides Endurance with long-term, repeat coverage (from SSTL User Guide).

I.1.1 COVERAGE

The Lunar Pathfinder orbit was selected to favor coverage for the southern hemisphere of the Moon, particularly the polar region. Depending on the location of the rover, the coverage by Lunar Pathfinder will vary as discussed in this section. Figure I-2 shows Average contact time as a function of lunar latitude, and Figure I-3 shows the maximum gap as a function of Lunar latitude. The range of traverse for the rover is between the South Pole and -35° . Per Figure I-2, average contact time for Endurance will be between 7 hours and 9.1 hours in a 12-hour period depending on its position on the Moon. The maximum gap will be between 2.9 hours for a location at the South Pole and 6 days for a location with -35° latitude, Figure I-3. Note that in every 28-day period (the Moon rotation period), there will be a communications gap of 6 days for a location at -35° latitude.

For a user on the surface of the Moon, the contact time between the user and Earth is an important figure of merit for a relay system because near-real-time communications is possible only when Earth is visible. This figure can be acquired from the cross section of two time periods, the contact time between the user and the relay and the contact time between the relay and Earth. Figure I-4A shows Earth-to-Lunar-frozen-Orbiter contact time. It is clear that the relay orbit has a favorable view of the Earth. Indeed, 98.2% of the time there is a line of sight from the orbiter to Earth. It should be noted that the gap in contact between the orbiter and Earth occurs mostly when the orbiter is in the Moon's Northern hemisphere. Therefore, for assets, such as the Endurance rover, which is traversing the southern hemisphere, this gap has no effect.

² Original plan was for Pathfinder to use the 12-hour frozen orbit; however, the latest plan is to use a slightly shorter orbital period of about 11 hours. However, all the analyses in this report are done for the 12-hour orbit.

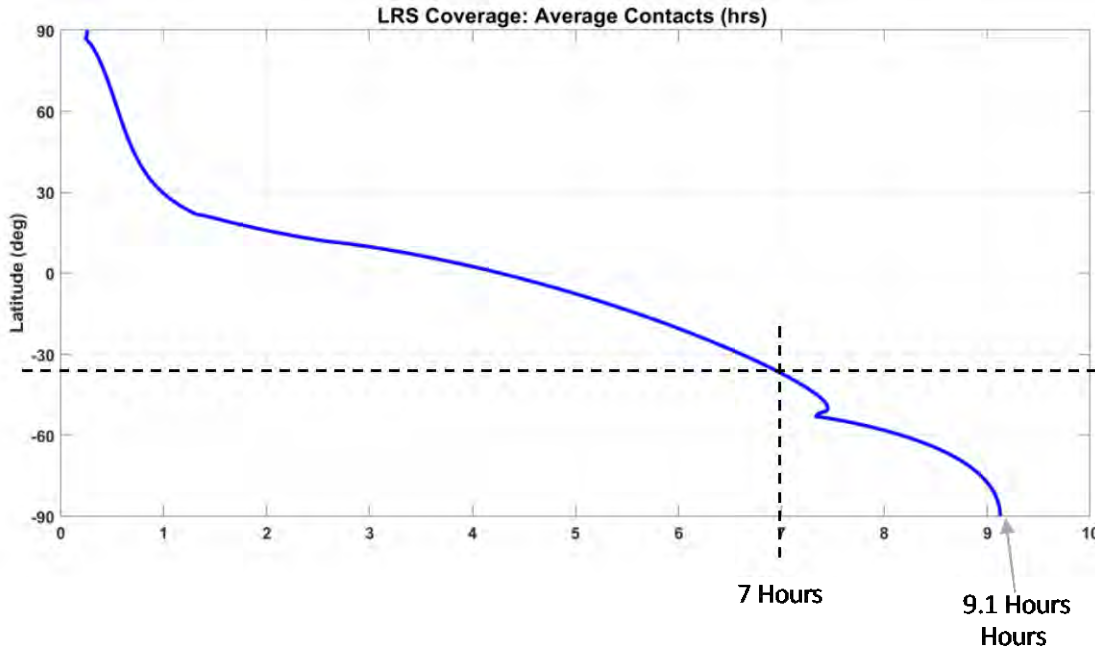


Figure I-2. Communications Pathfinder Relay Satellite Average Contact Time per 12-hour orbit (Credit: C. Lee).

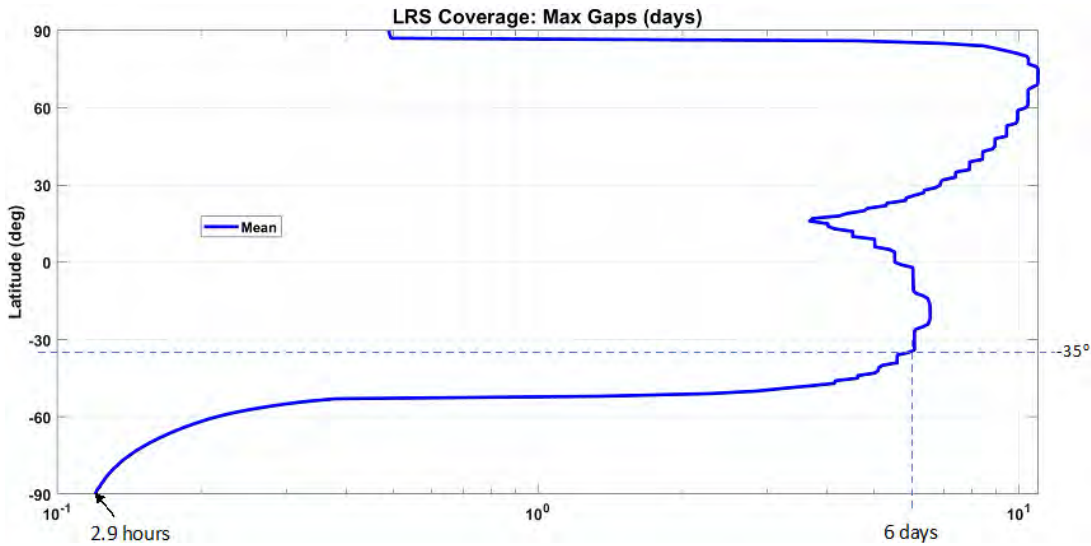


Figure I-3. Lunar Communications Pathfinder Relay Satellite Maximum Contact Gap Duration per 12-hour Orbit (Credit: C. Lee).

Figure I-4B shows rover to relay orbiter gap times for a 28-day period, assuming the rover is at -35° latitude. There is a 6-day gap plus other gaps that are shorter than 10 hours with an average availability of 46%. In a 28-day period, there are 44 contact events with minimum contact time of 2.57 hours and maximum contact time of 9.38 hours. Note that considering Endurance's traverse range, -35° latitude experiences the longer gaps with respect to locations at lower latitudes.

Figure I-4C is obtained from merging 4A with 4B. It provides the end-to-end gap profile for a location with -35° latitude. Figures I-4B and I-4C look similar because the relay has a clear view of Earth while serving a user at -35° latitude. Figure I-5 illustrates the path (rover-to-relay) elevation angle. As can be seen, there is a long period with the duration of 6 days in a 28-day period where elevation angle is less than 10° . Note that 10° is the threshold below which the relay is assumed not visible to the rover.

End-to-End Visibility for 35 degrees South

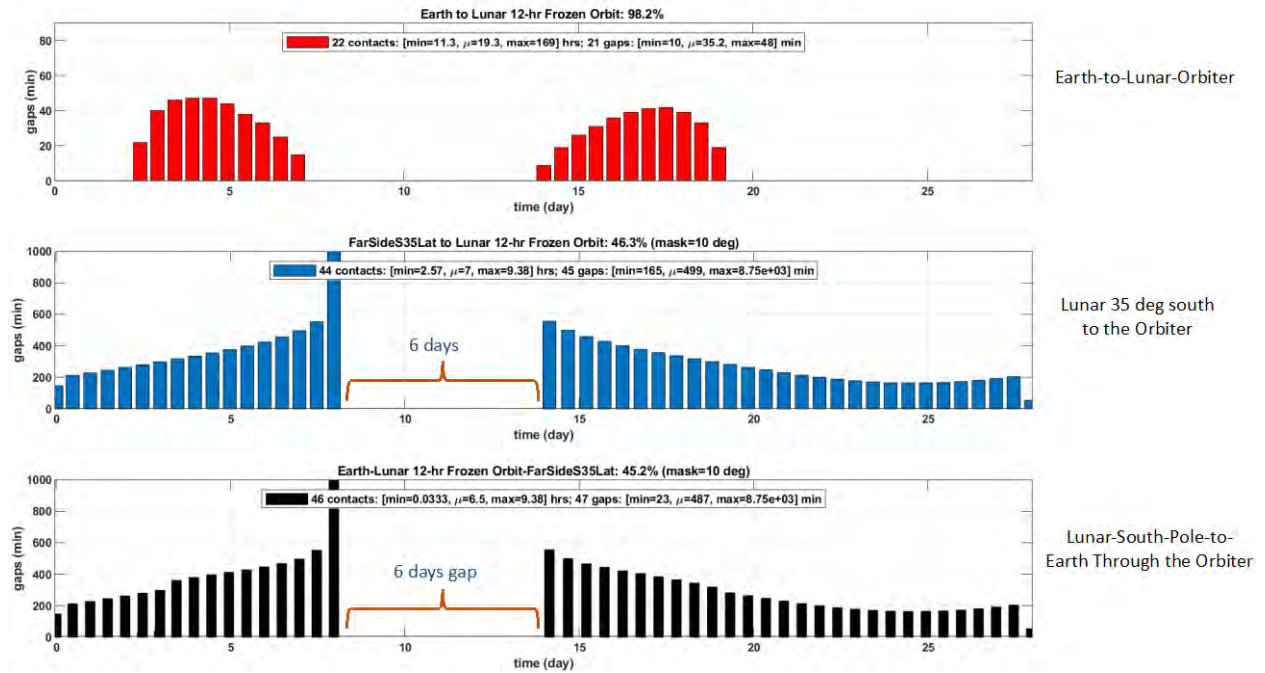


Figure I-4. A) Earth-to-Lunar-Orbiter Contact Gap Profile; B) Lunar 35° South to the Orbiter Contact Gap Profile C) Lunar 35° South to the Orbiter Contact Gap Profile (Credit: C. Lee).

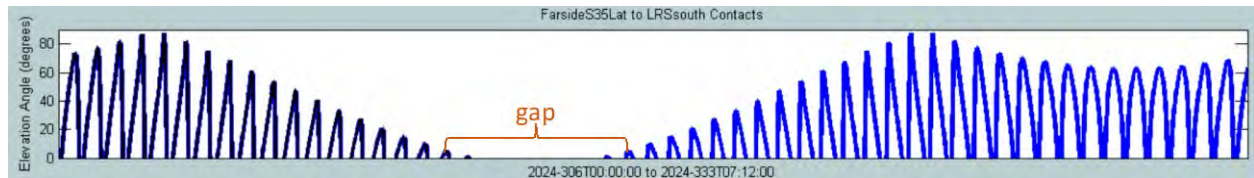


Figure I-5. Six days of continuous gap in every 28-day period, 35 degrees south (Credit: C. Lee).

Figure I-6 shows the average relay coverage as a function of latitude. Per the Endurance schedule, the rover position on the Moon will be between the South Pole and -35° latitude.

There are a few noteworthy points regarding relay coverage:

- Earth visibility to the relay orbiter is very high
- Maximum Earth visibility gap period is 48 minutes
- Lunar 35-degree south latitude to the relay visibility is 46% with a mask of 10 degrees (path elevation angle minimum is assumed 10°)
- Bent-pipe visibility from -35° to Earth (to allow near real time operation) is also about 46% with a 6-day gap in any 28-day period
- Assuming ground station availability, operation can be bent-pipe rather than store-and-forward

Figure I-7 illustrates the maximum and minimum in-view range of the relay from lunar surface as a function of lunar latitude. Note that from -35° latitude, the maximum distance is about 9,400 km and the minimum distance is about 2,600 km.

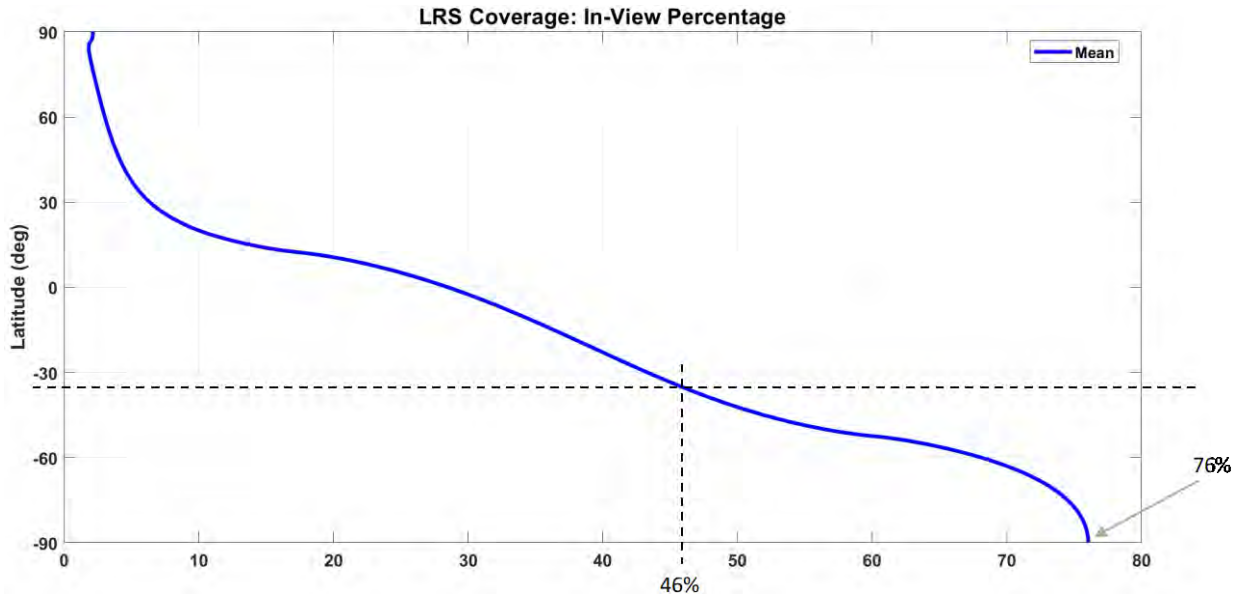


Figure I-6. Average relay coverage as a function of latitude (Credit: C. Lee).

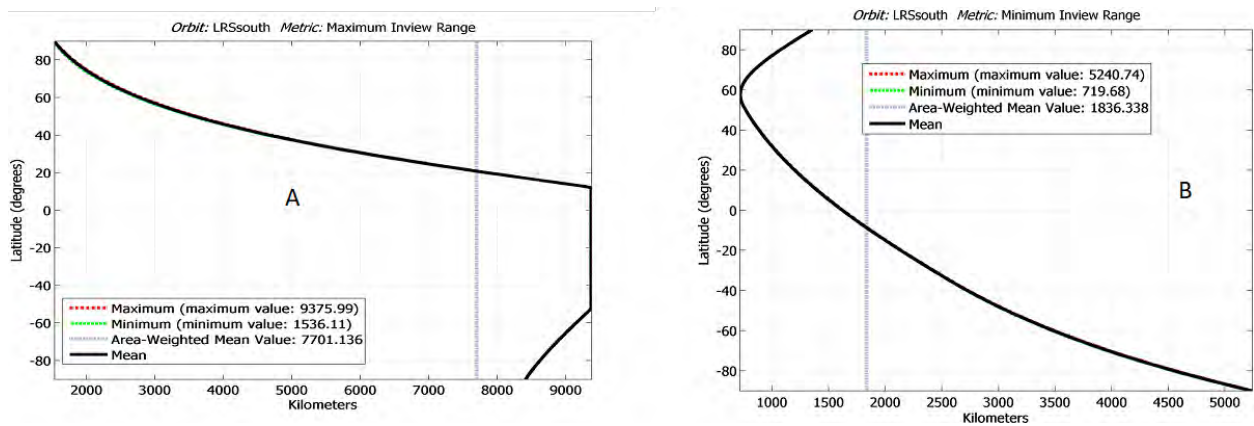


Figure I-7. Relay orbiter range from lunar surface; A) maximum distance and B) minimum distance (Credit: C. Lee).

I.1.2 EMERGENCIES

The Relay User Manual does not address user emergencies at this time. However, the service provider will develop an emergency plan at a later date. This plan will address emergency events and how a user can contact its mission control in such events.

I.2 COMMUNICATIONS LINK

This section provides an analysis of the link for calculating rover antenna size and amplifier power. The Pathfinder User Guide [101] provides technical data on the relay-to-rover link. The important points are summarized in Table I-2.

Since it is desired to operate the rover radio at the maximum transmit data rate of 2 Mbps, the rover communications system must produce an Effective Isotropic Radiated Power (EIRP) of 26.5 dBW per the above table. With a margin of 3 dB, the required EIRP is 29.5 dBW. This value can be obtained from the combination of a 5-W (7 dBW) power amplifier and an antenna with gain of 22.5 dBi. The size of the antenna can be

Table I-2. Important link information copied from Lunar Communications Pathfinder User Guide.

Transmit data rate (Endurance to relay)	<2 Mbps
Receive data rate (relay to Endurance)	<128 kbps
Required Endurance EIRP	26.5 dBW
Required Endurance G/T	-6 dB/T
Protocol	CCSDS Prox-1
Forward Frequency	2025-2110 MHz
Return Frequency	2200-2290 MHz

obtained from Figure I-8 to be 75 cm. The antenna must track the satellite as the relay slowly moves over the sky. Satellite tracking does not have to be extremely precise because the antenna beam is not very narrow. Figure I-9 shows antenna gain loss as a function of tracking error. For example, a 3° tracking error will result in a small gain loss of 0.5 dB.

For rover emergencies, the high-gain antenna will not be used. In this case, a S-band low gain antenna with a gain of 3 dBi will be employed. Assuming a 5-W amplifier, the low gain antenna can support a data rate of 22.4 kbps; this figure is obtained from reducing high gain antenna data rate of 2 Mbps by 19.5 dB ($19.5 = 22.5 - 3$). Similarly, the receive (commanding) rate of the low-gain antenna can be calculated. The required G/T for a receive data rate of 128 kbps, per Pathfinder User Manual, is -6 dB/T. With a 3 dBi antenna gain and a system noise temperature of 400 K, antenna G/T becomes -23 dB/T. The difference between the low gain antenna G/T and the required G/T is 17 dB (50 decimal). Therefore supported rate is $128/50 = 2.56$ kbps. To operate the link with a 3-dB margin, we reduce the above rate by a factor of 2 to get 1.2 kbps.

Note that in the above calculation we have used 400 K as the receiver system noise temperature which is a conservative assumption. This noise temperature does account for day time operation when sun is present. The overall effect of sun on the noise temperature is about or less than 10 K [102].

I.2.1 THE RADIO

The rover needs a radio with certain features. These features include the Proximity-1 standard, transmission rates up to 2 Mbps, and a risk posture of Class B. We identified three radio products for Endurance that can provide the above features. Although, these radios range in their maturity, capability, and cost, all three can meet Endurance's communications requirements. Table I-3 shows these options.

The UST-Lite transponder is a JPL design based on the UST radio (power amplifier is not included with the radio). One version of UST, a Ka-band modulator called KaM [103], is slated to fly on the NISAR Earth Orbiting mission in 2022. The KaM flight units are being integrated into the S/C now. UST-Lite is currently under development at JPL; it has a mass of 1 kg and uses only 14 Watts when engaged in simultaneous reception and transmission. The Frontier-Lite radio is designed by the Applied Physics Laboratory (APL) based on their TRL-9 Frontier radio. It offers the lowest mass and power among the three options. Frontier radio (not Frontier Lite) has flown before on multiple missions. The L3Harris transponder has the highest mass and power, however, it is very mature at TRL 9, and it comes with its own 8-W Solid State Power Amplifier (SSPA). This radio requires the lowest lead time among the options. None of the above radios is equipped with Proximity-1 protocol at the

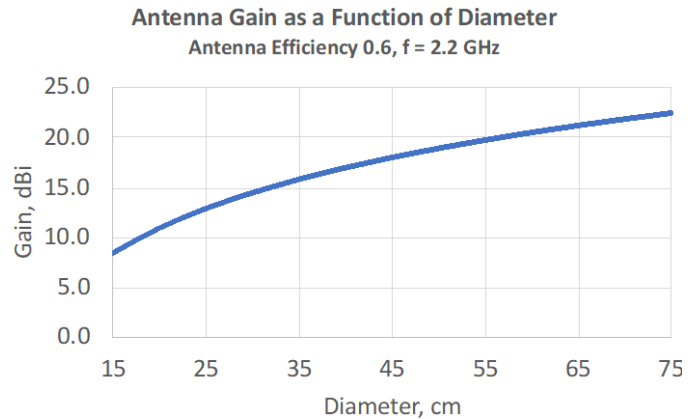


Figure I-8. Antenna gain as a function of diameter for a parabolic antenna.

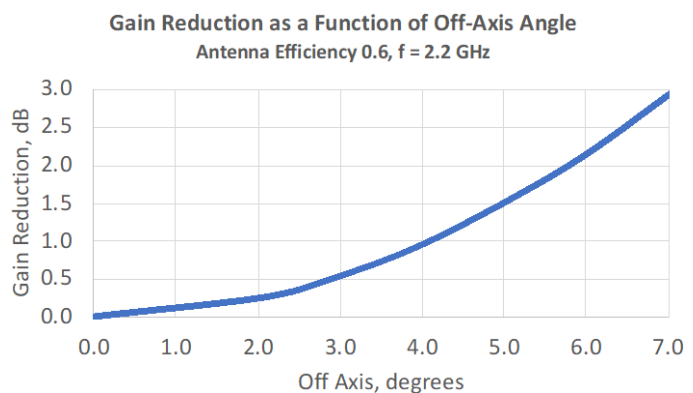


Figure I-9. Antenna gain loss as function of antenna mispointing.

Table I-3. S-band radio options.



	UST-L Transponder	Frontier Lite S-Band Transponder	L3Harris KG-150 (CX5-2000/C) Transponder
Mass	1 kg	0.5 kg (not incl SSPA)	5 kg max, with triplexer (includes 8W SSPA)
Volume	16x10x9 cm ³	15.2 x 9.7 x 2.2 cm ³	22.5x17.4x14.3 (cm ³)
Power	14 W (PA not included), 10W for receive only	4.5 W	63 W
RF Power	SSPA not included	0.7 W	8 W
TX rate	10bps-1Gbps	100sps - 10Msps	8 Mbps
RX rate	7.8 bps-1Gbps	100sps - 1Msps	2 Mbps
S/C interface	RS-422 & Spacewire	Spacewire,	RS-422
Encryption	AES256	No, likely can add	External, Can support AES256 or Suite-A solutions
Protocol	Prox-1/USLP	AOS, Prox-1 can be added	Prox-1 can be added
Lead time	30 months	28 months	18 months nominal, can be improved with advance notice
Price	\$5M for the first unit, \$2M per additional unit, Class B	\$450K, quantity of 10, Class D; Class B and C are possible	Varies based on Qty, notionally \$1.5M, Class B

present time, but this option can be added to them. In this study, we are using UST-Lite as the baseline with the understanding that any of the above radios can be used.

Proximity-1 is a Consultative Committee for Space Data Systems (CCSDS) hardware and link layer protocol for proximity links [104-106], and it is anticipated to be used widely in the future. Furthermore, it is expected that, by the time of the launch of Endurance, additional lunar relay satellites will be available providing backup to Pathfinder. The use of Proximity-1 will provide a standard interface for using other relay satellites.

Although the Proximity-1 standard allows for the relay as well as the rover to initiate communications through the hailing channel, the plan is for the relay (Pathfinder) alone to initiate communication sessions. We believe this limitation is likely to be removed by the time Endurance becomes operational, hence, also allowing for the rover to initiate contacts.

I.2.2 THE ANTENNA

The high-gain antenna will consist of a dish and a gimbal with azimuth and elevation rotation. One of Mars antennas could be modified for this application, or a new design can be used.

I.2.3 FUNCTIONAL BLOCK DIAGRAM OF THE COMMUNICATIONS SYSTEM

The functional block diagram of the communications system is provided in Figure I-10. Because the rover is a Class B asset, there are two radios and two power amplifiers for redundancy. Switches are provided to allow for switching between the radios. Each power amplifier is associated with only one of the radios. Table I-4 shows parts count of the telecom subsystem. It is recommended that the radio, SSPA, and antennas be configured in close proximity of each other to reduce coax losses, and the antennas should not be blocked by the body of the rover to prevent loss of data. Furthermore, science payloads, rover power system, etc., should not cause harmful interference to the communication system.

Table I-4. Rover Communications Subsystem Parts Count.

Item	Number
Radio	2
SSPA	2
Antenna	1 HGA and 1 LGA
Switch	2
Coax Cable	12
Diplexer	2

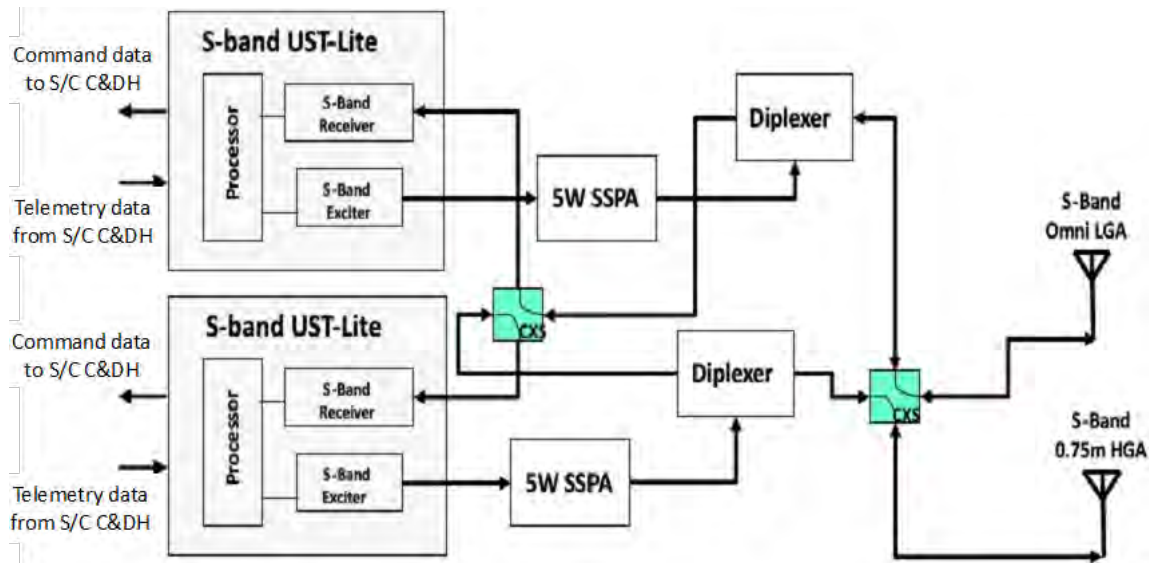


Figure I-10. The functional block diagram of Endurance communications System consisting of two redundant radio, two redundant power amplifiers, two switches, two diplexers, one tracking high-gain antenna, one low gain antenna, and coax cables (Credit: T. Voss).

J THERMAL DESIGN

Thermal control of low latitude rovers that must survive diurnal cycles is challenging due to the extreme cold and hot conditions, each of significantly long duration. This places an importance on the thermal analyses to accurately model the environmental conditions such that a high degree of model uncertainty does not drive an excessive need for system resources for rover survival.

Terrain features can have significant effects on the rover's thermal energy. Data from the Apollo program showed noticeable temperature increases when in view of distant hills. In the case of a rover with a scale factor on the order of nearby boulders and terrain features in combination with random tilts as it drives over an irregular surface, the thermal design must be coordinated with the operations plan to ensure a sufficiently high probability of success. This includes the ability to drive through unacceptable orientations that would otherwise result in high temperature limit violations.

Dust effects on thermo-optical properties of radiating surfaces must also be modeled accurately. An overly conservative approach would preclude a radiator design that receives an appreciable amount of solar flux while maintaining standard avionics temperature limits, thus requiring either an articulated radiator, dust mitigation provisions, or impractical orientation restrictions placed on the rover. Depending on the lander design, plume interaction analyses may be required to ensure an acceptably low amount of dust contamination on thermal control surfaces.

These environmental loads and influences must then be modeled onto the rover and its resulting thermal design. Heater energy predictions during the lunar night must be accurately predicted because of its driving effect on the power system and science-returning operability. Conservative, worst-case hot analyses are necessary for RPS hardware due to the strict interface requirements.

Lunar Surface Modeling. The effect of terrain features requires, at a minimum, representative cases to be run that include surface topography. Such cases are used to establish sensitivity analyses, or better yet, uncertainty quantification that can be used to assess temperature violation probabilities. Wider-swath topology data can be used to assess the effect of more distant terrain features. Custom scripts have been developed at JPL for translating Lunar Reconnaissance Orbiter (LRO) data to finite element mesh for direct use in the Thermal Desktop® analysis software. Both higher resolution LRO data (LROC NAC data) and lower resolution data (WAC and SELENE TC + LRO WAC) are accessible by the JPL tool. A 2-D mesh is generated depending on the user-specified resolution. In Figure J-1, example snapshots of processed LRO surface data are shown at user specified lat/long, area, and discretization and a resulting surface temperature prediction.

The in-depth model of the regolith or basalt is a 1-D model with sufficient skin depth to negate edge effects and is based on the penetration depth of a periodic temperature wave corresponding to the diurnal. Based on properties given in reference [107], this penetration depth corresponds to 7 cm for regolith and 68 cm for basalt. The thermal model then simulates a depth 10x this amount for conservatism with a nodal resolution of 1/10th the skin depth.

Dust Effects. Thermal analyses assume sensitive thermal control surfaces are protected from ballistic impacts of regolith or basalt particles. Thermal control surfaces that lack any dust mitigation mechanisms are assumed to eventually be covered by a monolayer of lunar regolith dust regardless of orientation and location. The nature of the dust, most importantly the solar absorptivity and IR emissivity, can vary depending on location on the moon. For conservatism, assuming a darker, mare-type dust is prudent when performing worst-case analysis. Testing done by [108], of NASA Glenn Research Center has shown that second surface silverized Teflon films are less susceptible to dust degradation than white paints for radiator surfaces. Because of the lack of actual regolith from the mare for testing, we assume the JSC-1AF simulant properties. Testing by [108], has shown that for such a monolayer over 5-mil silverized Teflon film, the solar absorptivity to IR emissivity ratio (α/ϵ) goes from 0.09/0.8 when pristine to 0.29/0.9 degraded.

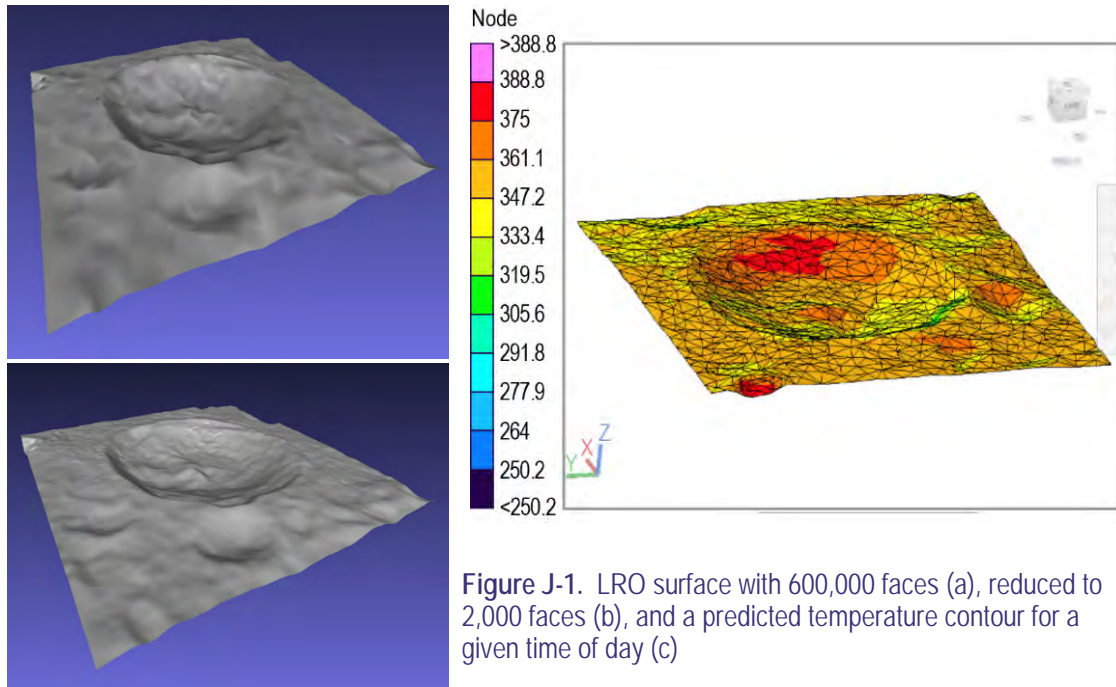


Figure J-1. LRO surface with 600,000 faces (a), reduced to 2,000 faces (b), and a predicted temperature contour for a given time of day (c)

For surfaces with lower IR emissivities, such as specular surfaces used on shields, JPL has found no reliable test data. And unlike for Martian dust, the particle size cannot be assumed sufficiently small as it is on Mars (~ 1 micron) to be effectively transparent to IR wavelengths. We are left to assume that particles are sufficiently large to not be IR transparent (> 10 microns) and that further testing is required to characterize the effects of dust on specular surfaces.

Intrepid Thermal Analyses. The thermal design is challenged by the extreme hot conditions of direct sun on the radiator or, worse, an orientation that also includes unfavorable views to the terrain that reach temperatures near $100\text{ }^{\circ}\text{C}$ at latitudes of 35 ° that are within Endurance's range. The primary challenge then is to allow for adequate heat rejection during the day while reducing it during the night when heating may be required. To minimize thermal resources, hardware temperature limits that span a wide range are most helpful. Such is the case with external elements such as mobility actuators and structure. But batteries, avionics, and some instruments require much narrower temperature ranges to operate and will require special provisions for them to remain within limits without employing excessive resources to do so. Table J-1 lists the driving temperature limits for Endurance hardware.

The extreme environment of the lunar surface and temperature limits drive the following thermal design:

- Where possible, items with narrow temperature limits such as batteries, avionics, and motor controllers are placed in a central Warm Electronics Box (WEB) that is well insulated.
- External elements should be qualified to a wide temperature range to prevent excessive amounts of localized survival heating and heat rejection surfaces and accompanying orientation restrictions.
- To minimize costs associated with mechanisms for an articulated radiator, a zenith-facing radiator is used to reject waste heat dissipations from the WEB. Obstructions that are within view of this radiator should be minimized.
- To reduce the amount of heat leak at night, a set of thermal switches are used that passively decouple the avionics within the WEB from the radiator. These switches work on the principle of differences in the coefficient of thermal expansion between materials and have an on/off heat conductance ratio of about 5 W/K to 0.002 W/K .

A block diagram schematic of the thermal design is shown in Figure J-2. The radiator is sized based on maintaining internal WEB components below 50 °C with a silverized Teflon coating whose properties are degraded by 100% coverage by a monolayer of lunar dust. The radiator surface area is sized at 1 m² and is capable of rejecting 100 W internal dissipation at 35° latitude with a 15° unfavorable rover tilt. During the night, 21 W of internal dissipation is required to maintain minimum WEB temperature of -20°C. For all cases except a safe or sleep mode, there is sufficient equipment dissipations without the need for electrical resistive heating. Figure J-3 and Figure J-4 show the solid model representation of the thermal design. Note that constant conductance heat pipes are embedded within the structure that runs between the dissipating components and the heat switches.

External Elements.

The actuators are expected to tolerate temperatures down to 90 K during the night while not operating. Prior to use, they will be heated by external heaters. Warm up times for larger actuators such as those used on the robotic arm can take about 7 earth hours to warm to a start-up temperature of -55°C using a 15 W heater wrapped around the external housing.

RTG Temperature. The GPHS-RTG has a maximum allowable fin root temperature of 260°C on its outer casing. The RTG placement was configured based on a conservative assumption of a heavy dust coating on the RTG’s white painted surface (IR emissivity = 0.9; solar absorptivity = 0.8). Figure J-5 shows that under a worst case 15° tilt at local noon at a latitude of 35°, fin root temperatures remain below the 260°C (533 K) limit.

Table J-1. Endurance Temperature Limits.

Intrepid Hardware	Allowable Flight				Protoflight or Qual			
	Operational		Nonoperational		Operational		Nonoperational	
	min	max	min	max	min	max	min	max
Sabertooth Board	-20	50	-30	50	-35	70	-45	70
Motor Controller Board	-40	50	-40	50	-55	70	-55	70
Power Board	-40	50	-40	50	-55	70	-55	70
Telecom and Multiplexer (MUX) Board	-20	50	-30	50	-35	70	-45	70
IMU	-39	51	-47	65	-54	71	-62	85
Li-Ion Battery	-20	50	NA	NA	-30	70	NA	NA
Motor Winding	-70	135	-100	135	-85	155	-120	155
Gearbox	-55	135	-131	91	-70	135	-146	111
APXS Sensor Head Housing	-170	-5	-170	50	-185	70	-185	70
APXS Electronics Housing	-45	50	-45	50	-60	70	-60	70
FarCam	-55	50	-120	50	-70	70	-135	70
GRNS Detector	-30	30	-35	50	-45	50	-50	70
GRNS Electronics	-30	30	-35	50	-45	50	-50	70
SW Suprathermal Sensor	-30	30	-50	60	-45	50	-65	80
SW Suprathermal Electronics	-30	40	-50	60	-45	60	-65	80
Solar Wind Sensor	-30	40	-50	60	-45	60	-65	80
Solar Wind Electronics	-30	40	-50	60	-45	60	-65	80
Engineering Camera Detector	-20	40	-40	70	-35	60	-55	90
Engineering Camera Electronics	-45	55	-40	70	-60	75	-55	90
EECAM (CMOS, Optics, Elec)	-55	50	-120	50	-70	70	-135	70

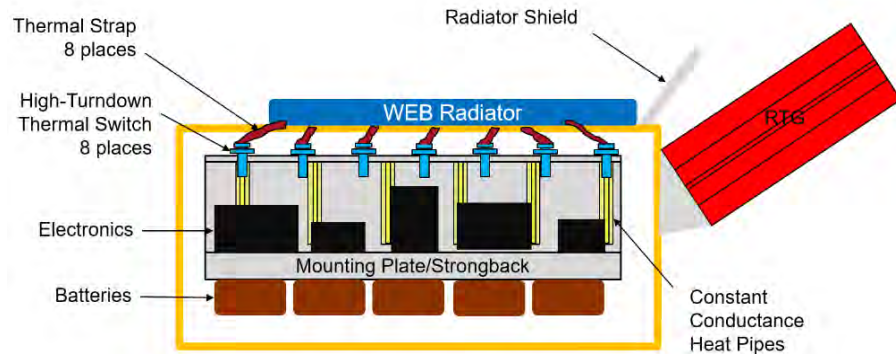


Figure J-2. Endurance WEB thermal control block diagram.

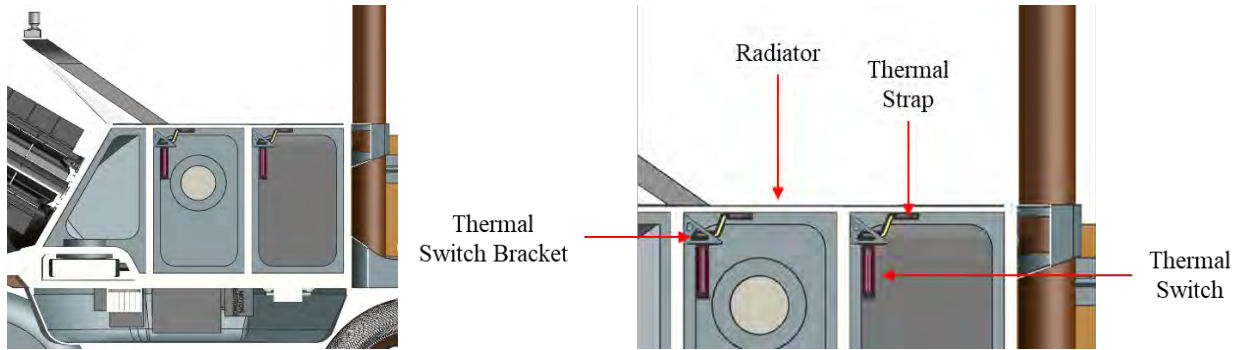


Figure J-3. Cut-away view showing the rover WEB thermal design with Constant Conductance Heat Pipes (CCHPs) embedded within honeycomb structure.

Instrument Thermal Control. The instrument with the most restrictive upper temperature limit is the APXS sensor head with an upper allowable of -5°C . Note that the internal sensor temperature is held colder by a built-in thermoelectric cooler and that the temperature limit applies to its hot-side interface. Maintaining this temperature with passive thermal control is not possible without a dedicated, shielded radiator that is accompanied by highly restrictive orientation requirements. At best, a passive thermal system with a zenith-facing radiator can operate during limited morning and afternoon windows. To provide greater science opportunities, a Ricor K508 cryocooler that can operate under warm conditions is baselined for the APXS (Figure J-6). It requires 8 W of input power that corresponds to a cryocooler heat sink temperature of 52°C which may be supplied by a local radiator. This allows nearly unrestricted operation of the APXS, barring extreme blockage of its local radiator.

Other instruments may be maintained below their upper allowable temperature limits with local radiating surfaces facing zenith.

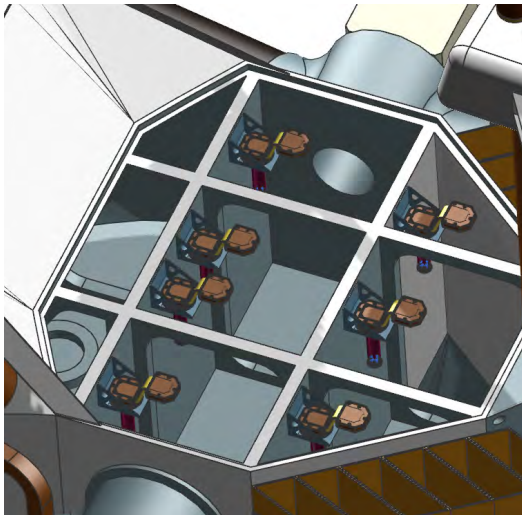


Figure J-4. Detail of the heat switch and flexible strap mounting assembly.

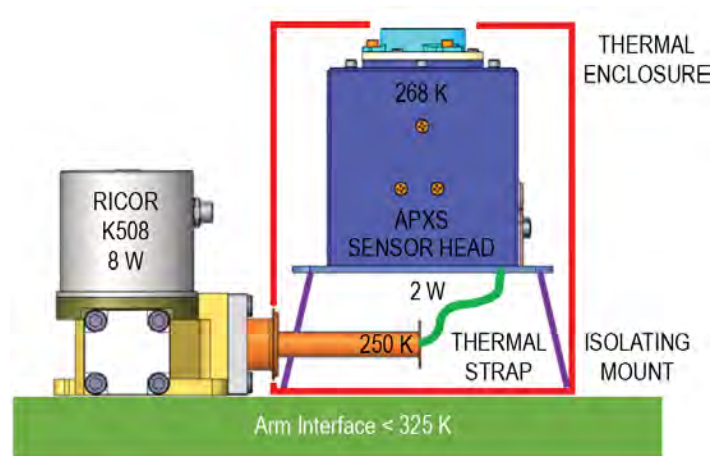


Figure J-6. APXS cryocooler configuration.

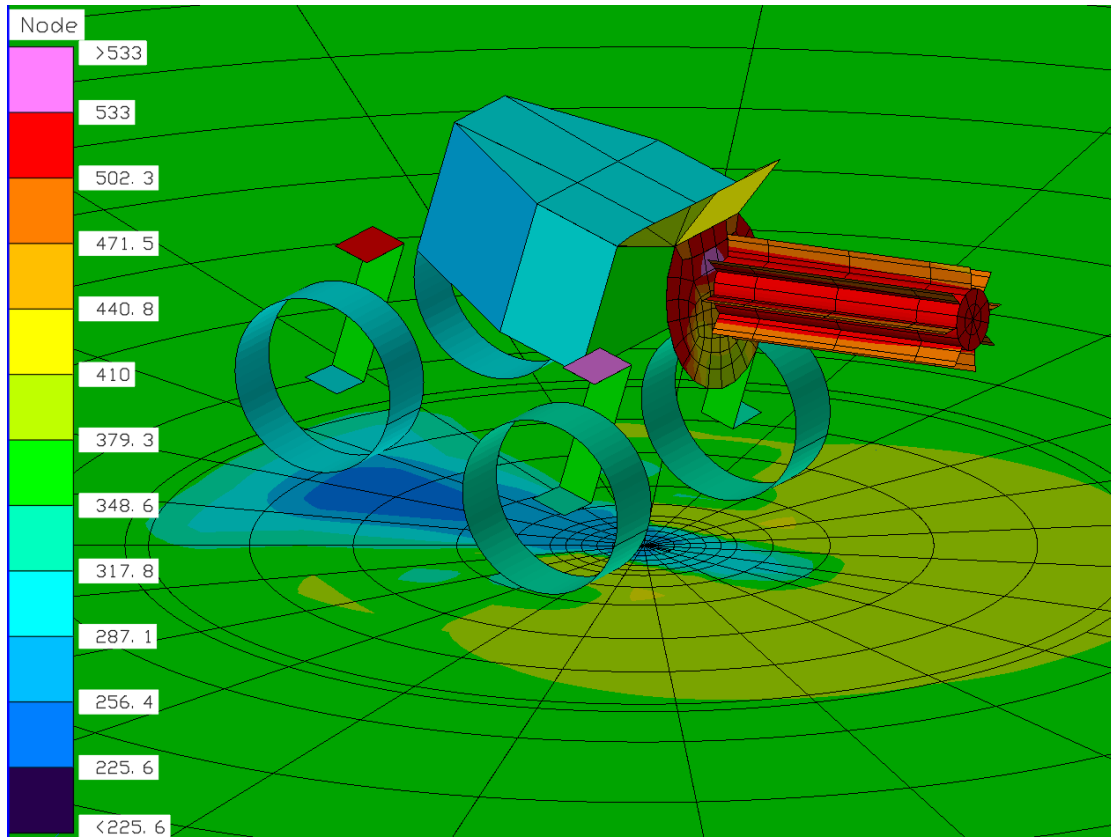


Figure J-5. RTG temperature prediction under worst case hot conditions.

K PATH PLANNING

The Endurance path planning involved an iterative process, starting with identification of the regions where the science stops would be selected, and finding of the datasets that were available for analysis within and between these regional sites. Notional paths between the regions were mapped. Higher resolution datasets which covered these regions were identified and used to support detailed path planning. Preliminary discussions with the mobility team resulted in a matrix of rover speed at slope for both lit and unlit regions. As the set of science sites were refined, a Version 1 of the path was baselined. Following iteration of science sites and the slope matrix, a Version 2 of the path was baselined. The results were fed into a mobility model in order to arrive at an estimated mission duration.

Two individual traverse paths have been generated:

1. The Northern Traverse – with a starting point located in Poincare (Site B) and the ending point located in the Apollo Crater (Site M).
2. The Southern Traverse – starting point located at Mafic Mound (Site H) and ending point located in Artemis Site 007.

Both the Northern and Southern Traverse were generated using ArcGIS's least cost path analysis. The least cost path algorithm works to determine the most cost-effective route between a user defined source and destination point based on the eight neighboring pixels of the cost dataset. The eight neighboring pixels are iteratively evaluated to determine the smallest accumulated cost value, thus determining the path direction. The resulting path is based on the smallest sum of pixel values between the two points. The cost value used for this analysis is based on the maximum degree of slope that can be traversed. Initially the slope constraint used to generate the paths was set to 15 degrees; however, increments and decrements to this constraint were also analyzed to observe alternate routes and to analyze sensitivity to traverse distances on slope constraint. The slope constraint was increased to 17 degrees and the cost dataset used for the least cost analysis was processed accordingly.

Two regional scale DEMs were selected for path planning. For portions of the path North of 60 degrees South, a 59 Meter per pixel DEM constructed from a merge of Kaguya and LOLA was used. For portions on the traverse south of 60 degrees south, a 20 meter per pixel DEM from Chang'e 2 was used. Both DEMs were converted to slope data products using ArcGIS's slope tool. All slope values greater than the defined 17 degree slope constraint were excluded from and not considered as viable path directions during the least cost path analysis as any value greater than 17 degrees slope was nulled.

Path generation from science station to science station has been conducted individually and outputted as polyline segments. All path segments were merged and dissolved together so that the final version of this path represents a single integrated polyline feature. Slope values were then extracted to obtain what percentage of the path is within a certain slope range. The following are the extracted slope statistics along the two traverse paths:

Table K-1. Northern Traverse.

Slope (degrees)	Path %
0 - 5	90.15
5 - 10	8.89
10 - 15	0.94
15 - 16	0.011
16 - 17	0.003

Table K-2. Southern Traverse.

Slope (degrees)	Path %
0 - 5	80.17
5 - 10	17.59
10 - 15	1.94
15 - 16	0.2
16 - 17	0.15

For the science sites more detailed data products were constructed. Ortho-image mosaics, stereo DEMs were constructed from NAC available imagery. Rock and Crater detectors were run on a set of NAC sample images from the science sites – and rock and crater size frequency distributions and hazard maps were constructed.

K.1 NORTHERN TRAVERSE

For the Northern traverse, the science sites listed in Table K-3 were selected. A traversable path between each of these sites was constructed.

Figures K-1, K-2, and K-3 depict the generated northern path.

Table K-3. Path Distance.

	Site	Latitude	Longitude	Geodesic (km)
Northern Traverse	B	-57.22227	162.6293	17.0
	A	-59.12448	161.051	63.0
	C	-61.25954	176.5608	241.9
	D	-57.23407	-171.9308	215.7
	E	-55.42484	-170.8276	57.9
	F	-56.6008	-166.6533	79.2
	G	-57.35599	-162.88	66.4
	H	-57.86208	-161.8022	23.3
	I	-54.60083	-162.5337	83.8
	J	-53.28576	-160.2125	57.5
	K	-51.1351	-163.1549	105.7
	N	-42.53054	-158.8416	275.7
	L	-40.37084	-157.2198	75.1
M	-37.71148	-153.0429	127.2	
	Total			1472.4

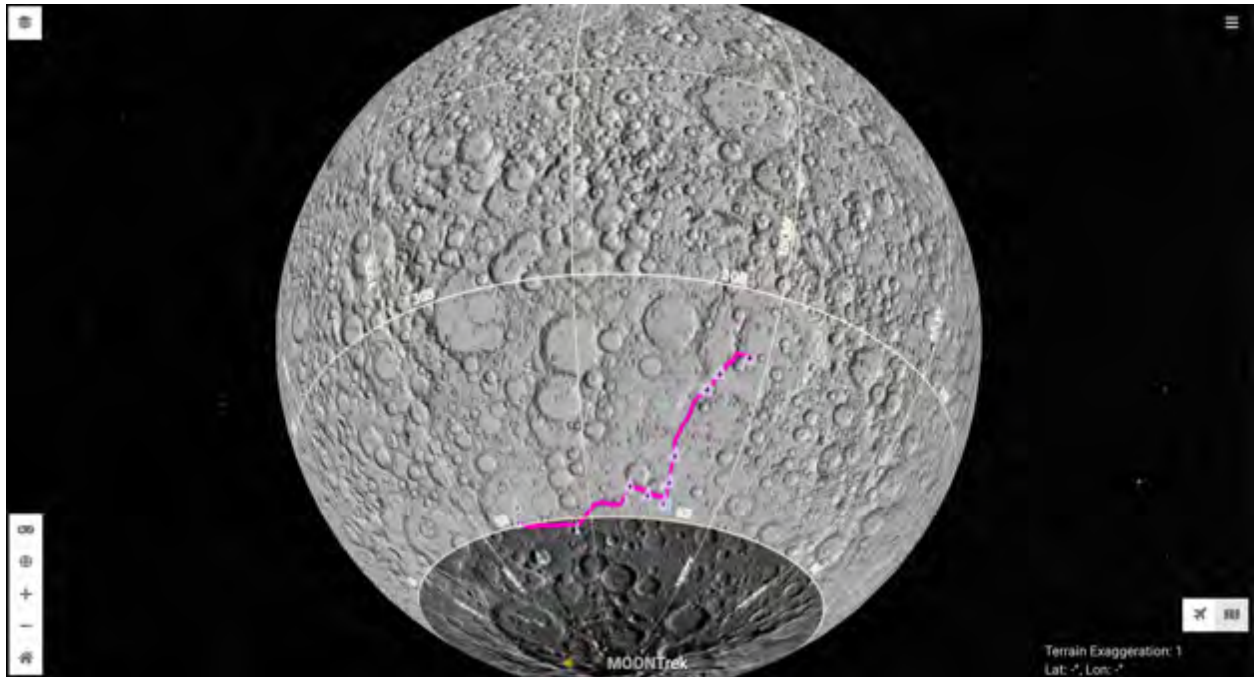


Figure K-1. Endurance Northern Traverse on LOLA Kaguya Merge, Globe View.

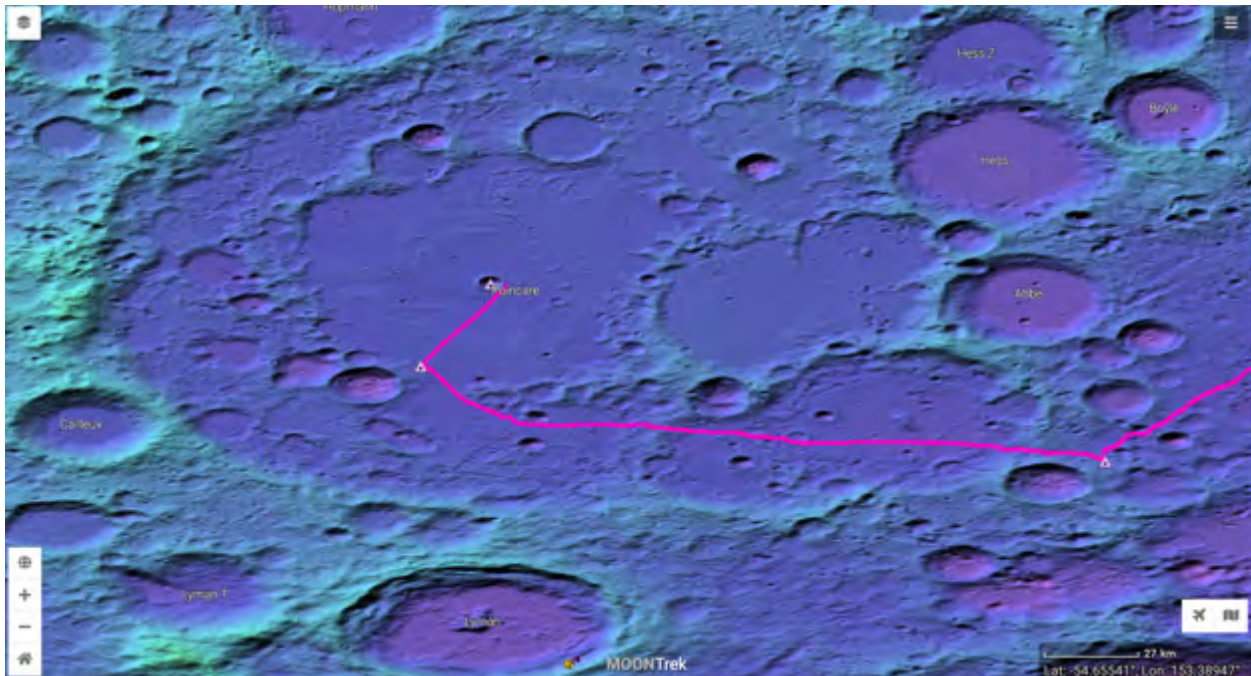


Figure K-2. Endurance Northern Traverse Part 1 on LOLA Color Hillshade, Global Projection.

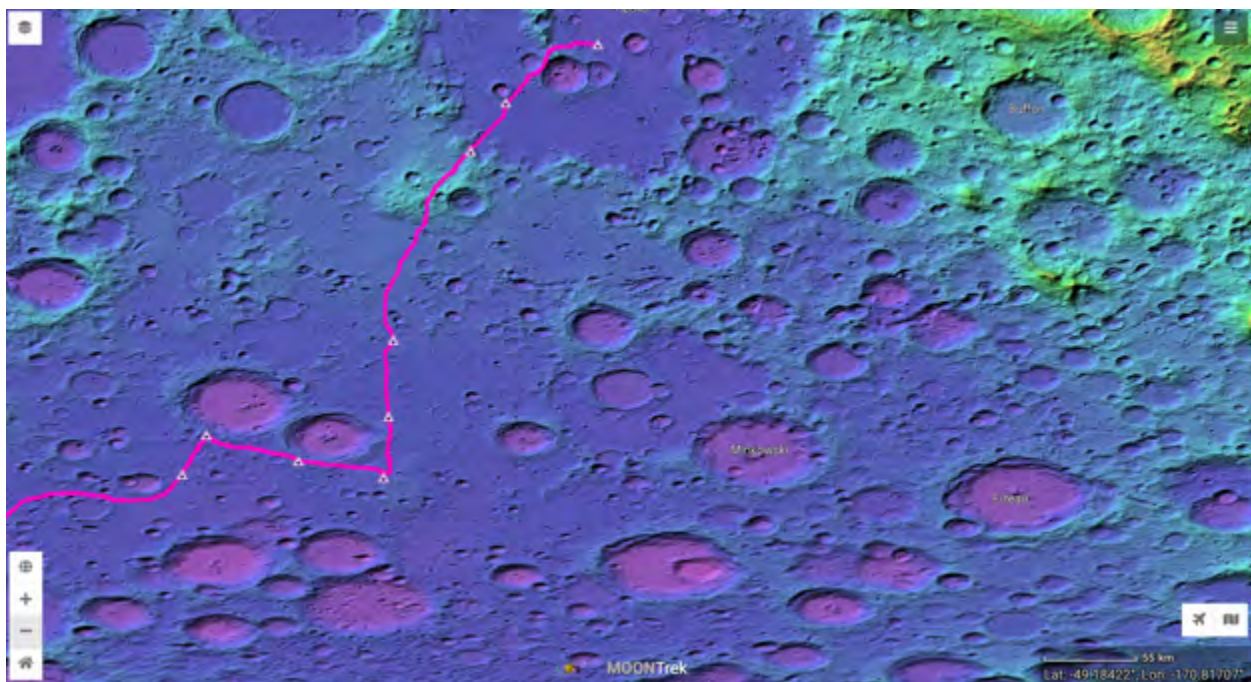


Figure K-3. Endurance Northern Traverse Part 2 on LOLA Color Hillshade, Global Projection.

K.2 SOUTHERN TRAVERSE

For the Southern traverse, the science sites listed in Table K-4 were selected. A traversable path between each of these sites was constructed.

Figures K-4, K-5, and K-6 depict the generated southern path.

Table K-4. Path Distance.

	Site	Latitude	Longitude	Geodesic (km)
Southern Traverse	G	-57.35599	-162.88	23.3
	F	-56.6008	-166.6533	66.4
	E	-55.42484	-170.8276	79.2
	D	-57.23407	-171.9308	57.9
	C	-61.25954	176.5608	215.7
	A	-59.12448	161.051	241.9
	O	-64.92944	162.4302	92.9
	P	-73.40344	135.3675	382.8
	Q	-75.29932	139.3307	66.0
	Artemis	-87	50.5	452.9
Total				1679.1

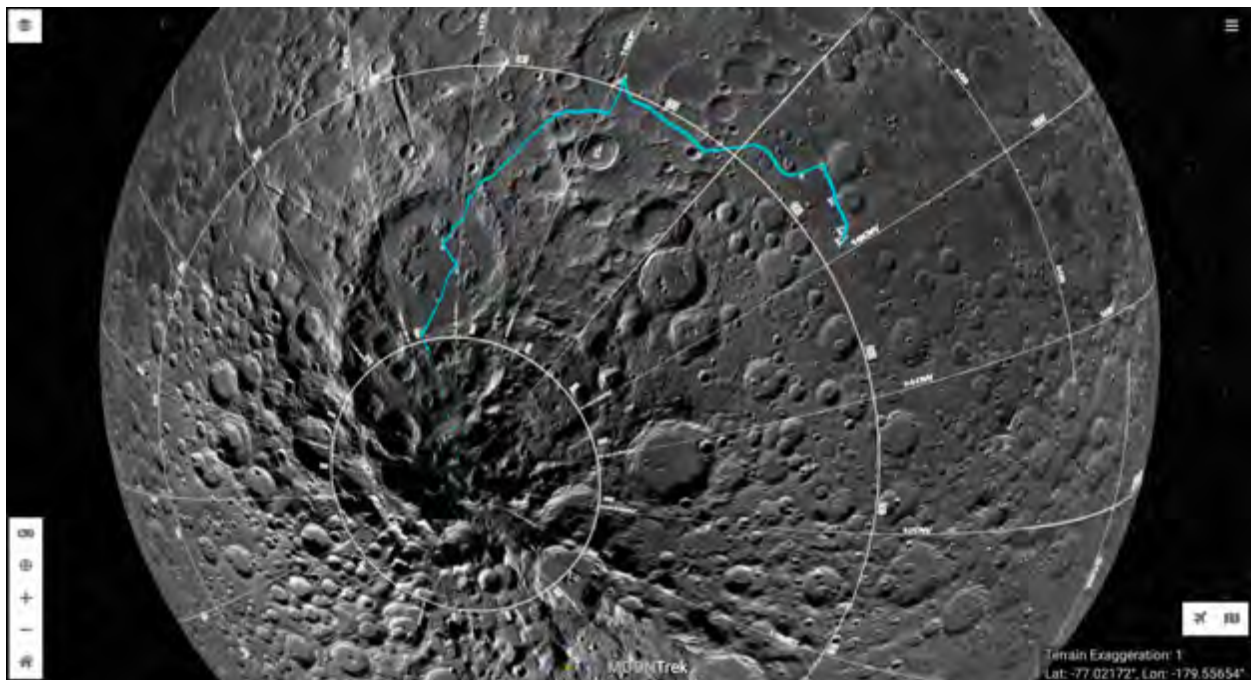


Figure K-4. Endurance South Traverse, Globe View.

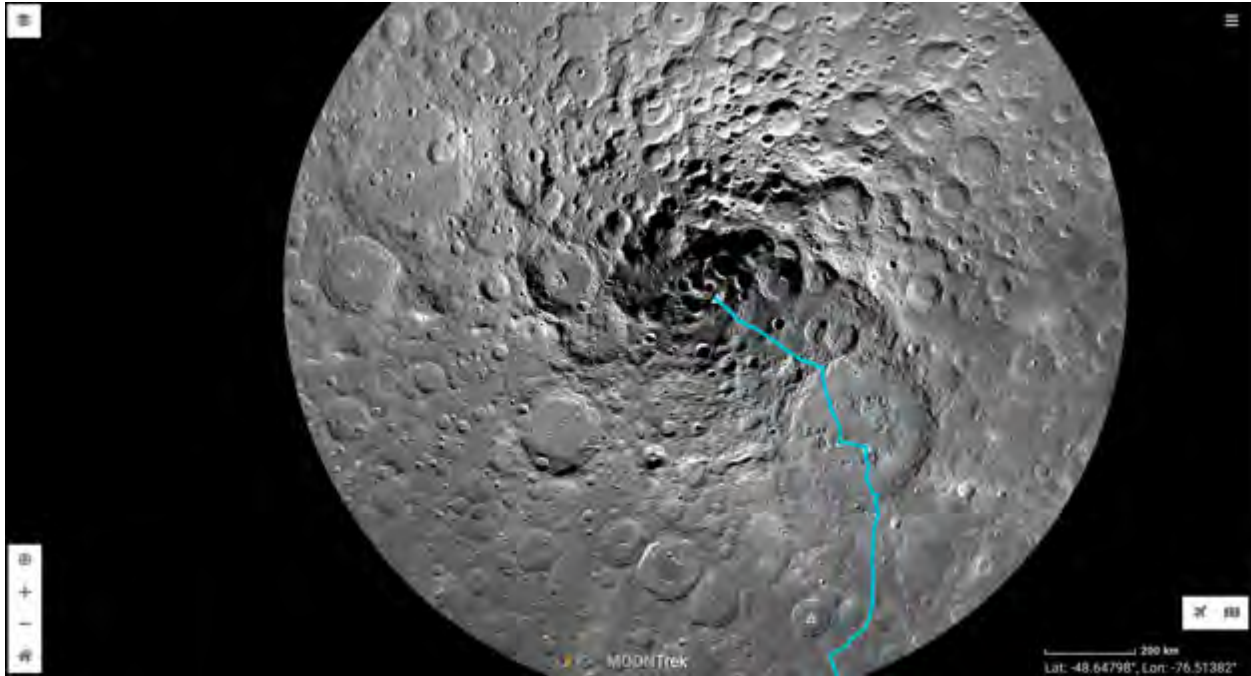


Figure K-5. Endurance South Traverse on LRO, South Pole Projection.

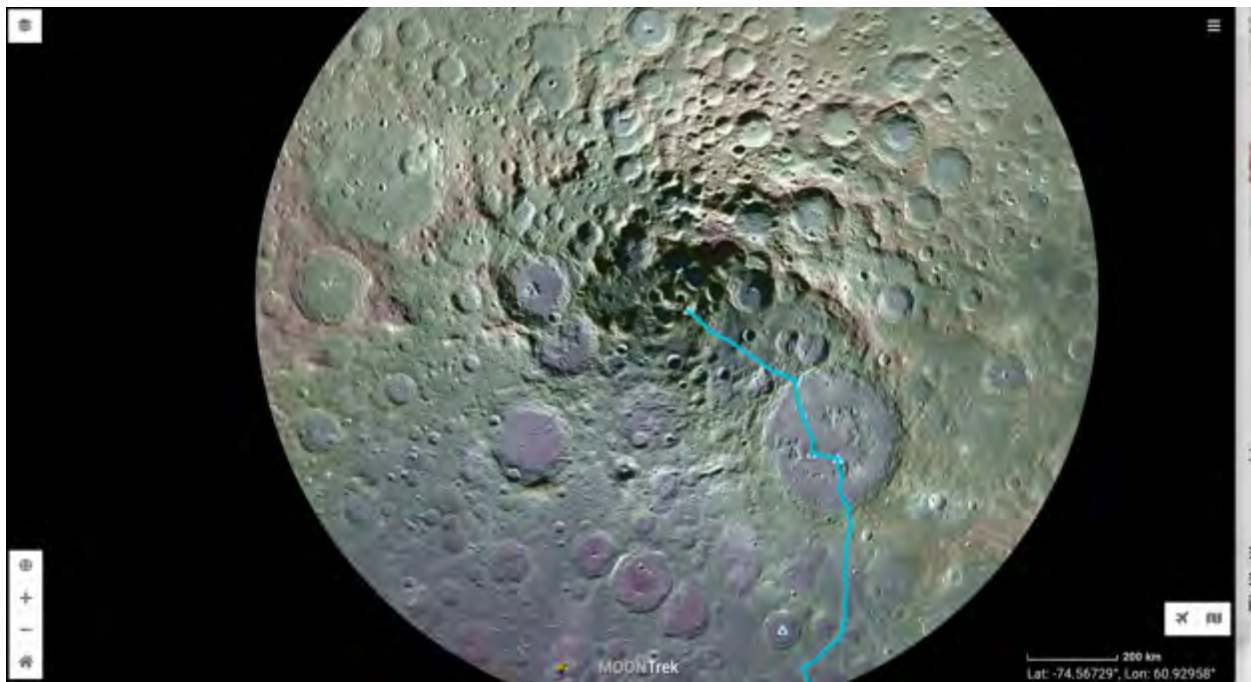


Figure K-6. Endurance South Traverse on Chang'e Color Hillshade, South Pole Projection.

K.3 TOOLS

K.3.1 LUNAR RECONNAISSANCE ORBITER (LRO) NAC SEARCH

A special tool was developed to simplify the construction of datasets to support path planning. The tool allows a user to draw a possible path on the lunar surface. Once the path is completed, a query is done to a backend database which contains NAC metadata. The results of the query are rendered on the map as shown in Figure K-7. Users also see the incidence, emission and phase angles associated with each image. For crater detection, rock detection and ortho-mosaic and stereo reconstruction appropriate images are selected from the available images covering the path.

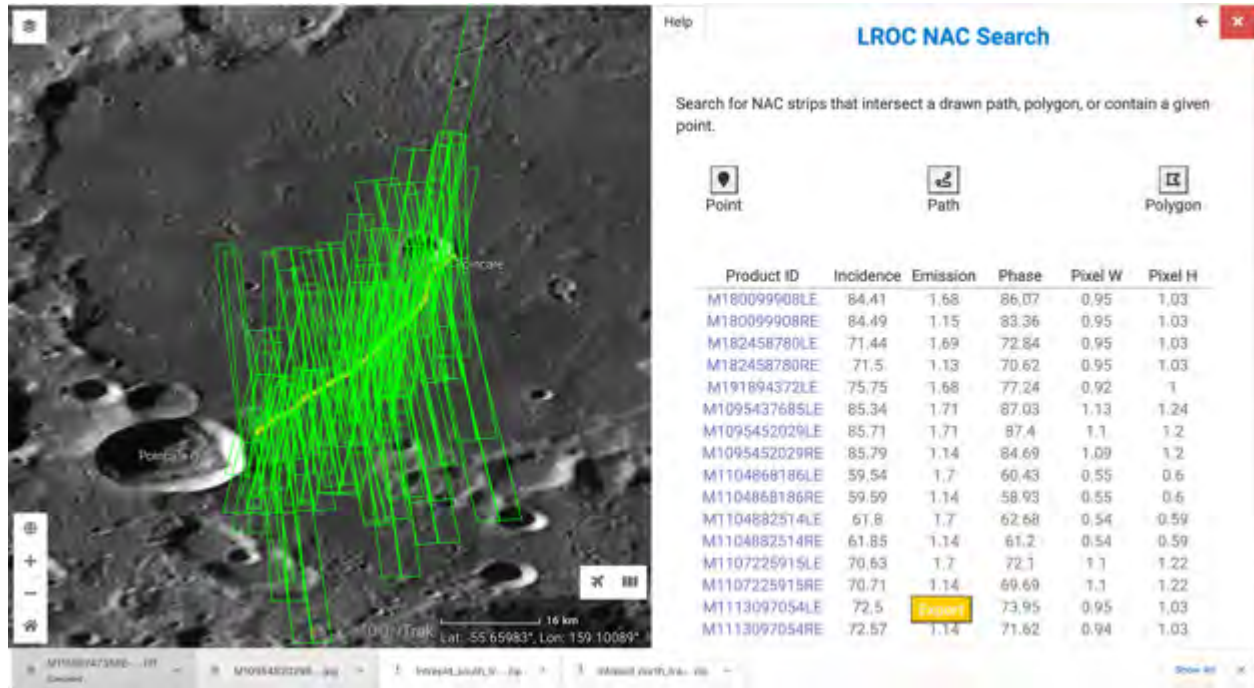


Figure K-7. Poincare (B to A) Path NAC Coverage.

K.3.2 DEM / MOSAIC PIPELINE

For ortho-mosaic and stereo DEM construction, a user takes the selected images and instructs the Solar System Treks Mosaic Pipeline (SSTMP) to construct the images. SSTMP is an internally developed tool recently released at <https://github.com/nasa-jpl/sstmp>. Figures K-8 and K-9 show SSTMP in action. SSTMP orchestrates data download, ingestion, and processing using a set of open-source applications running in containers on a Kubernetes cluster with Argo Workflows.

Figure K-10 shows an example of the output of the pipeline, the set of NAC resolution Ortho images and stereo DEMs inside of the Schrodinger crater, with the Endurance path superimposed.



Figure K-8. Solar System Treks Mosaic Pipeline web interface allows initiating and monitoring LRO NAC orthomosaic and stereo DEM creation.

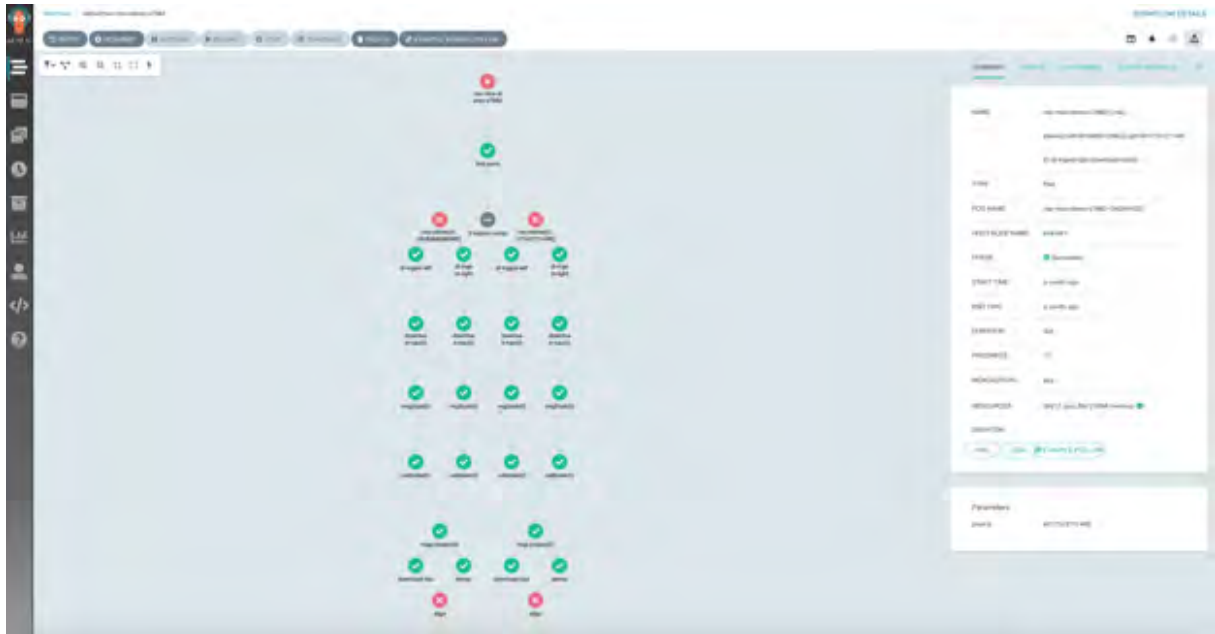


Figure K-9. Kubernetes Workflow Orchestration Pipeline.



Figure K-10. Endurance South Traverse Schrodinger Crater, Science Sites P, Q, LROC NAC Image Mosaic.

K.3.3 LIGHTING

Lighting tool is a geometrical and an irradiant model of the solar lighting on the surface of the moon. The model uses the ephemeris positions and the accepted sizes and orientations of the Sun, Moon and Earth, as a function of time. The NAIF/Spice toolkit is integrated into this tool.

The Lighting tool models the direct and reflected/scattered light by invoking the commercial ray tracing software POV-Ray. This is a fully physics-based model of incident and diffusely reflected light from a spherical light source (the Sun), which allows for accurate resolving of the quantitative nature of the lunar incident and reflected irradiance.

Suitable DEM is selected and fed in to the tool where POV-Ray performs the irradiance calculation for every triangular plate of the surface. At each time step, Moon-to-Sun and Earth-to-Sun vectors in the J2000 reference frame are calculated via Navigation and Ancillary Information Facility (NAIF)/Spice calls. The exact distance from the Sun to the Moon at each time step is used directly in deriving the current value of solar irradiance at the lunar distance from the Sun.

A set of lighting maps were made to show the ambient light levels as a function of time of day, time of year and latitude. The Figure K-11, K-12 and K-13 show a selected lighting map during the lunar morning, lunar midafternoon and lunar evening.

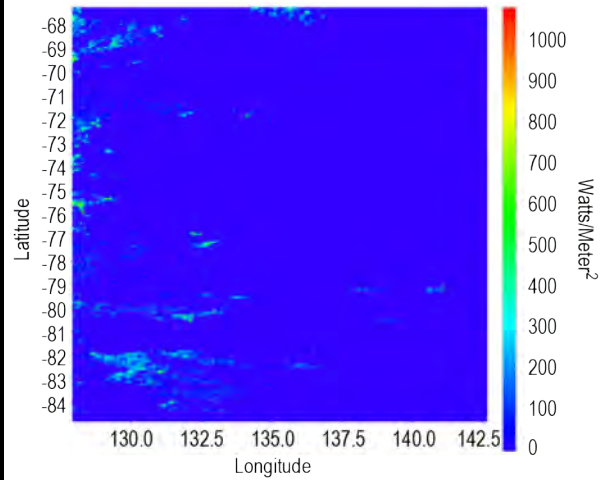


Figure K-11. Endurance Lighting Site P Lunar Morning.

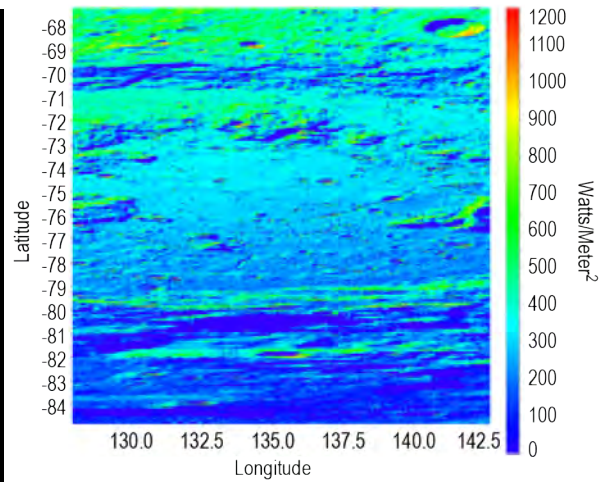
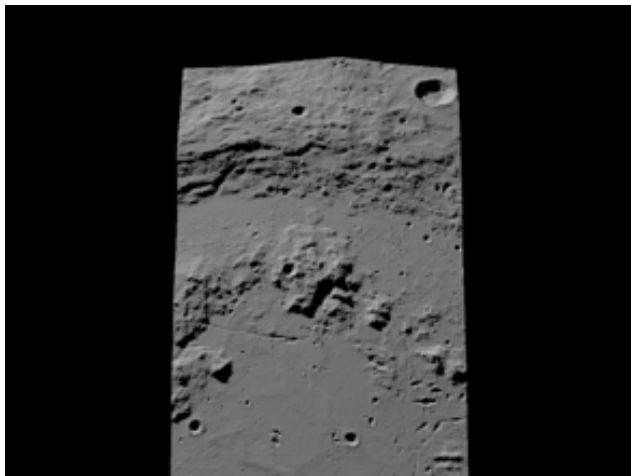


Figure K-12. Endurance Site P Lunar Noon.

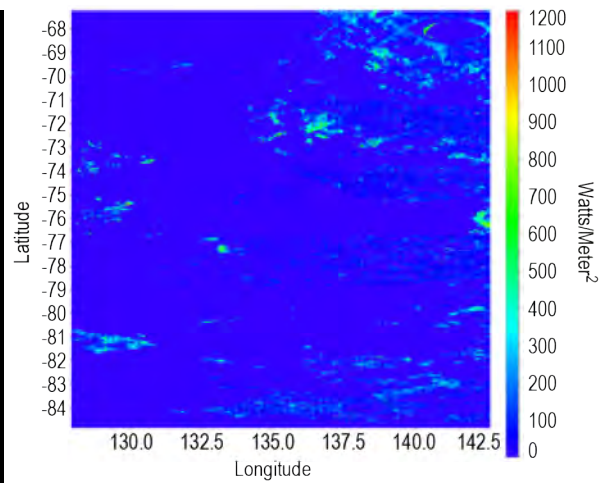
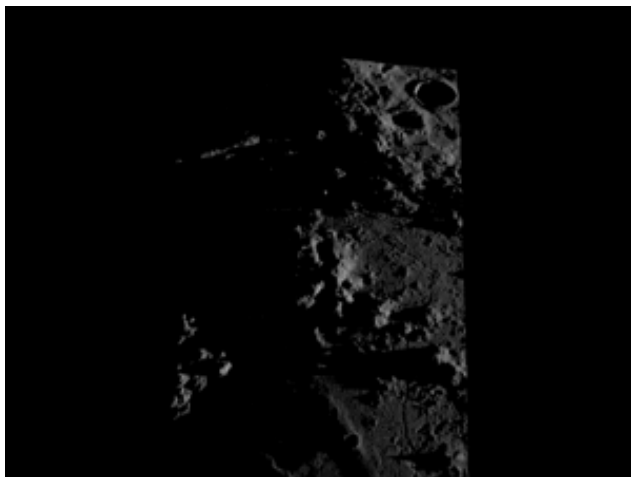


Figure K-13. Endurance Site P Lunar Evening.

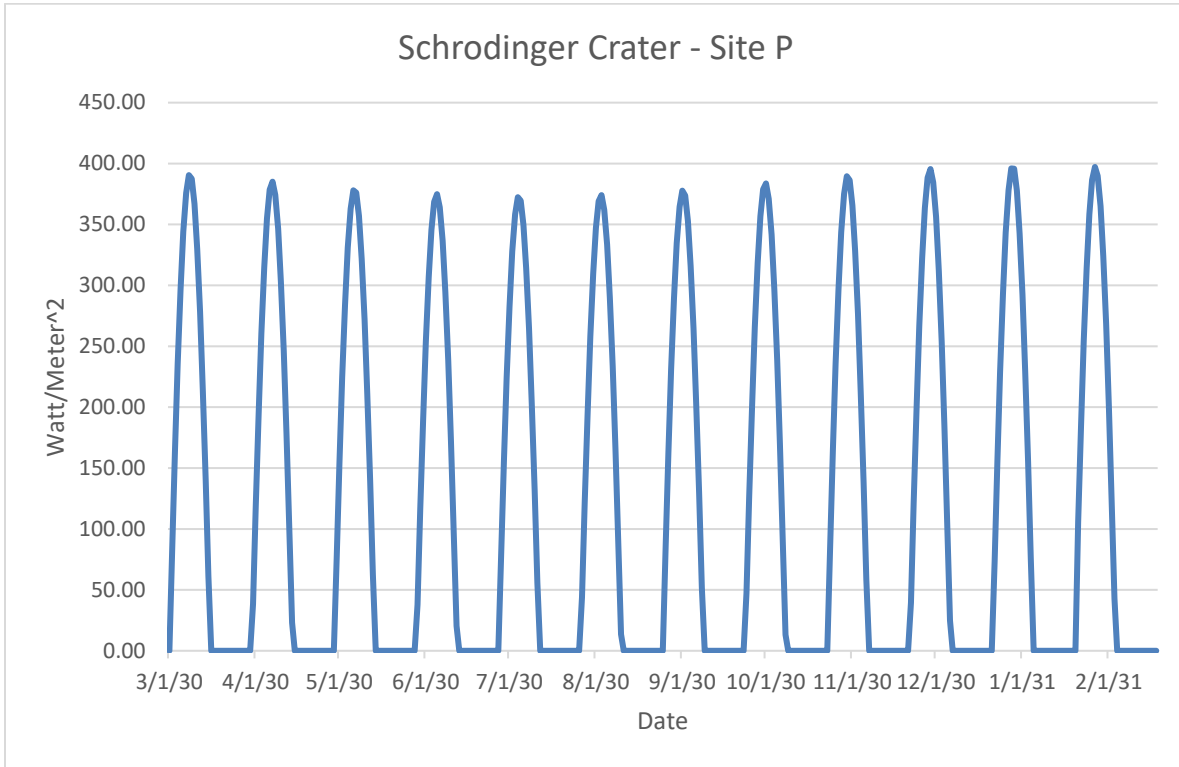


Figure K-14. Lighting at Site P for the period of 1 year.

K.3.4 COMMUNICATIONS

A Line of Sight tool was developed to compute possible communications windows. This tool uses SPICE (Spacecraft ephemeris, Planetary/satellite ephemeris and constants, Instruments, C Pointing Matrix, Event Info. [Kernels]) software to compute planetary geometries coupled with high resolution DEMs to find windows of possible communications between rovers, orbiters, and topographical surface points. The DEM dataset and path information are loaded into the tool to allow construction of communications windows with a prospective relay communication to an orbiter. A frozen orbit from a 2009 ephemeris was used to compute the visibility windows. Figure K-15 shows an example of the variation of the windows over a lunar day. Also shown is the illumination angle. The tool allows for detailed analysis to be performed. It takes into account the lunar rotation, the position of the rover on the surface of the moon, and the surrounding terrain all of which have an impact on

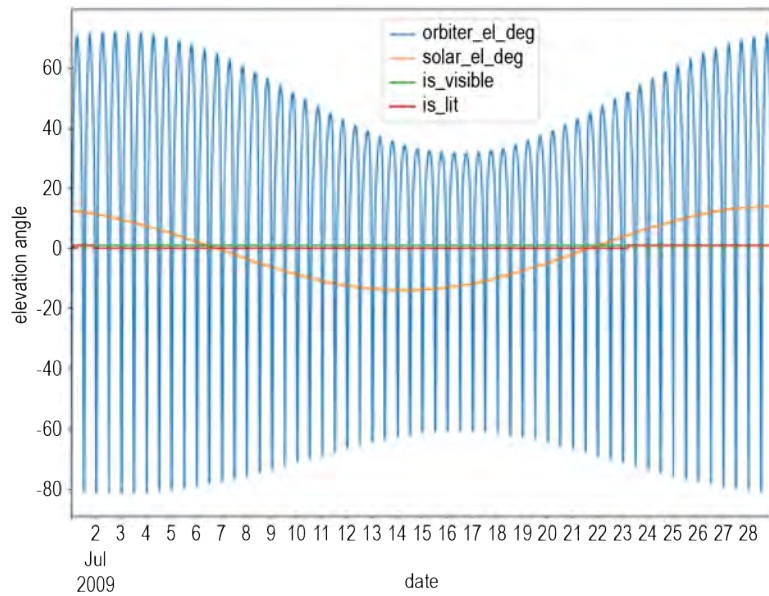


Figure K-15. P2 Line of Sight Analysis for an example Lunar Day (July 2009). The plot shows periods of communication or “visibility” as a binary value (0 for False and 1 for True). Likewise, the times when the terrain is illuminated by the sun are denoted by binary values.

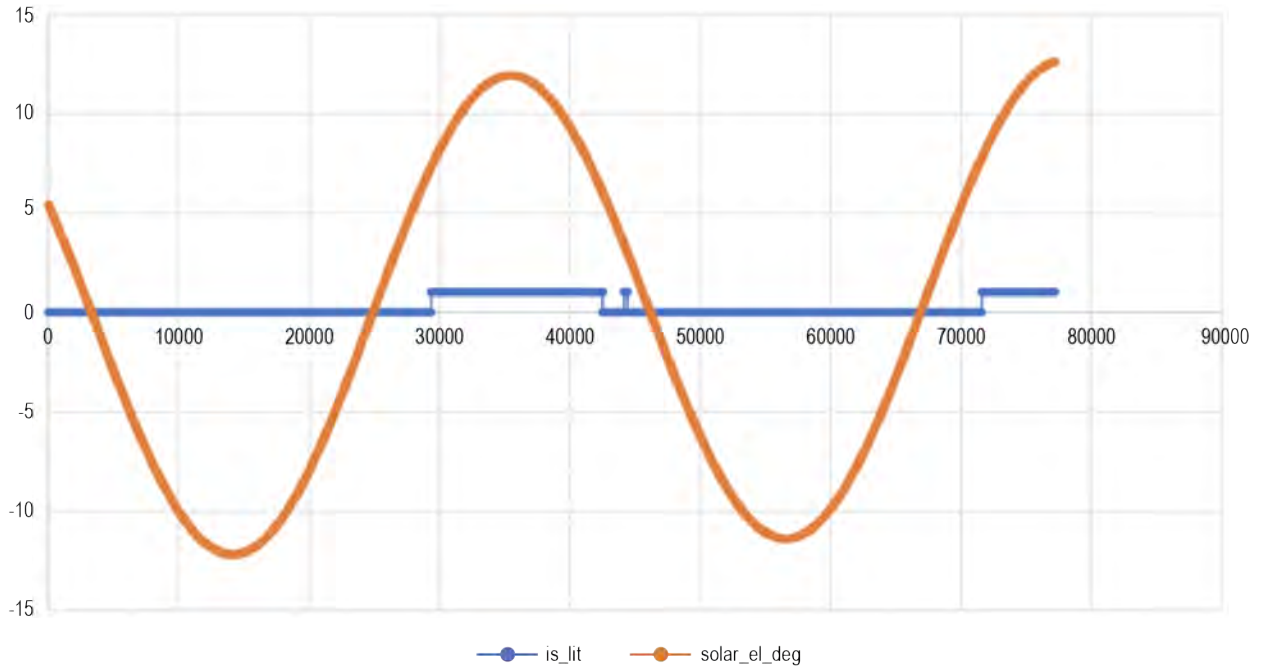


Figure K-16. Solar illumination Angle - occultation by terrain example. This graph shows that the terrain in a particular location is illuminated solar elevation is over the horizon by a certain degree. This also shows an interruption in “illumination” caused by terrain obstruction.

communications and lighting. Figure K-16 shows an example of a point on the path where the sun is above the horizon but is being occulted by the local terrain.

The computed path was generated using DEMs that spanned the traverse of 20 to 60 meters per pixel. In order to confirm path feasibility at higher resolutions, a few NAC-based DEMs were constructed and are shown below in Figure K-17, K-18 and K-19 for Site E, F and G. The path was superimposed on the DEM and it was verified that the path was indeed feasible in these areas – as corroborated by the higher resolution DEMs.

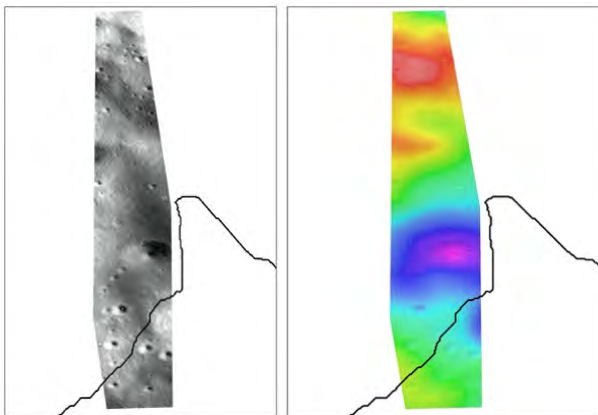


Figure K-17. Endurance Site E NAC Ortho-mosaic (1.48 mpp) and DEM (4.42 mpp) with Path Overlay.

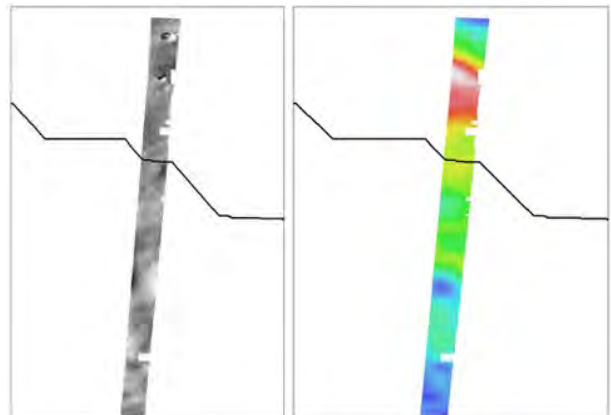


Figure K-18. Endurance Traverse Site F Ortho-mosaic (1.18 mpp) and DEM (3.54 mpp) with Path Overlay.

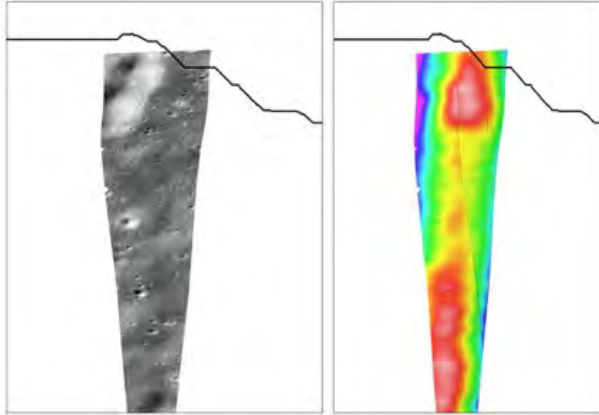


Figure K-19. Endurance Traverse Site G Ortho-mosaic (1.06 mpp) and DEM (3.18 mpp) with Path Overlay.

K.4 CRATERS AND ROCKS

Crater detection algorithms were run on a set of NAC images selected from the science sites. The crater detector uses NAC panchromatic images as input, and uses classical computer vision for crater detection, a convolutional neural network for crater recognition. The outputs of the tool include images with crater labels, hazard maps, and ascii files with crater details such as diameter estimates and coordinates. Figure K-20 shows a NAC image closeup of a section near site E with superimposed detected craters. For each crater detected a size and depth estimate is made. The crater data is then summarized in a Hazard map in which color is superimposed for every 500 square meters. The color red signifies areas with over 40% crater coverage, yellow represents areas with less than 40% coverage but over 20% crater coverage, and finally green signifies areas with less than 20% crater coverage. Figure K-21 shows a plot of the size frequency distribution of the craters found in this image. Craters with sizes larger than 10 meters are binned for better

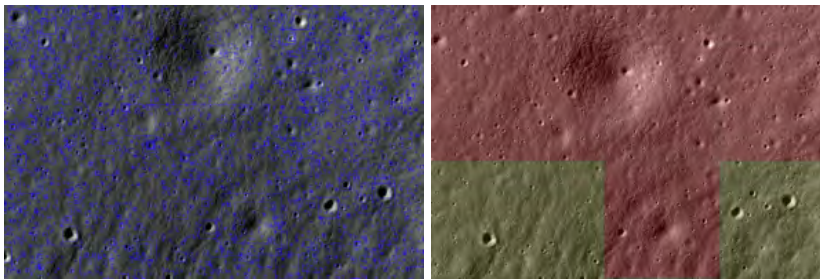


Figure K-20. Endurance Site A: M1159074735RE Crater Detections labeled with blue bounding boxes (left). Hazard Map with color imposed based on percentage of crater area coverage (right).

Crater Size Distributions: M1159074735RE

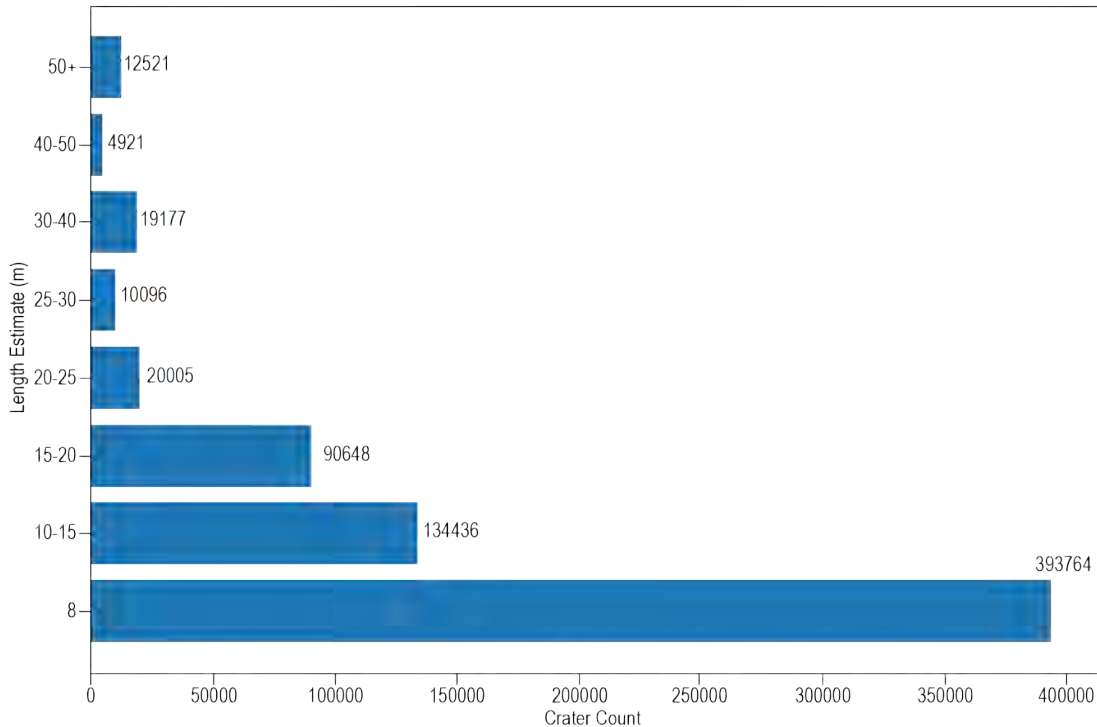


Figure K-21. Crater Size Frequency Distribution. Craters larger than 10 meters are binned.

viewing. Diameter estimates are rounded for binning and are dependent on the resolution of the input NAC image. Figure K-22 and Figure K-23 show the same information for site K.

Similarly, the rock detection algorithm uses NAC images as input and relies on classical computer vision for the detection of rocks. The outputs of this tool include images with detection labels, ascii files with rock locations, and density maps. Figure K-24 shows a region near site D with superimposed rock detections and densities summarized in a hazard map. The hazard maps impose color for every 500 square meters. Only areas with over 0.01 rock coverage have color imposed. Areas in red have rocks that cover over 2% rock coverage. Yellow areas have between 2% and 0.05% rock coverage. Green areas have between 0.05% and 0.01% rock coverage. Figure K-25 shows rock density distribution for the image. Figures K-26 and K-27 show the same information for site O.

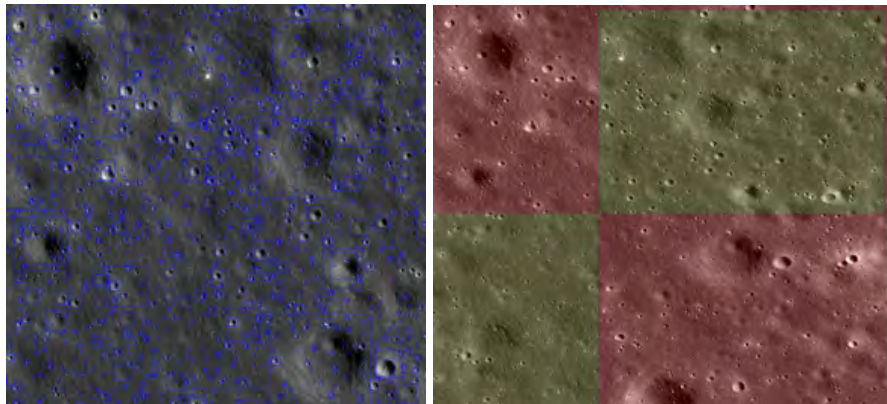


Figure K-22. Endurance Site K M1137559244RE Crater Detections with blue bounding box as label (left). Hazard Map with colors superimposed on image based on crater area coverage (right).

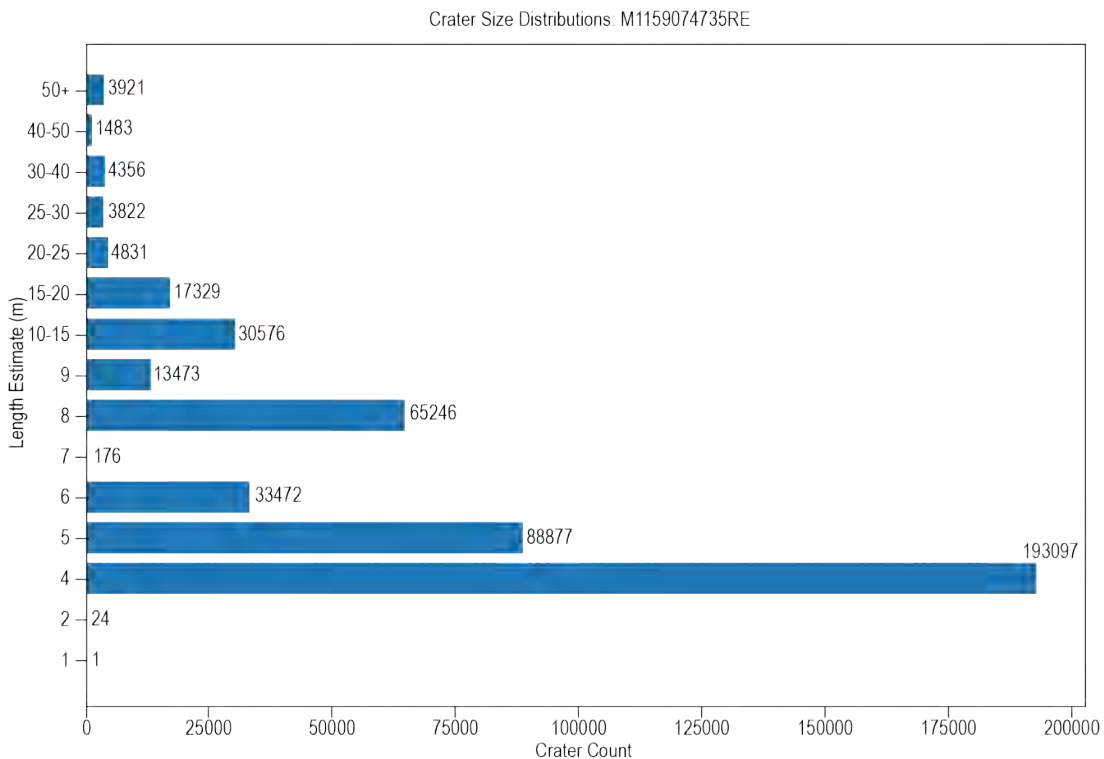


Figure K-23. Crater Size Frequency Distribution. Craters larger than 10 meters are binned.

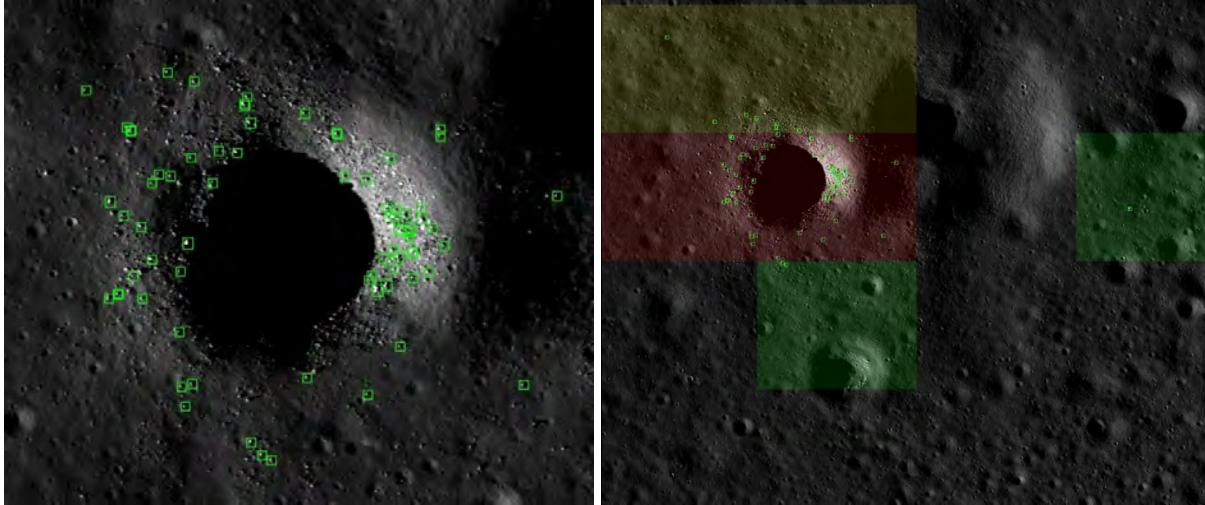


Figure K-24. Endurance Site D M1275325491RC Rock detections labeled with green bounding boxes (left). Hazard Map with color impose by rock area coverage (right).

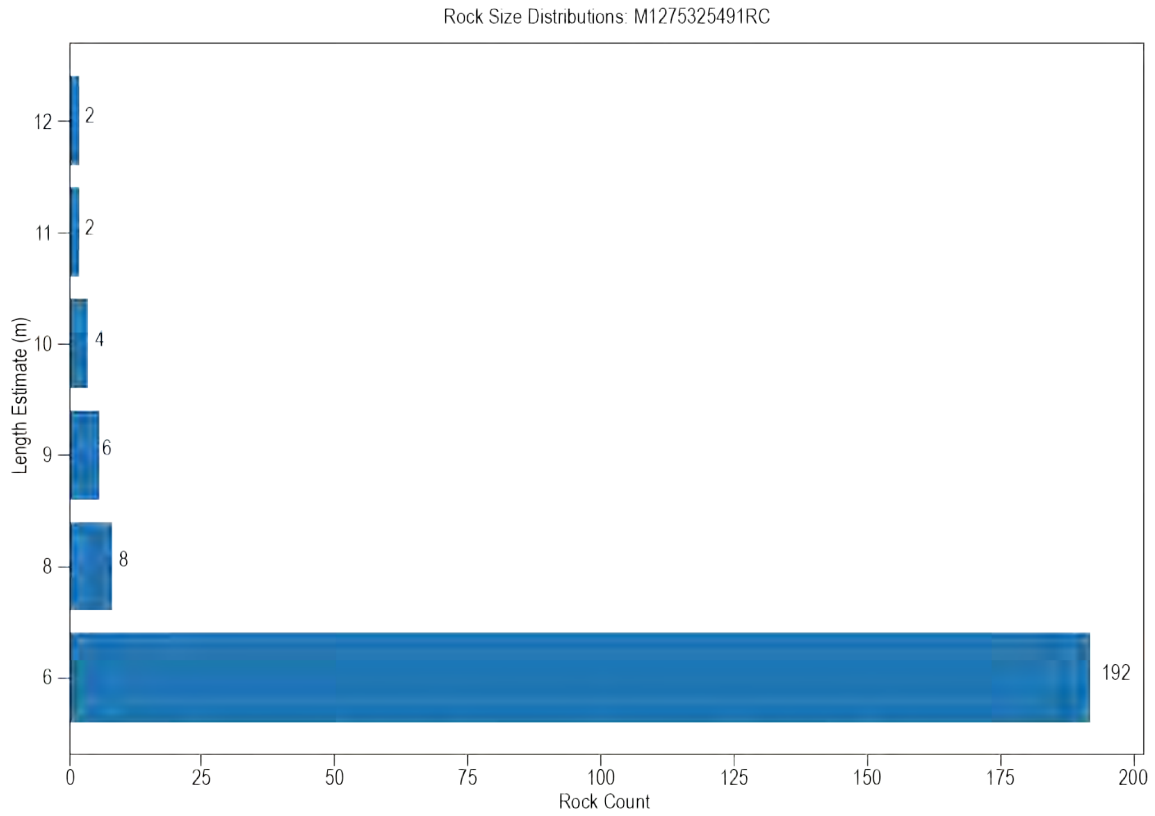


Figure K-25. Rock Size Frequency Distribution on image M1275325491RC near site D.

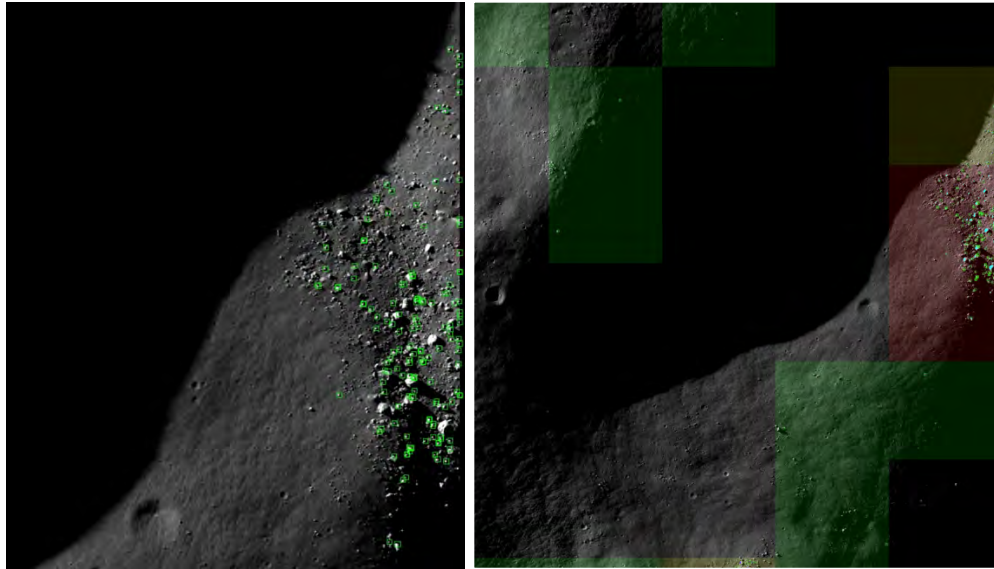


Figure K-26. Endurance Site O M1107233195RC Rock detections labeled with green bounding boxes (left). Hazard Map with color impose by rock area coverage (right).

Rock Size Distributions: M1107233195RC

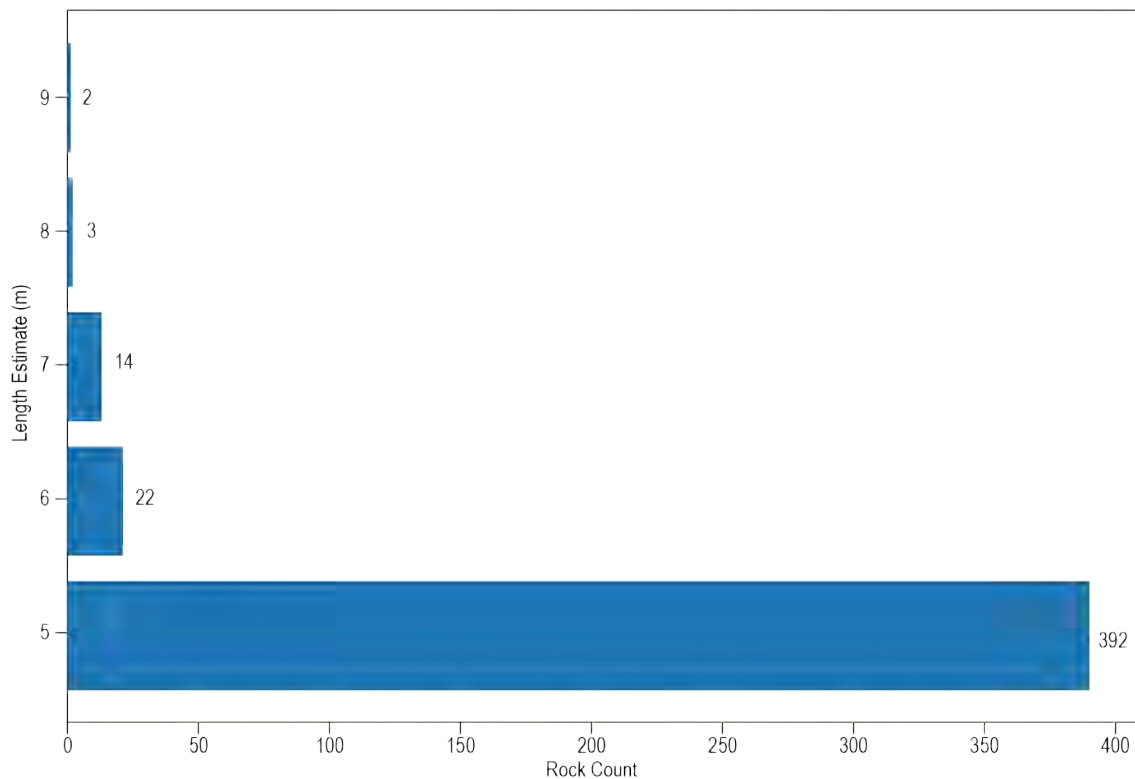


Figure K-27. Rock Size Frequency Distribution on image M1107233195RC near site O.

K.5 VISUALIZATION

Trek 3D path visualization tool uses the follow data to construct 3D visualization. First, it generates shape of entire moon using collections of DEMs from Moon Trek ranges from LRO LOLA global DEM to sparsely covered high resolution LRO NAC DEMs, second, it overlays map data from Moon Trek such as LRO WAC global imagery map, colorized Hillshade maps and colorized slope maps on

the Moon 3D model. Third, generated traversal path and marked science stations are converted into shapefiles and loaded to Trek infrastructure. Using Trek infrastructure, elevation value is retrieved for each point in the traversal path or roughly equidistance points in the path to characterize the path in 3D and to estimate surface distance along the path. These cartographic 3D points are used to draw path on the Moon model. Estimated surface distance allow user to interactively navigate the path from this tool.

A video of the Northern Traverse is available here:
<https://www.youtube.com/watch?v=31mEewiaWR4>

A video of the Southern Traverse is available here:
<https://www.youtube.com/watch?v=VqC0z2Z9zys>

L ROVER ARCHITECTURE**L.1 BLOCK DIAGRAM**

The block diagram for the Endurance rover is presented in Figure L-1.

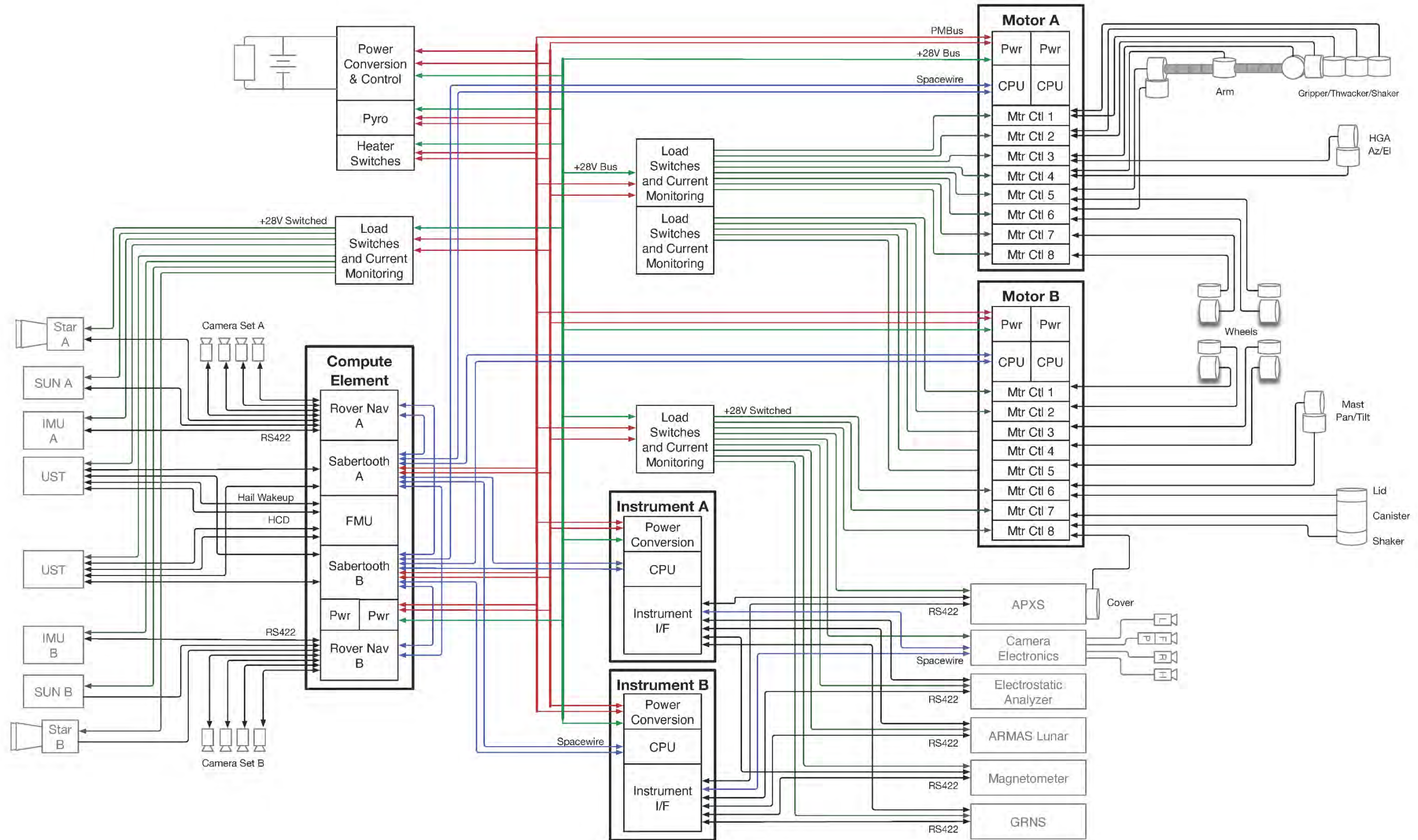


Figure L-1. Endurance Block Diagram.

L.2 CONFIGURATION

Both versions of the Endurance rover have an architecture based around a central warm electronics box (WEB) chassis which carries most of the avionics and payload electronics and which is connected to the wheels via two rockers and a differential.

The rover is supported on four 80-cm compliant mesh wheels, and each is connected via its structure to a steering actuator as well as a drive actuator. The rover belly has >60 cm clearance on flat terrain, and the rocker provides stability over uneven terrain.

The Endurance-A and Endurance-R variants share the same structural design. The WEB is a composite structure that is mostly hollow and has the internal payload and avionics on the underside. The RTG is attached to the back, and there is a central structural “spine” from the RTG to the front of the rover to provide additional support.

Because the RTG can provide power at all times, there is no need for a large number of batteries, and thermal isolation is less of a concern because systems remain powered and heaters can be used during the night. The internal avionics on the bottom of the WEB are shielded with a lightweight bottom cover.

The back wheels of the rover also are shielded from RTG radiant heat by thermal shields.

Some of the instruments that require height, such as the sun sensors and star trackers, are mounted on a lightweight aluminum structure on the back of the rover which also provides thermal shielding of the radiator from the RTG. The rear navigation cameras, along with their illuminators, are mounted on a separate aluminum structure on the back of the rover, below the RTG to ensure clear visibility.

L.2.1 ENDURANCE-A: ASTRONAUT VERSION

The Endurance-A rover has 6 sample canisters on each side of the rover body, totaling to 12, that will allow the double-sided scoop to obtain samples and pour them into all canisters on both sides without structural interference. Handles mounted on the sample containers will allow astronauts to detach the canisters from the rover for return to Earth. Aside from details of scoop design, the robotic arm assembly is the same for both versions.

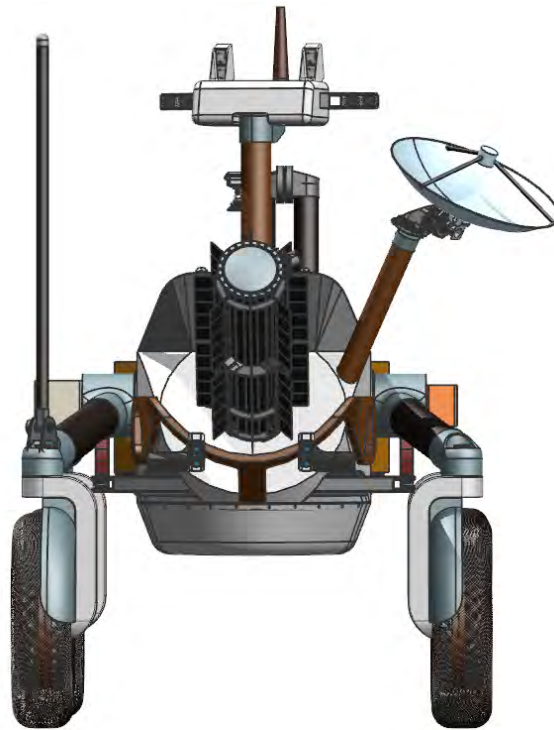


Figure L-2. Rear view of the rover showing RTG, HGA, Magnetometer, Illuminators, and rear navigation cameras.

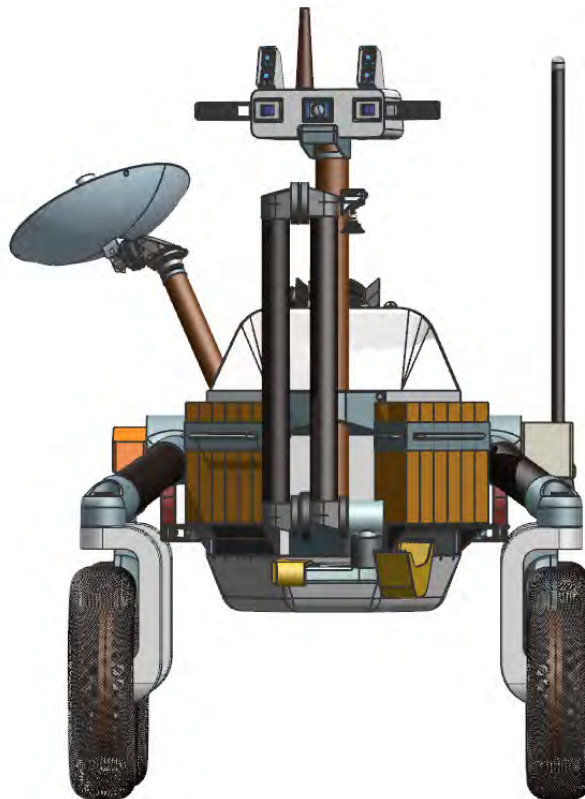


Figure L-3. Front view of the rover with the camera head, robotic arm, and sample canisters.

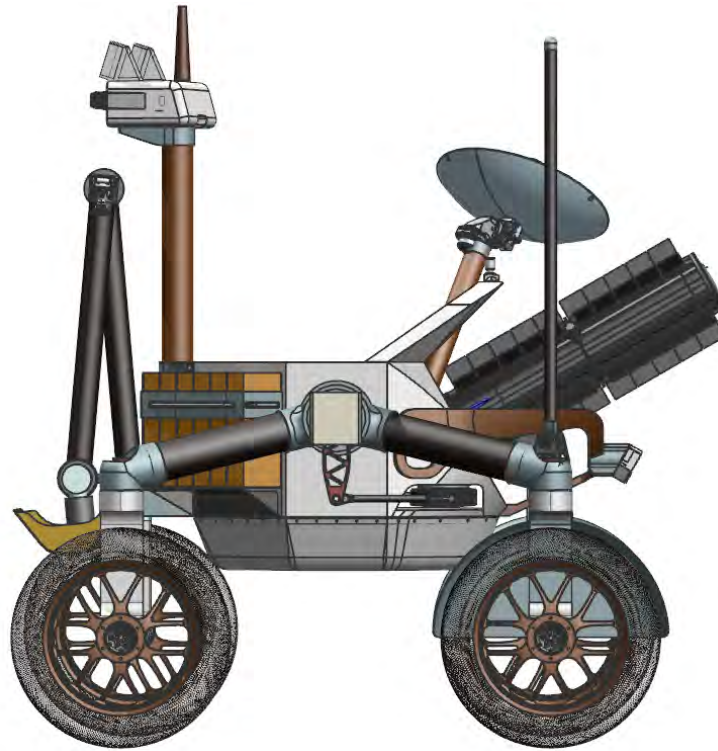


Figure L-4. Left view of the rover.

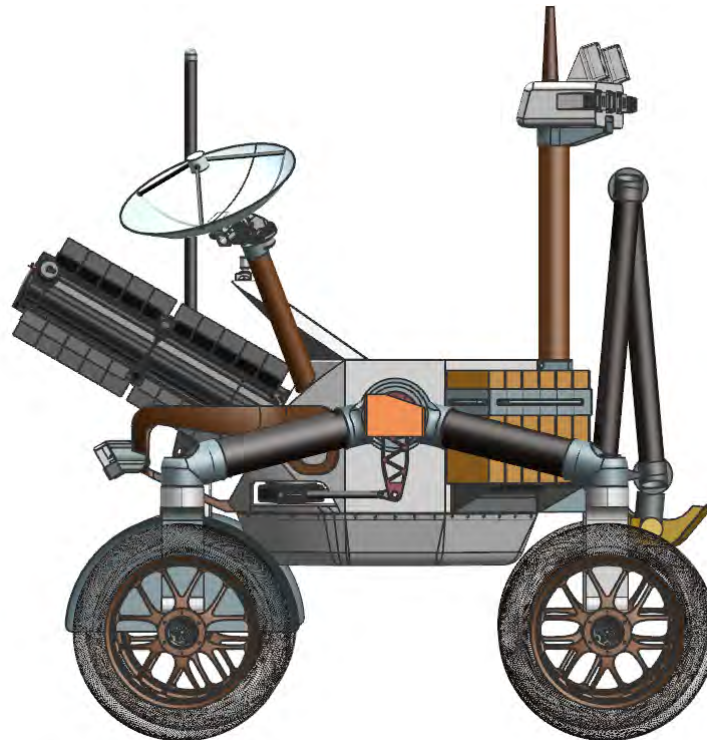


Figure L-5. Right view of the rover.

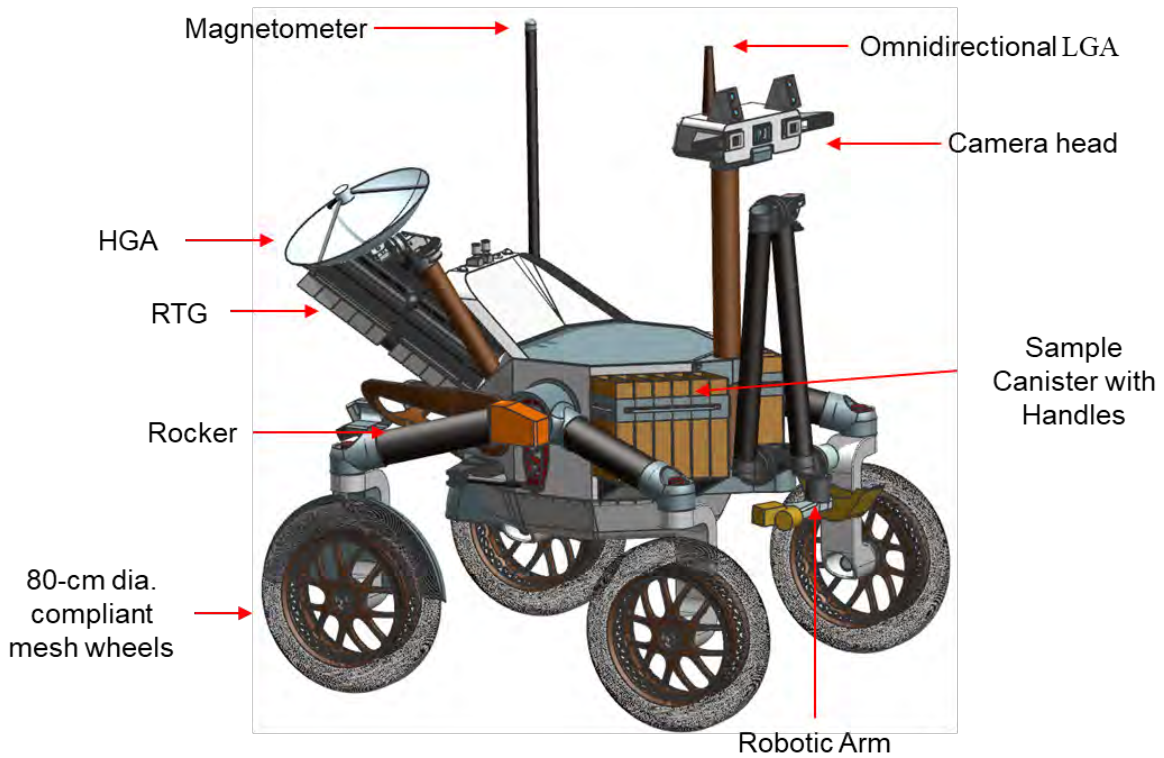


Figure L-6. Isometric view of the rover with robotic arm stowed.

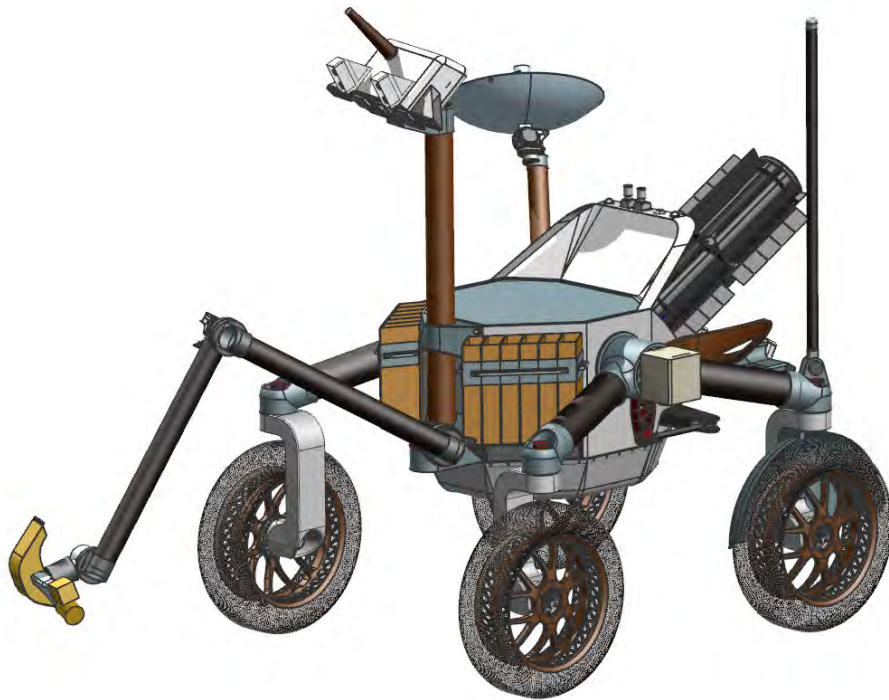


Figure L-7. Isometric view of the rover with the camera head pointing down, and the robotic arm extended and scooping.

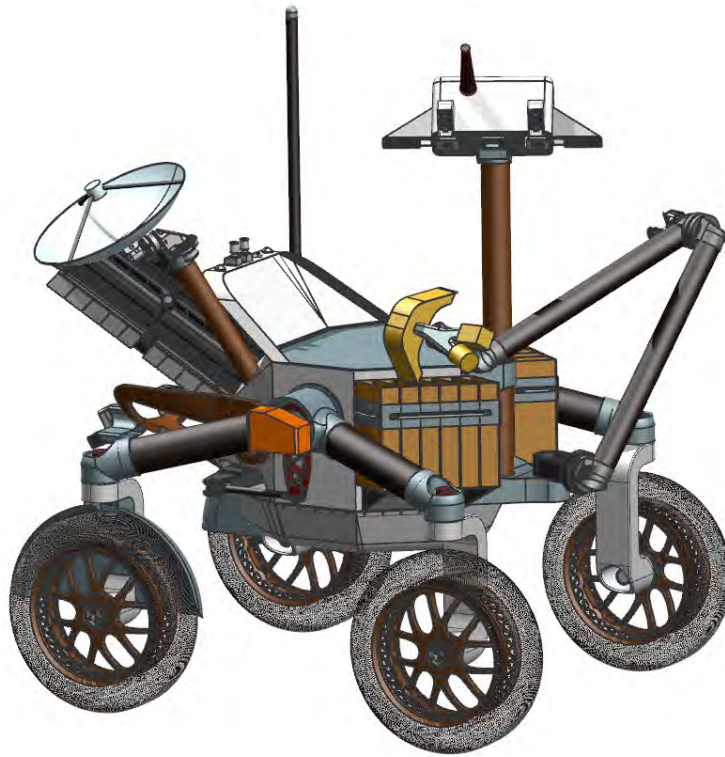


Figure L-8. Isometric right view of the rover with the camera head pointing down, and the robotic arm pouring sample into canister.

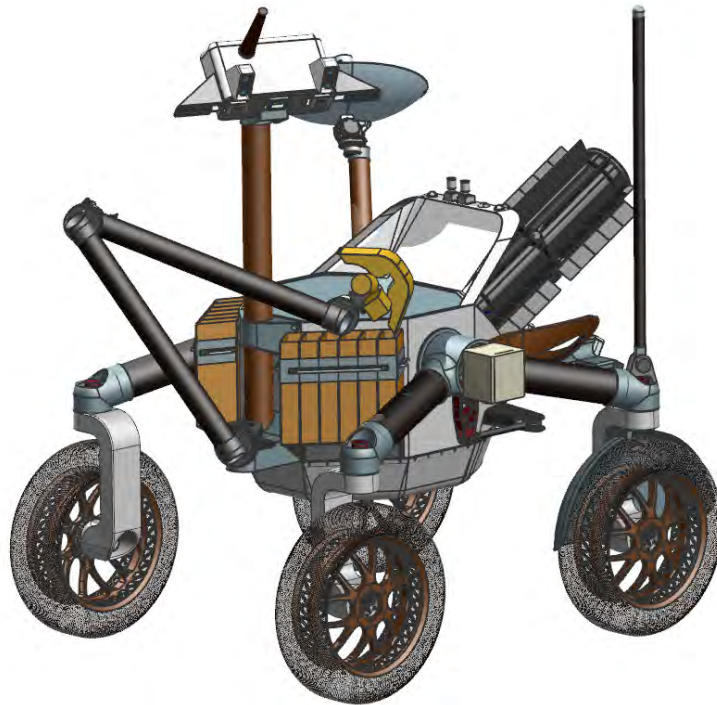


Figure L-9. Isometric left view of the rover with the camera head pointing down, and the robotic arm pouring sample into canister.

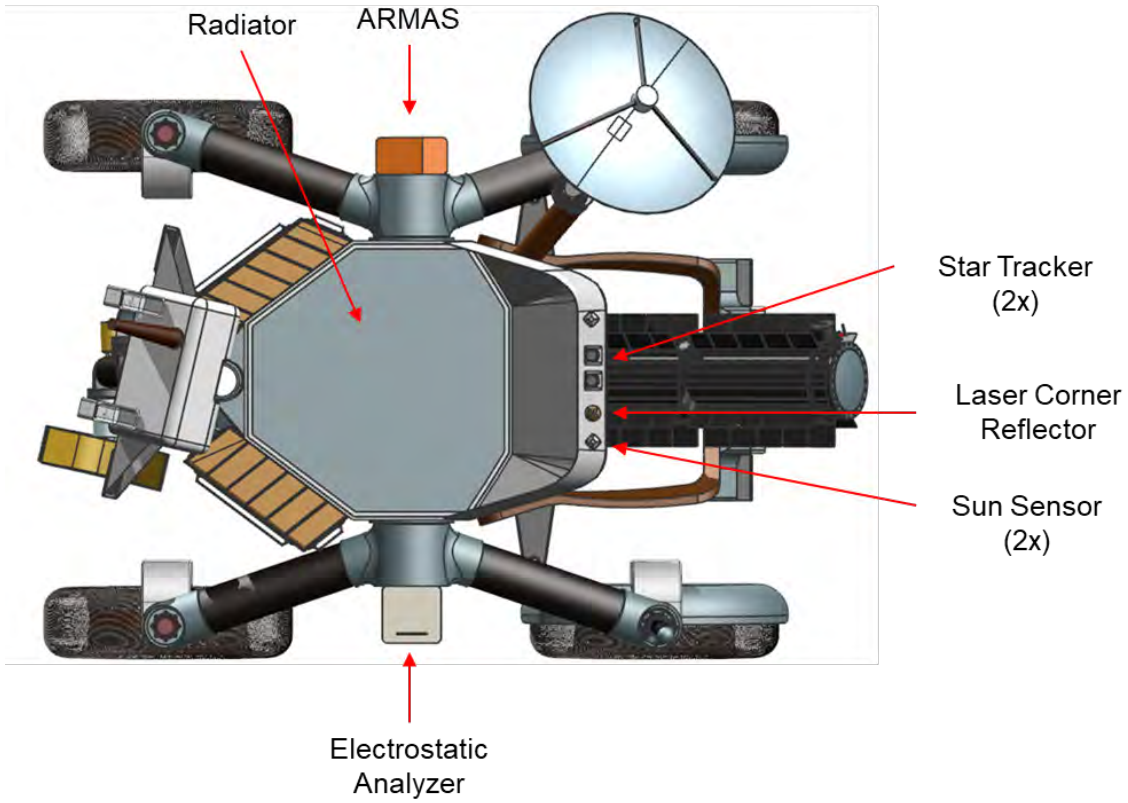


Figure L-10. Top view of the rover.

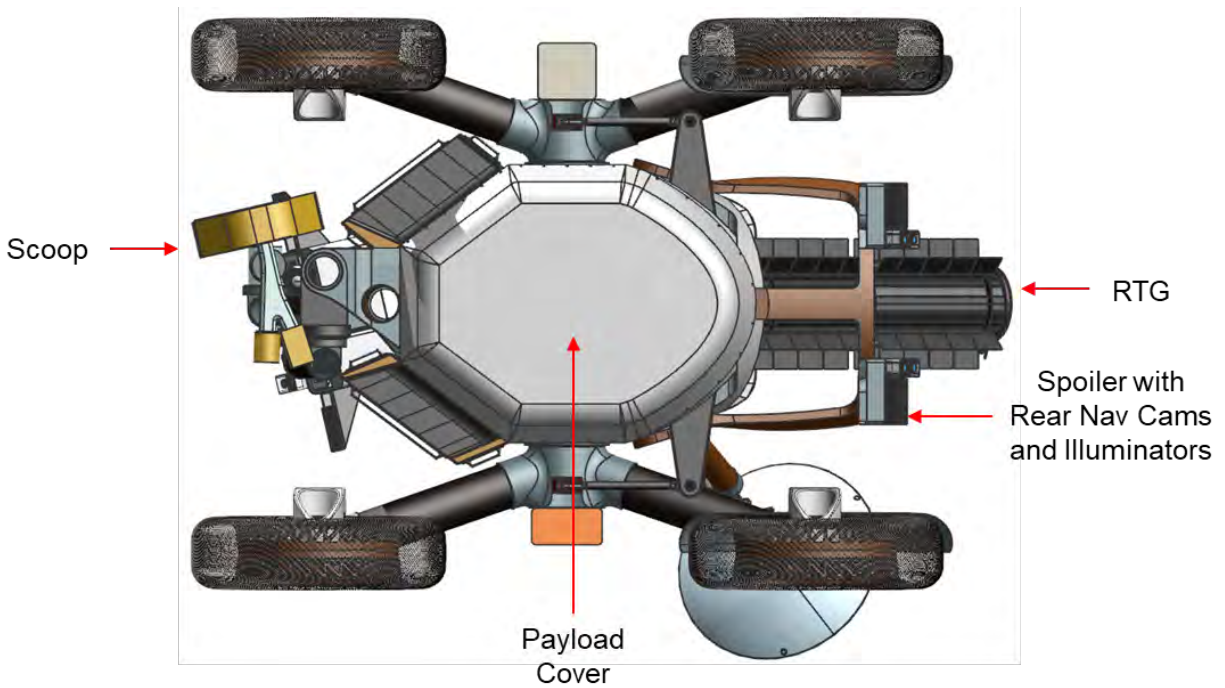


Figure L-11. Bottom view of the rover.

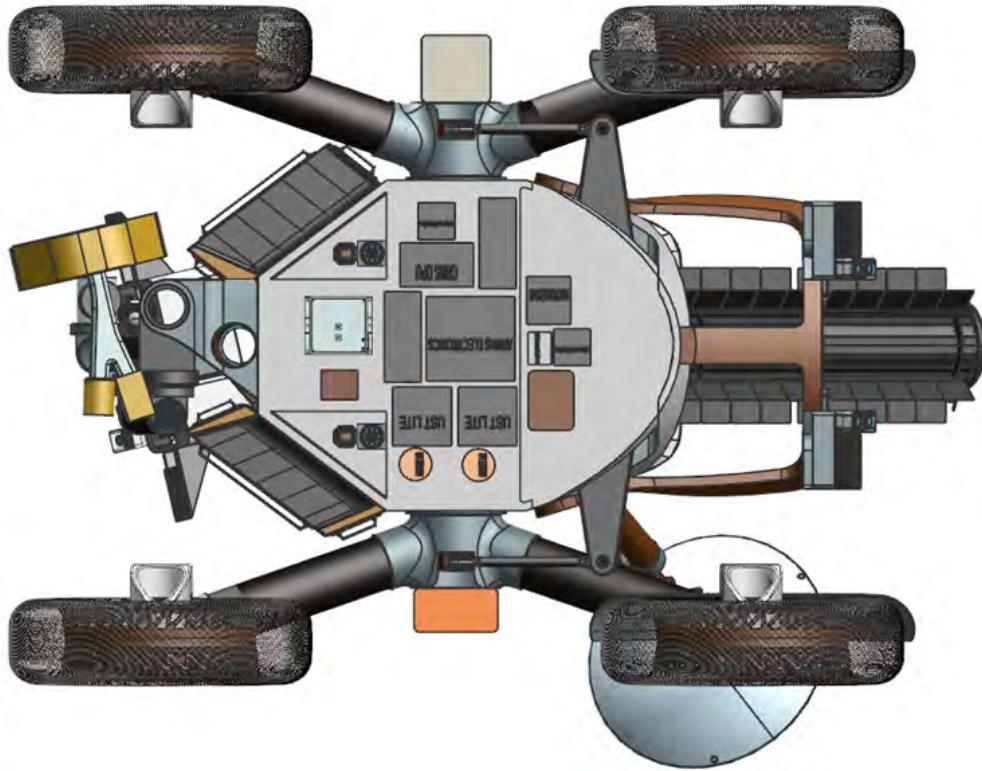


Figure L-12. Bottom view of the rover with the avionics shown.

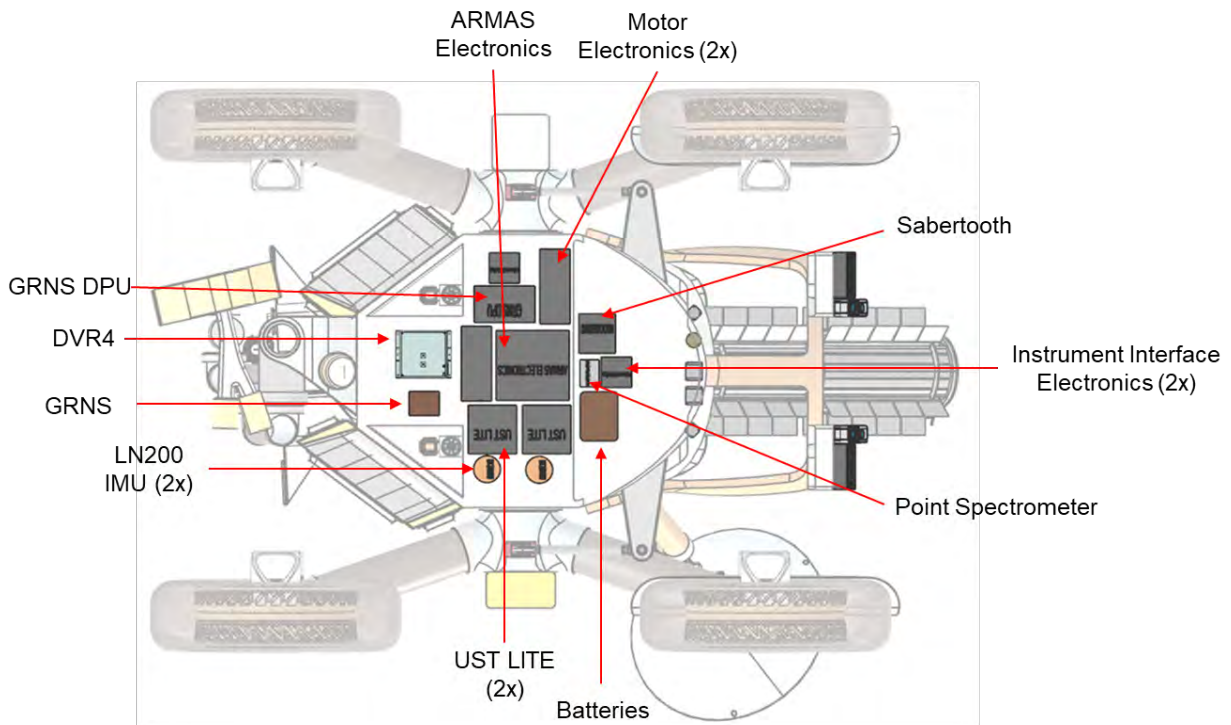


Figure L-13. Bottom view of the payload (same for Endurance-A and Endurance-R).

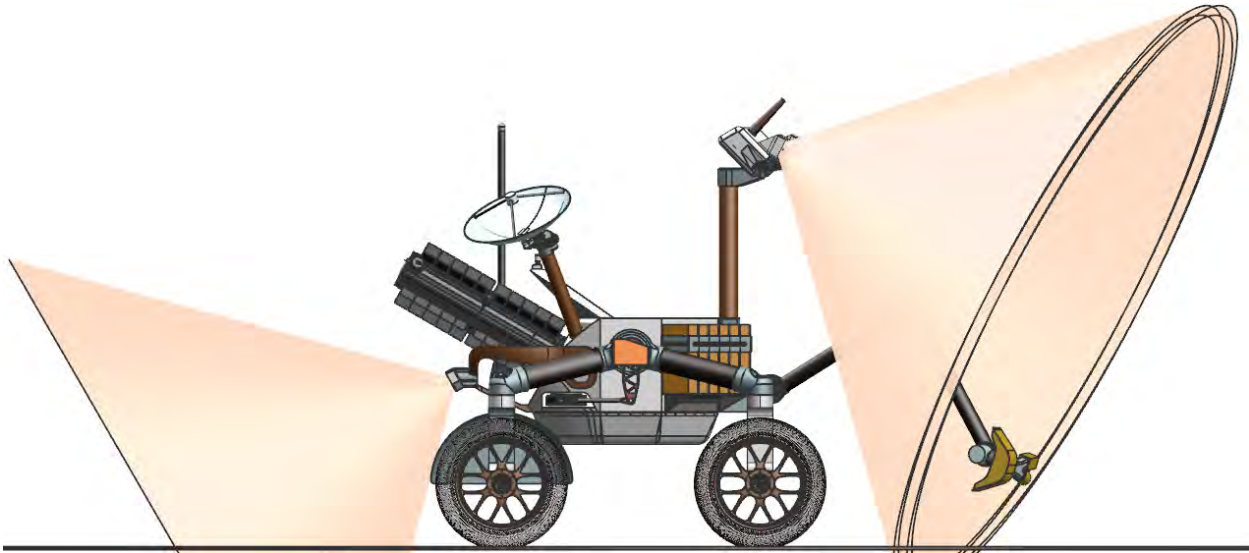


Figure L-14. Right side view of rover with the navigation camera FOVs shown (front and rear).

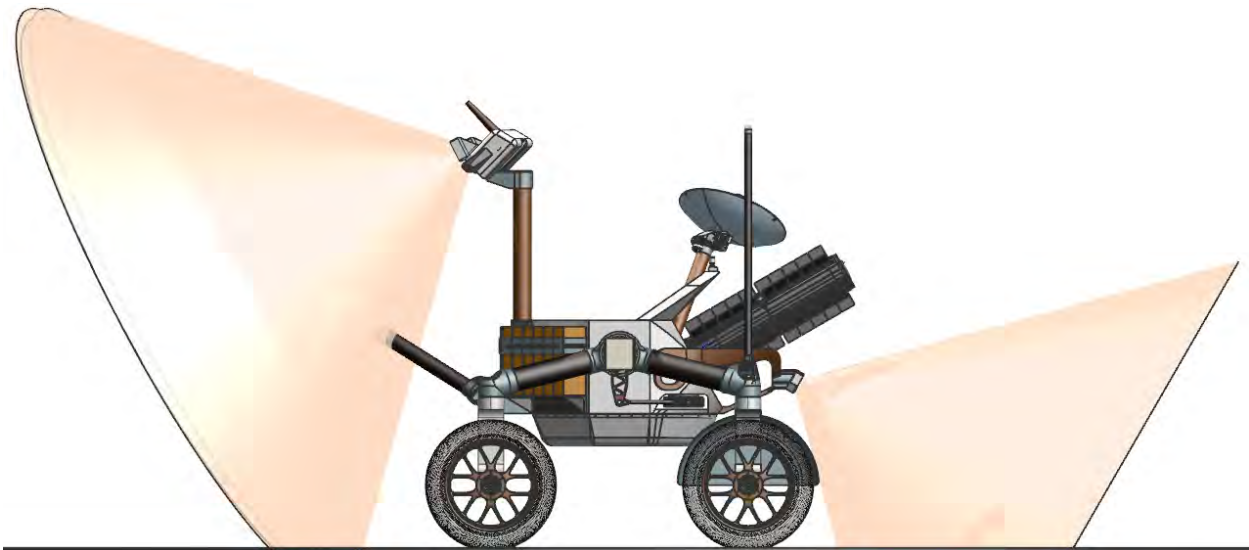


Figure L-15. Left side view of rover with the navigation camera FOVs shown (front and rear).

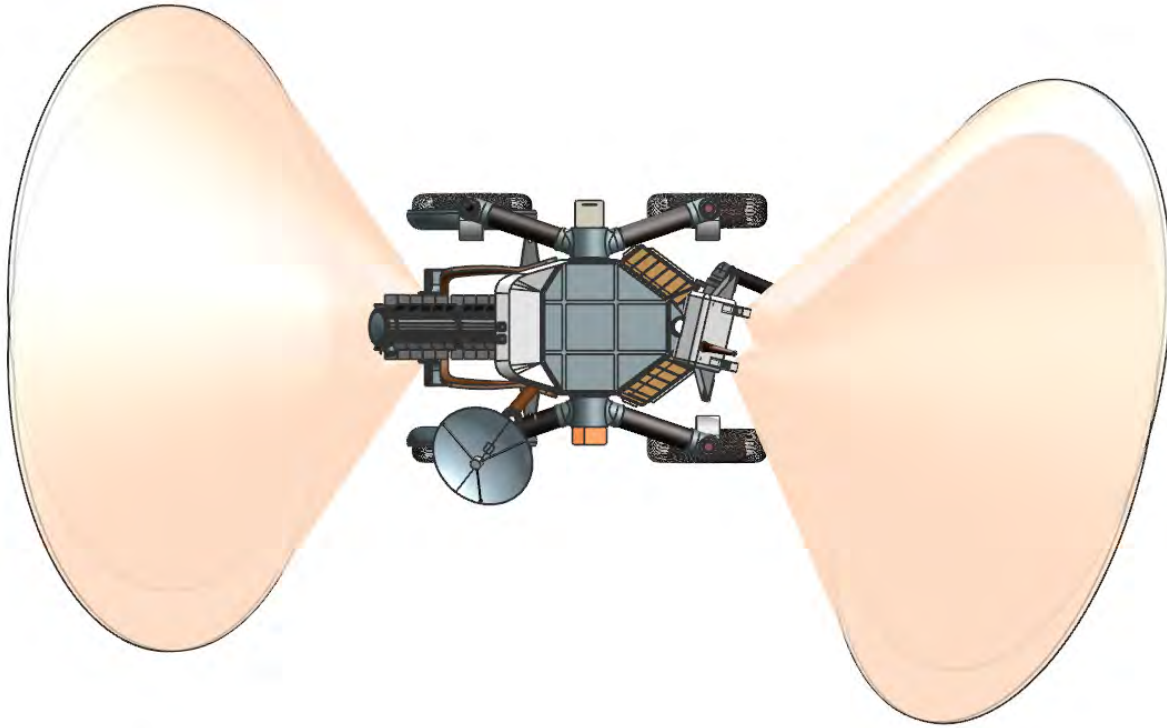


Figure L-16. Top view of the rover with the navigation camera FOVs shown (front and rear).

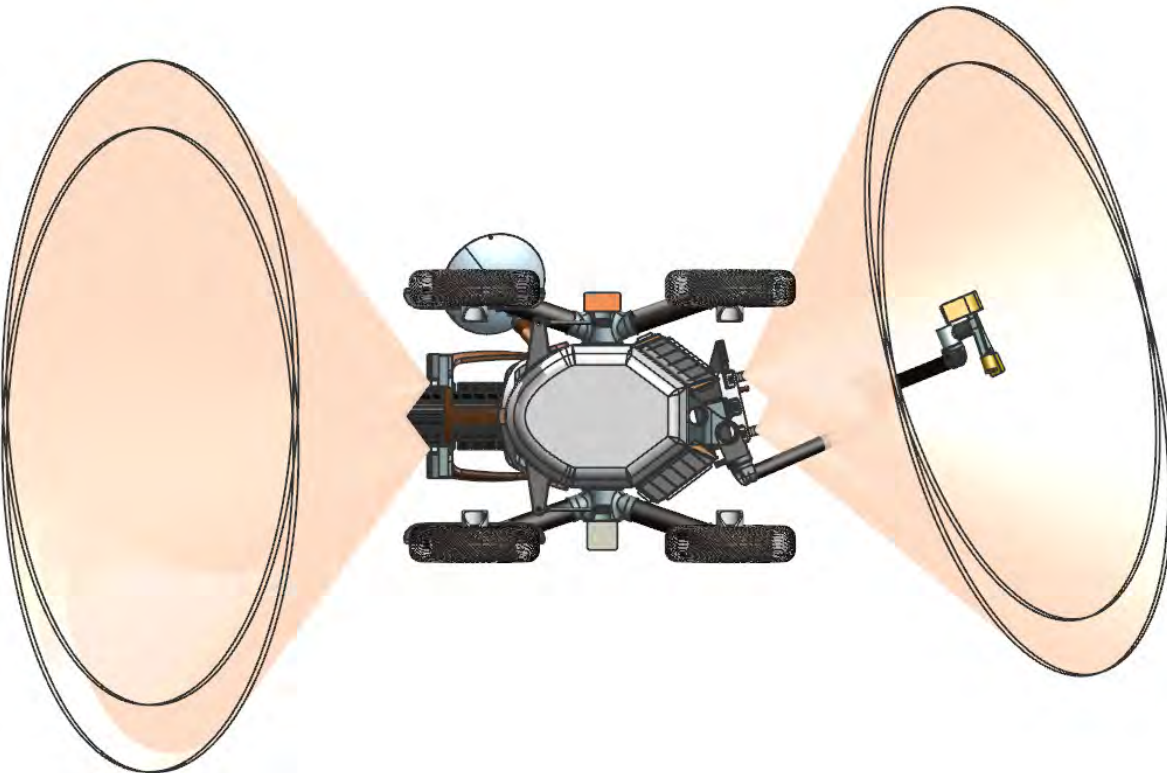


Figure L-17. Bottom view of the rover with the navigation camera FOVs shown (front and rear).

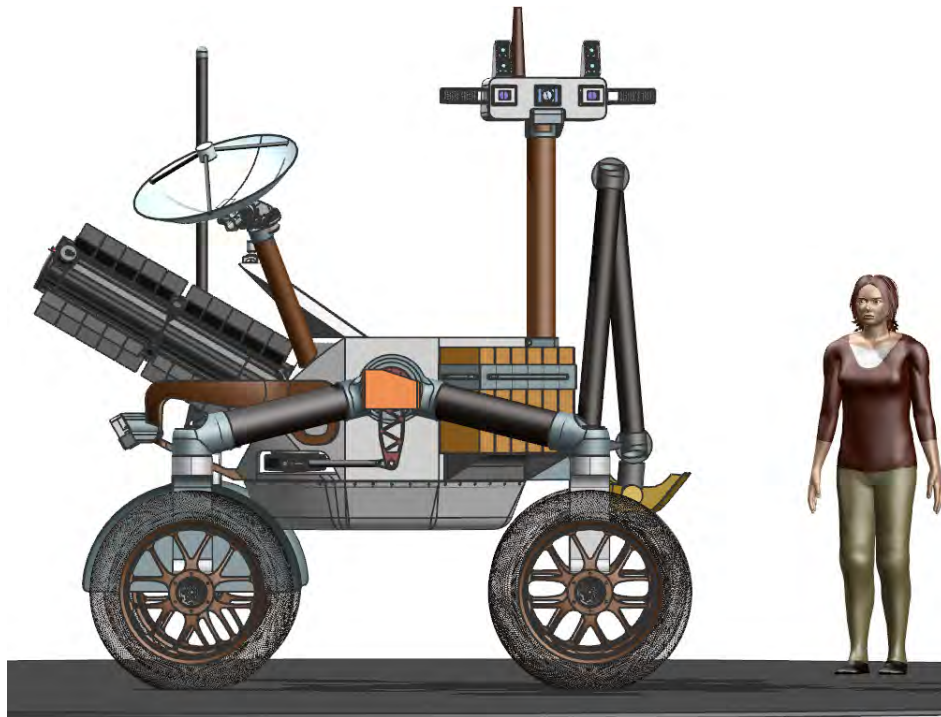


Figure L-18. Right side view of the rover with a human shown for scale.

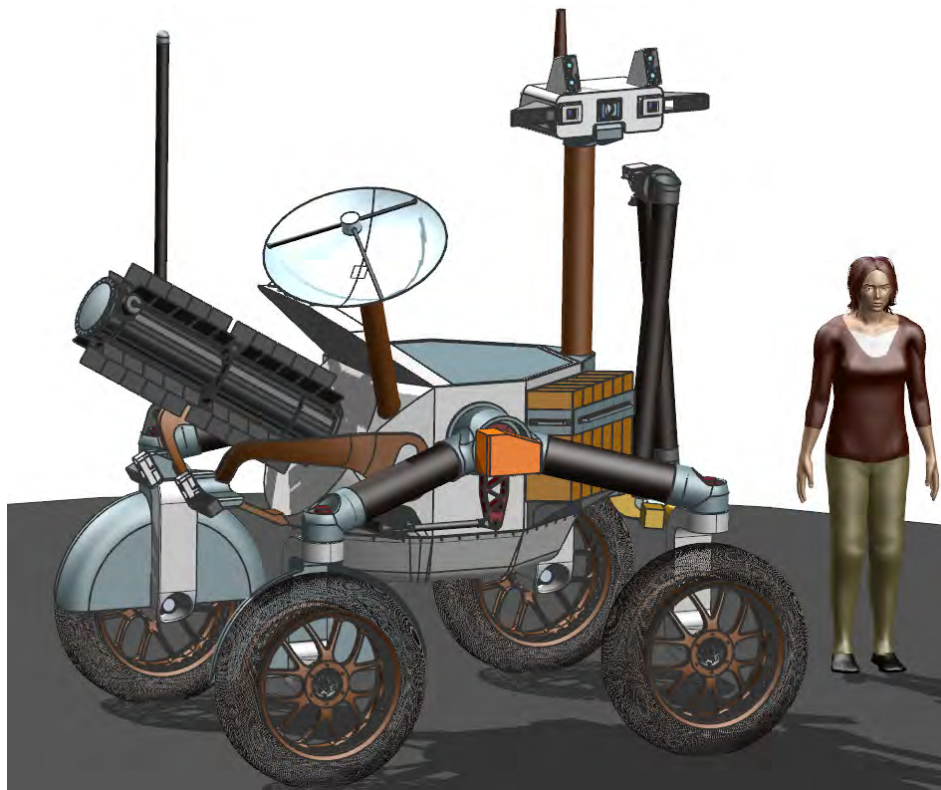


Figure L-19. Isometric view of the rover with a human shown for scale.

L.2.2 ENDURANCE-R: ROBOTIC SAMPLE RETURN

The Endurance-R rover has a sample carousel attached to the structure by a mast bracket. Each opening on the carousel has a lid, which only opens once the sample is being poured into it by the one-sided scoop of the robotic arm assembly. Once the carousel is full, the robotic arm will transfer it to the Earth Return Vehicle for transport to Earth.

Aside from the scoop, the robotic arm assemblies are identical on both rovers. The other difference between these two versions are the sample storage methods.

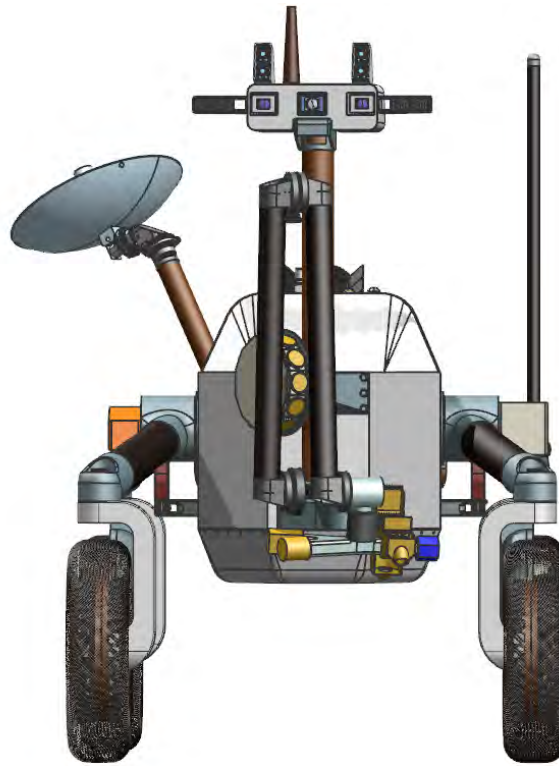


Figure L-20. Front view of the rover showing the camera head and robotic arm.

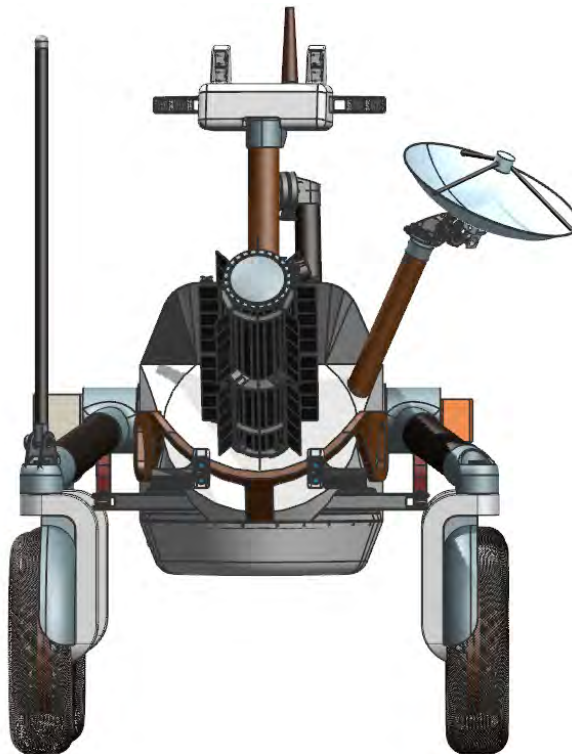


Figure L-21. Rear view of rover showing LGAs and navigation cameras.

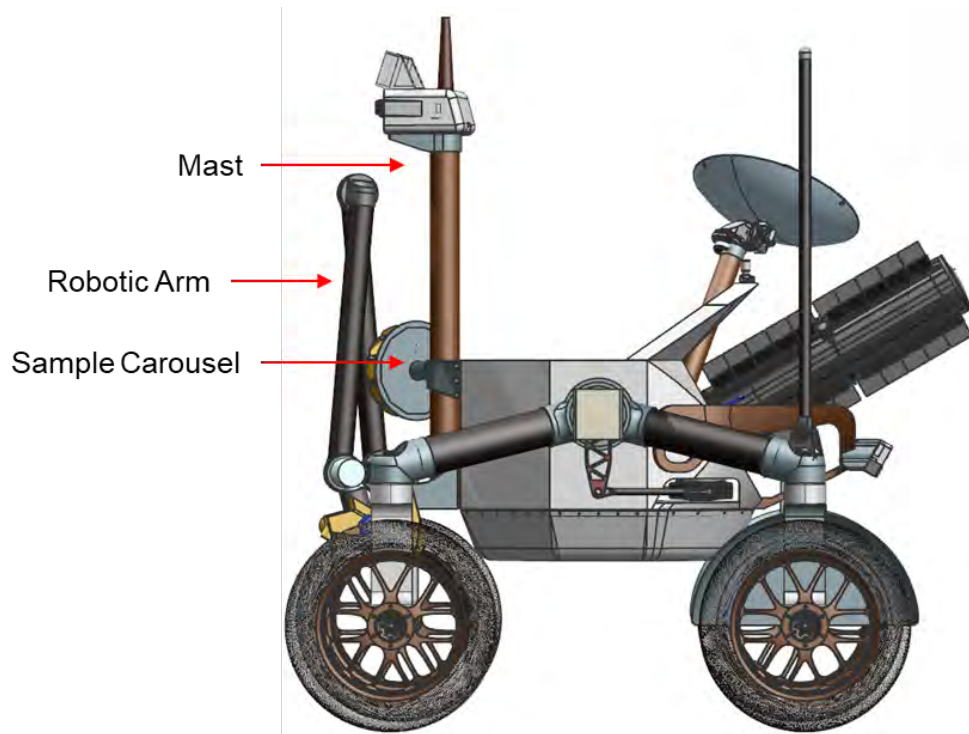


Figure L-22. Left side view of the rover.

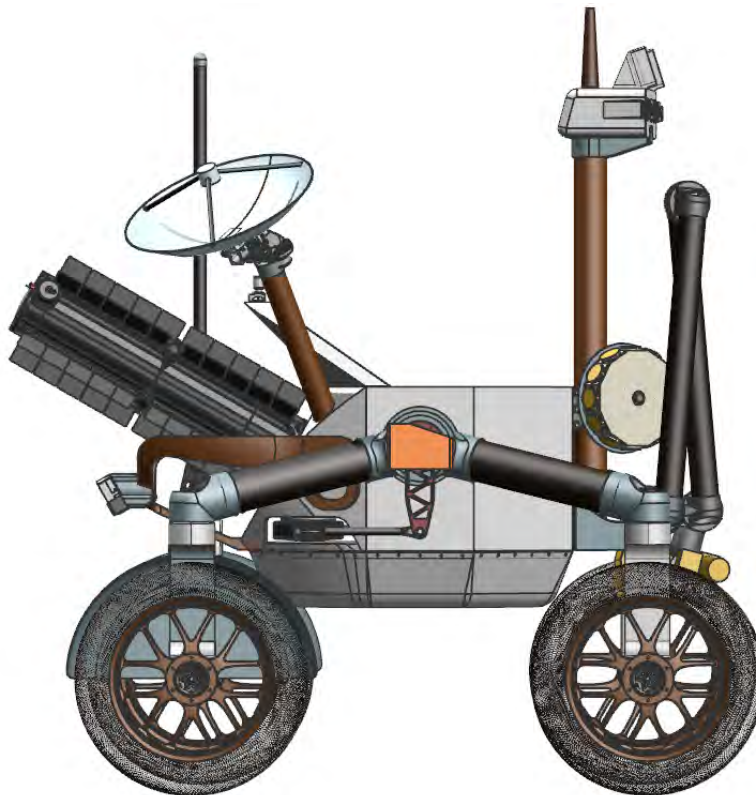


Figure L-23. Right side view of the rover.

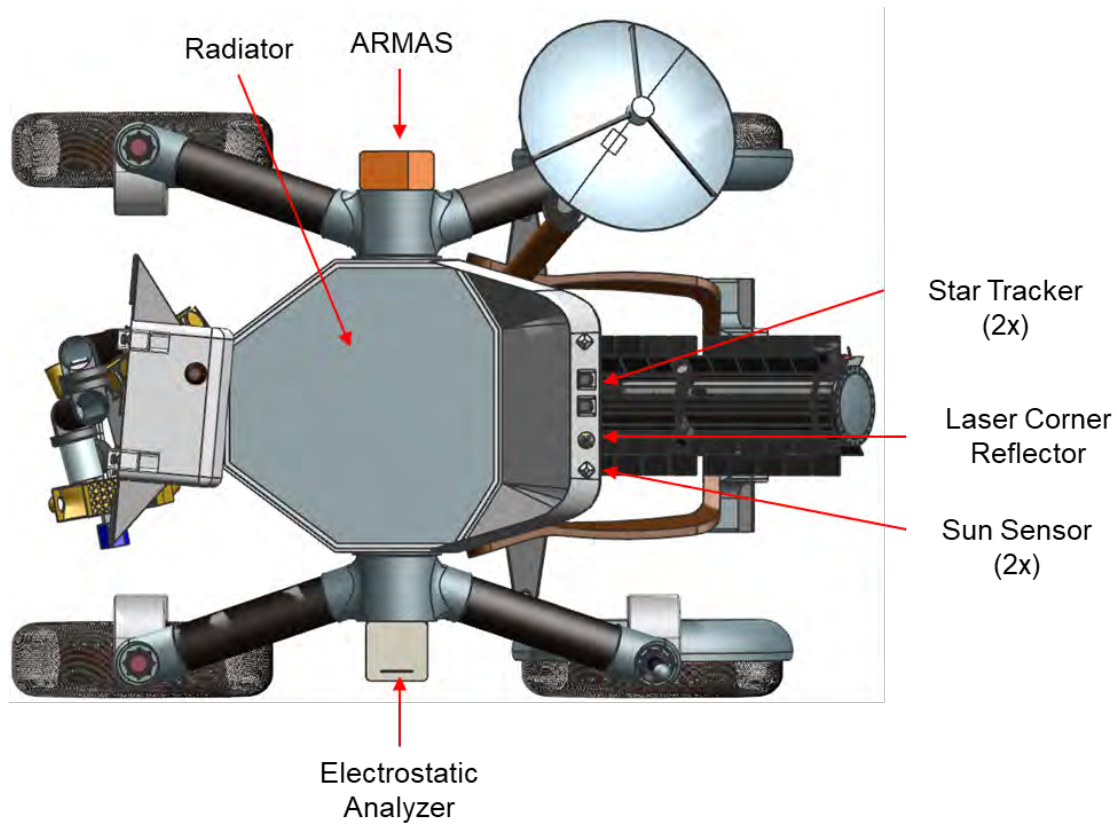


Figure L-24. Top view of the rover showing the radiator.

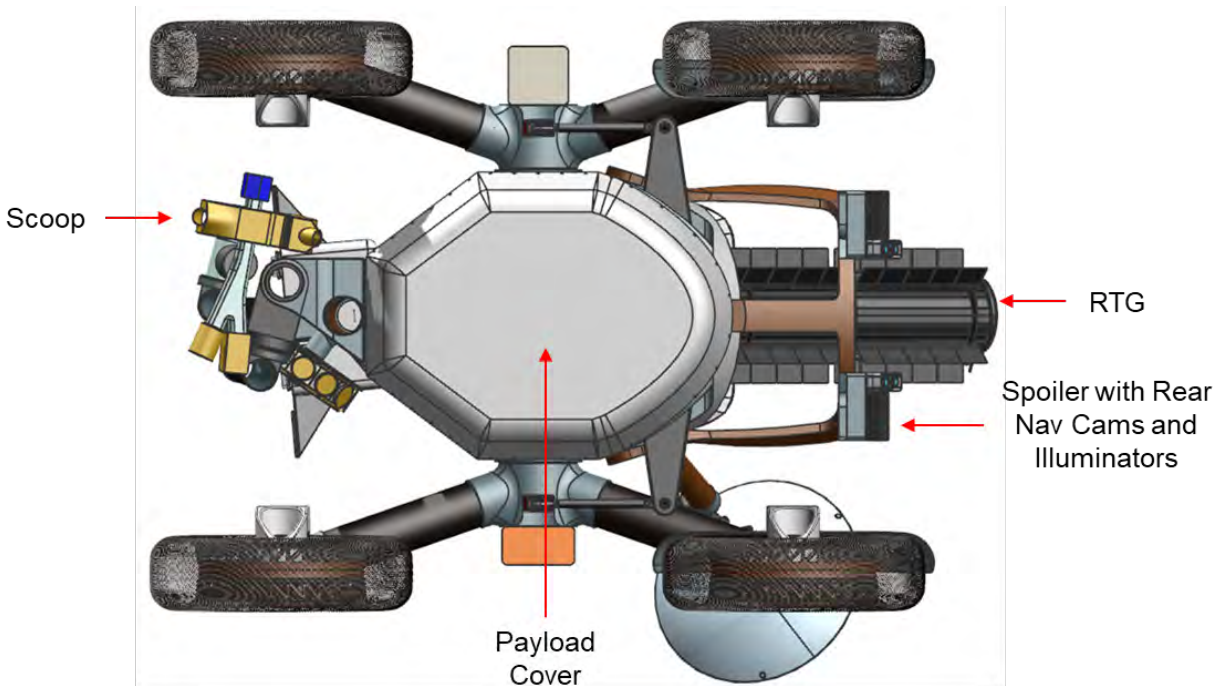


Figure L-25. Bottom view of the rover showing the radiator.

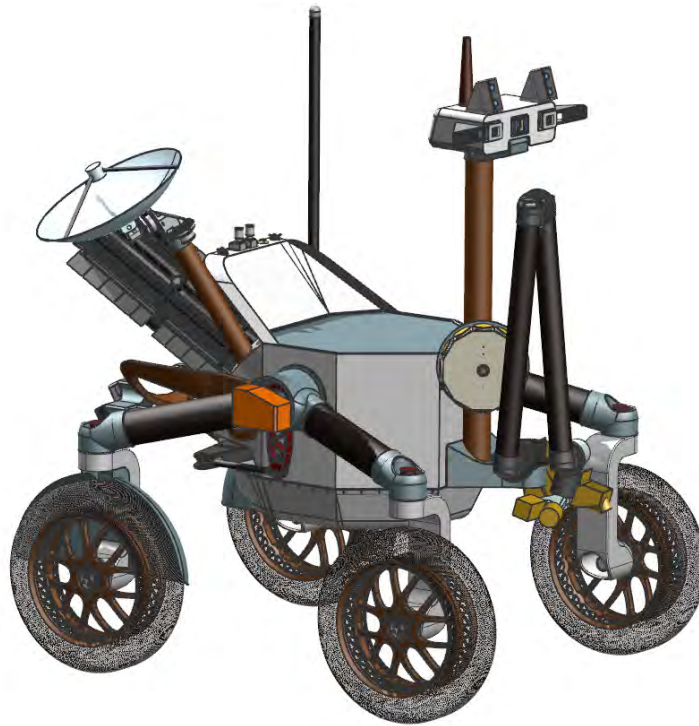


Figure L-26. Isometric view of the rover.

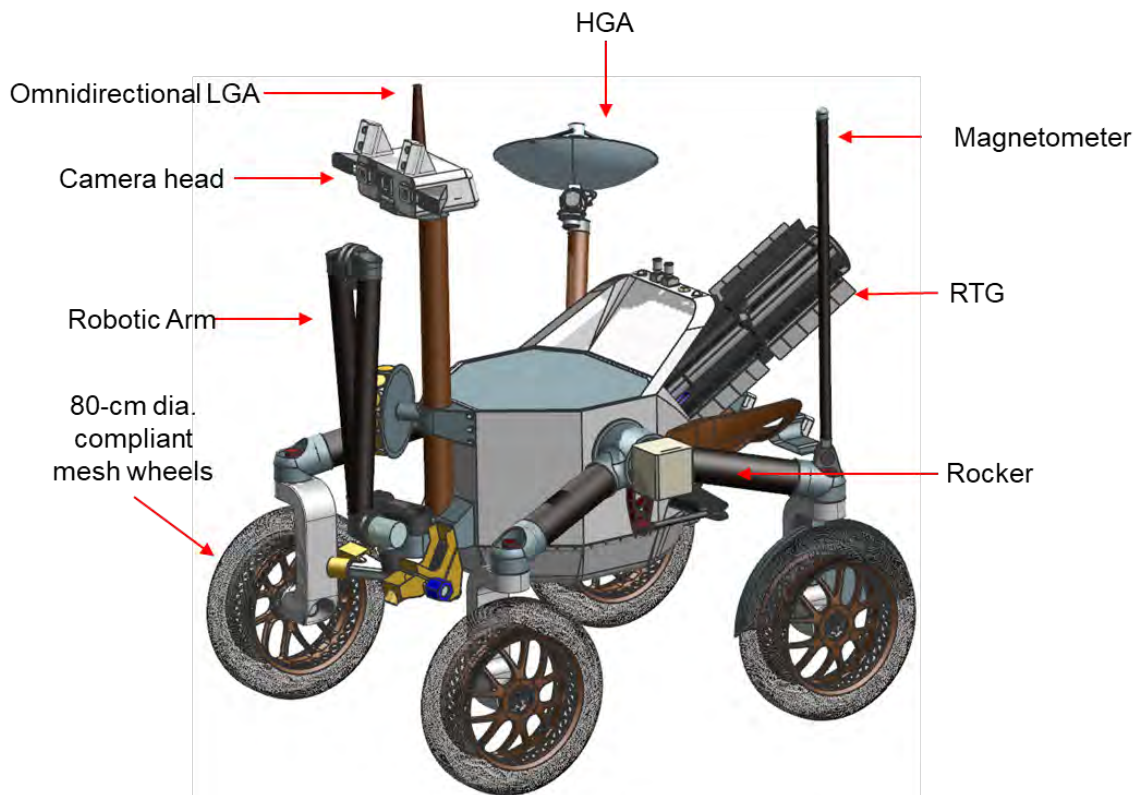


Figure L-27. Isometric view of the rover.

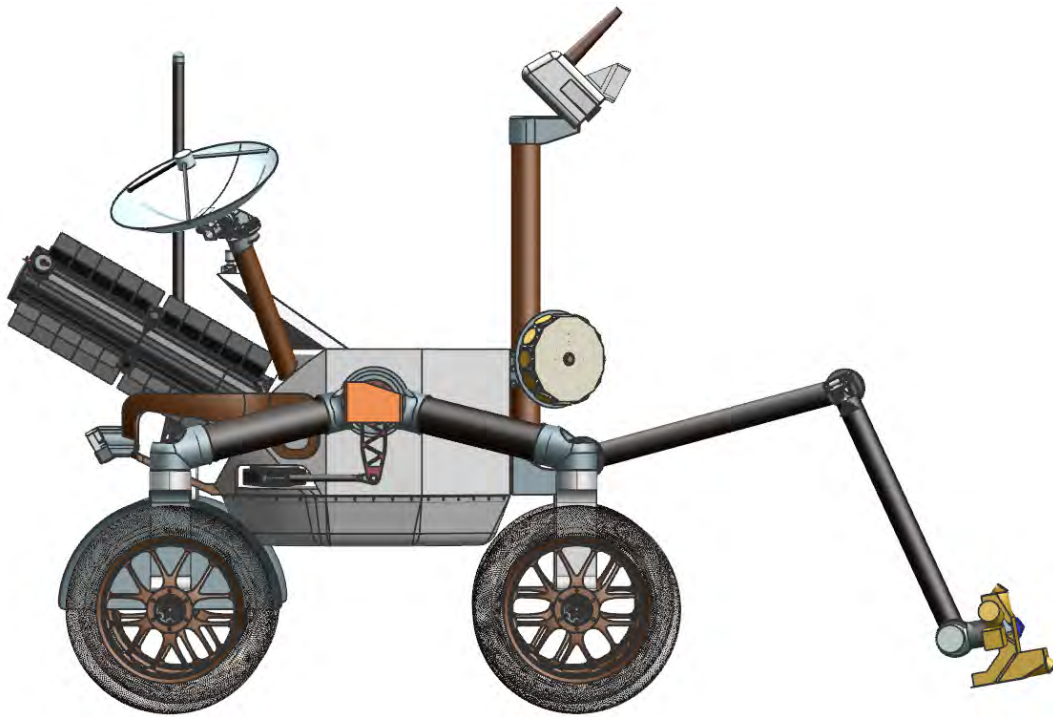


Figure L-28. Right side view of the rover with the arm extended and the camera head pointed down.

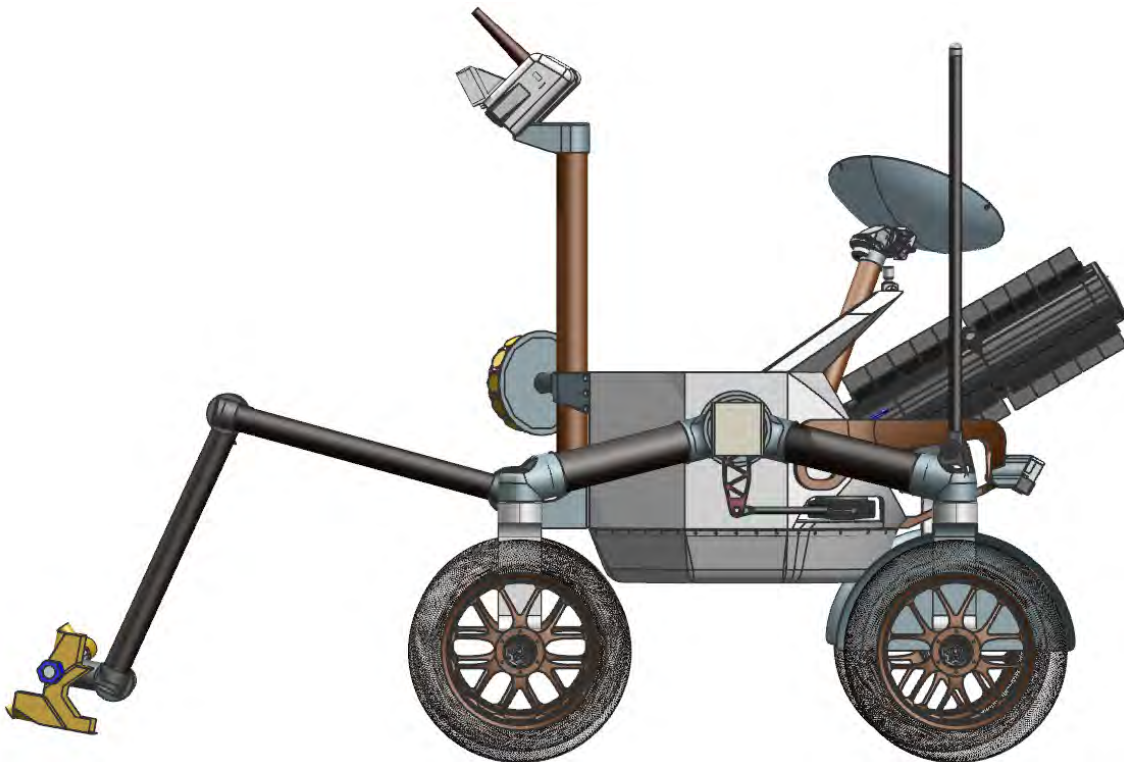


Figure L-29. Left side view of the rover with the arm extended and the camera head pointed down.

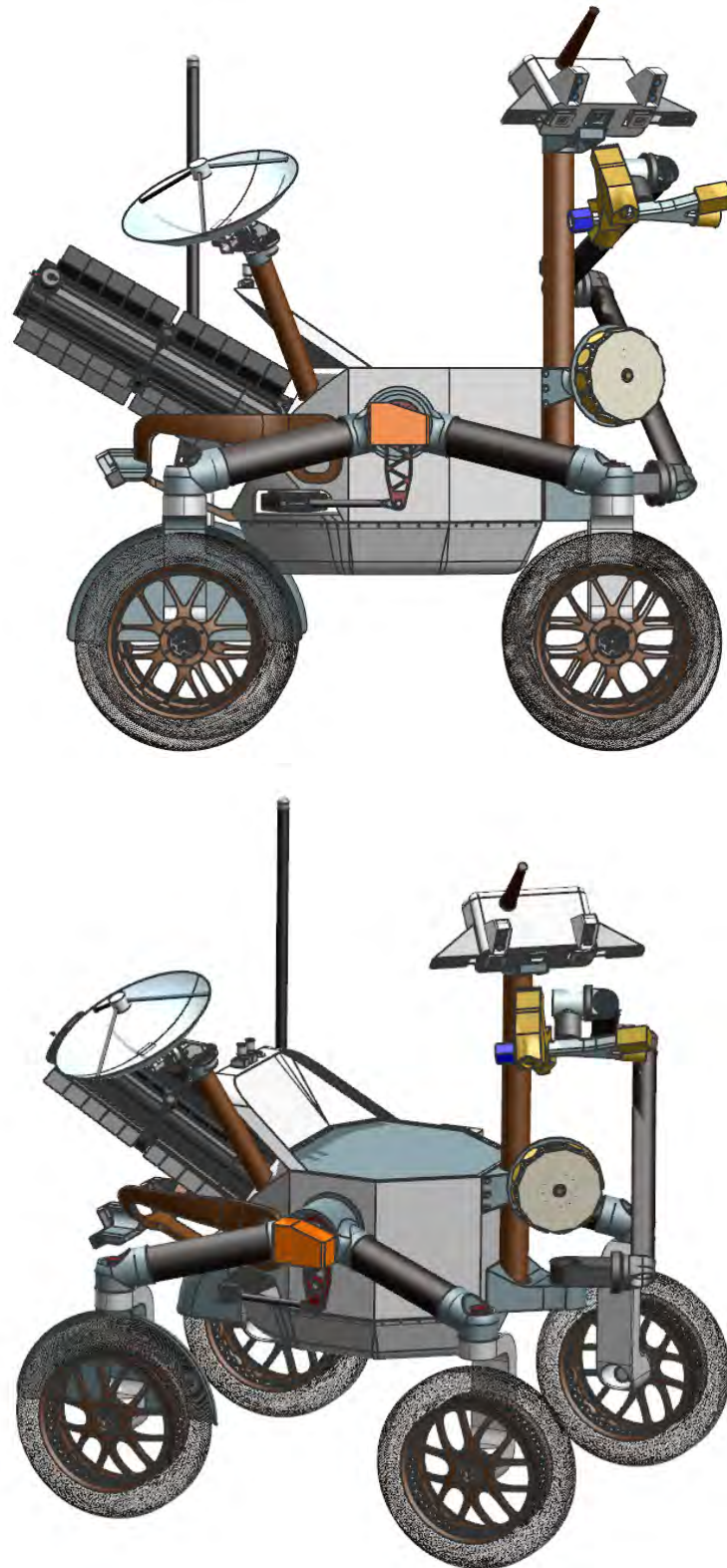


Figure L-30. Right and Isometric view of sample pouring.

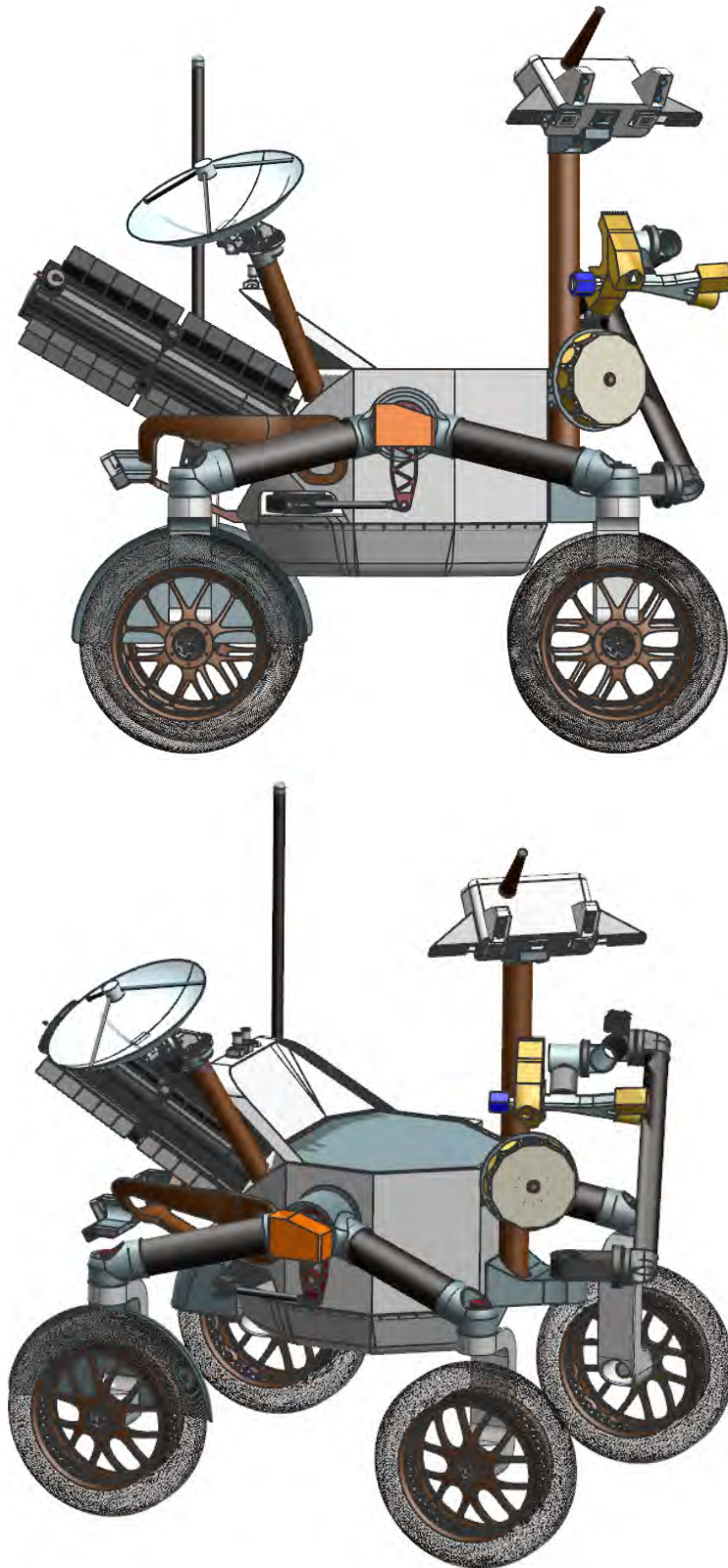


Figure L-31. Right and Isometric view of sample pouring.

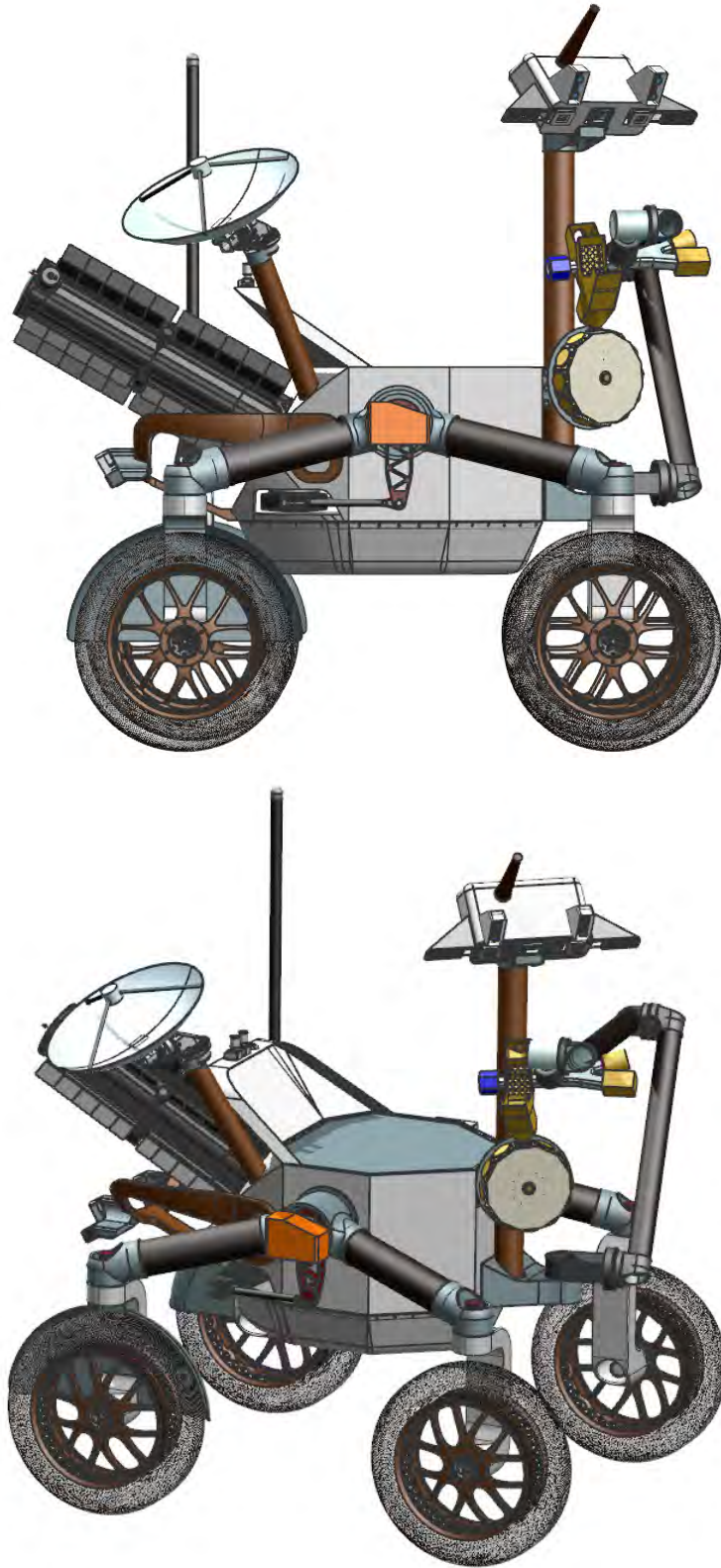


Figure L-32. Right and Isometric view of sample pouring.

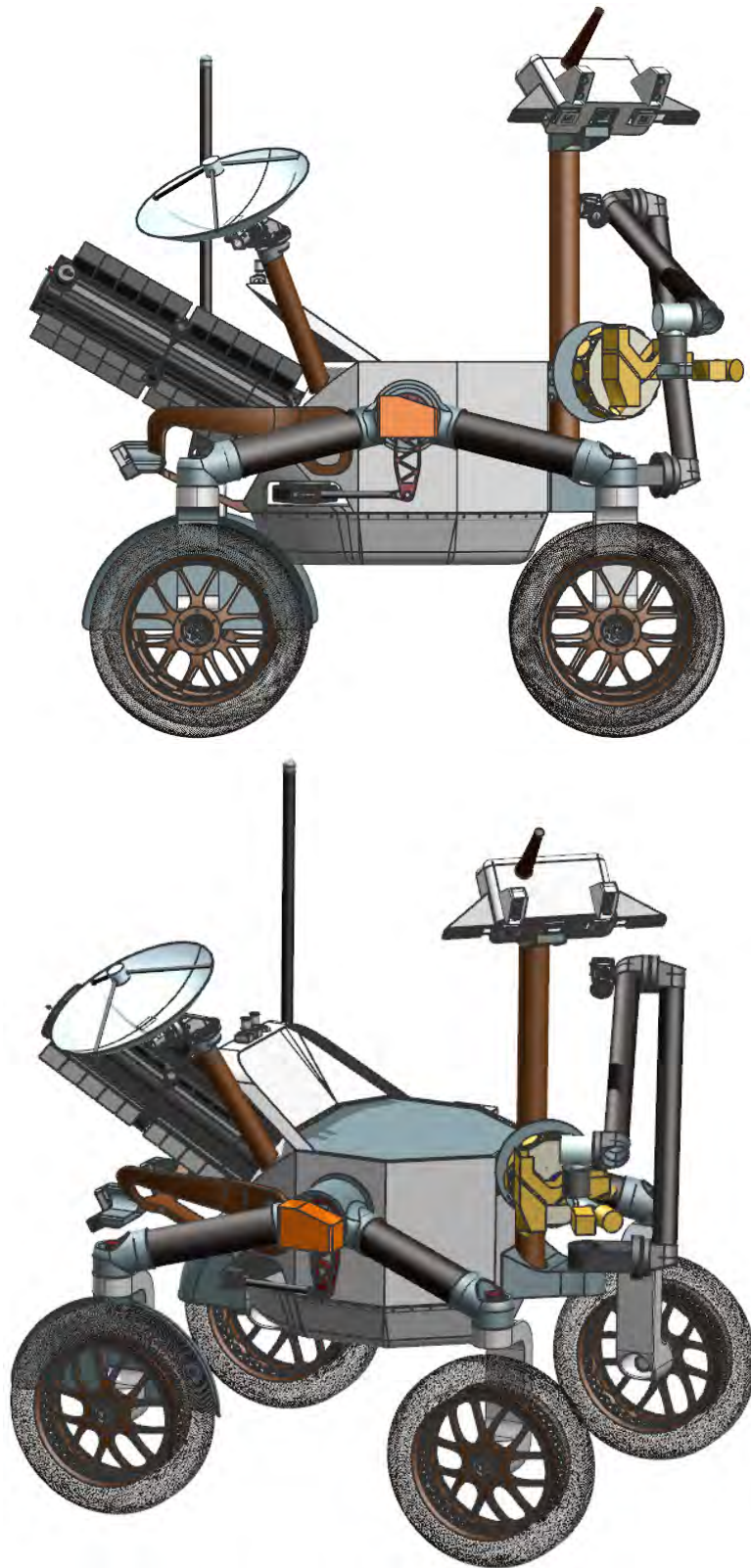


Figure L-33. Right and Isometric view of arm removing sample carousel.

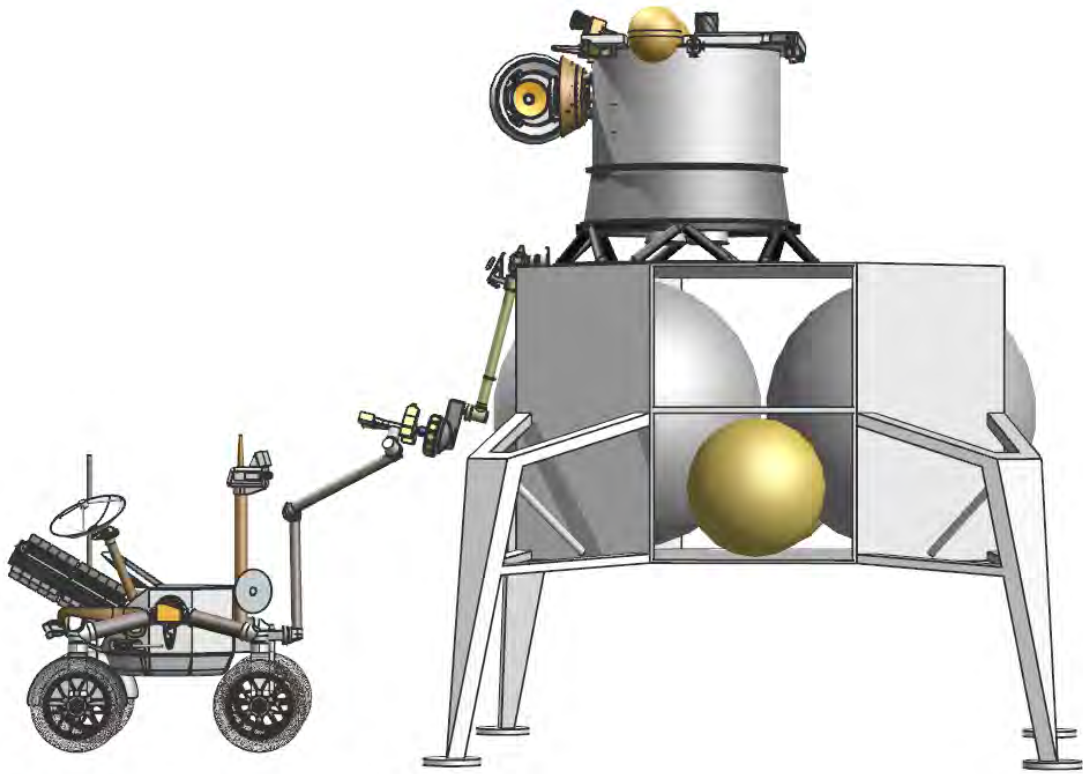


Figure L-34. Right view of arm passing the sample carousel to the Earth Return Vehicle (ERV).

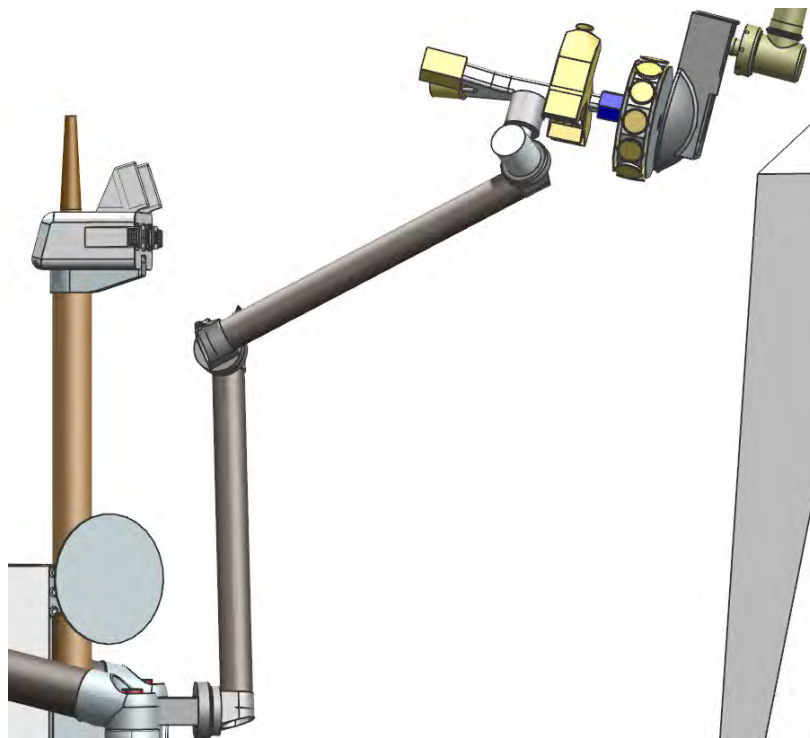


Figure L-35. Close-up of arm passing the sample carousel to the ERV.

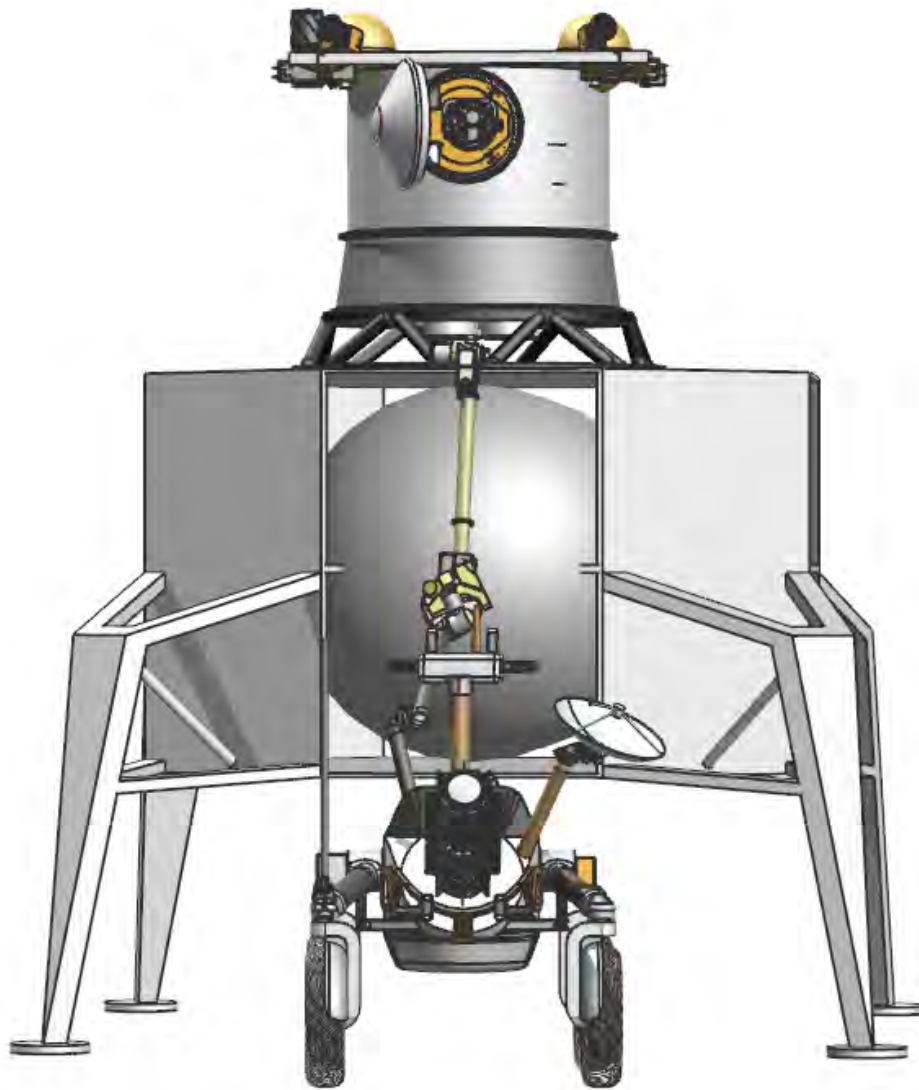


Figure L-36. Back view of the arm passing the sample carousel to the ERV.



Figure L-37. Right side view of the rover with the navigation camera FOVs shown (front and rear).

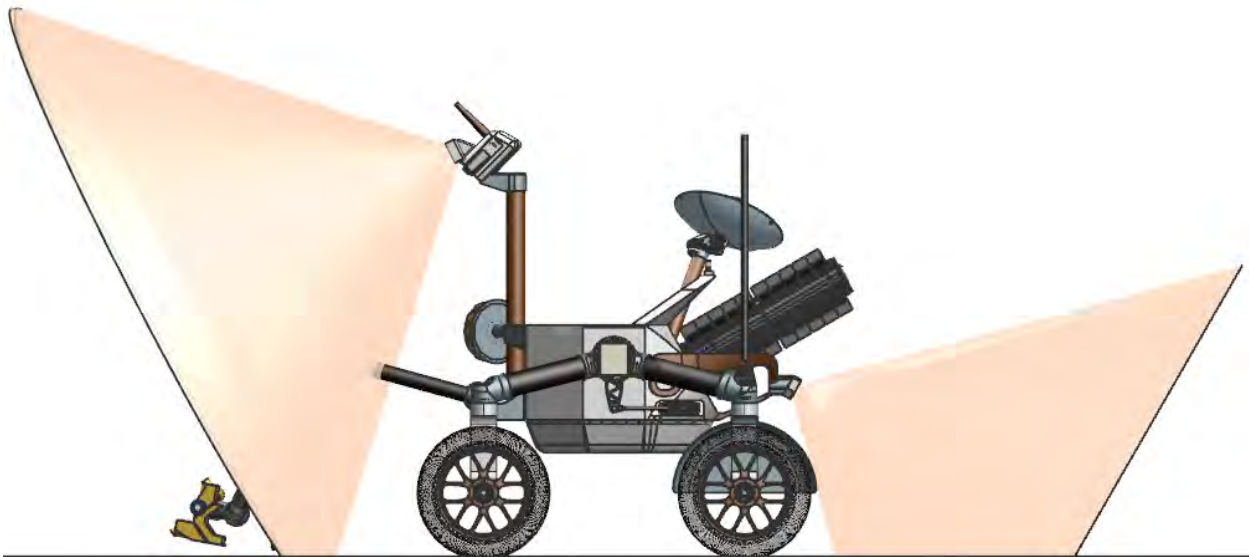


Figure L-38. Left side view of the rover with the navigation camera FOVs shown (front and rear).

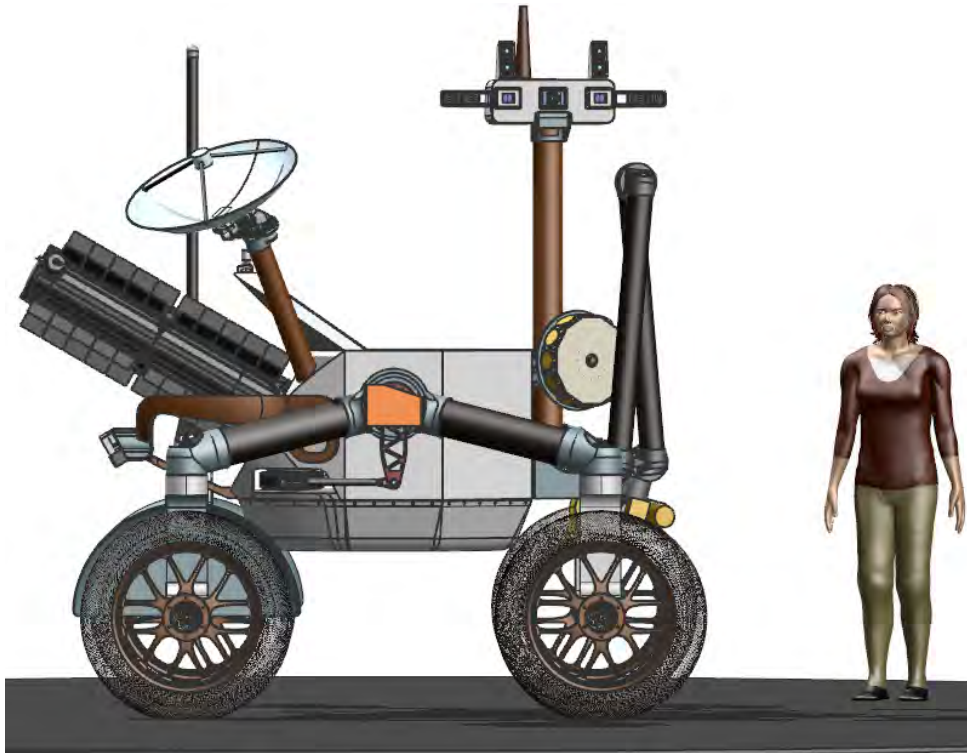


Figure L-39. Left side view of the rover with a human shown for scale.

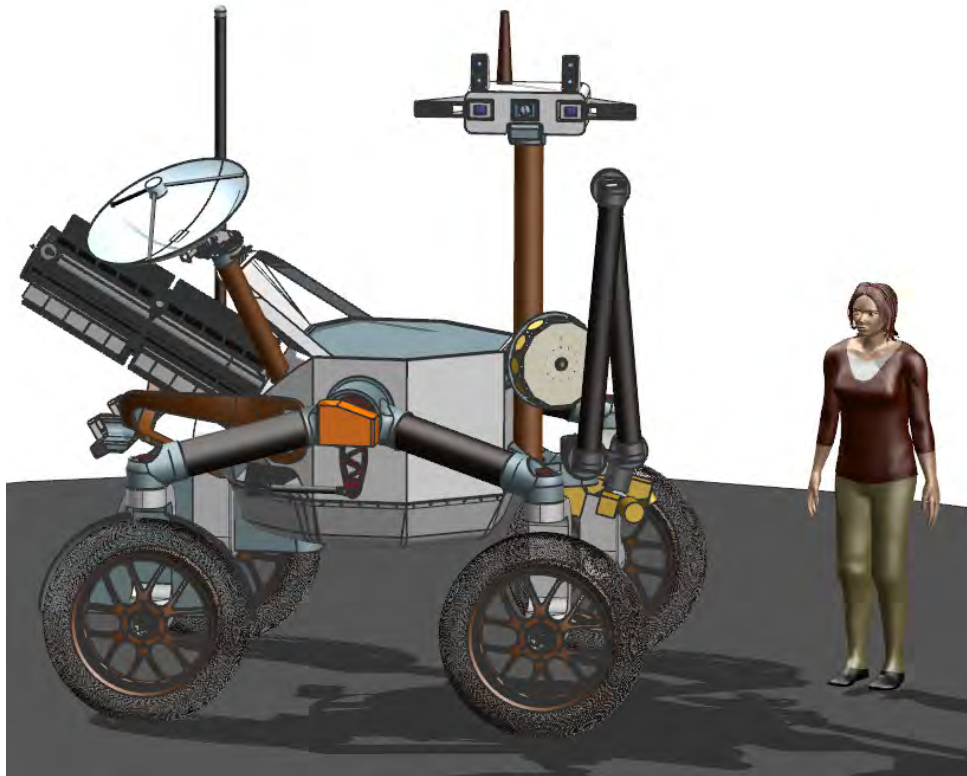


Figure L-40. Isometric view of the rover with a human shown for scale.

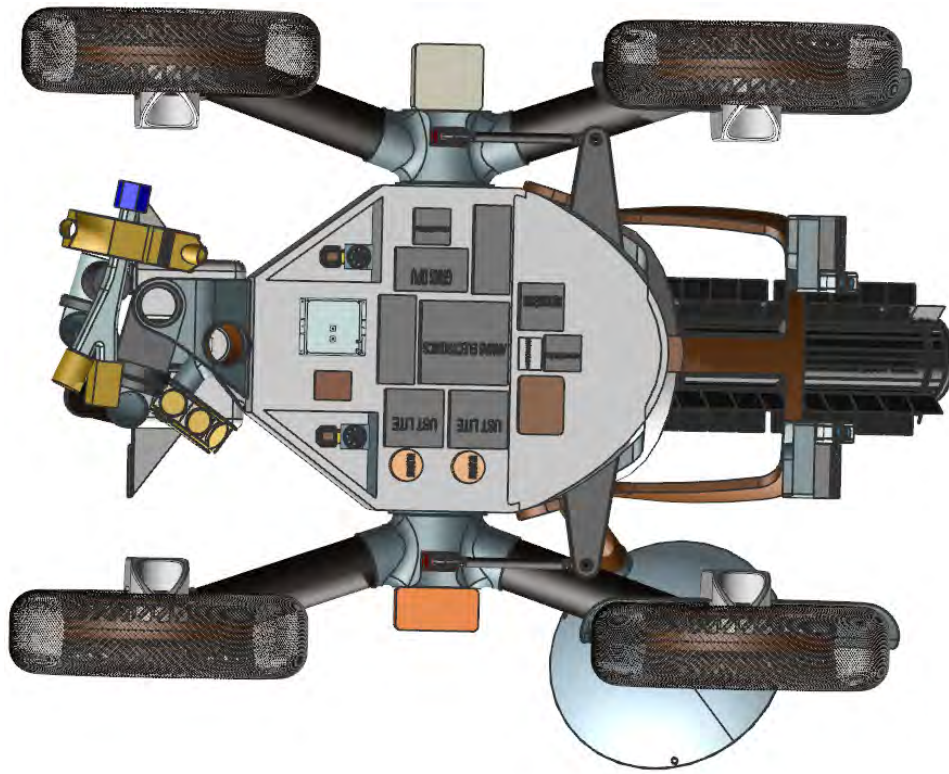


Figure L-41. Bottom view of the payload.

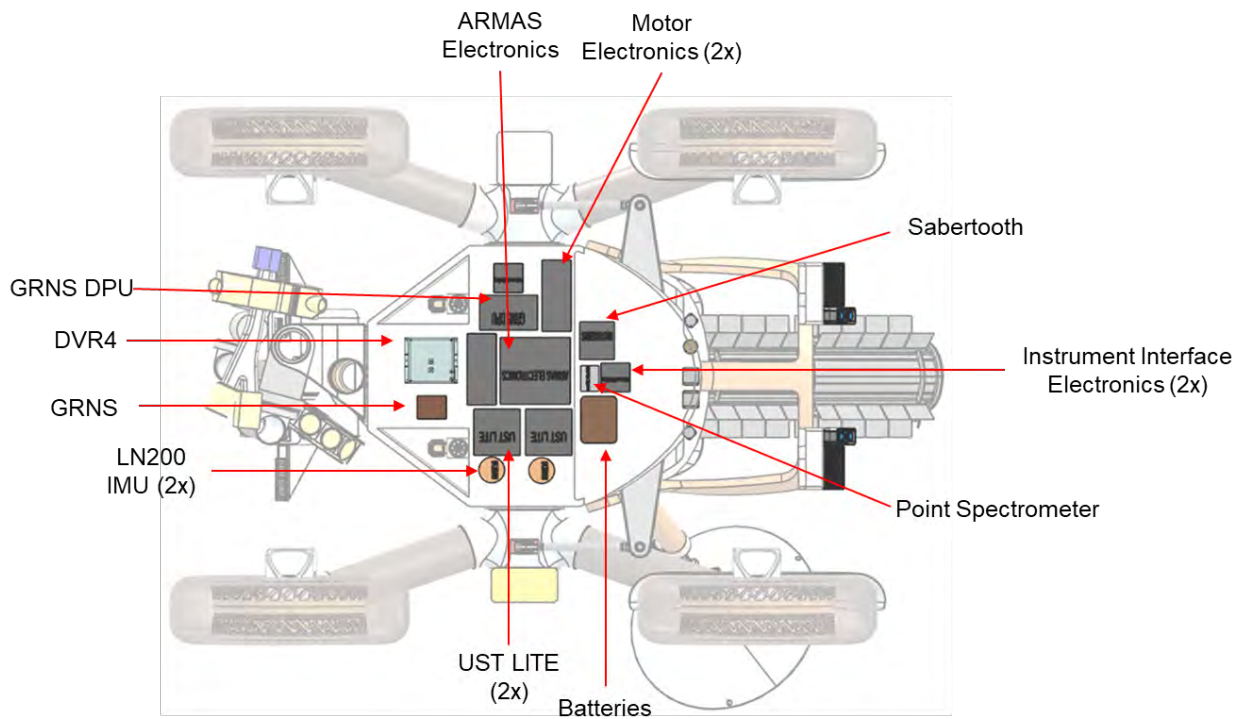


Figure L-42. Bottom view of the payload (same for Endurance-A and Endurance-R).

L.2.3 ENDURANCE ROVER (A AND R VERSIONS) THERMAL SYSTEM

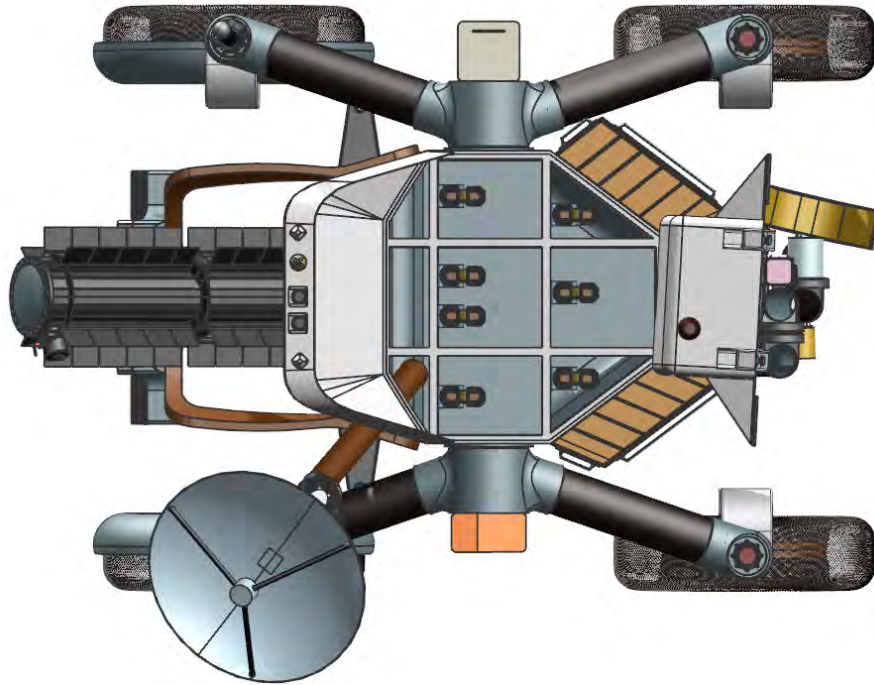


Figure L-43. Top view of thermal system without radiator.

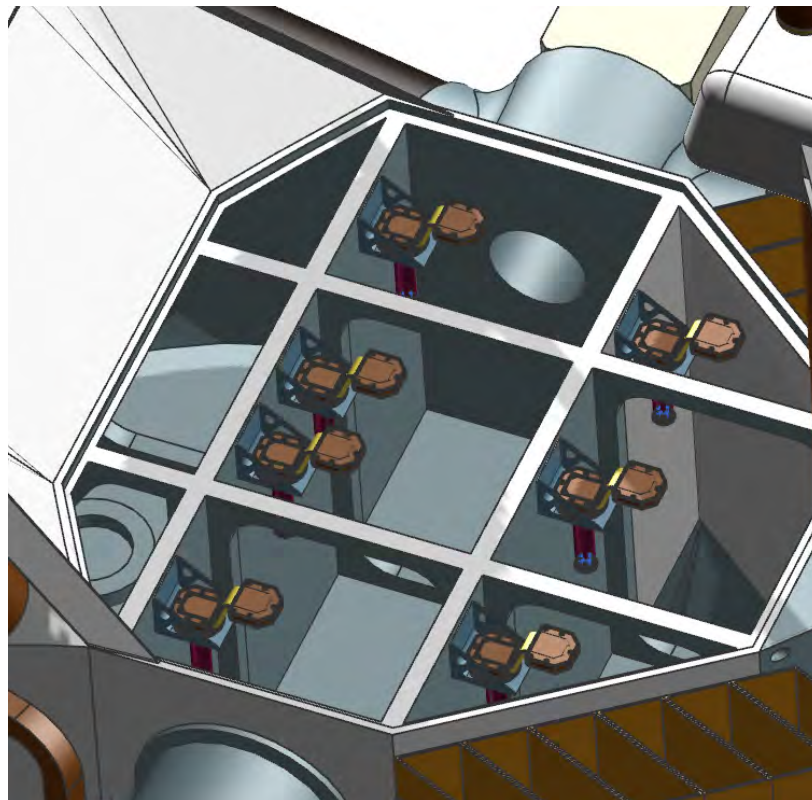


Figure L-44. Isometric view of thermal system without radiator.

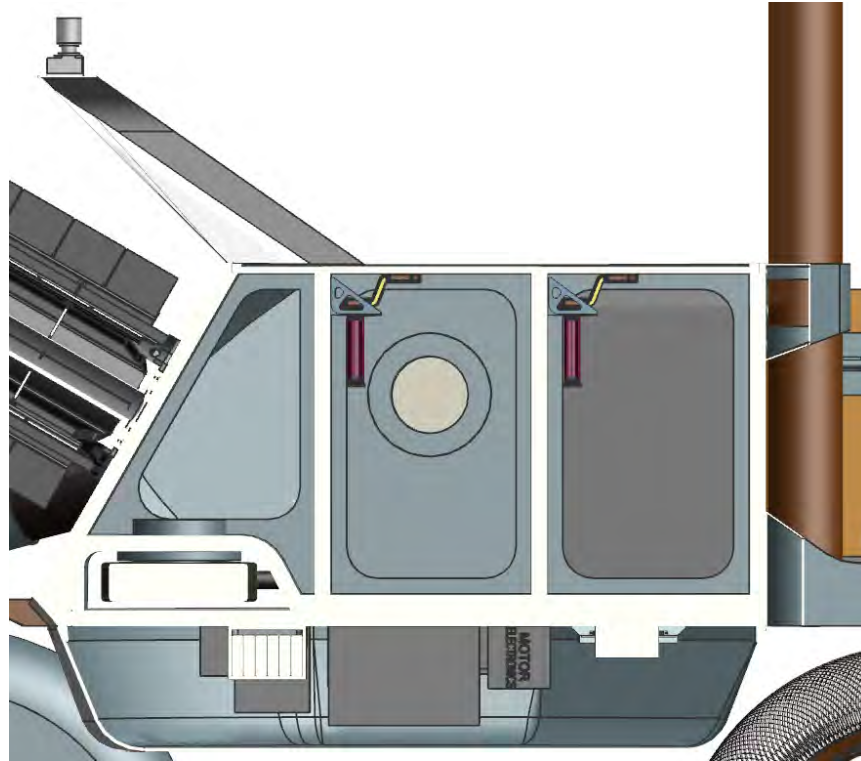


Figure L-45. Cross-sectional view of thermal system with radiator.

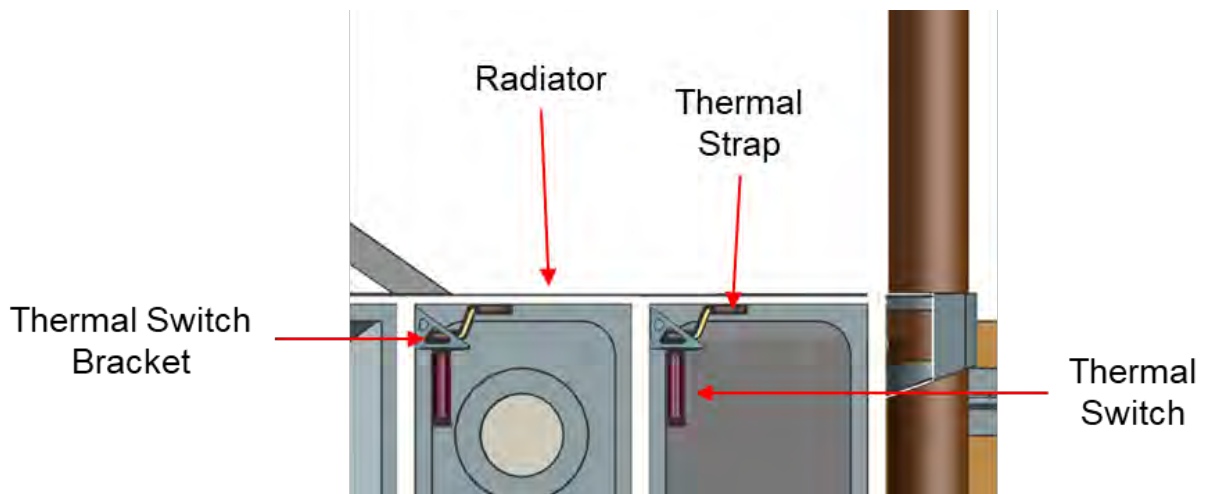


Figure L-46. Cross-sectional, close-up, view of thermal system with radiator.

L.2.4 ENDURANCE ROVER (A AND R VERSIONS) MASTHEAD

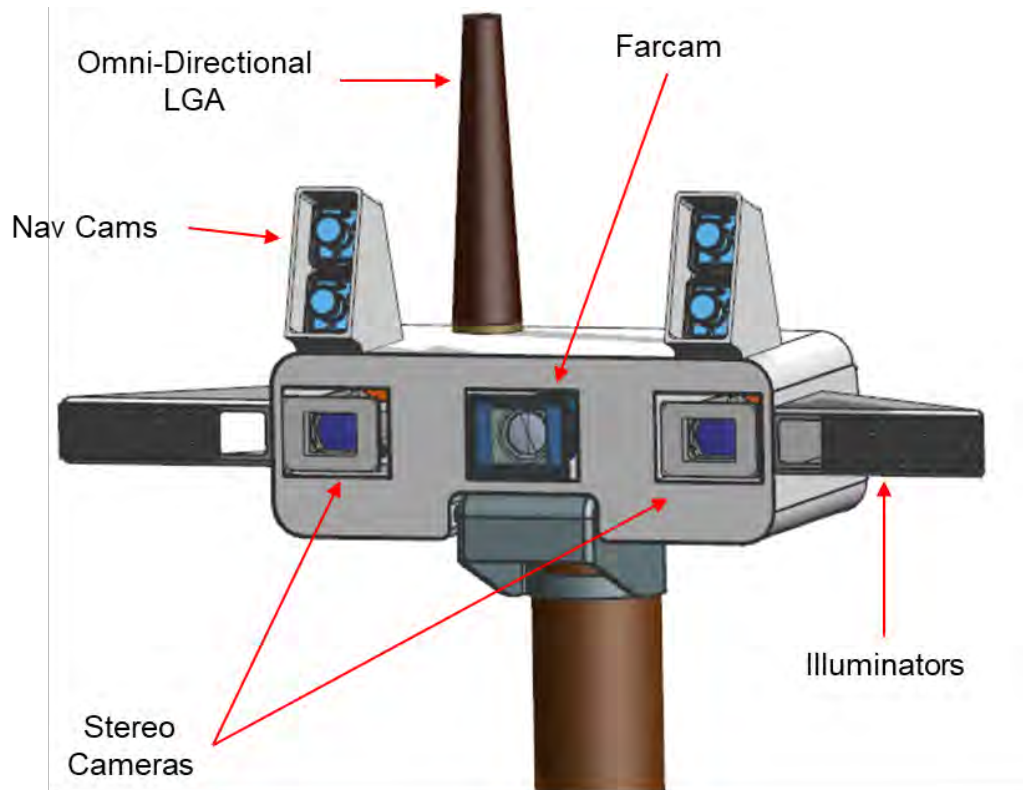


Figure L-47. Isometric view of the camera head, including the front navigation cameras and science cameras.

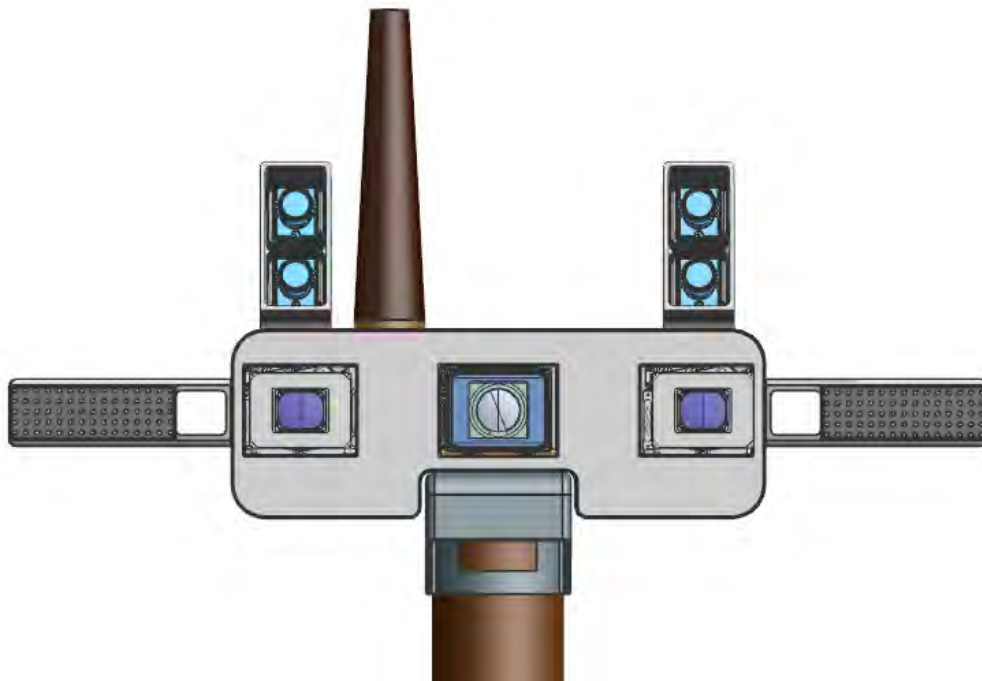


Figure L-48. Front view of the rover camera head, including the front navigation cameras and science cameras.

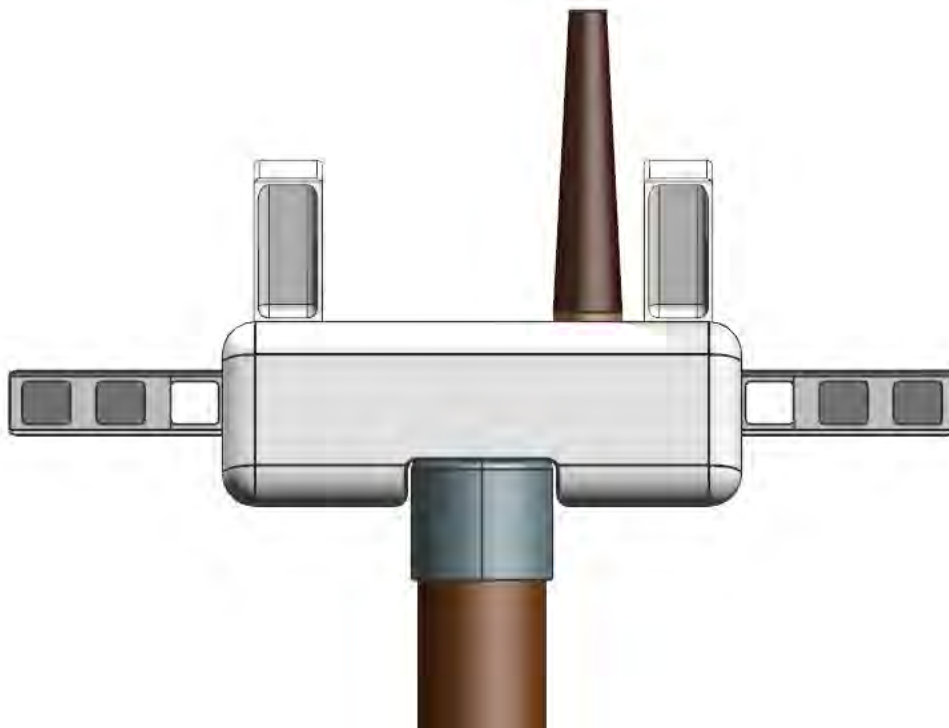


Figure L-49. Rear view of the rover camera head.

M ADDITIONAL COST MODELING INFORMATION

JPL's business organization performed an additional assessment of the Endurance costs using the following methodologies.

- Historical wrap factors for science, mission operations system, and ground data system that are level-of-effort.
- SEER (System Evaluation and Estimate of Resources) and TruePlanning for the payload and lander systems.
- Space Operations Cost Model (SOCM) for Phases E-F mission operations and data analysis costs

The cost results from these parametric estimates are summarized in Table M-1 for the Endurance-R options and Table M-2 for the Endurance-A option. The reserves are 50% for Phase A–D (excluding LV and the RTG) and 25% for Phase E/F (excluding tracking costs) as called for in the Decadal study ground rules.

In addition to the parametric model validations, a top-level crosscheck of the lunar rover (WBS 06) plus system I&T (WBS 10) was performed by looking as cost versus mass. Figure M-1 plots \$/kg for the Mars rover missions (Pathfinder, MEL, and MSL) and the two Endurance options. A trendline through the Mars missions show that both Endurance options are above the trendline. This indicates that the estimates for both lunar rover options are reasonable.

Phase A costs were added to the cost model estimates. As a gauge for the amount to apply, the pre-release draft of the NF 5 AO was used as the basis. New Frontiers 5 specifies a value of \$5M RY for Phase A.

Table M-1. Cost model results for Endurance-R option (FY25\$M). Highlighted cells represent **Wraps** and **SOCM**

WBS Element	Team X	SEER	TruePlanning (MSL Calibrated)	TruePlanning (Space Msn Catalog)	Model Average	Model Avg – Team X Delta (\$)	Delta (%)
Phase A Concept Study	Incl. below	5.0	5.0	5.0	5.0	-	-
01 Project Management	44.8	71.3	41.9	45.1	142.4	-6.4	-4%
02 Project System Engineering	52.3	99.5	29.9	38.0			
03 Safety & Msn Assurance	51.7	Incl. above	38.8	62.6			
04 Science	35.0	35.5	38.2	12.2	28.6	-6.4	-18%
05 Payload	77.1	76.8	105.3	110.7	97.6	20.6	27%
06 Flight System	795.3	766.3	756.4	666.3	729.6	-65.7	-8%
07 Mission Ops	43.7	44.9	48.3	30.3	41.1	-2.6	-6%
09 Ground Data System	47.4	41.7	44.9	40.1	42.2	-5.2	-11%
10 Project System I&T	61.5	63.4	135.6	95.1	98.0	36.5	59%
Total Dev. w/o Reserves	1,208.8	1,204.3	1,244.2	1,105.4	1,184.6	-24.2	-2%
Development Reserves (50%)	569.4	567.1	587.1	517.7	557.3	-12.1	-2%
Total A-D Development Cost	1,778.2	1,771.4	1,831.3	1,623.1	1,741.9	-36.3	-2%
01/02 PM/PSE	11.0	2.2	2.2	2.2	2.2	-8.8	-80%
04 Science	81.6	105.2	105.2	105.2	105.2	23.6	29%
07 Mission Operations System	79.5	77.2	77.2	77.2	77.2	-2.3	-3%
09 Ground Data System	33.1	27.8	27.8	27.8	27.8	-5.3	-16%
Total Ops w/o Reserves	205.2	212.4	212.4	212.4	212.4	7.3	4%
Operations Reserves (25%)	47.0	48.8	48.8	48.8	48.8	1.8	4%
Total E-F Operations Cost	252.1	261.2	261.2	261.2	261.2	9.1	4%
08 Launch System	400.0	400.0	400.0	400.0	400.0	0.0	0%
Total Cost	2,430.3	2,432.6	2,492.5	2,284.3	2,403.2	-27.2	-1%

Table M-2. Cost model results for Endurance-A option (FY25\$M). Highlighted cells represent Wraps and SOCM.

WBS Element	Team X	SEER	TruePlanning (MSL Calibrated)	TruePlanning (Space Msn Catalog)	Model Average	Model Avg – Team X Delta (\$)	Delta (%)
Phase A Concept Study	Incl. below	5.0	5.0	5.0	5.0	-	-
01 Project Management	23.7	45.6	24.7	26.4	86.1	1.2	1%
02 Project System Engineering	32.0	62.9	17.7	21.8			
03 Safety & Msn Assurance	29.2	Incl. above	23.2	36.1			
04 Science	32.2	21.4	23.4	11.8	18.9	-13.3	-41%
05 Payload	73.5	71.9	101.1	106.5	93.2	19.7	27%
06 Flight System	471.6	441.1	418.5	373.0	410.9	-60.7	-13%
07 Mission Ops	32.8	27.1	29.6	17.8	24.8	-8.0	-24%
09 Ground Data System	32.3	25.2	27.5	24.6	25.8	-6.5	-20%
10 Project System I&T	32.8	34.9	77.6	56.5	56.3	23.5	72%
Total Dev. w/o Reserves	760.0	735.2	748.2	679.5	720.9	-39.1	-5%
Development Reserves (50%)	345.0	332.6	339.1	304.7	325.5	-19.5	-6%
Total A-D Development Cost	1,105.0	1,067.8	1,087.3	984.2	1,046.4	-58.6	-5%
01/02 PM/PSE	6.7	2.0	2.0	2.0	2.0	-4.7	-71%
04 Science	78.2	97.6	97.6	97.6	97.6	19.4	25%
07 Mission Operations System	70.8	61.6	61.6	61.6	61.6	-9.2	-13%
09 Ground Data System	32.5	24.5	24.5	24.5	24.5	-8.0	-24%
Total Ops w/o Reserves	188.2	185.7	185.7	185.7	185.7	-2.5	-1%
Operations Reserves (25%)	44.9	44.3	44.3	44.3	44.3	-0.6	-1%
Total E-F Operations Cost	233.1	230.0	230.0	230.0	230.0	-3.1	-1%
08 Launch System	200.0	200.0	200.0	200.0	200.0	0.0	0%
Total Cost	1,538.1	1,497.7	1,517.3	1,414.2	1,476.4	-61.7	-4%

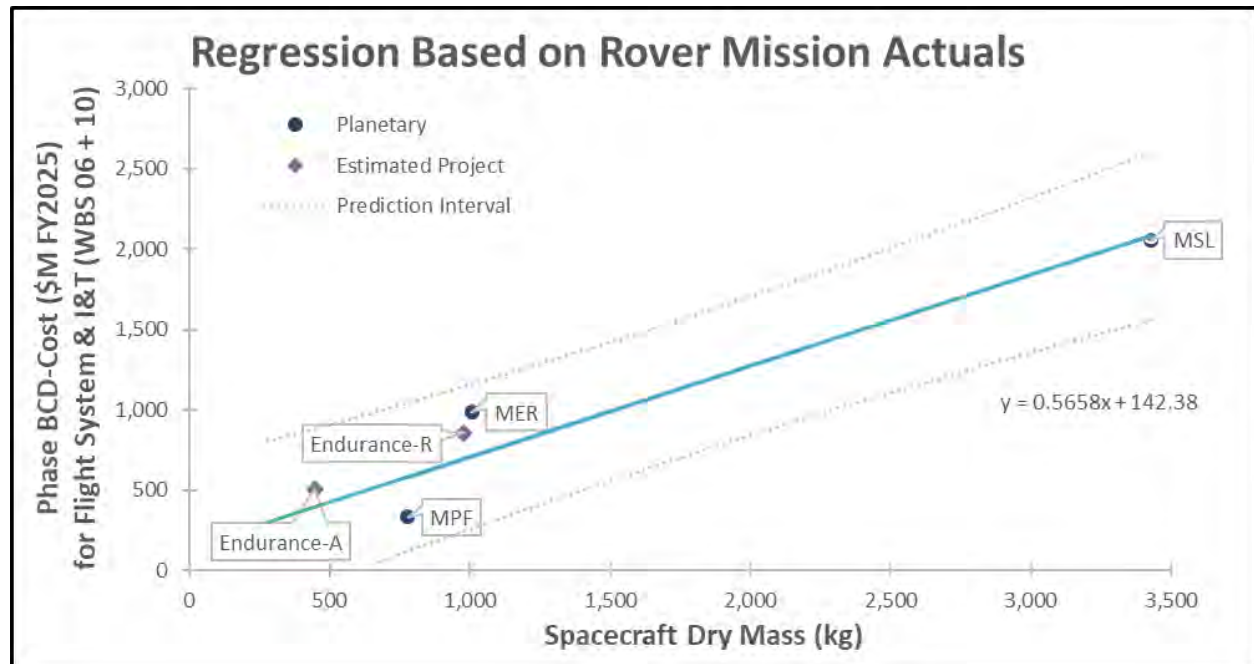


Figure M-1. \$/Kg Comparison of Endurance to Mars Rover Missions for WBS 06 and 10.

M.1 WRAP FACTORS

Wrap factors were developed from historical costs of selected JPL missions. The mission set includes:

- Mars Pathfinder, MER, and MSL – Rover missions developed in-house at JPL
- Stardust, Genesis, Deep Impact, Dawn, GRAIL, Phoenix, Insight – Discovery class missions managed by JPL
- Juno – New Frontiers class mission managed by JPL

Historical cost data comes from the NASA Cost Analysis Data Requirement (CADRe) for Launch or End of Mission. Wrap factors for WBS 04, 07, and 09 are computed as a percentage of total Phase B/C/D cost without LV or Reserves. Figure M-2 shows the calculated historical wrap factor for each WBS that was applied to the SEER and TruePlanning models which do not estimate these costs.

M.2 SEER

SEER (version 7.4.13) is a component level cost tool that is recognized for its built-in Knowledge Bases (KBases) that pre-populate most inputs with appropriate industry values and optional calibration adjustments. In particular, the Application and Acquisition Category KBases are important for defining the hardware component, the level of maturity, and how it will be acquired. As an additional aid for using the tool, a companion document, SEER-H Space Guidance (Rev 3.1), is available to the user. It presents a standardize approach for setting up an estimate and provides recommended setting for important inputs.

Table M-3 lists the Application and Acquisition Category KBase selections for each hardware component in the rover MEL that is applicable to both options. Table M-4 lists the Application and Acquisition Category KBase selections for each hardware component in the ERV MEL that is applicable to Endurance-R only. Table M-5 lists user-entered data that override the KBase default values. Software costs were added using a wrap factor of 10% on the hardware cost, which is based on historical data.

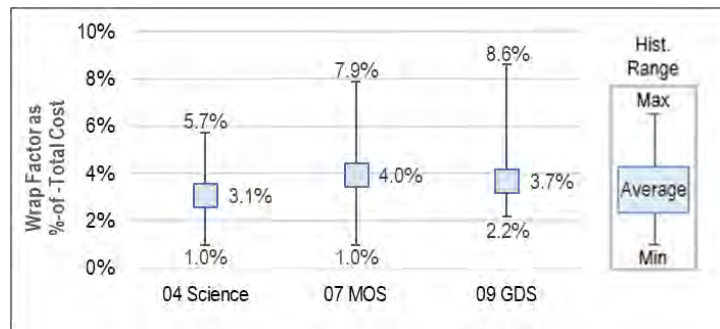


Figure M-2. Historical wrap factors for WBS 04, 07, and 09.

Table M-3. Application and Acquisition Category KBase Settings for Rover System that is Common to Both Options.

Hardware Element	Application	Acquisition Category
Science Payload	Space System - Payload/Instrument, Science	
ARMAS	Photon Detector - Space	Buy and Integrate
Magnetometer	Field Sensor - Space	Buy and Integrate
TriCam	Electro-Optical Sensor	Buy and Integrate
GRNS	Field Sensor - Space	Buy and Integrate
Point Spectrometer	Electro-Optical Sensor	Buy and Integrate
HLI	Electro-Optical Sensor	Buy and Integrate
APXS + Cryocooler	Photon Detector - Space	Buy and Integrate
Electrostatic Analyzer	Field Sensor - Space	Buy and Integrate
Laser Corner Reflector	Laser - Space	Buy and Integrate
Flight System	Spacecraft Bus	
Lunar Rover	Spacecraft Bus	
C&DH Subsystem		
Sabertooth based Compute Element	Processor - Central Processing Unit	Make
Instrument Interface	Interconnect - Data Bus	Make

Table M-3. Application and Acquisition Category KBase Settings for Rover System that is Common to Both Options.

Hardware Element	Application	Acquisition Category
Motor Control	Controller - Electro-Mechanical Control	Modification - Major
Telecom Subsystem		
UST-Lite	Transponder - S-Band, Deep Space	Modification - Average
5-W SSPA	Power Amplifier - Solid State (SSPA)	Modification - Average
Coax Transfer Switches	Radio Frequency (RF) Components - Space	Make
S-band Diplexer	RF Components - Space	Make
S-band Omnidirectional LGA	Antenna - Conical/Horn, Space	Modification - Major
S-band HGA & Feed (0.75m diameter)	Antenna - Dish, Space	Modification - Major
S-band HGA Gimbal	Gimbal Mechanism	Modification - Major
Coax Cabling	Cabling	Make
GN&C Subsystem		
LN 200 IMU	Inertial Measurement Unit - Space	Space Procure To Print
Sun Sensor	Sun Sensor - Space	Space Procure To Print
Front Nav Cameras (EECAM)		
Detector	Area Si charge-coupled device (CCD)	Modification - Minor
Optics	!-Optical General	Modification - Minor
Back Nav Cameras (EECAM)		
Detector	Area Si CCD	Modification - Minor
Optics	!-Optical General	Modification - Minor
Illuminators	!-Optical General	Modification - Average
Power Subsystem		
RTG	Auxiliary Power Unit	Buy and Integrate
Battery	Battery - Lithium, Space	Modification - Major
Placeholder SBIS/ PBC - Shunt & Battery I/F / Power Bus Control	Power Supply	Modification - Major
Load and Heater Switching	Controller - Process Control	Modification - Major
Placeholder Pyro Drivers	Controller - Electro-Mechanical Control	Modification - Major
Thermal Control Subsystem		
Avionics radiator	Radiator/Heat Pipe - Space	Make
Thermal switch	Thermal Control - Active	Make
Thermal strap	Thermal Control - Passive	Make
MLI	Thermal Control - MLI/Paint/Coating	Make
CCHPS	Radiator/Heat Pipe - Space	Make
Platinum Resistance Thermometer (PRT) temperature sensors	Thermal Control - Active	Make
Mechanical thermostats	Thermal Control - Active	Make
Heaters	Thermal Control - Active	Make
Structures & Mechanisms Subsystem		
Structures		
Web Chassis	Spacecraft Structure	Make
Chassis Bottom Platform	Spacecraft Structure	Make
Chassis Bottom Cover	Spacecraft Structure	Make
Wheel Fender	Spacecraft Structure	Make
Spoiler	Spacecraft Structure	Make
Spoiler Brackets	Spacecraft Structure	Make
Magnetometer Boom	Spacecraft Structure	Make
Mag. Bracket	Spacecraft Structure	Make
Mag Restraint	Spacecraft Structure	Make
Antenna Mast	Spacecraft Structure	Make
Camera Mast Bracket	Spacecraft Structure	Make
Robotic Arm Bracket	Spacecraft Structure	Make
Radiator Shield	Thermal Control - MLI/Paint/Coating	Make

Table M-3. Application and Acquisition Category KBase Settings for Rover System that is Common to Both Options.

Hardware Element	Application	Acquisition Category
Fasteners	!-Structural General	Make
Ballast	!-Structural General	Modification - Major
Rover Launch Restraint	Separation Mechanism	Modification - Major
Mobility		
Drive Actuators	Precision Mechanism	Make
Steer Actuators	Precision Mechanism	Make
Drive Actuator housing	Spacecraft Structure	Make
Steer Actuators Housing	Spacecraft Structure	Make
Wheels (+ Tires)	Spacecraft Structure	Make
Wheel Structure	Spacecraft Structure	Make
Rocker Booms	Spacecraft Structure	Make
Rocker Articulation Wheel	Spacecraft Structure	Make
Rocker Articulation Boom Fitting	Spacecraft Structure	Make
Rocker Lever	Spacecraft Structure	Make
Rocker Hub	Spacecraft Structure	Make
Dif Rotator	Spacecraft Structure	Make
Dif Lever	Spacecraft Structure	Make
Launch Locks / wheel-steer restraints / rocker restraints	Separation Mechanism	Make
Arm		
Arm	Precision Mechanism	Make
End Effector (including gripper mechanism)	Precision Mechanism	Make
Mast		
Camera Mast	Spacecraft Structure	Make
Camera Head Bracket	Spacecraft Structure	Make
Camera Mast Head	Spacecraft Structure	Make
Camera Mast Illuminator Bracket	Spacecraft Structure	Make
Sample Handling		
Sampling Handling Mechanism	Precision Mechanism	Make
Sample Container Release Mechanism	Separation Mechanism	Make
Vertical Pizza Sample Container	Precision Mechanism	Make
Harnesses		
Harnessing	Harness - Space	Make

Table M-4. Application and Acquisition Category KBase Settings for ERV Flight System Unique to Endurance-R.

Hardware Element	Application	Acquisition Category
Science Payload	Space System - Payload/Instrument, Science	
Cameras (EECAM)		
Detector	Area Si CCD	Modification - Minor
Optics	!-Optical General	Modification - Minor
Flight System		
Earth Return Vehicle	Space System - Unmanned Mission, Science	
GN&C Subsystem		
Sun Sensors	Sun Sensor - Space	Space Procure To Print
Star Trackers	Star Tracker - Complex, Space	Space Procure To Print
IMUs	Inertial Measurement Unit - Space	Space Procure To Print
C&DH Subsystem		
Processor: Sphinx	Processor - Central Processing Unit	Modification - Major
Custom_Board: Sphinx Interface	Interconnect - Data Bus	Modification - Major
Custom_Board: Motor Control	Controller - Electro-Mechanical Control	Modification - Major
Analog_I_F: physically in Power but bookkept in CDS	Interconnect - Data Bus	Modification - Major
Power: CEPCU	Power Supply	Modification - Major

Table M-4. Application and Acquisition Category KBase Settings for ERV Flight System Unique to Endurance-R.

Hardware Element	Application	Acquisition Category
Chassis: CDH chassis (4 slot)	Electronic Enclosure - Space	Modification - Major
Power Subsystem		
Solar Array, GaAs TJ Rigid, Non Deployable, 1.55m ²	Solar Array - Deployable, Earth Space	Modification - Major
500 W Array/Battery/Bus Interface - Fault Tolerant	Power Supply	Modification - Major
Battery, Secondary Battery Li-ION	Battery - Lithium, Space	Modification - Major
Autonomous Adaptive Power Ctrl - Fault Tolerant 3x redundancy	Power Supply	Modification - Major
Switch Function - Embodies 16 Distributed Switch Module Gumsticks High and Low Side	Controller - Process Control	Modification - Major
Htr Ctrl Function - Embodies 16 Distributed Linear Htr Controller	Controller - Process Control	Modification - Major
Prop Latch Valve Driver Function - Embodies 16 Distributed Latch Valve Drivers	Controller - Electro-Mechanical Control	Modification - Major
Prop Thruster Driver Function - Embodies 16 Distributed Thruster Drivers	Controller - Electro-Mechanical Control	Modification - Major
250 W Power Converter	Power Supply	Modification - Major
Propulsion Subsystem		
Gas Service Valve	Propulsion Components - Single Mode, Space	Make
HP Latch Valve	Propulsion Components - Single Mode, Space	Make
Solenoid Valve	Propulsion Components - Single Mode, Space	Make
HP Transducer	Propulsion Components - Single Mode, Space	Make
Gas Filter	Propulsion Components - Single Mode, Space	Make
NC Pyro Valve	Propulsion Components - Single Mode, Space	Make
Temp. Sensor	Thermal Control - Active	Make
Liq. Service Valve	Propulsion Components - Single Mode, Space	Make
Test Service Valve	Propulsion Components - Single Mode, Space	Make
Low Pressure (LP) Transducer	Propulsion Components - Single Mode, Space	Make
Liq. Filter	Propulsion Components - Single Mode, Space	Make
LP Latch Valve	Propulsion Components - Single Mode, Space	Make
Normally Closed (NC) Pyro Valve	Propulsion Components - Single Mode, Space	Make
Mass Flow Control	Propulsion Components - Single Mode, Space	Make
Temp. Sensor	Thermal Control - Active	Make
Lines, Fittings, Misc.	Propulsion Components - Single Mode, Space	Make
DM Monoprop Thrusters 1	Propulsion Thruster - Single Mode, Space	Modification - Average
DM Monoprop Thrusters 2	Propulsion Thruster - Single Mode, Space	Modification - Average
Biprop Main Engine	Propulsion System - Liquid Rocket	Modification - Average
Fuel Pressurant Tank	Propulsion Tankage - Single Mode, Space	Modification - Major
Ox Pressurant Tank	Propulsion Tankage - Single Mode, Space	Modification - Major
Fuel Tanks	Propulsion Tankage - Single Mode, Space	Modification - Major
Oxidizer Tanks	Propulsion Tankage - Single Mode, Space	Modification - Major
Mechanical Subsystem		
Primary Structure	Spacecraft Structure	Make
Secondary Structure	Spacecraft Structure	Make
Tertiary Structure	Spacecraft Structure	Make
Integration Hardware: Fasteners, etc.	!-Structural General	Make
Power Support Structure	Spacecraft Structure	Make
Telecom Support Structure	Spacecraft Structure	Make
Harnesses		
Harness	Harness - Space	Make
Telecom Subsystem		
S-band LGA, SMAP Helix	Antenna - Conical/Horn, Space	Modification - Major
UST-Lite Single RX, Single TX	Transponder - S-Band, Deep Space	Modification - Average
S-band SSPA, RF=11W	Power Amplifier - Solid State (SSPA)	Modification - Major

Table M-4. Application and Acquisition Category KBase Settings for ERV Flight System Unique to Endurance-R.

Hardware Element	Application	Acquisition Category
Coax Transfer Switch (CXS)	RF Components - Space	Make
S-Band Diplexer	RF Components - Space	Make
Coax Cable, flex (190)	Cabling	Make
Thermal Subsystem		
Multilayer Insulation (MLI)	Thermal Control - MLI/Paint/Coating	Make
General Thermal Surfaces	Thermal Control - Passive	Make
Paints/Films	Thermal Control - MLI/Paint/Coating	Make
General Conduction Control	Thermal Control - Passive	Make
Catalogue Heaters	Thermal Control - Active	Make
Propulsion Tank Heaters	Thermal Control - Active	Make
Propulsion Line Heaters	Thermal Control - Active	Make
PRT's	Thermal Control - Active	Make
Mechanical Thermostats	Thermal Control - Active	Make
Launchpad & Transfer Arm		
Transfer Arm Structure	Spacecraft Bus	
Launch Platform	Primary Structure - Complex	Make
ERV Support Structure	Precision Mechanism	Make
Transfer Arm Actuator	!-Mechanism General	Make
ERV Support Launch Locks	Separation Mechanism	Make
Harness	Harness - Space	Make
Sample Return Capsule		
Sample Return Capsule (SRC) without samples	Spacecraft Bus	
SRC Spin-up device - Bus side	Primary Structure - Complex	Make
SRC Release Device - Bus Side	Precision Mechanism	Make
SRC Mounting	Separation Mechanism	Make
Sample Canister without Samples	Primary Structure	Make
Sample Canister without Samples	Primary Structure - Complex	Make

Table M-5. User-specified inputs for SEER.

Input Parameter	Least	Likely	Most	Notes
<i>Global Settings applied across the entire SEER Estimate for both options</i>				
Weight (kg)	CBE	CBE + contingency	1.3 * (CBE + Contingency)	SEER-H Space Guidance applied to all Mechanical elements.
Prototype Quantity		0.65 per unit		SEER Rule of Thumb for an engineering model (EM). It was assumed all subsystems would build an EM.
Certification Level	Hi	Hi	Hi+	SEER-H Space Guidance for a Class B mission applied to all elements.
Reliability Standard	Hi+	VHi-	VHi-	SEER-H Space Guidance for a Class B mission applied to all EOS elements.
<i>Rover Specific Hardware Settings applicable to both options</i>				
<i>Sabertooth based Compute Element - Total PCBs</i>	5	6	7	Assume ~1 kg per board
<i>Motor Control in C&DH Subsystem - Total PCBs</i>	7	7	7	Each motor control box contains 7 motor control cards
<i>Camera Detectors - Array Size Rows</i>	5,120	5,120	5,120	Based on EECAM for Mars2020.
<i>Camera Detectors - Array Size Columns</i>	3,840	3,840	3,840	Based on EECAM for Mars2020.
<i>Camera Detectors - Pitch</i>	6	6	6	Based on EECAM for Mars2020.
<i>Hardware Elements using the "Spacecraft Structure" Application KBase - Complexity of Form</i>	VHi	VHi+	VHi+	Adjusted to reflect 9 instruments on the rover. Based on the SEER-H Space Guidance for 8 instruments and then increased the Likely value to VHi+ to account for 9 instruments instead.

Table M-5. User-specified inputs for SEER.

Input Parameter	Least	Likely	Most	Notes
<i>ERV Specific Hardware Settings applicable to the Endurance-R option</i>				
<i>Processor: Sphinx - Total PCBs</i>	1	1	1	Single custom board
<i>Custom_Board: Sphinx Interface - Total PCBs</i>	1	1	1	Single custom board
<i>Custom_Board: Motor Control - Total PCBs</i>	1	1	1	Single custom board
<i>Analog_I_F: physically in Power but bookkept in CDS - Total PCBs</i>	1	1	1	Single custom board
<i>Hardware Elements using the "Spacecraft Structure" Application KBase - Complexity of Form</i>	VHi	VHi+	VHi+	SEER-H Space Guidance for 3 instruments to account for the 2 Cameras plus the SRC with samples

M.3 TRUEPLANNING

TruePlanning (version 16.1 SR1) was used two ways to develop an estimate. One method was at the subsystem level using MSL as an analogy to calibrate the model and the other was at the component level using the Space Missions catalog.

For the calibrated estimate., the MSL Launch CADRe was the source for the cost and mass data. A subsystem level estimate is developed with the mass information. Then the built-in calibration tool is used to solve for the value of Manufacturing Complexity for Structure and Manufacturing Complexity for Electronics with the known cost as the target. With the calibrated complexity factors in hand, these settings can now be applied to Endurance by simply replacing and entering the mission’s subsystem mass.

For the second estimate, Endurance was modeled using the Space Missions Model with the Component Type Calculator. Inputs for the Component Type Calculator include Subsystem Type, Component Type, Platform, Parts Class, Unit Mass, Quantities, Heritage for Structure and Electronics, Advanced Technology Development, and a few other element unique parameters. The calculator uses these inputs to define values for Operating Specification, Weight of Structure, Weight of Electronics, Volume, Manufacturing Complexity for Structure, Manufacturing Complexity for Electronics, Percent New for Structure and Electronics, and Engineering Complexity. Software costs are included as part of the hardware estimate, so it does not need to be modeled. The model inputs used for each component in the MEL is provided in Table M-6 and Table M-7. For Platform and Parts Type, the same setting of “Planetary” and “S1” was used for all elements.

For the Payload System cost object, data was entered for the following inputs.

- Number of Production Units – set to 1
- Number of Prototypes – set to 1 for the assumption that there will at least one EM or prototype built for every instrument.
- Payload – set to Yes
- Mission Class – set to Class A/B
- Likewise for the Rover, ERV, and SRC System cost objects, the data entered was:
- Number of Production Units – set to 1
- Number of Prototypes – set to 1 for the assumption that there will at least one EM or prototype built for every instrument.
- Payload – set to No
- Mission Class – set to Class A/B

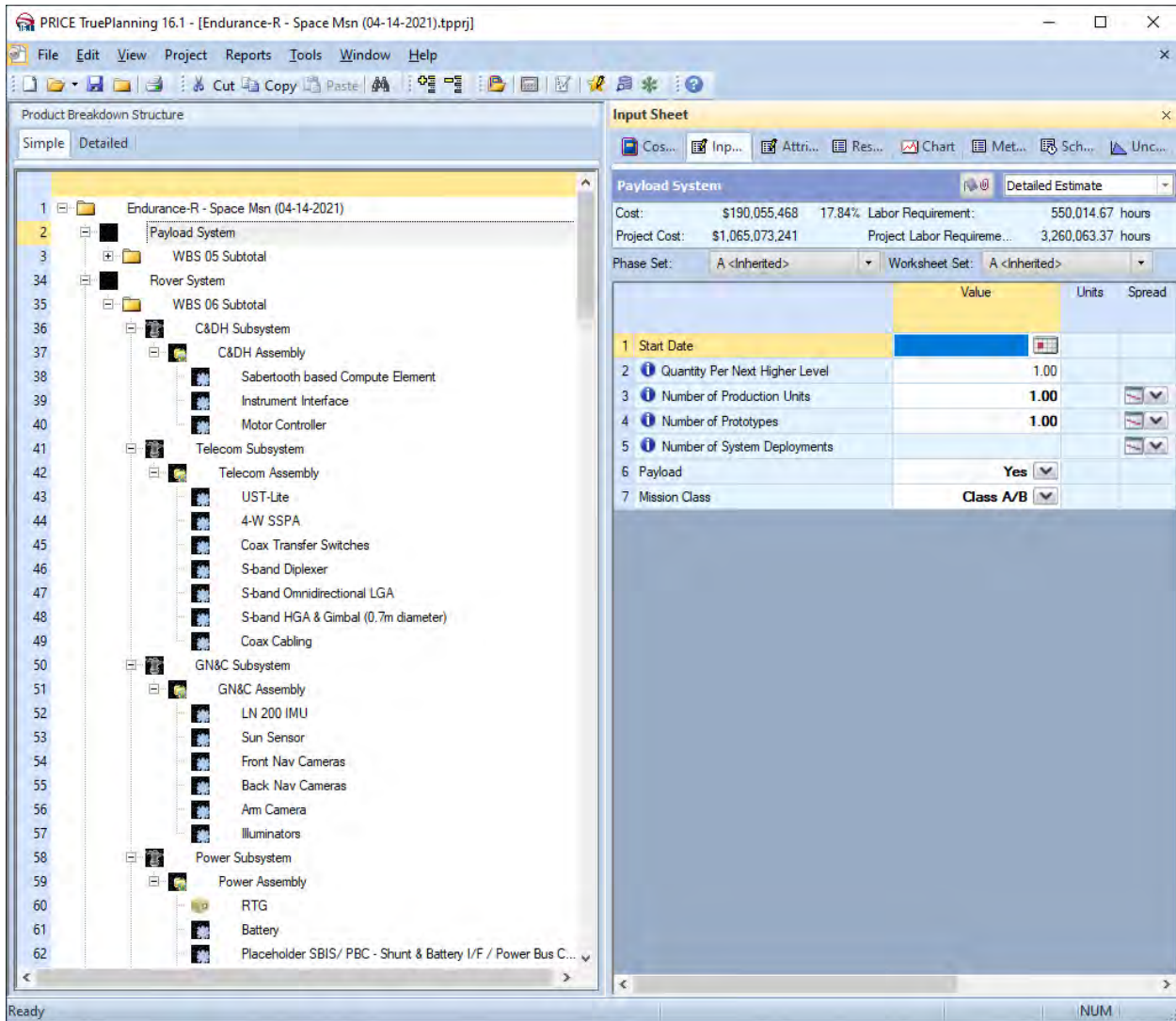


Figure M-3. TruePlanning Structure for Space Missions Model.

Table M-6. Inputs for Space Missions Model Component Type Calculator that is Common to Both Options.

Hardware Element	Subsystem Type	Component Type	Unit Mass (kg)	Heritage	Additional Input
Science Payload					Payload set to Yes; Mission Class set to A/B
ARMAS	Sensor Systems	Sensors/Detectors	1.1	Minimal Mod	Type set to Simple
Magnetometer	Sensor Systems	Magnetometer	0.55	Minimal Mod	Type set to Advanced
TriCam	Sensor Systems	Charge Coupled Device Detectors	6.49	Minimal Mod	Type set to Silicon-based Charge Coupled Device
GRNS	Sensor Systems	Gamma Sensor	3.3	Minimal Mod	Type set to Standard
Point Spectrometer	Sensor Systems	Sensors/Detectors	2.6	Minimal Mod	Type set to Nominal
HLI	Sensor Systems	Charge Coupled Device Detectors	0.66	Minimal Mod	Type set to Silicon-based Charge Coupled Device
APXS + Cryocooler	Sensor Systems	Neutron Sensor	2.53	Minimal Mod	Type set to Standard
Electrostatic Analyzer	Sensor Systems	Electro-Static Analyzer Sensor	4.62	Minimal Mod	Type set to Simple
Laser Corner Reflector	N/A	N/A	0.55	Minimal Mod	Used the Space Laser cost object
Lunar Rover					Payload set to No; Mission Class set to A/B

Table M-6. Inputs for Space Missions Model Component Type Calculator that is Common to Both Options.

Hardware Element	Subsystem Type	Component Type	Unit Mass (kg)	Heritage	Additional Input
C&DH Subsystem	Command and Data Handling				
Sabertooth based Compute Element	Command and Data Handling	Command/Data Processing	7.458	New	Type set to Most Microprocessors, RAD6000
Instrument Interface	Command and Data Handling	Command/Data Processing	1.7515	New	Type set to Simple or non-Programmable
Motor Control	Command and Data Handling	Command/Data Processing	2.2035	Major Mod	Type set to Advanced Devices
Telecom Subsystem	Communications				
UST-Lite	Communications	Transponder	1.25	Minimal Mod	Frequency Band set to S - band
5-W SSPA	Communications	Amplifier	1.725	Major Mod	Frequency Band set to Most S and X-Band Solid State Power Amplifiers
Coax Transfer Switches	Communications	Miscellaneous RF Electronics	0.1495	Major Mod	Frequency Band set to S - band
S-band Diplexer	Communications	Miscellaneous RF Electronics	0.1725	Major Mod	Frequency Band set to S - band
S-band Omnidirectional LGA	Communications	Medium Gain Antenna/Low Gain Antenna	0.33	Major Mod	Frequency Band set to S - band; Antenna set to Array
S-band HGA & Feed (0.75m diameter)	Communications	High Gain Antenna	8.47	Major Mod	Frequency Band set to S - band
S-band HGA Gimbal	Guidance, Navigation and Control	Gimbals	8.58	Major Mod	Material set to Composite
Coax Cabling	Communications	Waveguides - Comm Cabling	0.819	New	Frequency Band set to S - band
GN&C Subsystem	Guidance, Navigation and Control				
LN 200 IMU	Guidance, Navigation and Control	IMU-Gyro	0.814	Minimal Mod	
Sun Sensor	Guidance, Navigation and Control	Sun Sensor	0.1463	Minimal Mod	Type set to Standard
Front Nav Cameras (EECAM)	Sensor Systems	Charge Coupled Device Detectors	0.6325	Minimal Mod	Type set to Advanced Visible Detector or UV/IR Detector
Back Nav Cameras (EECAM)	Sensor Systems	Charge Coupled Device Detectors	0.6325	Minimal Mod	Type set to Advanced Visible Detector or UV/IR Detector
Arm Camera	Sensor Systems	Charge Coupled Device Detectors	0.638	Minimal Mod	Type set to Advanced Visible Detector or UV/IR Detector
Illuminators	Sensor Systems	Photodiode	0.12	Major Mod	Type set to Advanced
Power Subsystem	Power				
RTG	Power	N/A	72.8	N/A	Used the Purchased Good cost object; Unit Cost set to \$70,000,000; Component Type set to Hardware; Component Integration Size set to Midsize Components or Assemblies; Component Complexity set to High; External Integration Complexity set to 4.00
Battery	Power	Batteries	5.07	Major Mod	Chemistry set to Li-ion
Shunt & Battery I/F / Power Bus Controller	Power	Power Management and Distribution	1.43	Major Mod	Type set to Nominal Space based Device
Load and Heater Switching	Power	Power Management and Distribution	2.0475	Major Mod	Type set to Complex Device with Advanced Switching
Placeholder Pyro Drivers	Power	Pyrotechnics	1.05	Major Mod	Type set to Standard
Thermal Control Subsystem	Thermal Control				
Avionics radiator	Thermal Control	Radiators/Louvers	4.875	New	Material set to Aluminum
Thermal switch	Thermal Control	Heaters, RHUs, Thermostats	0.208	New	Material set to Composite
Thermal strap	Thermal Control	Heaters, RHUs, Thermostats	0.26	New	Material set to Composite

Table M-6. Inputs for Space Missions Model Component Type Calculator that is Common to Both Options.

Hardware Element	Subsystem Type	Component Type	Unit Mass (kg)	Heritage	Additional Input
MLI	Thermal Control	MLI, Paints, Coatings	5.85	New	
CCHPs	Thermal Control	Heat Pipes	0.195	New	Material set to Aluminum
PRT temperature sensors	Thermal Control	Heaters, RHUs, Thermostats	0.0013	New	Material set to Stainless Steel
Mechanical thermostats	Thermal Control	Heaters, RHUs, Thermostats	0.0325	New	Material set to Stainless Steel
Heaters	Thermal Control	Heaters, RHUs, Thermostats	0.065	New	Material set to Stainless Steel
Structures & Mechanisms Subsystem	Structure and Mechanisms				
Structures					
Web Chassis	Structure and Mechanisms	Primary Structure	48.0	New	Material set to Aluminum; Advanced Technology Development set to New
Chassis Bottom Platform	Structure and Mechanisms	Primary Structure	2.4	New	Material set to Aluminum; Advanced Technology Development set to New
Chassis Bottom Cover	Structure and Mechanisms	Primary Structure	3.6	New	Material set to Aluminum; Advanced Technology Development set to New
Wheel Fender	Structure and Mechanisms	Primary Structure	0.6	New	Material set to Aluminum; Advanced Technology Development set to New
Spoiler	Structure and Mechanisms	Primary Structure	3.48	New	Material set to Aluminum; Advanced Technology Development set to New
Spoiler Brackets	Structure and Mechanisms	Secondary Structure	0.12	New	Material set to Aluminum
Magnetometer Boom	Structure and Mechanisms	Primary Structure	0.384	New	Material set to Aluminum; Advanced Technology Development set to New
Mag. Bracket	Structure and Mechanisms	Secondary Structure	1.08	New	Material set to Aluminum
Mag Restraint	Structure and Mechanisms	Mechanism	0.24	New	Type set to Standard
Antenna Mast	Structure and Mechanisms	Primary Structure	1.44	New	Material set to Aluminum; Advanced Technology Development set to New
Camera Mast Bracket	Structure and Mechanisms	Secondary Structure	0.72	New	Material set to Aluminum
Robotic Arm Bracket	Structure and Mechanisms	Secondary Structure	2.04	New	Material set to Aluminum
Radiator Shield	Structure and Mechanisms	Shielding	1.08	New	Material set to Aluminum
Fasteners	Structure and Mechanisms	Secondary Structure	5.46	New	Material set to Aluminum
Ballast	Structure and Mechanisms	Secondary Structure	10.79	New	Material set to Aluminum
Rover Launch Restraint	Structure and Mechanisms	Mechanism	3.9	New	Type set to Standard
Mobility					
Drive Actuators	Structure and Mechanisms	Motor-Actuator	3.3125	New	Type set to Advanced; Advanced Technology Development set to New
Steer Actuators	Structure and Mechanisms	Motor-Actuator	3.3125	New	Type set to Advanced; Advanced Technology Development set to New
Drive Actuator housing	Structure and Mechanisms	Primary Structure	1.8	New	Material set to Aluminum; Advanced Technology Development set to New

Table M-6. Inputs for Space Missions Model Component Type Calculator that is Common to Both Options.

Hardware Element	Subsystem Type	Component Type	Unit Mass (kg)	Heritage	Additional Input
Steer Actuators Housing	Structure and Mechanisms	Primary Structure	1.8	New	Material set to Aluminum; Advanced Technology Development set to New
Wheels (+ Tires)	Structure and Mechanisms	Mechanisms	6.84	New	Type set to Very Advanced; Advanced Technology Development set to New
Wheel Structure	Structure and Mechanisms	Primary Structure	3	New	Material set to Aluminum; Advanced Technology Development set to New
Rocker Booms	Structure and Mechanisms	Primary Structure	1.2	New	Material set to Aluminum; Advanced Technology Development set to New
Rocker Articulation Wheel	Structure and Mechanisms	Primary Structure	8.4	New	Material set to Aluminum; Advanced Technology Development set to New
Rocker Articulation Boom Fitting	Structure and Mechanisms	Secondary Structure	3.0	New	Material set to Aluminum; Advanced Technology Development set to New
Rocker Lever	Structure and Mechanisms	Primary Structure	2.04	New	Material set to Aluminum; Advanced Technology Development set to New
Rocker Hub	Structure and Mechanisms	Primary Structure	4.8	New	Material set to Aluminum; Advanced Technology Development set to New
Dif Rotator	Structure and Mechanisms	Mechanisms	2.916	New	Type set to Advanced; Advanced Technology Development set to New
Dif Lever	Structure and Mechanisms	Mechanisms	0.312	New	Type set to Advanced; Advanced Technology Development set to New
Launch Locks / wheel-steer restraints / rocker restraints	Structure and Mechanisms	Mechanisms	0.6	New	Type set to Standard; Advanced Technology Development set to New
Arm					
Arm	Robotic Arm	Robotic Arm - Joint-Actuator	36.0	New	Type set to Very Advanced; Advanced Technology Development set to New
End Effector	Structure and Mechanisms	Mechanisms	9.6	New	Type set to Very Advanced; Advanced Technology Development set to New
Mast					
Camera Mast	Structure and Mechanisms	Primary Structure	0.3	New	Material set to Composite; Advanced Technology Development set to New
Camera Head Bracket	Structure and Mechanisms	Secondary Structure	1.68	New	Material set to Aluminum
Camera Mast Head	Structure and Mechanisms	Primary Structure	4.2	New	Material set to Aluminum; Advanced Technology Development set to New
Camera Mast Illuminator Bracket	Structure and Mechanisms	Secondary Structure	0.1524	New	Material set to Aluminum
Sampling Handling					
Sampling Handling Mechanism	Structure and Mechanisms	Mechanisms	6.5	New	Type set to Very Advanced; Advanced Technology Development set to New
Sample Container Release Mechanism	Structure and Mechanisms	Mechanisms	0.0275	New	Type set to Advanced; Advanced Technology Development set to New
Vertical Pizza Sample Container	Structure and Mechanisms	Primary Structure	7.28	New	Material set to Composite; Advanced Technology Development set to New
Harness Subsystem	Power				

Table M-6. Inputs for Space Missions Model Component Type Calculator that is Common to Both Options.

Hardware Element	Subsystem Type	Component Type	Unit Mass (kg)	Heritage	Additional Input
Harnessing	Power	Power Harness/Cabling	26.52	New	

Table M-7. Inputs for Space Missions Model Component Type Calculator that applies to ERV on Endurance-R.

Hardware Element	Subsystem Type	Component Type	Unit Mass (kg)	Heritage	Additional Input
Science Payload					Payload set to Yes; Mission Class set to A/B
Cameras	Sensor Systems	Charge Coupled Device Detectors	0.46	Minimal Mod	Type set to Silicon- based Charge Coupled Device
Earth Return Vehicle					Payload set to No; Mission Class set to A/B
GN&C Subsystem	Guidance, Navigation and Control				
Sun Sensor	Guidance, Navigation and Control	Sun Sensor	0.143	Minimal Mod	Type set to Standard
Star Trackers	Guidance, Navigation and Control	Star Tracker	3.63	Minimal Mod	Type set to Standard
IMUs	Guidance, Navigation and Control	IMU-Gyro	4.4	Minimal Mod	
C&DH Subsystem	Command and Data Handling				
Processor: Sphinx	Command and Data Handling	Command/Data Processing	0.1019	Major Mod	Type set to Most Microprocessors, RAD6000
Custom_Board: Sphinx Interface	Command and Data Handling	Command/Data Processing	0.1067	Major Mod	Type set to Advanced Devices
Custom_Board: Motor Control	Command and Data Handling	Command/Data Processing	0.1067	Major Mod	Type set to Advanced Devices
Analog_I_F: physically in Power but bookkept in CDS	Command and Data Handling	Command/Data Processing	0.1067	Major Mod	Type set to Advanced Devices
Power: CEPUCU	Power	Power Management and Distribution	1.2075	Major Mod	Type set to Complex Device with Advanced Switching
Chassis: CDH chassis (4 slot)	Structure and Mechanisms	Electronics Box	2.47	Major Mod	Material set to Aluminum
Power Subsystem	Power				
Solar Array, GaAs TJ Rigid, Non Deployable, 1.55m ²	Power	Solar Cells/Electrical	3.266	Major Mod	Type set to Multi- Junction and High Efficiency
500 W Array/Battery/Bus Interface - Fault Tolerant	Power	Power Management and Distribution	4.8012	Major Mod	Type set to Nominal Space based Device
Battery, Secondary Battery Li-ION	Power	Batteries	5.7323	Major Mod	Chemistry set to Li-ion
Autonomous Adaptive Power Ctrl - Fault Tolerant 3x redundancy	Power	Power Management and Distribution	1.6731	Major Mod	Type set to Nominal Space based Device
Switch Function - Embodies 16 Distributed Switch Module Gumsticks High and Low Side	Power	Power Management and Distribution	2.145	Major Mod	Type set to Complex Device with Advanced Switching
Htr Ctrl Function - Embodies 16 Distributed Linear Htr Controller	Command and Data Handling	Command/Data Processing	2.145	Major Mod	Type set to Simple or non-Programmable
Prop Latch Valve Driver Function - Embodies 16 Distributed Latch Valve Drivers	Command and Data Handling	Command/Data Processing	2.145	Major Mod	Type set to Simple or non-Programmable
Prop Thruster Driver Function - Embodies 16 Distributed Thruster Drivers	Command and Data Handling	Command/Data Processing	2.145	Major Mod	Type set to Simple or non-Programmable

Table M-7. Inputs for Space Missions Model Component Type Calculator that applies to ERV on Endurance-R.

Hardware Element	Subsystem Type	Component Type	Unit Mass (kg)	Heritage	Additional Input
250 W Power Converter	Power	Power Management and Distribution	0.3575	Major Mod	Type set to Nominal Space based Device
Propulsion Subsystem	Propulsion				
Gas Service Valve	Propulsion	Propulsion-Lines/Valves/Fittings	0.2346	New	Material set to Aluminum
HP Latch Valve	Propulsion	Propulsion-Lines/Valves/Fittings	0.357	New	Material set to Aluminum
Solenoid Valve	Propulsion	Propulsion-Lines/Valves/Fittings	0.3468	New	Material set to Aluminum
HP Transducer	Propulsion	Pressure Regulator-Transducer	0.2754	New	Type set to Standard
Gas Filter	Propulsion	Propulsion-Lines/Valves/Fittings	0.1122	New	Material set to Aluminum
NC Pyro Valve	Propulsion	Propulsion-Lines/Valves/Fittings	0.1836	New	Material set to Aluminum
Temp. Sensor	Thermal Control	Heaters, RHUs, Thermostats	0.0102	New	Material set to Stainless Steel
Liq. Service Valve	Propulsion	Propulsion-Lines/Valves/Fittings	0.2856	New	Material set to Aluminum
Test Service Valve	Propulsion	Propulsion-Lines/Valves/Fittings	0.2346	New	Material set to Aluminum
LP Transducer	Propulsion	Pressure Regulator-Transducer	0.2754	New	Type set to Standard
Liq. Filter	Propulsion	Propulsion-Lines/Valves/Fittings	0.459	New	Material set to Aluminum
LP Latch Valve	Propulsion	Propulsion-Lines/Valves/Fittings	0.357	New	Material set to Aluminum
NC Pyro Valve	Propulsion	Propulsion-Lines/Valves/Fittings	0.1836	New	Material set to Aluminum
Mass Flow Control	Propulsion	Propulsion-Lines/Valves/Fittings	0.0306	New	Material set to Aluminum
Temp. Sensor	Thermal Control	Heaters, RHUs, Thermostats	0.0102	New	Material set to Stainless Steel
Lines, Fittings, Misc.	Propulsion	Propulsion-Lines/Valves/Fittings	3.75	New	Material set to Aluminum
DM Monoprop Thrusters 1	Propulsion	Thrusters	1.0605	Major Mod	Material set to Stainless Steel
DM Monoprop Thrusters 2	Propulsion	Thrusters	0.3465	Major Mod	Material set to Stainless Steel
Biprop Main Engine	Propulsion	Thrusters	7.665	Major Mod	Material set to Stainless Steel
Fuel Pressurant Tank	Propulsion	Tanks	11.907	Major Mod	Material set to Titanium
Ox Pressurant Tank	Propulsion	Tanks	11.907	Major Mod	Material set to Titanium
Fuel Tanks	Propulsion	Tanks	8.862	Major Mod	Material set to Titanium
Oxidizer Tanks	Propulsion	Tanks	8.4735	Major Mod	Material set to Titanium
Mechanical Subsystem	Structure and Mechanisms				
Primary Structure	Structure and Mechanisms	Primary Structure	122.2032	New	Material set to Composite; Advanced Technology Development set to New
Secondary Structure	Structure and Mechanisms	Secondary Structure	6.2519	New	Material set to Composite; Advanced Technology Development set to New
Tertiary Structure	Structure and Mechanisms	Secondary Structure	2.5483	New	Material set to Aluminum
Integration Hardware: Fasteners, etc.	Structure and Mechanisms	Secondary Structure	9.1702	New	Material set to Aluminum
Power Support Structure	Structure and Mechanisms	Secondary Structure	2.8288	New	Material set to Aluminum
Telecom Support Structure	Structure and Mechanisms	Secondary Structure	0.0423	New	Material set to Aluminum

Table M-7. Inputs for Space Missions Model Component Type Calculator that applies to ERV on Endurance-R.

Hardware Element	Subsystem Type	Component Type	Unit Mass (kg)	Heritage	Additional Input
Telecom Subsystem	Communications				
S-band LGA, SMAP Helix	Communications	Medium Gain Antenna/Low Gain Antenna	0.2875	Major Mod	Frequency Band set to S – band; Antenna set to Array
UST-Lite Single RX, Single TX	Communications	Transponder	1.65	Major Mod	Frequency Band set to S - band
S-band SSPA, RF=11W	Communications	Amplifier	2.3	Major Mod	Frequency Band set to Most S and X- Band Solid State Power Amplifiers
CXS	Communications	Miscellaneous RF Electronics	0.156	Major Mod	Frequency Band set to S - band
S-Band Diplexer	Communications	Miscellaneous RF Electronics	0.18	Major Mod	Frequency Band set to S - band
Coax Cable, flex (190)	Communications	Waveguides-Comm Cabling	0.0819	New	Frequency Band set to S - band
Thermal Control Subsystem	Thermal Control				
Multilayer Insulation (MLI)	Thermal Control	MLI, Paints, Coatings	0.4875	New	
General Thermal Surfaces	Thermal Control	Radiators/Louvers	0.0325	New	Material set to Composite
Paints/Films	Thermal Control	MLI, Paints, Coatings	2.184	New	
General Conduction Control	Thermal Control	Heaters, RHUs, Thermostats	0.4787	New	Material set to Composite
Catalogue Heaters	Thermal Control	Heaters, RHUs, Thermostats	0.065	New	Material set to Stainless Steel
Propulsion Tank Heaters	Thermal Control	Heaters, RHUs, Thermostats	0.13	New	Material set to Stainless Steel
Propulsion Line Heaters	Thermal Control	Heaters, RHUs, Thermostats	0.13	New	Material set to Stainless Steel
PRT's	Thermal Control	Heaters, RHUs, Thermostats	0.013	New	Material set to Stainless Steel
Mechanical Thermostats	Thermal Control	Heaters, RHUs, Thermostats	28.0	New	Material set to Stainless Steel
Harness Subsystem	Power				
Harness	Power	Power Harness/Cabling	20.0969	New	
Launchpad & Transfer Arm					Payload set to No; Mission Class set to A/B
Mechanical Subsystem	Structure and Mechanisms				
Transfer Arm Structure	Structure and Mechanisms	Primary Structure	6.5	New	Material set to Composite; Advanced Technology Development set to New
Launch Platform	Structure and Mechanisms	Primary Structure	19.5	New	Material set to Composite; Advanced Technology Development set to New
ERV Support Structure	Structure and Mechanisms	Primary Structure	39.0	New	Material set to Composite; Advanced Technology Development set to New
Transfer Arm Actuator	Structure and Mechanisms	Mechanisms	6.5	New	Type set to Advanced; Advanced Technology Development set to New
ERV Support Launch Locks	Structure and Mechanisms	Mechanisms	0.65	New	Type set to Standard
Harness Subsystem	Power				
Harness	Power	Power Harness/Cabling	13.0	New	
Sample Return Capsule					Payload set to No; Mission Class set to A/B
Mechanical Subsystem	Structure and Mechanisms				

Table M-7. Inputs for Space Missions Model Component Type Calculator that applies to ERV on Endurance-R.

Hardware Element	Subsystem Type	Component Type	Unit Mass (kg)	Heritage	Additional Input
Sample Return Capsule (SRC) without samples	Structure and Mechanisms	Primary Structure	60.4513	New	Material set to Composite; Advanced Technology Development set to New
SRC Spin-up device - Bus side	Structure and Mechanisms	Mechanisms	2.7508	New	Type set to Advanced; Advanced Technology Development set to New
SRC Release Device - Bus Side	Structure and Mechanisms	Mechanisms	5.2949	New	Type set to Advanced; Advanced Technology Development set to New
SRC Mounting	Structure and Mechanisms	Primary Structure	2.99	New	Material set to Composite
Sample Canister without Samples	Structure and Mechanisms	Primary Structure	7.28	New	Material set to Composite; Advanced Technology Development set to New

M.4 SOCM

The Space Operations Cost Model (SOCM) was used for the validation of Phase E/F. SOCM estimates the costs and staffing for space operations projects using high-level project characteristics that are typically known at the early stages of a project's lifecycle. Running the cost model at Level 1 generates an estimate with an accuracy of $\pm 30\%$. The Level 1 Earth Orbiting inputs selected to reflect the Endurance mission are identified in Figure M-4 and Figure M-5. The only difference is contract type and number of imaging instruments. The Endurance-A option only has a rover flight element that will be an augmented hybrid development where a significant portion is done in-house and some hardware is contracted out. The Endurance-R option has additional flight elements for the ERV and SRC which will most likely be contracted out. The ERV also has a set of instrument cameras that will be used to observe the transfer of the samples from the rover to the ERV.

The Level 2 Earth Orbiting inputs may also be adjusted to refine the estimate and improve the accuracy. Figure M-6 provides the Level 2 settings that was the same for both options.

The Space Operations Cost Model (SOCM) estimates all Phase E/F costs, with the exception of ground station tracking (WBS 07.03) and costs for sample curation. Therefore, the Team X estimates for tracking (\$17.3M for the Endurance-R option and \$8.6M for the Endurance-A option) and sample curation (\$24.5M) were used as pass-throughs and added to the SOCM results. The final outputs from SOCM are provided in Figure M-7 and Figure M-8.

EARTH ORBITING - LEVEL 1 INPUTS							
	Value ->	1	2	3	4	5	6
MISSION CHARACTERIZATION							
Mission Type	4	Survey - Earth Science	Survey - Space Science	Targeted - Earth Science	Targeted - Space Science		
Tracking Network	3	Ground	TDRSS	DSN			
Orbit	4	LEO, circular	L1, halo	Highly Elliptical	Non-Standard/"Evolving"		
# of Identical Flight Systems	1	1	2	3	4	5	6
Nominal Mission Duration (mo)	50						
Extended Mission Duration (mo)	0						
Post-Flight Data Analysis Duration (mo)	6						
PROGRAMMATICS CHARACTERIZATION							
Mission Risk Class	4	Technology Demo (tech > sci)	SMEX	MIDEX/ESSP	Explorers	Great Observatories	
Development Schedule	3	Fast (< 2.5 yrs)	Moderate (2.5-4 yrs)	Long (> 4 yrs)			
Management Mode	1	PI	NASA				
Contract Type	3	In-House	Augmented Hybrid	Hybrid	Out-of-House		
GDS/MOS CHARACTERIZATION							
Operations Approach	2	Dedicated MOC	Multimission MOC	Remote MOC/SOC	Contracted		
Architecture Design	2	COTS	Heritage/GOTS	New/Custom			
Science Team Role	3	Data Processing	Instrument Health	Sequence Planning			
PAYLOAD CHARACTERIZATION							
# of Non-Imaging Instruments	7					Science Instrument Score	
# of Imaging Instruments	3					Score	13
Pointing Requirements	2	Low	Medium	High		Max Score	20
Conflicts Among Instruments	2	Low	Medium	High			
Scope of Guest Investigator Program	3	Small	Medium	Large			
# of Separate Science Investigations	4	1-2	3-5	6-10	11-15	> 15	
Science Team Size (not all FT)	3	Less than 10	10-20	more than 20	more than 50		
Science Team Location/Distribution	4	Colocated at 1 facility	Central SOC, 1-2 remotes	Central SOC, 3+ remotes	Central SOC, wide distr.	2 - 3 SOC locations	Multiple SOCs, wide distr
S/C DESIGN CHARACTERIZATION							
S/C Design Implementation	2	High Heritage	Cost-Capped	Requirements-Driven			
Design Complexity	3	Low (few flight rules)	Medium	High (unique engrng reqs)			

Figure M-4. SOCM Level 1 Cost Inputs for the Endurance-R option.

EARTH ORBITING - LEVEL 1 INPUTS							
	Value ->	1	2	3	4	5	6
MISSION CHARACTERIZATION							
Mission Type	4	Survey - Earth Science	Survey - Space Science	Targeted - Earth Science	Targeted - Space Science		
Tracking Network	3	Ground	TDRSS	DSN			
Orbit	4	LEO, circular	L1, halo	Highly Elliptical	Non-Standard/"Evolving"		
# of Identical Flight Systems	1	1	2	3	4	5	6
Nominal Mission Duration (mo)	50						
Extended Mission Duration (mo)	0						
Post-Flight Data Analysis Duration (mo)	6						
PROGRAMMATICS CHARACTERIZATION							
Mission Risk Class	4	Technology Demo (tech > sci)	SMEX	MIDEX/ESSP	Explorers	Great Observatories	
Development Schedule	3	Fast (< 2.5 yrs)	Moderate (2.5-4 yrs)	Long (> 4 yrs)			
Management Mode	1	PI	NASA				
Contract Type	2	In-House	Augmented Hybrid	Hybrid	Out-of-House		
GDS/MOS CHARACTERIZATION							
Operations Approach	2	Dedicated MOC	Multimission MOC	Remote MOC/SOC	Contracted		
Architecture Design	2	COTS	Heritage/GOTS	New/Custom			
Science Team Role	3	Data Processing	Instrument Health	Sequence Planning			
PAYLOAD CHARACTERIZATION							
# of Non-Imaging Instruments	7					Science Instrument Score	
# of Imaging Instruments	2					Score	11
Pointing Requirements	2	Low	Medium	High		Max Score	20
Conflicts Among Instruments	2	Low	Medium	High			
Scope of Guest Investigator Program	3	Small	Medium	Large			
# of Separate Science Investigations	4	1-2	3-5	6-10	11-15	> 15	
Science Team Size (not all FT)	3	Less than 10	10-20	more than 20	more than 50		
Science Team Location/Distribution	4	Colocated at 1 facility	Central SOC, 1-2 remotes	Central SOC, 3+ remotes	Central SOC, wide distr.	2 - 3 SOC locations	Multiple SOCs, wide distr
S/C DESIGN CHARACTERIZATION							
S/C Design Implementation	2	High Heritage	Cost-Capped	Requirements-Driven			
Design Complexity	3	Low (few flight rules)	Medium	High (unique engrng reqs)			

Figure M-5. SOCM Level 1 Cost Inputs for the Endurance-A option.

EARTH ORBITING - LEVEL 2 INPUTS						
LEVEL 2 ESTIMATE		Earth-Orbiting - LEVEL 2 INPUTS				
Endurance-A						
LEVEL 2 INPUTS						
Selected Cost Drivers:		Use Low or High when driver is known; Medium is default value			units	Definitions
Mission Implementation	Low	Medium	High			
Engineering Event Complexity	<input checked="" type="radio"/> Routine, Non-hazardous events	<input type="radio"/> Repetitive/No Hazardous Events	<input type="radio"/> Risky events/Significant Real-Time Contact			Number of unique engineering command sequences
Targeted Observations	<input checked="" type="radio"/> No targeted observations or >24 hours to implement	<input type="radio"/> Targeted observations implemented in 6-24 hours	<input type="radio"/> Targeted observations implemented in less than 6 hours			High level characterization of operation concept
Science Event Complexity	<input type="radio"/> Survey	<input type="radio"/> Few constraints	<input checked="" type="radio"/> Constrained, Multiple observation modes			Number of unique science instrument command sequences
Programmatic Implementation	Low	Medium	High			
Staff Experience	<input type="radio"/> More than 2 similar missions	<input checked="" type="radio"/> 1 or 2 similar missions	<input type="radio"/> New OPS team			Experience of ops staff with similar systems
Risk Plan - S/C	<input type="radio"/> Small S/C, No redundancy, Tech demo mission	<input type="radio"/> Class C, \$100M flt system development	<input checked="" type="radio"/> Redundant S/C, several \$100M development			Measure of the S/C operational risk based on design implementation
Risk Plan - Instruments/Payload	<input type="radio"/> Simple payload, No redundancy	<input checked="" type="radio"/> Few hazardous OPS, Limited redundancy	<input type="radio"/> Complex, redundant S/C			Measure of the instrument/payload operational risk based on design implementation
Risk Plan - GDS/MOS	<input type="radio"/> Accept min risk to msn safety, and mod data loss	<input checked="" type="radio"/> Accept mod risk to efficiency and data loss < 5%	<input type="radio"/> Accept min risk to efficiency and data loss < 1%			Measure of the GDS/MOS operational risk based on design implementation
Crosstraining/Staffing Overlaps	<input type="radio"/> Fully crosstrained	<input checked="" type="radio"/> Crosstrained within functions	<input type="radio"/> Limited crosstraining			Number of staff assigned/trained to perform same function
H/W Redundancy	<input type="radio"/> Limited or no redundancy	<input checked="" type="radio"/> Selected redundancy	<input type="radio"/> Full redundancy with rapid switchover			GDS/MOS system redundancy
Spacecraft Design Impl.	Low	Medium	High			
S/C Autonomy	<input type="radio"/> Proven sophisticated autonomy	<input checked="" type="radio"/> Simple robust safe mode; Onboard telemetry monitor	<input type="radio"/> Complex safe modes or experimental approach			Ability of the s/c to operate without ground control
Maneuver Frequency	<input type="radio"/> Once per year or less	<input type="radio"/> Couple of times per year	<input checked="" type="radio"/> Once a month or more			Frequency of S/C maneuvers over nominal operations period
Data Return Margin	<input checked="" type="radio"/> > 2	<input type="radio"/> 1.1 - 2	<input type="radio"/> < 1.1			Ratio of max amount of data that can be downlinked to the average amount required per downlink
Power Margin	<input type="radio"/> > 1.2	<input checked="" type="radio"/> 1 - 1.2	<input type="radio"/> < 1			Ratio of max avail power to peak power demand
Memory Margin	<input checked="" type="radio"/> > 2	<input type="radio"/> 1.5 - 2	<input type="radio"/> < 1.2			Ratio of on-board storage capacity to max quantity of data to be downlinked in a single pass

Figure M-6. SOCM Level 2 Cost Inputs for both options.

GDS/MOS Implementation		Low	Medium	High		
Command Frequency - Sequences	<input checked="" type="radio"/>	Loaded less than once per day	<input type="radio"/> Daily	<input type="radio"/> Loaded more than once per day		Frequency of developing sequences for uplink
Data Processing - Data Completeness	<input type="radio"/>	< 95%	<input checked="" type="radio"/> 95-98%	<input type="radio"/> > 98%	%	Measure of data return requirement vs. minimal acceptable data return
Data Processing - Data Delivery Time	<input type="radio"/>	More than 24 hours	<input checked="" type="radio"/> 6 to 24 hours	<input type="radio"/> Less than 6 hours	hrs	Time allowed to deliver data products after raw data is downlinked
Data Processing - Autonomy	<input type="radio"/>	Extensive	<input checked="" type="radio"/> Nominal	<input type="radio"/> Minimal		Measure of the degree of autonomy in ground data handling system
Data Processing - Heritage/Reuse	<input type="radio"/>	More than 85%	<input checked="" type="radio"/> 75%	<input type="radio"/> Less than 60%	%	% of ground data processing system based on existing designs
Command Frequency - Generation Time	<input checked="" type="radio"/>	More than one day before upload	<input type="radio"/> One day before upload	<input type="radio"/> Less than one day before upload		Time allowed to generate commands to modify/affect mission ops
Command Frequency - Real-Time Commands	<input type="radio"/>	No commands on some passes	<input checked="" type="radio"/> Routine commands on most passes	<input type="radio"/> Special commands on some passes		Frequency of real-time commands for uplink
Data Processing - Max. Downlink Rate	<input type="radio"/>	less than 1	<input checked="" type="radio"/> 1 to 2	<input type="radio"/> 10s to 100s	Mbps	Maximum downlink data rate accommodated
Data Processing - Max. Bits/Day	<input type="radio"/>	< 10	<input checked="" type="radio"/> 10-100	<input type="radio"/> > 100	Gb	Maximum # of bits downlinked per day
Data Processing - On-Line Storage	<input type="radio"/>	> 20	<input checked="" type="radio"/> 2 - 20	<input type="radio"/> < 2	GB	Size/capacity of onboard data storage system
Data Processing - Storage/Playback Frequency	<input type="radio"/>	Once per day or less	<input checked="" type="radio"/> Several times per day	<input type="radio"/> Once per orbit		Number of days that data can be stored without downlink
Payload Implementation		Low	Medium	High		
Instrument Support Complexity	<input type="radio"/>	Simple instrument with few operations	<input checked="" type="radio"/> Routine calibrations, few sched constraints	<input type="radio"/> Constrained operation, Complex instr interactions		Relates to # of instruments, conflicts, flight rules for instr operation
Payload Flight Heritage	<input type="radio"/>	Most instruments have flown together; No advanced technology	<input checked="" type="radio"/> Most instruments have flight heritage	<input type="radio"/> New instruments; Payload includes advanced technology		Measure of individual instruments and total payload package flight experience
Instrument/Payload Operating Modes	<input checked="" type="radio"/>	2-3 operating modes per instrument; One observing mode for all instruments	<input type="radio"/> Less than 3 operating modes per instrument; 2-3 observing modes	<input type="radio"/> Several instruments with multiple operating modes; 3+ observing modes		Number of operating modes for each instrument and observing modes for total payload; Modes include calibration

Figure M-6. SOCM Level 2 Cost Inputs for both options.

LEVEL 2 MISSION OPERATIONS COST Endurance-R	ESTIMATE				2025 constant FY \$K		JPL WBS	
	Phase E	Phase E	Post-Flight DA	Phase E Total	Mapping	Cost		
	Nominal	Extended						
1.0 MISSION PLANNING & INTEGRATION	4066.1	0.0		4066.1	MOS	7 MOS	59,930.5	
2.0 COMMAND/UPLINK MANAGEMENT	9646.3	0.0		9646.3	MOS			
3.0 MISSION CONTROL & OPS	11214.7	0.0		11214.7	MOS	9 GDS	27,809.7	
4.0 DATA CAPTURE	10543.6	0.0		10543.6	GDS			
5.0 POS/LOC PLANNING & ANALYSIS	551.5	0.0		551.5	MOS			
6.0 S/C PLANNING & ANALYSIS	1861.4	0.0		1861.4	MOS			
7.0 SCI PLANNING & ANALYSIS	32590.4	0.0		32590.4	MOS			
8.0 SCIENCE DATA PROCESSING	41351.9	0.0	4962.2	46314.1	Science	4 Science	80,682.2	
9.0 LONG-TERM ARCHIVES	20803.4	0.0	2496.4	23299.8	Science			
10.0 SYSTEM ENGINEERING, INTEG, & TEST	11358.9	0.0		11358.9	GDS			
11.0 COMPUTER & COMM SUPPORT	5274.3	0.0	632.9	5907.2	GDS			
12.0 SCIENCE INVESTIGATIONS	9882.4	0.0	1185.9	11068.3	Science			
13.0 MANAGEMENT	2213.5	0.0		2213.5	Mgmt	1 Mgmt	2,213.5	
Project Direct Total	161,358.4	0.0	9,277.4	170,635.9				

Operations Services

Tracking costs from Team X 17,300.0
 Sample Curation costs from Team X 24,497.1

Figure M-7. SOCM Level 2 Cost Results for the Endurance-R option.

LEVEL 2 MISSION OPERATIONS COST Endurance-A	ESTIMATE				2025 constant FY \$K		JPL WBS	
	Phase E	Phase E	Post-Flight DA	Phase E Total	Mapping	Cost		
	Nominal	Extended						
1.0 MISSION PLANNING & INTEGRATION	3668.3	0.0		3668.3	MOS	7 MOS	52,998.1	
2.0 COMMAND/UPLINK MANAGEMENT	8660.9	0.0		8660.9	MOS			
3.0 MISSION CONTROL & OPS	10003.8	0.0		10003.8	MOS	9 GDS	24,545.0	
4.0 DATA CAPTURE	8910.7	0.0		8910.7	GDS			
5.0 POS/LOC PLANNING & ANALYSIS	501.0	0.0		501.0	MOS			
6.0 S/C PLANNING & ANALYSIS	1593.7	0.0		1593.7	MOS			
7.0 SCI PLANNING & ANALYSIS	28570.4	0.0		28570.4	MOS			
8.0 SCIENCE DATA PROCESSING	38078.5	0.0	4569.4	42647.9	Science	4 Science	73,106.6	
9.0 LONG-TERM ARCHIVES	18504.6	0.0	2220.5	20725.1	Science			
10.0 SYSTEM ENGINEERING, INTEG, & TEST	10278.4	0.0		10278.4	GDS			
11.0 COMPUTER & COMM SUPPORT	4782.0	0.0	573.8	5355.9	GDS			
12.0 SCIENCE INVESTIGATIONS	8690.7	0.0	1042.9	9733.6	Science			
13.0 MANAGEMENT	1957.0	0.0		1957.0	Mgmt	1 Mgmt	1,957.0	
Project Direct Total	144,200.0	0.0	8,406.7	152,606.7				

Tracking costs from Team X 8,600.0
 Sample Curation costs from Team X 24,497.1

Figure M-8. SOCM Level 2 Cost Results for the Endurance-A option.

N REFERENCES

N.1 SECTIONS 1 – 5

- [1] M. S. Robinson *et al.*, "Intrepid Planetary Mission Concept Study Report," NASA, 2020. [Online]. Available: <https://science.nasa.gov/science-red/s3fs-public/atoms/files/Lunar%20INTREPID.pdf>
- [2] NRC, *New Frontiers in the Solar System: An Integrated Exploration Strategy*. Washington, DC: The National Academies Press (in English), 2003, p. 248.
- [3] NRC, *Vision and Voyages for Planetary Science in the Decade 2013-2022*. Washington, DC: The National Academies Press (in English), 2011, p. 398.
- [4] D. Nesvorný, "Dynamical Evolution of the Early Solar System," *Annual Review of Astronomy and Astrophysics*, vol. 56, no. 1, pp. 137-174, 2018, doi: 10.1146/annurev-astro-081817-052028.
- [5] K. Tsiganis, R. Gomes, A. Morbidelli, and H. F. Levison, "Origin of the orbital architecture of the giant planets of the Solar System," *Nature*, vol. 435, pp. 459-461, 2005/05/01 2005, doi: 10.1038/nature03539.
- [6] A. Morbidelli, K. J. Walsh, D. P. O'Brien, D. A. Minton, and W. F. Bottke, "The Dynamical Evolution of the Asteroid Belt," in *Asteroids IV*, P. Michel, F. E. Demeo, and W. F. Bottke Eds. Tucson: University of Arizona Press, 2015, pp. 493-507.
- [7] R. Gomes, H. F. Levison, K. Tsiganis, and A. Morbidelli, "Origin of the cataclysmic Late Heavy Bombardment period of the terrestrial planets," *Nature*, vol. 435, pp. 466-469, 2005/05/01 2005, doi: 10.1038/nature03676.
- [8] W. F. Bottke and M. D. Norman, "The Late Heavy Bombardment," *Annual Review of Earth and Planetary Sciences*, vol. 45, no. 1, pp. 619-647, 2017, doi: 10.1146/annurev-earth-063016-020131.
- [9] W. K. Hartmann, "History of the Terminal Cataclysm Paradigm: Epistemology of a Planetary Bombardment That Never (?) Happened," *Geosciences*, vol. 9, no. 7, p. 285, 2019, doi: 10.3390/geosciences9070285.
- [10] G. Ryder, "Lunar samples, lunar accretion and the early bombardment of the Moon," *Eos, Transactions American Geophysical Union*, vol. 71, no. 10, pp. 313-323, 1990, doi: 10.1029/90EO00086.
- [11] F. Tera, D. A. Papanastassiou, and G. J. Wasserburg, "Isotopic evidence for a terminal lunar cataclysm," *Earth and Planetary Science Letters*, vol. 22, no. 1, pp. 1-21, 1974/04/01/ 1974, doi: 10.1016/0012-821X(74)90059-4.
- [12] L. A. Haskin, "The Imbrium impact event and the thorium distribution at the lunar highlands surface," *Journal of Geophysical Research: Planets*, vol. 103, no. E1, pp. 1679-1689, 1998, doi: 10.1029/97JE03035.
- [13] G. A. Schaeffer and O. A. Schaeffer, "³⁹Ar-⁴⁰Ar ages of lunar rocks," in *Lunar Science Conference*, Houston, TX, March 14-18 1977, vol. 2: Pergamon Press, Inc., pp. 2253-2300.
- [14] P. D. Spudis, D. E. Wilhelms, and M. S. Robinson, "The Sculptured Hills of the Taurus Highlands: Implications for the relative age of Serenitatis, basin chronologies and the cratering history of the Moon," *Journal of Geophysical Research: Planets*, vol. 116, no. E12, 2011, doi: 10.1029/2011JE003903.
- [15] N. E. B. Zellner, "Cataclysm No More: New Views on the Timing and Delivery of Lunar Impactors," *Origins of Life and Evolution of Biospheres*, vol. 47, no. 3, pp. 261-280, 2017/09/01 2017, doi: 10.1007/s11084-017-9536-3.
- [16] L. T. Elkins-Tanton, S. Burgess, and Q.-Z. Yin, "The lunar magma ocean: Reconciling the solidification process with lunar petrology and geochronology," *Earth and Planetary Science Letters*, vol. 304, no. 3, pp. 326-336, 2011/04/15/ 2011, doi: 10.1016/j.epsl.2011.02.004.
- [17] J. A. Wood, J. S. Dickey, Jr., U. B. Marvin, and B. N. Powell, "Lunar anorthosites and a geophysical model of the moon," *Geochimica et Cosmochimica Acta Supplement*, vol. 1, p. 965,



- January 01, 1970 1970. [Online]. Available: <https://ui.adsabs.harvard.edu/abs/1970GeCAS...1..965W>.
- [18] L. T. Elkins-Tanton, "Magma Oceans in the Inner Solar System," *Annual Review of Earth and Planetary Sciences*, vol. 40, no. 1, pp. 113-139, 2012, doi: 10.1146/annurev-earth-042711-105503.
- [19] K. de Kleer, R. Park, and A. McEwen, "Tidal Heating: Lessons from Io and the Jovian System," 2019. [Online]. Available: https://www.kiss.caltech.edu/final_reports/Tidal_Heating_final_report.pdf
- [20] K. K. Khurana, X. Jia, M. G. Kivelson, F. Nimmo, G. Schubert, and C. T. Russell, "Evidence of a Global Magma Ocean in Io's Interior," *Science*, vol. 332, no. 6034, pp. 1186-1189, 2011, doi: 10.1126/science.1201425.
- [21] W. G. Henning *et al.*, "Highly Volcanic Exoplanets, Lava Worlds, and Magma Ocean Worlds: An Emerging Class of Dynamic Exoplanets of Significant Scientific Priority," White Paper, 2018. [Online]. Available: <https://arxiv.org/abs/1804.05110>
- [22] R. Tartèse *et al.*, "Constraining the Evolutionary History of the Moon and the Inner Solar System: A Case for New Returned Lunar Samples," *Space Science Reviews*, vol. 215, no. 8, p. 54, 2019/12/02 2019, doi: 10.1007/s11214-019-0622-x.
- [23] H. J. Melosh *et al.*, "South Pole–Aitken basin ejecta reveal the Moon's upper mantle," *Geology*, vol. 45, no. 12, pp. 1063-1066, 2017, doi: 10.1130/g39375.1.
- [24] C. K. Shearer, S. M. Elardo, N. E. Petro, L. E. Borg, and F. M. McCubbin, "Origin Of The Lunar Highlands Mg-Suite: An Integrated Petrology, Geochemistry, Chronology, And Remote Sensing Perspective," *American Mineralogist*, vol. 100, no. 1, pp. 294-325, 2015, doi: 10.2138/am-2015-4817.
- [25] A. Roy, J. T. Wright, and S. Sigurðsson, "Eathshine on a Young Moon: Explaining the Lunar Farside Highlands," *The Astrophysical Journal*, vol. 788, no. 2, p. L42, 2014/06/09 2014, doi: 10.1088/2041-8205/788/2/L42.
- [26] D. E. Loper and C. L. Werner, "On lunar asymmetries 1. Tilted convection and crustal asymmetry," *Journal of Geophysical Research: Planets*, vol. 107, no. E6, 2002, doi: 10.1029/2000JE001441.
- [27] E. M. Parmentier, S. Zhong, and M. T. Zuber, "Gravitational differentiation due to initial chemical stratification: origin of lunar asymmetry by the creep of dense KREEP?," *Earth and Planetary Science Letters*, vol. 201, no. 3, pp. 473-480, 2002/08/15/ 2002, doi: 10.1016/S0012-821X(02)00726-4.
- [28] S. Zhong, E. M. Parmentier, and M. T. Zuber, "A dynamic origin for the global asymmetry of lunar mare basalts," *Earth and Planetary Science Letters*, vol. 177, no. 3, pp. 131-140, 2000/04/30/ 2000, doi: 10.1016/S0012-821X(00)00041-8.
- [29] M. Ohtake *et al.*, "Asymmetric crustal growth on the Moon indicated by primitive farside highland materials," *Nature Geoscience*, vol. 5, no. 6, pp. 384-388, 2012/06/01 2012, doi: 10.1038/ngeo1458.
- [30] I. Garrick-Bethell, F. Nimmo, and M. A. Wieczorek, "Structure and Formation of the Lunar Farside Highlands," *Science*, vol. 330, no. 6006, pp. 949-951, 2010, doi: 10.1126/science.1193424.
- [31] A. C. Quillen, L. Martini, and M. Nakajima, "Near/far side asymmetry in the tidally heated Moon," *Icarus*, vol. 329, pp. 182-196, 2019/09/01/ 2019, doi: 10.1016/j.icarus.2019.04.010.
- [32] M. T. Zuber, D. E. Smith, F. G. Lemoine, and G. A. Neumann, "The Shape and Internal Structure of the Moon from the Clementine Mission," *Science*, vol. 266, no. 5192, pp. 1839-1843, 1994, doi: 10.1126/science.266.5192.1839.
- [33] M. Jutzi and E. Asphaug, "Forming the lunar farside highlands by accretion of a companion moon," *Nature*, vol. 476, no. 7358, pp. 69-72, 2011/08/01 2011, doi: 10.1038/nature10289.



- [34] M.-H. Zhu, K. Wünnemann, R. W. K. Potter, T. Kleine, and A. Morbidelli, "Are the Moon's Nearside-Farside Asymmetries the Result of a Giant Impact?," *Journal of Geophysical Research: Planets*, vol. 124, no. 8, pp. 2117-2140, 2019, doi: 10.1029/2018JE005826.
- [35] J. C. Andrews-Hanna, M. T. Zuber, and W. B. Banerdt, "The Borealis basin and the origin of the martian crustal dichotomy," *Nature*, vol. 453, no. 7199, pp. 1212-1215, 2008/06/01 2008, doi: 10.1038/nature07011.
- [36] P. H. Schultz and D. A. Crawford, "Origin of the Nearside/Farside Dichotomy," in *NLSI Lunar Science Conference*, NASA Ames Research Center, Moffett Field, California, July 20-23 2008, vol. 1415, p. 2118. [Online]. Available: <https://ui.adsabs.harvard.edu/abs/2008LPICo1415.2118S>.
- [37] J. H. Roberts and O. S. Barnouin, "The effect of the Caloris impact on the mantle dynamics and volcanism of Mercury," *Journal of Geophysical Research: Planets*, vol. 117, no. E2, 2012, doi: 10.1029/2011JE003876.
- [38] C. A. Denton, B. C. Johnson, S. Wakita, A. M. Freed, H. J. Melosh, and S. A. Stern, "Pluto's Antipodal Terrains Imply a Thick Subsurface Ocean and Hydrated Core," *Geophysical Research Letters*, vol. 48, no. 2, p. e2020GL091596, 2021, doi: 10.1029/2020GL091596.
- [39] J. T. Keane, I. Matsuyama, S. Kamata, and J. K. Steckloff, "Reorientation and faulting of Pluto due to volatile loading within Sputnik Planitia," *Nature*, vol. 540, no. 7631, pp. 90-93, 2016/12/01 2016, doi: 10.1038/nature20120.
- [40] F. Nimmo *et al.*, "Reorientation of Sputnik Planitia implies a subsurface ocean on Pluto," *Nature*, vol. 540, no. 7631, pp. 94-96, 2016/12/01 2016, doi: 10.1038/nature20148.
- [41] R. W. K. Potter, G. S. Collins, W. S. Kiefer, P. J. McGovern, and D. A. Kring, "Constraining the size of the South Pole-Aitken basin impact," *Icarus*, vol. 220, no. 2, pp. 730-743, 2012, doi: 10.1016/j.icarus.2012.05.032.
- [42] I. Garrick-Bethell and M. T. Zuber, "Elliptical structure of the lunar South Pole-Aitken basin," *Icarus*, vol. 204, no. 2, pp. 399-408, 2009, doi: 10.1016/j.icarus.2009.05.032.
- [43] (2020). 332, *Sample Return from the Moon's South Pole-Aitken Basin*.
- [44] LEAG, "Advancing Science of the Moon: Report of the Lunar Exploration Analysis Group Special Action Team," August 7-8 2017. [Online]. Available: <https://www.lpi.usra.edu/leag/reports/ASM-SAT-Report-final.pdf>
- [45] NRC, *The Scientific Context for Exploration of the Moon*. Washington, DC: The National Academies Press (in English), 2007, p. 120.
- [46] B. Cohen *et al.*, "In Situ Geochronology for the Next Decade," 2020. [Online]. Available: <https://science.nasa.gov/science-red/s3fs-public/atoms/files/Geochronology%20Report.pdf>
- [47] B. Cohen *et al.*, "In Situ Geochronology for the Next Decade: Mission Designs for the Moon, Mars, and Vesta," 2021.
- [48] C. M. Mercer *et al.*, "Refining lunar impact chronology through high spatial resolution $^{40}\text{Ar}/^{39}\text{Ar}$ dating of impact melts," *Science Advances*, vol. 1, no. 1, p. e1400050, 2015, doi: 10.1126/sciadv.1400050.
- [49] C. A. Crow, K. D. McKeegan, and D. E. Moser, "Coordinated U–Pb geochronology, trace element, Ti-in-zircon thermometry and microstructural analysis of Apollo zircons," *Geochimica et Cosmochimica Acta*, vol. 202, pp. 264-284, 2017, doi: 10.1016/j.gca.2016.12.019.
- [50] B. Jolliff, J. J. Gillis, L. A. Haskin, R. L. Korotev, and M. A. Wiczorek, "Major lunar crustal terranes: Surface expressions and crust-mantle origins," *Journal of Geophysical Research: Planets*, vol. 105, no. E2, pp. 4197-4216, 2000, doi: 10.1029/1999JE001103.
- [51] T. L. Jackson, W. M. Farrell, and M. I. Zimmerman, "Rover wheel charging on the lunar surface," *Advances in Space Research*, vol. 55, no. 6, pp. 1710-1720, 2015, doi: 10.1016/j.asr.2014.12.027.



- [52] I. A. Nesnas, M. W. Maimone, and H. Das, "Rover Maneuvering for Autonomous Vision-Based Dexterous Manipulation," in *IEEE International Conference on Robotics and Automation*, San Francisco, CA, April 24-28 2000: IEEE, in ICRA 2000 Proceedings, pp. 2296–2301, doi: 10.1109/ROBOT.2000.846369.
- [53] V. Asnani, D. Delap, and C. Creager, "The development of wheels for the Lunar Roving Vehicle," *Journal of Terramechanics*, vol. 46, no. 3, pp. 89–103, 2009, doi: 10.1016/j.jterra.2009.02.005.
- [54] (1965). *A dimensionless consolidation of WES data on the performance of sand under tire loads*.
- [55] M. Sutoh, J. Yusa, T. Ito, K. Nagatani, and K. Yoshida, "Traveling performance evaluation of planetary rovers on loose soil," *Journal of Field Robotics*, vol. 29, no. 4, pp. 648–662, 2012, doi: 10.1002/rob.21405.
- [56] J. Yoshida, "Full AV Stacks: Who, What, Where, etc.," *EE | Times*. [Online]. Available: <https://www.eetimes.com/full-av-stacks-who-what-where-etc/#>



N.2 APPENDICES

- [1] M. S. Robinson *et al.*, "Intrepid Planetary Mission Concept Study Report," NASA, 2020. [Online]. Available: <https://science.nasa.gov/science-red/s3fs-public/atoms/files/Lunar%20INTREPID.pdf>
- [2] R. W. K. Potter, G. S. Collins, W. S. Kiefer, P. J. McGovern, and D. A. Kring, "Constraining the size of the South Pole-Aitken basin impact," *Icarus*, vol. 220, no. 2, pp. 730-743, 2012, doi: 10.1016/j.icarus.2012.05.032.
- [3] D. P. Moriarty III and C. M. Pieters, "The Character of South Pole-Aitken Basin: Patterns of Surface and Subsurface Composition," *Journal of Geophysical Research: Planets*, vol. 123, no. 3, pp. 729-747, 2018, doi: 10.1002/2017JE005364.
- [4] D. P. Moriarty III and C. Pieters, "Impact Melt and Magmatic Processes in Central South Pole—Aitken Basin," in *Lunar and planetary science conference*, 2016, no. 1903, p. 1735.
- [5] D. P. Moriarty III, C. Pieters, and P. Isaacson, "Compositional heterogeneity of central peaks within the South Pole-Aitken Basin," *Journal of Geophysical Research: Planets*, vol. 118, no. 11, pp. 2310-2322, 2013.
- [6] R. Nakamura *et al.*, "Ultramafic impact melt sheet beneath the South Pole–Aitken basin on the Moon," *Geophysical Research Letters*, vol. 36, no. 22, 2009.
- [7] D. M. Hurwitz and D. A. Kring, "Differentiation of the South Pole–Aitken basin impact melt sheet: Implications for lunar exploration," *Journal of Geophysical Research: Planets*, vol. 119, no. 6, pp. 1110-1133, 2014.
- [8] C. Fassett *et al.*, "Lunar impact basins: Stratigraphy, sequence and ages from superposed impact crater populations measured from Lunar Orbiter Laser Altimeter (LOLA) data," *Journal of Geophysical Research: Planets*, vol. 117, no. E12, 2012.
- [9] J. H. Pasckert, H. Hiesinger, and C. H. van der Bogert, "Lunar farside volcanism in and around the South Pole–Aitken basin," *Icarus*, vol. 299, pp. 538-562, 2018.
- [10] D. A. Kring, G. Y. Kramer, G. S. Collins, R. W. Potter, and M. Chandnani, "Peak-ring structure and kinematics from a multi-disciplinary study of the Schrödinger impact basin," *Nature Communications*, vol. 7, no. 1, pp. 1-10, 2016.
- [11] M. Ivanov, H. Hiesinger, C. Van Der Bogert, C. Orgel, J. Pasckert, and J. Head, "Geologic History of the Northern Portion of the South Pole-Aitken Basin on the Moon," *Journal of Geophysical Research: Planets*, vol. 123, no. 10, pp. 2585-2612, 2018.
- [12] M. Taguchi, T. Morota, and S. Kato, "Lateral heterogeneity of lunar volcanic activity according to volumes of mare basalts in the farside basins," *Journal of Geophysical Research: Planets*, vol. 122, no. 7, pp. 1505-1521, 2017, doi: 10.1002/2016JE005246.
- [13] M. A. Wieczorek *et al.*, "The Crust of the Moon as Seen by GRAIL," *Science*, vol. 339, no. 6120, pp. 671-675, 2013, doi: 10.1126/science.1231530.
- [14] E. Czaplinski *et al.*, "Human-assisted Sample Return Mission at the Schrödinger Basin, Lunar Far Side, Using a New Geologic Map and Rover Traverses," *The Planetary Science Journal*, vol. 2, no. 2, p. 51, 2021.
- [15] N. J. Potts *et al.*, "Robotic traverse and sample return strategies for a lunar farside mission to the Schrödinger basin," *Advances in Space Research*, vol. 55, no. 4, pp. 1241-1254, 2015, doi: 10.1016/j.asr.2014.11.028.
- [16] G. Y. Kramer, D. A. Kring, A. L. Nahm, and C. M. Pieters, "Spectral and photogeologic mapping of Schrödinger Basin and implications for post-South Pole-Aitken impact deep subsurface stratigraphy," *Icarus*, vol. 223, no. 1, pp. 131-148, 2013.
- [17] D. Kring, G. Kramer, D. Bussey, and D. Hurley, "Prominent volcanic source of volatiles in the south polar region of the Moon," in *Annual Meeting of the Lunar Exploration Analysis Group*, 2014, vol. 1820, p. 3057.



- [18] D. P. Moriarty III *et al.*, "Evidence for a Stratified Upper Mantle Preserved within the South Pole–Aitken Basin," *Journal of Geophysical Research: Planets*, p. e2020JE006589, 2020.
- [19] R. Ghent, N. Zellner, I. Daubar, J.-P. Williams, S. Marchi, and N. Schmerr, "Assessing the Recent Impact Flux in the Inner Solar System," in *Lunar and Planetary Science Conference*, 2020, no. 2326, p. 2329.
- [20] J. P. Williams *et al.*, "Lunar cold spots and crater production on the moon," *Journal of Geophysical Research: Planets*, vol. 123, no. 9, pp. 2380-2392, 2018.
- [21] M. S. Robinson and M. Ravine, "Telephoto Reconnaissance Imaging for Lunar Rover Applications (FARCAM)," in *International Workshop on Instrumentation for Planetary Missions*, 2012. [Online]. Available: <https://www.lpi.usra.edu/meetings/ipm2012/pdf/1064.pdf>.
- [22] G. H. Heiken, D. T. Vaniman, and B. M. French, *Lunar Sourcebook, A User's Guide to the Moon*. Cambridge University Press, 1991.
- [23] B. P. Weiss and S. M. Tikoo, "The lunar dynamo," *Science*, vol. 346, no. 6214, p. 1246753, 2014, doi: 10.1126/science.1246753.
- [24] K. W. Lewis *et al.*, "A surface gravity traverse on Mars indicates low bedrock density at Gale crater," *Science*, vol. 363, no. 6426, pp. 535-537, 2019, doi: 10.1126/science.aat0738.
- [25] L. P. Keller and D. S. McKay, "The nature and origin of rims on lunar soil grains," *Geochimica et Cosmochimica Acta*, vol. 61, no. 11, pp. 2331-2341, 1997.
- [26] R. Arvidson, R. Drozd, C. Hohenberg, C. Morgan, and G. Poupeau, "Horizontal transport of the regolith, modification of features, and erosion rates on the lunar surface," *The Moon*, vol. 13, no. 1-3, pp. 67-79, 1975.
- [27] H. J. Melosh *et al.*, "South Pole–Aitken basin ejecta reveal the Moon's upper mantle," *Geology*, vol. 45, no. 12, pp. 1063-1066, 2017, doi: 10.1130/g39375.1.
- [28] W. M. Vaughan, J. W. Head, L. Wilson, and P. C. Hess, "Geology and petrology of enormous volumes of impact melt on the Moon: A case study of the Orientale basin impact melt sea," *Icarus*, vol. 223, no. 2, pp. 749-765, 2013.
- [29] W. M. Vaughan and J. W. Head, "Impact melt differentiation in the South Pole-Aitken basin: Some observations and speculations," *Planetary and Space Science*, vol. 91, pp. 101-106, 2014.
- [30] J. P. Cassanelli and J. W. Head, "Did the Orientale impact melt sheet undergo large-scale igneous differentiation by crystal settling?," *Geophysical Research Letters*, vol. 43, no. 21, pp. 11,156-11,165, 2016.
- [31] D. P. Moriarty III and C. M. Pieters, "The nature and origin of mafic mound in the South Pole-Aitken Basin," *Geophysical Research Letters*, vol. 42, no. 19, pp. 7907-7915, 2015.
- [32] M. J. Cintala and R. A. Grieve, "Scaling impact melting and crater dimensions: Implications for the lunar cratering record," *Meteoritics & Planetary Science*, vol. 33, no. 4, pp. 889-912, 1998.
- [33] H. J. Melosh, "Impact cratering: A geologic process," *icgp*, 1989.
- [34] M. Schmieder and F. Jourdan, "The Lappajärvi impact structure (Finland): Age, duration of crater cooling, and implications for early life," *Geochimica et Cosmochimica Acta*, vol. 112, pp. 321-339, 2013.
- [35] E. D. Young, I. E. Kohl, P. H. Warren, D. C. Rubie, S. A. Jacobson, and A. Morbidelli, "Oxygen isotopic evidence for vigorous mixing during the Moon-forming giant impact," *Science*, vol. 351, no. 6272, pp. 493-496, 2016.
- [36] P. J. Isaacson *et al.*, "The lunar rock and mineral characterization consortium: Deconstruction and integrated mineralogical, petrologic, and spectroscopic analyses of mare basalts," *Meteoritics & Planetary Science*, vol. 46, no. 2, pp. 228-251, 2011.
- [37] D. P. Moriarty III and C. Pieters, "Complexities in pyroxene compositions derived from absorption band centers: Examples from Apollo samples, HED meteorites, synthetic pure

- pyroxenes, and remote sensing data," *Meteoritics & Planetary Science*, vol. 51, no. 2, pp. 207-234, 2016.
- [38] B. Cohen *et al.*, "In Situ Geochronology for the Next Decade," 2020. [Online]. Available: <https://science.nasa.gov/science-red/s3fs-public/atoms/files/Geochronology%20Report.pdf>
- [39] B. Cohen *et al.*, "In Situ Geochronology for the Next Decade: Mission Designs for the Moon, Mars, and Vesta," 2021.
- [40] C. M. Mercer *et al.*, "Refining lunar impact chronology through high spatial resolution $^{40}\text{Ar}/^{39}\text{Ar}$ dating of impact melts," *Science Advances*, vol. 1, no. 1, p. e1400050, 2015, doi: 10.1126/sciadv.1400050.
- [41] C. A. Crow, K. D. McKeegan, and D. E. Moser, "Coordinated U–Pb geochronology, trace element, Ti-in-zircon thermometry and microstructural analysis of Apollo zircons," *Geochimica et Cosmochimica Acta*, vol. 202, pp. 264-284, 2017, doi: 10.1016/j.gca.2016.12.019.
- [42] (2020). 332, *Sample Return from the Moon's South Pole-Aitken Basin*.
- [43] W. S. Kiefer, R. J. Macke, D. T. Britt, A. J. Irving, and G. J. Consolmagno, "The density and porosity of lunar rocks," *Geophysical Research Letters*, vol. 39, no. 7, 2012.
- [44] D. Lauretta *et al.*, "OSIRIS-REx: sample return from asteroid (101955) Bennu," *Space Science Reviews*, vol. 212, no. 1, pp. 925-984, 2017.
- [45] M. D. Norman, R. A. Duncan, and J. J. Huard, "Identifying impact events within the lunar cataclysm from ^{40}Ar – ^{39}Ar ages and compositions of Apollo 16 impact melt rocks," *Geochimica et Cosmochimica Acta*, vol. 70, no. 24, pp. 6032-6049, 2006.
- [46] L. E. Borg, A. M. Gaffney, and C. K. Shearer, "A review of lunar chronology revealing a preponderance of 4.34–4.37 Ga ages," *Meteoritics & Planetary Science*, vol. 50, no. 4, pp. 715-732, 2015, doi: 10.1111/maps.12373.
- [47] R. W. Carlson, L. E. Borg, A. M. Gaffney, and M. Boyet, "Rb-Sr, Sm-Nd and Lu-Hf isotope systematics of the lunar Mg-suite: the age of the lunar crust and its relation to the time of Moon formation," *Philosophical Transactions of the Royal Society A: Mathematical, Physical and Engineering Sciences*, vol. 372, no. 2024, 2014, doi: 10.1098/rsta.2013.0246.
- [48] M. Boyet, R. W. Carlson, L. E. Borg, and M. Horan, "Sm–Nd systematics of lunar ferroan anorthositic suite rocks: constraints on lunar crust formation," *Geochimica et Cosmochimica Acta*, vol. 148, pp. 203-218, 2015.
- [49] P. Sprung, T. Kleine, and E. E. Scherer, "Isotopic evidence for chondritic Lu/Hf and Sm/Nd of the Moon," *Earth and Planetary Science Letters*, vol. 380, pp. 77-87, 2013.
- [50] S. J. Wentworth, L. P. Keller, D. S. McKAY, and R. V. Morris, "Space weathering on the Moon: Patina on Apollo 17 samples 75075 and 76015," *Meteoritics & Planetary Science*, vol. 34, no. 4, pp. 593-603, 1999.
- [51] J. Barnes *et al.*, "Accurate and precise measurements of the D/H ratio and hydroxyl content in lunar apatites using NanoSIMS," *Chemical Geology*, vol. 337, pp. 48-55, 2013.
- [52] F. M. McCubbin, A. Steele, E. H. Hauri, H. Nekvasil, S. Yamashita, and R. J. Hemley, "Nominally hydrous magmatism on the Moon," *Proceedings of the National Academy of Sciences*, vol. 107, no. 25, pp. 11223-11228, 2010.
- [53] M. Brounce *et al.*, "The oxidation state of sulfur in lunar apatite," *American Mineralogist: Journal of Earth and Planetary Materials*, vol. 104, no. 2, pp. 307-312, 2019.
- [54] J. M. Day, "Geochemical constraints on residual metal and sulfide in the sources of lunar mare basalts," *American Mineralogist: Journal of Earth and Planetary Materials*, vol. 103, no. 11, pp. 1734-1740, 2018.
- [55] E. H. Hauri, T. Weinreich, A. E. Saal, M. C. Rutherford, and J. A. Van Orman, "High pre-eruptive water contents preserved in lunar melt inclusions," *Science*, vol. 333, no. 6039, pp. 213-215, 2011.



- [56] F. M. McCubbin *et al.*, "Magmatic volatiles (H, C, N, F, S, Cl) in the lunar mantle, crust, and regolith: Abundances, distributions, processes, and reservoirs," *American Mineralogist*, vol. 100, no. 8-9, pp. 1668-1707, 2015.
- [57] M. J. Spicuzza, J. M. Day, L. A. Taylor, and J. W. Valley, "Oxygen isotope constraints on the origin and differentiation of the Moon," *Earth and Planetary Science Letters*, vol. 253, no. 1-2, pp. 254-265, 2007.
- [58] E. Füri, E. Deloule, and R. Trappitsch, "The production rate of cosmogenic deuterium at the Moon's surface," *Earth and Planetary Science Letters*, vol. 474, pp. 76-82, 2017.
- [59] A. E. Saal, E. H. Hauri, J. A. Van Orman, and M. J. Rutherford, "Hydrogen isotopes in lunar volcanic glasses and melt inclusions reveal a carbonaceous chondrite heritage," *Science*, vol. 340, no. 6138, pp. 1317-1320, 2013.
- [60] Z. Sharp, C. Shearer, K. McKeegan, J. Barnes, and Y. Wang, "The chlorine isotope composition of the Moon and implications for an anhydrous mantle," *Science*, vol. 329, no. 5995, pp. 1050-1053, 2010.
- [61] B. A. Wing and J. Farquhar, "Sulfur isotope homogeneity of lunar mare basalts," *Geochimica et Cosmochimica Acta*, vol. 170, pp. 266-280, 2015.
- [62] C. Kato, F. Moynier, M. C. Valdes, J. K. Dhaliwal, and J. M. Day, "Extensive volatile loss during formation and differentiation of the Moon," *Nature communications*, vol. 6, no. 1, pp. 1-4, 2015.
- [63] R. C. Paniello, J. M. Day, and F. Moynier, "Zinc isotopic evidence for the origin of the Moon," *Nature*, vol. 490, no. 7420, pp. 376-379, 2012.
- [64] K. Wang and S. B. Jacobsen, "Potassium isotopic evidence for a high-energy giant impact origin of the Moon," *Nature*, vol. 538, no. 7626, pp. 487-490, 2016.
- [65] J. Mortimer, A. Verchovsky, and M. Anand, "Predominantly non-solar origin of nitrogen in lunar soils," *Geochimica et Cosmochimica Acta*, vol. 193, pp. 36-53, 2016.
- [66] H. Vollstaedt, K. Mezger, and I. Leya, "The selenium isotope composition of lunar rocks: Implications for the formation of the Moon and its volatile loss," *Earth and planetary science letters*, vol. 542, p. 116289, 2020.
- [67] X. Wang, C. Fitoussi, B. Bourdon, B. Fegley, and S. Charnoz, "Tin isotopes indicative of liquid-vapour equilibration and separation in the Moon-forming disk," *Nature Geoscience*, vol. 12, no. 9, pp. 707-711, 2019.
- [68] E. A. Pringle and F. Moynier, "Rubidium isotopic composition of the Earth, meteorites, and the Moon: Evidence for the origin of volatile loss during planetary accretion," *Earth and Planetary Science Letters*, vol. 473, pp. 62-70, 2017.
- [69] N. X. Nie and N. Dauphas, "Vapor drainage in the protolunar disk as the cause for the depletion in volatile elements of the Moon," *The Astrophysical Journal Letters*, vol. 884, no. 2, p. L48, 2019.
- [70] C. Kato and F. Moynier, "Gallium isotopic evidence for extensive volatile loss from the Moon during its formation," *Science Advances*, vol. 3, no. 7, p. e1700571, 2017.
- [71] J. M. Day, E. M. van Kooten, B. A. Hofmann, and F. Moynier, "Mare basalt meteorites, magnesian-suite rocks and KREEP reveal loss of zinc during and after lunar formation," *Earth and Planetary Science Letters*, vol. 531, p. 115998, 2020.
- [72] S. M. Tikoo, B. P. Weiss, D. L. Shuster, C. Suavet, H. Wang, and T. L. Grove, "A two-billion-year history for the lunar dynamo," *Science Advances*, vol. 3, no. 8, p. e1700207, 2017.
- [73] J. M. Day, R. J. Walker, O. B. James, and I. S. Puchtel, "Osmium isotope and highly siderophile element systematics of the lunar crust," *Earth and Planetary Science Letters*, vol. 289, no. 3-4, pp. 595-605, 2010.



- [74] M. Fischer-Gödde and H. Becker, "Osmium isotope and highly siderophile element constraints on ages and nature of meteoritic components in ancient lunar impact rocks," *Geochimica et Cosmochimica Acta*, vol. 77, pp. 135-156, 2012.
- [75] NRC, *The Scientific Context for Exploration of the Moon*. Washington, DC: The National Academies Press (in English), 2007, p. 120.
- [76] NRC, *Vision and Voyages for Planetary Science in the Decade 2013-2022*. Washington, DC: The National Academies Press (in English), 2011, p. 398.
- [77] B. Jolliff *et al.*, "Selecting and certifying a landing site for moonrise in South pole-Aitken basin," 2017.
- [78] "Artemis III Science Definition Team Report," NASA, 2020.
- [79] J. M. Devine, D. S. McKay, and J. J. Papike, "Lunar regolith: Petrology of the < 10 μm fraction," *Journal of Geophysical Research: Solid Earth*, vol. 87, no. S01, pp. A260-A268, 1982.
- [80] D. S. McKay *et al.*, "The lunar regolith," in *Lunar sourcebook*, vol. 7: Citeseer, 1991, pp. 285-356.
- [81] R. J. Walker and P. J. J., "The relationship of the lunar regolith <10 μm fraction and agglutinates. Part II: Chemical composition of agglutinate glass as a test of the 'fusion of the finest fraction' (F3) model," presented at the Lunar and Planetary Science Conference, 1981.
- [82] B. Denevi *et al.*, "Lunar Simulant Assessment," Johns Hopkins Applied Physics Laboratory, 2020.
- [83] P. C. Hess and E. Parmentier, "A model for the thermal and chemical evolution of the Moon's interior: Implications for the onset of mare volcanism," *Earth and Planetary Science Letters*, vol. 134, no. 3-4, pp. 501-514, 1995.
- [84] L. T. Elkins-Tanton, J. A. Van Orman, B. H. Hager, and T. L. Grove, "Re-examination of the lunar magma ocean cumulate overturn hypothesis: melting or mixing is required," *Earth and Planetary Science Letters*, vol. 196, no. 3-4, pp. 239-249, 2002.
- [85] (1970). *Performance evaluation of wheels for lunar vehicles*.
- [86] I. A. Nesnas, M. W. Maimone, and H. Das, "Rover Maneuvering for Autonomous Vision-Based Dexterous Manipulation," in *IEEE International Conference on Robotics and Automation*, San Francisco, CA, April 24-28 2000: IEEE, in ICRA 2000 Proceedings, pp. 2296–2301, doi: 10.1109/ROBOT.2000.846369.
- [87] V. Asnani, D. Delap, and C. Creager, "The development of wheels for the Lunar Roving Vehicle," *Journal of Terramechanics*, vol. 46, no. 3, pp. 89–103, 2009, doi: 10.1016/j.jterra.2009.02.005.
- [88] M. G. Bekker, "The Development of a Moon Rover," *Journal of the British Interplanetary Society*, vol. 38, p. 537, 1985.
- [89] (1965). *A dimensionless consolidation of WES data on the performance of sand under tire loads*.
- [90] M. Sutoh, J. Yusa, T. Ito, K. Nagatani, and K. Yoshida, "Traveling performance evaluation of planetary rovers on loose soil," *Journal of Field Robotics*, vol. 29, no. 4, pp. 648–662, 2012, doi: 10.1002/rob.21405.
- [91] S. J. VanBommel *et al.*, "Modeling and mitigation of sample relief effects applied to chemistry measurements by the Mars Science Laboratory Alpha Particle X-ray Spectrometer," *X-Ray Spectrometry*, vol. 46, no. 4, pp. 229–236, 2017, doi: 10.1002/xrs.2755.
- [92] M. Fleder, I. A. Nesnas, M. Pivtoraiko, A. Kelly, and R. Volpe, "Autonomous rover traverse and precise arm placement on remotely designated targets," in *2011 IEEE International Conference on Robotics and Automation*, Shanghai, China, 2011: IEEE, pp. 2190–2197.
- [93] M. Heverly *et al.*, "Traverse Performance Characterization for the Mars Science Laboratory Rover," *Journal of Field Robotics*, vol. 30, no. 6, pp. 835-846, 2013, doi: 10.1002/rob.21481.
- [94] H. Kanamori, S. Udagawa, T. Yoshida, S. Matsumoto, and K. Takagi, "Properties of Lunar Soil Simulant Manufactured in Japan," in *Sixth ASCE Specialty Conference and Exposition on Engineering*,

- Construction, and Operations in Space*, 1998, pp. 462-468, doi: 10.1061/40339(206)53. [Online]. Available: <https://ascelibrary.org/doi/abs/10.1061/40339%28206%2953>
- [95] L. Ding, H. Gao, Z. Deng, J. Guo, and G. Liu, "Longitudinal slip versus skid of planetary rovers' wheels traversing on deformable slopes," in *2013 IEEE/RSJ International Conference on Intelligent Robots and Systems*, 3-7 Nov. 2013, pp. 2842-2848, doi: 10.1109/IROS.2013.6696758.
- [96] M. Sutoh, K. Nagaoka, K. Nagatani, and K. Yoshida, "Evaluation of Influence of Wheel Surface Shapes on Tractive Efficiencies of Planetary Rovers in Various Soil Environments," in *International Symposium on Artificial Intelligence, Robotics and Automation in Space (i-SAIRAS)*, 2012, vol. Proceedings of the International Symposium on Artificial Intelligence, Robotics and Automation in Space.
- [97] Interagency Operations Advisory Group - Lunar Communications Architecture Working Group (IOAG/LCAWG), "The Future Lunar Communications Architecture," 2019. [Online]. Available: <https://www.ioag.org/Public%20Documents/Lunar%20communications%20architecture%20study%20report%20Final%2009-25-2019.docx>
- [98] M. Boucher, "NASA's Plans to Commercialize Communications and Navigation from the Earth to the Moon," in *The Space Economy*, ed: SpaceQ, 2021.
- [99] A. Patro, private communication.
- [100] J. Friend, private communication.
- [101] "Lunar Pathfinder Service User Guide," 2020. [Online]. Available: <https://irp-cdn.multiscreensite.com/19e31c60/files/uploaded/LunarPathfinder-UserManual-WebSite-v002-2.pdf>
- [102] (2008). *IPN Progress Report 42-175, Solar Brightness Temperature and Corresponding Antenna Noise Temperature at Microwave Frequencies*. [Online] Available: https://ipnpr.jpl.nasa.gov/progress_report/42-175/175E.pdf
- [103] M. Pugh, I. Kuperman, M. Kobayashi, F. Aguirre, M. Kilzer, and C. Spurgers, "High-rate Ka-band modulator for the NISAR mission," in *2018 IEEE Aerospace Conference*, March 3-10 2018, pp. 1-13, doi: 10.1109/AERO.2018.8396451.
- [104] (2004). *CCSDS 211.1-B-2, PROXIMITY-1 SPACE LINK PROTOCOL—PHYSICAL LAYER BLUE BOOK*.
- [105] (2004). *CCSDS 211.0-B-3, PROXIMITY-1 SPACE LINK PROTOCOL—DATA LINK LAYER BLUE BOOK*.
- [106] (2003). *CCSDS 211.2-B-1, PROXIMITY-1 SPACE LINK PROTOCOL—CODING AND SYNCHRONIZATION SUBLAYER BLUE BOOK*.
- [107] P. O. Hayne *et al.*, "Global Regolith Thermophysical Properties of the Moon From the Diviner Lunar Radiometer Experiment," *Journal of Geophysical Research: Planets*, vol. 122, no. 12, pp. 2371-2400, 2017, doi: 10.1002/2017JE005387.
- [108] J. R. Gaier, M. C. Hicks, and R. M. Misconin, "Studies of Simulated Lunar Dust on the Properties of Thermal-Control Surfaces," *Journal of Spacecraft and Rockets*, vol. 50, no. 4, pp. 848-852, 2013, doi: 10.2514/1.A32135.